The Role of Protein Kinase C Epsilon in the Pathogenesis and Treatment Resistance of Acute Myeloid Leukaemia

A thesis submitted to Cardiff University in candidature for the degree of Doctor of Philosophy

Rachael Louise Nicholson

Division of Cancer and Genetics,

School of Medicine,

Cardiff University

May 2021

Abstract

Acute myeloid leukaemia (AML) is a heterogeneous group of haematological malignancies, characterised by the accumulation of abnormally differentiated blast cells in the bone marrow. For most patients, prognosis remains poor due to the prevalence of relapse. Protein kinase C epsilon (PKCε) is a pleiotropic regulator of cell signalling which has demonstrated oncogenic properties and in solid cancers, high PKCε expression is associated with poor outcomes. The aim of this study was to determine the clinical significance and functionality of PKCε in AML.

Existing protein expression data showed that PKCε was significantly upregulated in 37% (26/70) of AML patient samples and was associated with reduced CR ($p<0.05$). To support this, I analysed an independent mRNA dataset where high *PKCε* expression correlated with significantly reduced overall ($p<0.05$) and disease-free survival ($p<0.05$). Together these data suggest that high PKCε expression is associated with poor outcomes in AML. Functionality was investigated by modulating PKCε in normal human haematopoietic cells where PKCε overexpression promoted monocyte differentiation. This finding is inconsistent with a role in leukaemogenesis. Instead, it was hypothesized that PKCε may promote chemoresistance. In two AML cell lines, PKCε overexpression conferred daunorubicin (DNR) resistance ($p<0.05$) without affecting cytarabine sensitivities. This was accompanied by reduced DNR accumulation, and the upregulation of the selective DNR efflux pump, P-GP. P-GP inhibition restored DNR accumulation and sensitivity, demonstrating P-GP drug efflux as the mechanism of PKCε-mediated DNR resistance. PKC agonist and inhibitor treatments suggested that PKCε modulates P-GP drug efflux through indirect mechanisms, but a correlation between PKCε and P-GP expression and function was supported by analysis of patient samples. However, reducing PKCε expression did not sensitize AML cells to DNR, potentially due to redundancy between PKC isoforms.

In conclusion, elevated PKCε expression is a poor prognostic indicator in AML. Functional studies did not support an oncogenic role for PKCε in normal haematopoietic cells or AML cell lines. Nonetheless, PKCε can influence the chemosensitivity of AML cells by promoting P-GP-mediated DNR efflux, providing a mechanism through which PKCε could contribute to poor outcomes in this malignancy.

Acknowledgements

I would like to express my deepest gratitude to Prof. Richard Darley and Prof. Alex Tonks for their invaluable expertise and guidance throughout this project. I am particularly grateful for their support and patience over the last year, considering the challenges caused by the unprecedented times of late. Their knowledge and encouragement have allowed me to develop as a scientist and they have provided me with some unforgettable experiences. I would also like to thank Dr Steven Knapper for his advice and affording me the opportunity to attend a haematology clinic. Meeting patients served as a constant reminder of why conducting AML research is so important. Furthermore, I would like to acknowledge Sara Davies for her technical support and training at the start of this project, and the technical support of members of the Central Biotechnology Service at Cardiff University, namely Dr Ann Kift-Morgan, Dr Catherine Naseriyan and Mark Bishop.

Due to the difficult circumstances of the pandemic, I must thank the School of Medicine and Division of Cancer and Genetics leadership teams for their hard work which facilitated my return to the laboratory, especially Pete Gapper and Amanda Gilkes. In addition, I would like to thank Dr Amanda Tonks (Director of PGR, School of Medicine at Cardiff University) for her support and advice throughout my studies but particularly for her help in securing a funding extension for my final few months of research.

Special thanks are extended to my colleagues (and friends) Catarina Menezes, Aleksandra Azevedo and Adam Leckenby, for being there to celebrate the little victories and providing an endless supply of tea and biscuits which saw me through the less successful research days. I am also endlessly grateful to my parents for their constant support, and to all my friends and loved ones for always reminding me of my strength and abilities.

This research was funded by the School of Medicine, Cardiff University and I am sincerely grateful to everyone who has made this project possible.

Publications and Presentations

Publications

ABSTRACT: PKC-Epsilon Overexpression is Associated with Poor Outcomes in AML and Promotes Chemoresistance and Hematopoietic Stem Cell Quiescence **RL Nicholson**, S Knapper, A Tonks, RL Darley Blood 2019 Nov;134 (supplement_1):2704. doi: https://doi.org/10.1182/blood-2019-128184

Oral Presentations

2020- Schools of Medicine and Dentistry PGR symposium, Cardiff University, UK

2018-Division of Cancer and Genetics PGR Symposium, Cardiff University, UK

2018-2021 Haematology Department Seminar Series, Cardiff University, UK

Poster Presentations

2019- American Society of Hematology Conference, Orlando, Florida, USA

Awards

2020-American Society of Hematology Abstract Achievement Award

2020- William Morgan Thomas Fund Travel Bursary, Cardiff University

2018-People's Choice Award at the 2018-Division of Cancer and Genetics PGR Symposium

Contents

Summary of Figures

Summary of Tables

List of Abbreviations

Abbreviation	Definition
ALL	Acute Lymphocytic Leukaemia
AML	Acute Myeloid Leukaemia
APC	Allophycocyanin
aPKC	Atypical Protein Kinase C Isoforms
APL	Acute Promyelocytic Leukaemia
Ara-C	Cytarabine
ATM	Antimycin A
ATO	Arsenic Trioxide
ATRA	All-Trans Retinoic Acid
BM	Bone Marrow
BME	2-Mercaptoethanol
BSA	Bovine Serum Albumin
CB	Umbilical Cord Blood
C/EBPα	CCAAT/Enhancer-Binding Protein alpha
CC	Calphostin C
CFC	Colony Forming Cells
CLL	Chronic Lymphocytic Leukaemia
CLP	Common Lymphoid Progenitors
CML	Chronic Myeloid Leukaemia
CMP	Common Myeloid Progenitors
cPKC	Conventional Protein Kinase C Isoforms
CR	Complete Remission
CSF	Colony Stimulating Factor
CTP	Cytarabine Trisphosphate
CXCL12	CXC-Chemokine Ligand 12
CXCR4	CXC-Chemokine Receptor 4
DAG	Diacylglycerol
dCK	Deoxycytidine Kinase
DepMap	The Broad Institute's Cancer Dependency Map Project Portal
dH_2O	Distilled Water
DMSO	Dimethyl Sulfoxide
DNR	Daunorubicin
DOX	Doxorubicin
DFS	Disease Free Survival
EC50	Half-Maximal Effective Concentration
ECM	Extracellular Matrix
EDTA	Ethylenediaminetetraacetic Acid
EGTA	Ethylene Glycol-bis (β-aminoethyl ether)-N-N-N'-N'-Tetra Acetic Acid
EPO	Erythropoietin
EPO-R	Erythropoietin Receptor
ETC	Electron Transport Chain

FAB	French American British
FACS	Fluorescently Activated Cell Sorting
FADD	Fas-Associated Death Domain
FBS	Foetal Bovine Serum
FLAG-Ida	Fludarabine,+Ara-C,+G-CSF+Idarubicin
FLT3	Fms-Like Tyrosine kinase 3
FSC	Forward Scatter
GATA	Globin Transcription Factor
GAPDH	Glyceraldehyde 3-Phosphate Dehydrogenase
G-CSF	Granulocyte Colony Stimulating Factor
GFP	Green Fluorescent Protein
GM-CSF	Granulocyte-Macrophage Colony Stimulating Factor
GMP	Granulocyte-Macrophage Progenitors
GO	Gemtuzumab Ozogamicin
GOx	Glucose Oxide
H_2O_2	Hydrogen Peroxide
HA	Hyaluronan
hENT	Human Equilibrative Nucleoside Transporter
HMA	Hypomethylating Agents
HR	Hazard Ratio
HRP	Horseradish Peroxidase
HSC	Haematopoietic Stem Cells
HSPC	Haematopoietic Stem and Progenitor Cells
IP_3	Inositol 3,4,5-trisphosphate
IT-HSC	Intermediate-term Haematopoietic Stem Cells
K_{ATP}	Potassium Channels
LSC	Leukaemic Stem Cell
LDAC	Low-dose Cytarabine
LDS	Lithium Dodecyl Sulphate
LPS	Lipopolysaccharide
LSC	Leukaemic Stem Cell
LT-HSC	Long-term Haematopoietic Stem Cells
MDR	Multidrug Resistance
MDS	Myeloid Dysplastic Syndromes
MEP	Megakaryocyte-Erythrocyte Progenitors
MNC	Mononuclear Cells
MRP1	Multidrug Resistance Related Protein-1
N.D	Not Determined
NEB	New England Biolabs
NOX2	NADPH Oxidase 2
nPKC	Novel Protein Kinase C Isoforms
NPM1	Nucleophosmin
NLS	Nuclear Localisation Sequence
NSCLC	Non-Small Cell Lung Cancer
OS	Overall Survival
PB	Peripheral Blood
pBCL-2	Phosphorylated BCL-2

PBS	Phosphate Buffer Saline
PDK-1	Phosphoinositide-dependent kinase -1
PFA	Paraformaldehyde
P-GP	P-Glycoprotein
Ph	Philadelphia Chromosome
PI3K	Phosphoinositide 3-Kinase
PKC	Protein Kinase C
PKCε	Protein Kinase C Epsilon
PLC	Phospholipase C
PMA	Phorbol 12-Myristate-13-Acetate
pPKCα	Phosphorylated PKCα
PS	Pseudo-substrate
Puro^R	Puromycin resistance gene
RACK	Receptors for Activated C Kinase
RLU	Relative Light Units
RMA	Robust Multi Array
ROI	Region of Interest
ROS	Reactive Oxygen Species
r_p	Pearson's Correlation Coefficient
RPMI	Roswell Park Memorial Institute-1640 medium
RT	Room Temperature
SA-PerCP	Streptavidin-Peridinin Chlorophyll Protein
SCF	Stem Cell Factor
SCLC	Small Cell Lung Cancer
SLC	Solute Carrier Protein
SSC	Side Scatter
ST-HSC	Short-term Haematopoietic Stem Cells
TPO	Thrombopoietin
TPM	Transcripts Per Million
TRAIL	Tumour Necrosis Factor-Related Apoptosis-Inducing Ligand
UC	Universal Containers
VCAM-1	Vascular Cell Adhesion Molecule-1
VLA-4	Very Late Antigen-4
WBC	White Blood Count
WHO	World Health Organisation
ZSQ	Zosuquidar Hydrochloride

Chapter 1: Introduction

1.1 Haematopoiesis

The haematopoietic system comprises of specialised cell types which are responsible for a range of biological functions including the transport of oxygen and CO_2 around the body, coagulation, and immune responses. Haematopoietic cells are continually produced throughout a lifetime, and production of specific cell types can rapidly increase upon demand. Haematopoiesis describes the intricate and highly orchestrated process by which all terminally differentiated haematopoietic cells are generated. For the first 6 months of gestation, blood cells are transiently produced by the yolk sac through extra-embryonic haematopoiesis and is succeeded by definitive haematopoiesis in the aorta-gonad-mesonephros (AGM; Ivanovs, *et al.*, 2017). In the later stages of development, blood cell production occurs in the placenta, foetal liver, spleen, and bone marrow (BM; Ivanovs, *et al.*, 2017). Postnatally, the BM is the primary site of life-long haematopoiesis, although the liver and spleen retain some capacity for haematopoietic cell production in the case of increased demand such as injury (Kim, 2010).

Haematopoiesis is regulated by a complex network of intrinsic factors and environmental cues (1.1.2). Historically, haematopoiesis was depicted as a hierarchical tree and was considered a unilateral, stepwise process. The overall structure of the hierarchical model is outlined in Figure 1.1, where haematopoietic stem cells (HSC), which possess pluripotent and self-renewing capacity (1.1.1), sit at the apex. In response to appropriate stimuli (1.1.2), HSC give rise to progeny with increased differentiation potential and reduced self-renewal capacity (Akashi, *et al.*, 2000, Kondo, *et al.*, 1997). Initially, HSC give rise to multipotent progenitors (MPP) which generate common myeloid (CMP) and lymphoid (CLP) committed progenitors. In turn, CMP and CLP are responsible for the development of the monocytic, granulocytic and erythro-megakaryocytic lineages, and lymphoid, B-, T-, and natural killer (NK) -cells, respectively. In terms of the myeloid lineage, CMP can differentiate into granulocyte-macrophage progenitors (GMP) or megakaryocyte-erythroid progenitors (MEP). GMP ultimately give rise to monocytes, macrophages, and granulocytic cells from which basophils, neutrophils, and eosinophils are derived, while erythrocytes and platelets arise from MEP (Rieger and Schroeder, 2012; Figure 1.1). Once progenitors become uni-lineage committed, they continue to develop until terminal differentiation is achieved. The mature

blood cells subsequently leave the BM to carry out their biological function within the circulatory system (Konieczny and Arranz, 2018, Robb, 2007).

Since the hierarchical model was first proposed, evidence has emerged that haematopoiesis is a much more dynamic process. High-throughput and single-cell methodologies such as RNA sequencing, mass cytometry, and immunophenotypic analysis, have shown a high degree of heterogeneity and plasticity within defined cellular populations, which were previously considered homogenous. For example, immunophenotypic cell sorting and single-cell cloning analysis of human BM-derived $CD34^+$ cells indicated that this cellular compartment primarily consists of uni-lineage myeloid or erythroid progenitors and only a small proportion of oligopotent progenitor cells (Notta, *et al.*, 2016). As a result, alternative models of haematopoietic cell development have been proposed. One such example is the "myeloid bypass model" which suggests that myeloid lineage committed progenitors can be derived directly from HSC (Yamamoto, *et al.*, 2013). Using single cell transplantation studies, distinct self-renewing lineage restricted progenitor populations were identified within the phenotypically defined HSC population, including megakaryocyte repopulating progenitors (MkRP) megakaryocyte-erythrocyte repopulating progenitors (MERP) and common myeloid repopulating progenitors (CMRP; Yamamoto, *et al.*, 2013). Such heterogeneity within the HSC compartment as well as other progenitor populations is indicative of a dynamic process of haematopoiesis (Cabezas-Wallscheid, *et al.*, 2014, Wilson, *et al.*, 2008). Although methods such as single cell RNAseq cannot provide temporal information, it has allowed the identification of additional cellular compartments, and provides a detailed outline of the similarities and discrepancies between the transcriptional landscape of individual cell types. Single cell analysis of murine bone marrow cells to assess the transcriptomic landscape did not identify cells which significantly express multiple lineage-specific genes or transcription factors, suggesting cells in an intermediate state of lineage commitment are rare (Paul, *et al.*, 2015). Examples of "revised" models of haematopoiesis using single cell analysis have been reviewed in Cheng, *et al.*, 2020, and all demonstrate that haematopoiesis is not a unilateral process as previously thought.

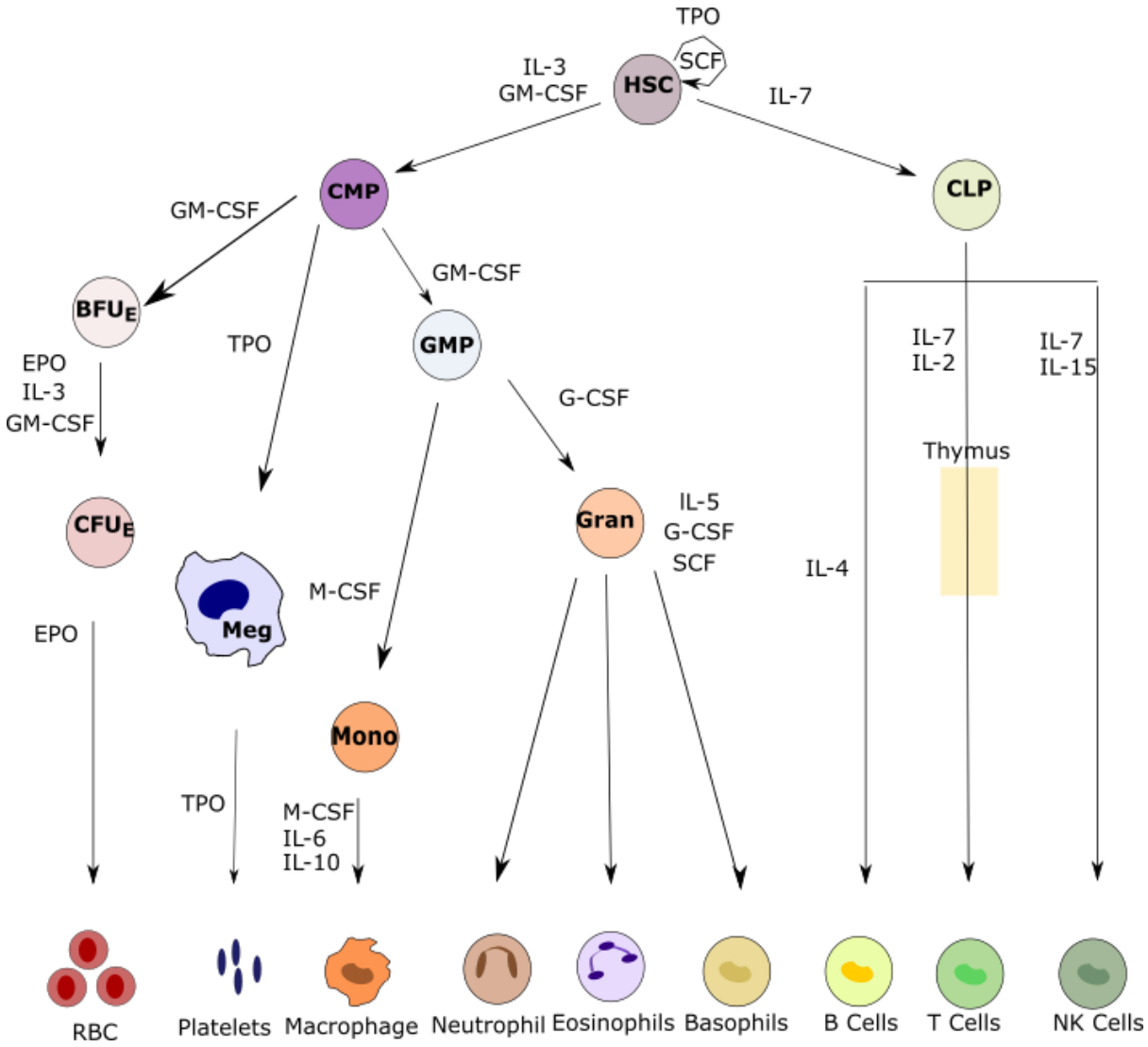

Figure 1.1: The hierarchical organisation of haematopoiesis

Schematic outlining the hierarchical model of haematopoiesis as described in 1.1 whereby, HSC differentiate into multipotent myeloid (common myeloid progenitor; CMP) and lymphoid (common lymphoid progenitor; CLP) cells. These progenitors subsequently undergo uni-lineage commitment and maturation until terminal differentiation is achieved. Some of the cytokines which support haematopoietic cell maintenance and differentiation are indicated. The transcriptional and cytokine regulation of haematopoiesis is outlined in greater depth in 1.1.2. Following the application of high throughput methods such as single cell RNAseq, haematopoiesis is thought to be a much more plastic process than is indicated by the hierarchical model (outlined in 1.1). Figure was adapted from Robb, 2007. *Abbreviations: HSC; Haematopoietic Stem Cell, CMP; Common Myeloid Progenitor; CLP; Common Lymphoid Progenitor, BFU_E; Erythroid burst forming units, CFU_E; Erythroid Colony forming units; RBC, Red Blood Cell; Mono; monocyte; Gran; Granulocytic progenitors; Meg; Megakaryocyte.*

1.1.1 Haematopoietic Stem Cells and the Bone Marrow Microenvironment

HSC reside within the BM and are defined by their self-renewal capacity and propensity to recapitulate the haematopoietic system in its entirety (Morrison and Weissman, 1994, Okada, *et al.*, 1992). As a rare population of cells, the degree of scalability required throughout haematopoiesis can only be achieved through the strict maintenance of an HSC pool. This occurs through the balance between HSC self-renewal and differentiation. The asymmetric division of HSC contributes to this (Wilson and Trumpp, 2006), but HSC maintenance is also facilitated by direct interactions and extrinsic signals from components of the BM microenvironment (1.1.1.1)

Most of the studies used to characterise HSC function have been conducted in murine transplantation models, where the ability of transplanted cells to restore the haematopoietic system is assessed. HSC were initially characterised as $CD34^{+}CD38^{-}$ cells as transplantation of this cellular compartment into immunodeficient mice showed a high level of engraftment and gave rise to myeloid- and lymphoid-committed progeny (Bhatia, *et al.*, 1997). Since the initial phenotypic characterisation of HSC, additional markers have been used to identify HSC such as Sca-1 and c-Kit in murine HSC (Okada, *et al.*, 1992), while CD90 positivity and the lack of CD45RA expression has been used to further characterise human HSC (Baum, *et al.*, 1992, Lansdorp, *et al.*, 1990, Majeti, *et al.*, 2007). In addition, the expression of CD49f on human haematopoietic cells can be used to distinguish between HSC and MPP (Notta, *et al.*, 2011).

Although often referred to as a single population of cells, molecular and functional analysis has identified distinct HSC sub-populations, which possess different self-renewal and differentiation capacities. Long-term (LT)-HSC ($CD34^{low/negative}$, c-Kit^{+}, Sca-1^{+}cells) have the capacity to reconstitute the haematopoietic system for between 3-4 months (Morrison and Weissman, 1994, Osawa, *et al.*, 1996), while short-term (ST)-HSC are $CD34^{+}$ but have a limited re-constitutive capacity (<1 month), and intermediate-term (IT)-HSC fall between LT- and SC-HSC in terms of self-renewal and re-constitutive capacity (Benveniste, *et al.*, 2010). Through cell sorting and mass cytometry analysis of primitive $CD34^{+}$ cells, Knapp *et al.* has also identified a high degree of heterogeneity, in terms of regenerative capacity, within this cellular compartment of human haematopoietic cells (Knapp, *et al.*, 2018). Although this could in part be due to the presence of primitive committed progenitors in addition to HSC, a

panel of markers were used to enrich for HSC as effectively as possible (Knapp, *et al.*, 2018). In addition to their differentiation and self-renewal properties, HSC also differ from more committed progenitor cells as they have a reduced mitochondrial (Vannini, *et al.*, 2016), and altered metabolic activity (Takubo, *et al.*, 2013).

1.1.1.1 The Bone Marrow Microenvironment

The concept of a stem cell niche was first proposed by Schofield, 1978 and subsequently, the importance of the microenvironment in which haematopoietic cells reside in normal haematopoiesis and haematological malignancies has been realised. The BM microenvironment is made up of a complex network of cells and secreted factors, as outlined in Figure 1.2, and contributes to the maintenance of HSC pluripotency and self-renewal. Broadly, the BM microenvironment can be divided into two niches: the endosteal and vascular niche. The endosteal niche is located near the bone surface and HSPC transplantation studies have shown that this is the preferred site of HSC homing within the BM (Nilsson, *et al.*, 2001). Traditionally, it was thought the endosteal niche primarily supported quiescent HSC, while the vascular niche supported proliferative and differentiating progenitors. However, evidence has emerged that the vascular niche also has the capacity to support quiescent HSC, with c65% of LT-HSC were maintained near sinusoids, facilitated by interactions with polydendrocytes and endothelial cells (Goulard, *et al.*, 2018).

Osteoblasts are a central component of the stromal BM support network, as demonstrated by conditional ablation of osteoblasts in mice which resulted in the loss of HSC, lymphoid, myeloid, and erythroid progenitor cells (Visnjic, *et al.*, 2004). In particular, the maintenance of HSC quiescence by osteoblasts is achieved through the production of cytokines such as thrombopoietin (TPO; Yoshihara, *et al.*, 2007) and angiopoietin-1 (Arai, *et al.*, 2004). In addition, interactions of the chemokine ligand 12 (CXCL12, also known as SDF-1) which is produced by the endosteal and vascular niches, with CXC-chemokine receptor 4 (CXCR4) expressed on the surface of HSC is an important axis in HSC maintenance. This has been demonstrated in mice, as conditional CXCR4 deficiency severely reduced the number of HSC in the BM (Sugiyama, *et al.*, 2006). As well as secreted factors, cellular interactions which modulate Notch (Calvi, *et al.*, 2003) and bone morphogenic protein signalling in HSC (Zhang, *et al.*, 2003) are also important in HSC maintenance and regulation by the BM microenvironment.

Cell adhesion molecules such as cadherins mediate the interactions of HSC and the BM microenvironment. The best studied cadherin in HSC maintenance is N-cadherin which is expressed on osteoblasts and HSC (Zhang, *et al.*, 2003). Despite the evidence that N-cadherin can mediate HSC proliferation and long-term self-renewal (Haug, *et al.*, 2008, Hosokawa, *et al.*, 2010), the requirement of N-cadherin has been disputed. Conditional deletion of N-cadherin in HSC revealed normal HSC frequency, while the reconstitution capacity of these cells in primary and secondary transplantations in irradiated mice was unaffected (Bromberg, *et al.*, 2012, Kiel, *et al.*, 2009). In addition to cadherins, integrins are also important in HSC homing and BM niche interactions (Grassinger, *et al.*, 2009, Potocnik, *et al.*, 2000).

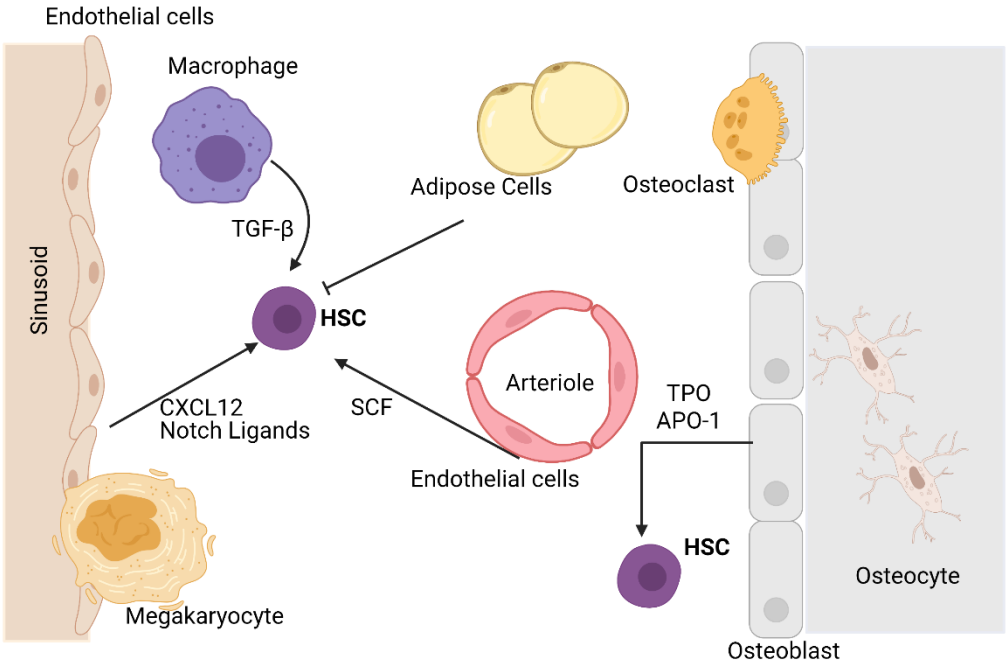

Figure 1.2: Schematic of HSC regulation by the BM microenvironment

Schematic showing components of the BM microenvironment which contribute to HSC maintenance (1.1.1.1). Image adapted from Pinho and Frenette, 2019. *Abbreviations; APO-1; angiopoietin-1, CXCL12; chemokine ligand 12, HSC; haematopoietic stem cell, SCF, stem cell factor, TGF-β, transforming growth factor beta, TPO; thrombopoietin.*

1.1.2 Regulation of Haematopoiesis

Homoeostatic regulation of haematopoiesis relies on the complex interactions of cytokines, transcription factors and signalling pathways, to direct cell fate. Haematopoietic cytokines are a group of soluble glycoproteins which were first identified in the 1960s and include interleukins (IL), colony stimulating factors (CSF), erythropoietin (EPO) and TPO (Robb, 2007). These factors can exert their function in a para-, endo- or autocrine fashion and influence haematopoietic stem and progenitor cell (HSPC) proliferation, lineage commitment and differentiation (Figure 1.1).

Cytokines and growth factors promote physiological changes in cells through interactions with cognate receptors expressed on the cell surface. The transduction of cytokine signals from cytokine-receptor interactions trigger homo-or hetero-dimerization of the receptors and the downstream phosphorylation of Janus kinases (JAK). This results in phosphorylation cascades and the subsequent activation of signal transducer and activator of transcription (STAT) proteins which induces differential gene expression (Spangler, *et al.*, 2015). In addition, some cytokines can activate the Akt and ERK signalling pathways, while signalling cascades including TGF-β, and Notch (Robert-Moreno, *et al.*, 2008), may also play a role in HSC specification, and differentiation (Kim, *et al.*, 2014).

In vitro studies have demonstrated that cytokines have different specificities, with some cytokines such as IL-3 promoting the proliferation of most lineages (Ihle, 1992), while EPO is an example of a cytokine which has lineage specific functions. Knockout of the EPO receptor (EPO-R) impairs erythroid colony formation and erythroblast development Lin, *et al.*, 1996. However, EPO-R deficient mouse embryos retained normal levels of early erythroid progenitors (Lin, *et al.*, 1996), highlighting that EPO is not required for erythroid lineage commitment or the generation of early committed progenitors but is critical in the terminal differentiation of erythroid cells. Murine studies have also shown a critical role for granulocyte colony stimulating factor (G-CSF) in myeloid cell development as knockout mice have chronic neutropenia because of impaired granulopoiesis and neutrophil mobilisation (Lieschke, *et al.*, 1994). Although most haematopoietic cytokines are pleotropic, the ability of some cytokines to promote the generation of specific cell types has also been of use clinically, as administration of recombinant cytokines can restore haematopoietic defects which occur as a complication of chemotherapy treatment (Antman, *et al.*, 1988, Gabrilove, *et al.*, 1988).

Despite the established importance of cytokine signalling in regulating haematopoiesis, there are two contrasting models which hypothesise the requirement of these factors in haematopoietic cell differentiation. The stochastic model was first proposed in the 1960s following a study in which multipotent progenitor cells (CFU-S) were injected into irradiated mice (Till, *et al.*, 1964). After two weeks the injected cells gave rise to a mixture of differentiated and undifferentiated cell types (Till, *et al.*, 1964). As the number of CFU-S cells within the generated colonies was highly variable it was suggested that differentiation was not tightly regulated for individual cells but is a stochastic event for which cytokines play a supportive role (Till, *et al.*, 1964). In contrast to the stochastic model, the instructive model suggests that cytokines transmit signals to multipotential haematopoietic cells and direct HSPC lineage commitment and differentiation (Robb, 2007). This hypothesis is supported by studies which forced the ectopic expression of cytokine receptors in HSPC. For example, overexpression of the G-CSF receptor in FDC-P1 mouse cells (which do not normally respond to G-CSF) promoted neutrophil differentiation (Fukunaga, *et al.*, 1993). Following such studies, the consensus is now towards an instructive role for cytokines in directing cell fate (Stanley, 2009).

Regardless of the relative contributions of cytokines in haematopoietic cell development, the signals transduced by these factors ultimately converge on haematopoietic transcription factors which direct cell fate by driving changes in gene expression. Several transcription factors have been implicated in myeloid differentiation including globin transcription factor (GATA) -1, GATA-3, Notch-1, friend of GATA-1 (FOG-1), putative oncogene Spi-1 (PU.1), and CCAAT/enhancer-binding protein alpha (C/EBPα) (Iwasaki and Akashi, 2007, Nerlov and Graf, 1998, Nerlov, *et al.*, 1998). As with the cytokine regulation of haematopoiesis, the co-operation of transcription factors can drive cell fate towards specific lineages. For example, the upregulation of PU.1 and GATA-1 promote the commitment of HSC to CMP (Zhu and Emerson, 2002), while GATA-1 and FOG-1 are involved in megakaryocyte and erythrocyte commitment in multipotent myeloid progenitors (Mancini, *et al.*, 2012, Shivdasani, *et al.*, 1997).

1.2 Acute Myeloid Leukaemia

Leukaemia describes a group of haematological malignancies which arise from the accumulation of genetic and epigenetic aberrations within haematopoietic progenitor cells and are broadly classified according to the type of haematopoietic cell affected. Myeloid leukaemia (also known as myelocytic or myelogenous leukaemia) manifests in myeloid progenitor cells, whilst lymphocytic leukaemia (also known as lymphoid or lymphoblastic leukaemia) impacts lymphocytic progenitors. Leukaemia can then be further classified into acute and chronic disease, according to the rate of progression. In acute leukaemia, blast accumulation occurs rapidly, while in chronic disease the accumulation of malignant blasts is considerably slower. With these classification systems in mind, there are four main types of leukaemia, chronic lymphocytic leukaemia (CLL), chronic myeloid leukaemia (CML), acute lymphocytic leukaemia (ALL) and acute myeloid leukaemia (AML). However, AML can be further classified according to the presence of specific cytogenetic and molecular aberrations, see 1.2.4.

1.2.1 Incidence and Aetiology

AML is a heterogeneous group of haematological malignancies that are characterised by the infiltration of the BM, peripheral blood (PB), and organs, such as the spleen and lymph nodes, by clonal, abnormally differentiated myeloid cells (Döhner, *et al.*, 2015). Collectively, AML represents a third of leukaemia cases in the United Kingdom (UK) and overall has a slightly higher prominence in men compared with women (Bhayat, *et al.*, 2009, Maksimovic, *et al.*, 2018). Although childhood leukaemia accounts for 15-20% of AML diagnoses, incidence increases with age and overall, the median age of diagnosis for AML is 65 years (Deschler and Lubbert, 2006, Shysh, *et al.*, 2017). Thus, with an aging population, the incidence of age-related malignancies such as AML are likely to increase in prevalence.

Development of an AML phenotype occurs following genetic reprogramming within myeloid progenitor cells which block their differentiation and confer a survival and/or proliferative advantage (1.2.2). Several factors are associated with an increased risk of developing AML, such as exposure to ionising radiation or cigarette smoke, and genetic disorders such as Down Syndrome, and Li-Fraumeni Syndrome (Deschler and Lubbert, 2006, Hasle, *et al.*, 2000, Pogoda, *et al.*, 2002, Swaminathan, *et al.*, 2019). AML can arise following chemotherapy or radiation, or from progressed myelodysplastic syndrome (MDS), and for

these patients, disease is particularly difficult to treat (Boddu, *et al.*, 2017). However, most patients will present with *de novo* disease, and will have no known predisposing risk factors.

1.2.2 Leukaemogenesis and Disease Evolution

AML develops from the progressive acquisition of genetic and epigenetic mutations within myeloid progenitor cells. The multi-step process of leukaemogenesis was initially modelled using the two-hit hypothesis. This model suggested that leukaemogenesis and the clonal expansion of malignant cells requires the acquisition and cooperation of at least two mutations from different classes (Conway O'Brien, *et al.*, 2014, Gilliland and Griffin, 2002). Class I mutations refer to aberrations which promote a proliferative advantage such as *FLT3*, *c-KIT* or *NRAS*, while mutations which inhibit differentiation such as *RUNX1-ETO* and *PML-RARA* are considered class II mutations. However, since this model was proposed, the involvement of mutations within epigenetic regulators in AML (class III mutations) such as *DMNT3A, TET2, WT1* and *IDH1* has been realised (Sun, *et al.*, 2018) and shown the two-hit hypothesis to be oversimplistic.

Similar to thyroid cancer and other haematological malignancies, AML has a relatively low mutational burden (<1 somatic mutation/megabase), compared with cancers such as melanoma which has a mutational burden of >10 somatic mutations/megabase (Alexandrov, *et al.*, 2013). As a result, recurrent mutations associated with AML are well defined (Table 1.1) and the presence of specific aberrations can be used to classify disease (1.2.4), infer prognosis (1.2.4) and direct treatment (1.3). The most frequently observed mutations in AML are in genes related to signalling pathways including *FLT3*, *c-KIT* and *RAS* which are found in over half of patients (Table 1.1). This is closely followed by epigenetic regulators such as *DNMT3A, TET2* and *IDH* which are mutated in around 40% of patients (Table 1.1). *DNMT3A* and *TET2* are somatic mutations which present in nearly all older individuals at very low frequencies, and likely arise because of the aging haematopoietic system (Buscarlet, *et al.*, 2017, Midic, *et al.*, 2020). For individuals who have such somatic mutations at an allelic frequency of $\geq$2% in the PB, without the diagnostic criteria of haematological disease, are deemed to have clonal haematopoiesis of indeterminate potential (Steensma, *et al.*, 2015) and are at increased risk of developing a haematological malignancy (Genovese, *et al.*, 2014). Despite their prevalence in AML, studies have identified *DNMT3A* and *TET2* mutations as pre-leukaemic aberrations, which alone are not sufficient to promote overt disease. In an inducible *DNMT3A* knock-out mouse model, *DNMT3A* deficiency resulted

in the expansion of HSC over serial transplantations compared to wild-type HSC (Challen, *et al.*, 2012). Nevertheless, despite this proliferative advantage, none of the *DNMT3A* mutant HSC recipients developed overt disease (Challen, *et al.*, 2012). Progression to leukaemia requires the acquisition of driver mutations, such as *PML-RARA*, which are not found in healthy individuals (Abelson, *et al.*, 2018, Welch, *et al.*, 2012).

Most cancers, including AML, are considered clonal malignancies, as they originate from a single mutated cell, but the instability of the cancer genome means that individual cancers can contain thousands of mutations and chromosomal alterations (Greaves and Maley, 2012). Although there appears to be some degree of order in the acquisition of the mutations required for leukaemogenesis, patients rarely present with a single malignant clone. Sequencing to determine the variant allele frequency of mutations can be used to estimate the size of the clones which make up a patient's disease at diagnosis and allows disease evolution to be followed over time. The evolution of cancer can occur through linear or branching patterns of mutation acquisition (Greaves and Maley, 2012, Morita, *et al.*, 2020). Linear evolution describes the stepwise acquisition of mutations which provide a survival advantage and allows the new clone to out compete previous clones. Contrastingly, in branching evolution clones diverge from a common ancestor, evolving in parallel giving rise to multiple clonal lineages (Davis, *et al.*, 2017). The molecular landscape of AML can change naturally over time or because of selective pressures, such as chemotherapy treatment. In this case, chemotherapy may eliminate the primary (chemo-sensitive) clone, but not affect lower frequency (chemoresistant) clones which can re-emerge, upon the termination of treatment, as the primary clone in relapsed disease (Vosberg and Greif, 2019). Therefore, understanding the molecular composition of AML throughout the disease course is an important factor in treatment and patient monitoring (1.3.3).

Table 1.1: Recurrent mutations in AML

Table outlining recurrent molecular and cytogenetic aberrations which are frequently observed in AML. Some of the example mutations encompass numerous aberrations which individually occur at a much lower frequency. For example, among other mutations, MLL-fusions describes MLL-AF6, MLL-AF9, and MLL-AF10. Table adapted from Grove and Vassiliou, 2014.

Type of Mutation	Example	Frequency (%)
Signal Transduction Genes	*FLT3,NRAS,c-KIT, PTPN11*	59
DNA Modification Genes	*DNMT3A,TET2,IDH1/2*	44
Chromatin Modifiers	MLL-fusions, *ASXL1, EZH2*	30
NPM1	-	27
Fusion Genes	*PML-RARA, MYH11-CBFB, RUNX1-ETO*	25
Myeloid transcription factors	*CEBPA,RUNX1*	22
Tumour Suppressor Genes	*TP53, WT1,PHF6*	16
Spliceosome Genes	*SF3B1,SRSF2,U2AF1*	14
Cohesins	*SMC1A,SMC3, RAD1, STAG2*	13

1.2.2.1 Leukaemic Stem Cells

In a similar manner to normal haematopoiesis (1.1), xenograft experiments suggest AML retains some degree of hierarchical organisation, whereby a small population of leukaemic stem cells (LSC) give rise to a larger pool of malignant cells that lack self-renewal capacity. LSC were first identified in AML through the transplantation of patient samples, fractionated into immature cells ($CD34^+CD38^-$) and more mature cells ($CD34^+CD38^+$), into immunodeficient mice (Bonnet and Dick, 1997). The $CD34^+CD38^-$ recipients developed the symptoms of overt disease; a finding which was not observed in recipients of the more mature $CD34^+CD38^+$ cellular population. Furthermore, the $CD34^+CD38^-$ cells were able to initiate disease upon serial transplantations (Bonnet and Dick, 1997). Thus, demonstrating the importance of this immature cellular compartment in the development and progression of AML. Since this discovery, there has been some evidence to suggest that $CD34^+CD38^+$ cells have some re-constitutive capacity (Hogan, *et al.*, 2002, McKenzie, *et al.*, 2006) and in some AML samples this fraction contains leukaemia initiating cells (Taussig, *et al.*, 2008). Together, these data are indicative of a heterogenous population of LSC which can contribute to disease progression and at present there is no unique phenotype which defines LSC.

Although a rare cellular population within the bulk of the disease, from a clinical perspective, eradicating LSC is essential for achieving long-term remission. Effective targeting of LSC has yet to be achieved, however the molecular characterisation of this cellular compartment has improved significantly. Several cell surface markers including CD44 (Jin, *et al.*, 2006), CD123 (Jin, *et al.*, 2009), and CD47 (Jaiswal, *et al.*, 2009) are upregulated in LSC compared to $CD34^+CD38^-$ HSC. Such discoveries not only allow for greater purification and characterisation of LSC, but also provide the potential to develop targeted therapies against this cellular population (1.3.2).

1.2.3 Clinical Presentation and Diagnosis of AML

The symptoms associated with AML arise due to the accumulation of leukaemic blasts within the BM and reflect the resulting reduction in normal haematopoietic output. Therefore, patients will typically present with general flu-like symptoms, fatigue, loss of appetite, recurrent infections, and bleeding tendencies (Khwaja, *et al.*, 2016). Full blood counts, which can identify thrombocytopaenia, anaemia, and neutropoenia are supported by BM aspirates, morphological analysis, and cytogenetic and molecular testing. An AML diagnosis is confirmed by >20% myeloblasts in the PB, however, lower levels do not necessarily rule out

an AML diagnosis (Döhner, *et al.*, 2017). Alongside morphological analysis, immunophenotypic analysis to determine the expression of MPO, CD13, CD33, CDw65 and CD117 in PB or BM samples can be used for diagnosing AML (Bain and Béné, 2019, Basharat, *et al.*, 2019). To identify AML-specific chromosomal aberrations such as *RUNX1-ETO* (t(8;21)(q22;q22)),) and *PML-RARA* (t(15;17)(q24;q21)), cytogenetic analysis (karyotyping) is conducted (Khwaja, *et al.*, 2016). The identification of these cytogenetic aberrations is not only an essential part of diagnosis but is also pertinent in disease classification and treatment stratification (1.2.4). However, not all risk stratifying abnormalities will be detected through this methodology. Thus, cytogenetic analysis is supported by next generation sequencing, real-time PCR and fluorescence *in-situ* hybridisation (Ottone, *et al.*, 2008).

1.2.4 Classification of Disease and Prognostic Stratification

The highly heterogeneous nature of AML renders disease classification an essential part of diagnosis, treatment stratification and determination of prognosis. The original strategy employed for the classification of AML was the French American British (FAB) system, which distinguishes subsets of disease according to cell morphology and cytology, and ranges from M0 disease (undifferentiated leukaemia) to M7 disease (megakaryocytic leukaemia; Table 1.2; Bennett, *et al.*, 1976, Estey and Döhner, 2006). This has since been superseded with the World Health Organisation (WHO) classification system which requires at least 20% of blasts to express surface antigens associated with myeloid differentiation, such as CD13 and CD33 (Estey and Döhner, 2006). The WHO classification system also incorporates cytogenetic and molecular analysis to distinguish between disease sub-types (Table 1.3). Based on this, the European LeukemiaNet (ELN) published guidelines for the use of these aberrations to infer prognosis (Estey, 2018), classifying leukaemia into favourable, intermediate, and poor prognostic disease (Table 1.4). For example, core binding factor malignancies, such as *RUNX1-ETO*, are considered a favourable risk disease type, with a 5-year survival of c60% following high-dose Ara-C chemotherapy (Ferrara and Schiffer, 2013).

Although cytogenetic analysis is a critical tool in the diagnosis and stratification of patients with AML, around 45% of patients present with a normal karyotype (Grimwade, *et al.*, 2001). Overall, normal karyotype AML is considered an intermediate risk disease, however, there is a high degree of heterogeneity in terms of clinical outcome in this cohort of patients. Therefore, molecular analysis to further characterise disease is important for prognostic outlook and patient stratification.

The most common molecular mutations in AML are in the cytokine receptor; Fms-Like Tyrosine kinase 3 (FLT3), and the cytoplasmic-nuclear shuttle protein, nucleophosmin (NPM1; Table 1.1). Within $FLT3^+$ AML, which occurs in around a third of patients (Kottaridis, *et al.*, 2001, Papaemmanuil, *et al.*, 2016), internal tandem duplication (*FLT3*-ITD) mutations occur most frequently, while point mutations in the tyrosine kinase domain (*FLT3*-TKD) occurs in 5% to 10% of patients (Daver, *et al.*, 2019). In terms of prognosis, *FLT*-ITD mutations are classified as a poor prognostic disease (Table 1.4) and is associated with an increased risk of relapse (Yanada, *et al.*, 2005). However, a significant association between *NPM1* and *FLT3*-ITD mutations has been determined and the occurrence of these two abnormalities results in differential prognostic classification. In general, *NPM1* mutations alone are associated with a favourable outcome while, the presence of both *NPM1* mutations and *FLT3*-ITD is indicative of an intermediate prognostic outlook (Table 1.4). Furthermore, a recent study in Sweden suggests that the prognostic implications of these mutations are age dependent. In this study, the presence of *FLT3*-ITD indicated poor survival in younger patients (<60 years) but not in older patients, while *NPM1* mutations indicated a better survival in older patients, but not in younger patients (Juliusson, *et al.*, 2020). In addition to disease related factors, patient specific characteristics have prognostic value and impact decisions regarding first-line therapy (1.3).

Of the patient-related factors, age has the strongest correlation with prognosis and is thought to reflect the higher incidence of co-morbidities present and a reduced tolerance for intensive therapies (Juliusson, *et al.*, 2009). Population studies have shown that compared to younger patients (<50 years) where the 5-year survival is c50%, for patients between 65 and 69 years, the 5-year survival is c15% and further decreases with increased age at diagnosis (Juliusson, *et al.*, 2009). This is thought to be linked to overall biological fitness and the increased incidence of co-morbidities in older individuals.

Table 1.2: French American British Classification of AML

Table outlining the FAB classification of AML malignancies, which differentiates sub-types of AML based upon morphological and cytological analysis (Bennett, *et al.*, 1976, Estey and Döhner, 2006).

FAB Classification	Description
M0	Undifferentiated AML
M1	Acute myeloblastic leukaemia with minimal maturation
M2	Acute myeloblastic leukaemia with maturation
M3	Acute promyelocytic leukaemia (APL)
M4	Acute myelomonocytic leukaemia
M4eos	Acute myelomonocyte leukaemia with eosinophilia
M5	Acute monocyte leukaemia
M6	Acute erythroid leukaemia
M7	Acute megakaryoblastic leukaemia

Table 1.3: WHO (2016) AML Classification

Table outlining the WHO classification system for AML malignancies with examples of cytogenetic and molecular aberrations which are associated with the disease sub-types (1.2.4). Adapted from Arber, *et al.*, 2016, Medinger and Passweg, 2017.

Disease Sub-Type	Cytogenetic and Molecular Characteristics
AML with recurrent Genetic Abnormalities	AML with t(8;21)(q22:22.1);*RUNX1-RUNX1T1*
	AML with inv(16)(p13.1q22) or t(16;16)(p13.1;q22);*CBFB-MYH11*
	APL with *PML-RARA*
	AML with t(9;11)(q23.1q26.2);MLLT3-BCR2A
	AML with t(6;9)(p23;q34.1);*DEK-NUP214*
	AML with inv(3)(q21.3q26.2) or t(3;3)(p13.3;q13.3);*RBM15-MKL*
	AML with mutant *NPM1*
	AML with biallelic mutations of *CEBPA*
AML with Myelodysplasia-related changes	
Therapy-Related Myeloid Neoplasms	Alkylating -agent or radiation-related type
	Topoisomerase-II-inhibitor related type
	Others
AML, not otherwise specified	AML with minimal differentiation
	AML without maturation
	AML with maturation
	Acute myelomonocytic leukaemia
	Pure erythroid leukaemia
	Acute megakaryoblastic leukaemia
	Acute monoblastic/monocytic leukaemia
	Acute basophilic leukaemia
	Acute panmyelosis with myelofibrosis
Myeloid Sarcoma	
Myeloid Proliferations related to Down Syndrome	Transient abnormal myelopoiesis
	Myeloid leukaemia associated with Down Syndrome

Table 1.4: European LeukemiaNet 2017 genetic risk stratification

Table outlining the European LeukemiaNet 2017 genetic risk stratification of AML (1.2.4), adapted from Estey, 2018.

Risk Category	Genetic Abnormality
Favourable	t(8;21)(q22;q22.1); *RUNX1-RUNX1T1* inv(16)(p13.1q22) or t(16;16)(p13.1;q22); *CBFB-MYH11* Mutated *NPM1* without *FLT3*-ITD or with *FLT3*-ITD^{low} = allelic ratio < 0.5 Biallelic mutated *CEBPA*
Intermediate	Mutated *NPM1* and *FLT3*-ITDhigh = allelic ratio > 0.5 Wild-type *NPM1* without *FLT3*-ITD or with *FLT3*-ITD^{low} (without adverse-risk genetic lesions) t(9;11)(p21.3;q23.3); MLLT3-KMT2A Cytogenetic abnormalities not classified as favourable or adverse
Adverse	t(6;9)(p23;q34.1); *DEK-NUP214* t(v;11q23.3); KMT2A rearranged t(9;22)(q34.1;q11.2); *BCR-ABL1* inv(3)(q21.3q26.2) or t(3;3)(q21.3;q26.2); *GATA2,MECOM(EVI1)* −5 or del(5q); −7; −17/abn(17p) Complex karyotype monosomal karyotype Wild-type *NPM1* and *FLT3*-ITD^{high} Mutated *RUNX1* Mutated *ASXL1* Mutated *TP53*

1.3 Treatment of AML

1.3.1 Conventional Therapeutic Strategies

The treatment strategies used for AML are typically divided into induction, consolidation, and maintenance therapy (Figure 1.3). The aim of induction chemotherapy is to reduce the tumour burden and achieve complete remission (CR), which is defined as <5% blasts in the BM, the absence of Auer rods and extramedullary leukaemia, a neutrophil count of >1,000/µL and a platelet count >100,000/µL (Döhner, *et al.*, 2017). For some patients, CR with incomplete haematological recovery (CRi) is achieved following induction therapy, whereby a reduction in blast burden to <5% is achieved but the neutrophil or platelet count does not recover enough to meet the criteria of CR (Döhner, *et al.*, 2017).

Induction therapy for young or biologically fit patients, typically relies on a 3+7 strategy, utilising an anthracycline (usually daunorubicin; DNR at 60mg/m^2/day) which is administered for 3 days, alongside 7 days of continuous cytarabine (Ara-C; 100mg/m^2/day) infusions (Ferrara and Schiffer, 2013). Ara-C is an antimetabolite pyrimidine nucleoside analogue which inhibits DNA synthesis and requires metabolism to exert its cytotoxic effects. Specifically, intracellular Ara-C is converted to its active form cytarabine trisphosphate (CTP) by deoxycytidine kinase (dCK). CTP can be incorporated into DNA during S phase and competitively inhibit DNA polymerase, preventing cell cycle progression (Li, *et al.*, 2017). Although the mechanism of DNR is not fully understood, DNR is thought to primarily act through the inhibition of topoisomerase II; an enzyme which regulates topological rearrangements of the DNA by generating double strand breaks (Lima and Mondragón, 1994). However, DNR can also undergo oxidation-reduction (REDOX) reactions which generate reactive oxygen species (ROS; Doroshow, 2019). Specifically, the quinone moiety of anthracyclines such as DNR can be reduced to semiquinone radicals which results in the generation of hydrogen peroxide (H_2O_2), superoxide and hydroxyl radicals (Doroshow, 2019, Jung and Reszka, 2001). A dose-dependent and significant increase in superoxide formation in the mitochondria following anthracycline treatment has been observed (Doroshow, 2019). Furthermore, the involvement of mitochondrial oxidative stress in the cytotoxicity of anthracyclines has been demonstrated in transgenic mice, where knocking out antioxidant components of the mitochondria such as manganese superoxide dismutase (MnSOD) leads to lethal cardiotoxicity following anthracycline treatment, while high levels of MnSOD attenuates

mitochondrial oxidative stress induced by the anthracycline Adriamycin (Li, *et al.*, 1995, Yen, *et al.*, 1999).

In younger patients (<60 years), the response to induction therapy is relatively successful, with > 70% achieving CR (Burnett, *et al.*, 2013, Ferrara and Schiffer, 2013). However, most AML patients are over the age of 65 years, and often present with additional co-morbidities, and as such are deemed unable to tolerate intensive therapeutic strategies. Due to this, outcomes are less favourable in this cohort, with CR rates between 45%-55% and survival rates of <6 months (Burnett, *et al.*, 2009, Ferrara and Schiffer, 2013). For older patients who are deemed unfit for intensive therapy, less intensive regimes can be administered including low-dose Ara-C (LDAC) or hypomethylating agents (HMA), such as Azacitidine (Dombret, *et al.*, 2015, Seymour, *et al.*, 2017). Alternatively, responses to induction chemotherapy can be improved with the addition of targeted therapies (1.3.2). Optimising the mode of drug delivery has also been beneficial. For example, Vyxeos® (CPX-351) a liposomal formulation of Ara-C and DNR is associated with significantly higher OS in older patients than these same agents when applied in the intensive chemotherapeutic strategies as described above (Lancet, *et al.*, 2018).

If CR is achieved following induction therapy, consolidation therapy is used to eliminate any residual leukaemic cells with the aim of preventing relapse (1.3.3). Consolidation therapy either involves a haematopoietic stem cell transplant or combination chemotherapy at similar or a reduced intensity to induction therapy (Figure 1.3). Following consolidation therapy, maintenance therapy will be administered to prevent relapse (Figure 1.3) and throughout, supportive care (such as anti-fungal and anti-bacterial agent, and prophylactic transfusions) will be administered as required (Figure 1.3).

1.3.2 Targeted Therapeutic Strategies

The emergence of next generation sequencing and the identification of specific genetic alterations in AML (1.2.4) has allowed the development of targeted therapies for this malignancy. The most successful application of targeted therapy in AML to date is the use of all-trans-retinoic acid (ATRA) and arsenic trioxide (ATO) for patients with acute promyelocytic leukaemia (APL). APL is characterised by the reciprocal translocation of chromosome 15 and 17 (t(15;17)(q22;q21) also known as PML-RARA) and was previously considered a poor prognosis disease, with OS rates like those of other AML sub-types.

However, with the addition of ATRA to induction chemotherapy, CR rates and long-term survival to now stand at around 90% (Sanz, *et al.*, 2019).

Since the approval of ATRA to treat patients with APL, the success of therapies targeted against specific mutations had been limited, although this has expanded considerably in recent years. A major area of research in the development of targeted therapy for AML has focused on FLT3 mutations, which are one of the most frequently observed aberrations (Table 1.1). The first FLT3 targeted therapy to be approved for AML treatment was Midostaurin. A phase 3 trial showed that in patients aged between 18 and 59 years with *FLT3* mutations, Midostaurin treatment significantly improved the median OS of patients compared to placebo treated patients and was associated with a HR of mortality of 0.78 (95% CI, 0.63 to 0.96; Stone, *et al.*, 2017). As Midostaurin is efficacious for multiple tyrosine kinases, more potent FLT3 inhibitors, including Gliterinib, Quizartinib and Crenolanib have been developed and have also shown promising results in improving outcomes. However, the success of these agents has been limited as the duration of clinical response is often short due to the rapid development of resistance (Wu, *et al.*, 2018).

Targeted therapies have also been raised against the apoptotic protein BCL-2 (1.4.1). Venetoclax; a BH3 mimetic with sub-nanomolar affinity to BCL-2 promoted apoptosis in AML cell lines and patient samples, as well as reducing disease progression in AML murine models (Pan, *et al.*, 2014). In a clinical setting, co-administration of Venetoclax with Azacitidine or decitabine is well-tolerated in older patients >65 years, and improved CR/CRi and OS to 73% and 17.5 months for patients who received 400mg Venetoclax +HMA (DiNardo, *et al.*, 2019). This compares to a median OS of 7-10 months for patients over 65 years who receive low-dose HMA (Dombret, *et al.*, 2015, Kantarjian, *et al.*, 2012). Furthermore, the benefits of Venetoclax in combination of Azacitidine was beneficial for patients across molecular subgroups, compared to Azaciditine alone, but patients with IDH1/2 mutations responding particularly well (Dombret, *et al.*, 2015).

Immunotherapy has also been incorporated into the treatment of AML. Gemtuzumab Ozogamicin (GO) also known as Mylotarg® ; a humanised anti-CD33 antibody conjugated to the DNA-intercalating agent calicheamicin (Wang, *et al.*, 2020). A phase I/II trial combining low doses of GO with Azacitidine appeared to be better tolerated than higher doses of GO as a monotherapy, with a similar response rate (Medeiros, *et al.*, 2018). Recently, the therapeutic potential of CD47 has been explored. Magrolimab; a first-in-class monoclonal antibody

against CD47 is now under investigation. CD47 is a transmembrane protein which is overexpressed in human and murine AML cells, compared to non-malignant cells, and is associated with poor patient outcomes (Majeti, *et al.*, 2009). The binding of CD47 to its cognate receptor, Signal Regulatory Protein α (SIRPα) expressed on macrophages prevents phagocytosis (Liu, *et al.*, 2015). Initial results from a phase 1b trial in which Magrolimab was administered in combination with Azacitidine to AML patients deemed unfit for intensive chemotherapy, showed that Magrolimab was well tolerated, and achieved a 64% (16/24 patients) response rate, with the response persisting in all these patients at the point of follow-up (8-9 months) (Sallman, *et al.*, 2020). Interestingly, the response for patients with TP53 mutations, an adverse aberration (Table 1.4), which is usually associated with a CR rate of c41% and OS at 2-years of 9% (Kadia, *et al.*, 2016), were particularly promising, achieving a 75% (9/12) response rate (Sallman, *et al.*, 2020). Therefore, this combination of therapy represents a potentially exciting development in the treatment of older individuals, and those harbouring TP53 mutations.

The application of chimeric antigen receptor (CAR)-T cell-based therapies is also being investigated in the context of AML. Identifying suitable targets for CAR-T therapy which are specific for AML blasts has been challenging. However, an initial study showed the anti-leukaemic potential of CD33 CAR-T therapy as a monotherapy, reducing the blast count in one patient from >50% to<6% two weeks after cellular infusion (Wang, *et al.*, 2015). Although this patient relapsed within 9 weeks, the efficacy of CD33-targeting CAR-T cells is currently being investigated in patients with relapsed or refractory AML. In addition to CD33, CAR-T cells targeting LSC markers such as CD123 (1.2.2.1), are potential candidate molecules for CAR-T therapy.

1.3.3 Relapse and Minimal Residual Disease Monitoring in AML

Most patients will have a degree of residual disease following the cessation of induction therapy which have the potential to re-emerge following the end of treatment. When AML blasts become >5% of cells in the BM, the patient has relapsed (Döhner, *et al.*, 2017). In part, relapse has been linked to the acquisition of mutations that confer drug resistance, as the dominant clone which presents in relapse can be a pre-existing genetically defined clone which has acquired additional mutations (Ding, *et al.*, 2012). Using techniques such as flow cytometry, PCR, and next generation sequencing, minimal residual disease monitoring can be

used to assess the progression of any residual cells (Ivey, *et al.*, 2016). As a result, treatment can be changed before relapse in the case of resurgent disease or discontinued in patients where relapse is deemed unlikely. This allows tailored and optimal treatment strategies to be administered, however, ultimately most patients will relapse, and prognosis for relapsed/refractory disease is particularly poor (Bose, *et al.*, 2017).

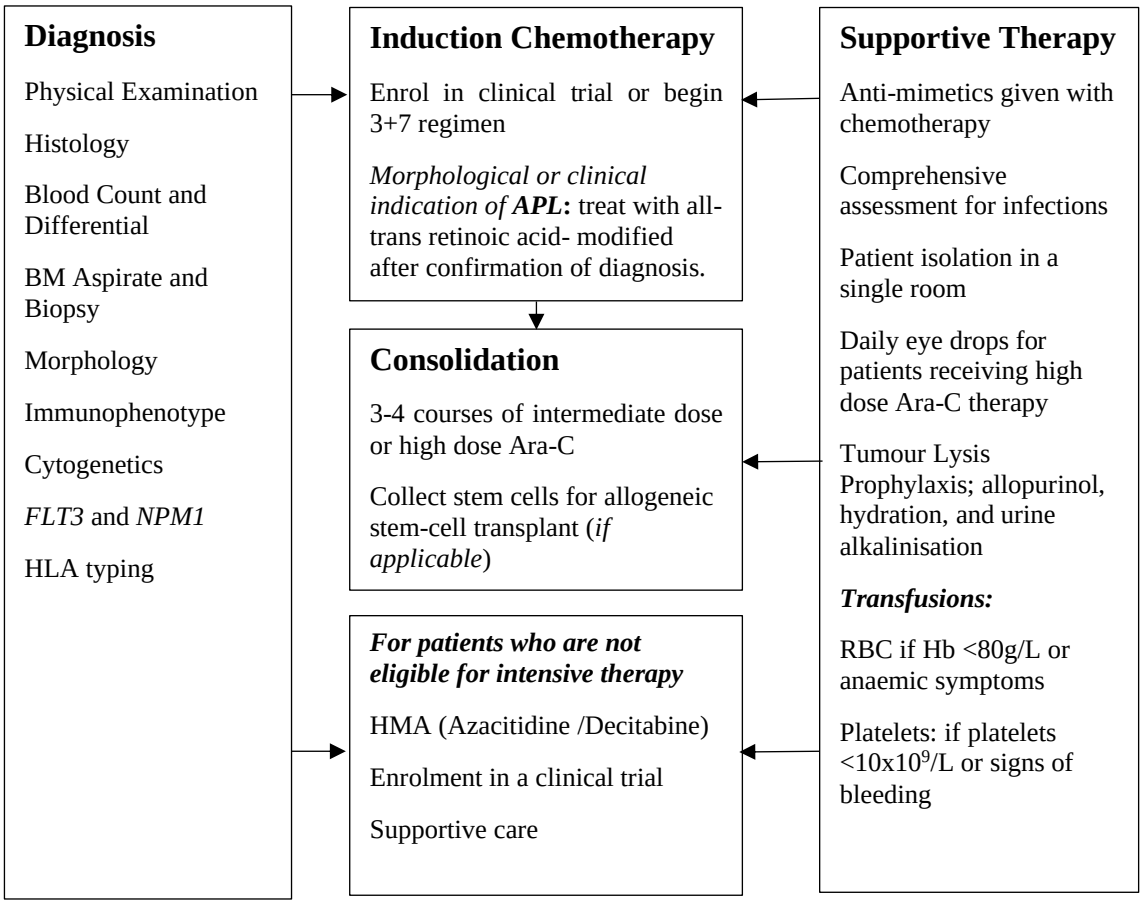

Figure 1.3: Flow Diagram of the patient pathway from diagnosis to treatment

Schematic outlining the clinical route for patients with AML including the diagnostic tests typically conducted, and the types of therapeutic options available. Adapted from Ferrara and Schiffer, 2013. *Abbreviations: APL; Acute Promyelocytic Leukaemia, Ara-C; Cytarabine, Hb; Haemoglobin, RBC; red blood cells.*

1.4 Mechanisms of Chemotherapy Resistance in AML

Chemotherapy is the most extensively used strategy in the treatment of AML, but the effectiveness of chemotherapeutic strategies is limited by the high proportion of patients who are considered unable to tolerate the intensive regimes which debulk disease most effectively (1.3). The efficacy of these treatments is further impacted by the emergence of drug resistance which can prevent patients from achieving CR in-response to first line therapy or promote relapse with refractory disease following a period of remission. Chemoresistance can arise due to a plethora of factors including those intrinsic to the malignancy such as intra-tumour heterogeneity, the persistence of quiescent cells, and the contribution of specific cytogenetic and molecular aberrations. In addition to intrinsic factors of chemoresistance, extrinsic signals such as those mediated by interactions with the ECM (1.4.2) and altered expression of transporter proteins (1.4.3), are also central mechanisms of chemoresistance in AML (Ross, 2000).

Some of the molecular aberrations associated with AML are thought to directly contribute to chemoresistance. Patients with *FLT3*-ITD have a short OS and increased risk of relapse (Kottaridis, *et al.*, 2001). Studying the clonal evolution of *FLT3* leukaemia has shown that maintaining *FLT3* mutations detected at diagnosis or at relapse is associated with a shorter OS than for patients with wildtype *FTL3* at either point of disease progression (Warren, *et al.*, 2012). In addition to the presence of *FLT3* mutations, the allelic frequency has prognostic implications with patients with a lower allelic frequency having a better outcome (Table 1.4). Moreover, patients with *FLT3*-ITD^{+} AML who received salvage therapy had a high risk of relapse even after allogeneic haematopoietic stem cell transplant, and *FLT3*-ITD allelic ratio correlated with survival (Wattad, *et al.*, 2017). Together these studies implicate a role for FLT3 mutations in promoting treatment resistance and disease progression. Although efforts to fully elucidate the underlying mechanisms are ongoing, *in vitro*, and murine studies have shown that FLT3-ITD mutations, which result in constitutive FLT3 activation, confers resistance to Doxorubicin (DOX) or combined Ara-C and DOX treatment requires p53 (Pardee, *et al.*, 2011).

RUNX1 loss-of-function mutations are also associated with poor outcomes and chemoresistance in AML (Gaidzik, *et al.*, 2011). A study using Ba/F3 cells; an IL-3 dependent murine haematopoietic progenitor cell line, and AML patient derived cells, has indicated that wild-type RUNX1 is upregulated in response to ionising radiation and Ara-C (Speidel, *et al.*, 2017). In this context, RUNX1-upregulation was accompanied by cell-cycle arrest and

apoptosis, while in Ba/F3 cells transduced with transcriptionally inactive RUNX1 mutants, loss of caspase 3 cleavage was observed, suggesting that loss-of function RUNX1 mutations contribute to chemoresistance by eliciting the loss of pro-apoptotic signals (Speidel, *et al.*, 2017).

1.4.1 Modulation of Survival and Apoptotic Signalling

Evasion of apoptosis is a hallmark of cancer (Hanahan and Weinberg, 2011), therefore, understanding the complex network of intracellular protein interactions which mediate cell survival and apoptotic signalling is an important area of cancer research. A prominent proliferative and pro-survival signalling cascade is the PI3K/Akt pathway. The canonical pathway in which PI3K and Akt are activated relies on phosphorylation following tyrosine kinase or G-protein coupled receptor-mediated signal transduction (Alessi, *et al.*, 1997). Constitutive phosphorylation of Akt has been identified in AML patient samples (Grandage, *et al.*, 2005) and is associated with poor OS (Gallay, *et al.*, 2009). A study in AML patient derived blasts has shown that modulating Akt activity using the PI3K inhibitor LY294002 can promote apoptosis, and potentiate responses to chemotherapy, including Ara-C (Grandage, *et al.*, 2005). This study also indicates that Akt potentially contributes to leukaemia cell survival through modulating MAPK, NF-κB and p53 signalling (Grandage, *et al.*, 2005).

The balance between pro- and anti-apoptotic proteins also contribute to AML cell survival and chemoresistance. Apoptosis is regulated by two pathways: the extrinsic pathway which is activated in response to ligands such as tumour necrosis factor α (TNFα), and the intrinsic pathway which is regulated by the BCL-2 family of proteins. In the extrinsic apoptotic pathway, tumour necrosis factor-related apoptosis-inducing ligand (TRAIL) promotes ligand-dependent trimerization of DR4 or DR5, and the subsequent activation of the death-inducing signalling complex (DISC), which is composed of Fas-associated death domain (FADD) and initiator procaspase-8 (Pan, *et al.*, 1997, Sprick, *et al.*, 2000). In contrast, the intrinsic pathway is activated by non-receptor stimuli and relies on the release of cytochrome c from the mitochondria to induce apoptosis. The BCL-2 family comprises of pro- (Bax, Bak, Bid, Bad, Bim) and anti-apoptotic proteins (BCL-2, BCL-x, BCL-XL) that together govern mitochondrial membrane permeability (Elmore, 2007).

Overexpression of BCL-2 is frequently observed in AML and is associated with short OS and low rates of CR induction (Campos, *et al.*, 1993, Tóthová, *et al.*, 2002). This pro-survival capacity of BCL-2 is in part mediated through sequestration of pro-apoptotic proteins (Certo, *et al.*, 2006). In addition, overexpression of MCL-1 and BCL-xL are associated with chemoresistance and poor outcomes in this malignancy (Kaufmann, *et al.*, 1998, Pallis, *et al.*, 1997), highlighting the importance of this family of proteins in treatment response. As a result, there have been significant efforts to develop targeted therapies against BCL-2 family members. The most successful of these agents to date is Venetoclax; a targeted BCL-2 inhibitor, which has improved OS and chemotherapy responses, across a broad range of AML subtypes (1.3.2).

1.4.2 Stromal interactions

As well as intrinsic mechanisms of chemoresistance, extrinsic factors such as the interactions between leukaemic cells and the BM microenvironment play an important role in treatment response and relapse. The ability of stromal interactions to protect against chemotherapy has been studied using mouse xenograft models and co-culture systems. These studies have implicated numerous mechanisms through which the BM microenvironment can influence leukaemia cell survival, including the secretion of soluble factors and cell-to-cell contact-mediated signalling pathways.

The CXCR4/CXCL12 axis is required for the maintenance of HSC quiescence (Sugiyama, *et al.*, 2006; 1.1.1.1) and has been implicated in LSC survival, migration, and retention, during the initiation and progression of leukaemia (Tavor, *et al.*, 2004). In AML, elevated CXCR4 expression is associated with reduced OS (Du, *et al.*, 2019). Mechanistically, this could be due to the activation of PI3K/Akt by CXCR4/CXCL12, promoting cell survival (Teicher and Fricker, 2010). The ability for the CXCL12/CXCR4 axis to mediate chemoresistance has also been demonstrated. Inhibition of CXCR4 with an inhibitory peptide (RCP168) reduced Akt and ERK activation in Jurkat cells, a T-ALL cell line, and partially overcame stromal mediated chemoresistance of AML patient derived cells in a co-culture model (Zeng, *et al.*, 2006). As a result of such findings, the therapeutic potential of targeting CXCR4 in AML is being investigated (Uy, *et al.*, 2012), though an initial (phase1b) trial has not demonstrated significant improvements in patient outcome using this approach (Roboz, *et al.*, 2018).

Adhesion of leukaemic blasts to the BM microenvironment, which is primarily mediated by cell adhesion molecules known as integrins, is also associated with chemoresistant phenotypes. One of the best characterised integrins is the very late antigen-4 (VLA-4) which mediates cell adhesion through binding to receptors and extracellular matrix molecules including vascular cell adhesion molecule-1 (VCAM-1) and fibronectin. In HSC, VLA-4 can be activated by SDF-1 promoting quiescence, and protection against cell-cycle dependent chemotherapeutic agents (Peled, *et al.*, 2000). VLA-4 mediated cell adhesion may also preserve residual disease or promote chemoresistance through modulating PIK3/AKT/BCL-2 signalling (Hazlehurst, *et al.*, 2007, Matsunaga, *et al.*, 2003). In addition, *in vitro* studies have shown the importance of the fibronectin-binding integrins α4β1 and α5β1 in promoting resistance to DOX in AML cells (Naci, *et al.*, 2019).

1.4.3 Drug Uptake, Efflux, and Inactivation

For chemotherapeutic agents to exert their cytotoxic effects, it is essential that sufficient intracellular concentrations within the target cell are achieved. This can be affected by multiple factors including perturbations in drug uptake, metabolism, and export. Drug transporters, primarily expressed at the plasma membrane, play an important role in the uptake and efflux of chemotherapeutic agents used in AML treatment. Broadly, transporter proteins can be divided into two classes: solute carrier proteins (SLC) which facilitate drug influx and efflux by diffusion or co-transport, and ATP-binding cassette (ABC) transporters; a group of active ATPase efflux pumps. While anthracyclines, including DNR, enter the cell by passive diffusion (Marbeuf-Gueye, *et al.*, 1999), some chemotherapeutic agents, such as Ara-C rely on transporter proteins to enter the cell. Uptake of Ara-C relies on the human equilibrative nucleoside transporter (hENT1; Rein and Rizzieri, 2014). Reduced hENT1 expression has been described in AML and is associated with an increased risk of relapse and reduced CR induction following first-line therapy (Galmarini, *et al.*, 2002).

In terms of drug efflux, there are 13 genes associated with drug resistance and ABC-mediated drug export (*ABCA2, ABCB1, ABCB4, ABCB11, ABCC1–6, ABCC10, ABCC11* and *ABCG2*), with *ABCB1*, which encodes P-glycoprotein (P-GP), being the best characterised in AML. Substrates for ABC efflux pumps such as P-GP include amino acids, organic ions, peptides, chemotherapeutic agents, and xenobiotics (Eckford and Sharom, 2009). In AML, P-GP overexpression is associated with poor outcomes in newly diagnosed and relapsed disease (Beck, *et al.*, 1996). Particularly pertinent in AML is the ability of pumps

such as P-GP to confer resistance to anthracyclines. An *in vitro* study in AML cell lines has shown the ability of P-GP to promote chemoresistance through reducing intracellular DNR accumulation (Nooter, *et al.*, 1990). However, there is some evidence that P-GP can affect cell fate through substrate efflux independent mechanisms (Johnstone, *et al.*, 2000, Pallis and Russell, 2000). Other than P-GP, aberrant expression of the multidrug resistance related protein-1 (*MRP1*; Schneider, *et al.*, 1995) and lung resistance protein (*LRP;* Hart, *et al.*, 1997) have also been described in AML. The contribution of individual efflux pumps is further complicated by the fact that AML cells can present with multiple active efflux pumps (Legrand, *et al.*, 1999a). Although the role of SLC carriers in AML have been studied to a lesser extent, increased *SLC2A* and *SLC2A10* expression in AML patients is associated with increased mortality (Lai, *et al.*, 2020).

The mechanisms regulating efflux pump expression and activity are highly complex and have not been fully resolved. Despite this, some aspects of efflux pump regulation are outlined below, with a focus on P-GP, as this is the best characterised drug transporter. A wide range of transcription factors including AP-1 and NF-κB have been implicated in P-GP regulation (Bark and Choi, 2010, Chen, *et al.*, 2014). The regulation of P-GP is post-translational as well as transcriptional. P-GP is exported from the endoplasmic reticulum as a 150-kDa protein which is subsequently glycosylated in the Golgi apparatus, and yields the mature 170-kDa protein which mediates drug efflux (Gribar, *et al.*, 2000). In addition to expression, the activity of efflux pumps is also central to drug transport. There is some evidence that phosphorylation of P-GP by protein kinase C (PKC) and A (PKA) isoforms could be linked to P-GP activity as several consensus sites have been identified within the linker region of P-GP (Chambers, *et al.*, 1992), however the evidence for this is conflicting (1.6.5.3).

Given the role of P-GP in AML, there have been considerable efforts to develop P-GP inhibitors that can be used in combination with conventional chemotherapeutic agents (Tang, *et al.*, 2008). However, first-generation inhibitors, such as Verapamil and cyclosporin A, were limited by a lack of specificity, high levels of associated toxicity, and ability to disrupt the pharmacokinetics of co-administered therapeutic agents (Thomas and Coley, 2003). Later generations of inhibitor such as Zosuquidar hydrochloride (ZSQ) have been safely administered to AML patients in combination with Ara-C and DNR (Gerrard, *et al.*, 2004), but the effects on patient outcome have been disappointing (Cripe, *et al.*, 2010, Kolitz, *et al.*, 2010). This may, in part, be due to the specificity of this inhibitor meaning that resistance in cells

where the co-expression of efflux pumps occurs cannot be overcome. In addition, P-GP specific inhibitors cannot inhibit the contribution of non-efflux mechanisms of resistance.

Altered drug metabolism is an important consideration for pro-drugs such as Ara-C that must be metabolised to exert their cytotoxic effects. Mutations which give rise to dCK deficiency; a key enzyme in the metabolism of Ara-C (1.3.1), is associated with reduced Ara-C cytotoxicity *in vitro* (Dumontet, *et al.*, 1999). Furthermore, low *dCK* mRNA expression in leukaemic blasts at diagnosis has been associated with poor clinical outcomes in patients treated with Ara-C (Galmarini, *et al.*, 2003). On the other hand, mutations or changes in topoisomerase II activity are pertinent to the efficacy of anthracyclines such as DNR (1.6.5.3).

1.5 Protein Kinase C Epsilon

1.5.1 Overview

The PKC family of serine/threonine kinases are a branch of AGM kinases and were first identified in the early 1980s as a target for phorbol esters which are natural products with tumour-promoting properties (Kikkawa, *et al.*, 1983, Nishizuka, 1984). Since their discovery, 11 PKC isoforms have been identified and are classified according to their structure, cofactor activation and substrate specificity (1.5.2). This classification system gives rise to three major groups; classical (cPKC; α, βI/II, γ), novel (nPKC; δ, ε, η, θ) and atypical (aPKC; ζ, λ/ι) PKC isoforms (1.5.2). Collectively, PKC enzymes are pleiotropic mediators of signal transduction, regulating cell proliferation, differentiation, migration, and survival. However, the role of individual isoforms is less clear given the high homology and suspected redundancy in function between isoforms. The *protein kinase C epsilon (PKCε)* gene, *PRKCE*, is located at chromosome 2p21, and following transcription and translation results in the production of a linear protein comprising of 737 amino acids. PKCε is expressed in most mammalian tissues, including heart, neuronal, endothelial, and immune cells (Totoń, *et al.*, 2011). As a nPKC isoform, PKCε is calcium-insensitive and is primarily activated by phospholipase C (PLC), diacylglycerol (DAG), and phosphoinositide-dependent kinase-1 (PDK-1) (1.5.3). In normal physiology, PKCε regulates a diverse range of signalling pathways and cellular outcomes (Figure 1.4) including proliferation, differentiation, and survival. Perturbed PKCε expression has been described in several diseases including heart disease (1.6.2) and cancer (1.6.5).

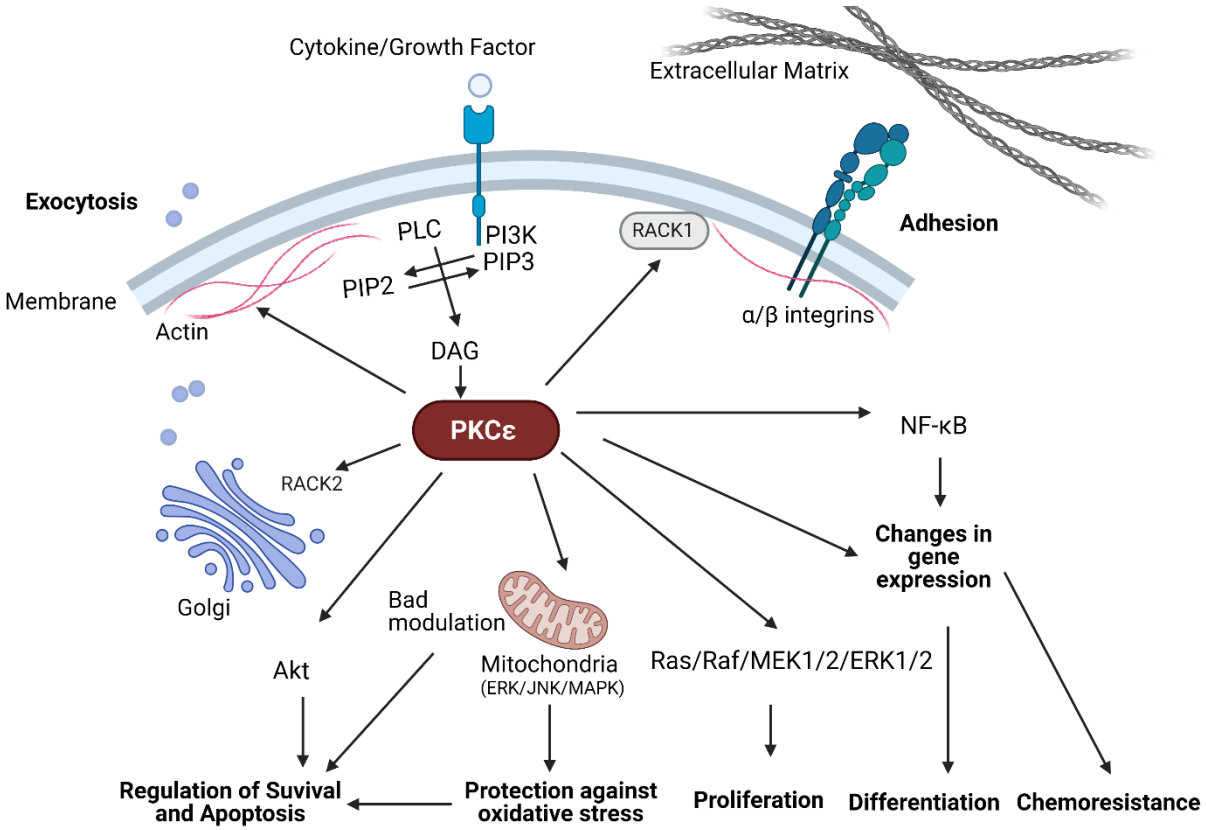

Figure 1.4: The role of PKCε in modulating cell physiology

Schematic highlighting downstream signalling and physiological impact of PKCε activation, adapted from Totoń, *et al.*, 2011. Briefly, PKCε is activated by DAG, PIP3 or fatty acids and exerts its function through translocation to various cellular compartments where it phosphorylates a range of downstream targets to regulate cell adhesion and motility, chemotherapy resistance, differentiation, apoptosis, and exocytosis. *Abbreviations; DAG; diacylglycerol, IP_3; inositol 3,4,5-trisphosphate, PI3K; phosphoinositide 3-kinase, PIP; phosphatidylinositol 3,4,5-trisphosphate, PLC; phospholipase C, RACK; receptor for activated C kinase.*

1.5.2 Structure of PKC Isoforms

The structural architecture of PKCε follows the archetypal organisation of PKC kinases, consisting of a regulatory, hinge and kinase domain (Figure 1.5; Steinberg, 2008). Despite the highly conserved structure, the composition of the modules contained within these regions differs between individual isoforms and determines the activity and binding specificity of the protein. The regulatory domain of PKC proteins encompasses the C1, C2 and pseudo-substrate (PS) modules. cPKC and nPKC isoforms contain tandem C1 and C2 regions, which interact with synthetic tumour-promoting esters such as phorbol 12-myristate-13-acetate (PMA, also known as TPA) and natural lipid metabolites, such as DAG (Newton, 2010). For cPKC isoforms this occurs in a Ca^{2+} dependent manner, however, the C2 domain of nPKC isoforms lack a residue rendering them insensitive to Ca^{2+}. As a result, the affinity of nPKC isoforms to DAG is around two orders of magnitude higher than cPKC enzymes (Giorgione, *et al.*, 2006). Furthermore, unlike cPKC and nPKC isoforms, aPKC proteins have a calcium in sensitive (PB1) C2 domain and an atypical C1 domain, made up of one cysteine-rich membrane targeting structure which can bind PIP3 or ceremide, as opposed to DAG (Steinberg, 2008).

Also contained within the regulatory domain is the PS which is conserved in all isoforms (Figure 1.5). The primary role of the PS is to maintain PKC isoforms in an inactive state in the absence of appropriate stimuli (1.5.3). In addition, and unique to PKCε, is an actin binding motif (LKKQET) which is situated between the C1A and C1B domains (amino acids 223-228; Figure 1.5; Akita, 2002, Prekeris, *et al.*, 1996), and allows direct interactions with the actin cytoskeleton and promotion of integrin mediated ECM attachment (1.6.5.4). The regulatory domain of PKC isoforms is connected to the kinase domain by a hinge region which facilitates the interaction of the PS and the C1 domain when PKC isoforms are in an inactive state. Finally, the kinase domain of PKC isoforms, which is situated at the C-terminus, contains motifs which are required for the catalytic activity of these enzymes. These include the activation loop which for nPKC isoforms contains a conserved TFCGTX motif and serine and threonine residues (T566, T710 and S729) which undergo phosphorylation for enzyme stability, competency, and activity (1.5.3), and an ATP binding motif (Figure 1.5).

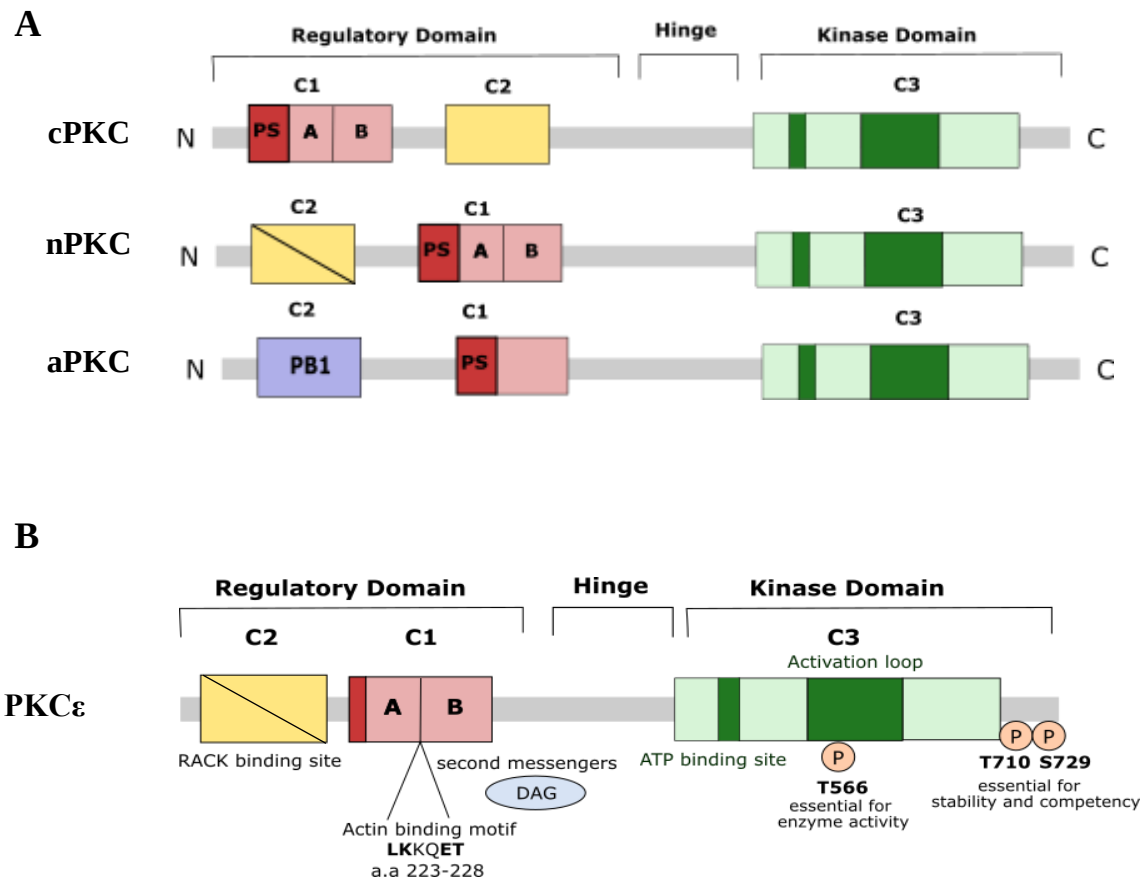

Figure 1.5: Structure of PKC isoforms

(A) Schematic showing the archetypal structure of classical (cPKC), novel (nPKC) and atypical (aPKC) PKC isoforms which are made up of a regulatory, hinge and kinase domain. Despite the conserved overall structure, nPKC isoforms contain a Ca^{2+}-insensitive C2 domain represented by a the hatching, while aPKC isoforms contain a PB1 domain and an atypical C1 domain which render these isoforms insensitive to Ca^{2+} and DAG (1.5.2) **(B)** Schematic showing the structure of PKCε, highlighting key components which are central to the function of this kinase (1.5.2), including the actin binding motif. *Abbreviations; PS; Pseudo-substrate.*

1.5.3 Maturation and Activation of PKC Isoforms

The molecular conformation, activation, and ability of PKC enzymes to respond to stimulants is regulated by reversible phosphorylation modifications. Typically, PKC isoforms reside in the cytosol in an inactive confirmation (1.5.2) and undergo maturation or "priming" before they can be activated and interact with downstream substrates. Studies have established that newly synthesized protein resides in an open (linear) confirmation and that binding of molecular chaperone protein such as Hsp90, is required for the subsequent phosphorylation and maturation of PKC isoforms (Aslam and Alvi, 2019, Gould, *et al.*, 2009). The first and rate-limiting phosphorylation step in the maturation of PKC isoforms is mediated by PDK-1 (Griner and Kazanietz, 2007, Le Good, *et al.*, 1998). PDK-1 phosphorylates the T566 residue contained within the activation loop of PKC enzymes (Figure 1.5). This results in a conformational change and exposes two further phosphorylation residues (S729 and T710), which are situated within the hydrophobic region of the C-terminal and the autophosphorylation site, respectively (Figure 1.5; Totoń, *et al.*, 2011). Phosphorylation of these sites leads to a stable form of the protein which is 'primed' for activation. Following phosphorylation of these serine and threonine residues, the PKC isoforms are maintained in a closed confirmation where the PS occupies the substrate binding site, located within the kinase domain, until it is activated by appropriate stimuli.

Under physiological conditions, binding of a ligand, such as a cytokine or growth factor, to its cognate tyrosine kinase or G-protein coupled receptor, stimulates the activation of PLC. This induces the hydrolysis of PIP2 which generates IP_3 and DAG (Figure 1.4). DAG activates PKC by binding to the C1 region of the regulatory domain. The energy generated from this interaction releases the PS from the substrate binding cavity, linearising the confirmation of the PKC protein (Newton, 2003). This facilitates translocation from the cytosol to intracellular compartments (1.5.4) where the activated protein exerts changes on cellular physiology by interacting with its downstream substrates (1.6).

In addition to DAG, phospholipids including phospholipase A2 and phospholipase D, exchange protein directly activated by cAMP 2 (Epac) GTPases and mTOR Complex 2 (mTORC2) can contribute to the activation of PKCε (Facchinetti, *et al.*, 2008). Although not a physiological stimulant, *in vitro* studies have shown that phorbol esters such as PMA can bind to cPKC and nPKC, with a high affinity, and promote activation by mimicking the action of DAG (Jain and Trivedi, 2014). Consequently, phorbol ester treatment is widely applied in

biochemical research into the effects of PKC expression and activation, however, although potent modulators of PKC, phorbol esters can also activate PKD, and other C1 domain-containing proteins (Jain and Trivedi, 2014). Furthermore, studies have also shown a variable response to PMA as exposure can ultimately promote PKC degradation (1.5.5).

1.5.4 Localisation of PKC Enzymes

All PKC isoforms reside within the cytosol prior to activation, as described above (1.5.3). Upon stimulation by an agonist, such as phosphatidylserine and DAG, the activated proteins relocate to specific sub-cellular compartments. The primary target of PKC translocation is the plasma membrane, and as a result, redistribution to this cellular compartment is frequently used as a surrogate measure of PKC activation. However, this does not account for the complex nature of PKC translocation. The rate of translocation to the membrane for nPKC isoforms is around one order of magnitude slower than cPKC isoforms due to the absence of calcium pre-targeting (Newton, 2003). Furthermore, PKC isoforms can also redistribute to the mitochondria (Baines Christopher, *et al.*, 2002, Majumder, *et al.*, 2001), Golgi (Xu, *et al.*, 2007), endoplasmic reticulum (Maissel, *et al.*, 2006), and the nucleus (Beckmann, *et al.*, 1994, Pierce, *et al.*, 1998).

PKC translocation to subcellular compartments relies on interactions with anchoring proteins such as receptors for activated C-kinase (RACK; Mochly-Rosen, *et al.*, 1991). Currently, two RACKs have been characterised; RACK1 which has shown some selectivity to PKCβ (Ron, *et al.*, 1994) but also binds PKCε (Pass, *et al.*, 2001) and RACK2 which is selective for PKCε (Csukai, *et al.*, 1997). These RACK proteins bind PKC in a saturable manner and maintain the activated PKC enzymes in the optimal location for modulating downstream signalling cascades and interactions with cytoskeletal and cell adhesion proteins (Mochly-Rosen, *et al.*, 2012). However, it is likely that there are multiple RACK for each isozyme given that activated PKC isozymes can localize at several subcellular compartments (Disatnik, *et al.*, 1994). In addition to RACK proteins membrane localisation of PKCε can also be facilitated by direct interactions with F-actin through its actin binding site (Prekeris, *et al.*, 1996).

Mitochondrial localisation of PKC isoforms is associated with protection against oxidative stress and several mitochondrial PKC substrates have been described (1.6.2). For nuclear translocation, some aPKC isoforms have a nuclear localisation sequence (NLS;

Perander, *et al.*, 2001), however, cPKC and nPKC isoforms lack this sequence, despite nuclear localisation of these isoforms being described. In yeast a protein interacting with C-kinase which is primarily expressed at the nuclear membrane has been identified as a substrate for PKCα (Staudinger, *et al.*, 1995). Alternatively, nuclear PKCε translocation could occur through co-transport, in association with proteins which contain a NLS, such as Matrin-3 or vimentin which have been identified as proteins which associate in the nucleus of PMA treated fibroblasts (Xu and Rumsby, 2004). In terms of what directs differential localisation of PKC isoforms, the second messenger which is bound to the C1 domain may play a role. One study has shown that in response to DAG or tridecanoic acid PKCε localises at the plasma membrane, while in response to arachidonic acid and linoleic acids this kinase localises at the Golgi apparatus (Shirai, *et al.*, 1998) through interactions with the PKC zinc finger domain (Lehel, *et al.*, 1995). Alternatively, this could be due to phosphorylation of different residues within PKC isoforms (Xu, *et al.*, 2007).

1.5.5 Downregulation and Degradation

Degradation is part of the natural life cycle for proteins, including PKC isoforms. Upon treatment with PKC modulators (Bryostatin-1 and PMA), proteasome inhibitors prevented down-regulation of these PKCα and PKCε, whereas inhibitors of calpain proteases, lysosomal enzymes, and vesicle trafficking had no effect on the expression of these kinases (Hansra, *et al.*, 1999). Therefore, indicating the ubiquitin-proteasome system (UPS) as the primary mechanism responsible for cPKC and nPKC degradation (Hansra, *et al.*, 1999). Briefly, the UPS of protein degradation is a non-lysosomal mechanism of degradation where proteins are labelled with ubiquitin. These ubiquitin-labelled proteins are recognised by the 26S proteasome which promotes the breakdown of ubiquitinated proteins to small peptides that are targeted by the proteasome machinery to undergo proteolysis and degradation (Herrmann, *et al.*, 2007).

As most studies investigating the downregulation of PKC isoforms utilise phorbol esters which are not physiologically relevant, the identification of intrinsic mechanisms which initiate PKC downregulation has not been fully established. However, activation of PKC may trigger its degradation. Mutation of the ATP binding site of PKCα negated phorbol ester-mediated degradation (Ohno, *et al.*, 1990), suggesting that the catalytic activity of PKC isoforms is required for their degradation. Furthermore, studies have shown that PKC degradation induced by chronic PMA or Bryostatin treatment, is preceded by

dephosphorylation (Lee, *et al.*, 1996). The dephosphorylation of PKC isoforms has recently been shown to involve PH domain leucine-rich repeat protein phosphatases (PHLPP; Brognard and Newton, 2008). Both PHLPP1 and PHLPP2 can dephosphorylate the hydrophobic motif of cPKC and nPKC isoforms (but not aPKC), while deletion mutagenesis of the PH domain of PHLPP isoforms results in increased expression of mature (phosphorylated) PKC (Gao, *et al.*, 2008). Despite this, hyperphosphorylation of PKCδ in NIH3T3 cells prior to PMA-mediated down-regulation has been observed (Srivastava, *et al.*, 2002), suggesting a role for phosphorylation in promoting PKC degradation may be isoform dependent.

1.6 Physiological and Pathophysiological Functions of PKCε

The nPKC isoform, PKCε is expressed in most mammalian tissues and has been shown to modulate a diverse range of cellular functions including cell proliferation, differentiation (Gobbi, *et al.*, 2007), and survival (Gray, *et al.*, 1997). Given these pleiotropic interactions, dysregulated PKCε expression has been described in a range of pathologies including; ischaemic heart disease (1.6.2) , Alzheimer's disease (1.6.3), diabetes (1.6.4), and cancer (1.6.5). This section briefly outlines some of the mechanisms through which PKCε modulates cellular processes and contributes to the pathogenesis of these diseases, while the role of PKC isoforms in haematopoietic cell regulation and haematological malignancies are outlined in sections 1.6.6 and 1.6.7, respectively.

1.6.1 The Role of PKCε in Cell Cycle Progression and Cell Division

Cell proliferation is fundamental in maintaining homeostasis and relies on the tight regulation of the mammalian cell cycle. The cell cycle is classically divided into 4 phases; G1 phase where cells prepare for DNA synthesis, S phase where DNA synthesis occurs, G2 phase in which cells prepare for cell division, and M (or mitosis) phase where sister chromatid separation and cell division occur (Vermeulen, *et al.*, 2003). Transition between the phases of the cell cycle relies on the phase specific expression of cyclins and cyclin-dependent kinases. PKC kinases have shown both positive and negative regulatory properties in respect to cell cycle progression (Black, 2000). The role of PKCε has predominantly been studied in an oncology setting so is discussed in greater depth in 1.6.5.1, however PKCε has also been implicated in mitotic and cell division processes (Brownlow, *et al.*, 2014, Martini, *et al.*, 2018, Saurin, *et al.*, 2009, Saurin, *et al.*, 2008).

The involvement of PKCε in cell division has been demonstrated in PKCε knockdown and knockout studies. Embryonic fibroblasts from PKCε knockout mice progressed normally through the cell cycle until cytokinetic abscission, where cells failed to separate and retained the microtubule bundle and contractile actin ring which are usually degraded to facilitate cytokinesis (Saurin, *et al.*, 2008). Reducing *PKCε* expression in Hela cells using interfering RNA systems has also supported the involvement of PKCε in this process as they exhibited the same cytokinesis defects (Saurin, *et al.*, 2008). A major player in mammalian cytokinesis is the small GTPase, RhoA, which activates formins, actin polymerisation and promotes myosin ATPase activity (Piekny, *et al.*, 2005). Saurin *et al*. have also shown that knocking down PKCε caused RhoA accumulation (Saurin, *et al.*, 2009). In addition, interactions between PKCε and 14-3-3 proteins are implicated in this process. 14-3-3 proteins are scaffold proteins that bind to phosphorylated serine and threonine motifs on target proteins. Three phosphorylation sites have been identified within PKCε that control its association with 14-3-3 (Saurin, *et al.*, 2008). Furthermore, the requirement of this interaction has been demonstrated as the cytokinesis defects caused by PKCε knockout or knockdown can only be reversed through the re-expression of PKCε protein which is competent for 14-3-3 association (Saurin, *et al.*, 2008).

1.6.2 Ischaemic Preconditioning and Protection Against Oxidative Stress

ROS such as superoxide anions, H_2O_2 and hydroxyl radicals are endogenously produced within the cell as by-products of aerobic respiration but can also be generated exogenously by chemotherapeutic agents (Doroshow, 2019, Ray, *et al.*, 2012). As part of normal signalling, ROS can act as localised second messenger molecules and influence cell signalling through oxidation of the cysteine and/or tyrosine residues of proteins (Corcoran and Cotter, 2013). This includes PKC isoforms which can be directly and indirectly activated by ROS (Steinberg, 2015). For example, oxidation of cysteine residues within the C1 domain leads to a reduced autoinhibitory capacity and co-factor-independent PKC activation (Knock and Ward, 2011).

As ROS are highly reactive molecules and have the capacity to oxidise DNA, proteins, and lipids (Valko, *et al.*, 2007), tight regulation of ROS homeostasis is required. The cell has a variety of mechanisms to detoxify ROS and maintain homeostasis. Antioxidants including catalase which converts H_2O_2 into H_2O and O_2 (George, 1947) and superoxide dismutase

(SOD) enzymes which catalyse the reduction of superoxide radicals into H_2O_2 (Fridovich, 1995), are central to this process. Oxidative stress is a phenomenon that arises when the levels of ROS outweigh the antioxidant capacity of the cell (Valko, *et al.*, 2007). The ability of PKCε to protect against oxidative stress has been studied most extensively in cardiac cells but has also been proposed in AML (1.6.7). In the context of the heart, studies using transgenic mice have highlighted a role for this kinase in ischaemic pre-conditioning; the phenomenon whereby repeated brief episodes of ischaemia and reperfusion increase the resistance to myocardial infarction and contractile dysfunction which are induced by subsequent sustained episodes of ischaemia (Iliodromitis, *et al.*, 2007). Inhibition of PKCε with a selective translocation inhibitor (εV1-2;1.7), has been shown to abolish the cyto-protective effect of PKCε in the hypoxic preconditioning of rabbit cardiac myocytes (Gray, *et al.*, 1997). Furthermore, PKCε knockout mice hearts do not develop tolerance to antimycin A (ATM)-induced ischemia (Kabir, *et al.*, 2006).

Cardiac preconditioning is associated with the activation of PI3K, upstream of PKCε (Tong, *et al.*, 2000), while the downstream consequences of PKCε activation is associated with mitochondrial translocation of this kinase. At the mitochondria, PKCε has several proposed substrates including mitochondrial potassium (K_{ATP}) channels and cytochrome c oxidase subunit IV of the electron transport chain (ETC; Jabůrek, *et al.*, 2006, Kabir, *et al.*, 2006, Kornfeld, *et al.*, 2015). Interaction of PKCε with the mitochondrial K_{ATP} channels leads to an influx of K^+ into the mitochondria and inhibits mitochondrial permeability transition (MPT) which is associated with ischemia-reperfusion injury induced necrotic cell death (Costa, *et al.*, 2006). There is also some evidence that PKCε can protect against MPT independently of K_{ATP} channels (Costa, *et al.*, 2006). PKCε also interacts with ERK, JNK, and p38 MAPK in normal and transgenic murine hearts at the mitochondria (Baines Christopher, *et al.*, 2002). Furthermore, in transgenic mice expressing a constitutively active PKCε mutant (A159E) increased activation of mitochondrial ERK, and phosphorylation of the apoptotic protein Bad was observed (Baines Christopher, *et al.*, 2002). Phosphorylation of Bad prevents the ability of this apoptotic protein to sequester anti-apoptotic BCL-2 family members (Zha, *et al.*, 1997). Therefore, PKCε may confer resistance to oxidative stress indirectly through modulating survival and apoptotic signalling.

1.6.3 Role of PKCε in Normal Brain Function and Alzheimer's Disease

PKC expression and activity are essential components of signal transduction within the brain (Sun and Alkon, 2012). Of the PKC isoforms, PKCε is thought to be the most abundant and plays a role in normal brain function and in neurological diseases, such as Alzheimer's disease. Through interactions with actin filaments via its actin binding site (1.5.2), PKCε has been shown to promote neurite outgrowth during differentiation (Zeidman, *et al.*, 2002). In response to retinoic acid, which promotes neuronal differentiation, the cytoskeletal localisation of PKCε in the human neuroblastoma cell line SK-N-BE(2) increased by 75%±30% (Zeidman, *et al.*, 2002). Furthermore, deletion of the PKCε actin binding motif reduced neurite outgrowth in SK-N-BE(2) and SH-SY5Y cells (Zeidman, *et al.*, 2002), demonstrating the importance of the actin binding site of PKCε in this process. PKCε-actin interactions have also been implicated in the exocytosis of the neurotransmitter glutamate (Prekeris, *et al.*, 1996), as well as regulating the expression of the metabotropic glutamate receptor, mGluR5 (Schwendt and Olive, 2017).

In terms of brain function, knockout mice models have suggested that PKCε plays a critical role in alcohol dependency through regulating the sensitivity of $GABA_A$ receptors (Hodge, *et al.*, 1999). PKC expression and activity are also associated with memory. Inhibition of PKCε with the translocation inhibitor εV1-2 reduced recognition memory in rats (Zisopoulou, *et al.*, 2013), while pharmacological activation of PKCε in rats improved synaptogenesis and memory (Hongpaisan, *et al.*, 2013). Reduced memory and cognitive function are characteristic features of Alzheimer's disease which arise in part from the formation of amyloid plaques within the brain. Reduced PKC signalling occurs in several dementias. In terms of Alzheimer's disease, the amyloid beta protein within amyloid plaques, contains a putative PKC pseudo-substrate domain which can directly inhibit PKC isoforms, including PKCα and PKCε (Lee, *et al.*, 2004), suggesting a mechanism of PKC downregulation which may have pathogenic implications in this disease.

1.6.4 Insulin Resistance and Diabetes

Two key factors in type II diabetes are β-cell dysfunction and insulin resistance which are frequently associated with increased lipid availability. As a lipid-dependent kinase, PKCε has been implicated in insulin resistance. Short-term (3-day) fat feeding of rats induces hepatic steatosis and a diminished ability of insulin to reduce endogenous glucose production (Samuel, *et al.*, 2004). This occurred in concert with increased membrane translocation and activation of PKCε (Samuel, *et al.*, 2004). Furthermore, in rats fed for 3 days on a high-fat diet, PKCε knockdown reversed the defect in insulin receptor kinase activity and supress hepatic glucose production (Samuel, *et al.*, 2007).

1.6.5 The Role of PKC Isoforms in Cancer

Changes in PKC expression is well established in cancer. Although the clinical associations of dysregulated PKC expression are context dependent and vary between isoforms, in general, elevated PKC expression is associated with aggressive disease phenotypes and poor patient outcomes (Table 1.5). Although the exact mechanisms which promote PKC dysregulation in cancer have not been established (Griner and Kazanietz, 2007), mutations within PKC isozymes are relatively rare. However, a point mutation in *PRKCA* (D294G) has been identified in a proportion of highly invasive pituitary tumours (Griner and Kazanietz, 2007), while a chromosomal rearrangement of the *PRKCE* gene has been described in a thyroid cancer cell line (Knauf, *et al.*, 1999). In addition, it is yet to be established whether the correlation between PKC isoform expression and disease progression is causal or associative. Difficulty in achieving this can in part be attributed to discrepancies between PKC mRNA and protein expression; as demonstrated in epithelial cancer, where PKCε expression is markedly upregulated at a protein level but marginal changes in mRNA expression are observed (Garg, *et al.*, 2014). This could be because mRNA datasets do not account for post-transcriptional/translational modifications which promote protein stability or affect the activation status of these kinases. Although all PKC isoforms have been implicated in cancer biology in some way, as reviewed by Garg, *et al.*, 2014, the rest of this section will focus on PKCε, as this is the isoform most relevant to this thesis.

PKCε overexpression has been described in numerous solid cancers (Table 1.5). In primary tumours from invasive ductal breast cancer patients, increased PKCε expression, determined by histological staining, correlated with established poor prognostic indicators in this malignancy including high tumour grade, positive ErbB2/Her2 status and negative oestrogen and progesterone receptor status (Pan, *et al.*, 2005). In addition, PKCε up-regulation has been reported in primary non-small cell lung cancer (NSCLC) cells compared to normal lung epithelium (Bae, *et al.*, 2007) and prostate cancer relative to benign prostatic epithelial cells (Cornford, *et al.*, 1999). Due to the promiscuous nature of PKC isoforms, the role of PKCε in cancer seems to be complex and context dependent, however, mouse models and *in vitro* studies have implicated PKCε in cancer cell transformation (1.6.5.1), survival (1.6.5.2), chemoresistance (1.6.5.3), and metastasis (1.6.5.4).

1.6.5.1 Cell Transformation and Proliferative Phenotypes

PKCε is the only isoform within its family to have shown transforming oncogene properties. Overexpression of PKCε in fibroblasts resulted in oncogenic transformation, demonstrated by the induction of anchorage-independent growth and tumorigenesis in mice (Mischak, *et al.*, 1993). Furthermore, transgenic PKCε overexpression in mouse skin epithelial cells leads to the development of metastatic squamous cell carcinomas and enhanced susceptibility to UV radiation-induced skin cancer (Verma, *et al.*, 2006). A recent study has also implicated PKCε in the tumorigenesis of KRAS mutant NSCLC cells. *KRAS* mutations are the most frequent oncogenic alterations reported in human lung adenocarcinoma, while PKCε is frequently overexpressed. In patients with *KRAS* mutant NSCLC, high (above median) *PKCε* expression was associated with significantly reduced OS than that of patients with low *PKCε* mRNA expression (below median; Garg, *et al.*, 2020). Subsequent analysis in KRAS mutant murine models showed that PKCε knockout significantly attenuated lesion formation, implicating a role for PKCε in the tumorigenesis of lung cancers harbouring KRAS mutations (Garg, *et al.*, 2020).

PKCε-mediated cell transformation has been linked to the activation of the Ras/Raf/MAPK pathway. PKCε overexpression and the resulting oncogenic transformation of rodent fibroblasts is associated with Raf hyperphosphorylation and increased Raf-1 and MAPK activity (Cacace, *et al.*, 1996). Furthermore, PKCε overexpression in fibroblasts harbouring a dominant negative Raf-1 mutation did not exhibit the increased growth or altered morphological changes associated with oncogenic transformation (Cacace, *et al.*, 1996). Thus,

demonstrating the requirement of Raf-1 in PKCε-mediated transformation in this context. A later study by the same group also identified that PKCε overexpression in rat fibroblasts have a reduced requirement for growth factors, and that the oncogenic properties of PKCε in these cells is, at least in part, due to increased TGFβ production (Cacace, *et al.*, 1998). The oncogenic properties of PKCε have been substantiated by an overexpression study in colon epithelial cells which resulted in oncogenic transformation, mediated through Ras signalling (Perletti, *et al.*, 1998). However, PKCε overexpression does not always result in oncogenic transformation. Prostate specific PKCε overexpression in transgenic mice caused the development of pre-neoplastic prostatic lesions but did not result in cancer progression (Benavides, *et al.*, 2011).

In several contexts PKCε upregulation has been associated with pro-proliferative phenotypes. In a rat embryo fibroblast cell line and mouse NIH3T3 fibroblast cells PKCε overexpression resulted in a decreased doubling time and an increased saturation density (Cacace, *et al.*, 1993 , Mischak, *et al.*, 1993). Furthermore, overexpression of PKCε in an androgen-sensitive human prostate adenocarcinoma cell line, LNCaP, promoted cell proliferation in the absence of androgen which usually results in G1-phase arrest (Wu, *et al.*, 2002). This phenotype was observed despite reduced androgen receptor expression. Furthermore, when injected into nude mice, tumours did not develop with in the control cell recipients but did in intact and castrated mice injected with the PKCε overexpression LNCaP cells (Wu, *et al.*, 2002). Together this suggests that PKCε overexpression can promote cancer cell growth and progression in the absence of proliferative stimuli.

Such proliferative phenotypes have been associated with accelerated cell cycle progression. For example, in the study described above, LNCaP cells overexpressing PKCε had an accelerated G1 to S phase progression, which was potentially mediated through altered expression of cell cycle proteins including Rb, E2F-1, and cyclin- D1, -D3, and -E (Wu, *et al.*, 2002). In line with this phenotype, NSCLC cells expressing a dominant negative PKCε mutant, or a PKCε-targeted interference RNA construct, showed a reduced G1-S cell cycle transition which was associated with reduced CDK2 complex activation and p21/Cip1 induction, a cyclin-dependent kinase inhibitor (Bae, *et al.*, 2007). Furthermore, a link between PKC signalling and cyclin D1 expression and activity, the cyclin involved in promoting G1/S phase cell cycle progression, has also been described in R6 fibroblasts overexpressing PKCε (Soh and Weinstein, 2003).

Table 1.5: Expression of PKC isozymes in human cancers

Table outlining the changes in PKC protein expression in different human cancers, alongside clinical attributes associated with these findings (1.6.5). Adapted from Griner and Kazanietz, 2007.

PKC	Tumour Type	Expression	Clinical associations	Reference
α	Urinary tract carcinoma	Increased	With tumour grade	Varga, *et al.*, 2004
	Ovarian	Decreased	With tumour grade	Weichert, *et al.*, 2003
βI/I	Urinary tract carcinoma	Decreased	With tumour grade	Varga, *et al.*, 2004
	Prostate	Decreased	Associated with early disease development and an increased risk of relapse	Cornford, *et al.*, 1999
δ	Bladder	Decreased	With tumour grade	Varga, *et al.*, 2004
	Colorectal	Increased	Not Determined	Pongracz, *et al.*, 1995
ε	Bladder	Increased	With tumour grade	Varga, *et al.*, 2004
	Breast	Increased	With tumour grade, metastasis, reduced OS and DSF	Pan, *et al.*, 2005
	Prostate	Increased	Implicated in early stages of tumour development	Cornford, *et al.*, 1999
	Lung Cancer	Increased	Adenocarcinomas> Squamous cell carcinoma T1 grade tumour>T2-T4 grade	Bae, *et al.*, 2007
	Head and Neck	Increased	Reduced OS and increased occurrence of relapse	Martínez-Gimeno, *et al.*, 1995
	Thyroid	Decreased	Not Determined	Knauf, *et al.*, 2002
	Urinary Bladder Carcinoma	Increased	Grade 2+3 tumours compared with normal tissues	Varga, *et al.*, 2004
η	Breast	Decreased	With tumour grade	Masso-Welch, *et al.*, 2001
θ	Gastrointestinal Stromal Tumour	Increased	Diagnostic Marker	Blay, *et al.*, 2004
ζ	Urinary Bladder Carcinoma	Increased	Increases with tumour grade	Varga, *et al.*, 2004
ι	Lung Cancer	Increased	Reduced OS	Regala, *et al.*, 2005

1.6.5.2 Survival and Apoptotic Signalling

In addition to the proliferative phenotypes described above, PKCε can promote cancer cell survival and protect against both the intrinsic and extrinsic pathway of apoptosis (1.4.1). PKCε modulate cancer cell survival through promoting Akt expression and activity (Lu, *et al.*, 2006, Okhrimenko, *et al.*, 2005); an important pro-survival protein which is frequently hyperactivated in cancer. In the breast cancer cell line MCF-7, PKCε protects against TNF-induced apoptosis through promoting Akt phosphorylation via DNA-dependent protein kinase (Lu, *et al.*, 2006). The propensity for PKCε to promote cell survival has also been associated with NF-κB activation. NF-κB is a dimer formed by proteins of the Rel family and is retained in the cytoplasm as a complex with inhibitory IB proteins. Androgen-dependent prostate cancer cells display high levels of PKCε compared to normal prostate epithelial cells (Benavides, *et al.*, 2011). Furthermore, pre-neoplastic lesions in PKCε overexpression mice display nuclear NF-κB staining which is indicative of NF-κB activation (Benavides, *et al.*, 2011). The requirement of PKCε in NF-κB activation in prostate cancer cells was subsequently demonstrated as RNAi-mediated knockdown of PKCε reduced intrinsic NF-kB activity in androgen dependent and independent prostate cancer cell lines, and significantly attenuated TNFα phosphorylation, IκBα degradation and nuclear translocation of NF-κB (Garg, *et al.*, 2012).

PKCε also promotes cell survival through the modulation of apoptotic signalling. The mechanisms through which PKCε mediates this apoptosis resistance are not fully understood. However, PKCε has been shown to inhibit TRAIL-induced apoptosis in glioma cells (Okhrimenko, *et al.*, 2005), while in the breast cancer cell line MCF-7 PKCε-mediated survival is associated with BCL-2 upregulation and simultaneous reductions in Bid expression (Sivaprasad, *et al.*, 2007). Although, BCL-2 and Bax expression in glioma cells was not affected by altered PKCε expression (Okhrimenko, *et al.*, 2005), the ability of PKCε to modulate BCL-2 family members has been substantiated in prostate cancer cells. Specifically, PKCε overexpression in LNCaP cells attenuated Bax induction in response to PMA treatment (McJilton, *et al.*, 2003). In addition, the propensity of PKCε to confer etoposide and DOX resistance in a small cell lung cancer (SCLC) cell line (H82) was associated with the inhibition of caspase-3 and caspase-9 cleavage and cytochrome c release from the mitochondria (Ding, *et al.*, 2002).

1.6.5.3 Chemoresistance

PKC isoforms may be able to promote chemoresistance by modulating survival and apoptotic proteins as described in 1.6.5.2 . However, PKC can also phosphorylate drug targets such as topoisomerase II. In U937 cells, topoisomerase II was identified as a downstream target of PKCζ (Plo, *et al.*, 2002) and in lysates of *Drosophila melanogaster* Kc tissue cells, PKC-mediated phosphorylation promoted ATP hydrolysis and the catalytic activity of topoisomerase II (Corbett, *et al.*, 1993). Such modifications can reduce the ability of topoisomerase inhibitors to stabilise topoisomerase-DNA complexes and induce apoptosis (DeVore, *et al.*, 1992). Although hypo-phosphorylation of topoisomerase II has also been associated with multidrug resistance (Ganapathi, *et al.*, 1996), this may represent a mechanism of PKC-mediated chemoresistance. Alternatively, PKC isoforms including PKCε, have been associated with efflux pump expression and activity which confer chemoresistance by reducing intracellular drug accumulation (1.4.3).

Associations between PKC activity and efflux pumps have primarily been established using PKC agonists and inhibitors (Mayati, *et al.*, 2017). Three PKC phosphorylation residues (ser661, Ser667 and Ser 671) have been identified within the intracellular linker region of the P-GP peptide, suggesting potential roles for this family of kinases in P-GP regulation (Chambers, *et al.*, 1992). PMA treatment has been shown to promote P-GP expression and drug efflux (Aftab, *et al.*, 1994, Chambers, *et al.*, 1992) while inhibiting PKC isoforms can overcome these phenotypes (Gupta, *et al.*, 1996). However, the causality of these findings has been complicated by the fact that some PKC inhibitors, including Chelerythrine and Enzastaurin can supress P-GP-mediated drug resistance by directly binding P-GP and inhibiting its function (Castro, *et al.*, 1999, Chambers, *et al.*, 1992, Michaelis, *et al.*, 2015). Furthermore, directed mutagenesis of the PKC phosphorylation sites did not affect P-GP expression or activity (Goodfellow, *et al.*, 1996). Thus, implicating a complex and potentially context dependent role for PKC isoforms in conferring chemoresistance through efflux pump regulation.

Despite conflicting mechanistic evidence linking P-GP and PKC kinases, PKCε has been associated with P-GP induction. In a prostate cancer cell line, the induction of P-GP in response to aspirin was significantly supressed upon PKCε inhibition using the translocation inhibitor εV1-2, compared to aspirin treatment alone (Flescher and Rotem, 2002a). Furthermore, through studies in a breast cancer cell line, it has been proposed that PKCε may

promote P-GP induction following CD44 and hyaluronan (HA) interactions. HA is a major component in the extracellular matrix of most mammalian tissues, and the adhesion molecule CD44 which selectively binds hyaluronan, have been implicated in chemotherapy resistance. HA-CD44 interactions promote Nanog protein expression and activity, where Nanog subsequently forms complexes with Stat-3 to promote *P-GP* gene expression (Bourguignon, *et al.*, 2008). HA-CD44 interactions also induced the binding of ankyrin, a cytoskeletal protein, to P-GP which resulted in drug efflux and chemoresistance (Bourguignon, *et al.*, 2008). A later study by the same group showed that HA-CD44 interaction in MCF-7 cells promoted PKCε activity resulting in the phosphorylation of Nanog (Bourguignon, *et al.*, 2009). The authors of this paper propose that Nanog, phosphorylated by PKCε, translocate to the nucleus and results in miR-21 production. miR-21then promotes chemoresistance through promoting IAP and P-GP expression (Bourguignon, *et al.*, 2009).

1.6.5.4 Cancer cell Metastasis and Invasion

Metastasis is an important aspect of cancer progression which involves the dissemination of malignant cells from the primary tumour to secondary sites. In many cancers PKCε expression is associated with invasive disease types (Gutierrez-Uzquiza, *et al.*, 2015, Jain and Basu, 2014a, Pan, *et al.*, 2005). In a human prostate cell line with a high bone metastatic potential, PKCε knockdown impaired metastasis upon injection into nude mice (Gutierrez-Uzquiza, *et al.*, 2015). In these cells, PKCε knockdown had limited effects on cell proliferation adhesion or motility, but instead significantly impaired the ability of this cell line to migrate through Matrigel, implicating a role for PKCε in promoting cell invasion (Gutierrez-Uzquiza, *et al.*, 2015). The requirement of PKCε for metastatic phenotypes has also been demonstrated in NSCLC cells where genetic and pharmacological inhibition of PKCε prevented cell migration and invasion (Caino, *et al.*, 2012).

A key aspect of metastasis is the epithelial-mesenchymal transition (EMT) where epithelial cells gain mesenchymal features such as a spindle shape and increased migratory and invasive potential (Geiger and Peeper, 2009). PKCε has been implicated in this process as overexpression in a non-malignant breast epithelial cell line (MCF-10A) promoted EMT, while PKCε knockout partially reversed the TGF-β-induced mesenchymal phenotype of these cells (Jain and Basu, 2014b). The EMT of this breast cancer cell line was associated with the loss of epithelial markers, such as E-cadherin, zonula occludens-1 (ZO-1), and claudin-1, and an increase in the mesenchymal marker vimentin (Jain and Basu, 2014b). This could be driven

by the ability of PKCε to modulate integrin expression and localisation (Chattopadhyay, *et al.*, 2014, Tuomi, *et al.*, 2009). In addition, the turnover of integrins is an important factor in metastasis and PKCε has been shown to play a role in the return of endocytosed β1-integrin to the membrane (Ivaska, *et al.*, 2002). Alternatively, PKCε-mediated cell adhesion has been associated with the activation, through phosphorylation, of ERK (Besson, *et al.*, 2001), Stat3 (Aziz, *et al.*, 2007) and Rho GTPases (Pan, *et al.*, 2006).

1.6.6 Normal Haematopoiesis and Immune Function

The expression of multiple PKC isoforms (α, β, δ, ε, η, ζ) has been identified in freshly isolated human $CD34^+$ cells from normal donors through western blot analysis (Bassini, *et al.*, 1999). The expression of these PKC isoforms is thought to be strictly regulated throughout haematopoiesis. In lineage-restricted murine 32D clones PKCα, PKCβI, PKCδ, PKCε, PKCη, and PKCζ were all expressed in mast, granulocytic/monocytic, and granulocytic restricted clones, while the expression of PKCε and PKCη was absent in erythroid-restricted cells (Bassini, *et al.*, 1999). This differential expression of PKC kinases between haematopoietic lineages implies a role for individual isoforms in the lineage commitment and differentiation of myeloid progenitors.

The ability of PKC isoforms to promote myeloid differentiation has long been established *in vitro* through the application of PKC agonists such as PMA (Aihara, *et al.*, 1991, Rossi, *et al.*, 1996). By exploiting the dose-dependent responses of cPKC and nPKC isoforms to PMA, Rossi *et al.* highlighted a role of PKC activity in promoting haematopoietic lineage commitment (Rossi, *et al.*, 1996). Specifically, this study showed that multipotency was maintained in transformed haematopoietic cells where PKC activity was low or absent (no PMA activation or high dose PMA treatment), while moderate PKC activity, was associated with monocytic differentiation, and high PKC activity with eosinophilic differentiation (Rossi, *et al.*, 1996). A separate study showed that PMA treatment promoted proliferation and macrophage development of human GM-colony forming cells (CFC), even in conditions which stimulate neutrophil development (Whetton, *et al.*, 1994). A role for PKC in haematopoietic cell differentiation has been supported by our group, where PKC was found to mediate the abnormal erythroid development and monocytic specification of human HSPC expressing mutant Ras (Pearn, *et al.*, 2007).

On an isoform specific level, the role of PKCε in haematopoiesis has been studied most extensively in the erythroid and megakaryocytic lineages. As described previously, PKCε expression was not detected in erythroid restricted 32D cells (Bassini, *et al.*, 1999). Furthermore, inhibition of PKCε using a specific peptide inhibitor promoted erythroid colony formation (Bassini, *et al.*, 1999), suggesting that PKCε is a negative regulator of erythroid commitment. Despite this, PKCε has been implicated in EPO signalling in erythroid cells. The differentiation and maturation of erythroid cells relies on the haematopoietic cytokine EPO (1.1.2). In Rauscher murine erythroleukaemia cells, knockdown of various PKC isoforms showed that only reduced PKCε expression impaired *c-myc* upregulation in response to EPO (Li, *et al.*, 1996). Although *c-myc* has been implicated in erythroid cell differentiation (Ohmori, *et al.*, 1992), PKCε knockdown did not affect the differentiation of the Rauscher murine erythroleukaemia cells but severely impaired EPO-induced cell growth (Li, *et al.*, 1996). PKCε can also promote erythroblast survival as PKCε inhibition increased TRAIL-induced apoptosis (Mirandola, *et al.*, 2006).

In the megakaryocytic lineage, western blot analysis of human HSPC cultured in conditions which support megakaryocyte differentiation showed temporal PKCε protein expression. Specifically, high levels of PKCε expression were observed in the early stages of megakaryocyte development but was subsequently downregulated during differentiation (Gobbi, *et al.*, 2007). The authors also showed that PKCε overexpression in TPO-treated HSPC impaired normal megakaryocytic differentiation, as demonstrated by reduced differentiation marker expression (CD61, CD41 and CD42b), polyploidization and platelet production (Gobbi, *et al.*, 2007). Although PKCε does not promote megakaryocyte differentiation, the high expression of PKCε in early megakaryocytic progenitors suggests a role for this kinase in megakaryocytic lineage commitment. This is supported by a study which showed that, ingenol-3,20-dibenzoate-induced megakaryocytic differentiation of K562 and HEL cells was associated with rapid nuclear translocation of PKCε (Racke, *et al.*, 2001). Mechanistically, PKCε expression may contribute to this by regulating the activity of the megakaryocyte-specific αIIb promoter, as PKCε inhibition reduced αIIb promoter activity. Furthermore, whilst modest αIIb promoter activation was observed with constitutively active PKCε mutants, functional cooperation with GATA-1, a known regulator of megakaryocytic differentiation, was observed (Racke, *et al.*, 2001).

Compared to the erythrocytic and megakaryocytic lineages, the role of PKCε in monocytic and granulocytic cells, which are primarily impacted in AML has been studied to a

lesser extent. Nevertheless, a role for PKCε in macrophage function has been identified as PKCε knockout mice had severely attenuated responses to lipopolysaccharide (Castrillo, *et al.*, 2001). In addition, PKCε has been implicated in myeloid cell differentiation. A study using U937 cells, showed that PMA-mediated monocyte differentiation was associated with onzin downregulation (Wu, *et al.*, 2010). Onzin is a small, widely conserved protein which is highly expressed in phagocytes, macrophages, neutrophils, intestine, and splenic cells (Ledford, *et al.*, 2007). shRNA-mediated PKCε knockdown in U937 cells prevented ERK phosphorylation and PMA-mediated onzin down-regulation; a finding which was not observed with other PKC isoforms (PKCβ). Thus implicating PKCε activity in PMA-mediated onzin down-regulation and differentiation in this context (Wu, *et al.*, 2010).

1.6.7 Role of PKC Isoforms in Leukaemia

As with solid cancers, upregulation of PKC isoforms has been described in haematological malignancies and although there is some heterogeneity in the contributions of individual isoforms, in general they are associated with poor outcomes (Redig and Platanias, 2008). For example, phosphorylated PKCα (pPKCα) was associated with worse OS compared with patients with negative pPKCα (p=0.054; hazard ratio (HR) 4.35 95% confidence interval (CI) (0.96-19.9) in a small cohort of AML patients (Kurinna, *et al.*, 2006), while in diffuse large-B cell lymphoma, patients with high PKCβ expression (upper quartile) had a significantly worse OS (p=0.0129) with a median OS of 1.9 years, compared to 10.6 years for patients with low PKCβ expression (lower quartile) (Li, *et al.*, 2007).

How PKC isoforms contribute to poor outcomes in leukaemia has not been studied to the same extent as solid cancers. However, our group has previously shown that the survival of AML blasts overexpressing PDK-1 (1.5.3) is mediated by PKC signalling (Zabkiewicz, *et al.*, 2014). PKCε has also been implicated in the survival of hairy cell leukaemia cells, potentially through the downstream activation of Rac1 and ERK (Slupsky, *et al.*, 2007). Treating AML cell lines with Enzastaurin; a selective PKCβ inhibitor (1.7) resulted in apoptosis induction (Ruvolo, *et al.*, 2011). Although at the μM concentrations used in this study, Enzastaurin inhibited PKCα phosphorylation and membrane localisation in OCIAML5 cells without affecting PKCβ localisation, this study suggests a role for PKC isoforms in AML cell survival. Furthermore, shRNA-mediated knockdown of PKCε in AML cell lines and

patient samples, reduced the fold expansion and viability, suggesting a specific role for PKCε in the intrinsic survival of AML cells (Di Marcantonio, *et al.*, 2018).

Mechanistically, dysregulated PKC expression and activity has been associated with altered survival and apoptotic signalling. PKCα has been shown to phosphorylate BCL-2 (pBCL-2; Ruvolo, *et al.*, 1998), which is required for the anti-apoptotic effects of BCL-2 (Ito, *et al.*, 1997, May, *et al.*, 1994, Ruvolo, *et al.*, 2001). Furthermore, in AML patient samples OS was reduced in patients with both pPKCα and pBCL-2 than in patients with these proteins alone (Kurinna, *et al.*, 2006). Furthermore, BCL-2 phosphorylation by PKCα in ALL cell lines has been associated with etoposide resistance (Jiffar, *et al.*, 2004). PKC isoforms have also been implicated in promoting cell survival and chemoresistance in Philadelphia (Ph) chromosome (t(9;22)(q34,q11)) positive CML and ALL cells. This study used a v-ABL, (the transforming agent of the Abelson murine leukaemia virus) cell line model to activate kinases in a similar manner to the Ph chromosome, to promote cell survival. In this model, the suppression of apoptosis was associated with perinuclear translocation and activation of PKCβII (Evans, *et al.*, 1995). The involvement of PKCβII in this was demonstrated through pharmacological inhibition assays, where Calphostin C (CC) treatment to inhibit the translocation of PKCβII overcame this phenotype in a dose dependent manner (Evans, *et al.*, 1995). In addition, microarray analysis of Ph^+ ALL patient samples identified that *PKCε* mRNA expression increased by at least 1.5-fold in response to Imatinib. Furthermore, in Ph^+ cell lines, PKCε overexpression was associated with Akt up-regulation and conferred resistance to imatinib, suggesting again that PKCε may contribute to imatinib resistance through pro-survival signalling (Loi, *et al.*, 2016).

PKCε may also promote leukaemia cell survival and chemoresistance through modulating ROS homeostasis. ROS has been implicated in haematopoietic cell differentiation (Sardina, *et al.*, 2010, Sardina, *et al.*, 2012, Sattler, *et al.*, 1999) as well as the development and progression of leukaemia (Hole, *et al.*, 2013, Sallmyr, *et al.*, 2008). For example, patients with *FLT3*-ITD mutations have elevated NADPH oxidase-derived ROS and a high frequency of double-strand breaks, which may contribute in some capacity to the poor prognosis of these patients (Sallmyr, *et al.*, 2008). As described previously, PKCε protects against oxidative stress in cardiac cells (1.6.2) and a recent study by Di Marcantonio *et al.* has implied a role for PKCε in mediating mitochondrial ROS homeostasis in AML cells. Furthermore, PKCε overexpression protected AML cell lines against ATM; a mitochondrial ROS-generating agent

(Di Marcantonio, *et al.*, 2018), suggesting PKCε could confer resistance to chemotherapeutic agents which induce oxidative stress.

1.7 Therapeutic Targeting of PKC Enzymes

Given that PKC isoforms have the capacity to regulate several cellular processes and are frequently perturbed in disease (1.6), this family of kinases have potentially far-reaching therapeutic potential. Although identifying isoform specific inhibitors has been challenging due to the high homology and potential overlapping roles of PKC isozymes.

Midostaurin has been approved for administration in combination with conventional chemotherapeutic agents to treat patients with *FLT3* mutations (1.3.2). Midostaurin is a multi-kinase inhibitor which has a high efficacy for PKC isoforms (Fabbro, *et al.*, 1999, Levis, 2017, Stone, *et al.*, 2018). Thus, the inhibition of PKC kinases may contribute to its efficacy. In support of the importance of the multi-targeted nature of Midostaurin is the fact that Midostaurin has shown some efficacy against nonmutant *FLT3* AML (Fischer, *et al.*, 2010) and that more specific FLT-3 inhibitors have not resulted in increased clinical efficacy (Majothi, *et al.*, 2020). Another potent but non-specific PKC modulator is Bryostatin-1; a macrocyclic lactone that binds to the regulatory domain of PKC isoforms. Bryostatin-1 can have both agonistic and inhibitory effects on PKC activity, where short-term exposure causes PKC activation (Kraft, *et al.*, 1986), and translocation to the nuclear membrane, while long-term exposure causes PKC degradation (Isakov, *et al.*, 1993). *In vitro*, Bryostatin-1 treatment of leukaemia cell lines promoted cell differentiation (Hu, *et al.*, 1993) and induced apoptosis (Wall, *et al.*, 2000). In clinical trials Bryostatin-1 as a single agent has been disappointing but trials investigating combination therapies have shown some promise (Kortmansky and Schwartz, 2003).

In terms of isoform specific inhibitors, Enzastaurin was initially thought to be selective for PKCβI/II but has since shown weaker affinities for other PKC isoforms including PKCε (Jasinski, *et al.*, 2008). Enzastaurin has shown promising anti-cancer properties in a range of cancers, including AML, in non-clinical settings and early phase clinical trials (Casey, *et al.*, 2010, Michaelis, *et al.*, 2015, Morschhauser, *et al.*, 2008, Rizvi, *et al.*, 2006, Ruvolo, *et al.*, 2011, Socinski, *et al.*, 2010). More recent efforts to inhibit PKC isoforms have focused on targeting PKC translocation through the design of isoform specific oligopeptides which resemble substrate recognition sequences but have a non-phosphorylatable alanine at the target

site. In the case of PKCε, a peptide (εV1-2) which mimics the region of PKCε (residues 1-148) that interacts with RACK2 has been developed (Johnson, *et al.*, 1996). Despite reversing PKCε-mediated phenotypes in non-clinical settings (Caino, *et al.*, 2012, Flescher and Rotem, 2002a, Zisopoulou, *et al.*, 2013), the application of this inhibitor is limited by the fact that the cells must be permeabilised to facilitate its uptake. For clinical applications, εV1-2 was conjugated to a carrier protein (marketed as KAI-1678) and in a safety and efficacy study investigating the application of this PKCε inhibitor for treating neuropathic pain, subcutaneous infusions of KAI-1678 were well tolerated. However, KAI-1678 administration did not significantly improve pain scores (Cousins, *et al.*, 2013). Furthermore, KAI-1678 is currently unavailable for commercial use and no oncological clinical data are available at present.

1.8 Aims

To identify the role of PKCε in AML, our group previously analysed the mRNA and protein expression of this kinase in AML patient samples. This preliminary analysis suggested that PKCε is frequently overexpressed in this malignancy and is associated with reduced CR following first-line therapy (3.3.1.2), however, these findings require substantiation. Furthermore, the mechanism through which PKCε may contribute to this clinical finding remains unclear. Therefore, the aim of this study is to investigate the role of PKCε in the pathogenesis and treatment resistance of AML, and will be achieved through the following objectives:

- **Determine the clinical associations of PKCε expression in AML patient samples**

  Publicly available mRNA datasets will be used alongside the existing protein analysis of AML patient samples, to further characterise the pathophysiological parameters associated with PKCε upregulation in this malignancy (Chapter 3).

- **Determine whether PKCε contributes to the pathogenesis of AML through disrupting myeloid cell development**

  The expression profile of PKCε in HSPC will be assessed using publicly available mRNA data and validated at a protein level by western blot analysis. Functional analysis using overexpression and knockdown systems will be conducted to

evaluate the role of PKCε in normal haematopoiesis and to determine whether PKCε contributes to the pathogenesis of AML by disrupting myeloid cell proliferation and differentiation (Chapter 3).

- **Determine whether PKCε confers chemoresistance in AML blasts**

The expression of PKCε in AML cell lines will be assessed using publicly available mRNA datasets and western blot analysis. To assess the role of PKCε in chemoresistance, PKCε expression in appropriately selected lines will be modulated using overexpression, knockdown, and knockout systems. The resulting impact on the chemosensitivity, in terms of the impact on growth and viability, of these lines to Ara-C and DNR will be assessed using flow cytometry (Chapter 4). Based on the findings of these studies, mechanistic analysis will be conducted (Chapter 5).

Chapter 2: Materials and Methods

2.1 Culture of Cell Lines

All tissue culture work was carried out in a Class II biosafety cabinet. Cells were cultured under aseptic conditions and maintained in a humidified incubator at 37^{o}C in 5% CO_2 unless stated otherwise. Culture medium was pre-warmed to 37^{o}C before use and tissue culture waste was disinfected with bleach or autoclaved.

2.1.1 Passage and Maintenance of Cell Lines

The origin and specific culture conditions for each cell line used in this study is outlined in Table 2.1. All cells were maintained in appropriate culture medium supplemented with 10% (*v/v*) heat-inactivated foetal bovine serum (FBS; 77133, Labtech International Ltd Sussex, UK), 2% (*v/v*) L-glutamine (Invitrogen, California, USA) and 20µg/mL Gentamycin (Life Technologies, California, USA) unless otherwise stated. Suspension cultures were maintained in log phase growth (1-8x10^5 cells/mL) in appropriate culture medium, while adherent cell lines were passaged when they reached 90% confluency. To passage adherent cultures, the culture medium was replaced with 3mL[F25] or 5mL [F75] of pre-warmed trypsin (Sigma-Aldrich, Dorset, UK) and incubated at room temperature (RT) for 3 min. An equal volume of culture medium was subsequently added to the cells to inactivate the trypsin before the harvested cells were transferred to universal containers (UC). Following centrifugation at 270*xg* for 10 min, the pelleted cells were resuspended in 10mL of culture medium, before being enumerated and seeded at an appropriate density for the requirements of subsequent assays or the continuation of the cultures.

2.1.2 Cryopreservation and Recovery of Cryopreserved Cell Lines

For cryopreservation, confluent cultures were centrifuged at 270*xg* for 5 min and resuspended in 500µL/vial of appropriate culture medium (Table 2.1). An equal volume of freezing medium (Iscove Modified Dulbecco's Medium (IMDM; Sigma-Aldrich), supplemented with 30% (*v/v*) FBS, and 20% (*v/v*) dimethyl sulfoxide (DMSO; Sigma-Aldrich)) was added to the cell suspensions which were subsequently transferred to 1.8mL cryovials (ThermoFisher Scientific, Massachusetts, USA) in 1mL aliquots. The cryovials were

immediately transferred to a controlled refrigerator vessel or Corning CoolCell® and placed at -80^{o}C overnight to allow the cells to equilibrate. For long-term storage, cryopreserved samples were transferred to liquid nitrogen containers. The number of vials frozen was proportional to the size of the culture at the time of freezing. For example, a confluent F75 culture was frozen down into a three cryovials.

When required, cryopreserved cell lines were recovered through rapid thawing in the presence of 1mL culture medium (Table 2.1), using a 37^{o}C water bath. The thawed cells were then transferred to a UC containing 5mL culture medium and centrifuged at 270*xg* for 5 min. For expansion, the pelleted cells were resuspended in 5mL culture medium and placed in a F25 tissue culture flask (ThermoFisher Scientific) overnight. The method used to recover haematopoietic stem and progenitor cells (HSPC) is described in 2.2.2 and AML patient derived lines in 2.3.

2.1.3 Cell Enumeration

The cellularity of cultures was determined using a Neubauer chamber (Hawksley, Brighton, UK). To do this, 10µL of cell suspension was removed from a known volume of culture and placed into the counting chambers, etched with ruled grids of a known volume. This volume is equally subdivided into cuboids equivalent to 100nL, allowing sample cellularity to be determined by averaging the number of cells in each cuboid and multiplying this average by $1x10^4$. Alternatively, cell cultures were enumerated by flow cytometry using the Accuri™ C6 plus flow cytometer (2.8.1). For this, 25µL samples of the culture were transferred to 1mL flow tubes before 10µL of was acquired by flow cytometry. Debris acquired during acquisition, defined as events with a forward scatter (FSC) of $< 5x10^4$, was excluded and the remaining number of events was multiplied by 100 to give the number of cells per mL. The accuracy and reliability of flow cytometric counts was ensured by counting, in triplicate, beads seeded at a known density prior to conducting the cell enumeration analysis.

Table 2.1: Description of cell lines

Table outlining the derivation, molecular characteristics, culture conditions and source of the cell lines used in this study. *Abbreviations: α-MEM; Minimum Essential Medium Eagle- alpha modification, APL; acute promyelocytic leukaemia, ATCC; American Type Culture Collection; DMEM; Dulbecco's modified Eagle's Medium DSMZ; Leibniz Institute DSMZ German collection of Microorganisms and Cell Culture, ECACC; European Council of Authenticated Cell Cultures, IMDM;* Iscove modified Dulbecco's medium, *RPMI; Roswell Park Memorial Institute-1640 medium*

Cell Line	Derivation	FAB classification and molecular characterisation	Medium	Culture	Source
HEK293	Human embryonic kidney cells	-	DMEM	Adherent	ATCC
HEL	30-year-old male erythroleukaemia patient	FAB M6; Carries JAK2 V617F mutation	RPMI	Suspension	ECACC
HL-60	PB cells from a patient with APL	FAB M2 t(5;17)	RPMI	Suspension	ATCC
K562	53-year-old female CML patient	BCR/ABL1- t(9;22)(q34;q11)	RPMI	Suspension	ECACC
KG-1	59-year-old man with erythroleukaemia that progressed to AML at relapse	FAB M1	IMDM+20% FBS	Suspension	ATCC?
MS5	Mouse stromal cells; C3H/HeMSlc mice	-	α-MEM	Adherent	ATCC
Mv4;11	10-year-old male myelomonocytic leukaemia	FAB M5, MLL translocation t(4;11)(q21;q23) $FLT3ITD^{+}$	IMDM	Suspension	ATCC
NOMO-1	31-year-old woman with AML at second relapse	FAB M5 ; MLL translocation t(9;11)(p22;q23)	RPMI	Suspension	DSMZ
OCI AML5	PB of a 77-year-old man with AML	M4, human hyper diploid karyotype t(1;19)(p13;p13	α-MEM, 20% FBS, 10ng/mL GM-CSF	Suspension	ATCC
SKNO-1	22-year-old man with AML in second relapse	FAB M2 t(8;21)(q22;q22),	RPMI+10ng/mL GM_CSF	Suspension	DSMZ?
TF-1	35-year-old male with erythroleukaemia	FAB M6	RPMI	Suspension	ATCC
THP-1	1-year-old boy with AML at the time of relapse	FAB M5; t(9;11)(p21;q23) leading to KMT2A-MLLT3 (MLL-MLLT3; MLL-AF9) fusion gene	RPMI	Suspension	ECACC
U937	Monocytic cells derived from a 37-year-old male with histiocytic lymphoma	FAB M5, MLL translocation; t(10;11)(p12;q14)	RPMI	Suspension	ATCC

2.2 Isolation and Expansion of Haematopoietic Stem and Progenitor Cells

Primarily, normal human umbilical cord blood (CB) was collected by midwives from full-term pregnancies during elective caesarean sections in the Women's Unit at the University Hospital of Wales in Cardiff, following informed consent. Samples were collected in 50mL Falcon tubes containing 200µL heparin (1000mU, Alfa Aesar, Heysham, UK). CB samples were maintained at RT for mononuclear cell (MNC) isolation (2.2.2) which was conducted within 24 hours of sample collection. Due to restrictions that were placed on local collection, CB was also purchased from the NHS Blood and Transplant Cord Blood Banks (supplied by Bristol and London laboratories), in line with the existing ethics approval. The London centre provided fresh CB and so these samples were processed in the same manner as the samples collected locally (2.2.2). In contrast, the Bristol laboratory provided frozen buffy coats which were delivered and stored in liquid nitrogen, and when required were directly processed for HSPC isolation (2.2.3).

2.2.1 Estimation of HSPC in Umbilical Cord Blood Samples

To estimate the number of HSPC ($CD34^+$ cells) within a given CB sample, which typically represents 0.1%-1.0% of the MNC fraction, 100µL samples of CB were transferred to a UC and concurrently labelled with 5µL CD45-APC (clone H130; BioLegend®, California, US) and 10µL of either CD34-PE (clone 581; BioLegend®) or IgG1-PE (MOPC-21; BioLegend®), for 30 min at 4°C. To lyse the red blood cells, the stained samples were diluted in 5mL 10% (*v/v*) FACS lysis buffer (Becton Dickinson, New Jersey, USA) diluted in tissue culture grade H_2O for 10 min at RT. Following this, 5mL of phosphate buffered solution (PBS; Sigma-Aldrich) was added to dilute the lysis reaction. The cells were then centrifuged at 270*xg* for 10 min, where the supernatant was removed, and the cells were resuspended in 200µL RPMI medium, supplemented with 10% (*v/v*) FBS and 10U/mL heparin. The resuspended cells were transferred to 1mL flow tubes for analysis by flow cytometry which is outlined in Figure 2.1.

2.2.2 Isolation of Mononuclear Cells from Umbilical Cord Blood Samples

MNC were isolated from CB by force gradient centrifugation using Ficoll-Hypaque (Sigma-Aldrich). To achieve this, the CB samples were diluted 1:1 in Hanks buffer (IMDM supplemented with 5% (*v/v*) FBS and 1/100 heparin). 8mL aliquots of the diluted CB were then layered onto 5mL Ficoll-Plaque™ in UC. The layered CB was then centrifuged at 400*xg* for 40 min to facilitate the separation of the haematopoietic fractions. To maintain the separate layers the acceleration and deceleration curves of the centrifuge were set to 4. Following centrifugation, the interface containing the MNC, located between the Ficoll-plaque™ and the plasma layer, were collected using a Kwill filling tube, attached to a 10mL syringe. The harvested cells were washed in 20mL heparin supplemented RPMI as described above, until the supernatant was clear, to ensure the removal of any contaminating residual platelets. The washed MNC were resuspended in 10mL heparin supplemented RPMI and for enumeration, a 10µL sample was further diluted in 190µL of heparin supplemented RPMI in the presence of 1.5µL Zaponin (BeckmanCoulter, Galway, Ireland) which was used to lyse residual red blood cells. Cell enumeration was subsequently carried out using a haemocytometer as described in 2.1.3. Following this, the isolated MNC were cryopreserved in heparin supplemented RPMI and freezing medium as described in 2.1.2, at a density of c5x10^7 MNC/vial.

When required, cryopreserved MNC were thawed rapidly at 37^{o}C using a water bath, in the presence of 1mL FBS and 200µg/mL deoxyribonuclease I (DNase; Sigma-Aldrich). The concentration of the cryoprotectant (DMSO) was gradually diluted through the dropwise addition of 5mM (*w/v*) $MgCl_2$ diluted in PBS over a period of 3 min. This process was repeated twice before the cells were recovered by centrifugation at 187xg for 10 min and resuspended in MACS buffer (PBS supplemented with 0.5% (*w/v*) bovine serum albumin (BSA; Sigma-Aldrich, A4503) and 5mM $MgCl_2$) to undergo HSPC enrichment through $CD34^+$ cell isolation (2.2.3). Prior to use, MACS buffer was de-gassed by filtering through a 0.40µM filter.

2.2.3 Isolation of HSPC from Mononuclear Cell Preparations

Cryopreserved MNC were thawed as previously described (2.2.2) and enriched (>90% purity) for HSPC, based on their $CD34^+$ expression. This was performed using MiniMACS™ positive selection columns (Miltenyi Biotech Ltd, Woking, UK). For cell suspensions of up 10^7 labelled cells an MS column was used but for samples which exceeded this an LS column was used, up to a maximum of 10^8 labelled cells per column.

For enrichment, the MNC were suspended in MACS buffer (2.2.2) and incubated at 4°C for 15 min in the presence of an anti-CD34 antibody (2 x 10^9cells/mL) and the Fc receptor blocking agent (2x10^9 cells/mL) from the CD34 MicroBead Kit (Miltenyi Biotech Ltd). Following a wash in MACS buffer (2 x 10^7 cells/mL), the cells were incubated at 4°C for 15 min in the presence of anti-Fc magnetic microbeads (2x10^9 cells/mL). The cells were then washed in MACS buffer and passed through a 40µM cell strainer before being applied to a MS or LS separation column, in the presence of a magnetic field, prior to which had been equilibrated with MACS buffer. Once the cells were applied to the column, the columns were washed with a total of 2mL MACS buffer. The MS or LS column was subsequently removed from the magnetic field to allow the magnetically labelled $CD34^+$ cells to be eluted in 1mL MACS buffer. The eluted cells were counted using a haemocytometer (2.1.3) and cultured for experimental use according to 2.2.4.

2.2.4 HSPC Culture Conditions

HSPC were maintained in a basal media of IMDM supplemented with 1% (*w/v*) BSA (PM-T1726/100; BioSera, Sussex, UK), 20% (*v/v*) FBS, 4.5x10-5M β-mercaptoethanol (Sigma-Aldrich), 360µg/mL of 30% iron-saturated human transferrin (Roche Diagnostics Basel, Switzerland). This basal medium was supplemented with specific combinations of cytokines, based on the requirements of the cells (Table 2.2). Immediately after isolation, HSPC were seeded at 2x10^5 cells/mL in cytokine rich media ($36S^{high}$) to promote recovery and cell cycle progression. After 3 days of culture and lentiviral infection (2.5) the cells were maintained in $3S^{low}$G/GM (Table 2.2) to support cell differentiation, where the media was replenished every 2-3 days to maintain optimal cytokine concentrations. The HSPC were seeded at densities which were appropriate for the proliferative capacity of the culture at each time point, whereby the cultures were seeded at 0.5x10^5 cells/mL from day 3 to day 6 as the cells have the highest rate of expansion. From day 6 to 8 the cells were seeded at 2x10^5 cells/mL, and at 3x10^5 cells/mL from day 10 onwards. For immunophenotypic analysis (2.8.4) transduced cells were selectively gated for according to their GFP expression by flow cytometry (2.8), while for morphological and western blot analysis a homogenous population of transduced (GFP^+) cells were generated using fluorescently activated cell sorting (FACS; 2.10).

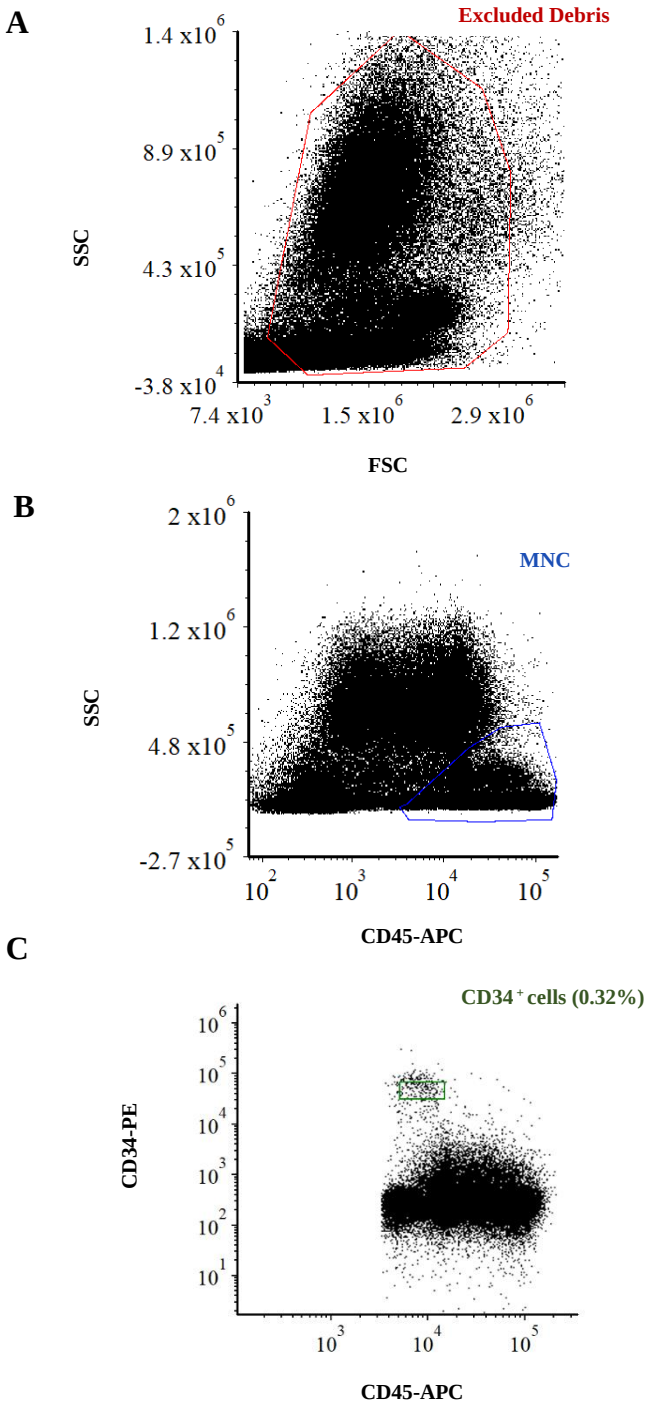

Figure 2.1: Estimation of CD34$^+$ cells in umbilical cord blood by flow cytometry

Representative bivariate density plots showing the gating strategy used for the estimation of CD34$^+$ cell content in CB samples. **(A)** Example gate used to exclude debris (events with an FSC < 5x10^4) recorded during sample acquisition (**B)** Using the "excluded debris" gate, the expression of CD45 was used to identify the mononuclear cell (MNC) population. **(C)** CD34$^+$ cells were then estimated from within the MNC gate based on the CD34 expression where an IgG1-PE antibody was used to determine the background level of staining (Table 2.12).

Table 2.2: HSPC culture medium

Table outlining the composition and concentration of the cytokines used to supplement complete IMDM for HSPC recovery and expansion as described (2.2.4). *Abbreviations; IL-3; interleukin 3, IL-6; interleukin 6; G-CSF; granulocyte-colony stimulating factor, GM-CSF; granulocyte-macrophage colony-stimulating factor, SCF; stem cell factor.*

Application	Medium	Cytokine	Concentration (ng/mL)
Cell recovery	$36S^{high}$	IL-3	50
		IL-6	25
		SCF	50
		G-CSF	25
		GM-CSF	25
		FLT-3	50
Long-term culture	$3S^{low}G/GM$	IL-3	5
		SCF	5
		G-CSF	5
		GM-CSF	5

2.3 Culture of AML Patient-Derived Cell Lines

The AML patient-derived cell lines used in this study were established from bone marrow samples collected from patients enrolled in the NCRI AML15 UK clinical trial (Table 2.3). Samples were obtained with ethical approval from the AML Clinical Trials Research Tissue Bank in the Haematology Department at Cardiff University, and cryopreserved as described in 2.1.2. Cells were thawed in 1mL of complete IMDM (2.2.4) to dilute the cryopreserving agent (DMSO), before being further diluted through the dropwise addition of 3mL complete IMDM. The cells were centrifuged at 270xg for 5 min before being resuspended in 1mL complete IMDM, supplemented with 5ng/mL IL-3, IL-6, SCF, GM-CSF, G-CSF, FLT-3, and M-CSF which were all purchased from BioLegend®.

Table 2.3: Description of AML patient derived cell lines

Table outlining the patient characteristics of the AML patient derived cell lines including the AML15 clinical trial patient ID, patient age, and gender, the FAB and karyotypic characteristic of the disease, and the survival and relapse status of each patient, fields where the clinical data is unknown is represented by a dash (-). *Abbreviations and definitions: CR; complete remission, censored; missing data, del; deletion; idem; Isoderivative chromosome, IND; investigational new drug.*

Cell line	Patient ID	Gender	Age	FAB	Karyotype	Survival	Relapse
AML92	-	-	-	-	-	-	-
AML148	15-2296	Male	46	M4	46, XY, del (9) (q13q22.3) [4]/46, XY [17]	Alive	CR
AML160	15-2422	Female	26	M4	46, XX [20]	Deceased	CR
AML162	15-2465	Male	40	-	46, XY [20]	Deceased	IND DEATH
AML164	15-2468	Female	56	M4	46, XX, del (7) (q32q36) [3]/47, idem, +14[7]	Deceased	CR
AML165	15-1121	-	-	-	-	-	-
AML172	15-2552	Female	52	M1	46, XX [20]	Alive	CENSORED
AML177	-	-	-	-	-	-	-

2.4 Virus Generation

2.4.1 Plasmid Overview

All plasmids were designed and purchased from VectorBuilder Inc., California, USA which were delivered in the form of chemically competent *Escherichia coli (E. coli*) glycerol stocks and maintained at -80^{o}C for long-term storage unless otherwise stated.

2.4.1.1 Lentiviral Overexpression Constructs

To force PKCε overexpression in AML cell lines and HSPC, a PKCε_GFP lentiviral vector was designed using VectorBuilder Inc. (Figure 2.2A). Briefly, the PRKCE gene (NM0-05400.3) was inserted into the open reading frame (ORF) of the plasmid, under the control of the human eukaryotic translation elongation factor 1 α1 (EF1A) promoter. Alongside this, a dual enhanced green fluorescent protein (EGFP) and puromycin resistance (puro^{R}) genes linked by a T2A sequence, were included as selectable markers, and placed under the control of a human cytomegalovirus (CMV) promoter. For all experiments an empty ORF GFP vector was used as a control (Figure 2.2B).

2.4.1.2 shRNA Constructs

The shRNA constructs used to promote targeted gene silencing in AML cell lines and HSPC are outlined in Table 2.4, and were identified using the Broad Institute Genetic Perturbation Platform (Yang, *et al.*, 2011). Constructs were selected based on their adjusted score; an indicator of the knockdown efficiency and gene specificity of each shRNA construct, while a shRNA sequence with no mammalian targets was used as a control throughout. Multiple shRNA candidate sequences, targeting a range of regions across the target mRNA sequence were selected and subsequently inserted into pLKO.1 U6-based shRNA expression vectors (Figure 2.3). For these constructs, dual EGFP and puromycin resistance or tag blue fluorescence protein (tagBFP) and neomycin resistance genes linked by a T2A sequence were used as selectable markers.

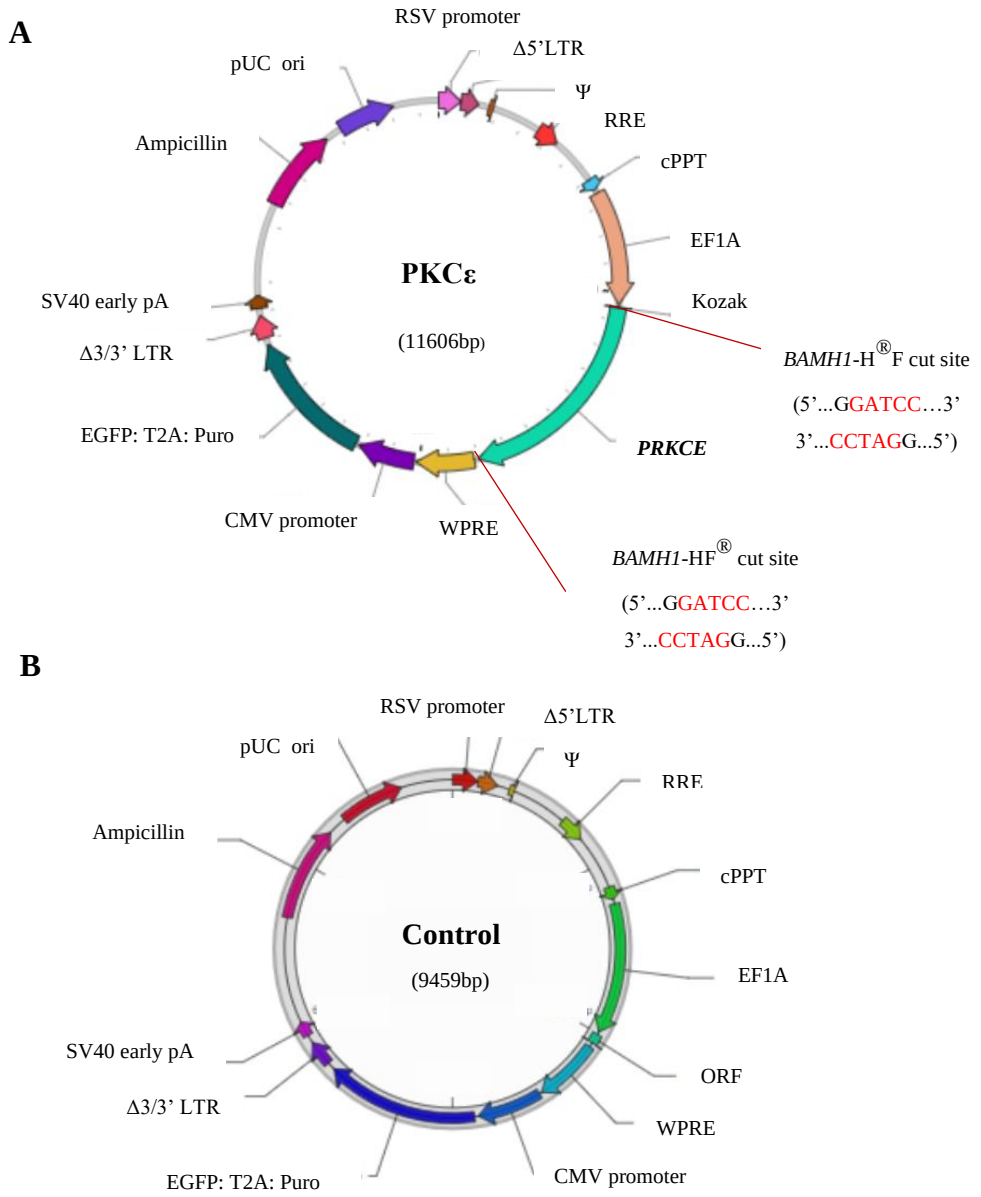

Figure 2.2: Lentiviral overexpression plasmid maps

Plasmid maps of the (**A**) PKCε overexpression construct (PKCε_GFP_Puro^{R}) and (**B**) control (empty GFP construct_Puro^{R}) which were generated by VectorBuilder (2.4.1.1). *Abbreviations; U6; RNA polymerase III U6 promoter, cPPT; central polypurine tract, Ampicillin; ampicillin resistance gene, pUC ori; pUC origin of replication, RRE; Rev response element, RSV promoter; Rous sarcoma virus promoter, Δ5' LTR; truncated HIV-1 5' long terminal repeat, Ψ; HIV-1 packaging signal, EGFP:T2A:Puro; EGFP and Puromycin linked by T2A, WPRE; woodchuck hepatitis virus post-transcriptional regulatory element, ΔU3/3' LTR; truncated HIV-1 3'long terminal repeat, SV40 early pA; simian virus 40 early polyadenylation signal; PRKCE; protein kinase C epsilon gene (NCBI NM0-05400.3*)

Table 2.4: Table of shRNA constructs

Table outlining the shRNA constructs used in cell line and primary cell experiments. *Abbreviations; 3UTR; 3-prime untranslated region, 5UTR; 5-prime untranslated region, BFP; blue fluorescent protein, CDS; coding sequence; GFP; green fluorescent protein, N/A; not applicable.*

shRNA Target	Construct Number	Clone ID	Target Sequence (5'→ 3')	Match Region	Adjusted Score	Fluorescent Marker	Antibiotic resistance
Control[1]	214		CCGGCAACAAGATGAAGAGCACCAACTCGAGTTGG TGCTCTTCATCTTGTTGTTTTT	N/A	N/A	N/A	Puromycin
	497		CCGGCAACAAGATGAAGAGCACCAACTCGAGTTGG TGCTCTTCATCTTGTTGTTTTT	N/A	-N/A	GFP	Puromycin
	531		CCGGCAACAAGATGAAGAGCACCAACTCGAGTTGG TGCTCTTCATCTTGTTGTTTTT	N/A	N/A	BFP	Geneticin™
PKCε	476	TRNC0000000846	CCACAAGTTCGGTATCCACAA	3UTR, CDS	5.67	N/A	Puromycin
	477	TRNC0000000845	CCCTTCAAACCACGCATTAAA	CDS	21.0	N/A	Puromycin
	478	TRNC0000219725	ATATGCTGTGAAGGTCTTAAA	3UTR, CDS	9.24	N/A	Puromycin
	479	TRNC0000219726	CTGCATGTTCAGGCATATTAT	3UTR	10.5	N/A	Puromycin
	480	TRNC0000195163	CATCCTAAGTTCCTAGCATAA	3UTR	7.56	N/A	Puromycin
	485	TRNC0000000845	CCCTTCAAACCACGCATTAAA	CDS	21.0	GFP	Puromycin
	486	TRNC0000000846	CCACAAGTTCGGTATCCACAA	3UTR, CDS	5.67	GFP	Puromycin

PKCθ	533	TRCN0000195559	CATCCTGATTGGGCATGAAAT	3UTR	9.24	BFP	Geneticin™
	535	TRCN0000197035	GCCAACCTTTGTGGCATAAAC	CDS	7.90	BFP	Geneticin™
	537	TRCN0000199654	GCGAGGCTGTTAACCCTTACT	5UTR	6.93	BFP	Geneticin™

[1] DNA sequence with no mammalian target

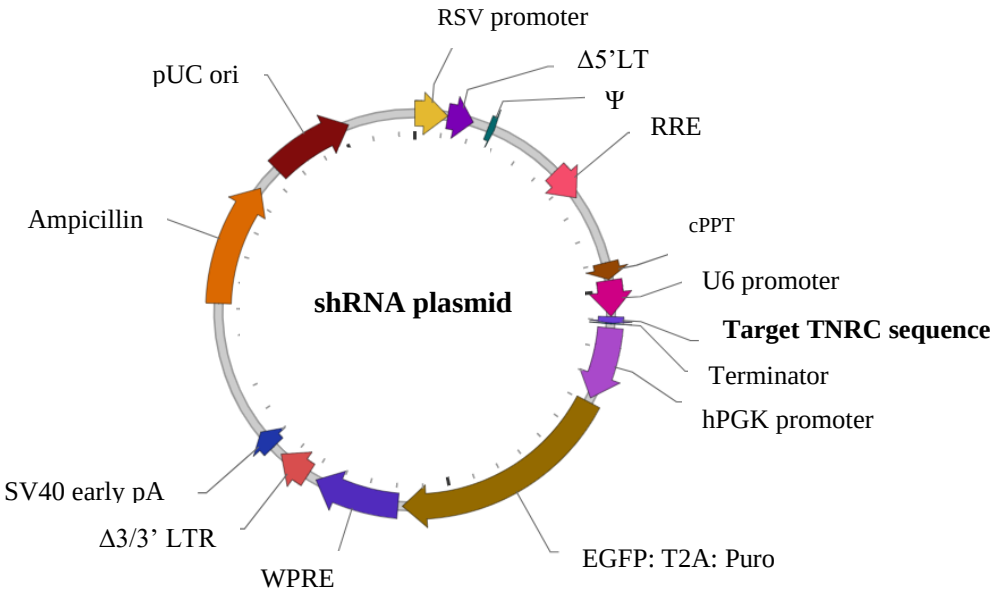

Figure 2.3: Example shRNA plasmid map

Example shRNA pHIV-EGFP: T2A: Puro-U6 (VectorBuilder Inc) plasmid map (2.4.1.2). *Abbreviations; U6; RNA polymerase III U6 promoter, cPPT; central polypurine tract, hPGK promoter; human phosphoglycerate kinase eukaryotic promoter, Ampicillin; ampicillin resistance gene, pUC ori; pUC origin of replication, RRE; Rev response element, RSV promoter; Rous sarcoma virus enhancer/promoter, Δ5' LTR; truncated HIV-1 5' long terminal repeat, Ψ; HIV-1 packaging signal, Terminator; Pol III transcription terminator, hPGK promoter; Human Phosphoglycerate kinase 1 promoter, EGFP:T2A:Puro; EGFP and Puro linked by T2A, WPRE; Woodchuck hepatitis virus posttranscriptional regulatory element, ΔU3/3' LTR; Truncated HIV-1 3' long terminal repeat, SV40 early pA; Simian virus 40 Early polyadenylation signal; target TNCR sequence* (as outlined in Table 2.4).

2.4.1.3 CRISPR/Cas9 gRNA Constructs

Guide RNA (gRNA) sequences were designed using CHOPCHOP™ v2 with the UCSC™ *homo sapiens* genome browser (hg38/GRCh38) where the gRNA sequences were ranked according to their Doench *et al.* 2016 efficiency score (Doench, *et al.*, 2016). From this screen, three PKCε-targeted gRNA with a high efficiency scores, low self-complementarity and no known off-target sites were selected (Table 2.5) and incorporated into CRISPR/*Cas9* plasmids (Figure 2.4) upstream of the human *Cas9* gene linked to a *puromycin resistance* gene by a T2A sequence was used as a selectable marker.

2.4.2 DNA Isolation and Quantification

Bacterial cells were plated on Luria Broth Agar (Sigma-Aldrich) plates supplemented with 100µg/mL ampicillin (Sigma-Aldrich) and incubated overnight at 37ºC. Single colonies were selected and used to inoculate 5mL ampicillin (100µg/mL) supplemented Luria Broth (Sigma-Aldrich) and were subsequently incubated for 8 hours at 37ºC in an orbital shaker, rotating at 225 revolutions per minute (rpm). These cultures were subsequently diluted 1:1000 with ampicillin-supplemented medium and returned to the orbital incubator overnight. The bacterial suspension was harvested and centrifuged at 6,000*xg* for 15 min at 4ºC before high-purity plasmid DNA was isolated from the bacteria using the hiSpeed Maxiprep DNA Isolation Kit (Qiagen, Crawley, UK), according to the manufacturer's instructions and was eluted in the kits elution buffer apart from DNA isolated for sequencing (2.4.4.2). The isolated DNA was eluted in distilled water (dH_2O) before the concentration, purity, and quality of the isolated plasmid DNA was assessed using a Nanodrop spectrophotometer (ThermoFisher Scientific) according to the manufacturer's instructions. Briefly, DNA concentration was estimated by measuring the absorbance at 260nm, however RNA can also absorb UV light at this wavelength, therefore the purity of the isolated DNA was assessed by determining the A_{260}/A_{280} ratio, where a ratio of between 1.7 and 2.0 is considered good quality.

2.4.3 Generation of Glycerol Stocks

Following culture in Luria Broth (2.4.2) 850µL bacterial suspension was combined with 150µL glycerol and transferred to a 1.8mL cryovial. The glycerol stocks were immediately transferred to -80ºC where they were kept for long-term storage.

Table 2.5: Table of CRISPR constructs

Table outlining the target site, gRNA sequences, predicted off-target effects and efficiency score of the PKCε-targeted constructs incorporated into the CRISPR/*Cas9* plasmids (Figure 2.4). Efficiency score aims to predict the strength of cleavage using the Doench *et al.* scoring system (Doench, *et al.*, 2016), normalised to a 0-1 interval.

Name	Chromosome Location	Exon	Target Sequence (5'→ 3')	Off Target Cuts	Efficiency Score
Control[1]	-	-	-	-	-
522	chr2:46001423	7	CCGTCGATGTGAGACCAACGTGG	0	0.75
524	chr2:45984589	6	AATGTGGACGACTCGCGATCGG	0	0.59
526	chr2:46184786	15	GTTCGGTATCCACAACTACAAGG	0	0.57

[1] Control gRNA contains the sequence (GCACTACCAGAGCTAACTCA) with no human or murine gene target.

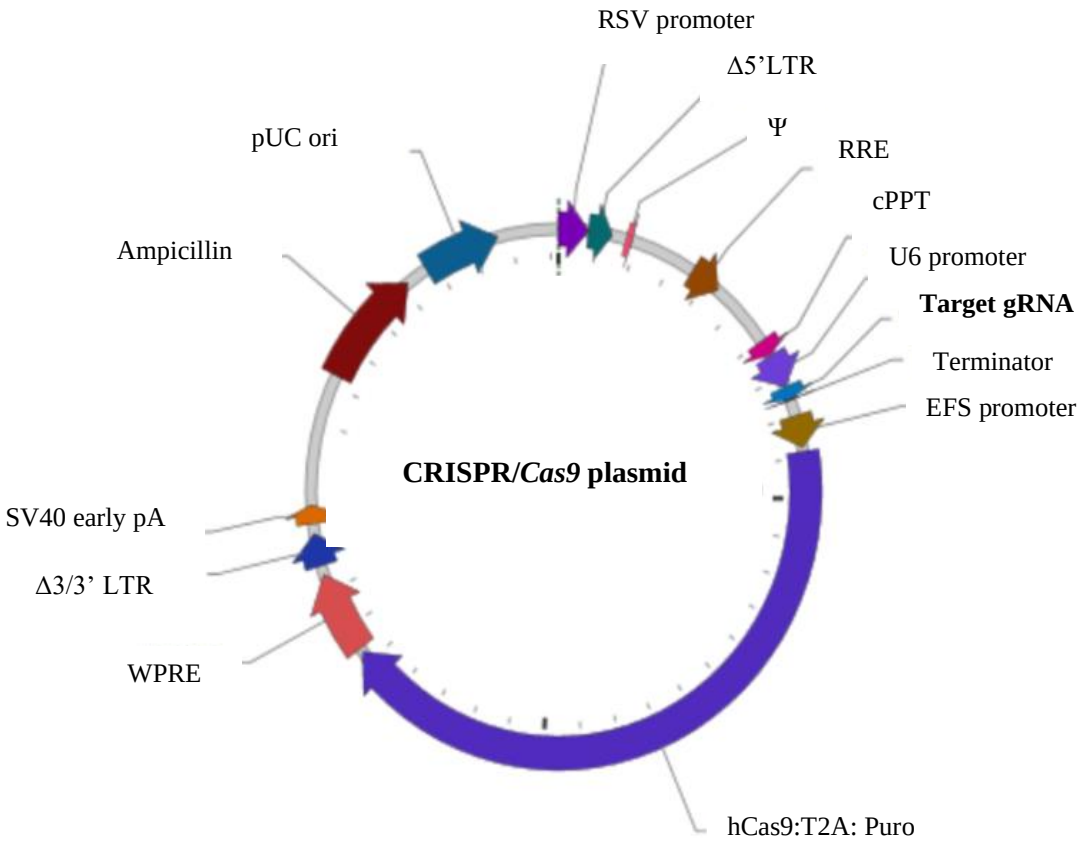

Figure 2.4: Example CRISPR/ *Cas9* plasmid map

Example CRISPR/Cas9 (VectorBuilder Inc) plasmid map (2.4.1.3). Abbreviations; U6 promoter; RNA polymerase III U6 promoter, cPPT; central polypurine tract, Ampicillin; ampicillin resistance gene, pUC ori; pUC origin of replication, RRE; Rev response element, RSV promoter; Rous sarcoma virus enhancer/promoter, Δ5' LTR; truncated HIV-1 5' long terminal repeat, Ψ; HIV-1 packaging signal, Terminator; Pol III transcription terminator, hCas9:T2A:Puro; human Ca9 and puromycin resistance gene linked by T2A, WPRE; Woodchuck hepatitis virus posttranscriptional regulatory element, ΔU3/3' LTR; Truncated HIV-1 3' long terminal repeat, SV40 early pA; Simian virus 40 Early polyadenylation signal; target gRNA sequence (outlined in Table 2.5).

2.4.4 Plasmid Validation

2.4.4.1 Restriction Enzyme Digests

A restriction enzyme digest was carried out on the PKCε plasmid complementary DNA (cDNA) to validate the presence of the *PRKCE* gene within the overexpression construct (2.4.1.1). To do this, plasmid DNA was incubated with the BamHI-high fidelity® (HF) restriction enzyme (New England Biolabs (NEB), Massachusetts, USA) for 30 min at 37ºC according to the manufacturer's instructions. The digest reactions were then separated by agarose gel electrophoresis) using a 0.8% (*w/v*) agarose gel, diluted in 1x Tris-borate-EDTA; TBE, (BioLine, Memphis, USA) containing 1µL PeqGreen (PeqLab, Lutterworth, UK). Samples were loaded with 2 µL loading buffer (NEB) and electrophoresed alongside 1kb DNA Ladder (NEB) to indicate the size of the restriction enzyme digest reaction products. Gels underwent electrophoresis at 80 volts for 1-2 hours and were documented using a UV box. An example restriction enzyme digest is outlined in Table 2.6.

Table 2.6: Table of an example restriction enzyme digest reaction

Table outlining the components and volumes of the reagents used in a typical restriction enzyme digest described in 2.4.4.1.

Reaction Components	**Volume (µL)**
Plasmid DNA	2
CutSmart® Buffer (x10)	1
BamHI (HF®)	1
Distilled water	16
Total Reaction Volume	**20**

2.4.4.2 Sanger Sequencing

Sanger sequencing was used to validate the *PRKCE* gene sequence contained within the PKCε overexpression plasmid cDNA (2.4.1.1). Sequence specific primers (Table 2.7) were purchased from Eurofins Scientific, Luxembourg and hydrated in dH_2O according to the manufacturer's instructions. For sequencing, 50ng of plasmid cDNA, eluted in nuclease-free H_2O, was made up to a volume of 15µL and combined with 10µM of the primer, giving a final reaction volume of 17µL. The pre-mixed sample reactions were sent to Eurofins Scientific for sequencing. The alignment of the *PRKCE* gene sequence generated from the Sanger sequencing was then compared with the corresponding sequence obtained from the NCBI database (NM_005400.3) using Clustal Omega Multiple Sequence Alignment software (EMBL-EBI; Madeira, *et al.*, 2019).

Table 2.7: Primers used to sequence the PKCε lentiviral overexpression vector

Table outlining the primer sequence (5' to 3'), sense and relative binding position within the *PRKCE* sequence for the three primers used for Sanger sequencing (2.4.4.2) and the evaluation of the sequence of the *PRKCE* gene inserted with in the PKCε-GFP overexpression (2.4.1.1). All primers were purchased from Eurofins Scientific and prepared as described in 2.4.4.2. *Abbreviations; bp; base pair.*

Description	**Binding position (bp)**	**Sense**	**Sequence (5'→3')**
*PRKCE*_Start	4098	Forward	GGCGTTACCCCAGACAAAAT
*PRKCE*_Middle	4518	Forward	GATGATGACGTGGACTG
*PRKCE*_End	5481	Reverse	CGTAAAAGGAGCAACATAGT

2.4.5 Transfection of HEK293 Cells

To generate assembled lentiviral particles, $5x10^6$ [F25] or $15x10^6$ [F75] HEK293 cells (Table 2.1) were seeded into tissue culture treated flasks, pre-coated with poly-D-lysine (Trevigen®, Maryland, USA) for 30 min at RT. Following seeding, the HEK293 cells were incubated overnight at 37°C to allow monolayer formation. The next day, 2.2µg [F25] or 6.6µg [F75] plasmid cDNA (transfer vector) was transfected into HEK293T cells using the Lipofectamine 3000™ transfection kit (Life Technologies) according to the manufacturer's instructions. Briefly, Opti-MEM 1 (Gibco, Paisley, UK) was equilibrated at RT before lipid-DNA complexes were generated through the combining the Lipofectamine transfection reagents and the transfer, packaging, and envelope plasmids (reactions A and B; Table 2.8). These reactions were prepared in separate UC and when combined were incubated at RT for 15 min, before being introduced to the cell cultures. During this incubation, the volume of DMEM medium within the tissue culture flasks was reduced to 3mL [F25] or 6mL [F75]. The primed lipid-DNA mixture (reaction A+B) was carefully added to the flasks and incubated for 6 hours at 37°C, after which the media was replaced with 3mL [F25] or 6mL [F75] DMEM.

The virus-containing medium was harvested at 24-hours and 48-hours post-transfection to a UC. Following the 24-hour harvest, the medium in the flasks was replenished with fresh DMEM (2.5mL [F25] and 7.5mL [F75]), while the harvested viral supernatant was stored at 4°C overnight. Once both viral harvests were completed and combined in the UC, the viral supernatant was centrifuged at 270*xg* for 10 min to pellet any contaminating cells. The supernatant was then divided into 1mL aliquots in 1.8mL cryovials and snap frozen in liquid nitrogen. For long-term storage, the aliquots were stored at -80°C until required.

Table 2.8: Lipofectamine reaction

Table outlining an example Lipofectamine reaction used for the transfection of HEK293 cells and the generation of lentiviral particles (2.4.5). All reaction quantities are based upon the requirement of 1xF25. For an F75 flask the amount of the reagents was increased by 3-fold to account for the larger surface area of the flask and number of cells seeded.

Reagents	Reaction A	Reaction B
Optimem™	677µL	675µL
pMD.2G envelope plasmid	2.2µg	-
psPAX2 packaging plasmid	4.0µg	-
Transfer vector	2.2µg	-
P3000 reagent	16µL	-
Lipofectamine 3000	-	19µL

2.4.6 Virus Titration

The titre of the generated viral particles was evaluated in K562 cells. For this, non-tissue culture treated 96 well plates were coated with RetroNectin® (30µg/mL; TAKARA Biotech Inc., Shiga, Japan) for 2 hours at RT before being replaced with 1% (*w/v*) BSA which was incubated for 30 min at RT. K562 cells were subsequently seeded at $1x10^5$ cells/mL in complete RPMI before 50µL viral supernatant was added and incubated with the cells for 48 hours. Following this, the cells were washed and resuspended in RPMI for analysis by flow cytometry where the proportion of cells expressing the fluorescent selectable marker of the constructs was assessed (2.4.1). Each lentiviral supernatant was plated in duplicate and assayed alongside a lentiviral supernatant of known concentration as a standard, allowing the titre of the lentiviral particles of interest to be quantified.

2.5 Generation and Selection of Lentiviral Transduced Cells

2.5.1 Gene Transduction

The lentiviral transduction protocols used in this project were based on the protocol outlined in Tonks, *et al.*, 2005. For overexpression lentiviral infection of AML cell lines, non-tissue culture treated plates were coated with 500µL RetroNectin® (30µg/mL; TAKARA) overnight at 4°C. The following day, the RetroNectin® was removed and immediately replaced with 250µL 1% (*w/v*) BSA (Sigma-Aldrich) for 30 min at RT, before this was replaced with 1mL lentivirus- containing medium. The plates were centrifuged at 2000*xg* for 1 hour 30 min before the supernatant was removed and replaced with an appropriate number of cells for gene transduction, typically $2\text{-}3x10^5$ cells/well. Following an overnight incubation, the cells were harvested and resuspended in 1mL fresh culture medium. For HSPC infection, the cells were harvested after 24 hours and a second viral coating was performed.

For shRNA and gRNA transduction in AML cell lines, pre-coating of the wells with lentiviral particles was unnecessary given the much higher titre of virus generated from these constructs. Instead, $2x10^5\text{-}6x10^5$ cells were resuspended in 1mL of media and seeded in a tissue culture treated 24 well plate and incubated with 300µL of virus-containing media for 24 hours. The next day, the cells were harvested into 1mL culture medium. In HSPC, knockdown lentiviral infection was carried out using the RetroNectin® pre-coating method (Tonks, *et al.*,

2005), however, in this case a second viral coating step was not performed. Instead, the cells were incubated with the lentiviral particles for 2 days, before being harvested on day 3 of culture. Transduction efficiencies were evaluated through the expression of the fluorescent selectable markers (2.4.1) using flow cytometry. After successful gene transduction had been confirmed, the cells were subjected to antibiotic selection (2.5.2) to enrich the cultures for transduced cells. For cells which were transduced with constructs without a fluorescent selectable marker (2.4.1), successful gene transduction could not be determined through this methodology and instead these cells immediately underwent antibiotic selection.

2.5.2 Selection of Transduced Cells

Transduced cells were selected with the appropriate antibiotic (2.4.1) whereby puromycin (Sigma-Aldrich; P8833) was used at 10µg/mL and Geneticin™ (a neomycin analogue, Gibco; 10131035) was used at 1000µg/mL, until parental un-transduced cultures were no longer viable, and a pure population of transduced cells was generated. Following selection, the transduced cell lines were maintained in normal growth medium until confluency was achieved, whereby aliquots were cryopreserved (2.1.2) and total protein lysates were taken (2.7.1.1) to validate ectopic protein expression by western blot analysis (2.7).

2.6 Morphological Analysis

For morphological analysis, cells were seeded at $0.3x10^5$ cells in 100µL of appropriate culture medium (2.1.1) before being loaded onto a cytospin assembly, consisting of a metal clasp, a glass slide, blotting paper and a plastic funnel. The cytospin assemblies were then centrifuged at 800 rpm for 5 min using a Shandon Cytospin3 (ThermoFisher) to separate the cells and deposit them in a monolayer on the slides whilst preserving cellular integrity and morphology. Following centrifugation, the glass slides were left to air dry before being stained with a combination of May-Grunwald and Giemsa stains. Staining was carried out in the Immunophenotyping Laboratory at the University Hospital of Wales, courtesy of Stephen Couzens. The stained air-dried slides were imaged at 20x magnification using the Zeiss Axioscan Z1 slide scanner which was accessed through Cardiff University's Central Biotechnology Services. Once documented, the images were analysed using the Zeiss Zen lite imaging software v2.6 (Blue Edition).

2.7 Western Blotting

2.7.1 Generation of Protein Lysates

2.7.1.1 Total Protein Lysates

To generate total protein lysates, the required number of cells (typically $1x10^6$) were harvested to UC and centrifuged at 270*xg* for 5 min. Following centrifugation, the supernatant was removed, and the pelleted cells were washed in 10mL tris-buffered saline (TBS) consisting of 50mM Tris (Sigma-Aldrich), which was dissolved in dH_2O and adjusted to pH 7.6 with HCl, and 150mM NaCl (Sigma-Aldrich) dissolved in dH_2O. Following a second centrifugation at 270*xg* for 10 min, the supernatant was once again removed, and the pelleted cells were snap frozen in liquid nitrogen before being stored at -80°C ready for protein extraction. When required, the frozen cell pellets were thawed on ice in the presence of 1µg/mL DNase for up to 5 min, before being resuspended in 50µL of homogenisation buffer (Table 2.9). The cells were incubated with the homogenisation buffer for 30 min on ice, and vortexed at regular intervals. Following this incubation, the cell suspension was transferred to ice cold 1.8mL Eppendorf tubes (Eppendorf, Stevenage, UK) and centrifuged for 5 min at 16,000*xg* at 4°C using a Biofuge fresco Heraeus centrifuge (ThermoFisher Scientific). The supernatant was then collected and transferred to a new pre-chilled 1.8mL Eppendorf, before lysates were stored at -80°C until required.

2.7.1.2 Cytosolic Protein Lysates

To generate cytosolic protein lysates, between $3x10^6$ and $5x10^6$ cells were fractionated using a nuclear/cytosolic fractionation kit (BioVision Inc., California, USA) according to the manufacturers' instructions. The cells were washed with 20mL TBS and centrifuged at 270*xg* for 10 min, before being resuspended in 200µL cytosolic extraction buffer (CEB)-A (cytosolic extraction buffer), containing 1mM dithiothreitol (DTT) and 1x protease inhibitor cocktail (PIC). This cell suspension was transferred to pre-chilled 1.5mL Eppendorf tubes, vortexed for 15 seconds, and incubated on ice for 10 min. Following this incubation, 11µL CEB-B was added to the cell suspension before a 5 sec vortex and 1 min incubation on ice. After this process was repeated twice, the samples were centrifuged at 16,000*xg* for 8 min at 4°C using a microcentrifuge and the supernatant, which represents the cytosolic fraction, was transferred

to separate pre-chilled Eppendorf tubes. The cytosolic lysates were quantified using a Bradford assay as described in 2.7.2 and stored at -80^{o}C until required.

2.7.2 Protein Quantification using the Bradford Assay

The quantity of protein contained within the generated lysates (2.7.1) were determined using a Bradford Assay. Lysates were diluted 1:100 in dH_2O before 10µL of the diluted lysates were plated in duplicate in a flat-bottomed 96-well plate, alongside 10µL protein standards (Sigma-Aldrich; 0-100µg/mL, diluted in dH_2O), which were plated in duplicate. Merck® Bradford's reagent (Sigma-Aldrich; B6916) was diluted 1:1 with dH_2O and 190µL of the diluted reagent was added to each well. The plate was then incubated at RT for 5 min, protected from light, before being analysed at 595nm using a Chameleon Luminescence Plate Reader (Hidex, Turku, Finland). The protein standards were used to generate a standard curve from which the concentration of protein within the cell lysates could be determined. The variation between the duplicate absorbance measurements for the protein standards was limited to a co-efficient variant of 5%, whilst a co-efficient variant of 10% was deemed acceptable for the samples.

Table 2.9: Details of the Homogenisation Buffer used for Total Lysate Generation

Table outlining the concentration of the components which make up the homogenisation used in the generation of total protein lysates (2.7.1.1). *Abbreviations: BME; 2-mercaptoethanol, EDTA; ethylenediaminetetraacetic acid, EGTA; ethylene glycol-bis (β-aminoethyl ether)-N-N-N'-N'-tetra acetic acid, HEPES; 4-(2-hydroyethyl)-1-piperazineethanesulfonic acid.*

Buffer	Composition	Concentration	Supplier
Homogenisation Buffer	Sucrose	0.25M	Sigma-Aldrich[1]
	HEPES-KOH pH7.2	10mM	Gibco[2]
	Magnesium Acetate	1mM	Sigma-Aldrich[1]
	EDTA	0.5mM	Sigma-Aldrich[1]
	EGTA	0.5mM	Sigma-Aldrich[1]
	BME	12.6M	Sigma-Aldrich[1]
	Distilled water	-	Sigma-Aldrich[1]
	EDTA free- protease inhibitor	1 tablet	Roche Diagnostics[3]
	Tween x-100	1% (*v/v*)	Sigma-Aldrich[1]

[1]Sigma-Aldrich, Dorset, UK, [2] Gibco Paisley, UK, [3] Roche Diagnostics, Basel, Switzerland.

2.7.3 Protein Electrophoresis

All reagents and equipment were purchased from Invitrogen and were prepared according to the manufacturer's instructions, unless otherwise stated. Prior to electrophoresis, cell lysates were denatured in a 70^{o}C water bath for 10 min in the presence of 4x NuPAGE™ lithium dodecyl sulphate (LDS) sample buffer (NP0007), 10x NuPAGE™ sample reducing agent (NP0009) and dH_2O. Protein gel electrophoresis was carried out using the NuPAGE™ XCell SureLock™ Mini-Cell and XCell II blot module system (EI0002). Before the samples were loaded, 200mL of 1x NuPAGE™ MOPS SDS running buffer (NP0001) supplemented with 500µL NuPAGE™ antioxidant (NP0005) was added to the central compartment of the gel tank containing the pre-cast polyacrylamide NuPAGE™ Novex 4-12% Bis-Tris, 1.0mm gels (12 well gels; NP0322). Between 10µg and 20µg of protein, in a maximum volume of 20µL per lane was loaded onto the gel. Samples were electrophoresed alongside 10µL prepared MagicMarker XP protein ladder (LC5602) which was diluted with 4x LDS sample buffer and dH_2O prior to loading. After loading the samples, the outer chamber of the gel tank was filled with 600mL 1x MOPS buffer before electrophoresis was conducted at 200 volts for 50 min.

2.7.4 Immunoblotting

During electrophoresis, 1x NuPAGE™ Transfer Buffer (NP00061) supplemented with 1mL NuPAGE™ antioxidant and 10% (*v/v*) methanol was prepared. The blotting pads, filter paper and nitrocellulose membrane 0.45µm pore size (LC2001) were submerged in the transfer buffer until required for immunoblotting. Following electrophoresis, the pre-cast gels were removed from their cassettes and sandwiched between the pre-soaked nitrocellulose membrane and pieces of filter paper. The gel-membrane assembly was subsequently placed within the transfer chamber, with blotting pads placed either side (Figure 2.5). The transfer cell was filled with transfer buffer until the sponges were completely submerged before the outer chamber was filled with 600mL dH_2O, and proteins were electroblotted for 1 hour at 30 volts. For the detection of larger proteins (>100kDa) Invitrolon™ polyvinylidene difluoride (PVDF) membranes (Life Technologies) were used. PVDF membranes were hydrated in methanol, opposed to transfer buffer, for 5 min prior to being place on the gel.

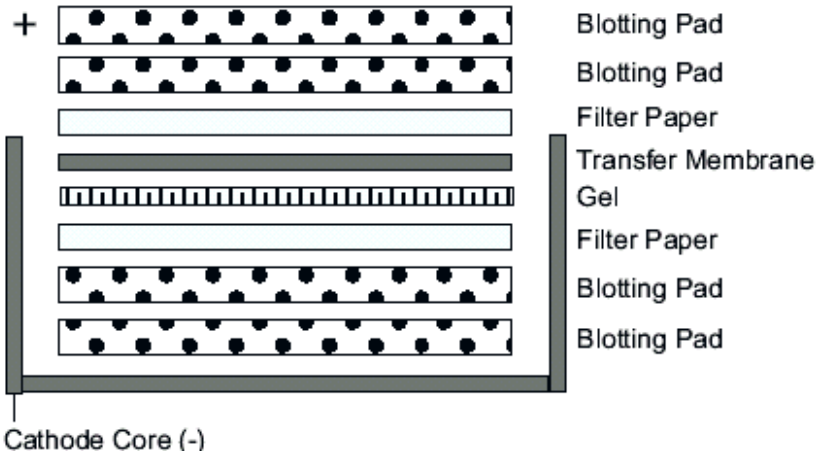

Figure 2.5: Schematic representation of the transfer chamber for immunoblotting

Schematic diagram showing the position of the gel and transfer membrane within the blotting module prior to immunoblotting. As described in 2.7.4, the pre-soaked nitrocellulose membrane was placed immediately against the gel and sandwiched between soaked pieces of filter paper. Any trapped air bubbles were removed, and the gel-membrane assembly was situated in the blotting module between pre-soaked blotting pads, with the gel closest to the cathode core.

Following transfer, residual transfer buffer was removed by washing the immunoblotted membranes twice with dH_2O for 5 min on an orbital shaker. The washed membranes were then incubated with 0.1% (*v/v*) Ponceau S (P7767; Sigma-Aldrich) for 30 sec to visualise the successful transfer of proteins from the gel to the membrane, and facilitate the division of membranes, if required. The Ponceau S stain was removed using dH_2O before the membranes were blocked for 45 min at RT in 2.5% (*w/v*) powdered milk, diluted in TBS supplemented with 0.1% (*v/v*) Tween-20 (Sigma-Aldrich; TBS-T). Blocked membranes were washed with TBS-T at RT for 30 min, before being incubated with the primary antibody (Table 2.10) in 2.5% (*w/v*) powdered milk diluted in TBS-T overnight at 4^oC. The following day, the primary antibody solution was decanted, and the membranes were washed with TBS-T for 30 min at RT. The washed membranes were then incubated with the appropriate anti-rabbit or anti-mouse horseradish peroxidase (HRP) conjugated secondary antibody (Table 2.10), diluted in 1% (*w/v*) milk for 1 hour at RT. Following imaging, membranes were briefly washed with TBS-T to remove residual ECL™ reagents (2.7.5) and re-probed with antibodies against Glyceraldehyde 3-phosphate dehydrogenase (GAPDH) which was used as a marker of protein loading (Table 2.10) for 1 hour at RT. The antibodies were diluted in 2.5% (*w/v*) milk and the membranes were protected from light throughout this incubation period. After a brief wash, DyLight conjugated antibodies (Table 2.10) were imaged directly (2.7.5), while the HRP antibodies were incubated with an appropriate secondary antibody (Table 2.10) as described above.

2.7.5 Immunodetection and Quantification

DyLight conjugated antibodies (Table 2.10) were imaged directly after probing using an Odyssey® Fc Imaging System (LI-COR Biosciences, Nebraska, USA) and an exposure time of 30 sec. In contrast, HRP-conjugated antibodies were detected through chemiluminescent reactions which were performed using either the Amersham™ ECL™ Prime (GE HealthCare Life Sciences) or Amersham™ ECL™ Select substrates (GE HealthCare Life Sciences), according to the manufacturers' instructions. Briefly, the Amersham™ ECL™ Luminol Enhancer solution (solution A) and Amersham™ ECL™ peroxide solution (solution B) were combined in equal volumes. Excess TBS-T was removed from the membrane and a total of 4mL chemiluminescent reaction (solution A+B) per full size membrane (10cm x 10cm) was used to saturate the membrane. This was left to develop, protected from light, for 5 min at RT

before the excess substrate was removed with filter paper. Membranes were sandwiched between two sheets of transparent acetate for imaging. Membranes probed with HRP-conjugated antibodies (Table 2.10) were documented using a LAS-3000 digital imager (FUJIFILM UK Ltd, Bedfordshire, UK), using an exposure time of up to 30 minutes.

The band intensity on documented membranes were semi-quantitatively measured by densitometric analysis using ImageJ (Fiji; v. 2.0.0.71), unless otherwise stated. To do this, a region of interest (ROI) was constructed around a specific band. From this, a histogram of peak intensity was generated, and a baseline of background intensity was set from the area surrounding the band within the ROI. The area under the curve was then calculated to give an arbitrary intensity value. The band intensities of the protein of interest were normalised to the band intensity of the loading control for each sample. Expression values are displayed relative to the control cell lines outlined in the figure legends.

Table 2.10: Table of antibodies for western blot analysis

Table outlining the supplier, clone, conjugate, and dilution of the antibodies used in western blot analysis as described in 2.7.4. Primary antibodies were stored at -20^{o}C and secondary antibodies at 4^{o}C. *Abbreviations: HRP; horseradish peroxidase*.

	Manufacturer	**Clone**	**Species**	**Conjugate**	**Dilution**
Primary Antibodies					
P-GP	Insight Biotchnology[1]	C219	Mouse	-	1:5000
PKCε	Cell Signaling Technologies[2]	22B10	Rabbit	-	1:1000-1:5000
PKCθ	Cell Signaling Technologies[2]	E1I7Y	Rabbit	-	1:5000
Secondary Antibodies					
Anti-mouse	GE HealthCare Life Scientific[3]	Polyclonal	Donkey	HRP	1:5000
Anti-rabbit	GE HealthCare Life Scientific[3]	Polyclonal	Donkey	HRP	1:5000
Loading Controls					
GAPDH	ThermoFisher Scientific[4]	GA1R	Mouse	DyLight 680	1:5000

[1]Insight Biotechnology, Middlesex, UK; [2]Cell Signaling Technologies Technology, Massachusetts, USA; [3] GE HealthCare Life Sciences, Chicago, USA, [4] ThermoFisher Scientific, Massachusetts, USA.

2.8 Flow Cytometry

2.8.1 Equipment and Analysis

Samples were analysed by flow cytometry using the Accuri™ C6 plus flow cytometer (Becton Dickinson) or the FACSCanto™ II (Becton Dickinson) flow cytometer. The technical specifications of these flow cytometers are outlined in Table 2.11. All flow cytometry data was analysed using FCS Express® v6 (De Novo Software, Pasadena, USA).

Table 2.11: Technical specifications of the Accuri™ C6 Plus and FACSCanto™II cytometers

Table outlining the instrument specifications of the Accuri™ C6 plus and FACSCanto™II flow cytometers which were used to assess the phenotypic impacts of modulating PKCε expression in HSPC and AML cells.

	Accuri™ C6 Plus	**FACSCanto™II**
Laser Excitation	488nm 640nm	405nm 488nm 633nm
Emission Detection	**FL1 533/30 nm** (FITC/GFP) **FL2 585/40 nm** (PE/PI) **FL3 > 670 nm** (PerCP-Cy™5.5) **FL4 675/25 nm** (APC)	*8 PMTs in 4-2-2 configuration* **Blue Laser:** 530/30; 585/42; >670; 780/60 nm **Red Laser:** 660/20; 780/60 nm
Flow rates	10 – 100 µL/min	10-120 µL/min

2.8.2 Determining Cell Growth and Viability using TOPRO-3 Staining

Cell growth and viability were determined through flow cytometry using TOPRO-3 (Invitrogen; T3605), a fluorescent dye with a high affinity for double stranded DNA and is only permeable in apoptotic cells where the integrity of the cell membrane is disrupted. Cells were seeded at $2x10^5$ cells/mL in 400µL/well in 48-well tissue culture treated plates. After 48 hours of culture, 225µL were harvested from each well and transferred to 5mL tubes (FACSCanto™ II) or 1mL flow tubes (Accuri C6 Plus) containing 25µL TOPRO-3 staining solution (RPMI supplemented with 100mM HEPES and 50nM TOPRO-3). For analysis on the Accuri C6 plus flow cytometer, 10µL of each sample was acquired at a high flow rate (100µL/min) to generate an absolute count, while on the FACSCanto™II samples were acquired for 5 seconds before any events were recorded to allow the flow rate to stabilise. Following this, 10 sec acquisitions were recorded for each sample to generate a relative count. For analysis of this data, debris acquired during sample acquisition, defined as TOPRO-3 negative events with a FSC of $<5x10^4$, were excluded and viability and viable cell counts were determined from within the viable cell population of TOPRO-3 negative events (Figure 2.6). From this, fold expansion was determined by dividing the viable counts/mL by the original seeding density (typically $2x10^5$).

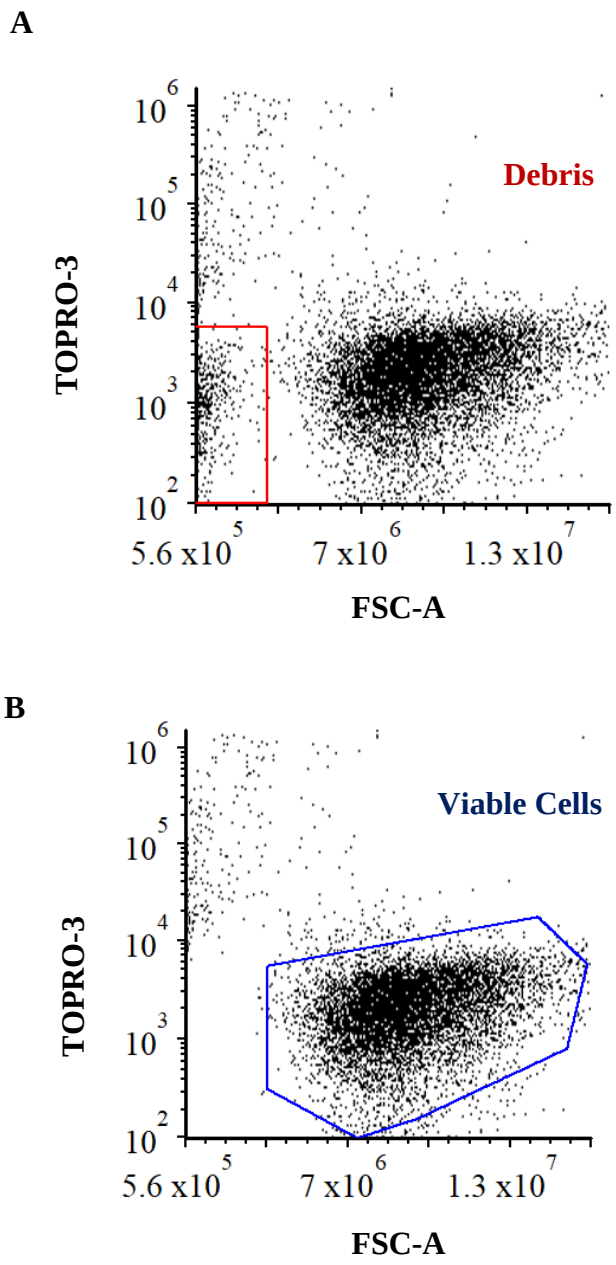

Figure 2.6: Flow cytometric gating strategy used to evaluate the fold expansion and viability of AML cell lines

Representative bivariate plots demonstrating the gating strategy employed to determine the viability and fold expansion of AML cell lines. **(A)** Cells were stained with TOPRO-3 and debris, defined as TOPRO3 negative events with FSC-A properties of less than $5x10^4$, were excluded before the **(B)** viable counts and percentage viability were calculated from gating around TOPRO-3 negative cells, as described in 2.8.2.

2.8.3 Intracellular Staining

For intracellular staining, $4x10^5$ cells were fixed using 4% (*w/v*) paraformaldehyde (PFA) diluted in PBS for 10 min at RT. During this incubation, the cell suspensions were transferred to labelled 1mL flow tubes and between each subsequent step in the protocol, the cells were centrifuged at 270*xg* for 3 min. Initially, cells were permeabilised using 0.25% (*w/v*) Triton X-100 (Sigma-Aldrich) diluted in PBS and 0.02% (*w/v*) sodium azide (Sigma-Aldrich) for 5 min at RT. The cells were then resuspended in 400µL blocking buffer (5% (*v/v*) goat serum (Sigma-Aldrich) and 0.2% (*v/v*) fish gelatin (Biotium Inc., California, USA) diluted in PBS supplemented with 0.02% (*w/v*) sodium azide), for 30 min at RT. Following blocking, the cells were resuspended in 100µL staining buffer (blocking buffer supplemented with 0.05% Tween (Sigma-Aldrich)) containing the primary rabbit anti-PKCε 22B10 (Cell Signaling) antibody or rabbit anti-PKCε polyclonal antibody; 20877-1-AP (Proteintech®, Illinois, USA) antibody which were diluted at 0.1 µg/mL-10µg/mL and incubated overnight at RT. The following day, samples were washed twice with 1% (*w/v*) BSA diluted in PBS before being resuspended in 150µL staining buffer containing the goat anti-rabbit IgG F(ab')2 Fragment AlexaFluor® 647 (Cell Signaling; CS4414) secondary antibody. The cells were subsequently incubated for 60 min at RT, after which the cells were washed twice as described above and resuspended in 100µL 1% (*w/v*) BSA diluted in PBS.

In subsequent experiments the cells were permeabilised with 90% (*v/v*) methanol for 10 min at RT. Following permeabilization, the cells were incubated with the primary antibodies for 30 min at RT and secondary antibodies for 20 min at RT following a wash step. For these experiments, a blocking buffer was not used, and all antibodies were diluted in 1% (*w/v*) BSA diluted in PBS and 0.02% (*w/v*) sodium azide. For all experiments, 20K events were acquired using the Accuri™ C6 plus flow cytometer (2.8).

2.8.4 Immunophenotyping

All antibodies used for immunophenotyping assays are outlined in Table 2.12. Both cell lines and HSPC were analysed using the same methodology, however the protocol outlined below focuses on HSPC immunophenotyping as this represents most of the data presented. Furthermore, cell lines were generally stained with a single antibody, while HSPC were concurrently labelled with multiple antibodies.

For HSPC cultures, transduced $CD34^+$ cells were analysed for the expression of lineage and differentiation markers, using four-colour cytometric analysis at the indicated time points (day 3, 6, 8 and 10 of culture following isolation; 2.2.3). For this, between $2.5x10^5$ to $5x10^5$ cells were resuspended in 80µL staining buffer (1% (*w/v*) BSA, diluted in PBS, supplemented with 0.02% (*w/v*) sodium azide). In U-bottom 96-well plates, 15µL cell suspension, with a maximum of $1x10^5$ cells/well, were concurrently labelled with APC conjugated CD13 antibody (BioLegend®; Table 2.12), a biotinylated CD36 antibody (Ancell Corporation, Minnesota, USA; Table 2.12) and one of the following phycoerythrin (PE) conjugated antibodies; IgG which was used as a negative control, CD34, CD11b, CD14 or CD15 (BioLegend®; Table 2.12) for 30 min at 4ºC. Following this incubation, the cells were washed with 150µL staining buffer and transferred to 1mL flow tubes, before the samples were labelled with streptavidin-peridinin chlorophyll protein (SA-PerCP cy5.5; Becton Dickinson Pharmingen, USA) for 20 min at 4ºC. The stained cells were washed once with staining buffer and resuspended in 150µL staining buffer for analysis using the Accuri™ C6 plus cytometer (2.8). The gating strategy used for HSPC analysis is detailed in Figure 2.7, for which, the whole 150µL culture was acquired for HSPC, while 10K events were acquired for the analysis of cell lines.

Table 2.12: Antibodies used for immunophenotypic analysis

Table outlining the supplier, clone, concentration, and manufacturer of the antibodies used for the immunophenotyping (2.8.4) of AML cell lines and HSPC. *Abbreviations: APC; Allophycocyanin, PE; phycoerythrin.*

Antibody	Conjugate	Clone	Isotype	Concentration	Manufacturer
IgG1	PE	-	-	5ng/µL	BioLegend®[1]
IgG1ka	APC	-	-	5ng/µL	BioLegend®[1]
CD11b	PE	ICRF4	IgG1	5ng/µL	BioLegend®[1]
CD13	APC	WM15	IgG	5ng/µL	BioLegend®[1]
CD14	PE	HCD14	IgG1	5ng/µL	BioLegend®[1]
CD15	PE	W6D3	IgG1	5ng/µL	BioLegend®[1]
CD34	PE	581	IgG1	5ng/µL	BioLegend®[1]
CD36	Biotinylated	SMO	-	1ng/µL	Ancell Corporation[2]
CD243	APC	UIC2	IgG2ka	5ng/µL	BioLegend®[1]

[1] BioLegend®, California, USA, [2] Ancell Corporation, Minnesota, USA.

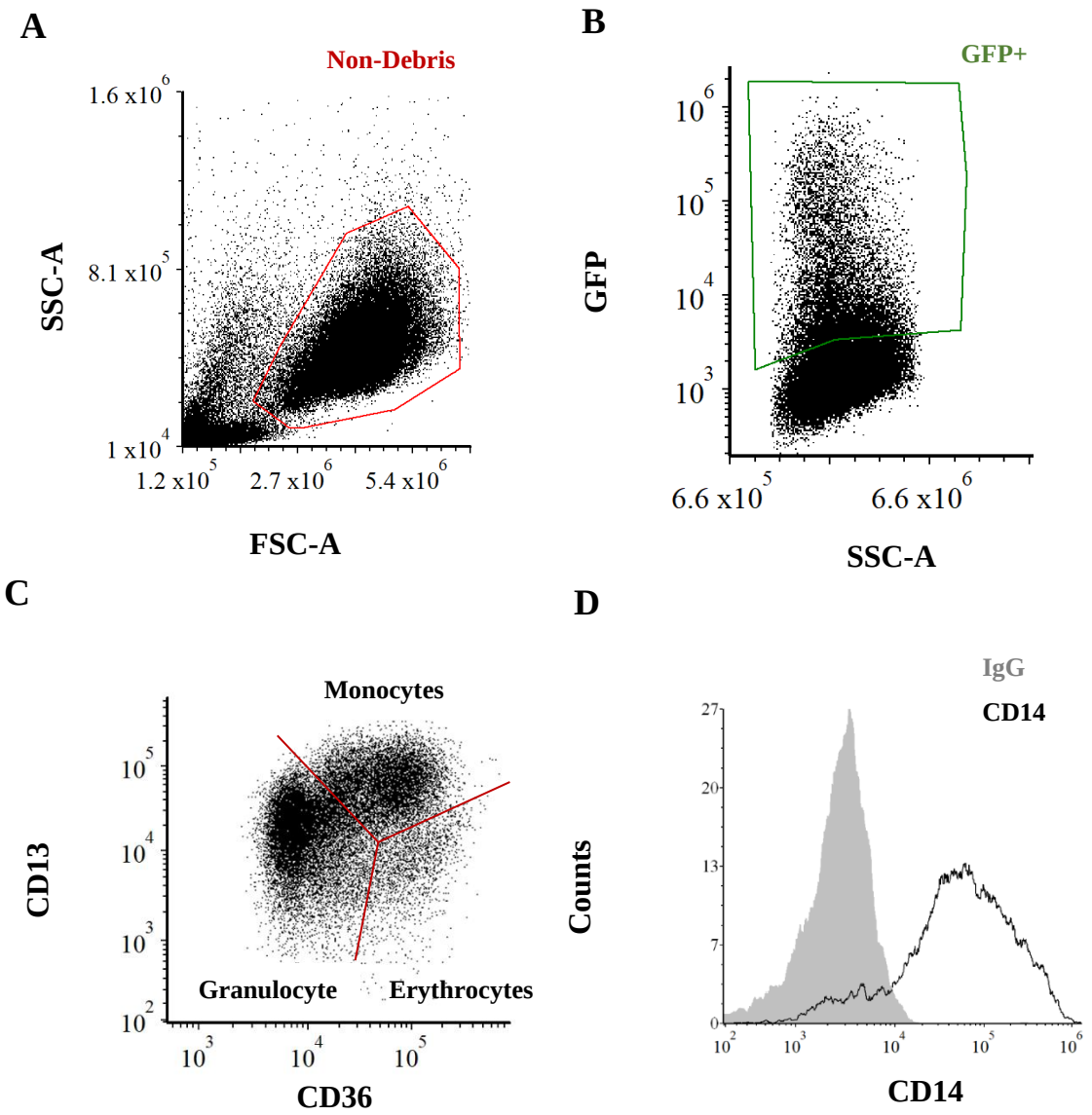

Figure 2.7: Gating strategy for HSPC immunophenotyping

Representative bivariate plots and histogram outlining the gating strategy used for immunophenotyping HSPC, as described in 2.8.4. **(A)** Debris, defined as events with FSC-A properties of $<5x10^4$, were excluded. **(B)** GFP expression was then used to limit subsequent analysis to transduced HSPC (GFP^+). **(C)** Expression of the lineage discriminating markers CD13 and CD36 was then used to resolve the monocytic, granulocytic and erythroid progenitor populations. **(D)** Within the monocytic and granulocytic progenitor populations the expression of maturation markers (outlined in 2.8.4), such as CD14 on monocyte, were assessed compared to the expression of an appropriate isotype control (Table 2.12).

2.8.5 Determining Mitochondrial Superoxide Levels using the MitoSOX™ Probe

The MitoSOX™ probe (ThermoFisher Scientific) is a cationic derivative of dihydroethidium. The cationic triphenyl phosphonium group allows the electrophoretic driven uptake of the probe by actively respiring mitochondria. Oxidation of the MitoSOX™ probe and the hydroxylation of dihydroethidium a the 2-position results in a fluorescence emission (at around 400nm). Thus, allowing the change in fluorescence of the MitoSOX™ probe to be used as an indicator of mitochondrial superoxide within the cell. The MitoSOX™ probe was diluted in DMSO according to the manufacturer's instructions. For this analysis, $1x10^6$ cells were harvested and centrifuged at 270xg for 5 min before being resuspended in 2mL of CO_2-independent medium (Gibco; 18045054), supplemented with 10% (*v/v*) FBS and 100nM TOPRO-3 and transferred to 5mL flow tubes. To each tube 10 µL MitoSOX™ probe (at a final concentration of 200nM) was added. The cells were incubated in a water bath at 37ºC for 75 min with the fluorescence of the MitoSOX™ probe being analysed at 15 min intervals using the FL-2 channel of the Accuri™ C6 plus (Table 2.11).

2.8.6 Determining NOX2-Derived Superoxide using the Diogenes™ Probe

NADPH oxidase 2 (NOX2)-derived superoxide was detected using the Diogenes™ chemiluminescent probe (National Diagnostics, Hessel, UK). Diogenes™ is a luminol probe that reacts with superoxide radicals to form an excited product which emits a photon as it returns to an unexcited state. The generated photon subsequently activates an enhancer within the probe which emits additional photons to amplify the signal. For the Diogenes™ assay, cells were counted and washed in 5mL PBS before being resuspended in standard buffer (Table 2.13) and seeded in a white FluoroNunc Maxisorp 96 well plate (50K/well) before 50µL Diogenes™ probe was added to each well. Immediately, 15µL PMA 10µM or PBS was added to the relevant wells. The plates were incubated at 37ºC and luminescence was measured at regular intervals over 100 min, using a Chameleon Hidex fluorescent plate reader, according to the manufacturer's instructions. Chemiluminescent traces were plotted according to the light emission rate, measured as relative light units (RLU), against time and the rate of superoxide photons produced/second.

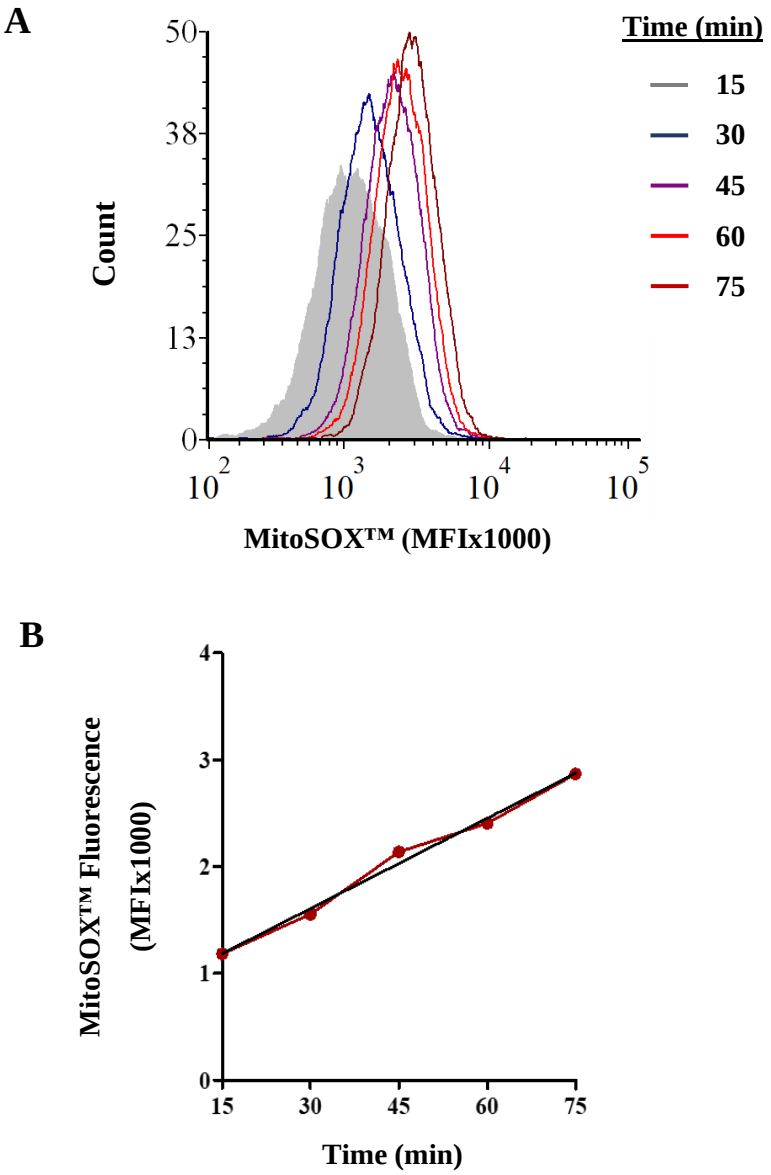

Figure 2.8: Assessing mitochondrial superoxide production in AML cell lines using MitoSOX™ fluorescence

(A) Representative histogram showing the increasing fluorescence intensity (MFI x1000) of the MitoSOX™ probe in the FL-2 channel (Table 2.11) over time (min) in U937 cells. **(B)** Representative line graph showing how the rate of change in MitoSOX™ fluorescence (MFI x1000) was used to evaluate the detectable levels of mitochondrial superoxide production as described in 2.8.5. The black line represents the linear regression line from which the rate of detectable levels of mitochondrial superoxide were determined.

Table 2.13: Composition of the standard buffer used in the Diogenes™ Assay

Table outlining the reagents that make up the standard buffer used in the Diogenes™ Assay (2.8.5). The pH of the standard buffer was adjusted to 7.4 before aliquoting and was stored at -20^{o}C until required. Each aliquot was thawed once, and any residual buffer was discarded.

Composition	Concentration	Supplier
PBS	-	Sigma-Aldrich
Sterile water	-	Sigma-Aldrich
Glucose	0.1 (*w/v*)%	Sigma-Aldrich
BSA (Low LPS)	0.1 (*w/v*)%	Sigma-Aldrich
Gentamycin	25 µg/mL	Sigma-Aldrich

2.8.7 Analysing Cell Cycle Distribution Through Determining Cellular DNA Content

Propidium Iodide (PI; Sigma-Aldrich) is a DNA binding dye which provides a proportional measure of the DNA content within cells, and so provides an indication of cell cycle distribution. For this analysis, cells were seeded at $2x10^5$ cells/mL and were expanded for 48 hours before being harvested to 1mL flow tubes and washed with 1mL PBS. The washed cells were subsequently resuspended in 300µL PBS and fixed for 30 min on ice by adding 700µL absolute ethanol. After fixation, the tubes were stored at -20ºC overnight. The next day, the cells were centrifuged at 270*xg* and washed with 1mL PBS before being resuspended in 50µL staining buffer (PBS+0.5% (*w/v*) BSA+ 0.02% (*w/v*) sodium azide). The cells were then stained with 25µL staining solution containing 40µg/mL propidium iodide, and 0.1mg/mL RNase (Sigma-Aldrich) diluted in PBS, for 30 min at 37ºC. Samples were acquired within 20 min of this incubation using the Accuri™ C6 Plus flow cytometer (2.8.1). For analysis, debris and doublets were excluded, before the cell cycle status was resolved using the fluorescence intensity of PI (Figure 2.9) which was measured on the FL-2 channel (Table 2.11). Cell cycle analysis was performed using the Multicycle AV DNA analysis tool plug-in for FCS Express.

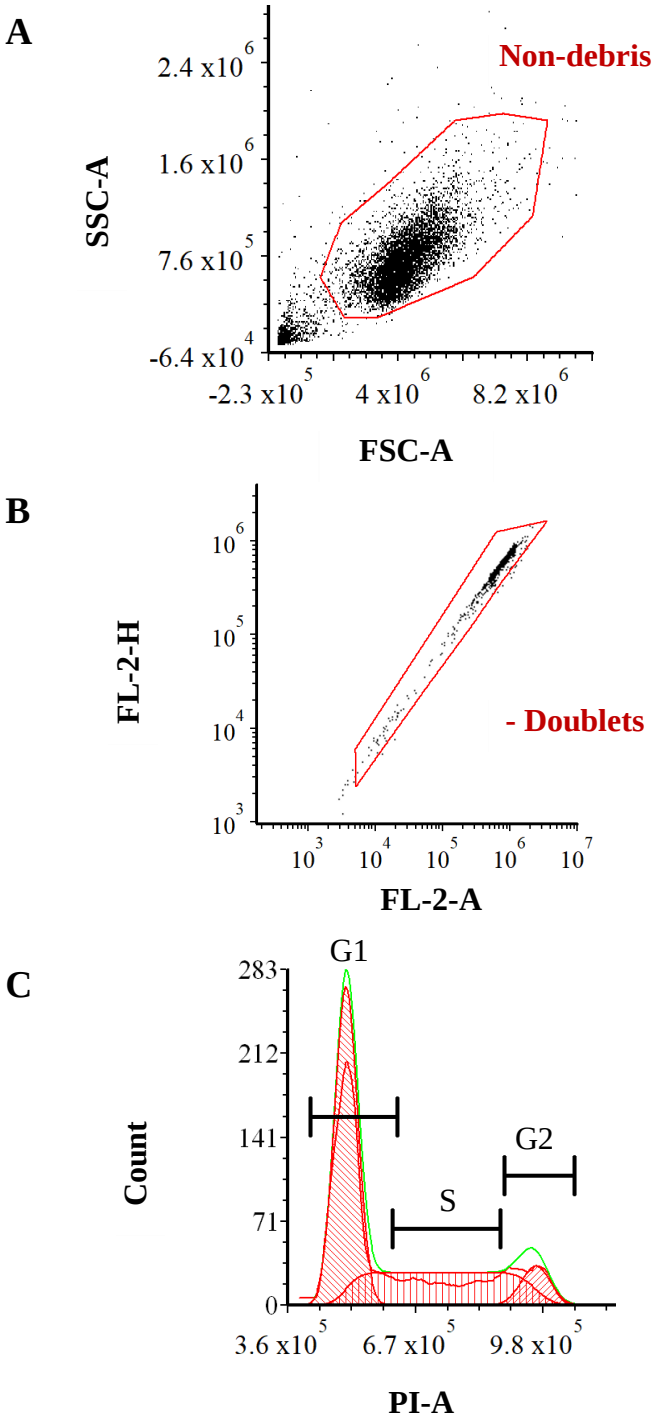

Figure 2.9: Flow cytometric gating strategy used for cell cycle analysis

Representative density plots and histogram depicting the gating strategy used for the analysis of cell cycle status by flow cytometry. **(A)** Debris acquired during the acquisition of cells, defined as events with an FSC <5x10^4 were excluded. **(B)** Height (FL-2-H) and area (FL-2-A) parameters were used to exclude doublets and cell aggregates. **(C)** Histogram showing the Multicycle AV DNA analysis tool plug-in for FCS Express 6 (model 1; "autofit") which was used to determine the proportions of cells with in the G1, S and G2 cell cycle phases which were resolved using propidium iodide (PI) staining (2.8.7).

2.8.8 Drug Sensitivity Assays

2.8.8.1 Drug Preparation and EC-50 Determination

Master stocks of each agent were generated according to the manufacturer's instructions and is outlined in Table 2.14. Once generated, all stocks were stored at -20^{o}C in 100µL aliquots for long-term storage unless otherwise stated. For the drug sensitivity assays, AML cell lines in log-phase growth were enumerated (2.1.3) and seeded at 2x10^{5} cells/mL in tissue-culture treated 48-well plates (Falcon), using 400µL/well. Following this, 4µL of the drug of interest (using the concentration ranges outlined in Table 2.14) was added, alongside the relevant vehicle control, before the cells were incubated for 48 hours. After this incubation, cell growth and viability were determined using TOPRO-3 staining (2.8.2) and the sensitivities of the cell lines to each agent was calculated by determining the half-maximal effective concentration (EC50) for cell growth and viability, whereby EC50^{G} refers to the impact on cell growth and EC50^{V} refers to the impact on cell viability.

2.8.8.2 Determining DNR Accumulation

DNR possesses fluorescent properties which can be detected by flow cytometry and used as an indicator of drug accumulation within the cell (Figure 2.10). To evaluate the impact of modulated PKCε expression on DNR uptake, AML cell lines were seeded in triplicate at 2x10^{6} cells/ml, in tissue culture treated 48-well plates, and were treated with 100nM DNR or the vehicle control (Table 2.14) for 2 hours at 37^{o}C. Following this, the cells were harvested into 5mL flow tubes and analysed by flow cytometry where 5,000 events were analysed. The FL-2 channel arithmetic mean fluorescence for each condition was determined using FCS Express (2.8) and the change in DNR fluorescence between the vehicle control and cells treated with 100nM DNR for each cell line was compared.

For the PKC agonist and antagonist studies, the cells were pre-incubated with PMA or Calphostin C (CC) for 30 min at 37^{o}C before DNR and ZSQ were added to the relevant wells and incubated at 37^{o}C for two hours, as described above. For the 2-day analysis, cells were harvested and stained with TOPRO-3 and DNR fluorescence (Figure 2.10) was measured within the viable (TOPRO-3 negative) population using the gating strategy described in 2.8.2.

Table 2.14: Agents used in the Drug Sensitivity Assays

Table outlining the agents and working concentrations used in the drug sensitivity assays. *Abbreviations: Ara-C; cytarabine, ATM; antimycin A, ATO; arsenic trioxide, CC; Calphostin C, DNR; daunorubicin, GOx; glucose oxidase, PMA; Phorbol 12-myristate 13-acetate; ZSQ; zosuquidar hydrochloride.*

Drug	Manufacturer	Preparation of Master and working stocks	Cat no.	Diluent/ vehicle control[1]	Concentration
Ara-C	Sigma-Aldrich	A 119mM Ara-C stock was generated by dissolving 100mg solid Ara-C in 3mL PBS. From this 840µL was diluted in 9.2mL PBS to generate a 10mM working solution.	C1768	PBS	0-800nM
ATM	Sigma-Aldrich	A 20Mm solution was generated by adding 2.3mL ethanol to 25mg ATM. From this a 2mM working stock was generated by adding 100uL ATM (20mM stock) to 900uL DMSO using a positive displacement pipette.	A8674	DMSO	0-20µM
ATO	Sigma-Aldrich	A 5mM stock was generated by dissolving c20mg of solid ATO in 31mL tissue-culture grade water (0.65mg/ml). This was passed through a 0.22µm filter and stored at RT.	71287	PBS	0-4µM
CC	ENZO	A 1.26mM stock was generated by dissolving 100mg of CC in 100µL DMSO and was stored at 20ºC. When required a 10µM working stock was generated by diluting 2µL in 250µL PBS.	BML-EI198-0100	PBS	100nM
DNR	Cayman Chemical	A 20mM master stock was generated by dissolving 5mg of solid DNR in 443µL DMSO.	14159	PBS	0-100nM
GOx	Sigma-Aldrich	GOx (specific activity 192U/mg) was solubilised at 1mg/mL (equivalent to 192,000mU/mL) in PBS. When thawed for use, aliquots were used once.	49180	PBS+1% (*w/v*) BSA	0-100mU
PMA	Cayman Chemical	A 100µM master stock was prepared in PBS and subsequently diluted 1/10 in PBS to generate a 10µM working stock.	400145	PBS	100nM
ZSQ	Cayman Chemical	A 1mM stock was generated by dissolving 1.57mL DMSO. This 1mM stock solution was further diluted 1/100 in DMSO to make a 10µM working stock.	21533	PBS+2.5% (*v/v*) DMSO	100nM

[1] Concentrations refer to the diluent, when used as a vehicle control these at 1µL/100µL of culture as described in 2.8.8.1.

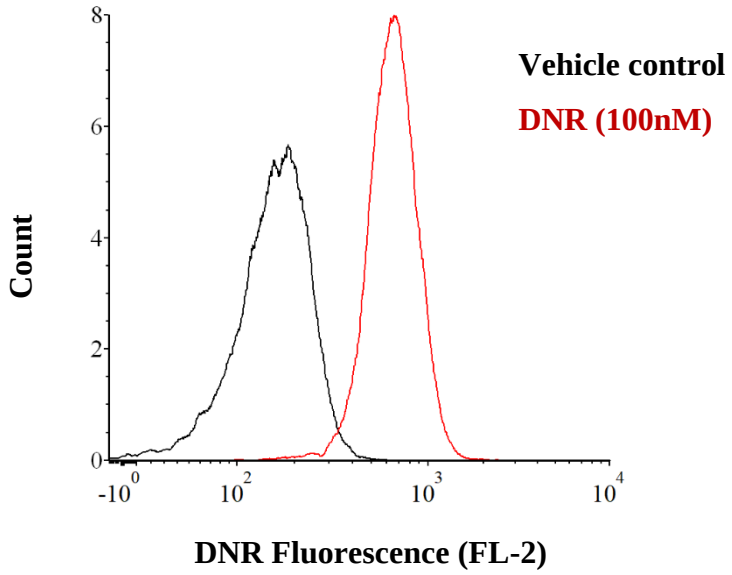

Figure 2.10: Using the fluorescent properties of DNR as an indicator of intracellular drug accumulation

Representative histogram showing the measurement of DNR fluorescence (FL-2) in U937 cells treated with 100nM DNR or vehicle control (PBS+0.01% BSA) following 2 hours of treatment as described in 2.8.8.2.

2.9 Stromal Co-culture Assays

2.9.1 Fold Expansion and Viability

MS5 stromal cells were trypsinised as described in 2.1.1 and enumerated using a haemocytometer (2.1.3). From this, a sufficient volume of cell suspension with a density of $0.5x10^5$ cells/mL was generated and seeded in 48 well tissue culture treated 48-well plates using 300µL/well. The MS5 cells were left to form monolayers overnight before the AML cell lines were seeded at $2x10^5$ cells/mL and treated with the chemotherapy agents or vehicle control as described above. After 48 hours of drug treatment, the cells were harvested and stained with TOPRO-3 as described in 2.8.2. Any contaminating MS5 stromal cells were excluded based on their FSC and side scatter (SSC) properties based on MS5 cells cultured without the addition of the AML cell lines.

2.9.2 Attachment Assays

To determine the attachment of AML cell lines to stromal cells, MS5 monolayers and co-cultures with the AML cell lines were set up in 48-well tissue culture treated plates as described in 2.9.1. Following 48 hours of co-culture, the supernatant was transferred to 5mL flow tubes and replaced with 400µL PBS. This was removed immediately, retrieving any loosely adhered cells, and combined with the cells collected in the supernatant harvest. The adherent cells were then trypsinised with 200µL trypsin for 3 min at RT before the trypsin was inactivated with an equal volume of culture medium. These cells were harvested to separate 5mL flow tubes for analysis. The number of cells within the adherent and non-adherent (supernatant) cultures were enumerated using 10µL acquisitions on the Accuri™ C6 plus cytometer (2.8.1). For the adherent cell counts, contaminating MS5 stromal cells were excluded, as described in 2.9.1 and counts were adjusted for the different volumes that the adherent and non-adherent cells were harvested in. The proportion of attached cells was calculated by dividing the number of cells in the adherent fraction by the total number of cells harvested from each well. .

2.9.3 Stromal Drug Sensitivity Assays

MS5 monolayers and AML co-cultures were set up as described in 2.9.1. Following seeding, the AML cell lines were incubated for 4 hours at 37°C before being treated with the chemotherapeutic agents described in 2.8.8. Following 48 hours of treatment, the non-adherent cells were collected by transferring the supernatant to 5mL tubes containing 80µLTOPRO-3 staining solution (2.8.8). The supernatant was replaced with 400µL PBS which was immediately removed and added to the collection tube. To harvest the adherent cells, 200µL pre-warmed trypsin was added to each well and incubated at RT for 3 min. Following this incubation, the trypsin was diluted 1:1 with growth medium and cells were harvested by systematic pipetting around the well. The harvested (adherent cells) were transferred to the corresponding collection tube. The wells were visually inspected to ensure that at least 90% of the cells had been harvested. The impact of drug treatment on the cell growth and viability was assessed as described in 2.8.2 with contaminating MS5 stromal cells being excluded, as described in 2.9.1

2.10 Fluorescence Activated Cell Sorting

For cell sorting, transduced HSPC were washed with PBS and resuspended in 500µL PBS supplemented with 5ng/mL IL-3, before being transferred to 15mL falcon tubes for sorting using FACS based on their GFP expression (Figure 2.11) using a BD FACSAriaIII™ which was accessed through Cardiff University's Central Biotechnology Service. FACS was conducted at RT, using a 100µM nozzle and sorted cells were collected in 15mL Falcon tubes containing 8mL IMDM supplemented with 10% (*v/v*) FBS. The sorted cells were then transferred to UC and centrifuged at 270*xg* for 10 min. Once the supernatant was removed the pelleted cells were resuspended in 1mL $3S^{low}G$/GM (Table 2.2) for enumeration by flow cytometry (2.1.3) and seeded at an appropriate seeding density, depending on the day of culture that the cells were sorted (2.2.4).

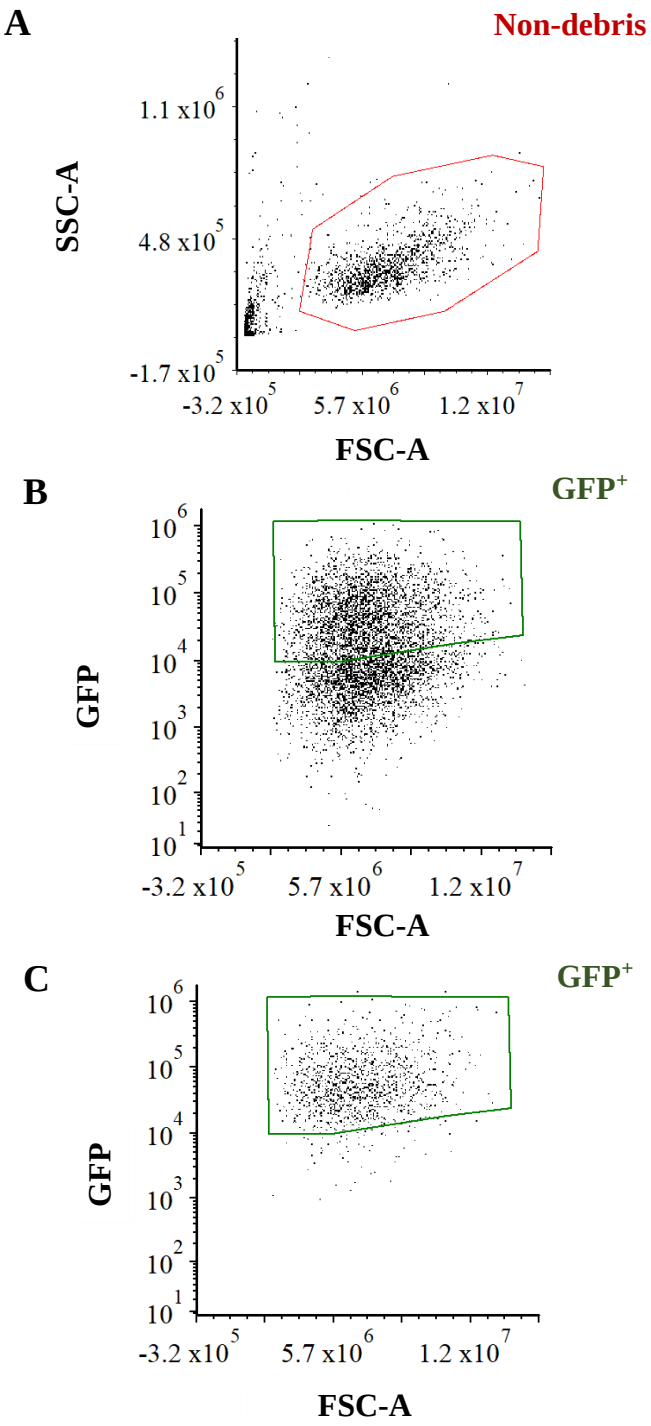

Figure 2.11: Gating Strategy used in the FACS of transduced HSPC

Representative bivariate dot plots showing the validation of FACS to enrich HSPC cultures for transduced (GFP^+) cells using the FACSAriaIII™ (2.10). **(A)** debris (events with an FSC $<5x10^4$) recorded during sample acquisition were excluded using the non-debris gate. **(B)** Before sorting, transduced cells were evaluated for GFP expression to confirm successful transduction, where the threshold for GFP positivity was established using the autofluorescence of un-transduced cells (negative control). **(C)** Following sorting the cultures were again analysed for GFP expression to ensure that >90% of the culture expressed GFP.

2.11 Evaluating *PKCε* mRNA Expression using Online Datasets

2.11.1 Bloodspot

The data regarding *PKCε* mRNA expression in human haematopoietic progenitor cells was accessed through the online database Bloodspot (Bagger, *et al.*, 2016;URL; http://servers.binf.ku.dk/bloodspot/) using the "normal haematopoiesis with AMLs" dataset where *PKCε* expression had been determined by microarray (GSE42519; Rapin, *et al.*, 2014). Overall, analysis was conducted using the mean expression from 3 of the 4 probe-sets available (206248_at, 236459_at and 226101_at). The fourth probe-set (239011_at) was excluded from this analysis as it showed a poor signal and was at discord with the other three datasets.

2.11.2 cBioPortal

mRNA expression in AML patient samples was obtained from cBioPortal (Cerami, *et al.*, 2012, Gao, *et al.*, 2013; URL; https://www.cbioportal.org/). Analysis was conducted using the TCGA, NEJM 2013 dataset comprising of whole-genome or whole-exome sequencing of where the complete set of data was available for 163 adult *de novo* AML samples (Ley, *et al.*, 2013). Untreated patients and those with APL were excluded from this analysis, and the remaining patients were stratified according to their *PKCε* expression into the upper (high *PKCε*) and lower (low PKCε) quartiles. The clinical attributes associated with high and low *PKCε* expression were assessed using cBioPortal including FAB classification of disease, cytogenetic and molecular abnormalities, OS, disease-free survival (DFS), age at diagnosis, sex, race, WBC, PB blast percentage, and bone marrow blast percentage. Cytogenetic and molecular aberrations were stratified into favourable, intermediate, and poor risk groups according to established systems (Döhner, *et al.*, 2017, Mrózek, *et al.*, 2012, Patel, *et al.*, 2012). All mRNA data from cBioPortal is represented as RNASeq RSEM; a software package used for the estimation of gene abundance (Li and Dewey, 2011), and corresponds to the rsem.genes.normalized_results file from TCGA.

2.11.3 Cancer Dependency Map Project Portal

Data regarding mRNA expression in AML cell lines was accessed through The Broad Institute's Cancer Dependency Map Project Portal (DepMap; URL; https://depmap.org/portal) using the Public 20Q1 dataset (Broad, 2020, Ghandi, *et al.*, 2019) where expression had been determined through RNAseq and is expressed as Log_2 (transcripts per million (TPM)+1).

2.12 Analysis of AML14 and AML15 Clinical Trial Patient Samples

Analysis of patient samples from the AML14 and AML15 NCRI clinical trials was conducted by Prof. Richard Darley and Prof. Alex Tonks before this PhD project commenced, however, the methodologies used in this analysis are briefly outlined below.

2.12.1 Affymetrix Microarray

PKCε mRNA expression was determined by Affymetrix DNA microarray. The raw data from the Hu133A GeneChip® was normalised using MAS5 or Robust Multi Array (RMA) analysis. The MAS5 analysis gave an indication of expression level as far as whether the gene was present, marginal, or absent, based on p-values and gives an indication as to the reliability of the data. On the other hand, RMA analysis adjusts for background readings, scales the data, and removes non-biological elements from the signal to decrease variability.

2.12.2 Protein Analysis

Evaluation of PKCε protein expression was assessed by western blot analysis in 70 AML patient samples using the methodology described in 2.8. However, for these samples, PKCε was detected using the C-15 anti-PKCε primary antibody (Santa Cruz Biotechnology, Texas, US), and donkey anti-rabbit HRP secondary antibody (NA934; GE HealthCare), while GAPDH was detected using an anti-GAPDH (sc-32233; Santa Cruz Biotechnology) antibody and donkey anti-mouse HRP secondary antibody (NA931; GE HealthCare Life Sciences). The expression of PKCε in normal BM-derived $CD34^+$ cells was used as a control. From this, PKCε overexpression within the AML samples was defined as 2 standard deviations (SD) above the mean expression of normal $CD34^+$ cell (108fg/1000 cells).

Western blots were documented using a Fuji Film LAS-3000 imager with an exposure as described in 2.8.6. The captured images were analysed semi-quantitatively using

post-acquisition software (Advanced Image Data Analyzer (AIDA) software version 4.26.038, Raytek Scientific, Sheffield, U.K). using the same methodology described in 2.7.5. PKCε expression normalised to loading (GAPDH expression) was then converted into fg/1000 by comparing the relative band intensity to a recombinant PKCε standard of a known concentration.

2.12.3 PKCε Expression and P-GP Expression and Functionality Analysis

P-GP expression and functionality data in AML14 and AML15 patient samples was kindly provided by Claire Seedhouse from the University of Nottingham. The methods utilised are outlined fully in Seedhouse, *et al.*, 2007. Briefly P-GP expression was determined by flow cytometry using an anti-P-GP (MRK16; Kamiya Biomedical) while P-GP function was measured by the efflux modulation of PSC-833, a P-GP inhibitor, using a rhodamine 123 accumulation assay. The impact of PSC-833 on rhodamine-123 accumulation was evaluated by calculating a Psc ratio, as described in Pallis and Das-Gupta, 2005, where the fluorescence of cells treated with rhodamine-123 and PSC-833 was divided by the fluorescence of the cells treated with rhodamine-123 and the vehicle control.

From this cohort of patients for which complete or partial P-GP expression and function data were available, PKCε expression had been determined by our group in 38 samples. These samples were subsequently grouped according to their PKCε expression, into samples with low PKCε protein expression (undetectable levels of protein by western blot analysis), and high PKCε (2SD above normal $CD34^+$ blasts; 2.12.2) and those within the upper quartile of samples with detectable PKCε protein expression (high PKCε expression). As described in P-GP data was generated across two independent centers, Cardiff University, and the University of Nottingham (Seedhouse, *et al.*, 2007). When assessing the MRK16 P-GP expression data were insufficiently reproducible to be pooled on a quantitative scale but when classified into high (above median) or low (below median) P-GP expression the two centres were able to distinguish the same cases as high or low in 87% (13 of 15 samples). So that samples from both centres could be used in this analysis, the relationship between PKCε and P-GP expression was assessed by comparing P-GP expression using this stratification system.

For the P-GP functional analysis, the Psc ratios were concordant across the two centres, therefore samples from both centres were included. In addition to the Psc ratio for each sample, P-GP function was stratified into those with negative (Psc ratio <1.7), low (Psc ratio 1.7-3.4) and high (Psc ratio>3.4) P-GP function (Seedhouse, *et al.*, 2007).

2.13 Statistical Analysis

All statistical analyses were conducted using GraphPad Prism (ver. 8) (GraphPad Software, California, USA). The statistical tests used are outlined in the figure legends. Statistical significance is denoted by *p-value<0.05, **p<0.01 and ***p<0.001.

Chapter 3: Characterising PKCε Expression in Normal Haematopoiesis and AML

3.1 Introduction

AML is a heterogeneous group of haematological malignancies which are characterised by abnormal myeloid cell development. Despite improvements in diagnosis and patient stratification, prognosis remains poor (1.2). Therefore, improving the understanding of the molecular mechanisms which underpin this malignancy, with the aim of identifying novel therapeutic targets is essential to improving patient outcomes. PKCε is an oncogenic kinase which is frequently upregulated in solid cancers (1.6.5) and is associated with aggressive disease phenotypes (Wu, *et al.*, 2002) and poor patient outcomes (Gorin and Pan, 2009). Although PKC signalling is thought to influence the proliferation, differentiation, and survival of haematopoietic cells (Aihara, *et al.*, 1991, Pearn, *et al.*, 2007, Redig and Platanias, 2008, Zabkiewicz, *et al.*, 2014), little is known about the role of specific PKC isoforms in the context of haematological malignancies, including AML.

Unlike other PKC isoforms, the role of PKCε in haematopoiesis has largely been studied in the context of the erythroid and megakaryocytic lineages (1.6.6). However, PKCε may be involved in myeloid cell development. PKCε knockout mice have severely attenuated macrophage activation in response to LPS (Castrillo, *et al.*, 2001), implicating a critical role of PKCε in the development and function of macrophages. Furthermore, PKCε-ERK signalling has been shown to promote differentiation in PMA-treated AML cells through onzin downregulation (Wu, *et al.*, 2010). In addition to the potential role of PKCε in myeloid cell differentiation, PKCε may contribute to the pathogenesis of AML through promoting cell survival. Our group has shown that the survival of primary AML blasts overexpressing PDK-1 is mediated by PKC signalling (Zabkiewicz, *et al.*, 2014). Furthermore, a recent study showed that reducing PKCε expression in AML cell lines and patient samples reduced cell survival, and prolonged disease progression in an MLL-AF9 murine model (Di Marcantonio, *et al.*, 2018). However, the exact role, including the frequency and clinical attributes associated with PKCε upregulation in AML has not been established.

3.2 Aims

The aim of this chapter is to establish the expression profile of PKCε in AML and assess whether PKCε contributes to the pathogenesis of this malignancy by acting as an oncogene in haematopoietic cells. This will be achieved through the following objectives:

- **Determine the expression profile and clinical features associated with high PKCε expression in AML patient samples**

  PKCε protein expression was previously established in patient samples from the AML14 and AML15 NCRI UK clinical trials using western blot analysis. This allowed the expression profile of PKCε protein to be determined, and the impact on OS and response to induction therapy of patients with high PKCε expression to be evaluated. This existing data will be supported with analysis of an independent RNAseq dataset (TCGA 2013; Ley, *et al.*, 2013), where the clinical attributes associated with high *PKCε* mRNA expression, including disease subtype, co-occurrence with cytogenetic and molecular abnormalities, OS, and DFS will be investigated.

- **Determine the impact of modulating PKCε expression on normal haematopoietic cell development**

  To determine whether PKCε overexpression contributes to the pathogenesis of AML by disrupting normal myeloid development, endogenous PKCε expression in haematopoietic progenitor cells will be assessed using online mRNA datasets. These findings will be validated at a protein level in CB-derived HSPC using intracellular flow cytometry and western blot analysis. Functional analysis will then be conducted using lentiviral overexpression and knockdown systems. The resulting impact on HSPC proliferation and differentiation will be assessed by flow cytometry.

3.3 Results

3.3.1 Assessing PKCε expression in AML patient samples

3.3.1.1 PKCε protein is upregulated in a third of AML patient samples

PKCε is associated with poor patient outcomes in solid cancers (1.6.5). *In vitro* studies have identified PKCε as an oncogene (Mischak, *et al.*, 1993), and in cancer cell lines has been implicated in chemoresistance (1.6.5.3). However, there is little published data on the role of this kinase in AML. To address this, our group previously analysed PKCε protein expression in 70 AML patient samples from the NCRI UK AML14 and AML15 clinical trials. PKCε expression was determined by western blot analysis, where overexpression was defined as 2 SD above the mean endogenous expression of BM-derived $CD34^+$ blasts from healthy donors (2.12.2). This analysis showed that PKCε was significantly overexpressed in 37% (26/70) of patient samples analysed, and heterogeneously expressed across samples within the same FAB classification, as well as across FAB disease sub-types (Figure 3.2). High PKCε protein expression was not associated with prognostic indicators such as a high white blood count (WBC), or with patient characteristics including age or gender (data not shown). In terms of patient outcome, there was no significant difference in OS (Figure 3.3A). However, using a model to adjust for age, gender, cytogenetics, and WBC, a Fisher's Exact test found that the proportion of patients achieving CR following first-line treatment with high PKCε protein expression was significantly lower than patients with low PKCε expression (Figure 3.3B; 65% (17/26 patients) high PKCε vs 84% (37/44 patients) low PKCε). This suggests that PKCε overexpression may be associated with a chemoresistance phenotype and an increased risk of relapse.

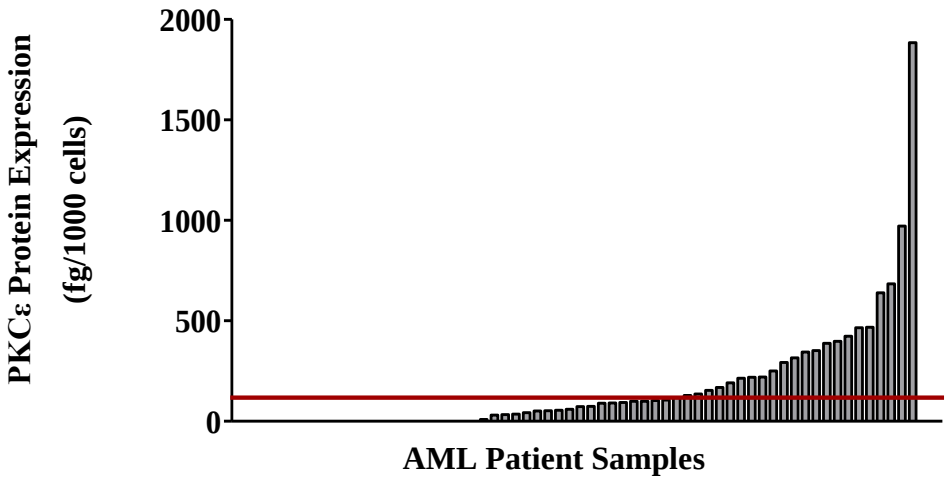

Figure 3.1: PKCε is frequently overexpressed in AML

Bar chart showing PKCε protein expression (femto-grams (fg) protein/1000 cells) across 70 AML patient samples, in ascending order, in samples from the AML14 and AML15 clinical trials. PKCε expression was determined by western blot (n=1 for each sample). Once normalised to loading (GAPDH expression), PKCε expression was converted to fg/1000 cells relative to a PKCε standard, as described in 2.12.2. The red line represents the threshold for overexpression, which was set at 2SD above the mean of normal $CD34^+$ blasts. A representative western blot is shown in Figure 3.2; *raw data provided by Prof. R. Darley*.

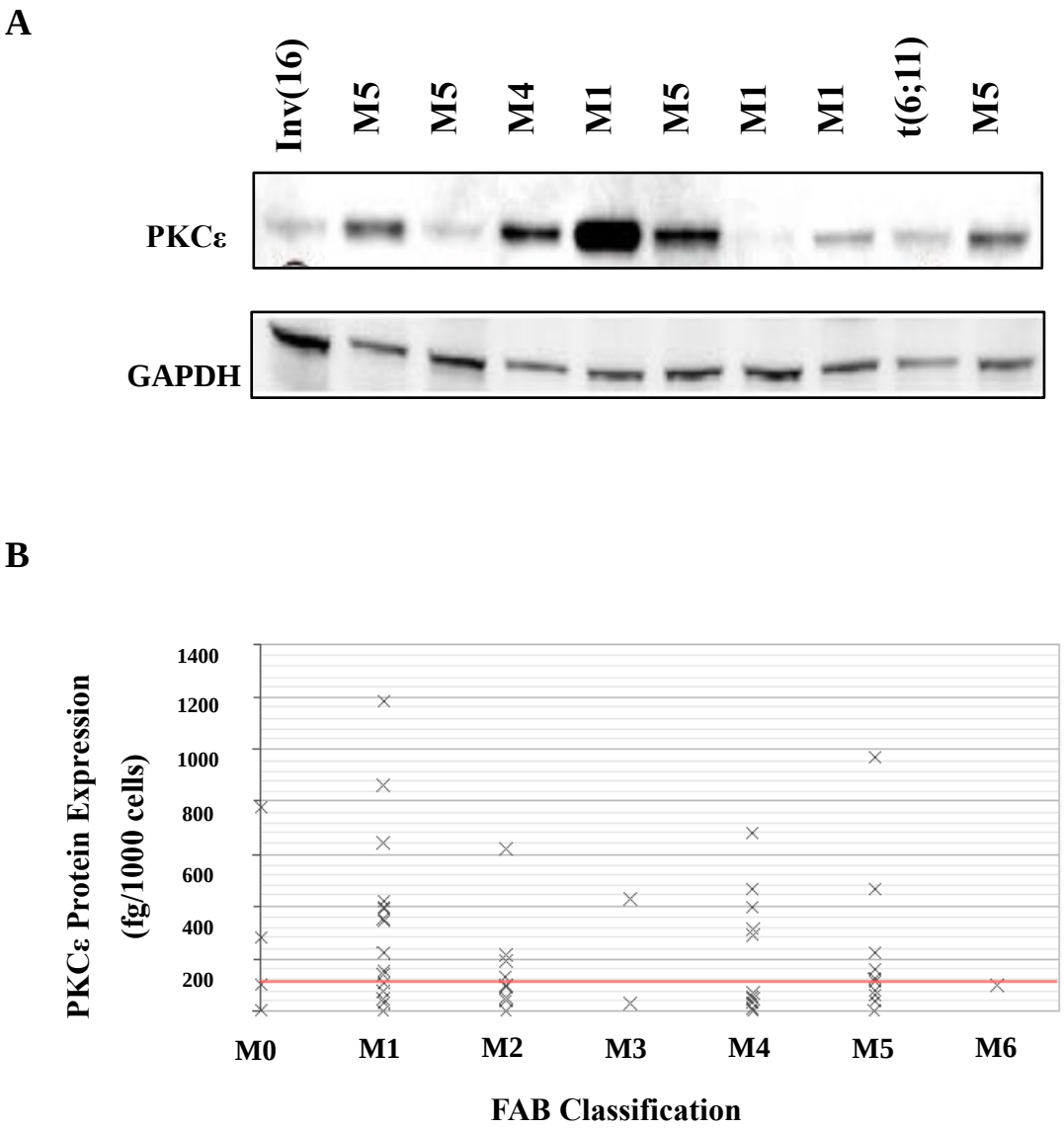

Figure 3.2: PKCε is heterogeneously expressed across AML FAB subtypes of disease

(A) Representative western blot showing PKCε (MW-84kDa) expression in AML patient samples from the AML14 and AML15 patient samples. PKCε expression was detected using the C-15 Santa Cruz antibody and is shown alongside GAPDH (MW-36kDa) expression which was used as a loading control and detected using the GAPDH (6c5) Santa Cruz antibody (2.12.2); *Data provided by Prof. R Darley.* **(B)** Graph showing PKCε protein expression in AML patient samples grouped by FAB subtype (n=58). The red line indicates the threshold for PKCε overexpression compared to normal $CD34^+$ blasts (108fg/1000 cells) as described in Figure 3.1. *Note: FAB type was not available for all patient samples analysed; Data and plot provided by Prof. R Darley.*

A

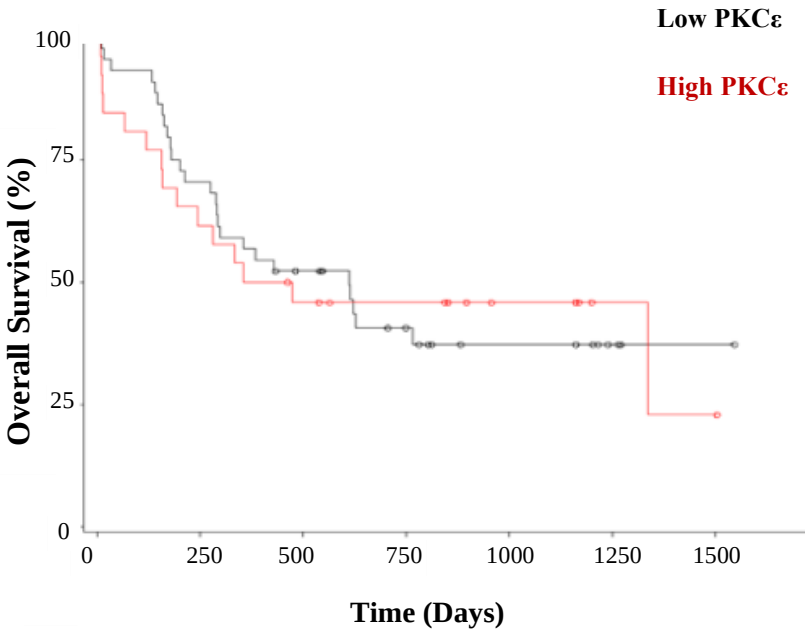

B

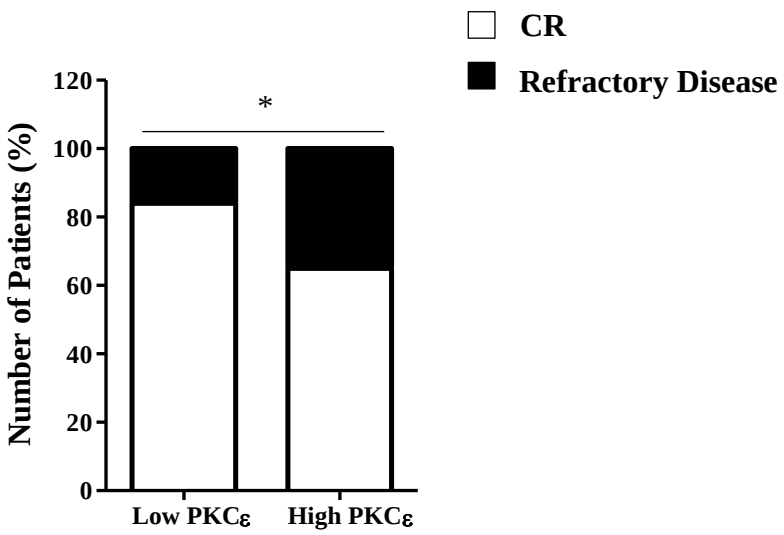

Figure 3.3: High PKCε protein expression is associated with reduced CR induction

(A) Kaplan-Meier curve comparing the OS (days) of AML patients from the AML14 and AML15 clinical trials with high (n=26) and low (n=44) PKCε expression, which were defined as described in Figure 3.1; *data and plot provided by R. Darley*. **(B)** Stacked bar chart showing the proportion of patients (%) that achieved complete remission (CR) or presented with refractory disease following induction chemotherapy for patients with high and low PKCε expression, as described above; *raw data provided by Prof. R. Darley*. Statistical significance was determined using a Fisher's Exact test and was deemed significant; *$p<0.05$.

3.3.1.2 PKCε mRNA and protein expression positively correlate in AML patient samples

Most of the clinical data which could be used to further determine the clinical attributes associated with PKCε upregulation in AML is linked with transcriptomic expression data. Correlations between mRNA and protein expression are variable (Maier, *et al.*, 2009). Therefore, to establish the extent of correlation between these factors for PKCε in AML patient samples, protein expression (Figure 3.1) was compared with mRNA expression data which had been determined using GeneChip® Affymetrix Microarray analysis (2.12.1). In the 18 samples for which PKCε protein and transcriptomic data was available, a significant positive correlation was observed (Figure 3.4). This indicates that mRNA expression is a reasonable predictor of PKCε protein expression in AML patient samples.

3.3.1.3 High PKCε mRNA expression is associated with poor OS and DFS

With a positive correlation between PKCε mRNA and protein expression in AML patient samples having been identified (Figure 3.4), I supported the preliminary analysis previously performed by the group (3.3.1.1), by analysing the TCGA 2013 RNAseq dataset (Ley, *et al.*, 2013). This dataset contains gene expression data for patients with *de novo* AML, across all major cytogenetic and morphological subsets of this malignancy. For this analysis, patients with APL and those who did not receive treatment were excluded, and the remaining patients were grouped according to their *PKCε* expression using the upper and lower quartiles to represent high and low *PKCε* expression, respectively. This stratification ensured clear separation, in terms of *PKCε* expression, between these two groups (Figure 3.5). Following this, the OS and DFS for patients with high *PKCε* mRNA expression was assessed. In addition, the association between high *PKCε* mRNA expression and disease subtypes, molecular and cytogenetic abnormalities, and patient characteristics were evaluated.

In terms of patient outcome, this analysis showed that high *PKCε* mRNA expression was associated with significantly reduced OS with a median survival of 11.2 months compared to 30.6 months for patients with low *PKCε* expression (Figure 3.6). Thus, suggesting that high *PKCε* expression is associated with an increased risk of mortality. Furthermore, high *PKCε* mRNA expression was associated with significantly reduced DFS. In this case, patients with high *PKCε* mRNA expression had a median DFS of 11.6 months, compared with 20.8 months

for patients with low *PKCε* expression (Figure 3.7). This was accompanied with a HR of 2.1 (95% CI (1.1-4.0)), which is indicative of an increased risk of relapse. This finding supports the original protein analysis, in that an increased risk of relapse could be caused by chemoresistance; a phenotype which was indicated by the reduced rate of CR induction for patients with high PKCε protein expression (3.3.1.1). However, this finding could not be directly validated using the mRNA analysis as information regarding CR induction was not available in this dataset.

Having identified that high *PKCε* mRNA expression is associated with poor patient outcomes, the co-occurrence with disease characteristics and prognostic indicators including FAB subtype of disease, cytogenetic and molecular abnormalities, WBC, and blast counts were investigated. As with the protein analysis, high *PKCε* mRNA expression occurred across FAB disease subtypes and was not associated with specific cytogenetic or molecular abnormalities, WBC, the percentage of blasts in the BM or peripheral blood (PB) (Figure 3.10) or patient characteristics such as age or gender (Figure 3.11). However, when the cytogenetic and molecular abnormalities were stratified according to risk, poor and intermediate risk aberrations were enriched in the high *PKCε* expression cohort (Figure 3.12). Although risk adjusted analysis would need to be conducted to determine the significance of this relationship, this suggests that, in part, the poor outcome associated with high *PKCε* expression may be due to an association with poor risk cytogenetic and molecular aberrations. Furthermore, this is in contrast with the protein analysis, where high PKCε expression occurred independently of known indicators of adverse risk. Although the causality of the relationship between PKCε and patient outcome in AML requires further clarification, overall, these findings support the protein analysis, highlighting the heterogeneous expression of PKCε in AML, and that high expression of this kinase is associated with poor patient outcomes.

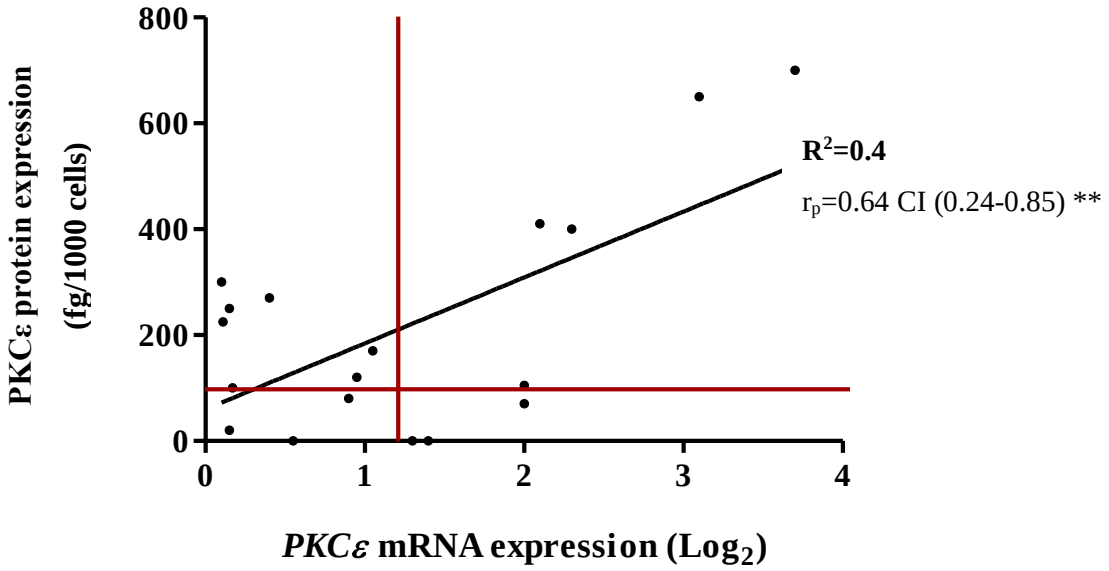

Figure 3.4: PKCε mRNA and protein expression positively correlate in patient samples

Dot plot showing the correlation between *PKCε* mRNA expression (Log_2), determined by microarray (2.12.1), and protein expression (fg/1000 cells), determined by western blot analysis, in AML patient samples from the AML14 and AML15 clinical trials (n=18). The vertical and horizontal red lines represent the thresholds for mRNA (1.42) and protein (108fg/1000 cells) overexpression, respectively compared to normal $CD34^+$ blasts. The linear regression line is represented by the black line (R^2=0.4) and the degree of correlation was assessed using Pearson's correlation analysis; r_p=0.6; 95% CI (0.24-0.85); **p< 0.01; *raw data provided by Prof. R. Darley.*

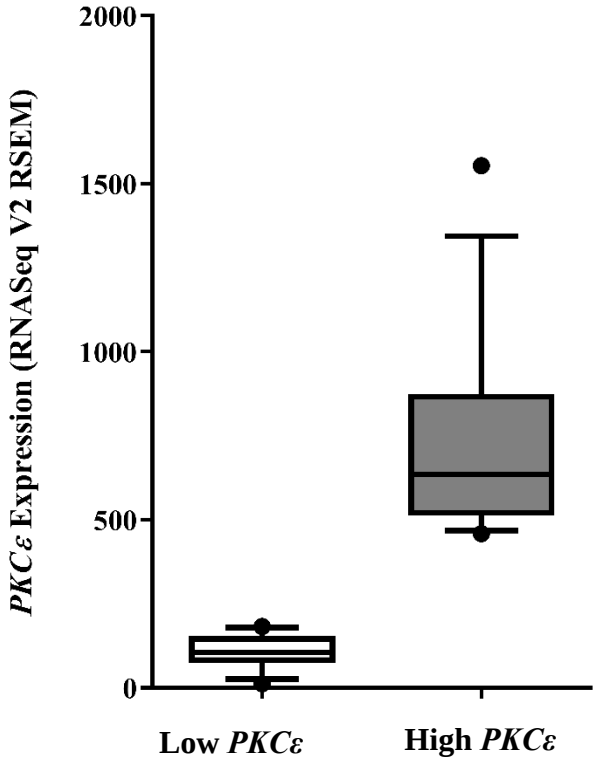

Figure 3.5: Stratification of AML patient samples according to their *PKCε* mRNA expression

Box and whisker plot showing *PKCε* mRNA expression (RNAseq V2 RSEM on a linear scale) in patient samples from the TCGA 2013 dataset (Ley, *et al.*, 2013). Patients were stratified based upon their *PKCε* expression, into high and low cohorts, using the upper (n=38) and lower (n=37) quartiles, respectively. The *PKCε* mRNA expression data was accessed using cBioPortal (Cerami, *et al.*, 2012, Gao, *et al.*, 2013; 2.11.2). The box represents the upper and lower quartiles of expression within each patient cohort, the solid line in the boxes represents the mean level of expression, while the whiskers represent the range. Samples which did not fall between the 5th and 95th quartiles are represented by black dots.

A

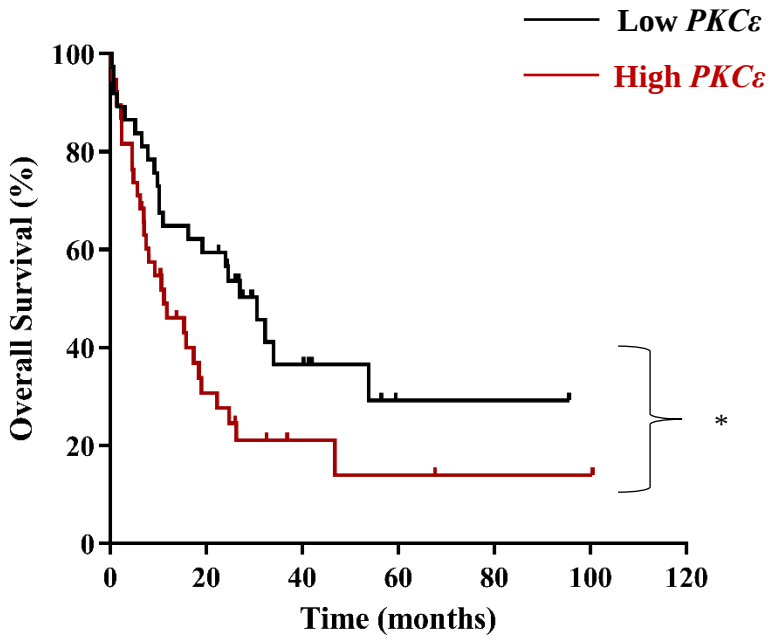

B

PKCε Expression	Number of patients	Number of deceased patients	Median OS (months)	Hazard Ratio	95% CI
High	38	29	11.2	1.8	1.1-3.3
Low	37	22	30.6		

Figure 3.6: High *PKCε* mRNA expression is associated with poor OS in AML patients

(A) Kaplan-Meier Curve of the OS (months) for AML patients from the TCGA 2013 dataset (Ley, *et al.*, 2013) with high (n=38) and low (n=37) *PKCε* expression as described in Figure 3.5. Data was obtained using cBioPortal (Cerami, *et al.*, 2012, Gao, *et al.*, 2013; 2.11.2). Statistical significance was determined using a Log-Rank Test and was deemed significant; *p<0.05. **(B)** Summary table showing the number of deceased patients from each cohort, the median survival for patients and the hazard ratio with 95% CI.

A

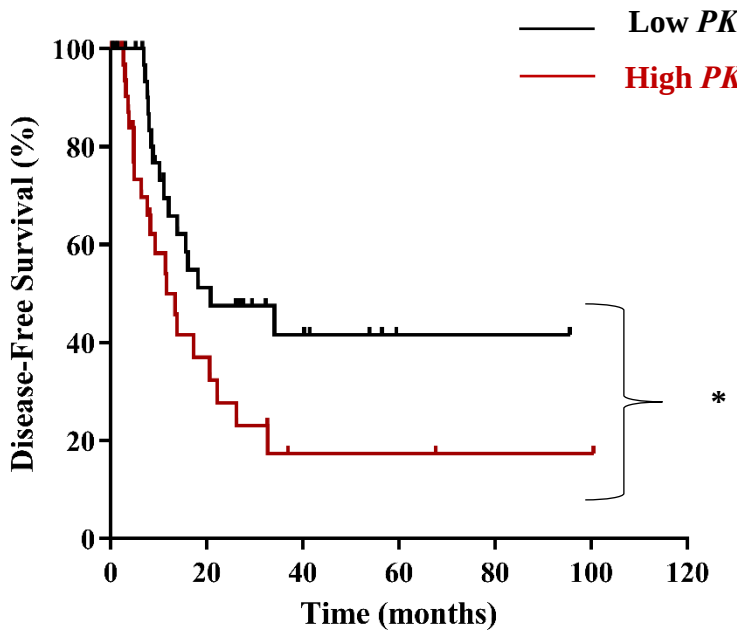

B

PKCε Expression	Number of patients	Number of relapsed/ progressed patients	Median DFS (months)	Hazard Ratio	95% CI
High	38	21	11.6	2.1	1.1-4.0
Low	37	16	20.8		

Figure 3.7: High *PKCε* mRNA expression is associated with reduced DFS

(A) Kaplan-Meier Curve of the DFS (months) for AML patients from the TCGA 2013 dataset (Ley, *et al.*, 2013) with high (n=38) and low (n=37) *PKCε* expression as described in Figure 3.5. Data was obtained using cBioPortal (Cerami, *et al.*, 2012, Gao, *et al.*, 2013; 2.11.2). Statistical significance was determined using a Log-Rank Test and was deemed significant; *p<0.05. **(B)** Summary table showing the number of relapsed/progressed patients, the median DFS for each cohort, and the hazard ratio with 95% CI.

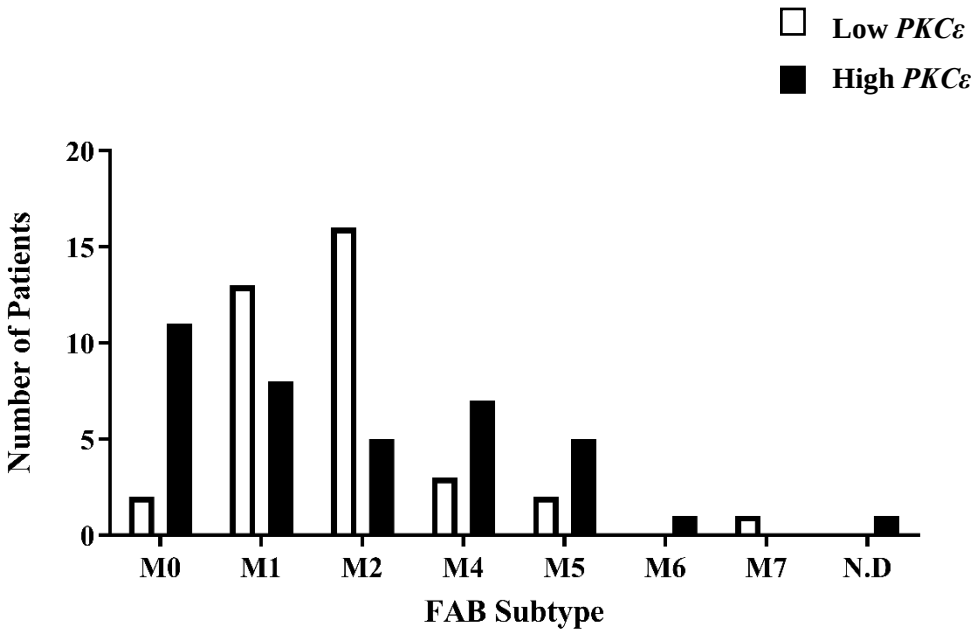

Figure 3.8: High *PKCε* mRNA expression occurs across AML disease subtypes

Bar chart representing the number of patients across the different FAB subtypes of AML (M0-M7) for samples from the TGCA 2013 dataset (Ley, *et al.*, 2013) with low (n=37) and high (n=38) *PKCε* expression as described in Figure 3.5. Data was obtained using cBioPortal (Cerami, *et al.*, 2012, Gao, *et al.*, 2013; 2.11.2). *Abbreviations: N.D; Not Determined.*

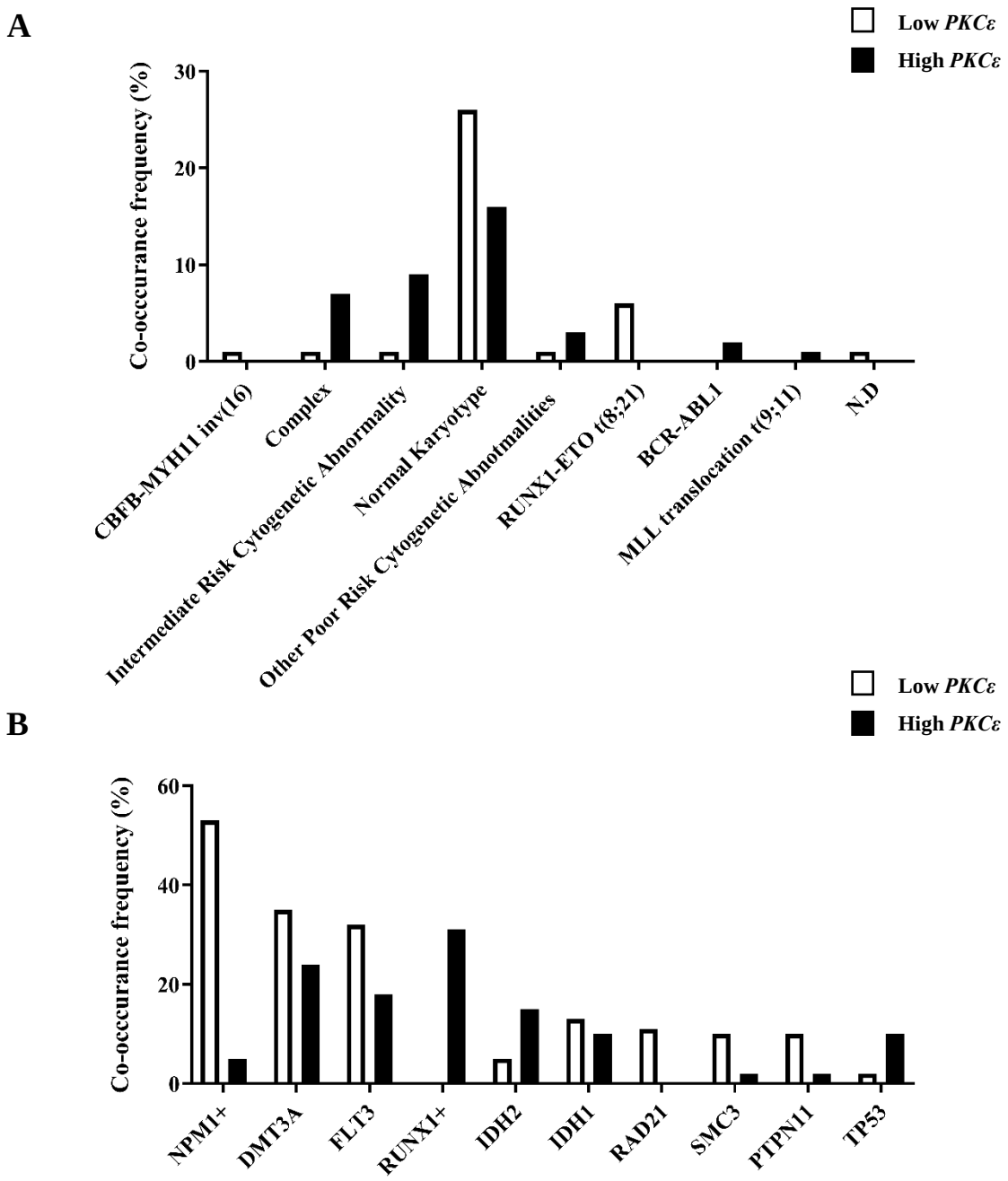

Figure 3.9: High *PKCε* mRNA occurs with a range of cytogenetic and molecular abnormalities

Bar charts representing the co-occurrence frequency (%) of specific **(A)** cytogenetic or **(B)** molecular abnormalities in AML patient samples from the TCGA 2013 dataset (Ley, *et al.*, 2013) with low (n=37) and high (n=38) *PKCε* expression as described in Figure 3.5. Data was obtained using cBioPortal (Cerami, *et al.*, 2012, Gao, *et al.*, 2013; 2.11.2). *Abbreviations: N.D; Not Determined.*

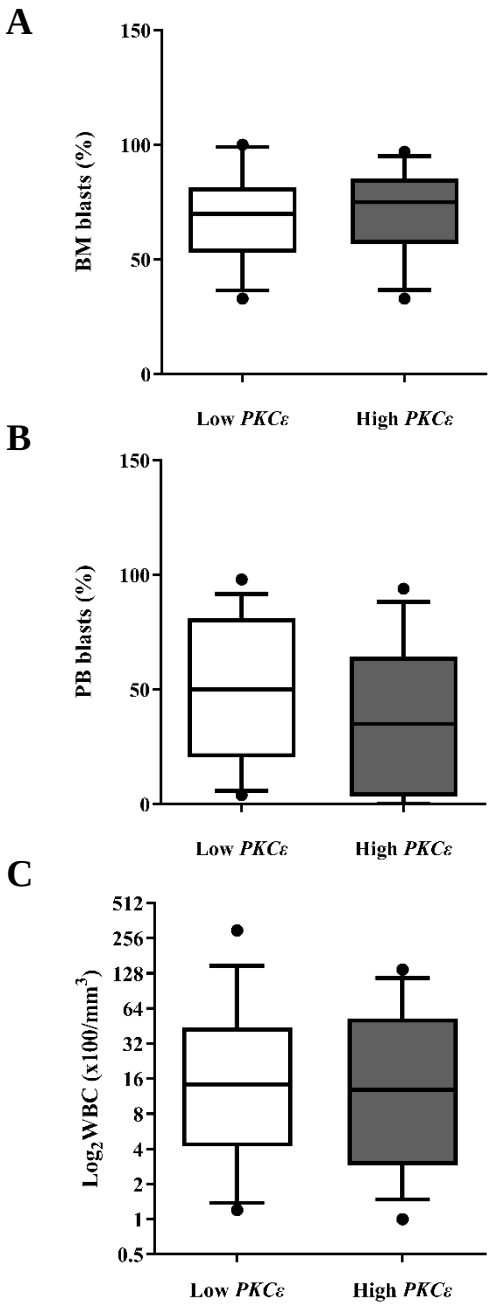

Figure 3.10: High *PKCε* mRNA expression is not associated with high PB and BM blast percentages, or WBC

Box and whisker plots showing the percentage of **(A)** peripheral blood (PB) blasts, **(B)** BM blasts and **(C)** WBC in samples for patient samples from the TCGA 2013 dataset (Ley, *et al.*, 2013) with low (n=37) and high (n=38) *PKCε* expression as described in Figure 3.5. Data was obtained using cBioPortal (Cerami, *et al.*, 2012, Gao, *et al.*, 2013; 2.11.2). The box represents the upper and lower quartiles, the solid line within the box represents the mean, while the whiskers represent the range. Samples which do not fall within the 5^{th} and 95^{th} quartiles are represented by black dots.

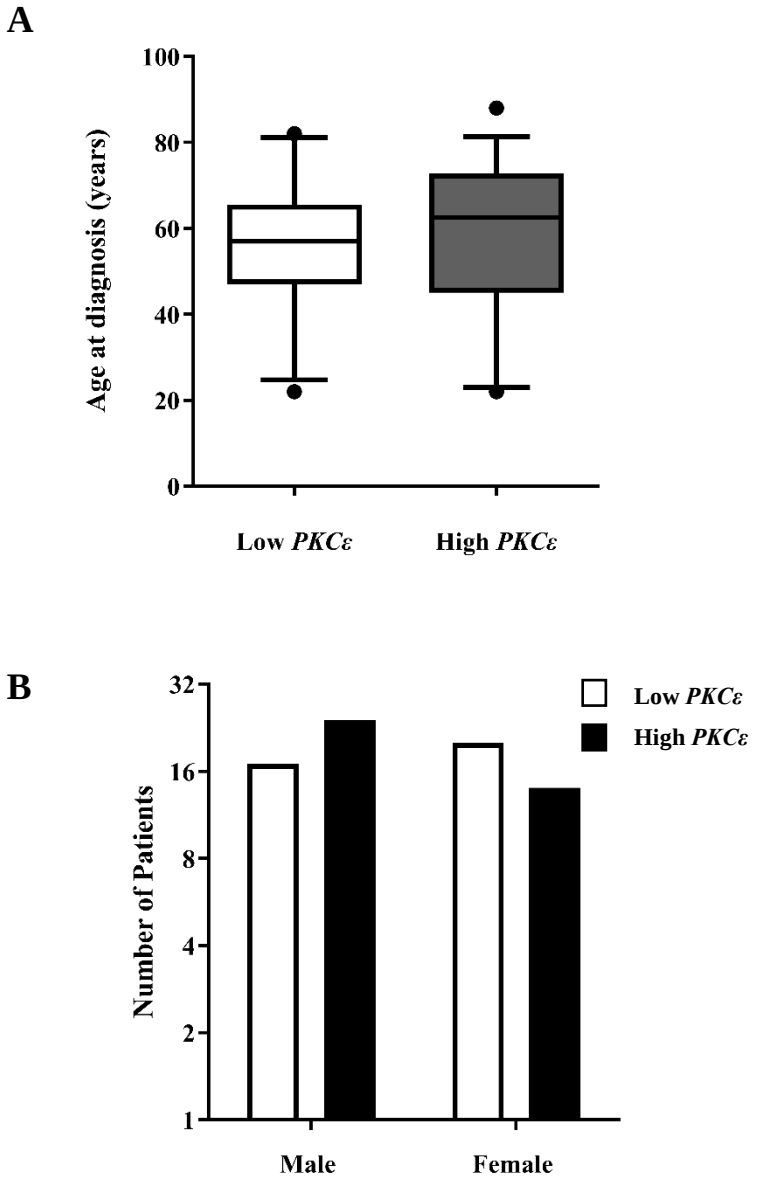

Figure 3.11: High *PKCε* mRNA expression is not associated with patient characteristics

(A) Box and whisker plot showing the age at diagnosis (years) of patients from the TCGA 2013 dataset (Ley, *et al.*, 2013) with low (n=37) and high (n=38) *PKCε* expression as described in Figure 3.5. Data was obtained using cBioPortal (Cerami, *et al.*, 2012, Gao, *et al.*, 2013; 2.11.2). The box represents the upper and lower quartiles, the solid line within the box represents the mean, while the whiskers represent the range. Samples which do not fall within the 5th and 95th quartiles are represented by black dots. Statistical significance was determined using Mann Whitney tests and was deemed non-significant. **(B)** Bar chart representing the proportion of male and female patients in the TCGA 2013 dataset (Ley, *et al.*, 2013) as described above. Statistical analysis was determined using Mann-Whitney tests and was deemed non-significant.

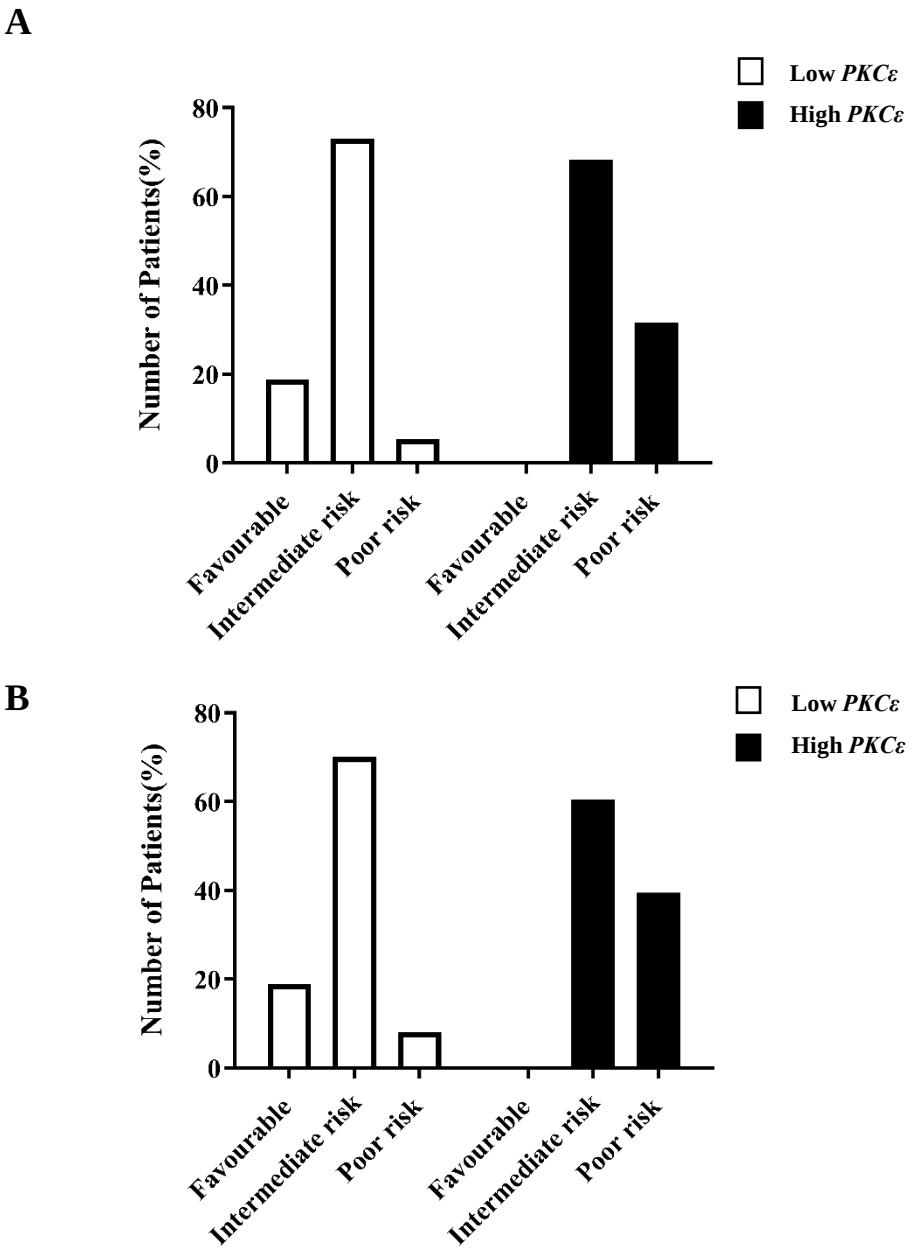

Figure 3.12: High *PKCε* mRNA expression occurs more frequently with intermediate and adverse risk cytogenetic and molecular abnormalities

Bar charts representing the number of patients (%) with known poor, intermediate, and favourable risk **(A)** cytogenetic and **(B)** molecular aberrations for patients from the TCGA 2013 dataset (Ley, *et al.*, 2013) with low (n=36) and high (n=37) *PKCε* expression as described in Figure 3.5. Data was obtained using cBioPortal (Cerami, *et al.*, 2012, Gao, *et al.*, 2013; 2.11.2). Patients where cytogenetic and molecular risk had not been determined were excluded from this analysis.

3.3.2 Characterising PKCε mRNA expression in human HSPC

PKC isoforms appear to play several roles in haematopoiesis (1.6.6), however, the expression and function of individual isoforms, including PKCε, in myeloid cell development is not well established. To determine *PKCε* expression in human haematopoietic cells, mRNA expression was assessed using publicly available microarray data through the online data repository, BloodSpot (Bagger, *et al.*, 2016; 2.11.1). Of the four probe-sets available (206248_at, 226101_at, 236459_at, and 239011_at), probe-set 239011_at, showed a poor signal and was discordant with the other three datasets. As a result, this probe-set was excluded, and an average of the remaining probe-sets was determined. This analysis showed that *PKCε* is expressed throughout haematopoiesis. The lowest levels of expression were found in MEP and metamyelocytes (MM), while the highest levels of expression were in GMP, monocytes and polymorphonuclear (PMN) cells (Figure 3.13). Within the monocytic and granulocytic lineages, *PKCε* expression was maintained, increasing slightly as cells reached terminal differentiation (Figure 3.13B and C). Although the range of *PKCε* expression across the different haematopoietic progenitor populations was small (c2-fold), the pattern of expression is similar within murine haematopoietic cells where *PKCε* expression had been determined by RNAseq (GSE60101; available from BloodSpot; data not shown). Overall, this pattern of expression suggests a potential role for *PKCε* in myeloid maturation.

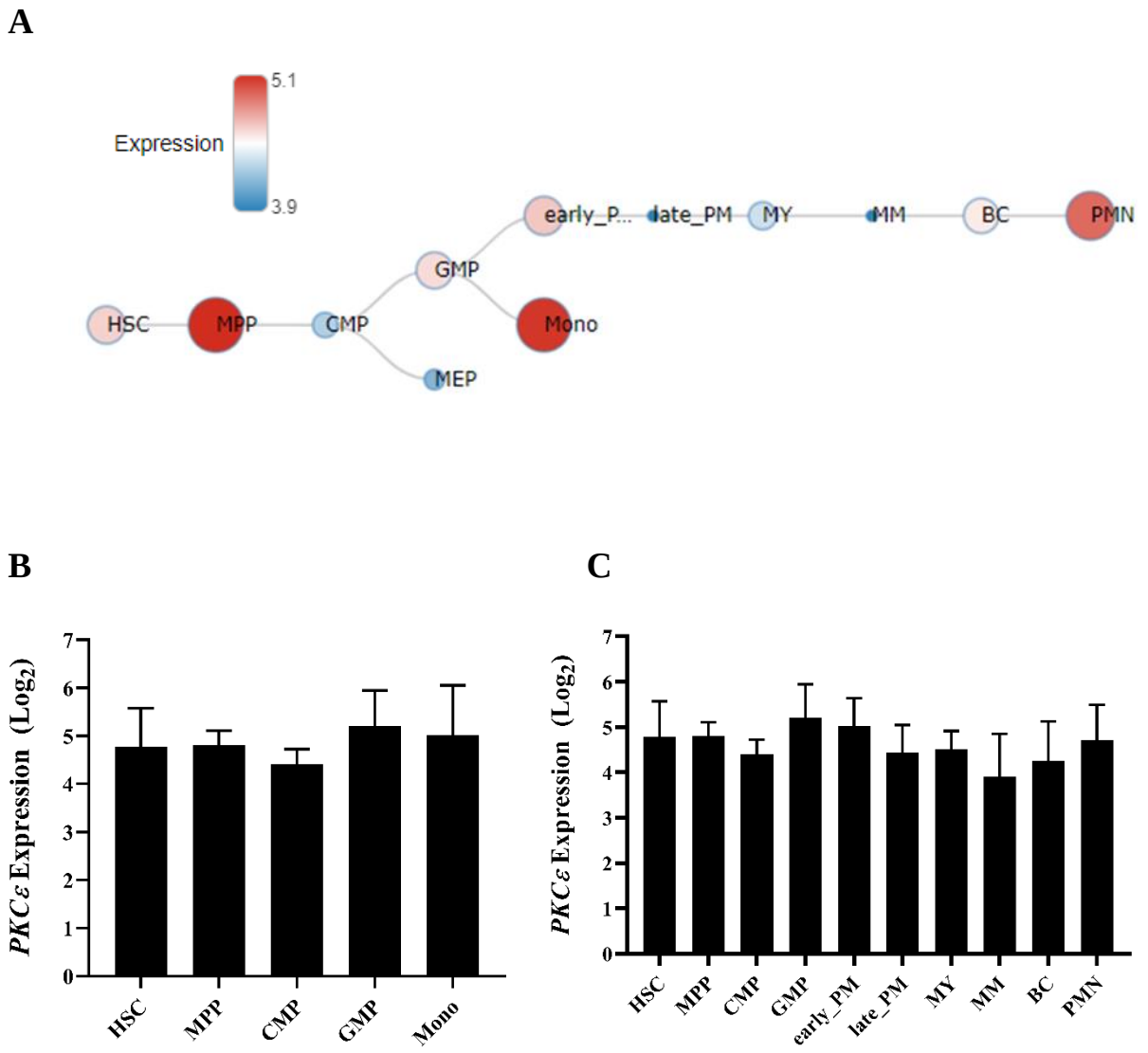

Figure 3.13: *PKCε* mRNA expression in HSC and myeloid progenitor cells

(A) Representative hierarchical differentiation tree showing *PKCε* mRNA expression (Log_2) in human haematopoietic progenitor cells, which had been determined by microarray (GSE42519; Rapin, *et al.*, 2014; probe-set 206248_at). The average *PKCε* expression in **(B)** monocytic and **(C)** granulocytic progenitors was determined by taking the mean of three probe-sets; 206248_at, 236459_at, and 226101_at; as described in 2.11.1; data represents mean+1SD. All probe-sets were accessed through Bloodspot (Bagger, *et al.*, 2016) which is where the hierarchical tree was generated. *Abbreviations; CLP; common lymphoid progenitor, HSC; haematopoietic stem cell; MMP multipotent progenitors; CMP; common myeloid progenitor, MEP; megakaryocyte-erythroid progenitor, GMP; granulocyte-macrophage progenitor, Early_P; early promyelocyte, Late_PM; late promyelocyte, MY; myelocyte, MM; metamyelocytes, BC; band cell, PMN; polymorphonuclear cells.*

3.3.3 Characterising PKCε protein expression in HSPC

To validate the mRNA expression data described above (3.3.2), PKCε protein expression was determined in human CB-derived HSPC (2.2) which comprise of committed progenitor cells and a small proportion (c10%) HSC. Protein expression is typically determined through western blot analysis; however, the complexity of the HSPC cultures means that identifying PKCε expression within specific populations using this methodology is challenging. In theory, this can be resolved using multi-parameter flow cytometry, as this methodology would allow HSPC to be concurrently labelled with a PKCε-specific antibody and markers associated with haematopoietic cell lineage commitment and differentiation. To optimise a flow cytometric method for determining endogenous PKCε protein expression in HSPC populations, two PKCε-specific antibodies, from different suppliers (2.8.3), were initially validated for their ability to detect intracellular PKCε in K562 cells overexpressing this protein. Both antibodies tested detected the ectopic expression of PKCε protein by western blot analysis (Figure 3.14A). However, neither the Cell Signalling or Protein Technology antibodies were able to detect the ectopic expression of PKCε through intracellular staining and flow cytometry, despite using different fixation and permeabilization approaches (Figure 3.14B-E). As a result, this methodology could not be used to determine endogenous PKCε protein expression in HSPC sub-populations. Although the resolution in terms of the cellular compartments which could be analysed was reduced, western blot analysis was instead used to determine the level of PKCε protein expression in normal haematopoietic cells.

In BM samples from 5 healthy donors, which were used to represent the total MNC compartment, western blot analysis showed that PKCε is endogenously expressed (Figure 3.15A). To determine PKCε protein expression throughout myeloid development, total protein lysates were generated from HSPC over 13 days of culture, in conditions which primarily support monocytic and granulocytic differentiation. These data showed that PKCε protein is expressed at undetectable levels in early myeloid progenitors (day 4 of culture) and that expression increases over time (Figure 3.15B). This supports the mRNA analysis (Figure 3.13) in suggesting that PKCε expression increases with myeloid cell differentiation. However, these total lysates are a combination of monocyte, granulocyte, and erythroid committed progenitors. Therefore, the lineage specific PKCε expression was examined in existing total protein lysates from monocytic-, granulocytic- and erythrocytic-committed progenitors (which had been selected for based on the differential expression of CD14 and CD36). This analysis showed

that PKCε protein is expressed in monocyte, granulocyte, and erythroid progenitors, at day 6 of culture (Figure 3.16). As normalisation to the loading control GAPDH, assumes that GAPDH expression within the samples is equivalent, it is only valid for making comparisons within the same cell type. However, although only conducted once due to the limited amount of material available, this lineage-specific expression profile is not inconsistent with the mRNA expression data (Figure 3.13). Furthermore, due to the number of cells required for western blot analysis, determining PKCε protein expression within the HSC compartment could not be achieved. Nevertheless, together with the mRNA expression profile (Figure 3.13), these data show that PKCε is endogenously expressed in myeloid committed progenitors and highlights a pattern of expression which is compatible with a role for PKCε in myeloid cell development.

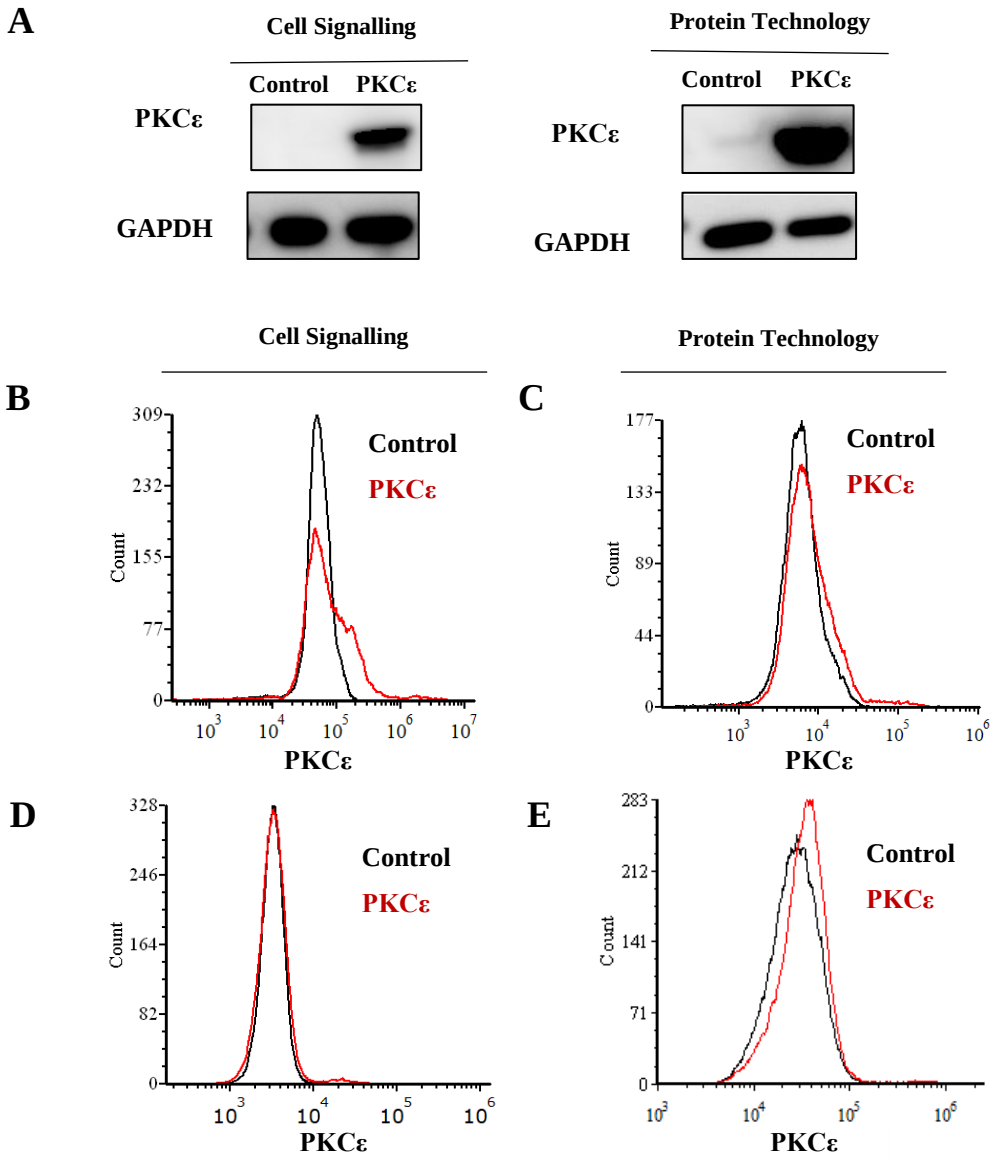

Figure 3.14: Ectopic PKCε protein expression could be determined by western blot analysis but not by flow cytometry

(A) Western blots showing PKCε expression in K562 cells transduced with the control or PKCε overexpression constructs (2.4.1.1). PKCε (MW-84kDa) expression was detected using the Cell Signalling Technologies antibody #2683 (clone 22B10; Table 2.10) or the Protein Technology polyclonal antibody (Table 2.10). PKCε expression is shown alongside GAPDH (MW-36kDa) expression, which was used as a loading control and detected using the ThermoFisher Scientific GAPDH antibody (clone GA1R; Table 2.10); n=1. The PKCε antibodies were applied to flow cytometry whereby K562 cells transduced with the control or PKCε overexpression constructs were permeabilized using the triton (**B** and **C**) or methanol (**D** and **E**) methodologies described in 2.8.3. Histograms show the staining profiles obtained with the Cell Signalling (**B** and **D**) and Protein Technology (**C** and **E**) antibodies in the control and PKCε overexpression K562 cells. *Validation of the PKCε construct is described in 3.3.4.1.*

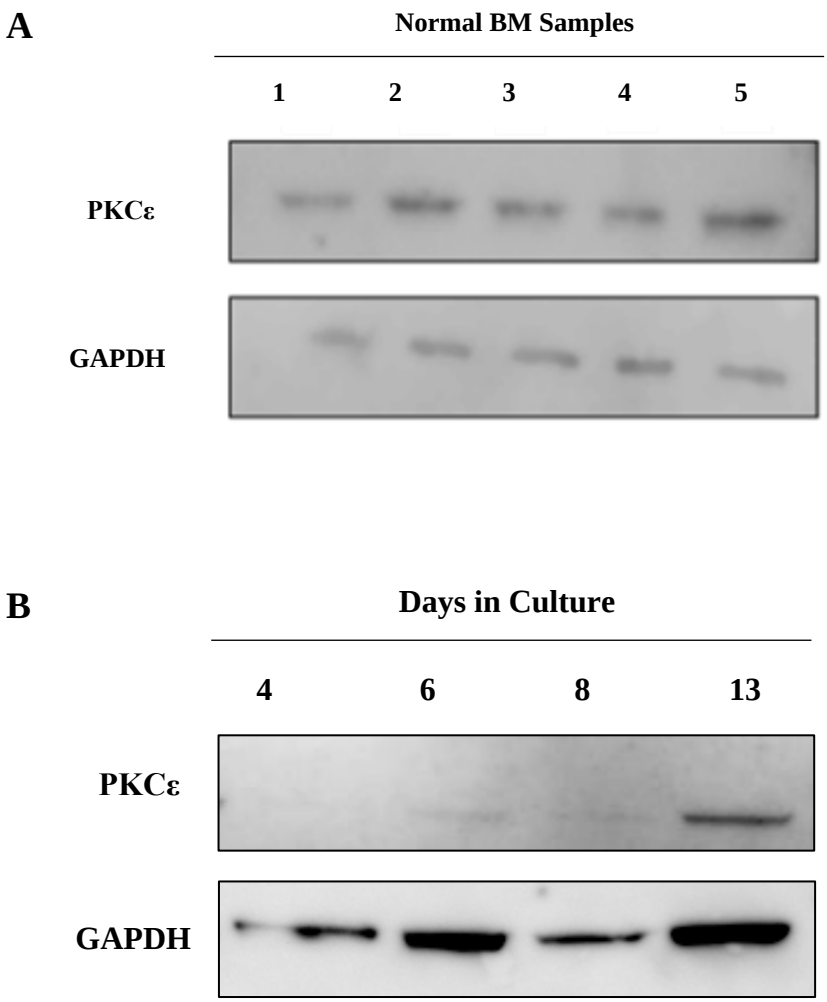

Figure 3.15: PKCε protein is endogenously expressed in normal bone marrow samples

Western blot showing PKCε (MW-84kDa) expression in **(A)** the cytosolic fraction of five independent bone marrow samples from healthy donors which were purchased from ALLCells and fractionated into cytosolic lysates as described in 2.7.1.2. *Lysates were provided by Prof. Alex Tonks;* n=1. PKCε expression was detected using the Cell Signalling Technologies antibody #2683 (clone 22B10; Table 2.10) and is shown alongside GAPDH expression (MW-36kDa), which was used as a loading control and detected using the ThermoFisher Scientific GAPDH antibody (clone GA1R; Table 2.10)*;* n=1 **(B)** Western blot analysis of HSPC over 13 days of culture in IMDM supplemented with IL-3, SCF, G-SCF and GM-CSF ($3S^{low}$G/GM; 2.2.4). PKCε expression was detected using the Cell Signalling Technologies antibody #2683 (clone 22B10; Table 2.10) and is shown alongside GAPDH expression (MW-36kDa), which was detected as described above (clone GA1R; Table 2.10)*;* n=1.

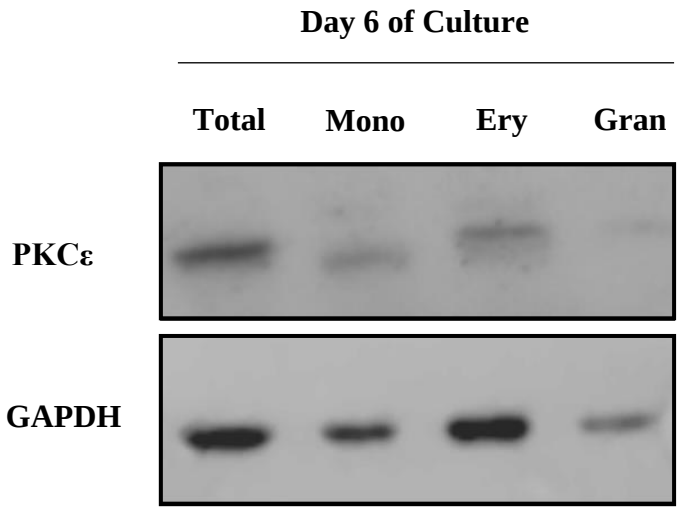

Figure 3.16: PKCε protein is expressed in lineage committed monocyte, granulocyte, and erythrocyte progenitor cells

Western blot of PKCε (MW-84kDa) expression in human HSPC, monocyte (mono; $CD14^{high}$), erythroid (ery; $CD14^{low}CD36^{high}$) and granulocyte (gran; $CD14^{low}CD36^{low}$) progenitors (Tonks, *et al.*, 2007) following 6 days of culture in $3S^{low}G/GM$ (2.2.4). PKCε expression was detected using the Cell Signalling Technologies antibody #2683 (clone 22B10; Table 2.10) and is shown alongside GAPDH (MW-36kDa) expression, which was used as an indicator of loading and was detected using the ThermoFisher Scientific GAPDH antibody (clone GA1R; Table 2.10); n=1; *Lysates were provided by Prof Alex Tonks.*

3.3.4 Assessing the effect of modulating PKCε expression on the growth and differentiation of human HSPC

3.3.4.1 Validating the PKCε overexpression construct

To force the ectopic expression of PKCε protein in cell lines and HSPC, a PKCε overexpression construct (PKCε_GFP_Puro^{R}; 2.4.1.1) was purchased from VectorBuilder™ and validated using a restriction enzyme digest (2.4.4.1) and Sanger sequencing (2.4.4.2). A restriction enzyme digest was carried out to validate the positional insertion of the *PRKCE* gene within the purchased plasmid. The plasmid was digested with the restriction enzyme, BamH1-HF®, as BamH1-HF® recognition sites were designed to flank the coding sequence of *PRKCE* gene (Figure 2.2). Following electrophoresis of the restriction enzyme digest products, the undigested DNA showed a single band (smear) at c11,000bp, representing the circular and supercoiled plasmid DNA (Figure 3.17A). In contrast, the digested cDNA migrated with two bands; one with a molecular weight of 9,380bp representing the linearized cDNA fragment, and a band at 2,226bp which corresponds to the molecular weight of the excised human *PRKCE* gene (Figure 3.17A). Therefore, this data indicates that the *PRKCE* gene is situated in the desired position within the plasmid sequence. However, this analysis could not confirm that the sequence of the *PRKCE* gene contained within the plasmid was correct. To determine this, Sanger sequencing was carried out by Eurofins Scientific (2.4.4.2). The resulting sequence aligned with the published human *PRKCE* gene sequence (NM_005400.3; Figure 3.17B), demonstrating the desired *PRKCE* gene sequence was contained within the plasmid.

Having validated the PKCε overexpression construct, the ectopic expression of PKCε protein following lentiviral transduction was evaluated in K562 cells using western blot analysis. This showed that K562 cells transduced with the PKCε overexpression construct had a higher PKCε expression than parental cells and the cells transduced with a control construct (GFP_Puro^{R}; 2.4.1.1) which showed undetectable levels of PKCε protein expression (Figure 3.18). This demonstrates the ability of the PKCε overexpression construct to drive ectopic PKCε protein expression in this cell line and suggests it would be suitable for studying the impact of PKCε overexpression in HSPC.

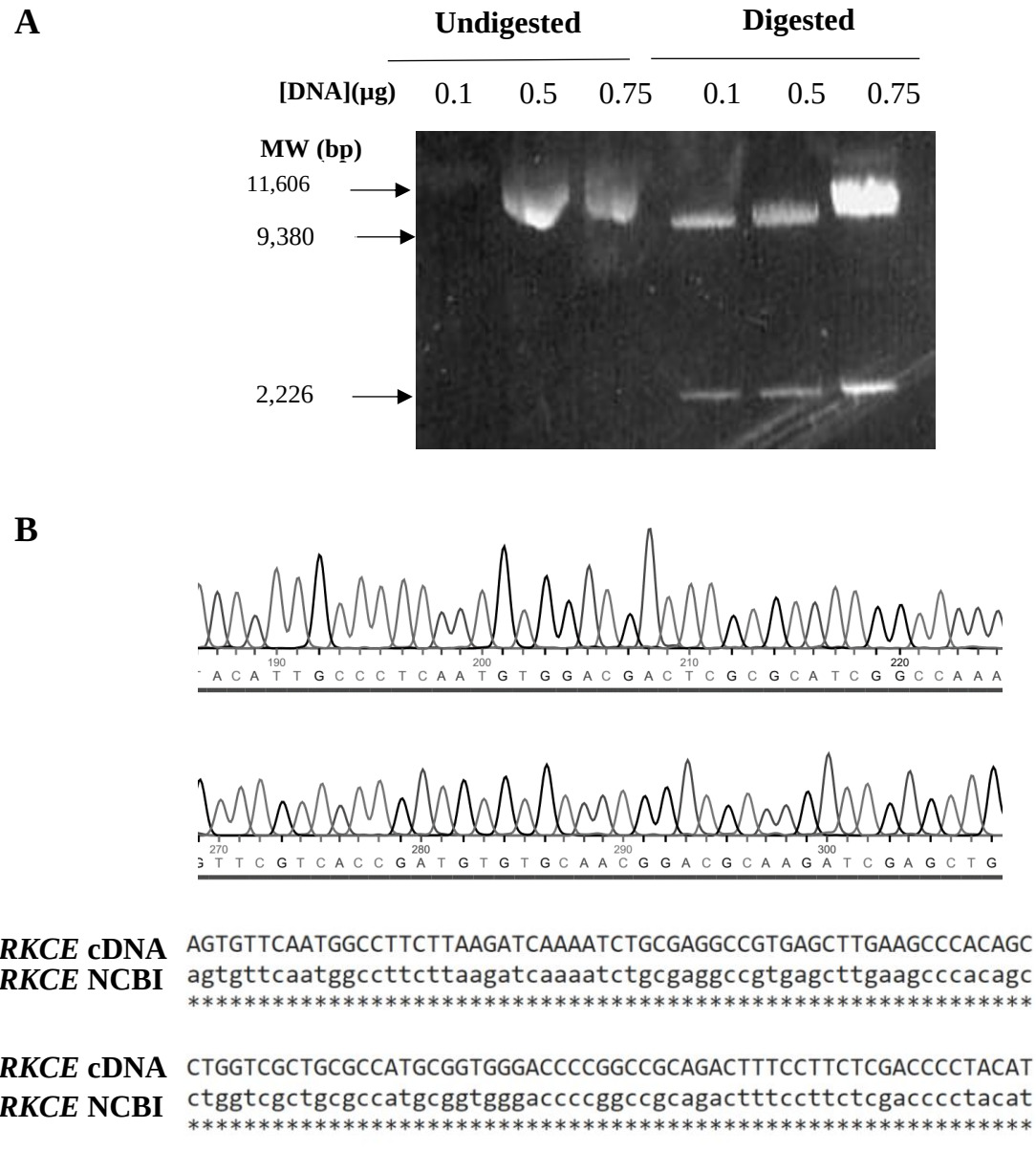

Figure 3.17: Validating the lentiviral PKCε overexpression construct

(A) Image showing the validation of the PKCε overexpression plasmid by restriction enzyme digest (2.4.4.1). Plasmid cDNA was incubated with the BamHI-HF® restriction enzyme (NEB), as described in 2.4.4.1. The image shows the bands detected using 0.1-0.75µg digested and undigested DNA following electrophoresis in a 1 (*w/v*) % agarose gel. **(B)** Representative sequencing data showing the *PRKCE* gene sequence contained within the PKCε overexpression plasmid (*PRKCE* cDNA), obtained by Sanger sequencing which was performed by Eurofins Scientific (2.4.4.2) using the *PRKCE* specific primers outlined in (Table 2.7). This is shown alongside the human *PRKCE* gene sequence obtained from the NCBI database (NM_005400.3; *PRKCE* NCBI) Sequence alignment between the two sequences is represented by *.

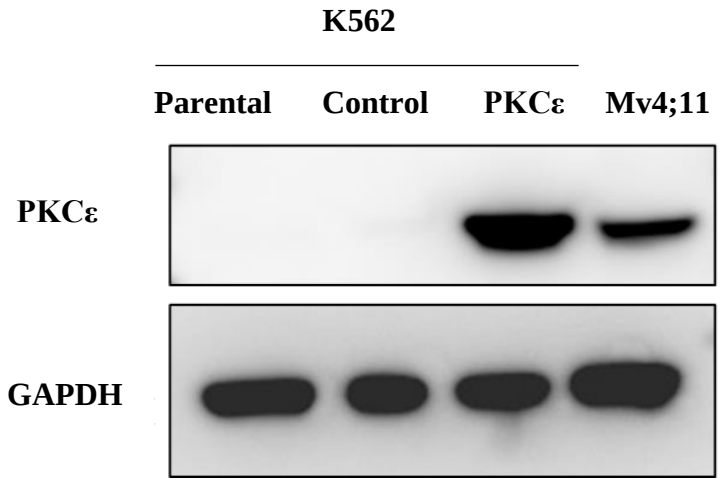

Figure 3.18: Validating ectopic PKCε protein expression in K562 cells

Western blot showing PKCε (MW-84kDa) expression in K562 cells transduced with the control or PKCε overexpression constructs (2.4.1.1). Before lysate generation, the AML cell lines underwent puromycin selection (10 µg/mL) to remove un-transduced cells (2.5.2). Parental K562 cells were used to show the endogenous PKCε expression in this cell line (not detectable), while Mv4;11 cells were used as a positive control. PKCε expression was detected using the Cell Signalling Technologies antibody #2683 (clone 22B10; Table 2.10) and is shown alongside GAPDH (MW-36kDa) expression, which was used as a loading control and detected using the ThermoFisher Scientific GAPDH antibody (clone GA1R; Table 2.10); n=1.

3.3.4.2 PKCε overexpression in HSPC promotes monocyte differentiation

Having validated the PKCε overexpression construct in a leukaemia cell line, the impact of PKCε overexpression in HSPC was assessed. HSPC were transduced with the control or PKCε overexpression lentiviral particles as described in 2.5.1. Following this, on day 3 of culture, the transduction efficiency was evaluated by flow cytometry through assessing the proportion of cells expressing the selectable marker GFP. The transduction efficiency in these cells was c10% for the PKCε overexpression construct and c20% for the control (Figure 3.19). This was sufficient for immunophenotypic analysis where transduced cells could be selectively gated for. However, for validating protein overexpression by western blot analysis, the cells needed to be sorted by FACS based on their GFP expression to remove the un-transduced (GFP^-) cells. This western blot analysis showed the ectopic expression of PKCε compared to the control cell lines (Figure 3.20), allowing the phenotypic consequences of PKCε overexpression in HSPC to be evaluated by flow cytometry.

For immunophenotypic analysis, the myeloid lineages were resolved using the lineage discrimination markers CD13 and CD36, into monocytic ($CD13^{high}CD36^{high}$) and granulocytic ($CD13^{low}CD36^{low}$) progenitor populations (Figure 2.7). The differentiation status of these lineage-committed progenitors was subsequently evaluated by assessing the expression pattern of specific myeloid maturation markers (CD34, CD11b, CD14, and CD15). In culture conditions which support myeloid differentiation, CD34 expression will decrease over time, as this transmembrane glycoprotein is restricted to early HSPC (Gustafson, *et al.*, 2015). In contrast, CD11b, CD14 and CD15 expression is progressively upregulated during differentiation, with mature monocytes being characterised by the expression of CD11b and CD14 and mature granulocytes by the expression of CD11b and CD15 (Gustafson, *et al.*, 2015). Although the culture conditions used (2.2.4) also support the differentiation of erythroid progenitors up to the EPO-dependent developmental stage, the impact of modulating PKCε expression on erythroid development was not investigated, as the monocyte and granulocyte lineages dominate these cultures. Furthermore, the role of PKCε expression in erythrocyte development has been reported extensively in the literature (Bassini, *et al.*, 1999, Li, *et al.*, 1996, Mirandola, *et al.*, 2006; 1.6.6).

Over 10 days of culture, PKCε overexpression significantly reduced the cumulative fold expansion of HSPC by 2.6-fold, compared to the control cells (Figure 3.21A). Using the lineage discriminator markers CD13 and CD36, the relative impacts on the fold expansion of the individual myeloid lineages was also assessed. This showed that at day 10, the expansion of monocyte progenitors was reduced by 1.6-fold in the PKCε overexpression cells compared to the control (Figure 3.21B). In contrast, the fold expansion of granulocytic progenitors was not affected by PKCε overexpression (Figure 3.21C). As cell proliferation and differentiation are often inversely linked, it was hypothesised that the reduced proliferation in the PKCε overexpression HSPC was a consequence of the induction of cell differentiation in the monocytic lineage.

Analysis of differentiation marker expression within the monocytic and granulocytic progenitor populations showed that, at day 10 of culture, PKCε overexpression promoted a 1.5-fold increase in CD11b expression and a 1.8-fold increase in CD14 expression, compared to the control cells (Figure 3.22 and Figure 3.23). This suggests that the reduction in monocytic proliferation is a result of increased differentiation. The ability of PKCε overexpression to promote monocytic differentiation was supported by morphological analysis. This indicated a higher proportion of macrophages in the PKCε overexpression culture compared to the control (Figure 3.26), however, this aspect of the analysis was only conducted once. In contrast, PKCε overexpression did not significantly affect the expression of CD11b or CD15 on granulocytic progenitors (Figure 3.24 and Figure 3.25). The pro-differentiation phenotype observed in HSPC overexpressing PKCε is concordant with the mRNA (3.3.2) and western blot (3.3.3) analysis, where PKCε expression increased with myeloid cell differentiation. Modulating PKCε expression in HSPC suggests that the propensity of PKCε to promote myeloid cell differentiation is selective for monocyte differentiation, although the granulocytic data is equivocal. Importantly, this data also indicates that PKCε upregulation in AML is unlikely to contribute to the pathogenesis of AML through perturbing myeloid cell differentiation.

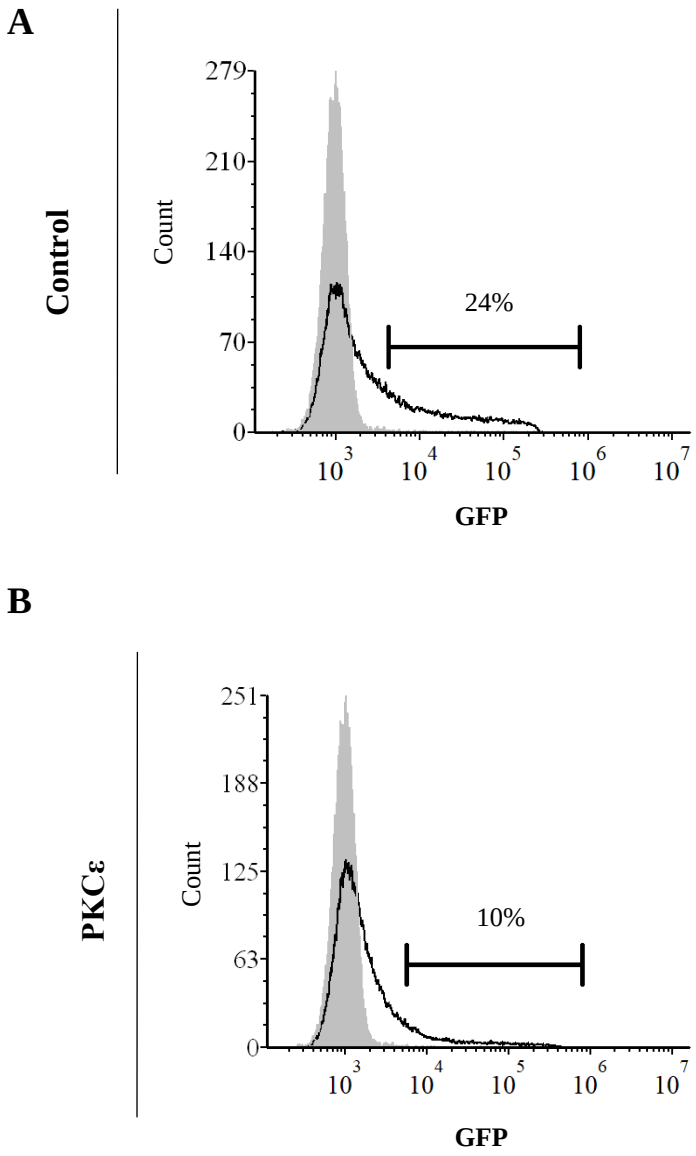

Figure 3.19: Assessing the transduction efficiency of the control and PKCε overexpression constructs in HSPC

Representative histograms showing the transduction efficiency of the **(A)** control and (**B)** PKCε overexpression constructs (Figure 3.18) in HSPC following two days of lentiviral infection (2.5.1). GFP expression was used as a marker of successful transduction, where un-transduced HSPC were to set the threshold for GFP expression (grey).

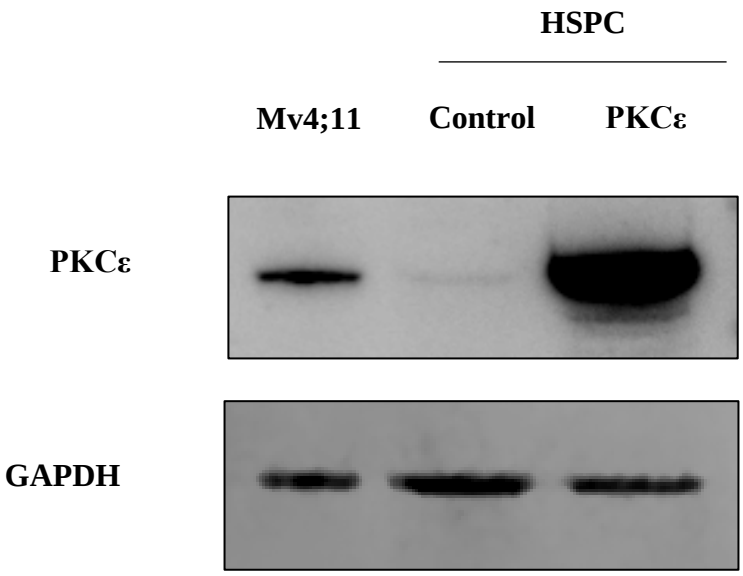

Figure 3.20: Validating PKCε protein overexpression in HSPC

Western blot showing PKCε (MW-84kDa) expression in HSPC transduced with the control or PKCε overexpression constructs (Figure 3.18) following 13 days of culture in $3S^{Low}G/GM$ (2.2.4). Before lysate generation, the cells were enriched (>90%) by FACS based on their GFP expression to remove any un-transduced cells (2.10). PKCε expression was detected using the Cell Signalling Technologies antibody #2683 (clone 22B10; Table 2.10), where Mv4;11 cells were used as a positive control. PKCε expression is shown alongside GAPDH (MW-36kDa) expression, which was used as a loading control and detected using the ThermoFisher Scientific GAPDH antibody (clone GA1R; Table 2.10); n=1.

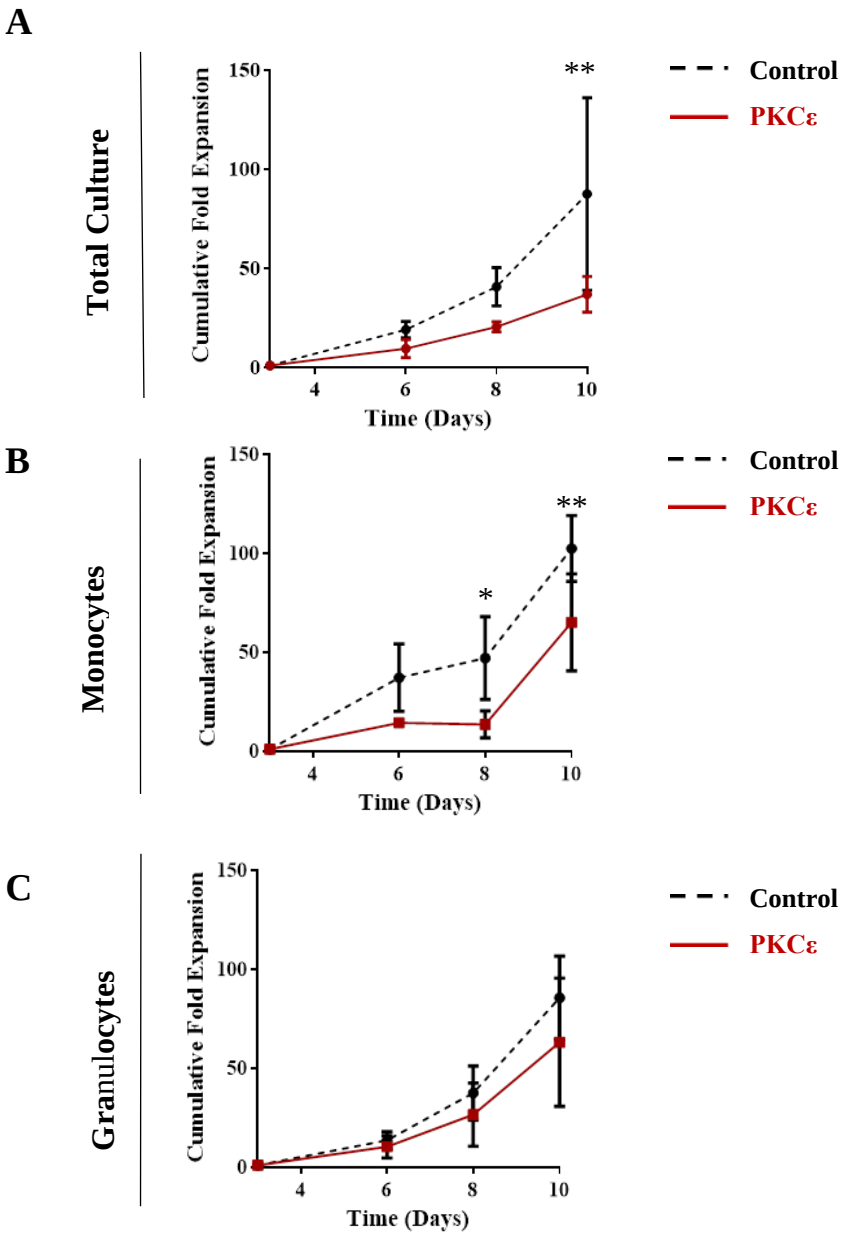

Figure 3.21: PKCε overexpression reduces the fold expansion of HSPC

Line graphs showing the cumulative fold expansion of HSPC transduced with the control or PKCε overexpression constructs (Figure 3.18) over 10 days of culture in $3S^{Low}G/GM$ (2.2.4); **(A)** total culture, **(B)** monocyte ($CD13^{high}CD36^{high}$) progenitors and **(C)** granulocyte ($CD13^{low}CD36^{low}$) progenitors. Analysis commenced at day 3 of culture; n=4, data represents the mean ±1SD. The statistical significance between the control and PKCε overexpression cultures at each time point was determined using a two-way ANOVA with Bonferroni post-test comparison and was deemed significant; * $p<0.05$, ** $p<0.01$.

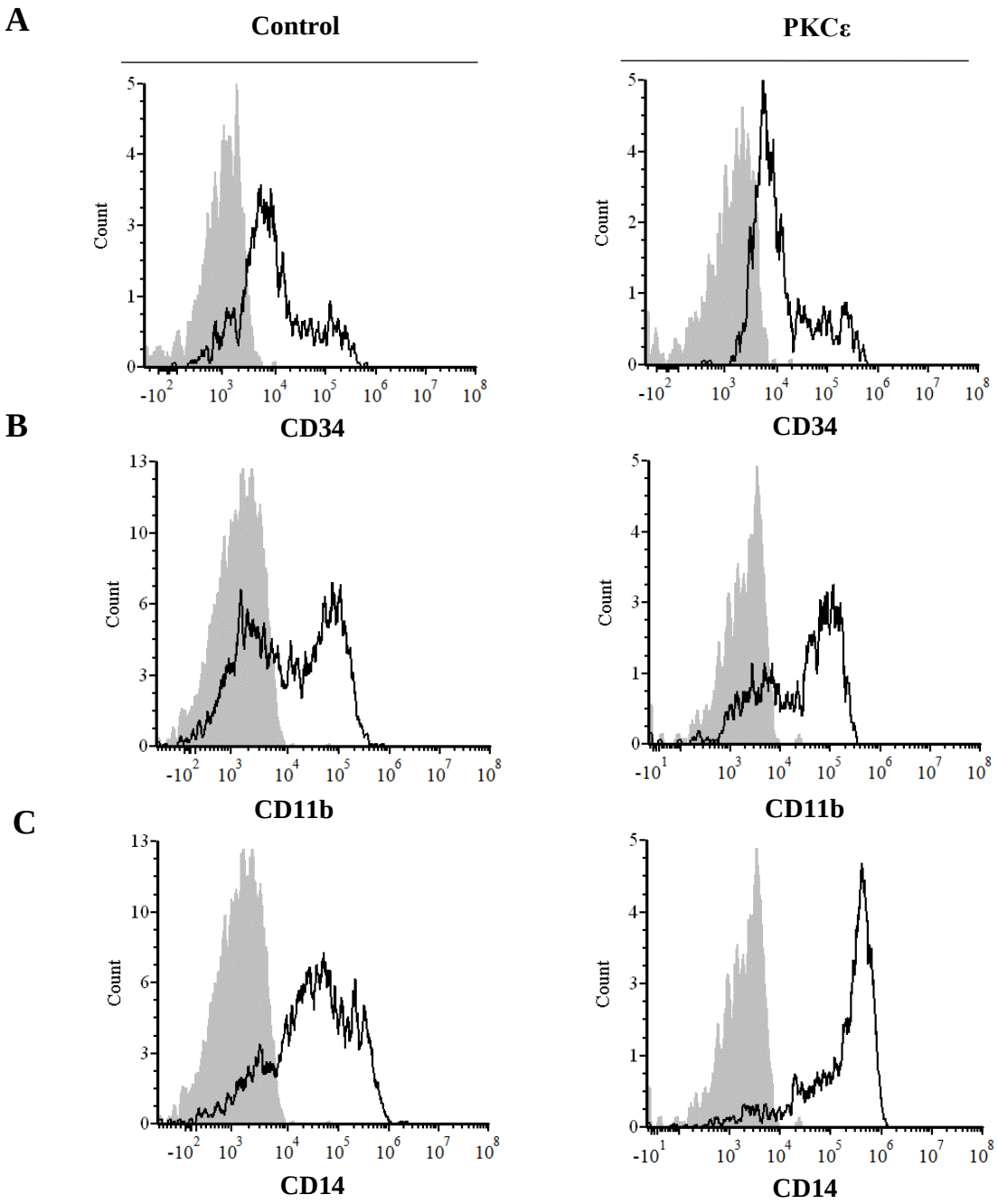

Figure 3.22: The effect of PKCε overexpression on monocyte differentiation marker expression

Representative histograms showing the expression of **(A)** CD34, **(B)** CD11b and **(C)** CD14 on monocyte progenitor cells ($CD13^{high}CD36^{high}$) transduced with the control or PKCε overexpression constructs (Figure 3.18), following 3 days for CD34 and 8 days of culture in for CD11b and CD14 in $3S^{Low}G/GM$ (2.2.4). The expression of these differentiation markers is shown alongside cells stained with an isotype control (grey).

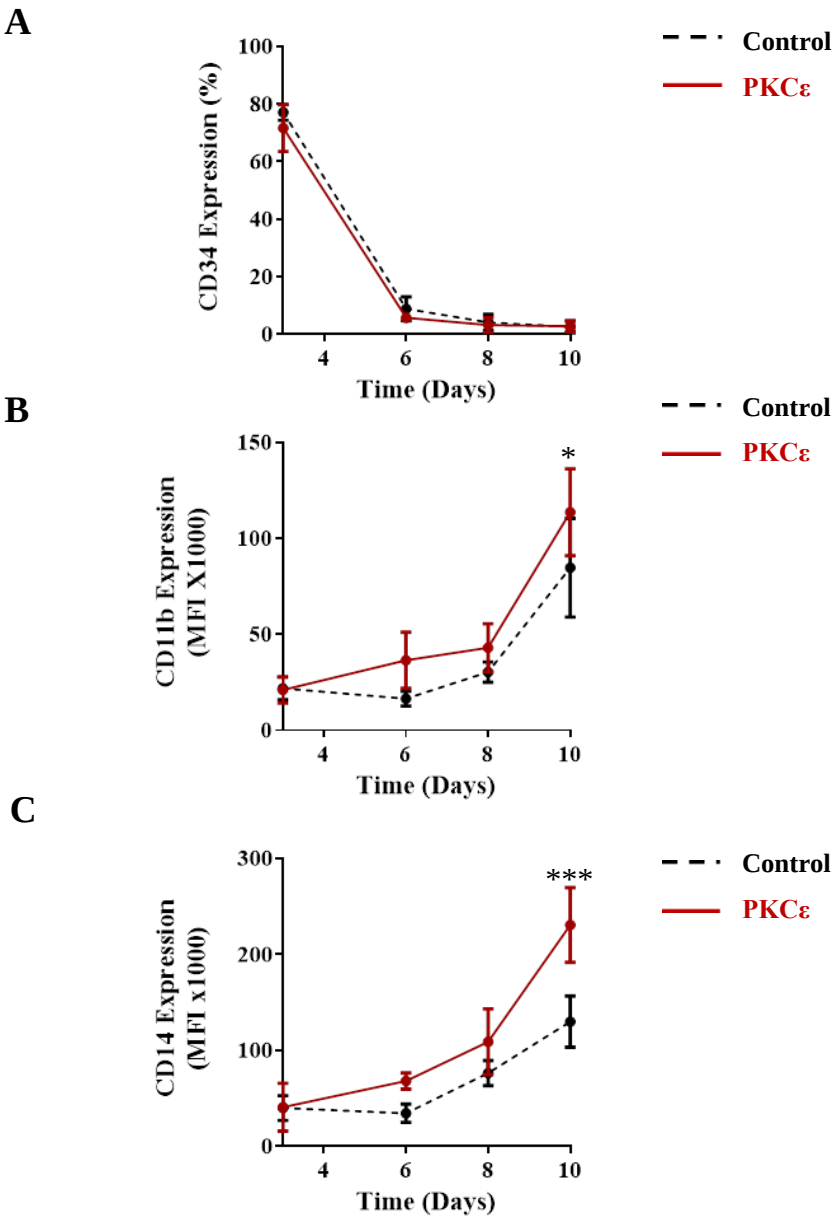

Figure 3.23: PKCε overexpression promotes the upregulation of maturation markers in monocyte progenitors

Line graphs showing the immunophenotypic profile of monocyte progenitors ($CD13^{high}CD36^{high}$) transduced with the control or PKCε overexpression constructs (Figure 3.18) over 10 days of culture in $3S^{low}G/GM$ (2.2.4). Analysis commenced at day 3 of culture. Cells were stained for **(A)** CD34, **(B)** CD11b and **(C)** CD14 expression (Figure 3.22); CD34 expression is represented by the proportion of positive cells (%) while CD11b and CD14 expression is represented using the fluorescence intensity (MFI x1000); n=3, data represent mean ± 1SD. Statistical significance between the marker expression of the control and PKCε overexpression cultures at each time point was determined using two-way ANOVA with Bonferroni post-test comparison and was deemed significant; *$p<0.05$, ***$p<0.001$.

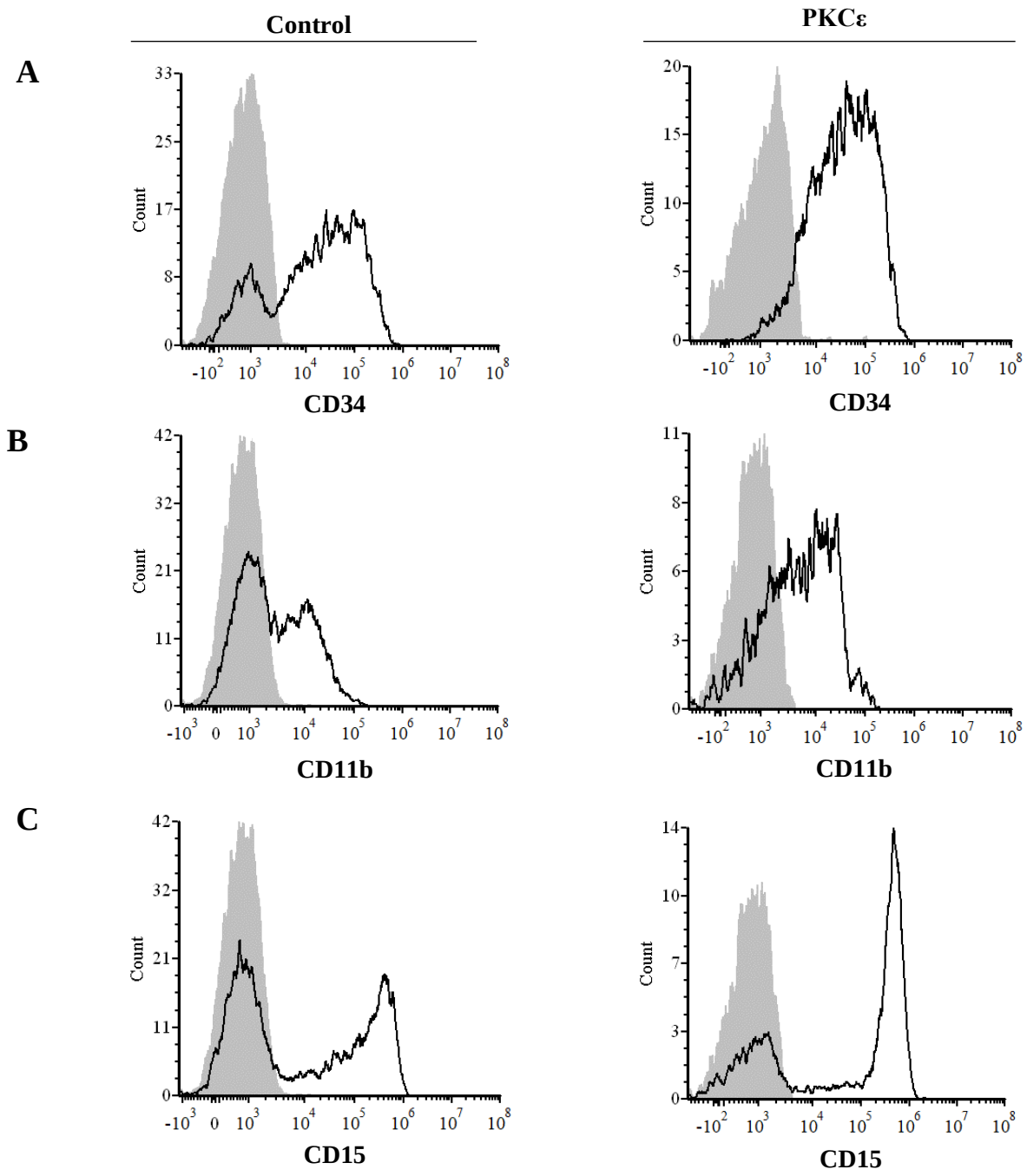

Figure 3.24: The effect of PKCε overexpression on granulocyte differentiation marker expression

Representative histograms showing the expression of **(A)** CD34, **(B)** CD11b and **(C)** CD15 on granulocyte progenitor cells ($CD13^{low}CD36^{low}$) transduced with the control or PKCε overexpression constructs (Figure 3.18) following 3 days for CD34 and 8 days of culture in for CD11b and CD14 in $3S^{Low}G/GM$ (2.2.4). The expression of these differentiation markers is shown alongside cells stained with an isotype control (grey).

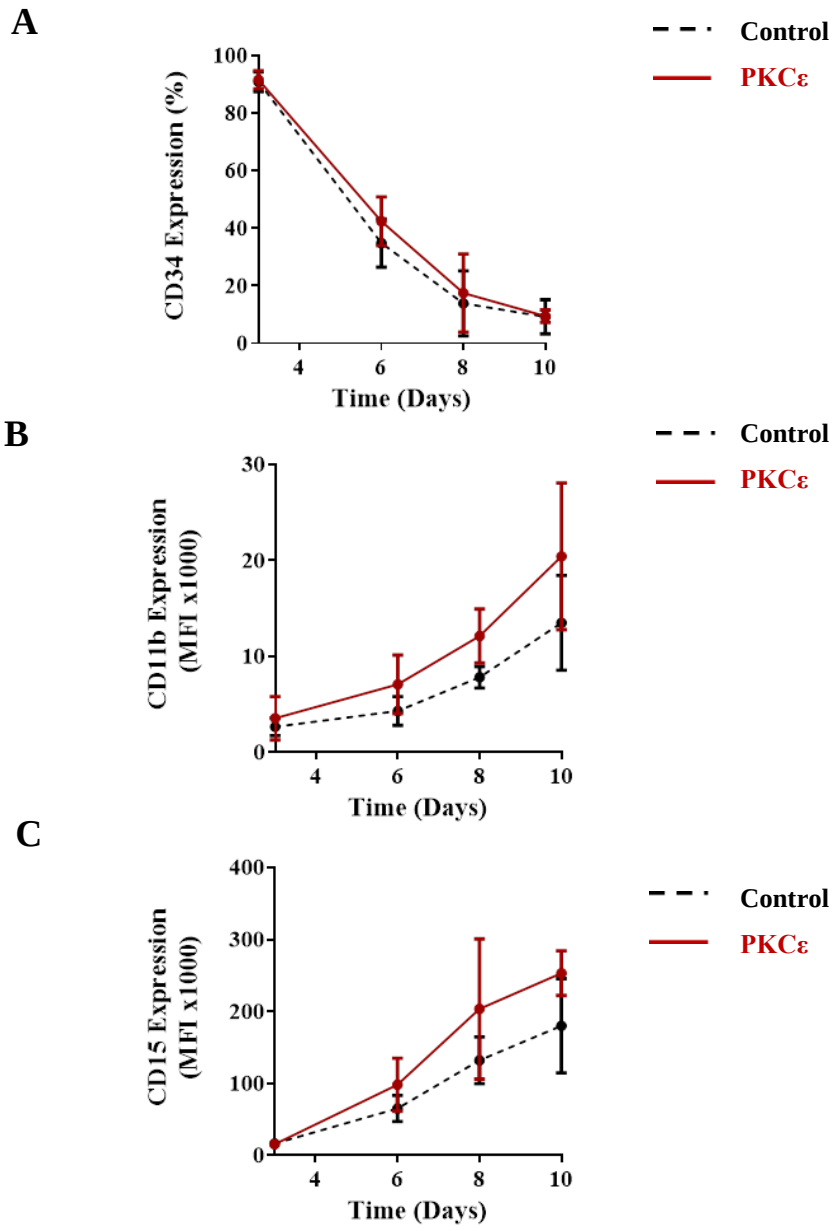

Figure 3.25: PKCε overexpression does not significantly affect granulocyte differentiation

Line graphs showing the immunophenotypic profile of granulocytic progenitor cells ($CD13^{high}CD36^{high}$) transduced with the control and PKCε overexpression constructs (Figure 3.18) over 10 days of culture in $3S^{Low}G/GM$ (2.2.4). Analysis commenced at day 3 of culture. Cells were stained for **(A)** CD34, **(B)** CD11b and **(C)** CD15 expression (Figure 3.24); CD34 expression is represented by the proportion of positive cells (%) while CD11b and CD15 expression is represented using the fluorescence intensity (MFI x1000); n=3, data represent mean ±1SD. Statistical significance was determined using two-way ANOVA with Bonferroni post-test comparison and was deemed non-significant.

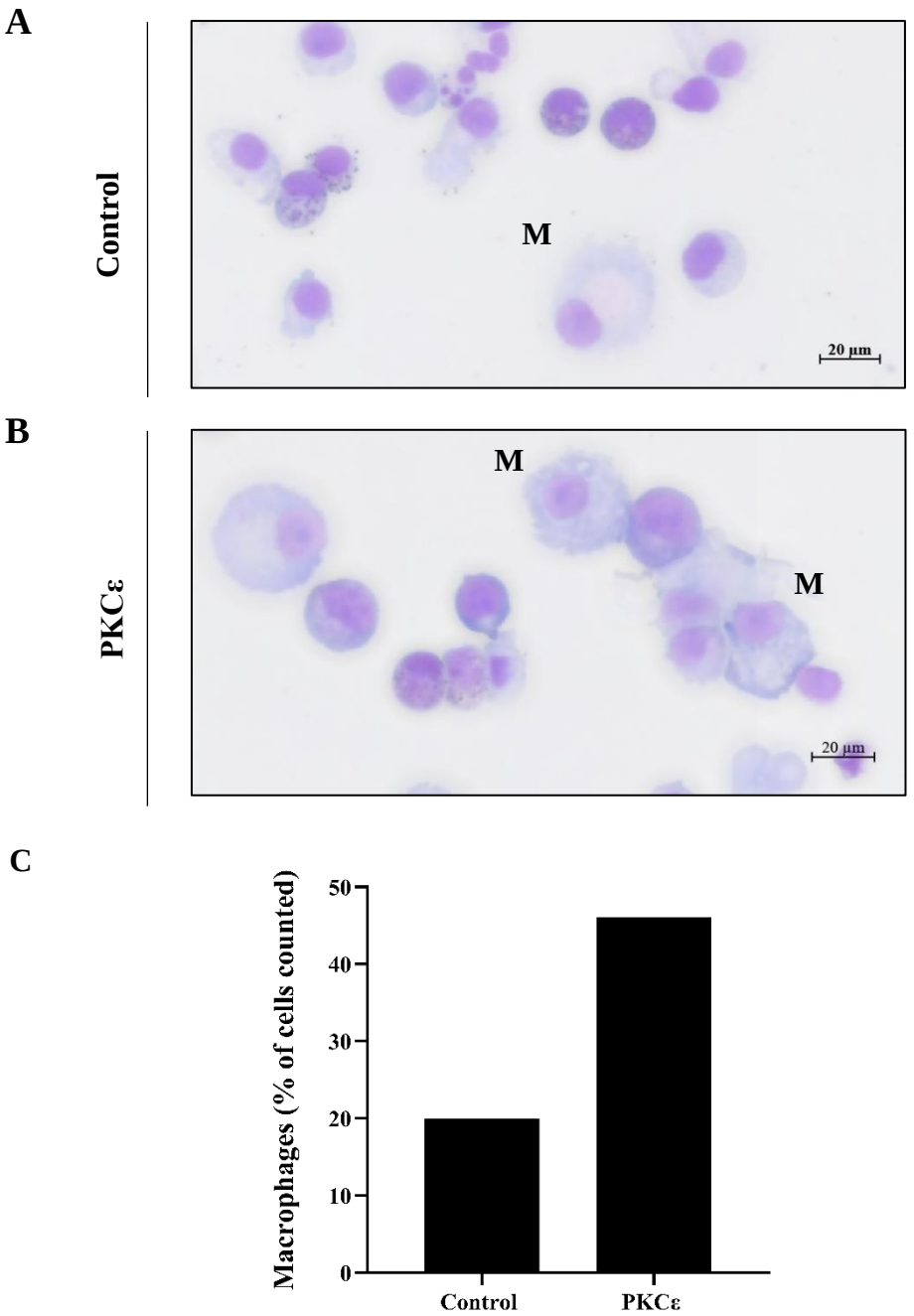

Figure 3.26: Effect of PKCε overexpression on the morphology of HSPC

Representative images showing the morphology of HSPC transduced with the **(A)** control and **(B)** PKCε overexpression constructs (Figure 3.18) following 10 days of culture $3S^{Low}G/GM$ (2.2.4). Cells were stained with a Giemsa differential stain and slides were imaged using a Zeiss Axioscan Z1 slide scanner at 20x magnification as described in 2.6; scale bar-20 µm; **M** indicates cells with macrophage-like morphology; n=1. **(C)** Bar chart showing the number of macrophages (% of cells counted) from the imaged cytospins of HSPC transduced with the control or PKCε constructs (control; 22/110 cells , PKCε; 53/116 cells).

3.3.4.3 PKCε knockdown does not significantly impact myeloid cell differentiation

Overexpression of PKCε in HSPC promoted monocyte differentiation (3.3.4.2). To establish whether PKCε is required for normal haematopoietic cell development, the impact of reducing PKCε expression in HSPC was investigated using shRNA-mediated knockdown systems. The knockdown efficiency of five PKCε-targeted shRNA constructs (Table 2.4) were first assessed in U937 cells, a cell line which endogenously expresses PKCε protein (Figure 3.27). This analysis showed that constructs 480 ,476, 477 were the most efficacious, reducing PKCε protein expression compared to the control (shRNA_Puro^R with no mammalian target; Table 2.4) by c70% to c80% (Figure 3.27). Whilst the 480-shRNA construct had a high efficacy of PKCε knockdown, the growth of these cells was severely impaired. As this was the only construct to demonstrate this phenotype it was assumed that this was due to off-target effects. Consequently, this construct was not used in subsequent analysis.

To explore the effects of reducing PKCε expression in HSPC, the PKCε-targeting shRNA constructs 476 and 477 were purchased in GFP co-expression constructs (486 and 485; Table 2.4), as the addition of GFP facilitates the analysis of transduced cells within a mixed population, where antibiotic selection is not suitable, such as HSPC cultures. The transduction efficiency of the shRNA constructs in HSPC was assessed using GFP expression and showed an efficiency of between 50% and 70% (Figure 3.28). As with the overexpression constructs, the cells were sorted by FACS based on their GFP expression to allow the reduction in PKCε expression by each construct to be determined by western blot analysis. Compared to HSPC transduced with the control (no mammalian target) shRNA construct, a c40% and c90% reductions in PKCε protein expression were observed in HSPC transduced with the 485 and 486 PKCε-targeted shRNA constructs respectively (Figure 3.29).

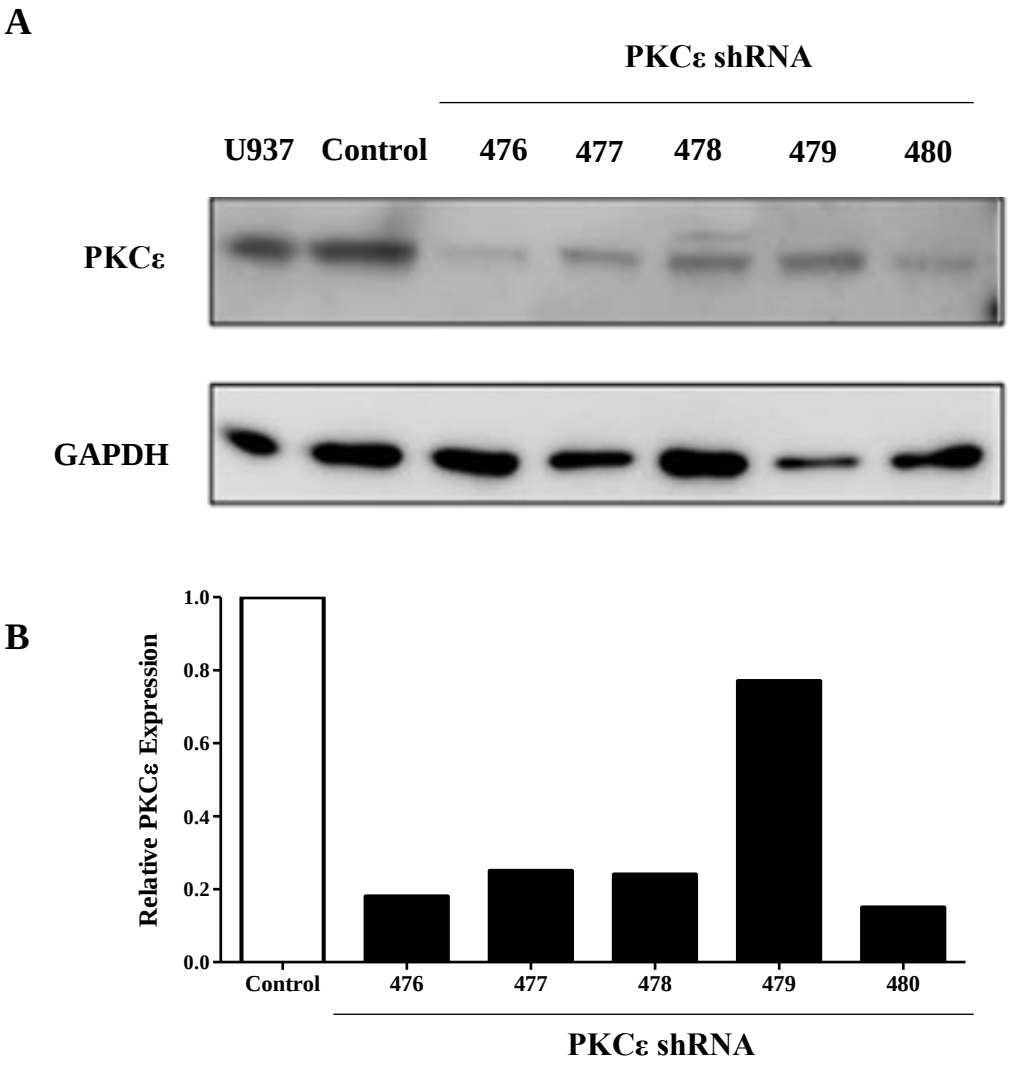

Figure 3.27: Assessing the efficacy of PKCε-targeted shRNA constructs in U937 cells

(A) Western blot showing PKCε (MW-84kDa) expression in U937 cells transduced with the control (shRNA_Puro^R with no mammalian target; 214 Table 2.4) or PKCε-targeted shRNA constructs (PKCε_shRNA_Puro^R;476-480; Table 2.4). Before lysate generation, the cell lines underwent puromycin selection (10 µg/mL) to remove un-transduced cells (2.5.2). PKCε expression was detected using the Cell Signalling Technologies antibody #2683 (clone 22B10; Table 2.10) and is shown alongside GAPDH (MW-36kDa) expression, which was used as a loading control and detected using the ThermoFisher Scientific GAPDH antibody (clone GA1R; Table 2.10). **(B)** Bar chart showing PKCε expression in U937 cells transduced with the PKCε-targeted shRNA constructs. PKCε expression was quantified by densitometry analysis using Image J (Fiji), normalised to loading (GAPDH expression) and is shown relative to the expression of U937 cells transduced with the control shRNA construct (2.7.5); n=1.

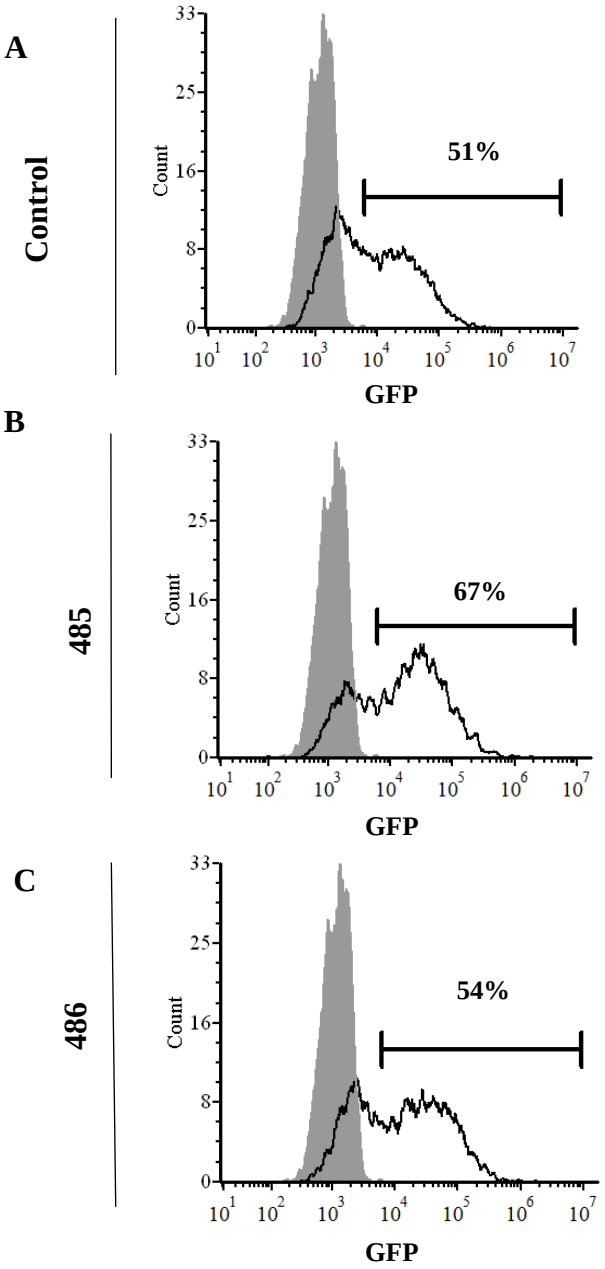

Figure 3.28: Representative histograms showing the transduction efficiency of the control and PKCε-targeted shRNA constructs in HSPC

Representative histograms showing the transduction efficiency of the **(A)** shRNA control and PKCε-targeted **(B)** 485 and **(C)** 486 knockdown constructs in HSPC on day 3 of culture (two days after infection; 2.5.1). GFP expression was used as a marker of transduction efficiency where un-transduced (GFP^-) HSPC were used to determine the threshold for GFP expression (grey).

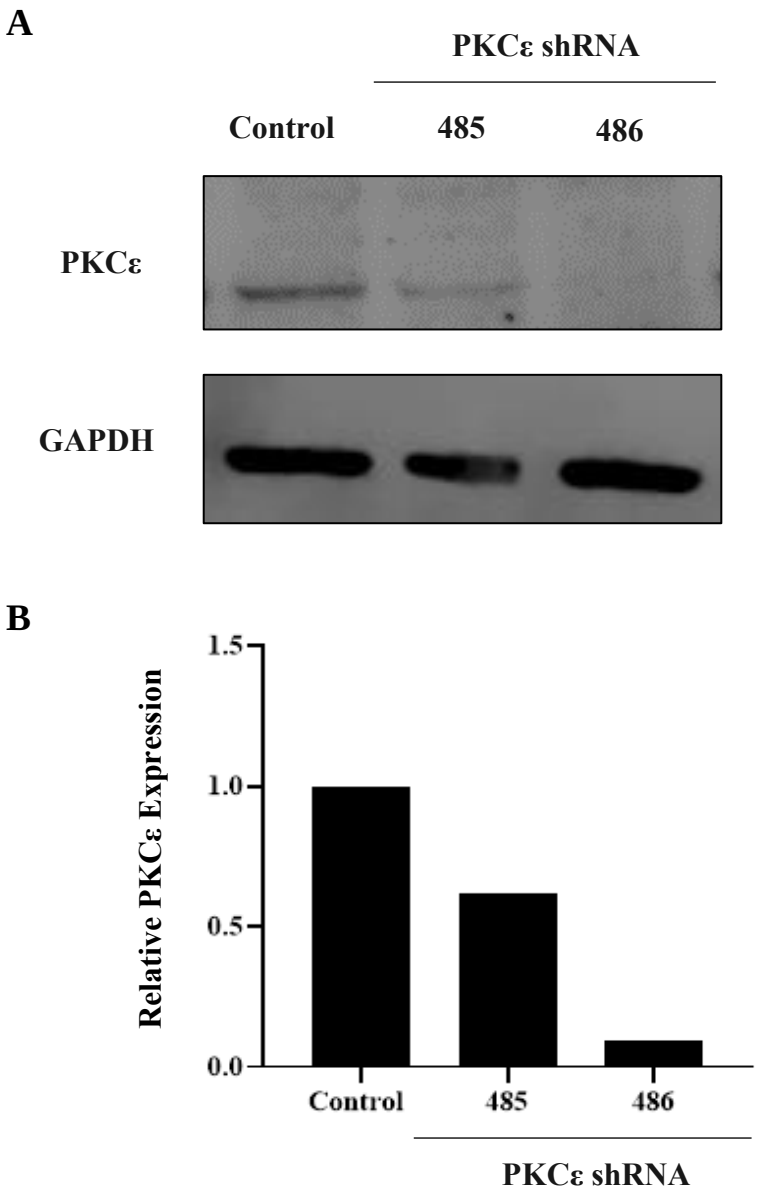

Figure 3.29: Validating PKCε knockdown efficiency in HSPC

(A) Example western blot and **(B)** densitometric quantification of PKCε (MW-84kDa) expression in HSPC transduced with the control (shRNA_GFP with no mammalian target;497; Table 2.4) or PKCε-targeted shRNA constructs (485 and 486; Table 2.4) after 10 days of culture in $3S^{Low}G/GM$ (2.2.4). Before lysate generation, the cells were enriched (>90%) by FACS based on GFP expression to remove any un-transduced cells (2.10). PKCε expression was detected using the Cell Signalling Technologies antibody #2683 (clone 22B10; Table 2.10) and is shown alongside GAPDH (MW-36kDa) expression, which was used as a loading control and was detected using the ThermoFisher Scientific GAPDH antibody (clone GA1R; Table 2.10). Densitometry analysis was conducted using Image J (Fiji). PKCε expression was calculated relative to loading (GAPDH expression) and normalised to the expression of HSPC cells transduced with the control shRNA construct (2.7.5); n=1.

Having determined the transduction and knockdown efficiency of the PKCε-targeted shRNA constructs in HSPC, the resulting impact of reduced PKCε expression on cell proliferation and differentiation was determined by flow cytometry as described in 3.3.4.2. Compared to the control, PKCε knockdown did not significantly impact the growth of HSPC over 10 days of culture, although a trend towards reduced growth in the culture with the highest knockdown efficiency (486-shRNA) was observed (Figure 3.30A). Given that PKCε overexpression suppressed the growth of HSPC (Figure 3.21), it was hypothesised that reducing PKCε expression may extend the proliferative capacity of these cells. As a result, the growth of the knockdown cultures was followed for a longer period (17 days), but no significant differences in growth were observed at the longer time point (n=2; data not shown). When assessing the impact of PKCε knockdown on the growth of the monocytic and granulocytic progenitor cells individually, the fold expansion of monocytic progenitors was not affected by PKCε knockdown (Figure 3.30B). In contrast, PKCε knockdown reduced the cumulative fold expansion of the granulocyte progenitors compared to the control, by 1.4-fold (485-shRNA) and 2.7-fold (486-shRNA; Figure 3.30C), where the effect size was concordant with the degree of knockdown efficiency. As granulocytes make up most of the cultures (60%-80%), it is likely that the slight reduction in the growth of the bulk PKCε knockdown cultures is due to the reduced proliferative output of the granulocytic progenitors.

In terms of the effect of reducing PKCε expression on myeloid differentiation, a trend of reduced CD11b and CD14 expression on monocyte progenitors was observed, although the small effect size meant that significance was not achieved (Figure 3.31). While this finding is not inconsistent with a role for PKCε in monocyte differentiation, implicated by the overexpression analysis, these data suggest that PKCε is not essential for monocyte development. Furthermore, PKCε knockdown did not affect the expression of CD11b or CD15 on granulocyte progenitors compared with the control cultures (Figure 3.32). Therefore, these data suggest that PKCε does not play an endogenous role in granulocyte development and that the reduction in granulocyte growth is not due to altered differentiation. Overall, although PKCε can promote monocyte differentiation in some capacity, expression of this kinase is not essential for monocyte development. In contrast, the impact on granulocyte growth suggests that reducing PKCε may impact the viability of this cellular compartment.

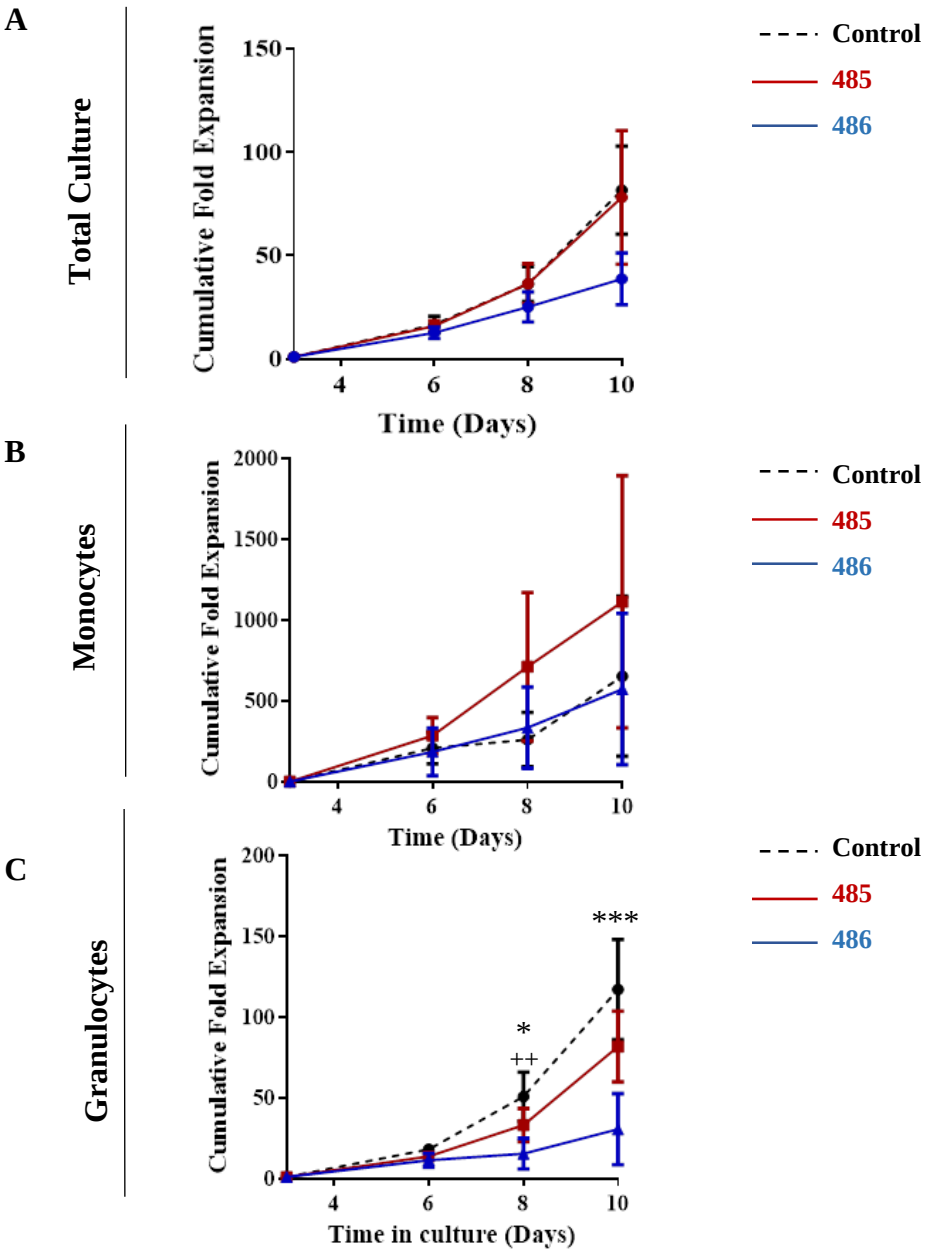

Figure 3.30: PKCε knockdown reduces the fold expansion of granulocyte progenitors

Line graphs showing the cumulative fold expansion of HSPC transduced with the control or PKCε-targeted shRNA constructs 485 and 486, over 10 days of culture in $3S^{Low}G/GM$ (2.2.4). **(A)** total culture, **(B)** monocyte ($CD13^{high}CD36^{high}$) and **(C)** granulocyte ($CD13^{low}CD36^{low}$) progenitors. Analysis commenced at day 3 of culture; n=4; data represents the mean ± 1SD. Statistical significance between the control and knockdown cultures at each timepoint was determined using two-way ANOVA with Bonferroni post-test comparison and was deemed significant (*control vs 485; +control vs 486);*p<0.05; ** p<0.01, ***p<0.001.

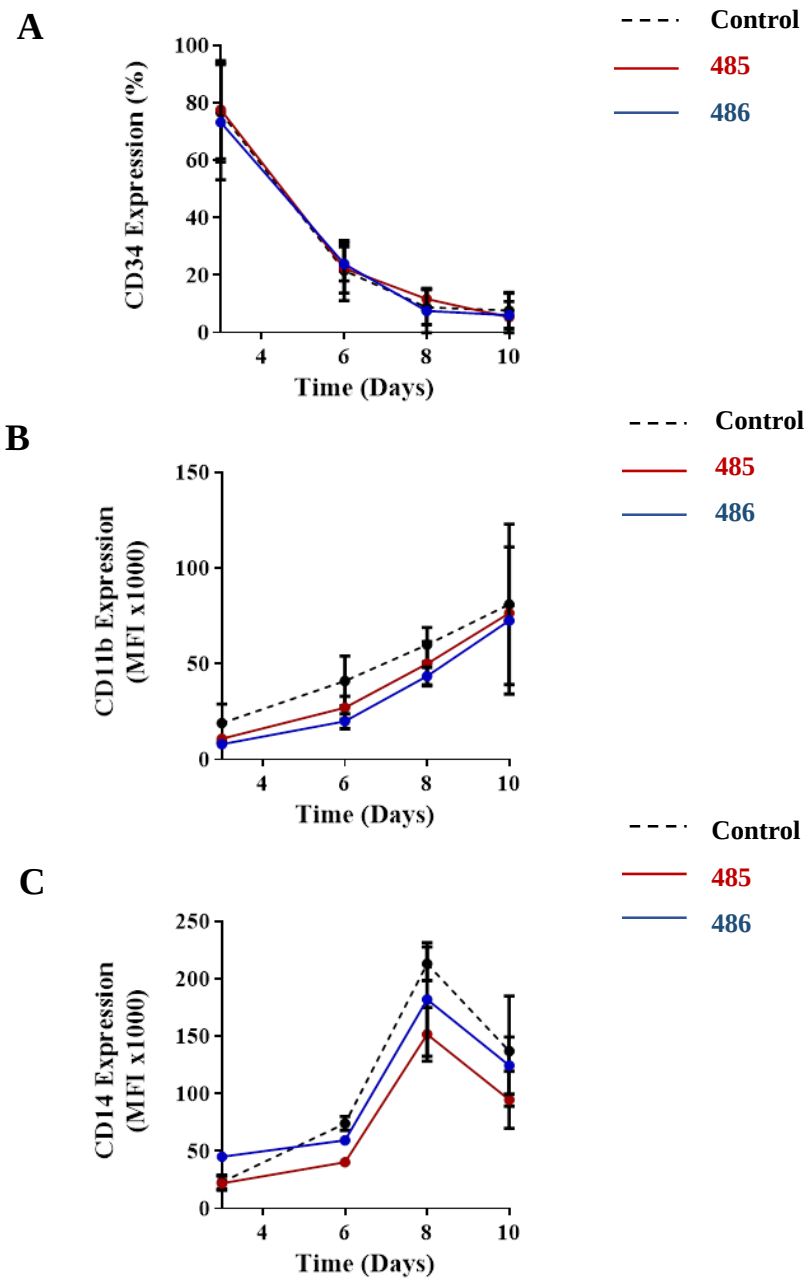

Figure 3.31: PKCε knockdown does not significantly affect monocyte differentiation

Line graphs showing the immunophenotypic profile of monocyte ($CD13^{high}CD36^{high}$) progenitor cells transduced with the control or PKCε-targeted shRNA constructs 485 and 486, over 10 days of culture in $3S^{Low}G/GM$ (2.2.4). Analysis commenced at day 3 of culture. Cells were stained for **(A)** CD34, **(B)** CD11b and **(C)** CD14 expression; CD34 expression is represented by the proportion of positive cells (%) while CD11b and CD14 expression is represented using the fluorescence intensity (MFI x1000); n=3, data represent mean ± 1SD. Statistical significance was determined by two-way ANOVA with Bonferroni post-test comparison; and was deemed non-significant.

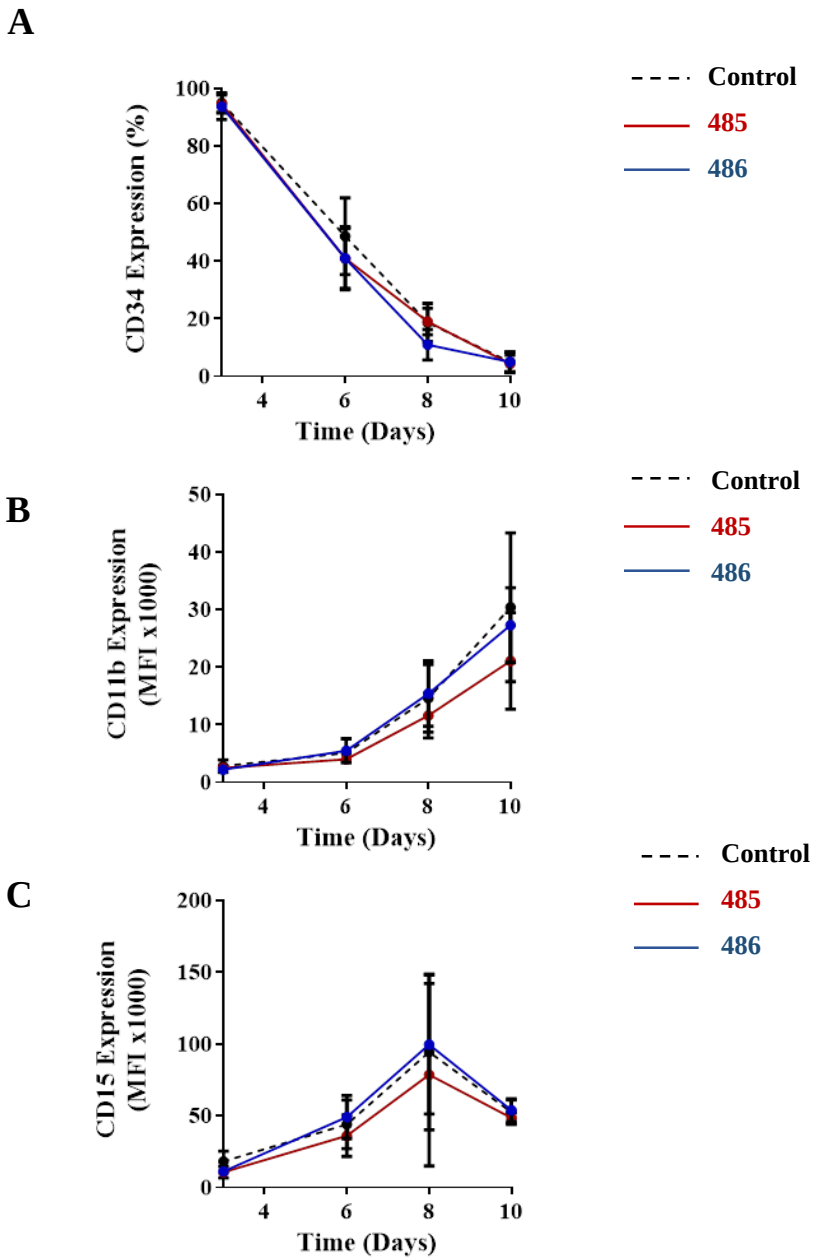

Figure 3.32: PKCε knockdown does not significantly affect granulocyte differentiation

Line graphs showing the immunophenotypic profile of granulocyte ($CD13^{low}CD36^{low}$) progenitor cells transduced with the control or PKCε-targeted shRNA constructs 485 and 486, over 10 days of culture in $3S^{Low}G/GM$ (2.2.4). Analysis commenced at day 3 of culture. Cells were stained for **(A)** CD34, **(B)** CD11b and **(C)** CD15 expression; CD34 expression is represented by the proportion of positive cells (%) while CD11b and CD15 expression is represented using the fluorescence intensity (MFI x1000); n=3, data represent mean ± 1SD. Statistical significance was determined by two-way ANOVA with Bonferroni post-test comparison and was deemed non-significant

3.4 Discussion

PKCε is frequently upregulated in solid cancers and is associated with aggressive disease phenotypes and poor patient outcomes. Furthermore, *in vitro* studies have identified PKCε as an oncogenic kinase and in solid cancers is implicated in promoting proliferation, metastasis and chemoresistant phenotypes (Garg, *et al.*, 2014). Although PKC signalling has been implicated in haematopoiesis, unlike in solid cancers, there is little published data on the role of PKCε in haematological malignancies, including AML. Therefore, the initial aim of this chapter was to determine whether PKCε is abnormally expressed in AML and establish whether mis-expression of this kinase affects the clinical outcome of patients.

To determine the frequency and clinical findings associated with high PKCε expression in AML, our group previously analysed the protein expression of this kinase in 70 AML patient samples from the NCRI UK AML14 and AML15 clinical trials. This analysis showed that PKCε protein is frequently overexpressed in AML (c30% of patients analysed) and that overexpression is not restricted to a particular disease sub-type. In terms of patient outcome, no significant difference in OS was observed for patients with high PKCε protein expression. However, risk adjusted analysis suggested that these patients were less responsive to induction chemotherapy (Figure 3.3). This finding suggests that PKCε could be an independent indicator of poor treatment response. However, the small size of the cohort used in these analyses, means that they are underpowered. Therefore, additional investigations were required to support these preliminary data, and further elucidate the pathophysiological attributes associated with PKCε upregulation in AML.

Although protein expression is a superior indicator of the role of PKCε in AML than mRNA expression, as protein expression directly correlates with functional potential, most clinical data is associated with mRNA expression due to the high throughput nature of methods such as RNAseq. It is frequently observed that the correlation between mRNA and protein expression is weak (Maier, *et al.*, 2009). Therefore, to draw meaningful conclusions from mRNA datasets, it is important that mRNA and protein expression positively correlate. From the 18 AML14 and AML15 patient samples, where mRNA and protein expression data were available, a positive correlation between PKCε mRNA and protein expression was observed. Therefore, indicating that *PKCε* mRNA expression is a reasonable indicator of protein expression in AML patient samples. Having identified this, I analysed the TCGA 2013 mRNA

dataset (Ley, *et al.*, 2013) to further explore the relationship between high PKCε expression and patient outcomes in AML.

Patients were stratified according to their *PKCε* expression using the lower and upper quartiles to represent patients with low and high *PKCε* expression, respectively. This data supported the findings of the protein analysis, in that high *PKCε* mRNA expression occurred across disease subtypes and with a range of cytogenetic and molecular abnormalities. Furthermore, no association with patient characteristics such as age and gender were observed. Furthermore, at an mRNA level, high *PKCε* expression was associated with significantly worse OS and DFS. Together with the protein analysis, these data suggest that PKCε upregulation in AML is associated with poor outcomes, especially in terms of response to induction chemotherapy and an increased risk of relapse. However, high *PKCε* mRNA expression tended to co-occur with intermediate and poor risk disease. Therefore, it cannot be ruled out that the poor outcomes associated with elevated *PKCε* mRNA expression may in part be driven by the co-occurrence of known adverse aberrations. To determine the significance of this association, risk adjusted analysis would need to be conducted, however, the support to conduct this analysis was not available at the time of writing. It is also important to note that as the analysis of PKCε protein expression is risk adjusted, making it more robust than the mRNA analysis. Although further analysis is required to establish whether PKCε is an independent prognostic indicator in AML, this analysis is supportive of the association between PKCε upregulation and poor patient outcomes in this malignancy.

The association between high PKCε expression and poor outcomes in AML reflects the observations in solid cancers (1.6.5). For example, in primary invasive breast carcinoma, immunohistochemistry determination of PKCε expression (n=144) showed that high PKCε protein expression occurred more frequently in high grade (grade 3) tumours compared with low grade disease (p=0.0206) and was significantly associated with negative oestrogen (p=0.0026) and progesterone (p=0.0008) receptor status; parameters which are established markers of poor outcome and response to hormone therapy (Pan, *et al.*, 2005). Furthermore, Kaplan-Meier analysis comparing the OS and DFS of patients with moderate/high PKCε staining (n=36) and samples with undetectable levels of PKCε (n=44), PKCε expression was associated with significantly worse OS (p=0.0414) and DSF (p=0.0478). Although when adjusted for prognostic markers such as hormone receptor status, significance in terms of OS or DFS was not achieved, this could partly be due to the small sample size used in this study

(Pan, *et al.*, 2005). Despite this, such studies highlight the potential of PKCε upregulation as a biomarker for aggressive disease and poor patient outcomes in solid cancer (1.6.5).

In the present study, although largely concordant, the discrepancies observed between the AML patient mRNA and protein analysis could, in part, be due to the moderate correlation between these factors. While a positive correlation between PKCε mRNA and protein expression was observed, the associated Pearson squared correlation coefficient was 0.64. This implies that c60% of the variation in protein concentration can be explained by knowing the abundance of mRNA, but that c40% of the protein expression cannot be explained by mRNA expression and may be a result of post-transcriptional regulation.

In addition to the level of PKCε expression, the activation status of this kinase is an important factor to consider. Phosphorylation of PKC isoforms is a central mechanism in regulating their activation. For nPKC enzymes including PKCε, the first and rate-limiting phosphorylation step occurs at the activation loop by PDK-1 (1.5.3). PDK-1 is frequently overexpressed in AML (Zabkiewicz, *et al.*, 2014). Furthermore, our group has previously shown a functional link between these two factors as the survival of AML cells overexpressing PDK-1 is mediated by PKC signalling (Zabkiewicz, *et al.*, 2014). Although phosphorylation of PKC isoforms by PDK-1 does not result in direct activation, it does promote autophosphorylation of the two additional phosphorylation residues at the C-terminus of PKC isoforms (Cenni, *et al.*, 2002). Thus, a positive feedback loop between upstream activators of PKCε, such as PDK-1, may contribute to PKCε overexpression in AML. This was not followed up in this study as data previously generated by our group showed a poor correlation between PKCε and PDK-1 protein expression in AML patient samples from the NCRI UK AML14 and AML15 clinical trials (R^2=0.14; data not shown). Alternatively, a study in breast cancer cell lines has highlighted a role of STAT-1 and Sip-1 in regulating PKCε transcription (Wang, *et al.*, 2014). PKCε has been shown to promote the phosphorylation of STAT-1 which is required for its transcriptional activity (Ivaska, *et al.*, 2003, Wang, *et al.*, 2014), raising the possibility that PKCε autoregulates its expression through a positive feedback loop involving STAT-1.

Overall, the clinical data analysed in this chapter indicate that PKCε upregulation is associated with poor outcomes and reduced response to first-line therapy in AML. A significant contribution to poor outcomes in AML is chemoresistance, which can be attributed to multiple factors including, the balance between apoptotic and survival signalling, the persistence of cancer stem cells, and the expression of drug specific efflux pumps which lead

to a decrease in drug accumulation (1.4.3). The results of functional studies to determine whether the relationship between PKCε and chemoresistance in AML is causal or associative, will be outlined and discussed in Chapter 4, however, some of the mechanisms through which PKCε may confer chemoresistance in AML are briefly described below.

PKCε is associated with chemoresistant phenotypes in cancer cell lines which have been linked to altered apoptotic and survival signalling (1.6.5.2). For example, in a prostate cancer cell line, PKCε has been shown to enhance the expression of anti-apoptotic proteins and downregulate pro-apoptotic BCL-2 family members such as Bid (Sivaprasad, *et al.*, 2007), while in SCLC cell lines, PKCε overexpression promotes increased expression of BCL-XL and X-linked inhibitor of apoptosis (XIAP) which was associated with etoposide resistance (Pardo, *et al.*, 2006). The propensity of PKCε to modulate apoptotic signalling in haematopoietic cells has also been described. PKCε was found to protect erythroid cells from TRAIL-induced apoptosis, while prolonged phorbol ester treatment and siRNA downregulation of PKCε sensitised AML cell lines and patient derived samples to the apoptotic effects of TRAIL (Gobbi, *et al.*, 2009). PKC isoforms have also been associated with the regulation of efflux pump expression, localisation, and activation (Mayati, *et al.*, 2017; 1.6.5.3), and in a prostate cancer cell line, PKCε activation has been shown to regulate P-GP expression (Flescher and Rotem, 2002a), an efflux pump which is frequently overexpressed in AML (Beck, *et al.*, 1996, van der Kolk, *et al.*, 2002, van der Kolk, *et al.*, 2000, Wuchter, *et al.*, 2000). This therefore represents a potential mechanism through which PKCε upregulation may contribute to chemoresistance and poor patient outcomes in AML.

The efficacy of chemotherapeutic agents is also highly dependent on the proliferation rate of the target cells. LSC are thought to possess chemoresistant properties, due to the quiescent state in which these cells reside (Passegué and Wagers, 2006) and persistence of LSC following the completion of treatment is a major contributor to relapse in AML. PKCε has been implicated in regulating HSC activity and self-renewal. Studies in murine HSPC showed that alongside *PKCα*, *PKCη* and *PKCθ*, *PKCε* was increased in LT-HSC, which have a greater self-renewal capacity, compared to ST- HSC (Hazen, *et al.*, 2011, Ivanova, *et al.*, 2002). This is supported by the observation in this study that *PKCε* is highly expressed at an mRNA level in human HSC and is downregulated as these cells become lineage committed progenitors. Due to technical constraints, the impact of modulating PKCε expression on the self-renewal capacity and activity of human HSC could not be investigated in this study. However, if high levels of PKCε are required for HSC maintenance and quiescence, in AML, PKCε upregulation

could promote chemoresistance and disease relapse through promoting these attributes in LSC and leukaemia cells.

As well as the potential to confer chemoresistance, it was hypothesised that PKCε may contribute to the pathogenesis of AML by promoting the growth of leukaemic cells and disrupting normal myeloid cell development. The expression of PKC isoforms has been demonstrated by western blot analysis in freshly isolated human HSPC (Bassini, *et al.*, 1999) and are thought to mediate the proliferation, differentiation, and survival of haematopoietic cells (Redig and Platanias, 2008). The role of PKCε in haematopoiesis has been studied most extensively in the erythroid and megakaryocytic lineages. However, the role of PKCε in monocytic and granulocytic development, the lineages which are primarily impacted in AML, has not been resolved to the same extent. To gain a better understanding of the role of PKCε in the development of monocytic and granulocytic progenitors, *PKCε* mRNA expression was assessed using publicly available transcriptomic datasets in human haematopoietic progenitor cells. This analysis showed that expression was maintained throughout monocytic and granulocytic development, suggesting a potential role for this kinase in GMP lineage commitment and monocyte development.

It was hoped that the role of PKCε in myeloid development could be further resolved by determining the endogenous expression of PKCε protein in specified cellular compartments, using flow cytometry. However, despite applying different fixation and permeabilization methodologies, even ectopic PKCε expression in K562 cells could not be detected using this methodology. Therefore, this approach could not be applied to the HSPC cultures, where the level of endogenous expression is considerably lower than in the overexpression context. The antibodies used for this analysis were validated for their ability to detect PKCε expression by western blot, where the conformation of the protein is highly linearized (Forsström, *et al.*, 2015). However, in flow cytometry, antibody binding to a native conformational epitope is a requirement. Therefore, this may explain why these antibodies were unable to detect ectopic PKCε expression using this methodology. A relatively recent study which assessed PKC expression in human haematopoietic cells by flow cytometry achieved positive PKCε staining compared to an isotype control in monocyte and neutrophil populations using the [EPR1482(2)] Abcam anti-PKCε antibody (Perveen, *et al.*, 2019). This antibody was tested in this study, but I was unable to validate this antibody by western blot analysis or flow cytometry in the K562 PKCε overexpression cell line (data not shown). Instead, the mRNA data was supported by the determination of PKCε protein expression in HSPC by western blot analysis.

This showed that at a protein level, PKCε is expressed in early monocyte, granulocyte, and erythrocyte progenitors (day 6). Furthermore, when HSPC are cultured in medium which primarily supports monocyte and granulocyte maturation, PKCε protein expression increased with maturation. Thus, supporting the potential role of this kinase in myeloid cell development.

To further elucidate this and determine whether high PKCε expression could contribute to the pathogenesis of AML by disrupting myeloid cell development, functional studies using genetic systems to overexpress and knockdown PKCε in HSPC were conducted. PKCε overexpression reduced the growth of HSPC, showing that PKCε does not act as an oncogene in this context. Reduced growth can be a result of perturbed cell cycle progression. Although in other settings, PKCε overexpression is associated with pro-proliferative phenotypes (Mischak, *et al.*, 1993), PMA-mediated PKC activation has been associated with both positive and inhibitory effects on cell cycle progression (Black, 2000). The propensity of PKC isoforms to impair cell cycle progression has previously been associated with G2-phase delay and ERK-dependent upregulation of p21; a negative regulator of cell cycle progression (Barboule, *et al.*, 1999, Kosaka, *et al.*, 1996). The relative contributions of perturbed cell cycle progression and the induction of apoptosis could not be resolved due to the heterogenous nature of the HSPC cultures and the small effect sizes observed. However, it was proposed that the slower growth of the PKCε overexpression cells could be associated with the induction of differentiation, given the inverse relationship of these parameters in a range of cell types (Ruijtenberg and van den Heuvel, 2016).

The differentiation status of HSPC was evaluated through the expression of myeloid specific maturation markers. PKCε overexpression promoted significant increases in monocyte maturation marker CD11b and CD14 expression. This suggests that the reduced proliferation of the monocytic progenitors is a result of differentiation induction whereby PKCε could be slowing cell cycle progression as its expression increases, leading to growth arrest and terminal differentiation. In contrast the impact of PKCε overexpression on granulocytic differentiation was equivocal as, although the trend of increased CD11b and CD15 expression on these cells was not inconsistent with a pro-differentiation phenotype, the magnitude of change did not result in statistical significance. Therefore, these data suggest that PKCε is primarily involved in monocytic development, as opposed to promoting myeloid differentiation more broadly

The small effect sizes observed in the HSPC PKCε overexpression studies, meant that elucidating the mechanisms through which PKCε promotes monocyte development, in this context, was not possible. However, the ability of PKCε to promote monocyte commitment and differentiation in HSPC is in concordance with the literature. One of the first studies implicating PKC in monocyte differentiation, demonstrated the ability of PMA treatment, a potent PKC activator, to promote monocytic differentiation in U937 cells (Hass, *et al.*, 1991). This phenotype has subsequently been shown in THP-1 cells (Schwende, *et al.*, 1996) and $CD14^+$ monocytes (Lin, *et al.*, 2011). PMA induced differentiation is thought to mimic cytokine signalling; a central aspect of haematopoiesis regulation (1.1.2). For example, a study in human PB monocytes showed that 7 days of treatment with PMA or GM-CSF promoted equivalent morphological and surface marker expression profiles, consistent with macrophage differentiation (Lin, *et al.*, 2007). In several contexts, PMA treatment has been associated with the translocation of the cPKC isoform PKCα (Chang and Beezhold, 1993, Lin, *et al.*, 2011, Whetton, *et al.*, 1994). However, one group anecdotally reported that translocation of PKCε in PMA treated human monocytes was observed in a similar manner to PKCα, although expressed at a lower level (Chang and Beezhold, 1993), suggesting that the phenotypic impact of PMA treatment could result from the activation of more than one PKC isoform.

Mechanistically, PMA induced differentiation of U937 cells is associated with *c-myc* downregulation and the upregulation of *c-jun* and *c-fms* (Hass, *et al.*, 1997). The *c-jun* gene products can cooperate with the transcription factors AP-1 and PU.1 which are associated with monocyte differentiation. PKC isoforms can also promote myeloid differentiation through modulating the phosphorylation status and DNA binding capacity of these transcription factors. For example, phosphorylation of PU.1 by PKCδ has been implicated in the differentiation of HSPC to dendritic cells (Hamdorf, *et al.*, 2011). Alternatively, one study has shown that myeloid differentiation in PMA treated AML cell lines and patient samples, demonstrated by the upregulation of CD11b, is associated with the downregulation of onzin (Wu, *et al.*, 2010). . Using chemical PKC inhibitors, RNA interference systems, and dominant negative and constitutively active forms of various PKC isoforms in AML cell lines, PKCε was identified as a central mediator of this phenotype. Specifically, in co-operation with ERK, PKCε facilitated PMA mediated suppression of onzin (Wu, *et al.*, 2010). Thus, PKCε-ERK-onzin interactions represents a potential mechanism of PKCε-mediated differentiation. PKCε can also modulate, and be activated by, the levels of ROS which influence monocytic

differentiation through the activation of JNK and FOXO in Drosophila and murine models (Sardina, *et al.*, 2012).

Regardless of the mechanism through which PKCε overexpression may promote monocyte differentiation in HSPC, this is not a phenotype associated with AML, in which, arrested myeloid development is a defining characteristic. Thus, the data presented in this chapter demonstrate that PKCε upregulation is unlikely to contribute to the pathogenesis of AML by disrupting myeloid development. However, PKCε knockout mice have severely impaired responses to LPS (Castrillo, *et al.*, 2001). This suggests a requirement of PKCε in the development and immunological function of these cells. To determine whether PKCε is essential for monocyte development the impact of reducing PKCε expression in HSPC was investigated. A trend of reduced CD11b and CD14 on monocyte progenitors was observed, which although not significantly reduced, is not inconsistent with a role for PKCε in monocyte development but does not support a critical role. Although PKCε knockdown reduced the fold expansion of granulocytic progenitors, differentiation was unaffected. This suggests that PKCε does not have an endogenous role in granulocyte differentiation but may impact the viability of this lineage. The impact of PKCε knockdown on cell viability was not studied extensively, however, Annexin V staining of HSPC after 11 days of culture was supportive of this premise, showing a reduced viability in PKCε knockdown bulk culture (control; 77%, 485; 70% and 486; 66%, data not shown; n=1).

In conclusion, the data presented in this chapter show that PKCε is unlikely to contribute to the pathogenesis of AML through disrupting myeloid development. However, it was found that PKCε is frequently upregulated in AML and that high mRNA expression may be a predictor of poor outcome in this malignancy. As a result, the capacity of PKCε to contribute to this, through mechanisms such as conferring chemoresistance, will be addressed in the subsequent chapters.

Chapter 4: The Relationship Between PKCε Expression and Chemoresistance in AML Cells

4.1 Introduction

Although the use of Ara-C and DNR is effective in achieving CR in younger AML patients, most older patients cannot tolerate intensive chemotherapy (1.3.1) and will either fail to achieve CR or relapse following a period of remission (Ramos, *et al.*, 2015). Thus, the prognosis for most patients with AML remains poor. The development of chemoresistance is thought to contribute to the poor outcomes associated with AML and as a result, research into factors which contribute to chemoresistance is essential to improving patient outcomes.

As mentioned previously, PKCε is the only PKC isoform known to behave as a transforming oncoprotein (Cacace, *et al.*, 1996, Mischak, *et al.*, 1993), which in addition to promoting disordered cell growth can contribute to oncogenesis by inhibiting cell death (1.6.5.2). Expression of PKCε has been shown to regulate both receptor- (Mirandola, *et al.*, 2006) and DNA damage-mediated (Basu and Weixel, 1995) apoptosis. Therefore, PKCε has the capacity to confer resistance to a range of chemotherapeutic agents. In NSCLC cells, increased PKCε expression is associated with chemoresistance while in SCLC cells, lack of PKCε has been associated with chemosensitivity (Ding, *et al.*, 2002). Furthermore, ectopic PKCε expression in SCLC cell lines promoted chemoresistance through inhibiting caspase activation (Ding, *et al.*, 2002), suggesting that PKCε may alter the apoptotic threshold of lung cancer cells. Alternative mechanisms of PKCε-mediated chemoresistance have also been described, including the upregulation and phosphorylation of efflux pumps such as P-GP (Chambers, *et al.*, 1992, Chaudhary and Roninson, 1992). P-GP confers drug resistance by reducing intracellular drug accumulation(Nooter, *et al.*, 1990) and is associated with low rates of CR induction in AML (van der Kolk, *et al.*, 2000). The data presented in the previous chapter, indicates that PKCε may contribute to poor outcomes in this malignancy through promoting chemoresistance and disease progression (3.3.1.1 and 3.3.1.3). Overexpression of PKCε in AML cells has been shown to protect against TRAIL-induced apoptosis (Gobbi, *et al.*, 2009), however, the ability of PKCε to confer chemoresistance in AML cells has not been established.

4.2 Aims

The aim of this chapter is to determine whether PKCε has the capacity to contribute to poor outcomes in AML by conferring chemoresistance. This will be achieved through the following objectives:

- **Determine PKCε expression in AML cell lines**

  To determine whether AML cell lines are a suitable model to investigate the role of PKCε in chemoresistance, the expression of this kinase in AML cell lines will be investigated at an mRNA and protein level using publicly available mRNA datasets and western blotting analysis, respectively.

- **Determine whether there is a causal relationship between PKCε expression and chemoresistance in AML cells**

  PKCε expression will be modulated in selected AML cell lines using overexpression, knockdown, and knockout systems. The resulting impact on the chemosensitivity, in terms of the impact on growth and viability, of these lines to Ara-C and DNR will be assessed using flow cytometry.

4.3 Results

4.3.1 Establishing PKCε expression in AML cell lines

To determine whether AML cell lines are a suitable model to study the biological role of PKCε in AML, endogenous PKCε mRNA and protein expression was assessed in a range of AML cell lines. mRNA expression was investigated using DepMap. This analysis showed heterogenous *PKCε* expression across the different AML cell lines investigated (Figure 4.1A). Subsequently, PKCε protein expression was validated by western blot analysis. This identified three cell lines (U937, Mv4;11 and OCIAML5) that expressed detectable levels of PKCε protein (Figure 4.1B). Comparing the expression of PKCε in AML cell lines using these two sets of analyses showed a poor correlation between *PKCε* mRNA and protein expression (Figure 4.2); a finding which is not in-line with the observation made in AML patient samples (Figure 3.3). However, the AML cell line analysis was conducted on a relatively small number of lines (n=10). Furthermore, the fact that the mRNA and protein data for the AML cell lines were not derived from an identical source of cells, may contribute to this poor correlation. Based on this, the identification of suitable AML cell lines to study the functional effects of modulating PKCε expression using genetic overexpression and knockdown or knockout systems was based upon their endogenous PKCε protein expression.

4.3.1.1 PKCε overexpression reduces the fold expansion of AML cell lines, potentially through disrupting cell cycle progression

The cell lines, U937, HEL, NOMO-1, and TF-1, were selected for the generation of PKCε overexpression cell lines based on their endogenous PKCε protein expression. All these lines had undetectable levels of protein by western blot analysis, except for U937 where protein expression was low (Figure 4.1). Transduced cell lines were generated using the control and PKCε overexpression constructs which were previously validated in K562 cells (Figure 3.17) and ectopic PKCε expression was validated by western blot analysis. In all four lines, the cells transduced with the PKCε overexpression construct had much higher levels of PKCε protein expression compared with cells transduced with the control construct (Figure 4.3). As a result, the phenotypic impact of PKCε overexpression including the effect on cell growth and viability were assessed by flow cytometry.

In U937 and HEL cells, PKCε overexpression promoted a reduction in cell viability of c10% compared to the control cell lines (Figure 4.4). However, this was accompanied by a respective 1.5-fold and 2.8-fold reduction in growth (Figure 4.5). This suggests that the apparent reduction in cell viability could be an artefact arising from the relative accumulation of non-viable cells because of the reduced proliferation rate of these cultures. In contrast, no significant differences in the viability (Figure 4.4) or growth (Figure 4.5) of NOMO-1 or TF-1 cells overexpressing PKCε was observed. Given the impact of PKCε overexpression on the proliferation of U937 and HEL cells, the DNA content of these lines was evaluated using flow cytometry to determine cell cycle progression (2.8.7). In both cell lines, the PKCε overexpressing cells had an increased proportion of cells in the G2-phase compared to the controls (Figure 4.6), suggesting that the reduced growth of these cell lines could be a result of disrupted cell cycle progression.

As shown in Chapter 3, PKCε overexpression in HSPC reduced proliferation and promoted monocyte differentiation (3.3.4.2). Therefore, it was hypothesised that the reduced cell growth in U937 and HEL cell lines could be associated with the induction of a more differentiated phenotype. Differentiated cells are typically larger than precursors, thus the size and morphology of the U937 and HEL cell lines was evaluated. This analysis showed that both U937 and HEL cells overexpressing PKCε had significantly higher forward scatter properties, a parameter related to cell size, compared to cells transduced with the control construct (Figure 4.7). This was supported by morphological analysis which also indicated that the PKCε overexpression U937 and HEL cells were larger than the control cell lines (Figure 4.8). These observations are indicative of a more differentiated phenotype, however, no associated change in the expression of myeloid differentiation markers including CD11b, CD14 and CD13 were observed (data not shown). Thus, suggesting that the reduced proliferation and increased size of the PKCε overexpression U937 and HEL cells is a result of partial G2 arrest as opposed to the induction of cell differentiation. These parameters were also assessed in the NOMO-1 and TF-1 cells and as expected, there was no difference in cell size, cell cycle progression or differentiation. Overall, PKCε overexpression in AML cell lines does not have a biologically significant impact on cellular viability but has the propensity to reduce cell growth, potentially mediated by perturbed cell cycle progression.

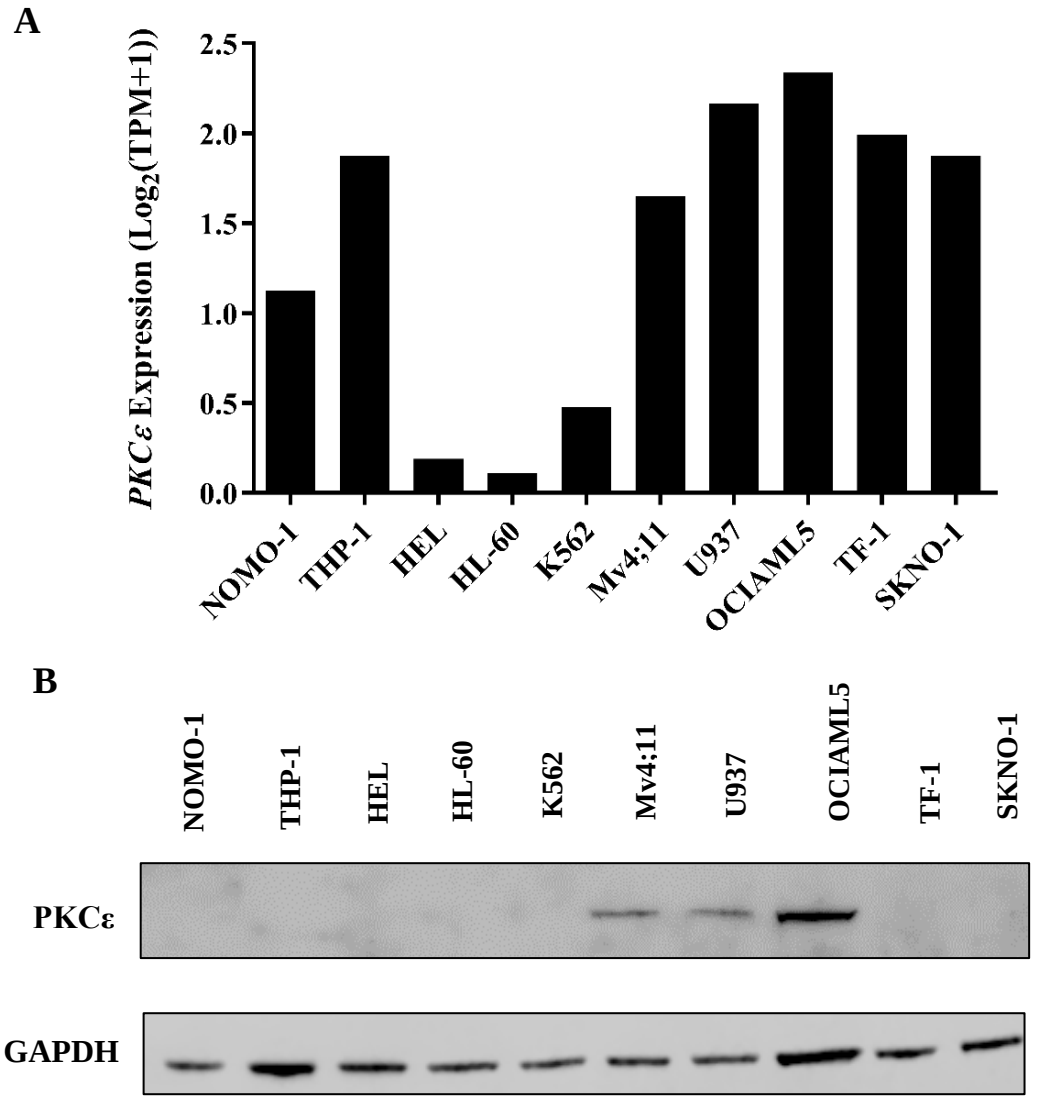

Figure 4.1: PKCε mRNA and protein is heterogeneously expressed in leukaemia cell lines

(A) Bar chart showing *PKCε* mRNA expression ($\log_2$ (TPM+1)) across different leukaemia cell lines. Data was obtained from DepMap (Barretina, *et al.*, 2012) as described in 2.11.3. **(B)** Western blot image showing PKCε protein (MW-84kDa) expression in leukaemia cell lines (Table 2.1). PKCε expression was detected using the Cell Signalling Technologies antibody #2683 (clone 22B10; Table 2.10) and is shown alongside GAPDH (MW-36kDa) expression, which was used as a loading control and detected using the ThermoFisher Scientific GAPDH antibody (clone GA1R; Table 2.10); n=1. *Abbreviations: TPM; transcripts per million.*

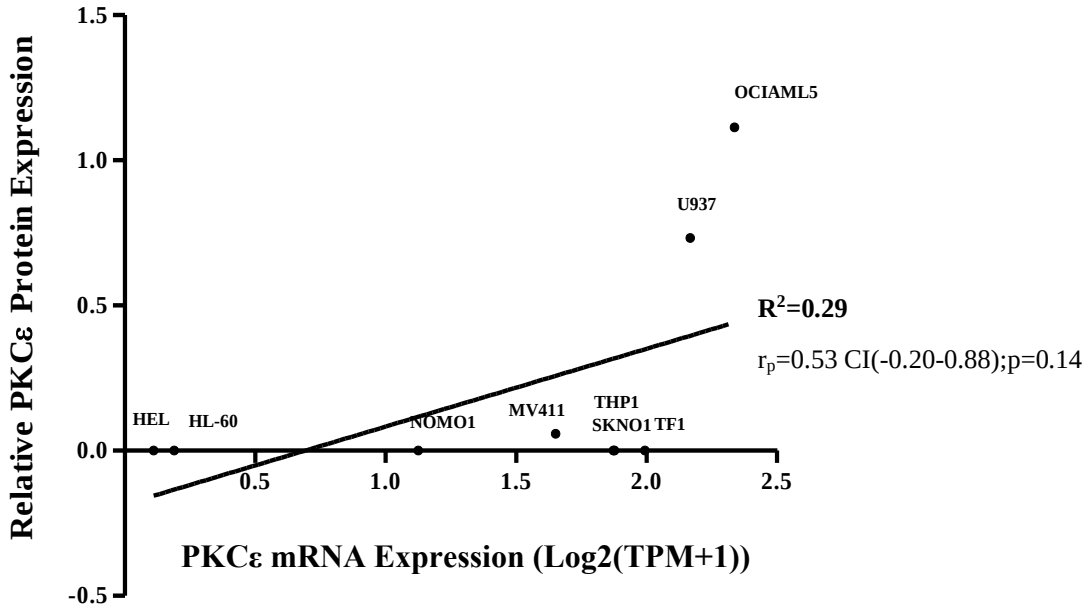

Figure 4.2: PKCε mRNA and protein show a poor correlation in AML cell lines

Dot plot showing the relationship between PKCε mRNA and protein expression in AML cell lines. mRNA expression was obtained from DepMap (Barretina, *et al.*, 2012), while protein expression was determined by western blot analysis as shown in Figure 4.1. The black line represents the linear regression line (R^2=0.29) and the degree of correlation assessed using Pearson's correlation analysis (r_p=0.53 CI(-0.20-0.88); p=0.14) and was deemed non-significant.

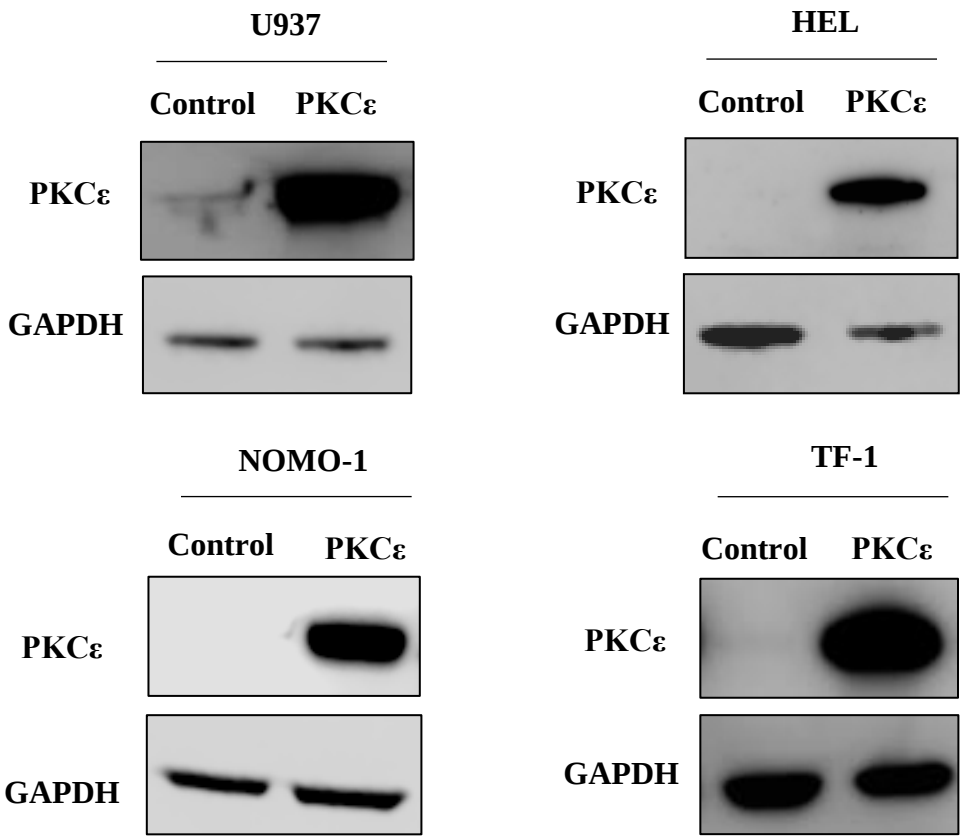

Figure 4.3: Validation of PKCε overexpression in AML cell lines by western blot

Representative western blots showing PKCε (MW-84kDa) expression of U937, HEL, NOMO-1, and TF-1 cells transduced with the control (GFP-Puro^R) or PKCε overexpression (PKCε-GFP-Puro^R) constructs (2.4.1.1). Before lysate generation, the AML cell lines underwent puromycin selection (10 µg/mL) to remove un-transduced cells (2.5.2). PKCε expression was detected using the Cell Signalling Technologies antibody #2683 (clone 22B10; Table 2.10) and is shown alongside GAPDH (MW-36kDa) expression, which was used as a loading control and was detected using the ThermoFisher Scientific GAPDH antibody (clone GA1R; Table 2.10); n=2.

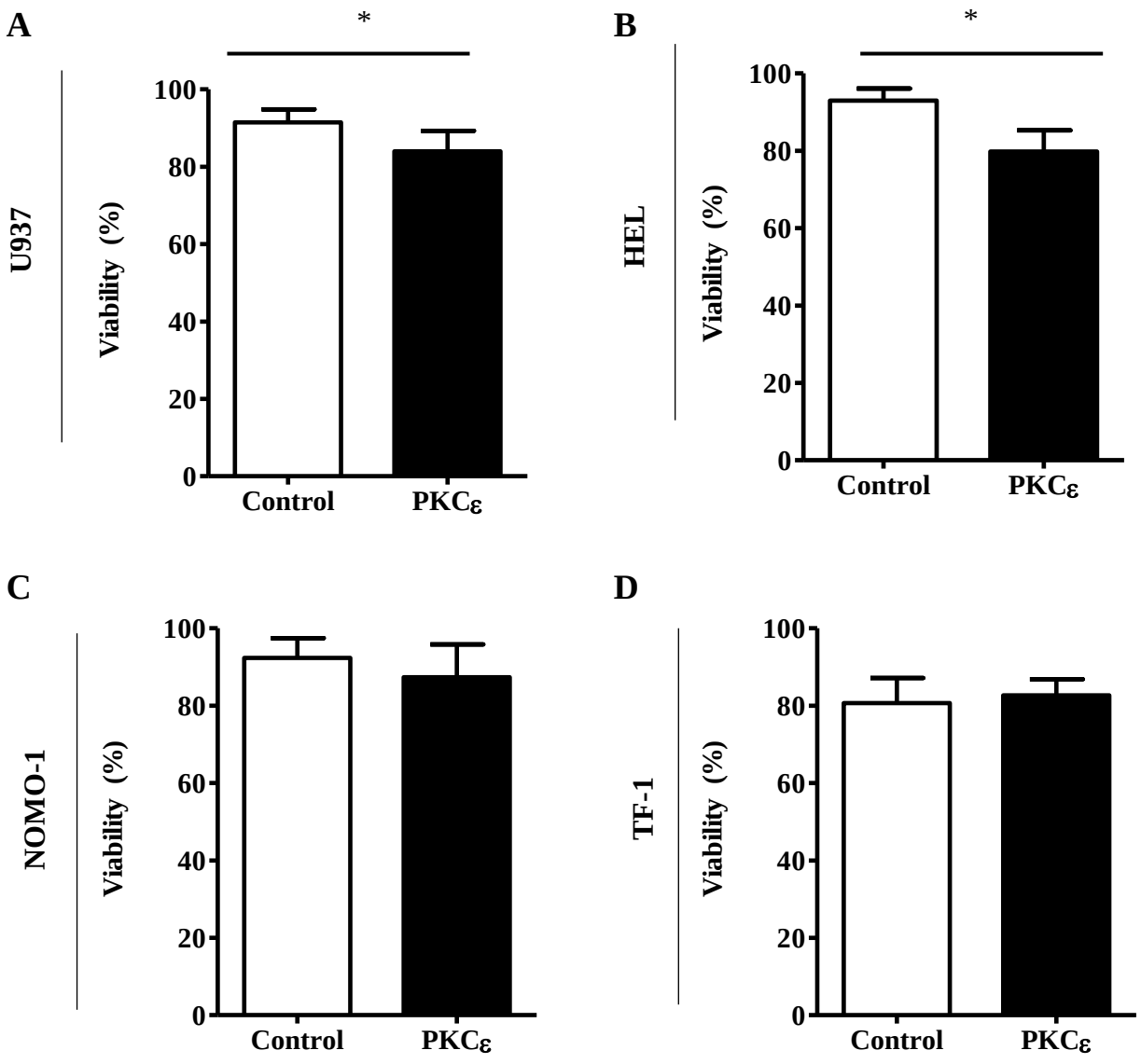

Figure 4.4: The effect of PKCε overexpression on the viability of AML cell lines

Bar charts representing the viability (%) of **(A)** U937, **(B)** HEL, **(C)** NOMO-1 and **(D)** TF-1 cells transduced with the control or PKCε overexpression constructs (Figure 4.3) following 48 hours of culture. Viability was determined by flow cytometry using TOPRO-3 staining as described in 2.8.2; data represents mean+1SD;U937 and HEL (n=4), NOMO-1, and TF-1 (n=3). Statistical significance was determined using a Mann-Whitney test; * $p<0.05$.

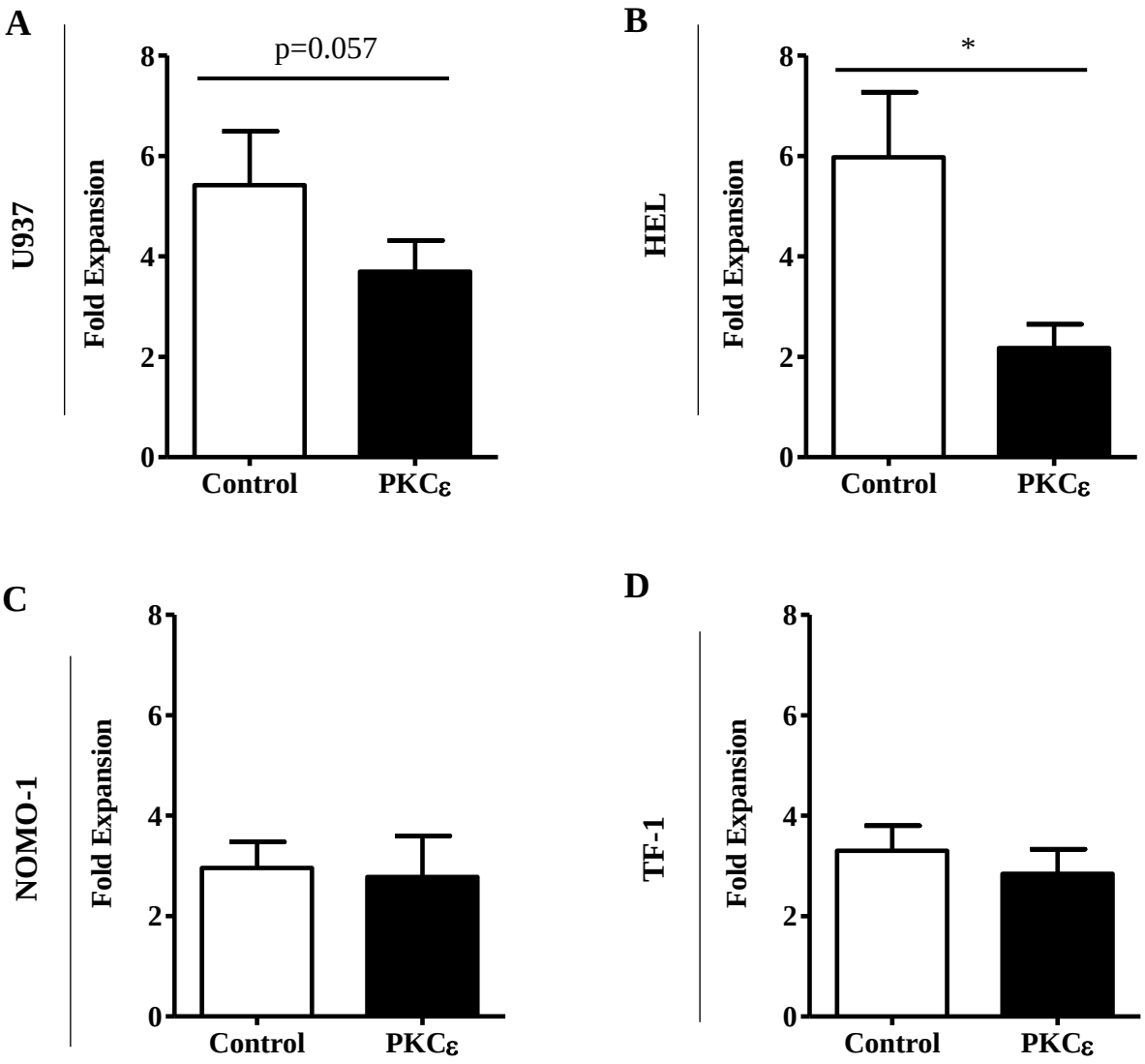

Figure 4.5: The effect of PKCε overexpression on the fold expansion of AML cell lines

Bar charts representing the fold expansion of **(A)** U937, **(B)** HEL, **(C)** NOMO-1 and **(D)** TF-1 cells transduced with the control or PKCε overexpression constructs (Figure 4.3) over 48 hours of culture. The fold expansion of the cells was calculated by dividing the viable growth determined using TOPRO-3 staining by the cell count at the time of seeding, as described in 2.8.2; data represents mean+1SD; U937 and HEL (n=4), NOMO-1 and TF-1 (n=3). Statistical significance was determined using a Mann-Whitney test, *$p<0.05$.

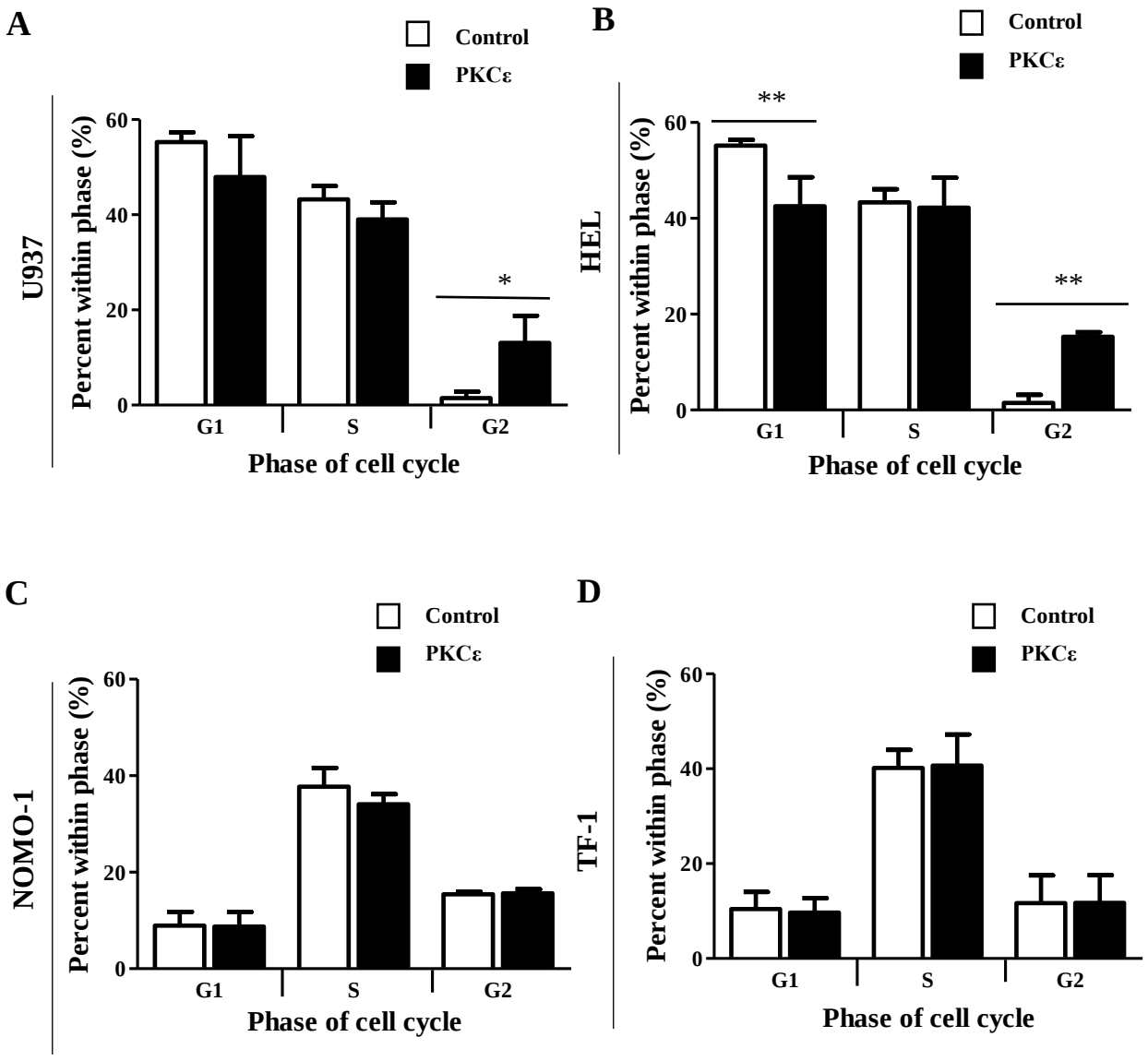

Figure 4.6: PKCε overexpression is associated an increased proportion of U937 and HEL cells in G2-phase of the cell cycle

Bar charts showing the proportion (%) of cells in the G1, S and G2 phase of cell cycle, determined by PI staining as described in 2.8.7 for **(A)** U937, **(B)** HEL, **(C)** NOMO-1 and **(D)** TF-1 cells transduced with the control or PKCε overexpression constructs (Figure 4.3) following 48 hours of culture (2.8.2); n=3, bar charts represent mean+1SD. Statistical significance was determined using a two-way ANOVA with Bonferroni post-test comparison, * $p < 0.05$, ** $p < 0.01$.

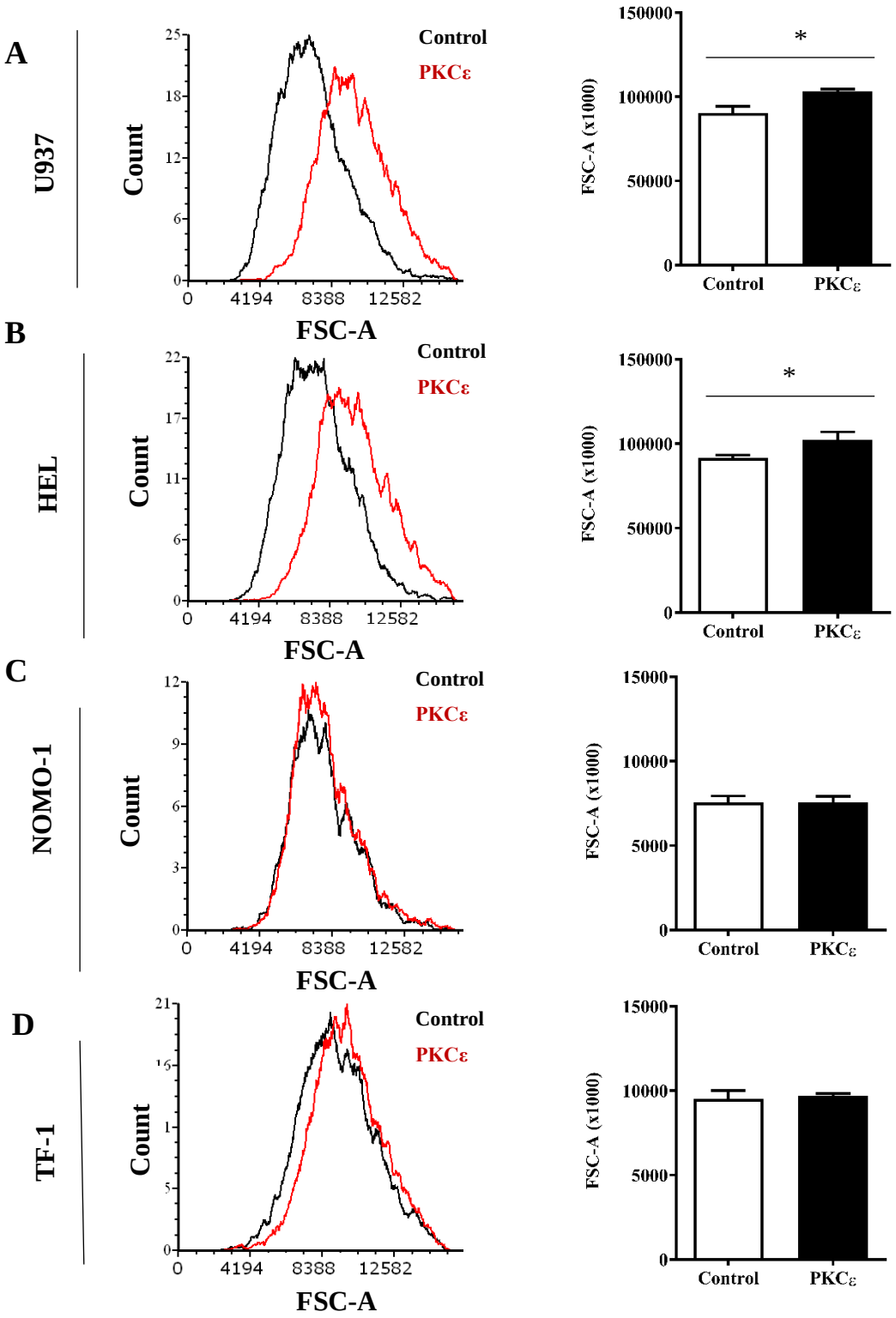

Figure 4.7: The effect of PKCε overexpression on the forward scatter of AML cell lines

Representative histograms (left) and the mean forward scatter properties (FSC-A x1000; right) of **(A)** U937, **(B)** HEL, **(C)** NOMO-1 and **(D)** TF-1 cells transduced with the control or PKCε overexpression constructs (Figure 4.3); U937 and HEL n=4, NOMO-1, and TF-1 n=3, data represents mean+1SD. Statistical significance was determined using a Mann-Whitney test;* $p<0.05$.

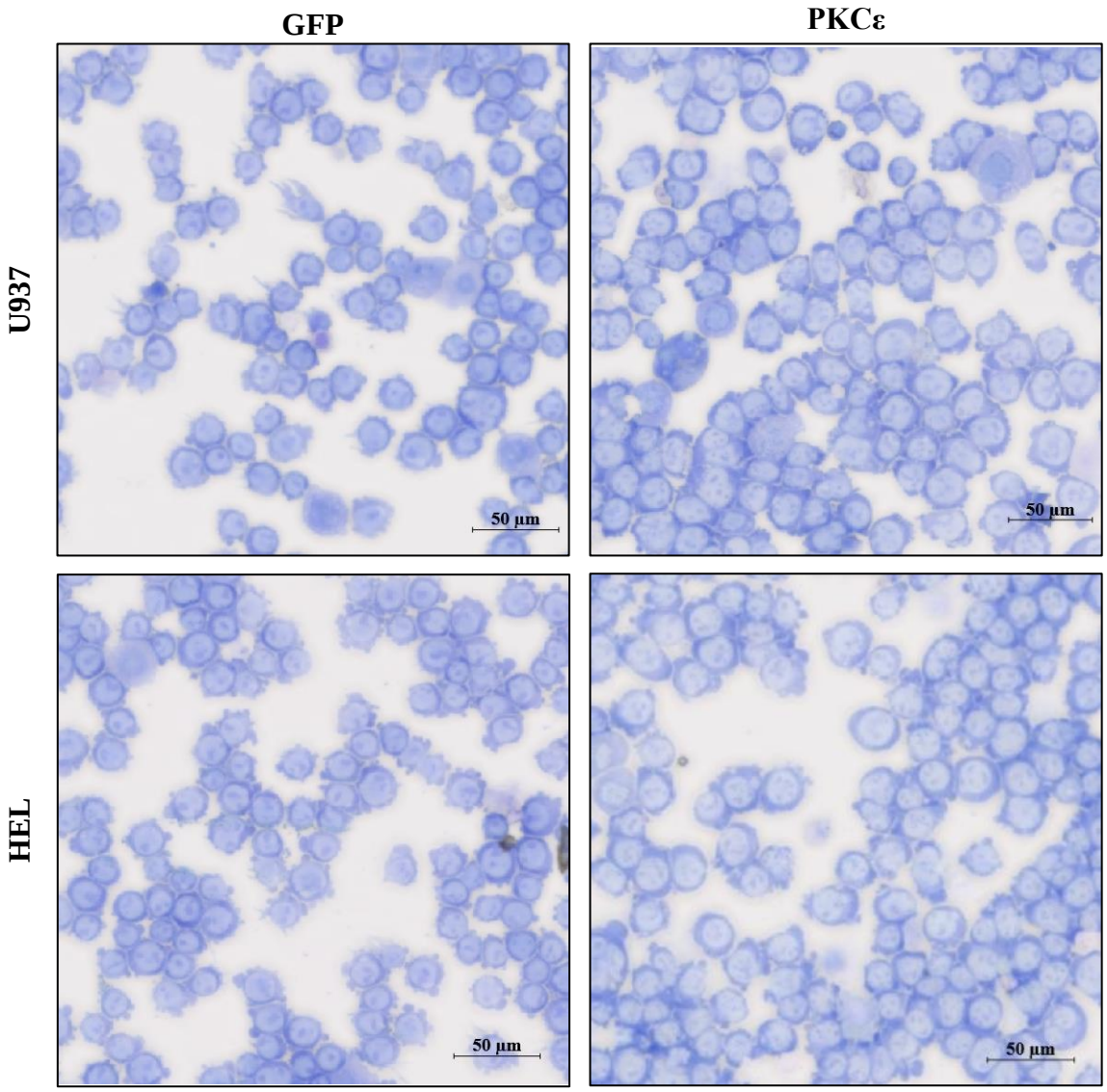

Figure 4.8: Morphological effects of PKCε overexpression in AML cell lines

Images showing the morphology of U937 (left) and HEL (right) transduced with the control or PKCε overexpression constructs (Figure 4.3). The cells were stained with a combination May-Grunwald and Giesma differential stains and imaged using a Zeiss Axioscan Z1 slide scanner at 20x magnification; scale bar-50µm stain as described in 2.6.

4.3.2 Assessing the relationship between PKCε overexpression and chemoresistance in AML cell lines

Given the previously described capacity of PKCε overexpression to promote chemoresistance in cancer (1.6.5) and the impact of PKCε overexpression on the proliferation of AML cell lines (4.3.1.1), the effect of modulating PKCε expression on the sensitivity of AML cell lines to Ara-C and DNR was investigated using flow cytometry (2.8.8). To partially resolve the relative contributions of the growth inhibitory and cytotoxic impact of chemotherapy treatment, both cell growth and viability were assessed. The sensitivities of each cell line to Ara-C and DNR were calculated by determining the EC50 of each agent, where $EC50^G$ refers to the impact on cell growth and $EC50^V$ refers to the impact on cell viability.

4.3.2.1 PKCε overexpression does not promote resistance to Ara-C in AML cell lines

U937 and HEL cells had an endogenous Ara-C $EC50^G$ of 142nM and 97nM (Figure 4.9) and $EC50^V$ of 536nM and > 800nM respectively (Figure 4.10). Comparing the $EC50^G$ and $EC50^V$ of these cell lines suggests that the impact of Ara-C treatment is primarily anti-proliferative at the concentrations used. Unexpectedly, given that the growth of U937 and HEL cells was reduced compared to the control lines, PKCε overexpression increased the sensitivity to Ara-C, reducing the $EC50^G$ by 2.9-fold and 1.9-fold respectively (Figure 4.9). This was accompanied by significant reductions in cell viability in response to Ara-C, where the $EC50^V$ were reduced by 3.5-fold in U937 cells and c5-fold in HEL cells (Figure 4.10). Together, this data show that PKCε overexpression in U937 and HEL cells sensitises these lines to Ara-C, likely due to increased levels of apoptosis. In contrast, intrinsically, NOMO-1 and TF-1 cells showed little sensitivity to Ara-C up to 800nM (Figure 4.9 and Figure 4.10) and PKCε overexpression had little impact on this. Higher doses of Ara-C were not assayed since the highest concentration investigated already exceeded the steady-state plasma level used in patients (c300nM; Fleming, *et al.*, 1995). Overall, this data suggests that in cell lines that are intrinsically sensitive to Ara-C treatment, PKCε overexpression enhances the growth inhibitory and cytotoxic effects of this chemotherapeutic agent. This finding was surprising given that PKCε overexpression reduced the intrinsic growth of the cell lines which exhibited increased Ara-C sensitivity. Furthermore, these data do not support the hypothesis that PKCε overexpression has the propensity to confer resistance to Ara-C.

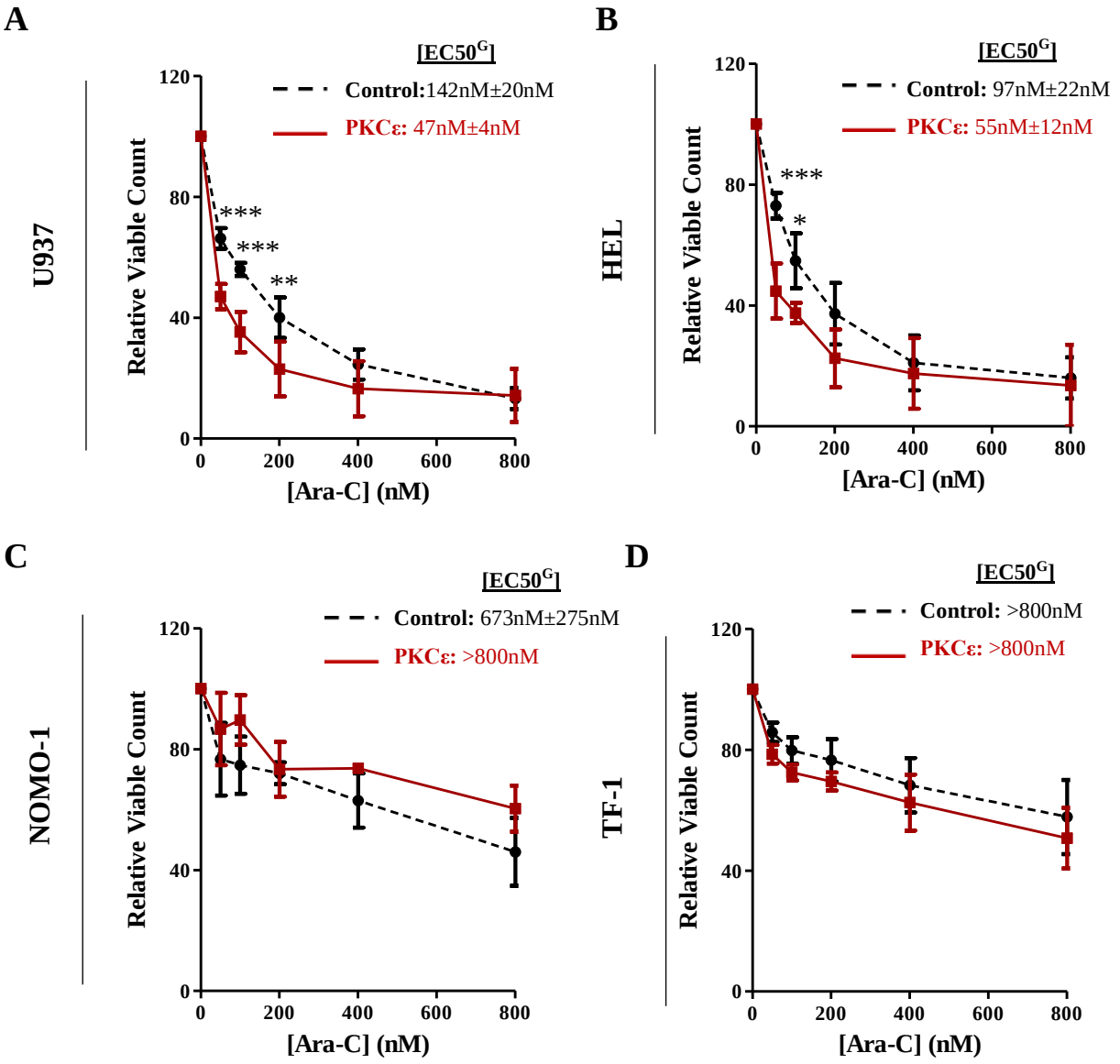

Figure 4.9: PKCε overexpression reduces the growth of AML cell lines in response to Ara-C

Line graphs showing the effect of increasing Ara-C concentration (nM) on the growth of **(A)** U937, **(B)** HEL, **(C)** NOMO-1 and **(D)** TF-1 cells transduced with the control or PKCε overexpression constructs (Figure 4.3), following 48 hours of treatment. Cell growth was determined by flow cytometry using TOPRO-3 staining and normalised to the growth of cells treated with the vehicle at the time of harvesting (2.8.2); n=3; data represents mean ± 1SD. Statistical significance between the sensitivities of the control and PKCε overexpression cell lines was determined using a two-way ANOVA with Bonferroni post-test comparison; *p<0.05, ** p<0.01, *** p<0.001.

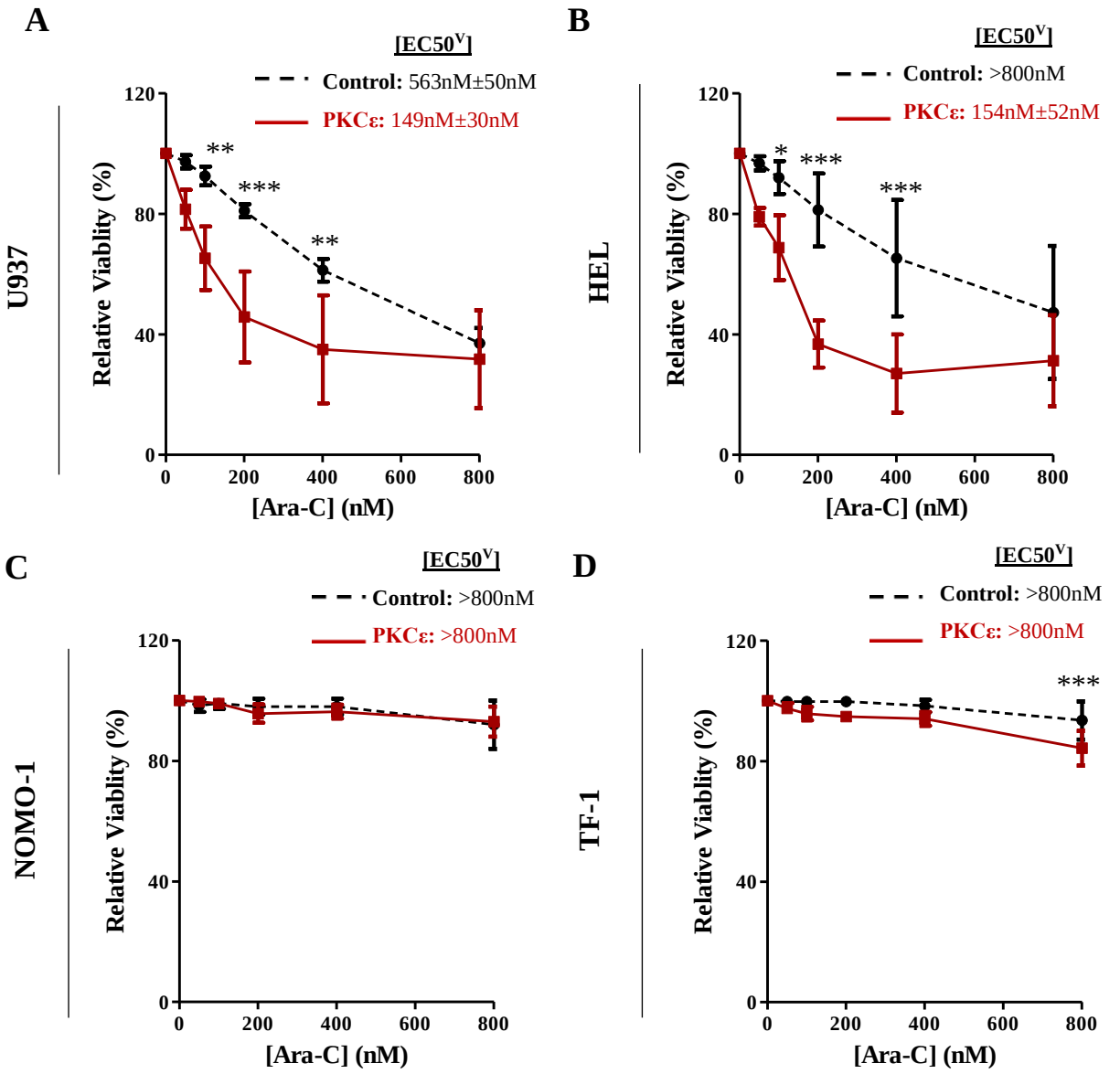

Figure 4.10: PKCε overexpression reduces the viability of AML cells in response to Ara-C

Line graphs showing the effect of increasing Ara-C concentration (nM) on the viability of **(A)** U937, **(B)** HEL and **(C)** NOMO-1 and **(D)** TF-1 cells transduced with the control or PKCε overexpression constructs (Figure 4.3), following 48 hours of treatment (2.8.8). Viability was determined by flow cytometry using TOPRO-3 staining and was normalised to the viability of cells treated with the vehicle control (PBS), at the time of harvesting (2.8.2); n=3; data represents mean ±1SD. Statistical significance between the sensitivities of the control and PKCε overexpression cell lines was determined using a two-way ANOVA with Bonferroni post-test comparison; * $p < 0.05$, ** $p < 0.01$, *** $p < 0.001$.

4.3.2.2 PKCε overexpression promotes DNR resistance in U937 and HEL cells

In contrast to Ara-C, all the lines tested demonstrated an intrinsic sensitivity to the anti-proliferative impact of DNR treatment, with $EC50^G$ of 16-31nM (Figure 4.11). The impact on cell viability was more heterogeneous. NOMO-1 cells showed a high degree of resistance (with an $EC50^V$ >100nM; Figure 4.12) ,while the sensitivities of U937, HEL and TF-1 cells were relatively comparable ($EC50^V$ of 42nM-67nM; Figure 4.12). Together, these values indicate that the reduced cell growth in these lines following DNR treatment, except for NOMO-1 cells, is a result of a combination of anti-proliferative and pro-apoptotic mechanisms. PKCε overexpression in U937 and HEL cells promoted a 2.7-fold and 2.9-fold increase in the $EC50^G$ of DNR, compared to the control cell lines (Figure 4.11), and conferred a significant survival advantage, with the $EC50^V$ increasing from c60nM to >100nM (Figure 4.12). This suggests that, in contrast to its impact on Ara-C sensitivity, PKCε overexpression promotes resistance to the cytotoxic effects of DNR in these cell lines. However, PKCε overexpression had no impact on the DNR sensitivity of NOMO-1 and TF-1 cells in terms of growth (Figure 4.11) or viability (Figure 4.12). Despite the heterogeneous responses across the four AML cell lines investigated, overall, these data show that in some AML cells PKCε overexpression has the propensity to selectively promote resistance to DNR.

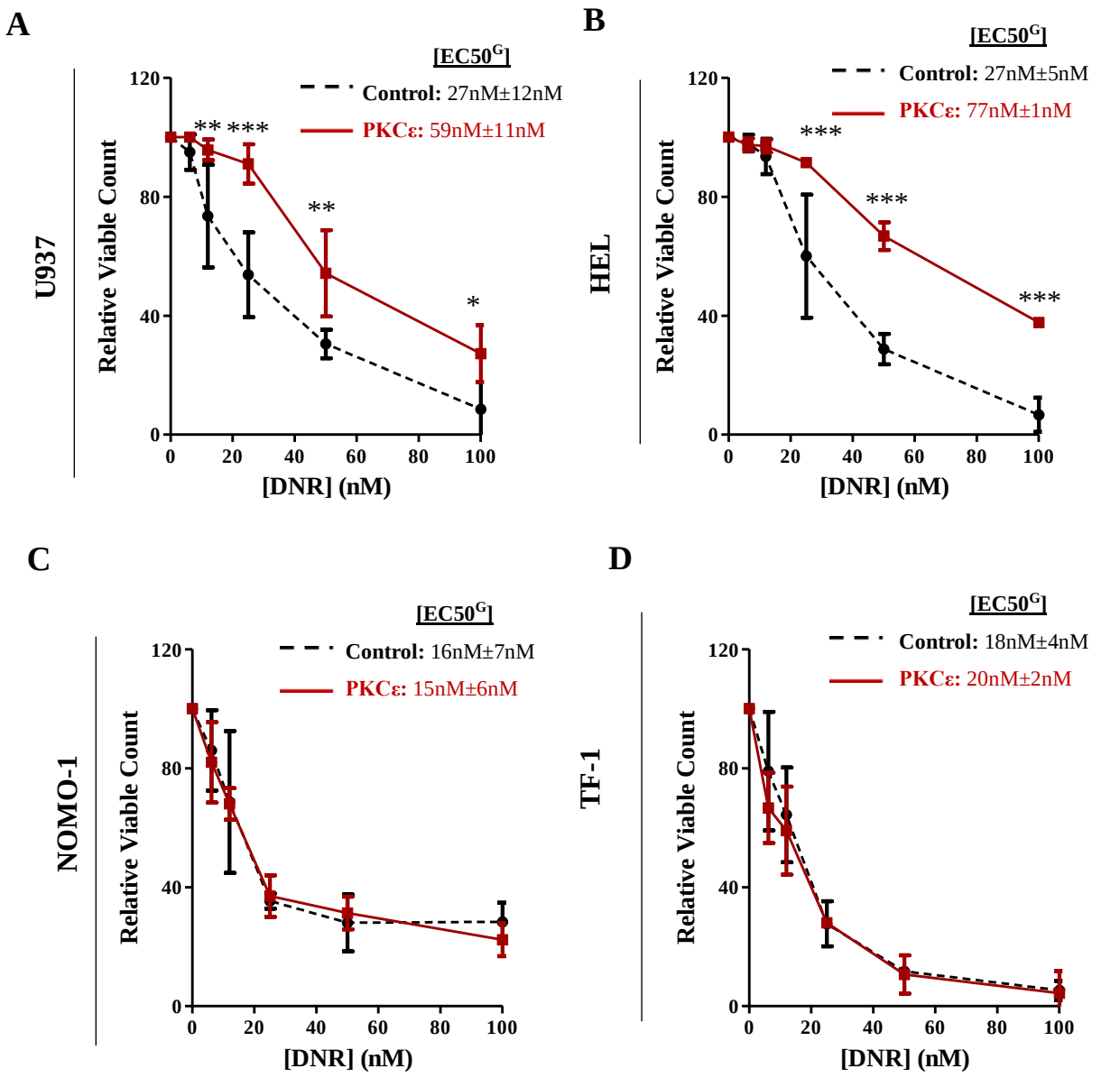

Figure 4.11: PKCε overexpression reduces the growth inhibitory impact of DNR in AML cell lines

Line graphs showing the effect of increasing DNR concentration (nM) on the growth of **(A)** U937, **(B)** HEL, **(C)** NOMO-1 and **(D)** TF-1 cells transduced with the control or PKCε overexpression constructs (Figure 4.3), following 48 hours of treatment (2.8.8). The counts were determined using TOPRO-3 staining and were normalised to the growth of the cells treated with the vehicle control (PBS; 2.8.2); U937 (n=4), HEL, NOMO-1, TF-1 (n=3); data represents mean ±1SD. Statistical significance between the sensitivities of the control and PKCε overexpression cell lines was determined using two-way ANOVA with Bonferroni post-test comparison; * p <0.05, **p<0.01, *** p<0.001.

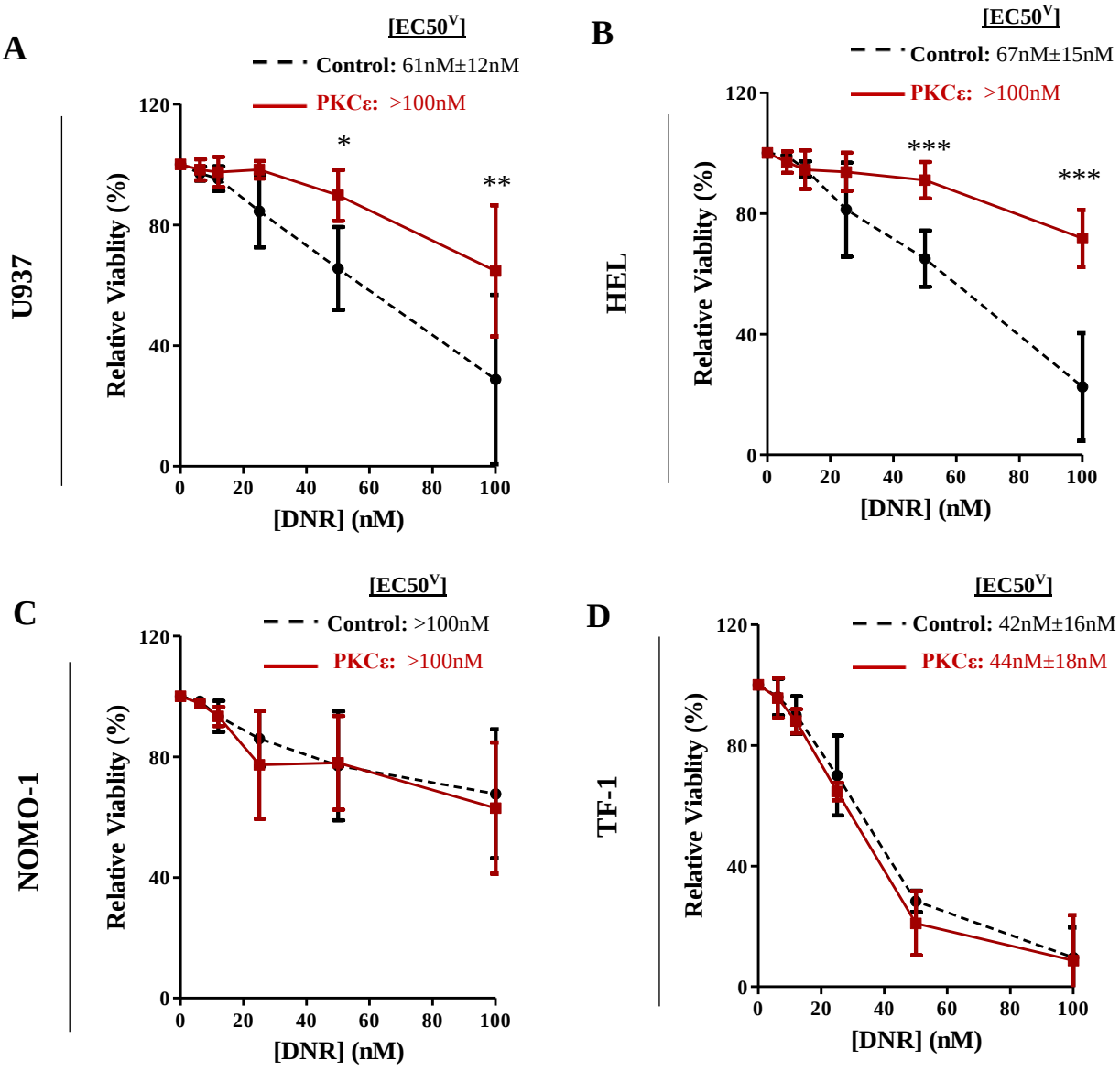

Figure 4.12: PKCε overexpression promotes cell survival in response to DNR treatment in U937 and HEL cells

Line graphs showing the effect of increasing DNR concentration (nM) on the viability of **(A)** U937, **(B)** HEL and **(C)** NOMO-1 and **(D)** TF-1 cells transduced with the control or PKCε overexpression constructs (Figure 4.3), following 48 hours of treatment (2.8.8). Viability was determined using TOPRO-3 staining and was normalised to the viability of cells treated with the vehicle control (PBS; 2.8.2); n=3; data represents mean ±1SD. Statistical significance between the sensitivities of the control and PKCε overexpression cell lines was determined using two-way ANOVA with Bonferroni post-test comparison; * $p<0.05$, ** $p<0.01$, *** $p<0.001$.

4.3.2.3 Establishing whether stromal interactions contribute to PKCε-mediated chemoresistance in AML cell lines

In vivo, leukaemia cells reside in the BM microenvironment (1.1.1.1) where interactions with the niche can impact leukaemia cell biology including promoting chemoresistance (1.4.2). Unlike other PKC isoforms, PKCε has an actin binding motif which allows it to modulate the cytoskeletal arrangement and integrin expression of cells and facilitate ECM interactions (1.6.5.4). Furthermore, stromal interactions can promote quiescence. As in normal culture conditions, DNR resistance was observed in the cell lines where proliferation was reduced, it was hypothesised that PKCε overexpression may promote stromal interactions which could further reduce cell proliferation and amplify the chemoresistance phenotype observed in the absence of stroma (4.3.2.2). To establish this, the AML cell lines overexpressing PKCε (4.3.1.1) were seeded on MS5 stromal monolayers and the impact of PKCε overexpression on the viability, growth, attachment to stromal, and chemosensitivity was assessed by flow cytometry as described in 4.3.2.

Although the magnitude of difference was not statistically significant, in U937 and HEL cells, PKCε overexpression promoted increases in the attachment of these lines to the MS5 cells by c60% compared to the control lines, while in NOMO-1 and TF-1 cells no differences in cell attachment were observed (Figure 4.13). Furthermore, no significant difference in cell viability or growth were observed in any of the cell lines compared to the absence of stroma (Figure 4.14). However, a trend towards increased proliferation in the presence of stroma was observed for both the control and PKCε overexpression cell lines. In terms of the chemosensitivity, stromal co-culture did not confer resistance to Ara-C (data not shown) and did not exacerbate DNR resistance (Figure 4.15). Compared to normal culture conditions (in the absence of stroma), stromal co-culture sensitised both the control and PKCε overexpression cell lines to DNR, opposed to being supportive and promoting DNR resistance (Figure 4.15). As a result of these findings, the impact of PKCε overexpression and stromal interaction was not pursued further and subsequent studies into the mechanism of PKCε-mediated DNR resistance were conducted in the absence of stroma (Chapter 5).

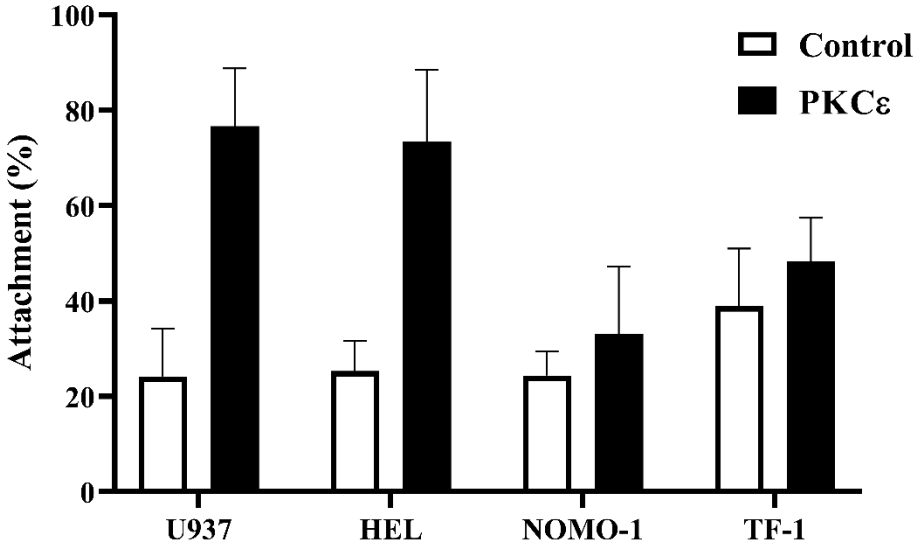

Figure 4.13: PKCε overexpression promotes U937 and HEL cell attachment to stroma

Bar charts representing the proportion (%) of U937, HEL, NOMO-1 and TF-1 cells transduced with the control or PKCε overexpression constructs (Figure 4.3) attached to MS5 stromal cells following 48 hours of culture (2.9.2). Data represents mean+1SD; n=3, except NOMO-1 where n=2. Statistical significance was determined using a Mann-Whitney test and was deemed non-significant.

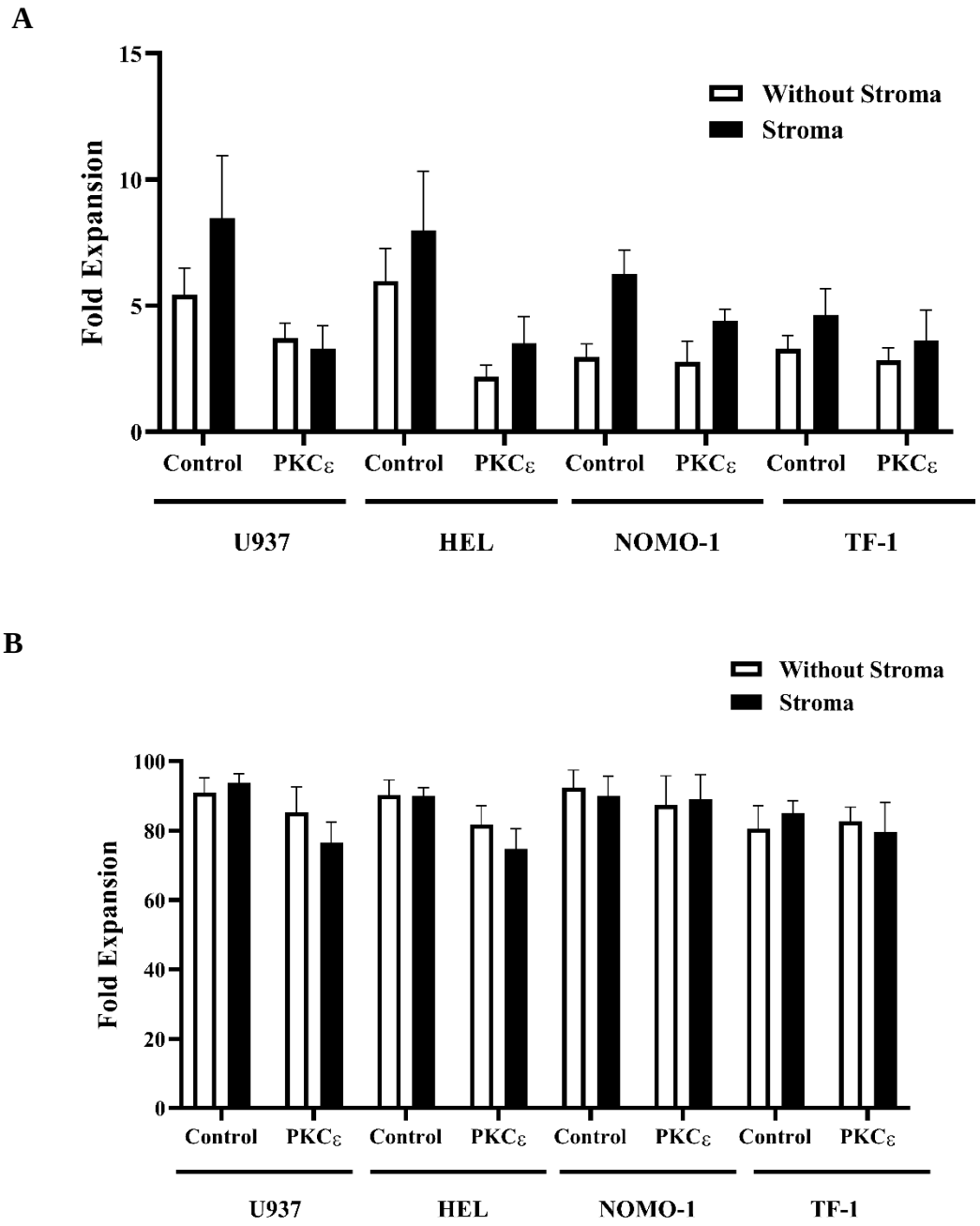

Figure 4.14: Stromal co-culture increased the proliferation of AML cell lines but had no effect of viability

Bar charts representing the **(A)** fold expansion and **(B)** viability of U937, HEL, NOMO-1 and TF-1 cells transduced with the control or PKCε overexpression constructs (Figure 4.3) over 48 hours of culture in the presence and absence of MS5 stromal cells (2.9.1). The counts and viability of the cells was determined by TOPRO-3 staining as described in 2.8.2; data represents mean+1SD; n=3, except NOMO-1 where n=2 for viability only. Statistical significance was determined using Mann-Whitney tests and was deemed non-significant.

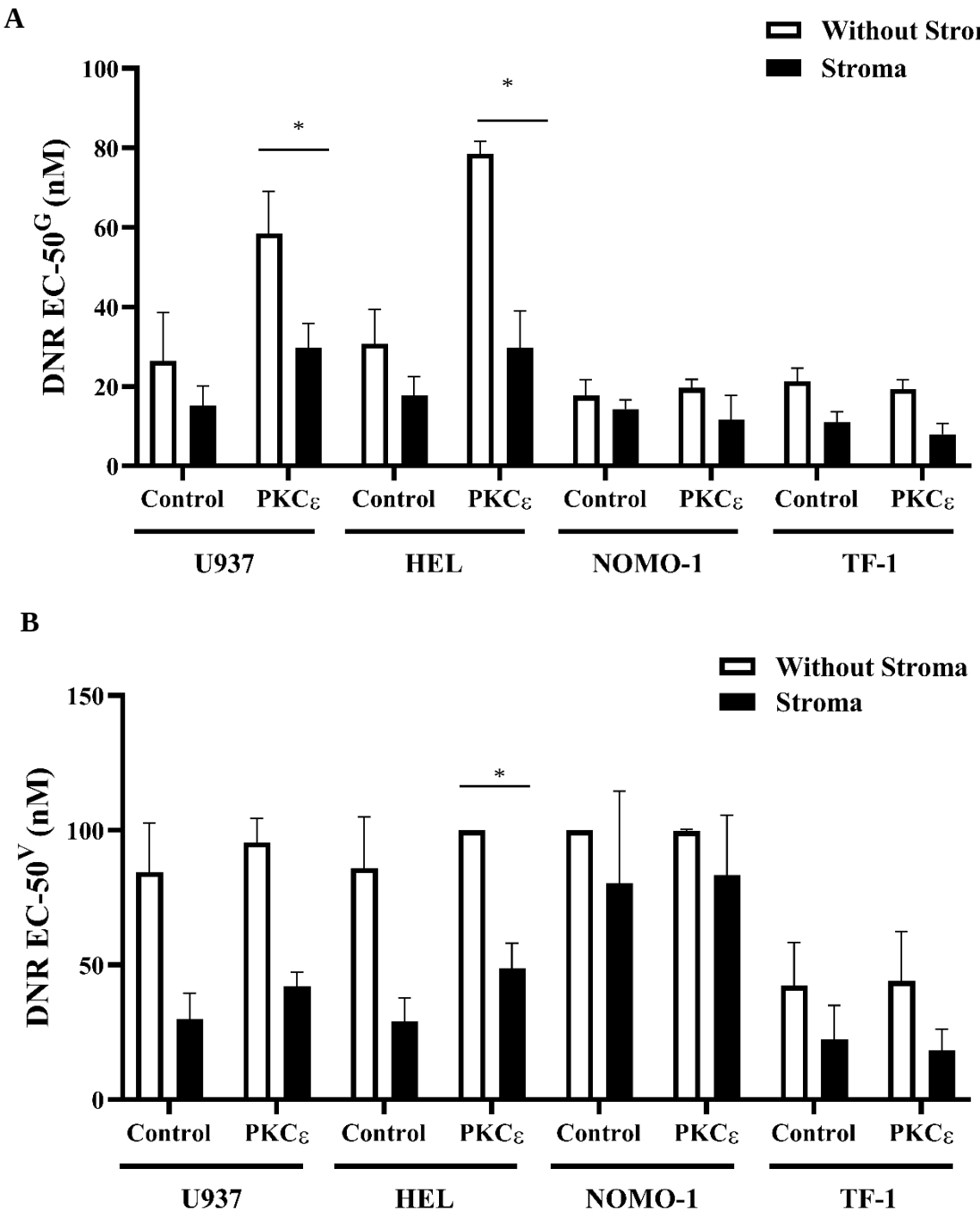

Figure 4.15: Stromal co-culture does not exacerbate PKCε-mediated DNR resistance in AML cell lines

Bar charts representing the **(A)** $EC50^G$ and **(B)** $EC50^V$ of DNR (nM) for U937, HEL, NOMO-1 and TF-1 cells transduced with the control or PKCε overexpression constructs (Figure 4.3) over 48 hours of culture on in the presence and absence of MS5 stromal cells (2.9.3). The viability of the cells was determined by TOPRO-3 staining (2.6.3); data represents mean+1SD; n=3, except NOMO-1 where n=2 for viability only. Statistical significance was determined using Mann-Whitney tests; *$p<0.05$.

4.3.3 Determining the impact of reducing PKCε expression in AML cell lines

Having determined that PKCε overexpression can selectively confer resistance to DNR in AML cell lines, experiments to determine whether reducing PKCε impacted the sensitivity of AML cells to Ara-C and DNR were conducted. To do this, PKCε-targeted shRNA and gRNA constructs were employed in cell lines with endogenous PKCε protein expression (U937, Mv4;11 and OCIAML5; Figure 4.1). The impact of reducing PKCε expression on cell growth, viability and chemosensitivity was assessed and compared to cells transduced with constructs which do not have a mammalian gene target (Table 2.4 and Table 2.5).

4.3.3.1 PKCε knockdown does not affect the sensitivity of AML cell lines to Ara-C or DNR

The effect of reducing PKCε expression was first examined using shRNA-mediated knockdown systems. Having been validated in HSPC (Figure 3.29), the knockdown efficiency of the PKCε-targeted shRNA constructs 485 and 486 were assessed in U937 and Mv4;11 cells (Figure 4.16). This analysis showed a respective reduction in PKCε protein expression of c70% and c80% in U937 cells and c70% in Mv4;11 cells (Figure 4.16). This reduction in PKCε expression had no significant impact on the growth or proliferation of U937 or Mv4;11 cells (Figure 4.17). Therefore, the consequence of reduced PKCε expression on the Ara-C and DNR sensitivity of these cell lines was assessed as previously described (4.3.2). In both U937 and Mv4;11 cells, PKCε knockdown did not significantly affect the Ara-C (Figure 4.18) or DNR (Figure 4.19) sensitivities, compared to the control lines in terms of $EC50^{G}$ or $EC50^{V}$, following 48 hours of treatment. Therefore, reducing PKCε expression is not sufficient to affect the intrinsic survival of these cell lines or the chemosensitivity to the agents investigated. However, this could be due to the efficiency of PKCε knockdown in this system in which 20%-30% of endogenous PKCε expression remained, which could be sufficient to prevent apoptosis or chemo-sensitisation.

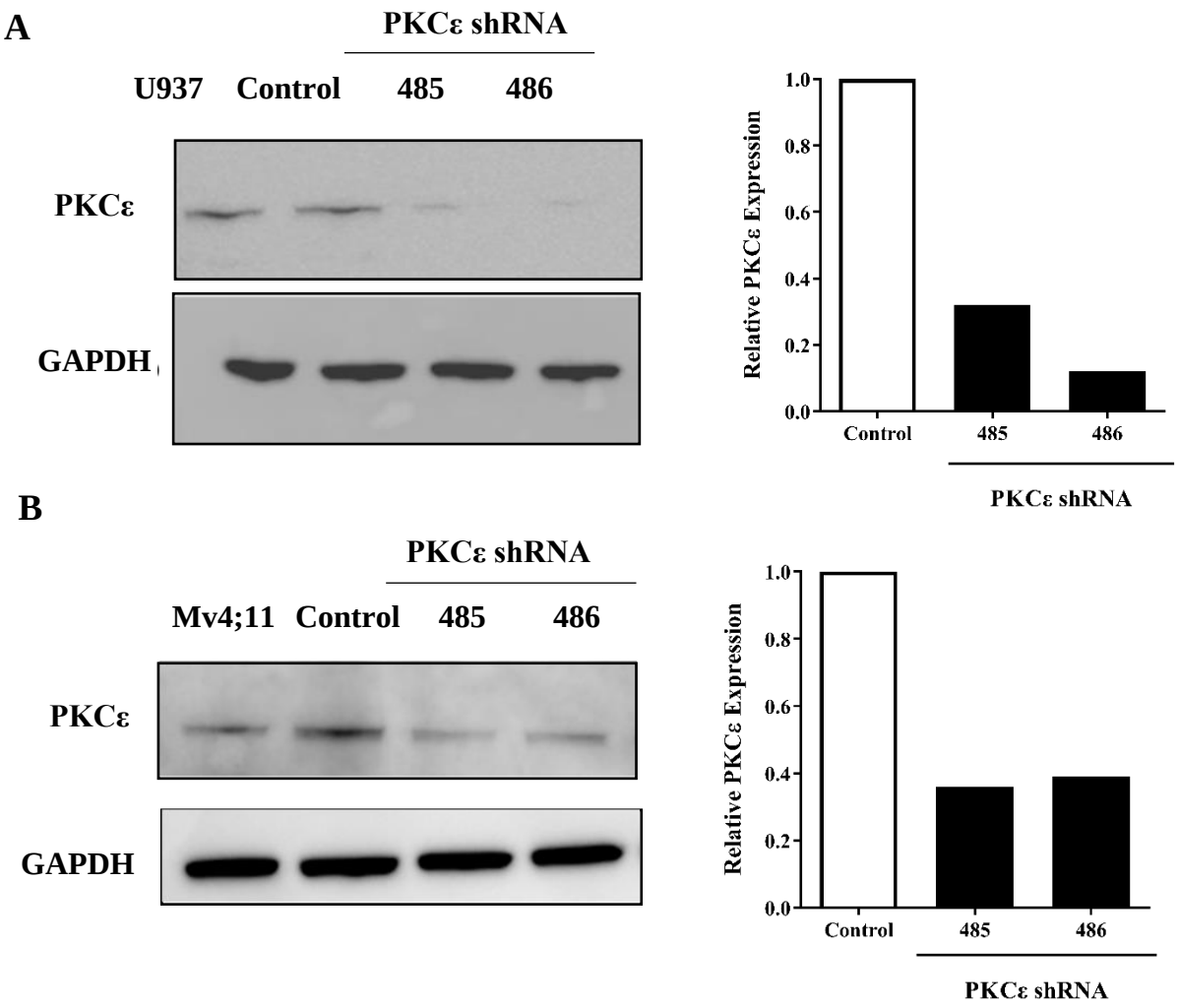

Figure 4.16: Validation of PKCε knockdown in AML cell lines

Western blot images (left) and quantification (right) showing PKCε (MW-84kDa) expression in **(A)** U937 and **(B)** Mv4;11 cells transduced control (shRNA_GFP_puro^R with no mammalian target;497; Table 2.4) and PKCε-targeted shRNA constructs (PKCε_shRNA_GFP_Puro^R; 485 and 486; Table 2.4). Before lysate generation, the transduced cell lines underwent puromycin selection (10 µg/mL) to remove un-transduced cells (2.5.2). Parental U937 and Mv4;11 cells were included in the western blot analysis to shown endogenous PKCε expression. PKCε expression was detected using the Cell Signalling Technologies antibody #2683 (clone 22B10; Table 2.10) and is shown alongside GAPDH (MW-36kDa) expression, which was used as a loading control and detected using the ThermoFisher Scientific GAPDH antibody (clone GA1R; Table 2.10). PKCε expression was quantified by densitometry analysis using Image J (Fiji). PKCε expression was calculated relative to loading (GAPDH expression) and normalised to the expression of U937 cells transduced with the control shRNA construct (2.7.5); n=1.

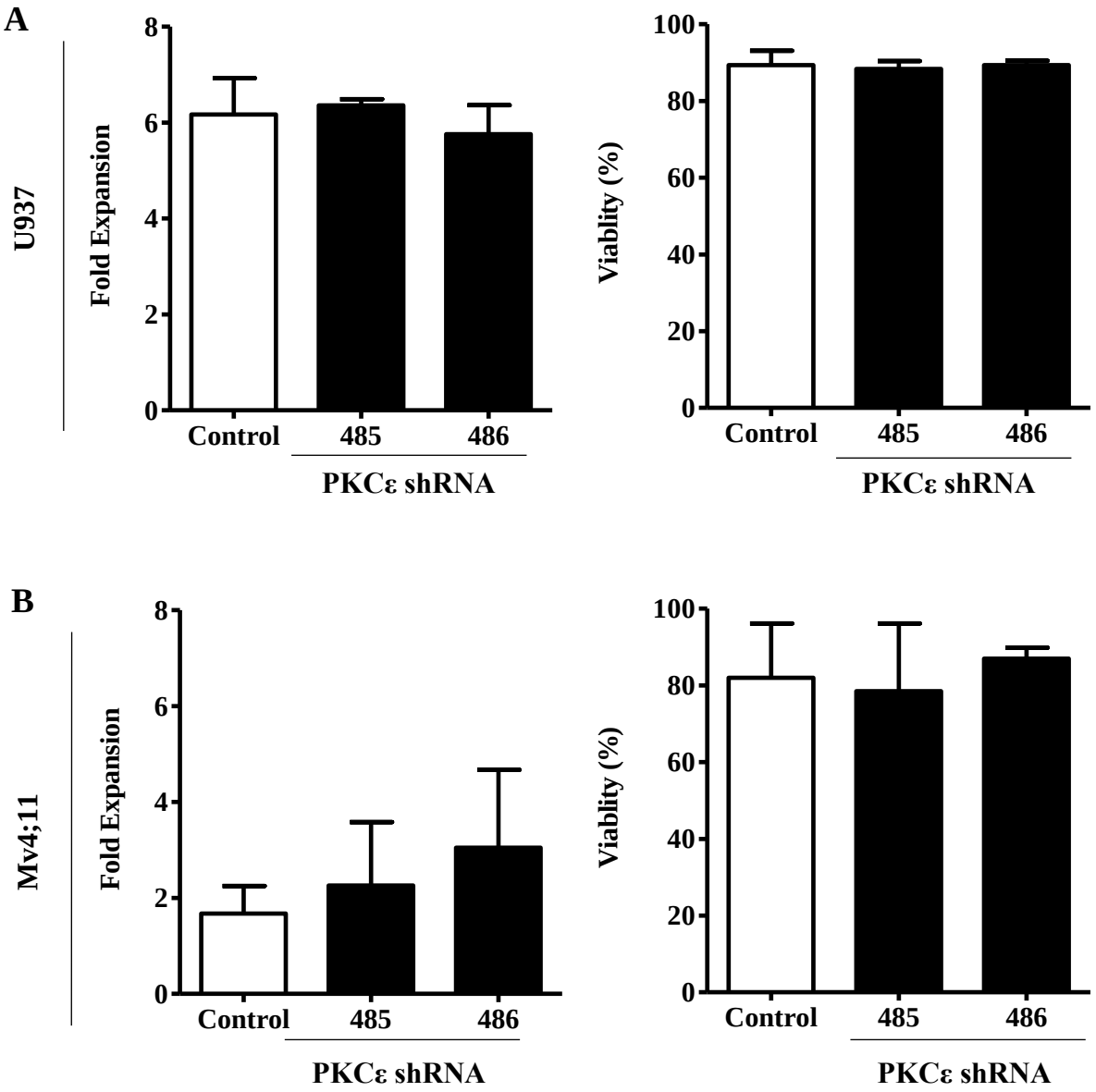

Figure 4.17: The effect of PKCε knockdown on the growth and viability of AML cell lines

Bar charts representing the fold expansion (right) and viability (%;left) of **(A)** U937 and **(B)** Mv4;11 cells transduced with the control or PKCε-targeted shRNA constructs (Figure 4.16) following 48 hours of culture. The fold expansion and viability of the cells was determined by TOPRO-3 staining as described in 2.8.2; data represents mean+1SD; U937 (n=3), Mv4;11 (n=2). Statistical significance was determined using a one-way ANOVA with Bonferroni post-test comparison and the data was deemed non-significant.

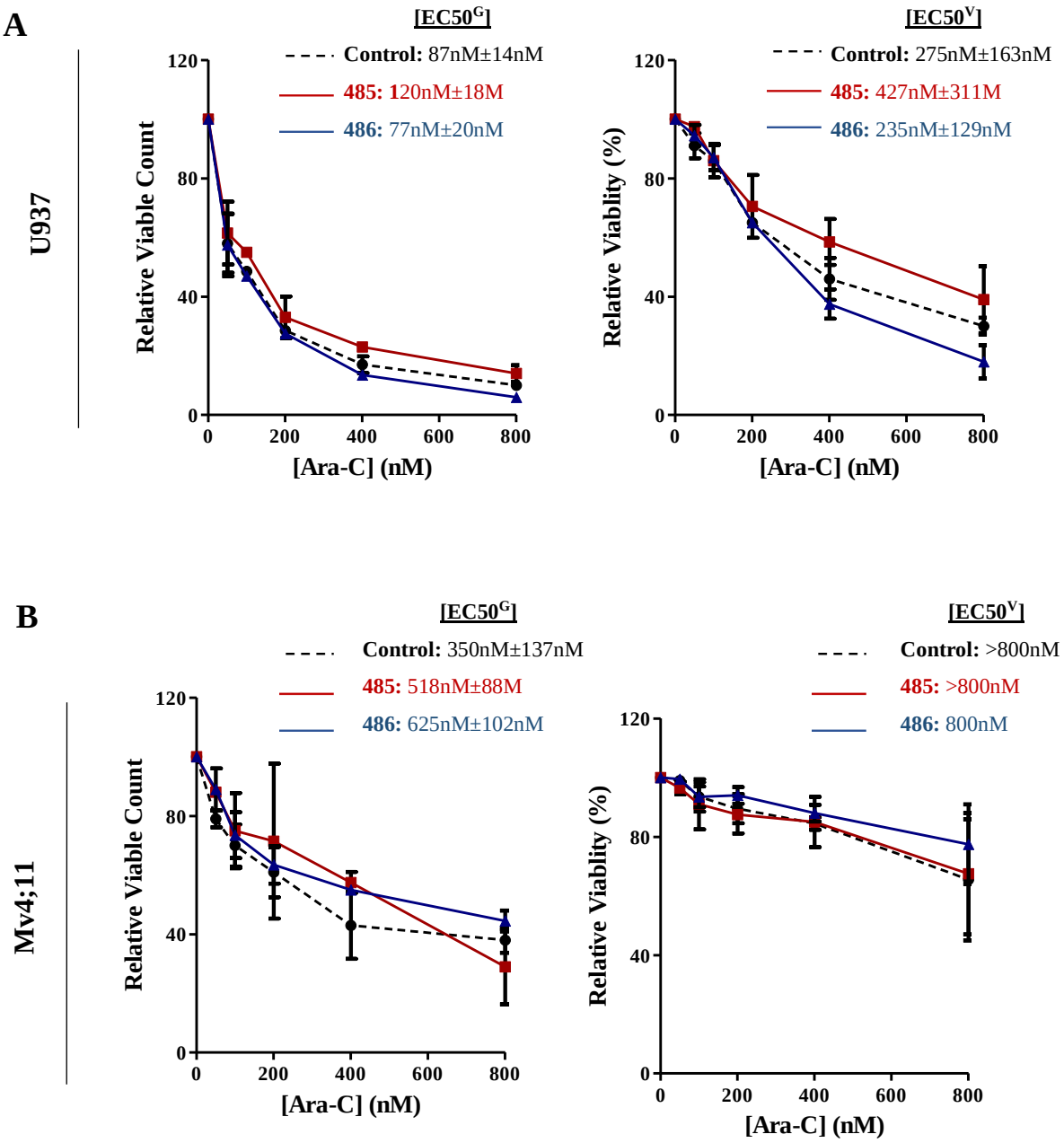

Figure 4.18: PKCε knockdown has no effect on the Ara-C sensitivity of AML cell lines

Line graphs showing the effect of increasing Ara-C concentration (nM) on the growth ($EC50^G$;left) and viability ($EC50^V$; right) of **(A)** U937 and **(B)** Mv4;11 cells transduced with the control or PKCε-targeted shRNA constructs (Figure 4.16), following 48 hours of treatment (2.8.8). Growth and viability were measured by flow cytometry and normalised to cells treated with the vehicle control; n=2; data represents mean ± 1SD.

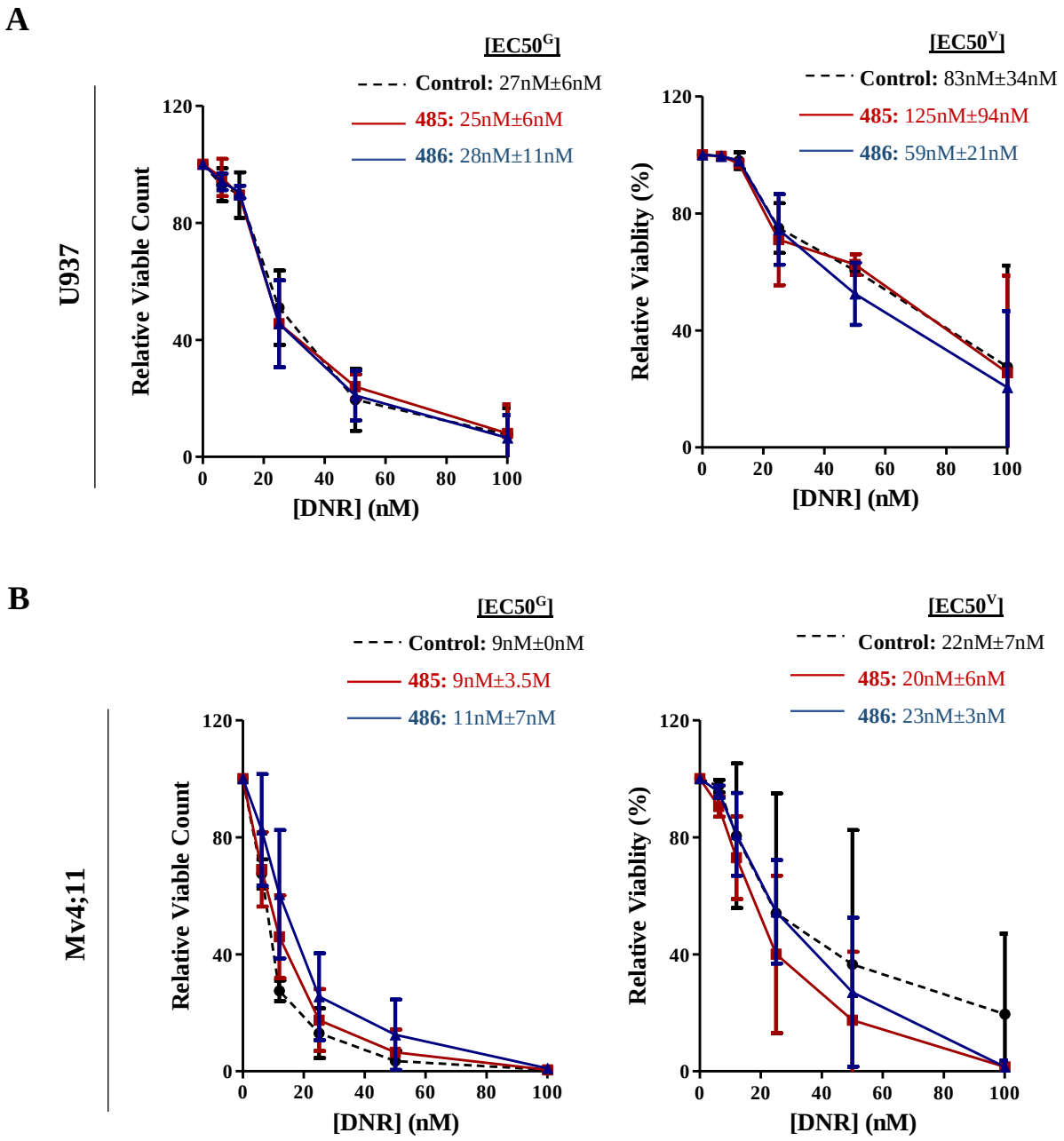

Figure 4.19: PKCε knockdown has no effect on the sensitivity of AML cell lines to DNR

Line graphs showing the effect of increasing DNR concentration (nM) on the growth ($EC50^G$; left) and viability ($EC50^V$; right) of **(A)** U937 and **(B)** Mv4;11 cells transduced with the control or PKCε-targeted shRNA constructs (Figure 4.16), following 48 hours of treatment (2.8.8). Growth and viability were measured by flow cytometry and normalised to cells treated with the vehicle control (PBS); n=2; data represents mean ± 1SD.

4.3.3.2 CRISPR/Cas9-mediated PKCε knockout does not sensitize AML cell lines to Ara-C or DNR

Unlike shRNA-mediated gene silencing in which post-transcriptional down-regulation means that functional mRNA will be translated albeit in a reduced capacity, CRISPR/*Cas9* technology has the capacity to generate complete loss-of-function mutations by inducing targeted double strand breaks which can result in frameshift mutations and a lack of functional protein expression. However, in practice CRISPR transduced cell cultures are highly heterogenous with the potential of some cells completely escaping genetic modification while others may harbour mutations which do not affect protein function such as in-frame insertion or deletion mutations. The cell lines described below are referred to as knockout lines, in order to distinguish them from the shRNA cell lines, however, this does not imply a complete knockout has been achieved.

To investigate the consequences of PKCε knockout in AML cell lines, three PKCε-targeted guide RNA (gRNA; 522, 524, 526; Table 2.5) were purchased alongside the control gRNA construct (Table 2.5). These constructs were transduced into U937 cells and the levels of reduction in PKCε protein by each construct was evaluated by western blot analysis. This showed that the 522-gRNA was the most efficient (Figure 4.20) reducing PKCε protein expression by c90% (Figure 4.21A). This construct was then transduced into an additional cell line. For this analysis, Mv4;11 cells were replaced with OCIAML5 cells which had the highest endogenous level of PKCε expression (Figure 4.1). The reason behind this decision being that the impact of knocking out PKCε may be more significant for these cells given their higher endogenous expression. Validation of OCIAML5 cells transduced with the PKCε-targeted 522-gRNA also showed c90% reduction in PKCε protein expression (Figure 4.21B). Subsequent flow cytometric analysis showed that the growth and viability of the PKCε knockout lines was no different from the respective control cell lines (Figure 4.22). Furthermore, PKCε knockout, did not significantly impact the sensitivity of U937 or OCIAML5 cells to Ara-C (Figure 4.23) or DNR (Figure 4.24). This data supports the conclusion of shRNA analysis in showing that solely targeting PKCε is not sufficient to alter the intrinsic survival or affect the chemosensitivity of the AML cell lines investigated, albeit with the caveats described above.

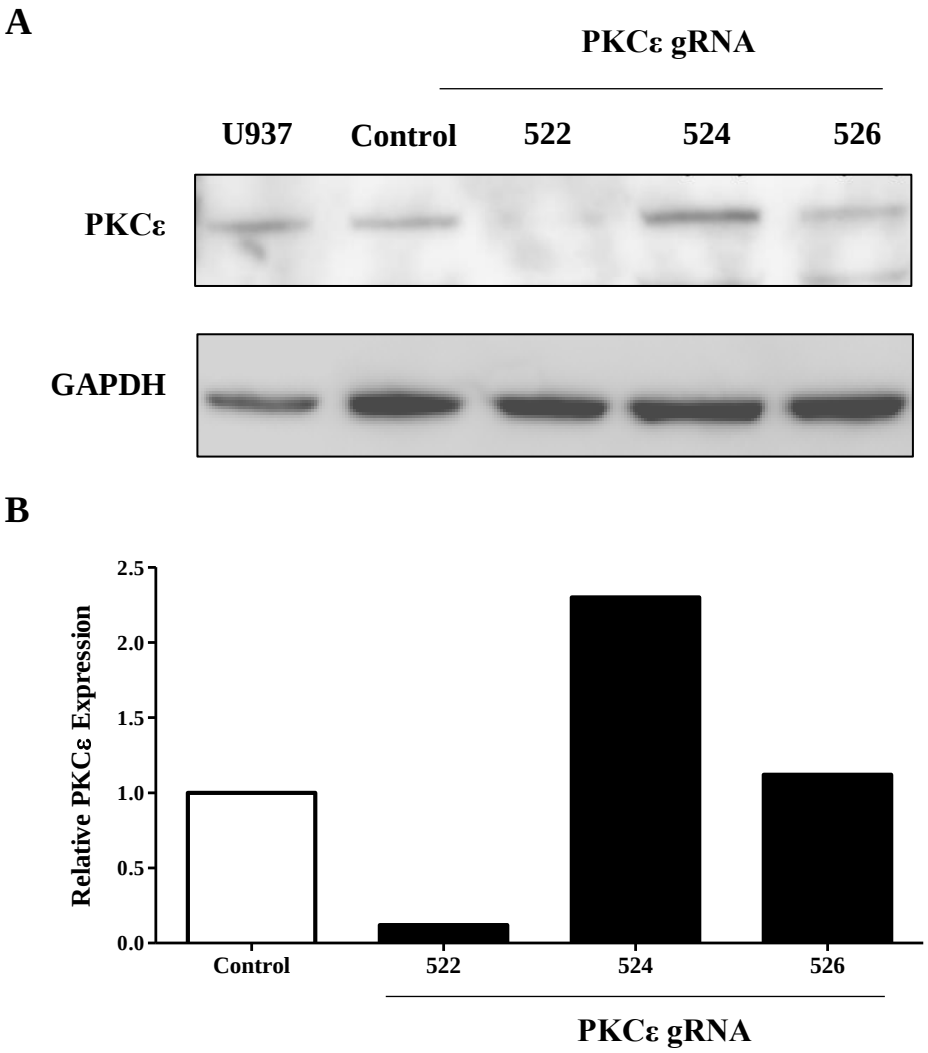

Figure 4.20: Validating the efficacy of PKCε-targeted gRNA constructs

(A) Western blot showing PKCε (MW-84kDa) expression in U937 cells transduced with the control (gRNA_puro^R with no mammalian target;463; Table 2.5) or PKCε-targeted gRNA constructs (PKCε_gRNA_puro^R;522, 524, 526; Table 2.5). Before lysate generation, the transduced cell lines underwent puromycin selection (10 µg/mL) to remove un-transduced cells (2.5.2). Parental U937 cells were included in the western blot analysis to show endogenous PKCε expression. PKCε expression was detected using the Cell Signalling Technologies antibody #2683 (clone 22B10; Table 2.10) and is shown alongside GAPDH (MW-36kDa) expression, which was used as a loading control and detected using the ThermoFisher Scientific GAPDH antibody (clone GA1R; Table 2.10). **(B)** Bar chart showing PKCε expression in U937 cells transduced with the PKCε-targeted gRNA constructs. PKCε expression was quantified by densitometry analysis using Image J (Fiji). PKCε expression was calculated relative to loading (GAPDH expression) and normalised to the expression of U937 cells transduced with the control gRNA construct (2.7.5); n=1.

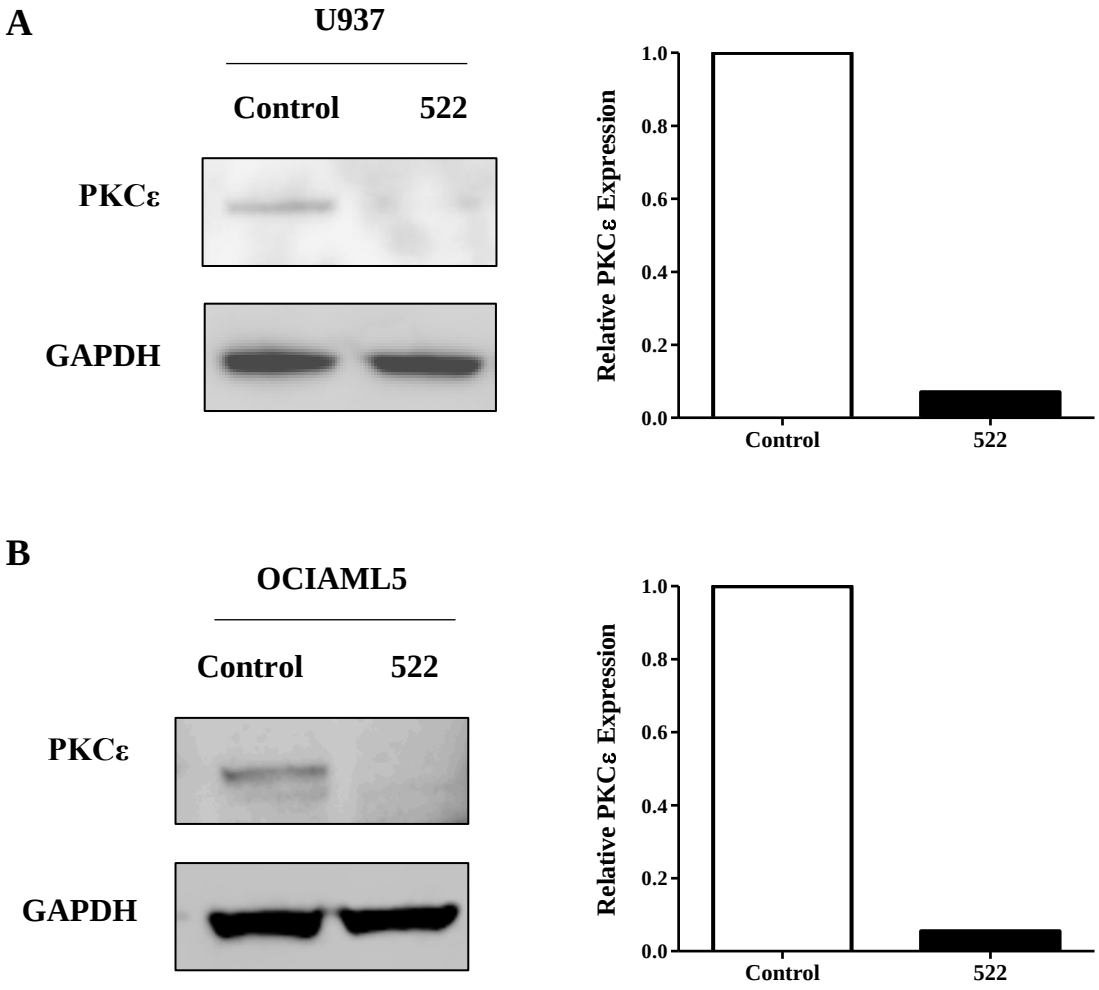

Figure 4.21: Validation of PKCε knockout in U937 and OCIAML5 cells

Western blots (left) and quantification (right) showing PKCε (MW-84kDa) expression in **(A)** U937 and **(B)** OCIAML5 cells transduced with the control (gRNA_puro^{R} with no mammalian target;463; Table 2.5) or PKCε-targeted gRNA construct (PKCε_gRNA_puro^{R};522; Table 2.5). Before lysate generation, the AML cell lines underwent puromycin selection (10 µg/mL) to remove un-transduced cells (2.5.2). PKCε expression was detected using the Cell Signalling Technologies antibody #2683 (clone 22B10; Table 2.10) and is shown alongside GAPDH (MW-36kDa) expression, which was used as a loading control and detected using the ThermoFisher Scientific GAPDH antibody (clone GA1R; Table 2.10). PKCε expression was quantified by densitometry analysis using Image J (Fiji). PKCε expression was calculated relative to loading (GAPDH expression) and normalised to the expression of cells transduced with the control gRNA (2.7.5); n=1.

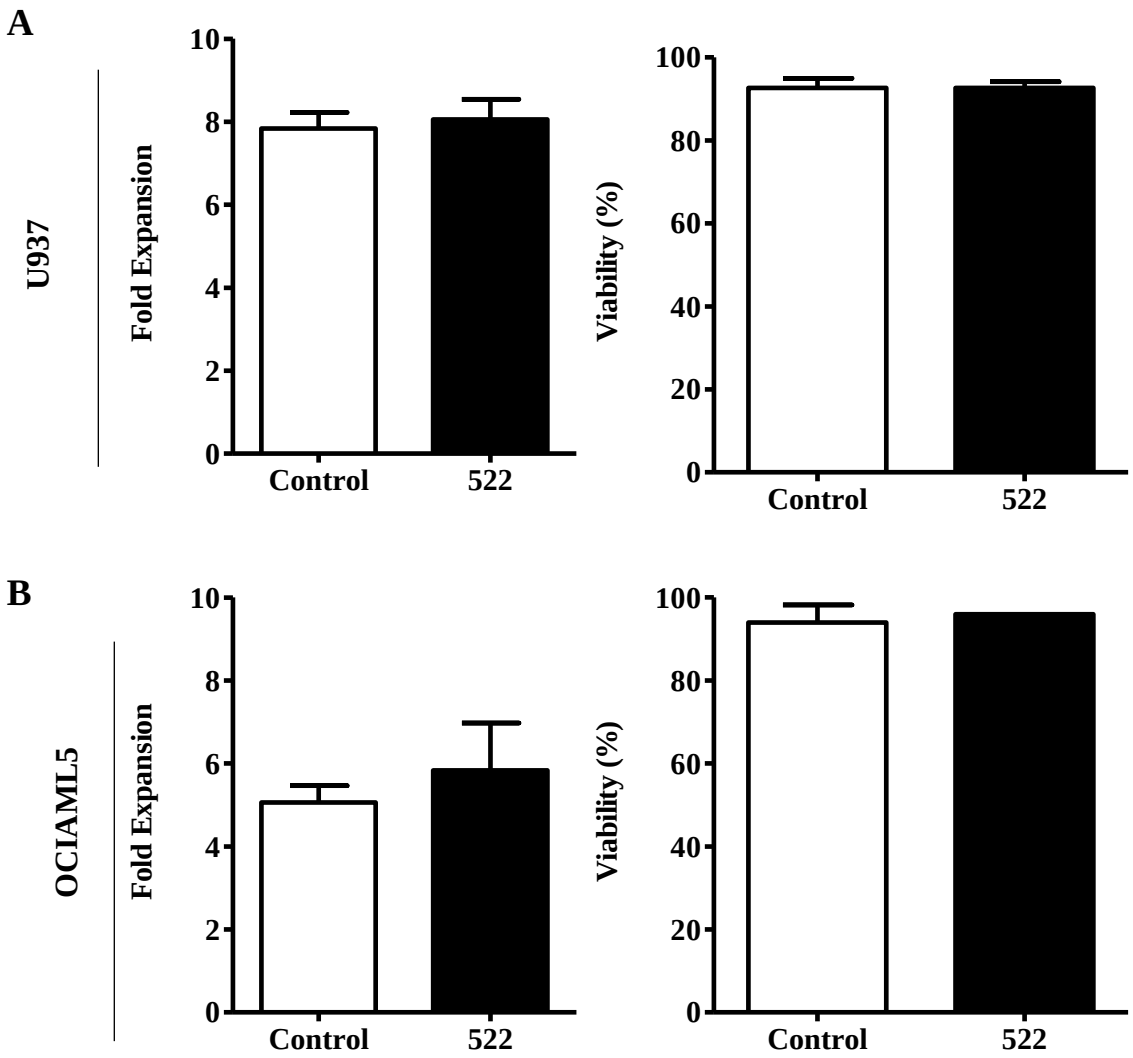

Figure 4.22: PKCε knockout has no effect on the growth and viability of AML cell lines

Bar charts representing the fold expansion (right) and viability (%;left) of **(A)** U937 and **(B)** OCIAML5 cells transduced with the control or PKCε-targeted gRNA constructs described in Figure 4.21, following 48 hours of culture. The fold expansion and viability of the cells was determined using TOPRO-3 staining as described in 2.6.3; data represents mean+1SD; U937 (n=3), OCIAML5 (n=2). Statistical significance was determined using Mann-Whitney tests and was deemed non-significant.

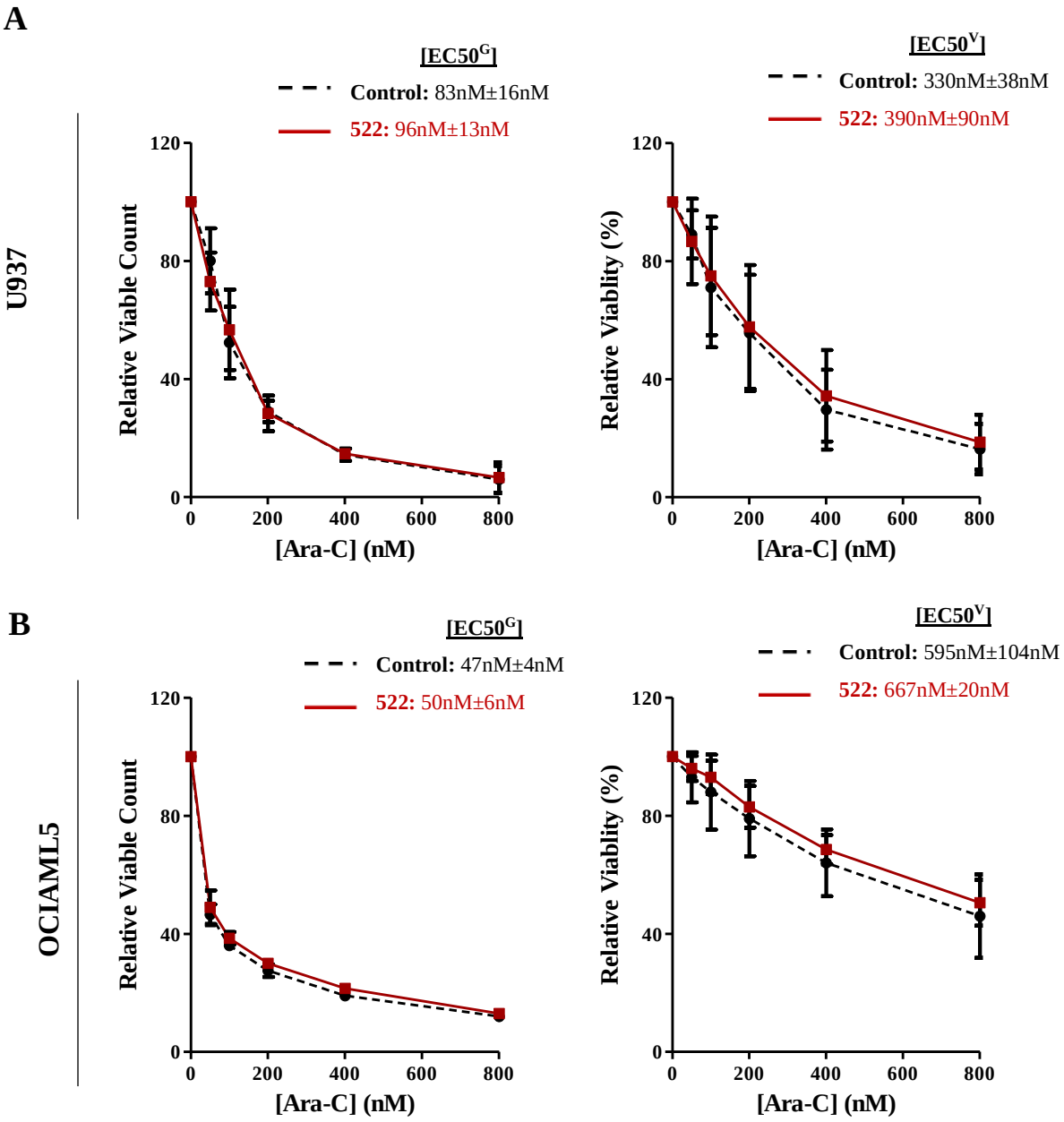

Figure 4.23: PKCε knockout has no effect on the sensitivity of AML cell lines to Ara-C

Line graphs showing the effect of increasing DNR concentration (nM) on the growth ($EC50^G$; left) and viability ($EC50^V$; right) of **(A)** U937 and **(B)** OCIAML5 cells transduced with the control or PKCε-targeted gRNA constructs (Figure 4.21), following 48 hours of treatment (2.8.8). Growth and viability were determined using TOPRO-3 staining as described in 2.6.3 and normalised to cells treated with the vehicle control (PBS); U937 (n=3) and OCIAML5 (n=2); data represents mean±1SD. Statistical significance between the sensitivities of the control and PKCε knockout cell lines was determined using two-way ANOVA with Bonferroni post-test comparison and was deemed non-significant.

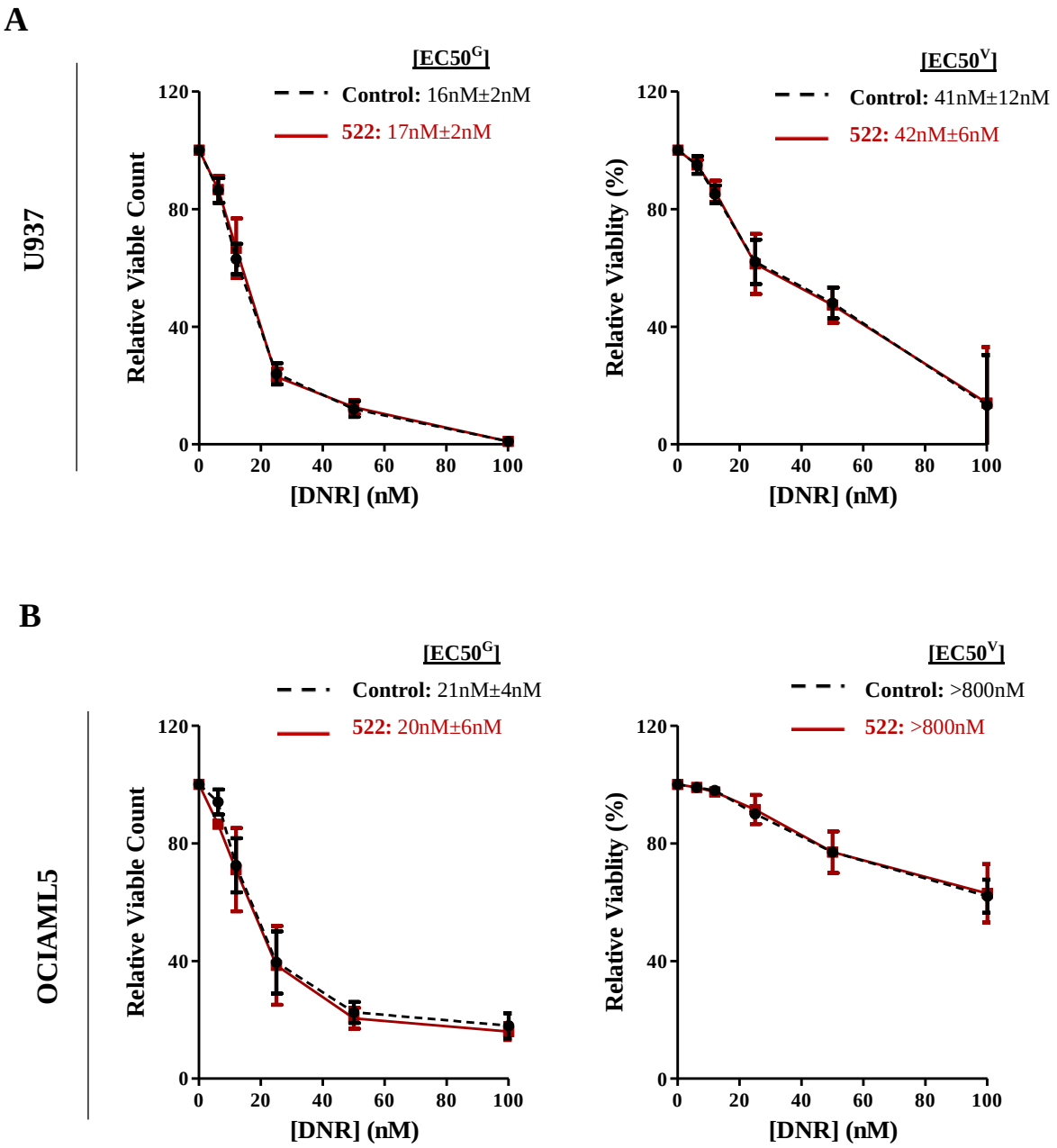

Figure 4.24: PKCε knockout has no effect on the sensitivity of AML cell lines to DNR

Line graphs showing the effect of increasing DNR concentration (nM) on the growth ($EC50^{G;}$ left) and viability ($EC50^{V}$; right) of **(A)** U937 and **(B)** OCIAML5 cells transduced with the control or PKCε-targeted gRNA constructs (Figure 4.21), following 48 hours of treatment (2.8.8). Growth and viability were determined by TOPRO-3 and normalised to cells treated with the vehicle control (PBS); U937 (n=3) and OCIAML5 (n=2); data represents mean ± 1SD. Statistical significance between the sensitivities of the control and PKCε knockout cell lines was determined using two-way ANOVA with Bonferroni post-test comparison and was deemed non-significant.

4.3.4 Determining potential redundancy in function between PKCε and other nPKC isoforms

The PKC family is made up of 11 homologous isoforms which may have overlapping biological functions. Therefore, it was hypothesised that reducing PKCε did not sensitise the AML cell lines to DNR due to redundancy in function between the different PKC isoforms. This analysis focused on the nPKC isoforms, PKCδ, PKCθ and PKCη, which are most closely structurally related to PKCε (1.5.1). The expression of ABC cassette efflux pumps has previously been associated with poor patient outcomes in AML (van der Kolk, *et al.*, 2000; 1.4.3), and drug efflux, mediated by such transporters, is a well described mechanism of anthracycline resistance (Eckford and Sharom, 2009). Therefore, to determine the relationship between the nPKC isoforms and chemoresistant phenotypes in AML, the correlation between the mRNA expression of *PKCδ, PKCθ* and *PKCη,* and ABC transporters for which DNR is a substrate and Ara-C is not (*ABCB1*,(P-GP), *ABCC1* (MRP1), and *ABCG2* (BRP1;de Jonge-Peeters, *et al.*, 2007) was investigated in AML patient samples using the TCGA 2013 dataset (Ley, *et al.*, 2013). This analysis showed that *PKCε* and *PKCδ* do not significantly correlate with *P-GP, MRP1 or BRP1*, while *PKCθ* and *PKCη* showed significant positive correlations with *P-GP, MRP1* and *BRP1* (Table 4.1). Therefore, PKCθ and PKCη may be associated with chemoresistance in AML and could be preventing DNR sensitisation in the AML cell lines upon reducing PKCε expression.

To further evaluate this hypothesis, the mRNA expression of *PKCε*, and *PKCθ* and *PKCη* was assessed in AML cell lines using DepMap (2.11.3). This analysis showed that *PKCη* was expressed at low levels in U937 and Mv4;11 cells (Figure 4.25A); lines in which reducing PKCε did not affect DNR sensitivity (4.3.3). In contrast, *PKCθ* was expressed at similar levels to *PKCε* in U937, Mv4;11 and OCIAML5 (Figure 4.25B), making PKCθ the more likely candidate for redundancy with PKCε in these cell lines. As a result, the expression profile of PKCθ in AML cell lines was validated by western blot. This supported the mRNA analysis, showing that the cell lines which expressed PKCε at a protein level (U937, Mv4;11 and OCIAML5) also expressed detectable levels of PKCθ (Figure 4.26). Therefore, supporting the premise that co-expression and potential redundancy between these two isoforms could be why reducing PKCε expression in these cell lines did not result in increased DNR sensitivity.

Table 4.1: Correlation between nPKC isoforms and DNR ABC cassette transporters

Table outlining the correlation between the novel PKC isoforms (*PKCε, PKCδ, PKCθ* and *PKCη*) and ABC cassette transporter proteins for which DNR is a known substrate. Data was obtained from the TCGA 2013 (Ley, *et al.*, 2013) dataset which was accessed using cBioPortal (Cerami, *et al.*, 2012, Gao, *et al.*, 2013). Values in bold indicate the Spearman's rank coefficient while the corresponding p-values are in parentheses.

ABC transporter (protein name)	***PKCε***	***PKCδ***	***PKCθ***	***PKCη***
ABCB1 (P-GP)	**0.041** (0.60)	**-0.464** (4.8×10^{-10})	**0.56** (8.3×10^{-15})	**0.554** (2×10^{-12})
ABCC1 (MRP1)	**-0.027** (0.78)	**-0.420** (2.7×10^{-8})	**0.64** (1.62×10^{-20})	**0.34** ($9.4 \times^{-6}$)
ABCG2 (BRP1)	**0.161** (0.04)	**-0.309** (6.4×10^{-5})	**0.40** (9.6×10^{-8})	**0.44** (5.7×10^{-9})

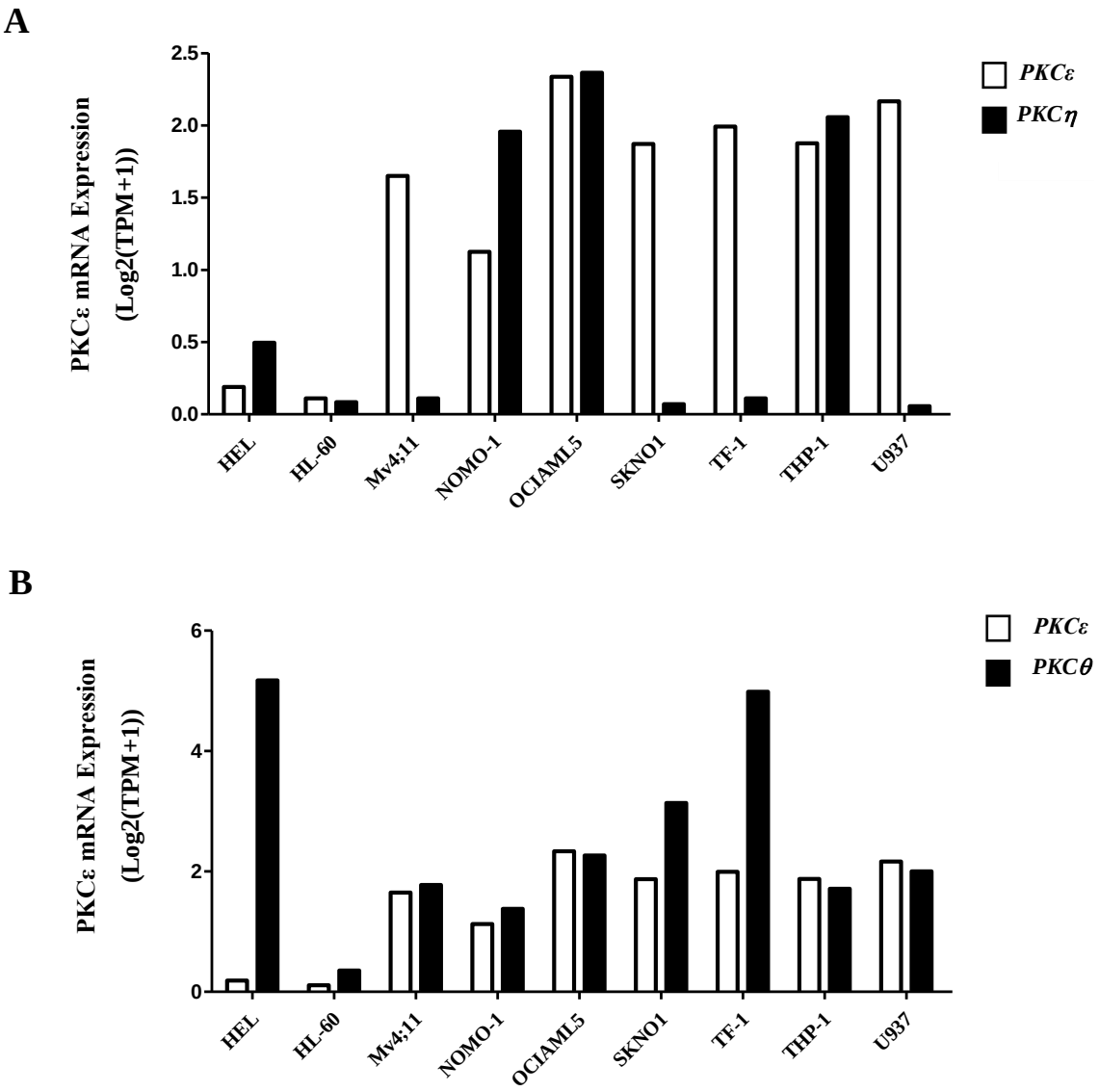

Figure 4.25: mRNA expression of *nPKC* isoforms in AML cell lines

Bar charts representing the mRNA expression (Log_2 (TPM+1)) of *PKCε* and **(A)** *PKCη* and **(B)** *PKCθ* in AML cell lines determined by RNAseq. Data was obtained from the DepMap using the Public 20Q1 dataset (Broad, 2020, Ghandi, *et al.*, 2019; 2.11.3).

4.3.4.1 PKCε knockout and PKCθ knockdown does not affect the chemosensitivity of OCIML5 cells

To investigate whether redundancy between PKCε and PKCθ prevented chemo-sensitisation of AML cell lines with reduced PKCε expression, the effect of reducing PKCθ expression in AML cell lines was investigated. To do this, the knockdown efficiency of three PKCθ-targeted shRNA constructs (533, 535 and 537; Table 2.4) was assessed in OCIAML5 cells; a cell line that endogenously expresses PKCθ and PKCε at a protein level (Figure 4.26A). Following quantification, this analysis showed that the shRNA construct 537 had the highest knockdown efficiency, reducing PKCθ protein expression by c90% compared to the control cell line (531;Figure 4.27). As a result, this construct was subsequently transduced into the OCIAML5 PKCε knockout cell line. The knockdown efficiency of this PKCθ targeted shRNA construct was assessed in this context using western blot analysis. As expected in this cell line, PKCε expression was undetectable by western blot analysis. Furthermore, a reduction in PKCθ expression of c60% compared to parental OCIAML5 cells was observed (Figure 4.28A). However, PKCθ expression was also reduced, by c45%, compared to the endogenous expression of OCIAML5 parental cells, in the PKCε knockout cells transduced with the control shRNA construct (531; Figure 4.28); a finding that was not observed in the original shRNA screen (Figure 4.27). Therefore, the knockdown efficiency achieved when comparing the PKCθ shRNA construct with the control shRNA construct, in the context of the PKCε knockout was modest at c25%.

Functional studies showed that PKCθ knockdown in the context of PKCε knockout did not affect cell proliferation and viability (Figure 4.29), or the sensitivity of these cells to either Ara-C or DNR (Figure 4.30), compared to cells transduced with the control shRNA construct (Figure 4.28). Furthermore, despite the reduction in PKCθ expression in both the control and PKCθ knockdown cells, compared to parental OCIAML5 cells (Figure 4.28), the chemosensitivity of the transduced PKCε knockout lines was not significantly different from the CRISPR/*Cas9* control which does not have a mammalian gene target (Figure 4.23 and Figure 4.24). Therefore, these data indicate that reducing both PKCε and PKCθ expression in OCIAML5 cells does not promote chemosensitivity. Consequently, redundant function between PKCε and PKCθ is unlikely to be responsible for the lack of chemosensitivity in the PKCε knockout cell lines (4.3.3.2).

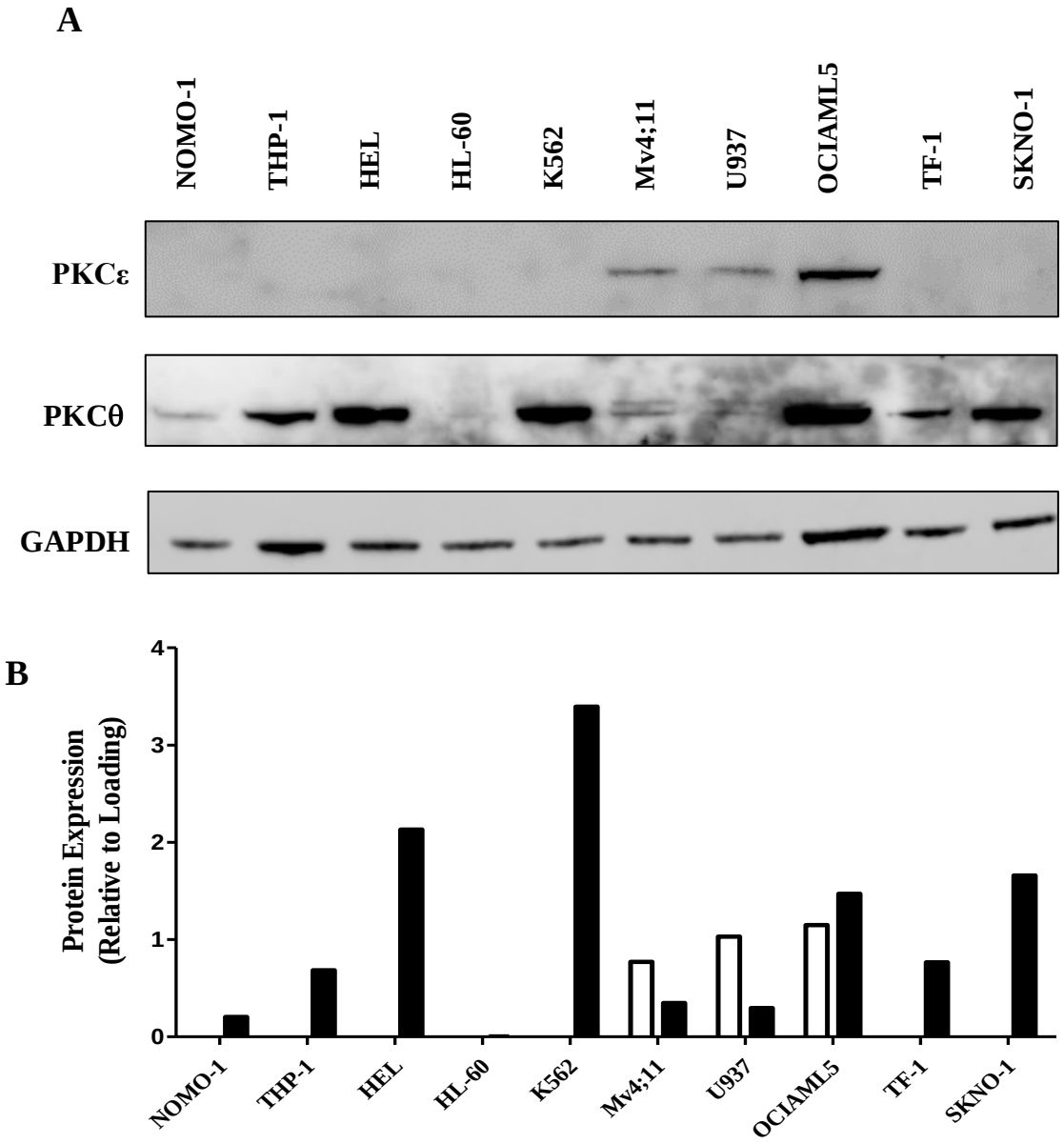

Figure 4.26: Validation of the expression of PKCε and PKCθ in AML cell lines

(A) Western blot showing PKCε (MW-84kDa) and PKCθ (MW-78kDa) expression in different AML cell lines. PKCε expression was detected using the Cell Signalling Technologies antibody #2681 (clone 22B10; Table 2.10) and PKCθ expression was detected using the Cell Signalling Technologies antibody #13643 (clone E1I7Y; Table 2.10). Expression of PKCε and PKCθ is shown alongside GAPDH (MW-36kDa) expression, which was used as a loading control and detected using the ThermoFisher Scientific GAPDH antibody (clone GA1R; Table 2.10). Western blot showing the expression of PKCε and PKCθ in different AML cell lines, GAPDH was used as a loading control. **(B)** Bar chart showing the expression of PKCε and PKCθ in different AML cell lines which were quantified by densitometry analysis using Image J (Fiji) as described in 2.7.5. PKCε and PKCθ expression was calculated relative to loading (GAPDH expression); n=1.

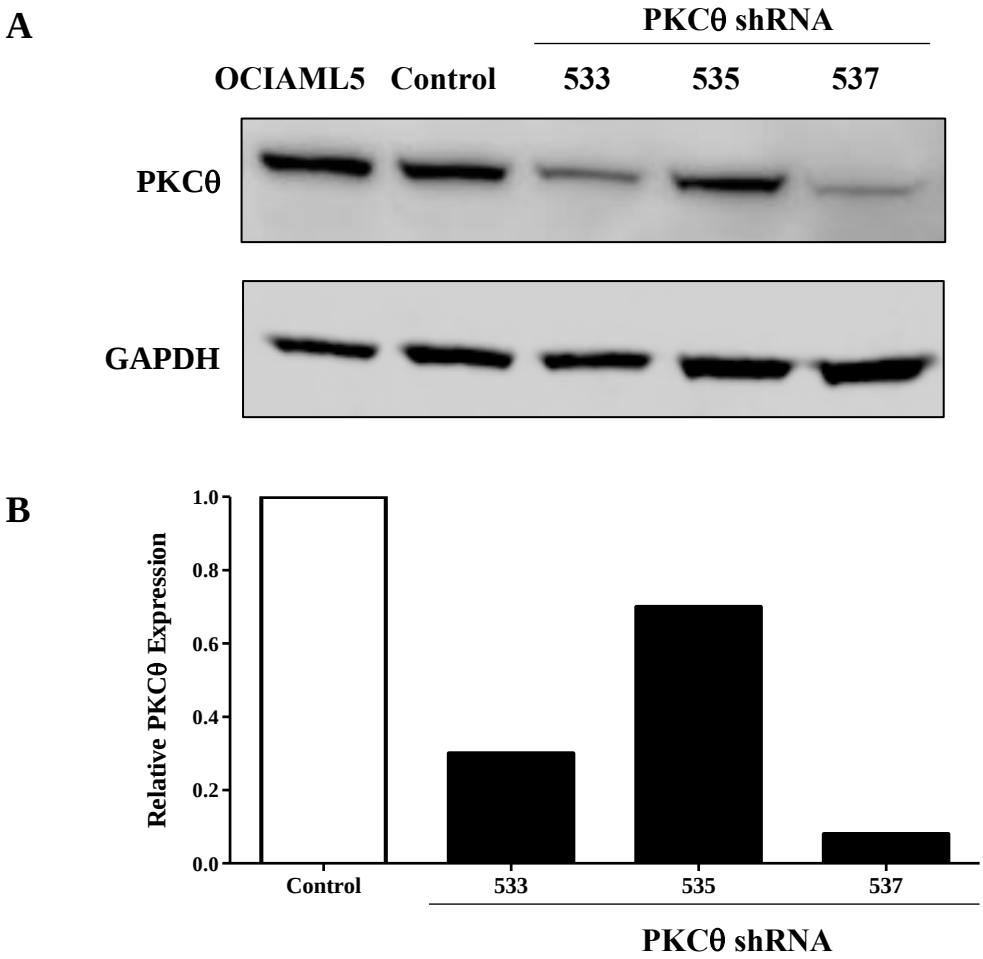

Figure 4.27: Validating the efficacy of PKCθ shRNA constructs by western blot

(A) Western blot showing PKCθ (MW-78kDa) expression in OCIAML5 cells transduced with the control (shRNA_BFP_Gen^R with no mammalian target;531) or PKCθ-targeted shRNA constructs (PKCθ_shRNA_BFP_Gen^R; 533, 535 and 537; Table 2.10). Before lysate generation, the transduced cell lines underwent Geneticin™ selection (1000 µg/mL) to remove un-transduced cells (2.5.2). Parental OCIAML5 cells were included in the western blot analysis to show endogenous PKCθ expression. PKCθ expression was detected using the Cell Signalling Technologies antibody #13643 (clone E1I7Y; Table 2.10) and is shown alongside GAPDH (MW-36kDa) expression, which was used as a loading control and detected using the ThermoFisher Scientific GAPDH antibody (clone GA1R; Table 2.10). **(B)** Bar chart showing PKCθ expression in OCIAML5 cells transduced with the PKCθ-targeted shRNA constructs. PKCθ expression was quantified by densitometry analysis using Image J (Fiji) as described in 2.7.5. PKCθ expression was calculated relative to loading (GAPDH expression) and normalised to the expression of OCIAML5 cells transduced with the control shRNA construct (531;Figure 4.28B); n=1.

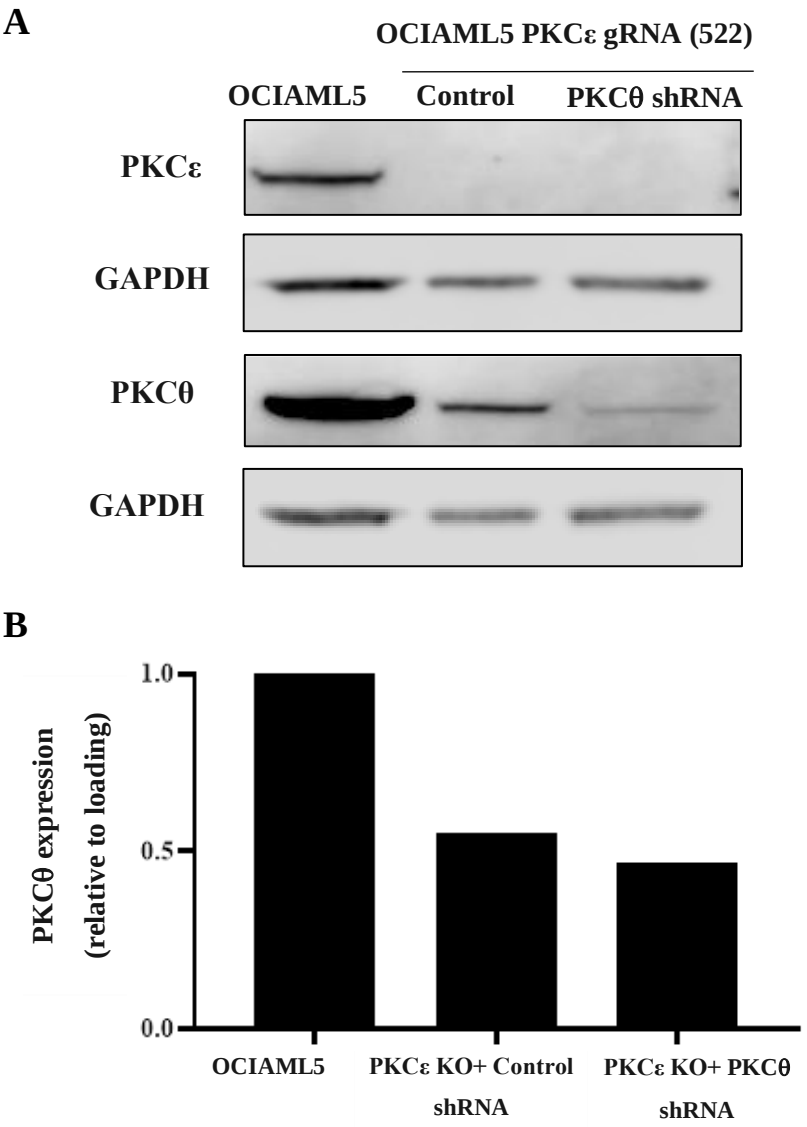

Figure 4.28: Validation of the PKCθ knockdown in OCIAML5 PKCε knockout cells

(A) Western blot showing the PKCε (MW-84kDa) expression and PKCθ (MW-74kDa) expression in OCIAML5 cells transduced with the PKCε-targeted gRNA (522; Figure 4.21) and either the control (531; Figure 4.27) or PKCθ-targeted shRNA construct (537; Figure 4.27). Parental OCIAML5 cells show endogenous expression of PKCε and PKCθ. Before lysate generation, the transduced AML cell lines underwent Geneticin™ (1000 µg/mL) selection to remove un-transduced cells (2.5.2). PKCε expression was detected using the Cell Signalling Technologies antibody #2681 (clone 22B10; Table 2.10) and PKCθ expression was detected using the Cell Signalling Technologies antibody #13643 (clone E1I7Y; Table 2.10). Expression of PKCε and PKCθ is shown alongside GAPDH (MW-36kDa) expression, which was used as a loading control and detected using the ThermoFisher Scientific GAPDH antibody (clone GA1R; Table 2.10). **(B)** Bar chart showing PKCθ expression in OCIAML5 cells transduced the with 522-PKCe gRNA and with the control or PKCθ-targeted shRNA constructs (Figure 4.27). PKCθ expression was quantified by densitometry analysis using Image J (Fiji) as described in 2.7.5; n=1.

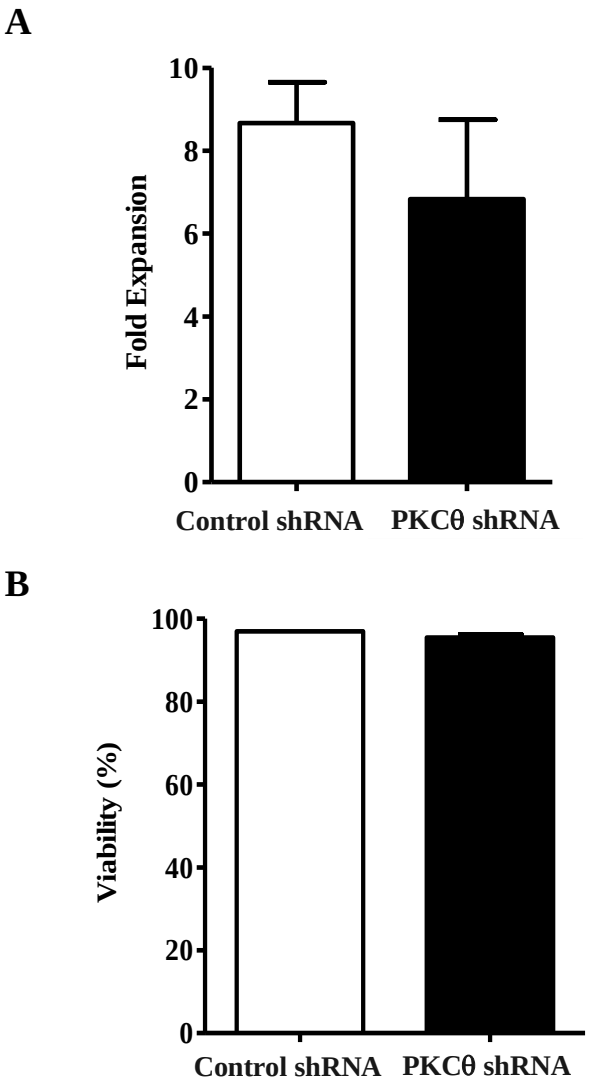

Figure 4.29: PKCθ knockdown in the context of PKCε knockout does not have a significant impact on the growth or viability of OCI AML5 cells

Bar charts representing the **(A)** fold expansion and **(B)** viability (%) of OCIAML5 cells transduced with the PKCε-targeted gRNA (522; Figure 4.20) and either the control or PKCθ-targeted shRNA construct (537; Figure 4.27) 48 hours after seeding. The fold expansion and viability of the cells was determined by TOPRO-3 staining as described in 2.8.2; n=2; data represents mean + 1 SD.

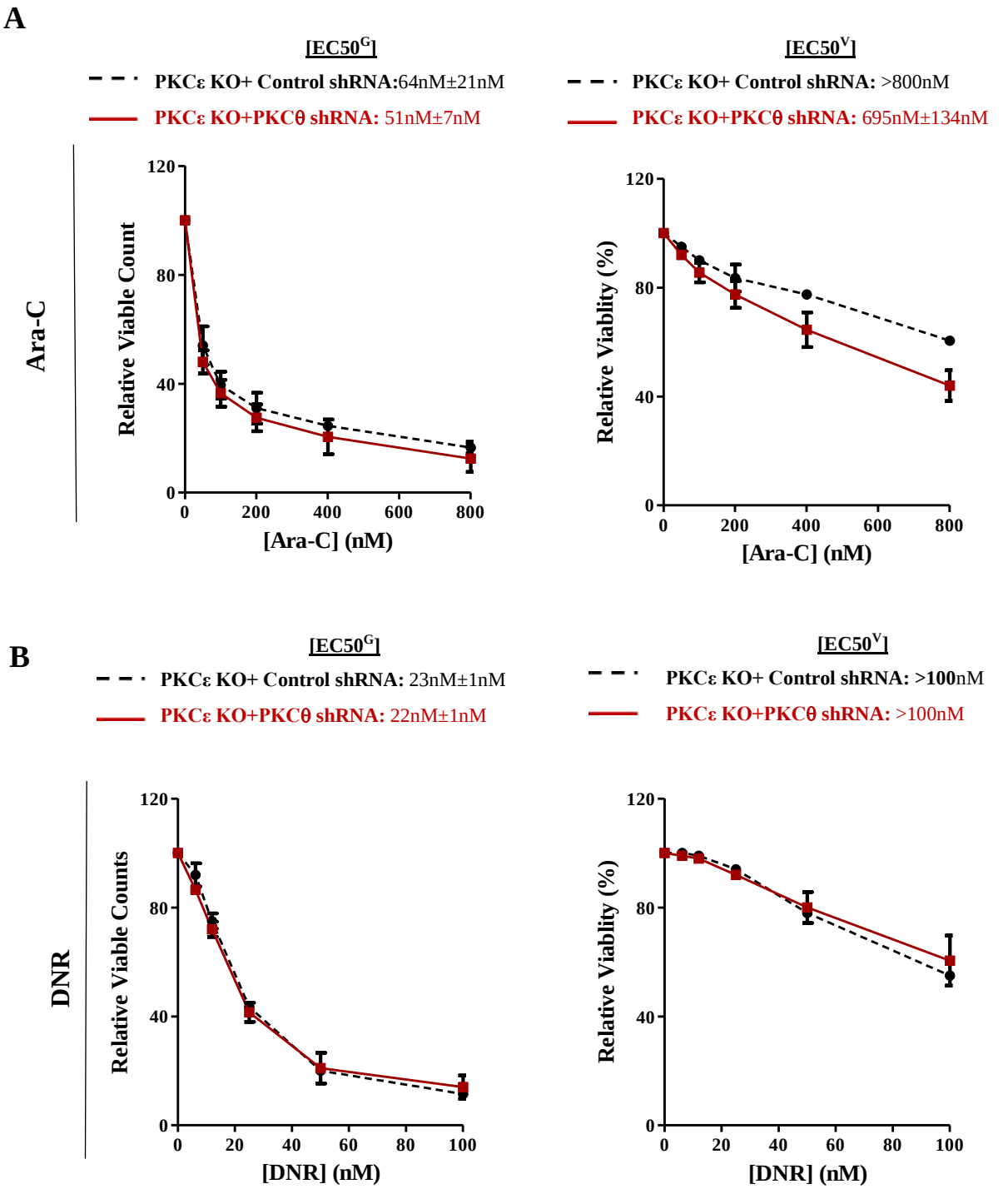

Figure 4.30: PKCθ knockdown in the context of PKCε knockout does not sensitise OCIAML5 cells to Ara-C or DNR

Line graphs showing the effect of increasing **(A)**Ara-C and **(B)** DNR concentration (nM) on the growth ($EC50^G$; left) and viability ($EC50^V$; right) of OCIAML5 cells transduced with the PKCε-targeted gRNA (522; Figure 4.20) and either the control (531; Figure 4.27) or PKCθ-targeted shRNA construct (537; Figure 4.27), following 48 hours of treatment (2.8.8). The growth and viability were measured using flow cytometry and were normalised to the cells treated with the appropriate vehicle control (PBS); n=2; data represents mean ± 1SD.

4.4 Discussion

In the previous chapter, high PKCε expression in AML patient samples was associated with poor outcomes and reduced CR following first-line therapy (3.3.1). Given that chemoresistance is a major factor in this malignancy, the aim of this chapter was to determine whether PKCε contributes to poor patient outcomes by conferring chemoresistance in AML cells. To explore this, the effect of modulating PKCε expression, using overexpression, knockdown, and knockout systems, on the chemosensitivity of AML cell lines was assessed by flow cytometry.

To establish suitable cell lines to conduct this analysis, endogenous PKCε mRNA and protein expression was evaluated in 10 leukaemia cell lines. Using the DepMap mRNA expression data, heterogenous *PKCε* expression was observed across the cell lines, while protein analysis by western blot was only able to detect PKCε expression in three of the cell lines analysed (U937, Mv4;11 and OCIAML5). Unlike in the patient samples where PKCε was endogenously expressed in samples across the different disease subtypes (3.3.1.1 and 3.3.1.3), the cell lines with detectable levels of PKCε expression all represent FAB M4/M5 disease. As a result, the studies into the effect of reducing PKCε expression through shRNA or CRISPR/*Cas9* technologies were limited to models of monocytic AML. Despite this, the heterogeneous expression of PKCε across the AML cell lines investigated allowed the impact of modulating the expression of this kinase on cell growth, viability and chemosensitivity to be studied.

In terms of cell growth, PKCε is frequently associated with pro-proliferative phenotypes (1.6.5.1), including in NIH3T3 fibroblasts where PKCε overexpression promotes oncogenic transformation, increased proliferation rate and tumour formation upon injection into murine models (Mischak, *et al.*, 1993). However, in the present study, PKCε overexpression significantly reduced the fold expansion of U937 and HEL cells. Although this was accompanied by a small reduction in cell viability (c10%), the small effect size means that this is unlikely to be biologically significant and is probably an artefact of accumulated cellular debris arising from the slower growth rate. Therefore, alternative reasons for the reduced proliferation rate in these PKCε overexpression cell lines were investigated. The anti-proliferative capacity of PKCε overexpression in these AML cell lines is in-line with the observations made in Chapter 3, where PKCε overexpression in HSPC reduced cell growth, which in this context, was accompanied by a pro-differentiation phenotype (3.3.4.2). In the

cell lines, significant increases in the forward scatter properties and an observable increase in cell size by morphological analysis in the PKCε overexpressing cells, suggested that PKCε may be promoting a more differentiated phenotype in this context. However, the induction of myeloid differentiation, as measured by the expression of the monocytic differentiation markers (CD11b, CD14 and CD13), could not be recapitulated. As the cell lines are transformed cells the expression of myeloid markers in AML cell lines are intrinsically perturbed compared to normal haemopoietic cells. Therefore, the capacity of PKCε to promote differentiation in this context cannot be conclusively ruled out.

Progress through the cell cycle directly influences cell proliferation, as well as being linked with the differentiation status of cells. Analysis of cell cycle status showed that in both U937 and HEL cells overexpressing PKCε, an apparent retardation of G2-phase exit was observed; a propensity of PKC which has been demonstrated in studies using PMA treatment to promote PKC activity (Barboule, *et al.*, 1999, Kosaka, *et al.*, 1996). This suggests that the reduction in growth and increased cell size could in part be due to perturbations in cell cycle progression. As alluded to previously, this could be caused by the induction of cell differentiation as these factors are inversely linked in several tissues. However, in non-dividing hypertrophic cardiac cells, PKCε overexpression has been shown to promote changes in cell size including increased cell length, length-to-width ratio, and perimeter-to-area ratio (Russell, *et al.*, 2010), suggesting that the changes in morphology may not be related to cell cycle progression. In myocytes the morphological changes occur due to the co-localisation of PKCε and focal adhesion kinase (FAK) at focal adhesions (Russell, *et al.*, 2010), thus, the morphological changes in the AML cells could be linked with the ability of PKCε to interact with actin and the cellular cytoskeleton.

The proliferation rate of the target cell is a major factor which influences the efficacy and cytotoxicity of anti-cancer agents (Valeriote and van Putten, 1975), with malignant cells generally being highly proliferative and more sensitive to chemotherapeutic agents than their non-malignant counterparts. Thus, it was hypothesised that the reduction in cell growth following PKCε overexpression could confer chemoresistance. This was supported by the observation that in both cell lines where proliferation had been impacted (U937 and HEL; 4.3.1.1), PKCε overexpression conferred DNR resistance. However, PKCε overexpression did not confer resistance to Ara-C which would have been anticipated if the anti-proliferative effects of PKCε overexpression was the true mechanism of DNR resistance.

As well as intrinsic mechanisms of resistance, extracellular signals including interactions with the BM microenvironment (1.1.1.1) can confer chemoresistance to agents such as Ara-C (Macanas-Pirard, *et al.*, 2017) through a range of mechanisms including adhesion mediated chemoresistance and the ability of the stroma to promote cellular quiescence (Tabe and Konopleva, 2015). PKCε has an actin binding motif which allows it to modulate the cytoskeleton arrangement and integrin expression which facilitate ECM interactions (1.3.2.2). Thus, it was hypothesised that the impact of PKCε-mediated stromal interactions may further confer chemoresistance in the AML cell lines. While in a co-culture setting PKCε overexpression promoted the level of attachment of U937 and HEL cells to MS5 stromal cells, co-culture did not result in Ara-C resistance in the PKCε overexpression lines or exacerbate the DNR phenotypes, compared to normal culture conditions. Thus, indicating that stromal interaction is not an important factor in PKCε-mediated DNR resistance and meant that subsequent analysis was conducted in the absence of stroma.

To support the overexpression data and determine the therapeutic potential of targeting PKCε in AML, targeted knockdown and knockout studies were carried out in AML cell lines. Reducing PKCε expression using shRNA mediated knockdown did not affect cell proliferation, viability, or the chemosensitivity of the AML cell lines investigated (U937, Mv4;11, and OCIAML5), suggesting that PKCε is not a central mediator of cell survival or chemosensitivity in these cell lines. This observation conflicts the findings of Di Marcantonio *et al*. where shRNA-mediated PKCε knockdown reduced the survival of THP-1, OCIAML3, NOMO-1 and U937 cells (Di Marcantonio, *et al.*, 2018). Of the cell lines used by Di Marcantonio *et al*., U937 cells were the least impacted by PKCε knockdown and is the only line which were used in both studies. This was because despite using the same western blot PKCε antibody to determine PKCε protein expression, in contrast to the Di Marcantonio *et al.* study, I was unable to detect PKCε expression in NOMO-1 and THP-1 cells (Figure 4.1). Although at the time of establishment cell lines represent a pure population of highly proliferative cells, it is widely recognised that sub-strains, arising from clonal evolution during prolonged culture, exist and can result in high degrees of heterogeneity between the cell lines of different laboratories (Ben-David, *et al.*, 2018) and this may in part explain the divergent findings of these two studies.

An additional consideration when comparing these two studies is the shRNA constructs used. In the Di Marcantonio *et al*. study two shRNA constructs were used: shRNA PKCε_1 (TRCN0000000848) and shRNA PKCε_2 (TRCN0000000846). The primary shRNA

construct (shRNA_1) is unique to the Di Marcantonio *et al*. study. In NOMO-1 cells, the impact on growth and viability using this construct was not in line with the degree of PKCε knockdown, in relation to the second shRNA construct used. Thus, raising some concerns regarding potential off-target effects with this shRNA construct. However, the shRNA_2 construct used in the Di Marcantonio *et al*. paper was the same as the 486-construct used in the study. The reason for the disparity between the effect of PKCε knockdown in U937 cells between the Di Marcantonio *et al*. and the current study is unclear given that an equivalent level of knockdown (c80%) was achieved in both studies. However, the endogenous expression of PKCε in the U937 cells used in the Di Marcantonio *et al*. paper appeared to be much higher than the cells used in this study.

In addition to experiments in AML cell lines, Di Marcantonio *et al.* conducted studies in murine cells and patient-derived samples. Such models are important in validating findings as the selective pressures involved in cell line generation mean that the complexity of the disease state is often lost. Through these assays, Di Marcantonio *et al.*, showed that reducing PKCε expression caused modest decreases in the expansion of murine MLLAF9 leukaemia cells and prolonged disease progression *in vivo*. Hence, supporting their findings of PKCε knockdown in the AML cell lines. However, unlike the AML cell line analysis, a single shRNA mouse-*pkcε* construct was employed. Therefore, experiments exploring the impact of other shRNA constructs, as well as pharmacological PKCε inhibitors, are required to substantiate this. The role of PKCε in promoting AML cell survival was supported by knockdown studies in patient-derived samples, where expression of the shRNA_1 construct was found to reduce the survival of 8 out of the 10 samples investigated (Di Marcantonio, *et al.*, 2018). Although this data suggests the potential vulnerability of AML cells to PKCε-targeted therapies, endogenous PKCε expression in these samples as well as the knockdown efficiencies achieved following shRNA transduction in these samples was not reported. Furthermore, in a similar manner to the murine studies, only one shRNA construct (shRNA_1) was utilised, which as discussed above could have been affected by off-target effects. The Di Marcantonio *et al*. paper did not assess the impact of reducing PKCε on chemosensitivity in patient derived samples and as a result, was briefly investigated in the present study (Chapter 5).

The shRNA findings of the present study were supported by CRISPR/*Cas9*-mediated knockout experiments which also showed that PKCε knockout in U937 and OCIAML5 cells did not affect the growth, viability or chemosensitivity of these cell lines. Although it is important to note that, as described in 4.3.2.3, the knockout cultures represent a heterogeneous

population of cells with different degrees of PKCε deletion. The definitive way to assess the effect of PKCε knockout on AML survival would have been to generate clones, sequence those with undetectable protein expression, and subsequently perform phenotypic analyses on the clones with biallelic mutations. However, the reduction of PKCε protein expression by c90% within the bulk culture suggests that in most cells homozygous mutation was achieved. Therefore, since in the bulk cultures PKCε knockout did not affect cell growth, viability or chemoresistance, clonal analysis was not conducted.

An additional limitation of the knockdown and knockout studies was that these experiments were restricted to models of monocytic (M4/M5) disease as only three cell lines (out of ten lines screened) expressed detectable levels of PKCε protein endogenously (Figure 4.1). However, the lack of chemosensitivity induced following reduced PKCε expression in these cell lines may be due to redundancy in function between PKCε and other PKC isoforms. Redundancy between PKC isoforms is supported by the fact that pan-PKC inhibitors have been shown to affect the survival of AML blasts. Our group has previously shown that PKC inhibition with Chelerythrine (a competitive PKC inhibitor) and BIM-1 (an ATP competitive PKC inhibitor) ablated the pro-survival effects of PDK-1 overexpression in THP-1 cells (Zabkiewicz, *et al.*, 2014). Furthermore, treatment of patient-derived AML cells with 5μM Enzastaurin promoted apoptosis (Ruvolo, *et al.*, 2011). Although Enzastaurin is selective for PKCβ at nM concentrations, at the μM concentrations used in this study inhibition of other PKC isoforms including PKCα and PKCε has been demonstrated (Jasinski, *et al.*, 2008).

A central mechanism of DNR resistance is drug efflux through ABC cassette transporters, which confer chemoresistance by reducing intracellular drug accumulation (Nooter, *et al.*, 1990). Expression of the ABC cassette efflux pumps is associated with chemoresistant phenotypes and poor patient outcomes (Liu, *et al.*, 2018). The most likely isoforms to have overlapping function with PKCε are the other nPKC isoforms (PKCδ, PKCθ and PKCη) which are most structurally related to PKCε. Therefore, the relationship between *PKCδ*, *PKCθ* and *PKCη* and ABC cassette transporters for which DNR is a substrate was assessed in AML patient samples. This analysis showed that both *PKCθ* and *PKCη* significantly positively correlated with the ABC cassette transporters *ABCB1*, *ABCC1* and *ABCG2* suggesting that these isoforms may be associated with chemo resistance. When the expression of these isoforms in AML cell lines was investigated all three of the lines used in the PKCε knockdown and knockout studies (U937, Mv4;11 and OCIAML5), co-expressed

PKCθ and *PKCε*, while *PKCη* was only expressed at very low levels in U937 and Mv4;11 cells, making PKCη a less likely candidate for redundancy in this context. In terms of overlapping function, PKCε and PKCθ have both been shown to promote T-cell survival through modulating apoptotic signalling cascades (Bertolotto, *et al.*, 2000), while in terms of conferring DNR resistance, PKCθ may have a causal role as it has been reported to bind to the *ABCB1* promoter (Gill, *et al.*, 2001). However, reducing PKCθ expression in the context of PKCε knockout did not alter the chemosensitivity of OCIAML5 cells. Even though only a modest PKCθ knockdown efficiency was achieved in the PKCε knockout cells compared to the control shRNA construct, a c50% reduction in protein expression compared to parental cells was observed. As the DNR sensitivity of PKCε knockout OCIAML5 cells transduced with the control and PKCθ shRNA constructs were equivalent to OCIAML5 cells transduced with a CRISPR/*Cas9* construct, which does not have a mammalian gene target, these data indicate that redundancy between PKCε and PKCθ is unlikely to be preventing DNR sensitisation in this cell line. Nevertheless, this does not rule out redundancy between PKCε and other PKC isoforms. Although the expression of PKCη was low in the AML cell lines at an mRNA level, protein expression was not assessed, and therefore redundancy between PKCε and PKCη cannot be ruled out (Chapter 6). It is also possible that other classes of PKC may contribute to DNR resistance. For example, inhibition of PKCα, using a cPKC inhibitor (Go6976), has been shown to promote apoptosis in human colon cancer cells in response to DOX (Lee, *et al.*, 2012), an anthracycline with similar biochemical properties to DNR.

In conclusion, the data presented in this chapter indicate that PKCε overexpression can selectively promote DNR resistance in AML cell lines and supports the premise that PKCε may contribute to poor patient outcomes in AML by conferring chemoresistance. Furthermore, these data suggest that as a single target, reducing PKCε expression does not impact the chemosensitivity of AML cells. However, it remains unclear as to whether pan-PKC inhibitors, such as Midostaurin which is currently used in the treatment of AML with *FLT3* mutations (1.3.2) for which part of its efficacy may result from PKC inhibition, could have wider therapeutic applications in this malignancy.

Chapter 5: Mechanisms of PKCε-Mediated Chemoresistance

3.1 Introduction

Development of drug resistance contributes significantly to the poor clinical outcomes associated with AML, making both the induction of CR and the maintenance of remission, if it is achieved, challenging. Chemoresistance can occur through a range of mechanisms including as a direct consequence of mutations, or indirectly through perturbed cell survival and apoptotic signalling (1.4.1). In several contexts, including in AML cells, PKCε has been shown to modulate the expression of apoptotic proteins, such as BCL-2 family members, as well as protect against TRAIL-induced apoptosis (Gobbi, *et al.*, 2009, McJilton, *et al.*, 2003). Although perturbed apoptotic signalling can contribute to chemoresistance, the data presented in Chapter 4 showed that PKCε overexpression can promote selective DNR resistance in AML cell lines, in the absence of altered Ara-C sensitivities (4.3.2.2). This suggests that the mechanism of PKCε-mediated chemoresistance, in this context, is linked to the mode of action of DNR, opposed to the evasion of apoptosis from altered survival signalling.

DNR is an anthracycline which exerts its cytotoxic effects through interactions with topoisomerase II and the generation of H_2O_2 and superoxide radicals which induce oxidative stress (Doroshow, 2019, Pommier, *et al.*, 2010). The ability of PKCε to protect against oxidative stress has been demonstrated in cardiac cells (Kabir, *et al.*, 2006), while a recent study in AML cells implicated PKCε in maintaining mitochondrial ROS homeostasis (Di Marcantonio, *et al.*, 2018). Therefore, altered ROS homeostasis may represent a potential mechanism of PKCε-mediated DNR resistance. Alternatively, anthracyclines, including DNR, are substrates for efflux pumps such as P-GP, for which Ara-C is not a substrate (Nooter, *et al.*, 1990). P-GP is expressed in c50% of AML blasts and is associated with chemoresistance and poor patient outcomes (Wuchter, *et al.*, 2000). Studies have shown that PKC activation promotes an increase in P-GP expression and activity (Chambers, *et al.*, 1992, Mayati, *et al.*, 2017), while inhibiting PKCε membrane translocation decreases aspirin-induced P-GP expression in a prostate cancer cell line (Flescher and Rotem, 2002a). However, the mechanism of PKCε-mediated DNR resistance in AML cells is unknown.

3.2 Aims

The aim of this chapter is to establish the mechanism through which PKCε overexpression confers chemoresistance in AML cells. This will be achieved through the following objectives:

- **Determine whether PKCε-mediated DNR resistance is caused by altered ROS homeostasis**

  To determine whether ROS homeostasis and resistance to oxidative stress contributes to PKCε-mediated DNR resistance in AML cell lines, the effect of PKCε overexpression on steady-state ROS will be assessed by flow cytometry. This will be supported by drug sensitivity assays to determine the sensitivity, in terms of growth and viability, of the cell lines to different ROS-generating agents.

- **Determine whether PKCε-mediated DNR resistance is caused by drug export via efflux pumps**

  To achieve this, the impact of PKCε overexpression on DNR accumulation in AML cell lines will be assessed using flow cytometry. The relationship between PKCε and P-GP; a well-characterised efflux pump in AML which selectively expels DNR but not Ara-C, will be assessed using online datasets, flow cytometry and western blot analysis. Furthermore, functional analysis will be conducted using ZSQ; a selective P-GP inhibitor. The resulting impact on DNR accumulation and cell viability will be assessed by flow cytometry.

3.3 Results

3.3.1 Altered redox homeostasis is not the mechanism of PKCε-mediated DNR resistance

As shown in Chapter 4, PKCε overexpression in AML cell lines promotes opposing phenotypes in response to Ara-C and DNR; sensitising cells to Ara-C (4.3.2.1) and conferring resistance to DNR (4.3.2.2). Therefore, mechanisms of chemoresistance specific to DNR were investigated. Although DNR-induced apoptosis is primarily mediated through interactions with topoisomerase II, metabolism of anthracyclines leads to the generation of superoxide anions and H_2O_2, in numerous cellular compartments, including the mitochondria (Doroshow, 2019). Thus, inducing oxidative stress contributes at least in part to the cytotoxicity of DNR. PKCε has been shown to modulate the antioxidant capacity of AML cells and protect against oxidative stress in several contexts (Di Marcantonio, *et al.*, 2018, Giorgi, *et al.*, 2010). Therefore, it was hypothesised that disrupted ROS homeostasis may represent the mechanism of PKCε-mediated DNR resistance. This was investigated by assessing the impact of PKCε overexpression on steady-state ROS levels, using a mitochondrial-targeted superoxide probe, MitoSOX™, as well as assessing the response of the PKCε overexpression cell lines to agents which induce oxidative stress.

3.3.1.1 PKCε overexpression reduces the levels of detectable mitochondrial superoxide in U937 and HEL cells

Oxidation of the MitoSOX™ probe by mitochondrial superoxide radicals results in a change in its fluorescent properties. Therefore, measuring changes in MitoSOX™ fluorescence by flow cytometry can be used as an indicator of the levels of intracellular mitochondrial superoxide (2.8.5). Using this probe, the rate of superoxide production in U937, HEL and NOMO-1 cells was comparable, at c0.015 MFI/hour, while TF-1 cells had a lower rate of 0.05MFI/hour (Figure 5.1). When evaluating the impact of PKCε overexpression, no differences in detectable superoxide levels were observed in NOMO-1 and TF-1 cells, compared to the control cell lines (Figure 5.1). In contrast, PKCε overexpression in U937 and HEL cells was accompanied by a 5-fold and 11-fold reduction in the rate of superoxide production, respectively (Figure 5.1). As these cell lines (U937 and HEL) demonstrated DNR

resistance, this data suggests that altered ROS homeostasis could contribute to the chemoresistant phenotype associated with PKCε overexpression.

The rate of change in MitoSOX™ fluorescence is a composite measure of mitochondrial superoxide production and the antioxidant capacity of the mitochondria. As PKCε overexpression reduced the proliferation rate of U937 and HEL cells compared to the control lines, the changes in mitochondrial superoxide levels could be attributable to a reduction in metabolic activity. Nevertheless, the ability of PKCε overexpression to confer resistance to the ROS-generating agents in AML cells has been suggested (Di Marcantonio, *et al.*, 2018). Therefore, to determine whether this reduction in mitochondrial ROS was also associated with resistance to oxidative stress, the impact of PKCε overexpression on the sensitivity to the ROS-generating agents GOx, ATM, and ATO was assessed in U937 and HEL cells; the lines where PKCε conferred DNR resistance and impacted steady-state mitochondrial ROS levels.

3.3.1.2 PKCε overexpression does not confer resistance to ROS-generating agents

GOx promotes oxidative stress by catalysing the oxidation of glucose to form β-D-glucono-δ-lactone and H_2O_2 (Ferri, *et al.*, 2011). As with DNR, both U937 and HEL cells were intrinsically sensitive to GOx, with $EC50^G$ of 3.3mU and 3.5mU and $EC50^V$ of 8.3mU and 5.3mU, respectively (Figure 5.2). As no viable cells were detected at concentrations of 12mU and above, this suggests that the reductions in growth in response to GOx is a result of apoptosis induction. Compared to the control cell lines, PKCε overexpression did not significantly affect the sensitivity to GOx in terms of the $EC50^G$ or $EC50^V$, although there was some evidence to suggest that PKCε sensitised these cell lines to the cytotoxic effects of GOx (Figure 5.2). Overall, this analysis shows that PKCε overexpression does not confer resistance to GOx, despite the reduced levels of endogenous mitochondrial ROS (3.3.1.1). Instead, there was some evidence that PKCε overexpression can sensitise cells to agents which generate broad spectrum ROS and induce H_2O_2-mediated apoptosis.

The Di Marcantonio *et al.* study implicated a role for PKCε in maintaining mitochondrial ROS homeostasis in AML cells (Di Marcantonio, *et al.*, 2018). Therefore, it was hypothesised that the ability of PKCε to confer resistance against ROS-generating agents is dependent on the type and localisation of the ROS generated. As a result, the effect of PKCε overexpression on the sensitivity of the cell lines to mitochondrial ROS-generating agents was

investigated. ATM and ATO promote mitochondrial ROS-generation and oxidative stress by disrupting the mitochondrial ETC (Piskernik, *et al.*, 2008, Pourahmad, *et al.*, 2016). The impact of ATM treatment on the growth of U937 and HEL cells was not linear, making it impossible to determine $EC50^{G}$ values for this agent, while the $EC50^{V}$ was >20µM in both U937 and HEL cells (Figure 5.3). With the impact on cell growth outweighing the effect on viability, the mode of action of ATM in these cell lines appears to be anti-proliferative. Compared to the control cell lines, PKCε overexpression reduced the growth inhibitory impact of ATM treatment in U937 and HEL cells by 1.3-fold and 1.5-fold, respectively. These findings support the proposed capacity of PKCε overexpression to confer resistance to mitochondrial ROS-generating agents. However, PKCε overexpression had a minimal impact on cell viability as the $EC50^{V}$ values for both cell lines remained > 20µM (Figure 5.3). Due to the kinetics of ATM treatment, it was difficult to demonstrate whether PKCε overexpression influenced AML cell survival, so to investigate this further the cell lines were challenged with a different mitochondrial ROS-generating agent; ATO.

In contrast to ATM, U937 and HEL cells responded to ATO in a dose-dependent manner with $EC50^{G}$ values of 2.8µM and 2.3µM respectively, while both lines had an $EC50^{V}$ value of >4µM (Figure 5.4). This suggests that ATO primarily acts through anti-proliferative mechanisms at the concentrations used. However, PKCε overexpression did not confer resistance to ATO in either U937 or HEL cells (Figure 5.4). Together these data dispute the premise that PKCε can confer resistance to ROS-generating agents as indicated by Di Marcantonio, *et al.*, 2018. Reasons for this discrepancy are discussed in 3.4, however, overall, these data demonstrate that altered ROS homeostasis and protection against oxidative stress is not the mechanism of PKCε-mediated DNR resistance.

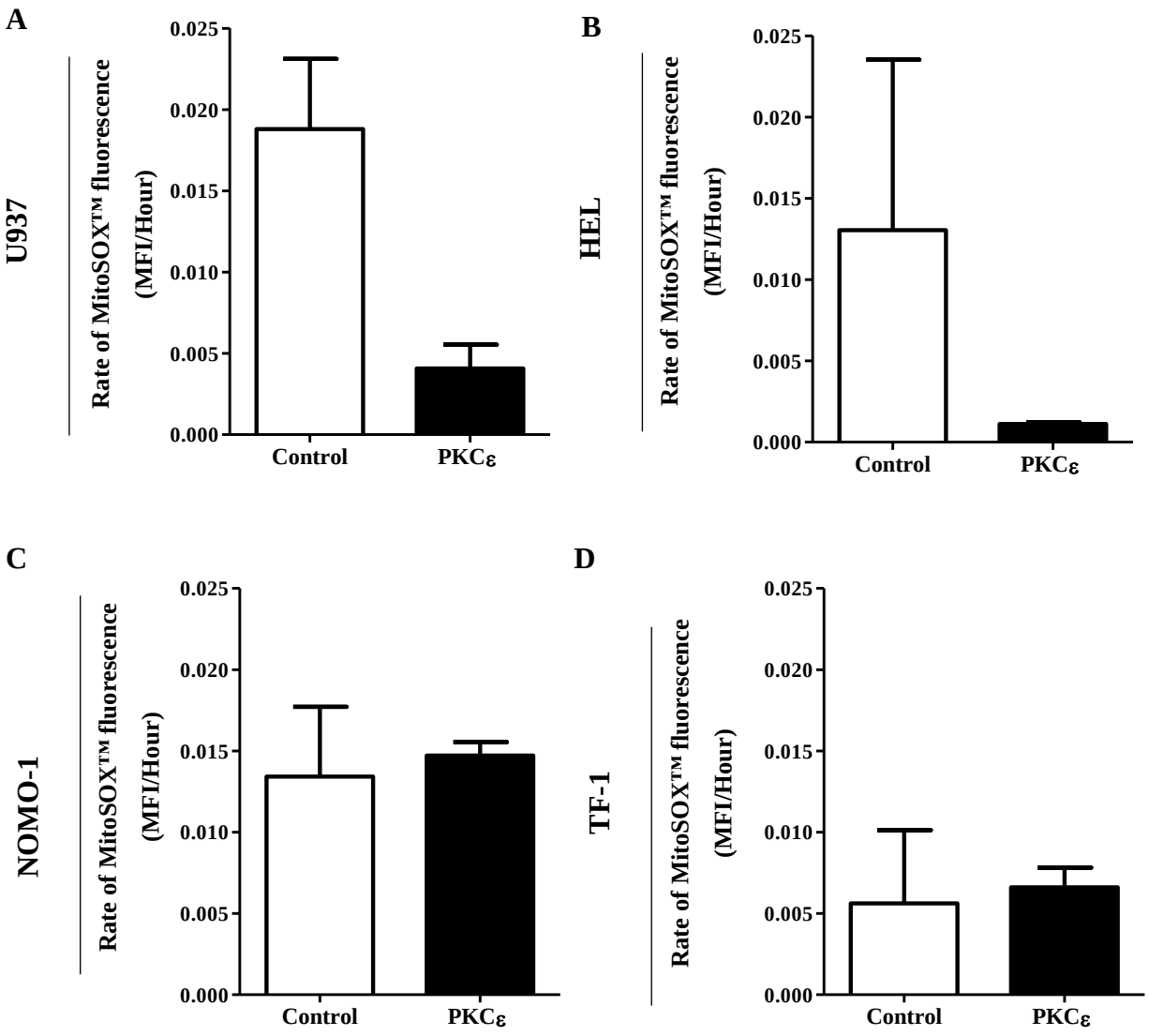

Figure 5.1: PKCε overexpression reduces detectable mitochondrial superoxide in U937 and HEL cells

Bar charts showing the rate of mitochondrial superoxide production by **(A)** U937, **(B)** HEL, **(C)** NOMO-1 and **(D)** TF-1 cells transduced with the control and PKCε overexpression constructs (Figure 4.3). The rate of superoxide production was determined from the rate of change in fluorescence of the MitoSOX™ probe (MFI/hour) as described in section 2.8.5; n=2; data represents mean +1SD.

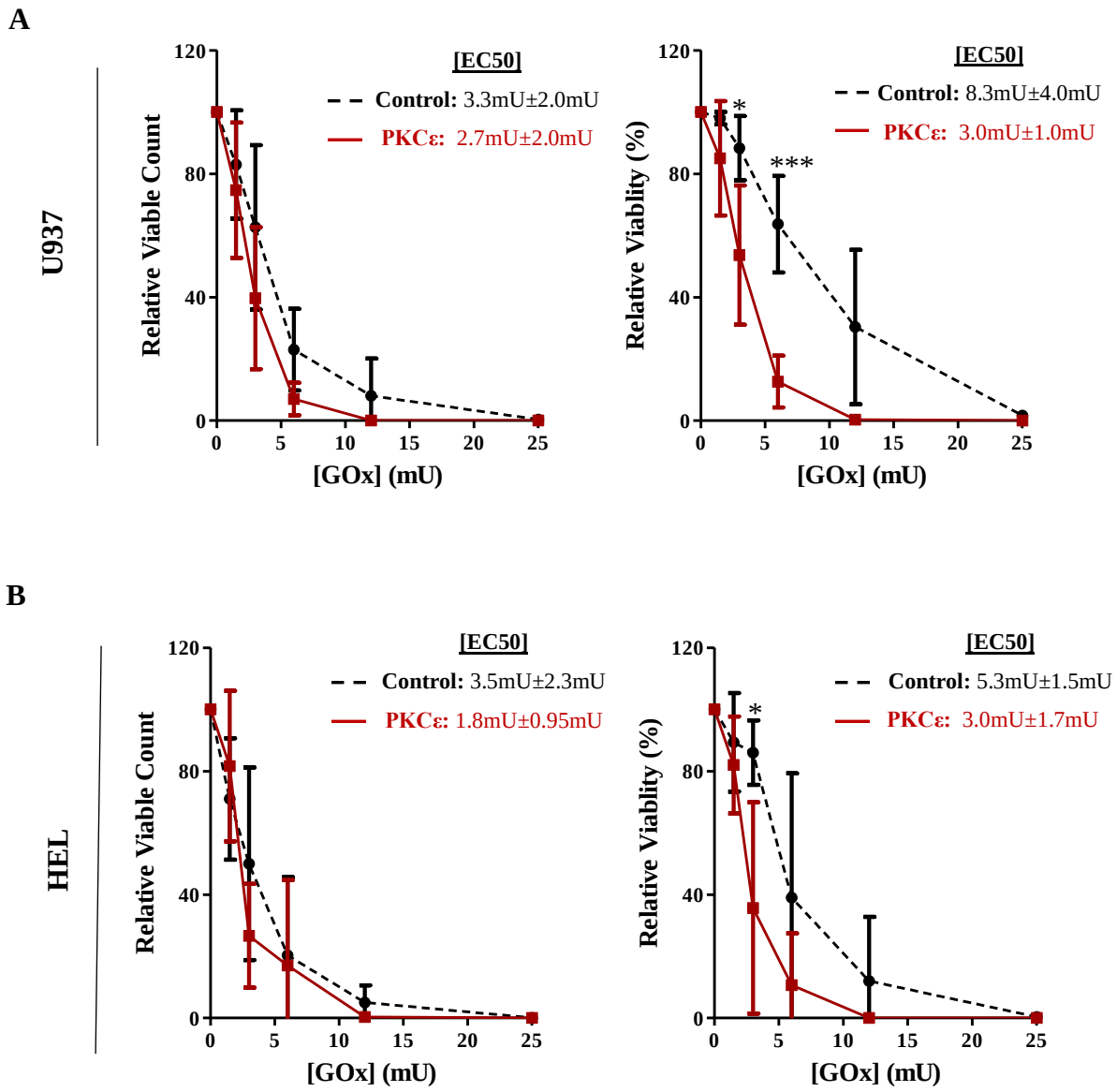

Figure 5.2: PKCε overexpression sensitises AML cell lines to GOx

Line graphs showing the effect of increasing GOx concentration (mU) on the growth (left) and viability (right) of **(A)** U937 and **(B)** HEL cells transduced with the control or PKCε overexpression constructs (Figure 4.3), following 48 hours of treatment as described in 2.8.8. The growth and viability were determined by flow cytometry using TOPRO-3 staining (2.8.2) and normalised to cells treated with the vehicle control (PBS+0.01%(*w/v*) BSA; 2.8.8.1); n=3; data represents mean±1SD. Statistical significance between the sensitivity of the control and PKCε overexpression cell lines at each concentration was determined using a two-way ANOVA with Bonferroni post-test comparison and was deemed significant;*p<0.05, **p<0.01.

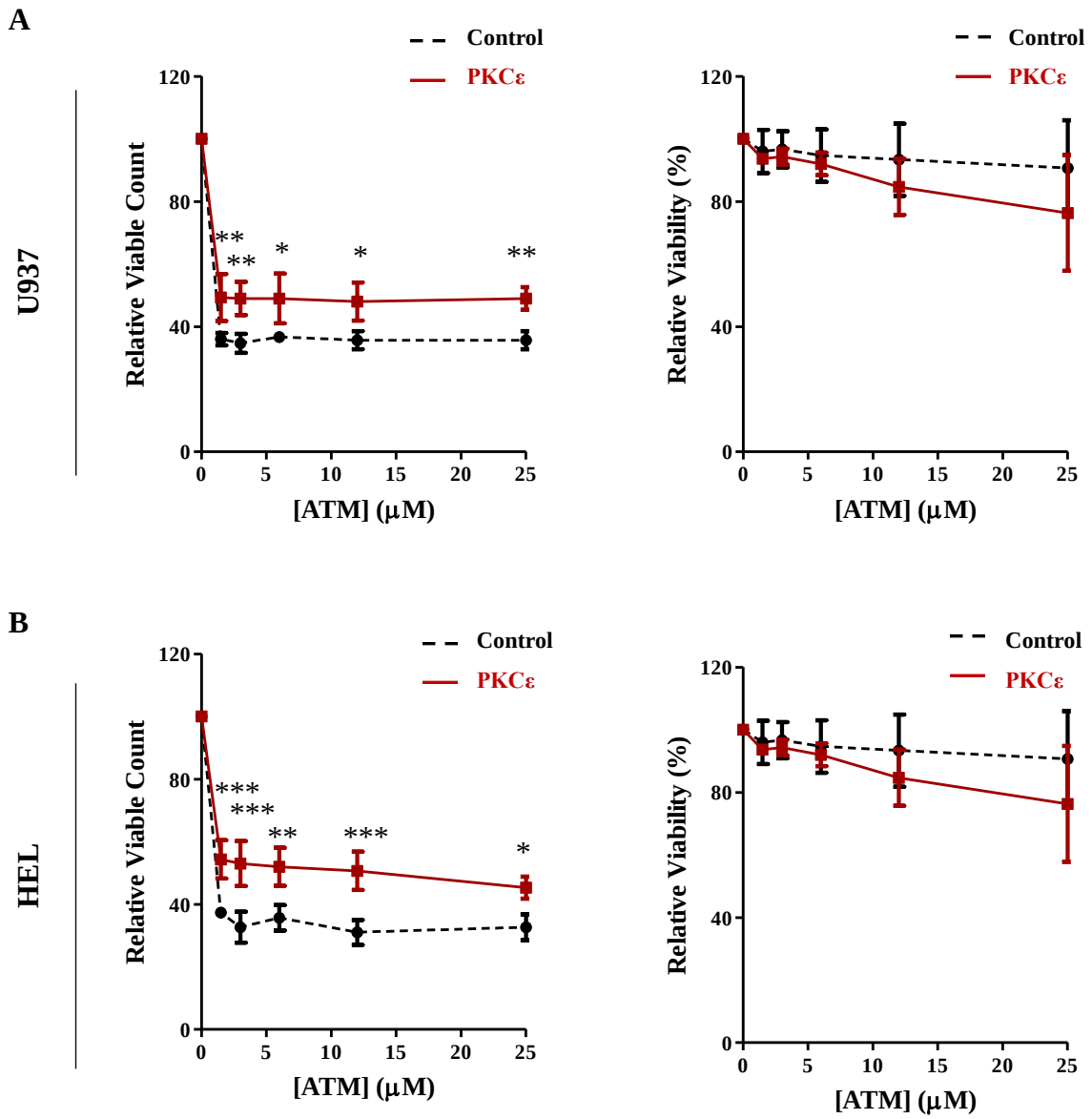

Figure 5.3: PKCε overexpression confers resistance to ATM in U937 and HEL cells

Line graphs showing the effect of increasing ATM concentration (μM) on the growth (left) and viability (right) of **(A)** U937 and **(B)** HEL cells transduced with the control or PKCε overexpression constructs (Figure 4.3), following 48 hours of treatment as described in 2.8.8. growth and viability were determined by flow cytometry using TOPRO-3 staining (2.8.2) and normalised to cells treated with the vehicle control (DMSO; 2.8.8.1); n=3; data represents mean±1SD. Statistical significance between the sensitivity of the control and PKCε overexpression cell lines at each concentration was determined using a two-way ANOVA with Bonferroni post-test comparison and was deemed significant;*p<0.05, **p<0.01,***p<0.001.

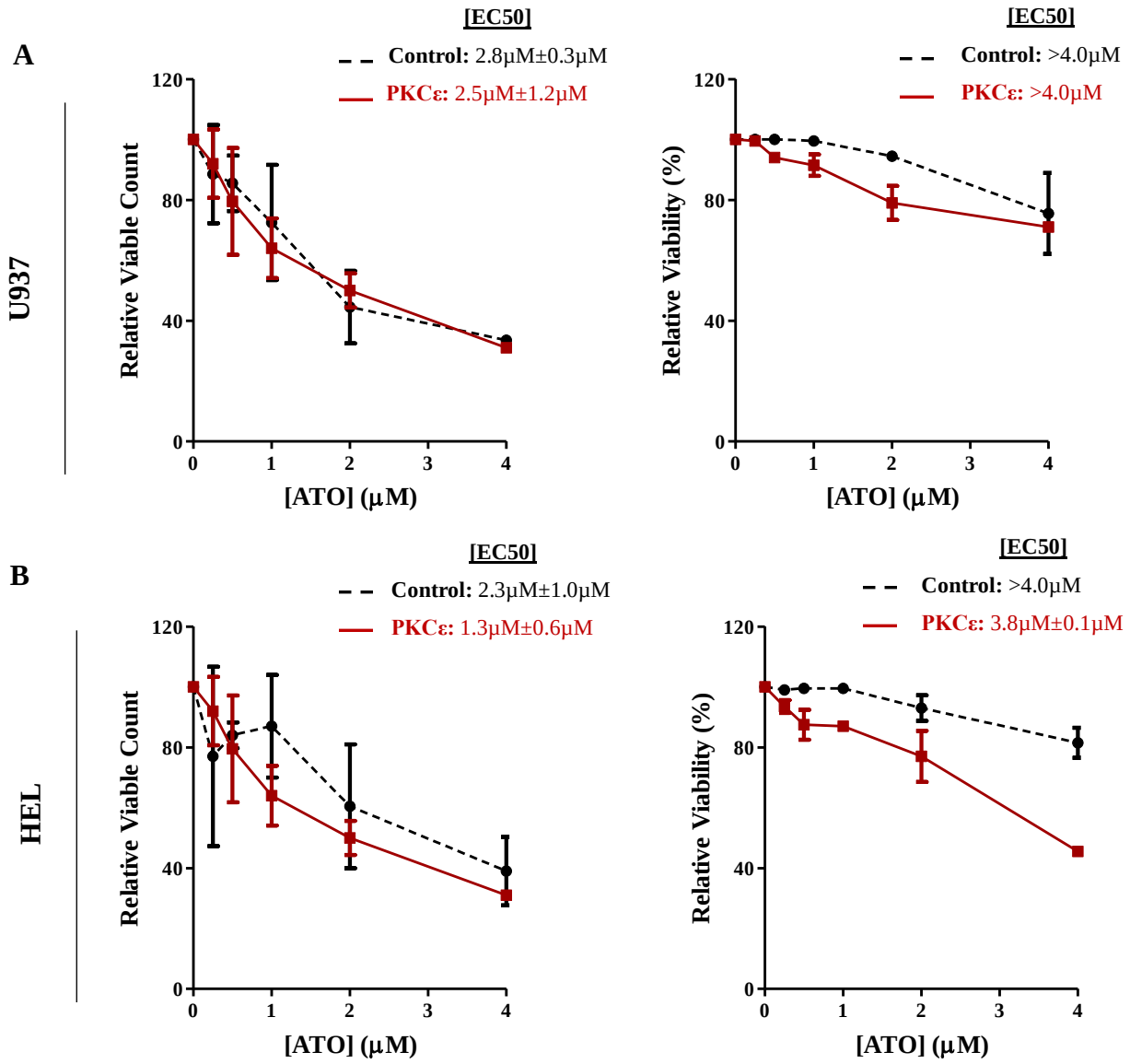

Figure 5.4: PKCε overexpression does not confer resistance to ATO in U937 and HEL cells

Line graphs showing the effect of increasing ATO concentration (µM) on the growth (left) and viability (right) of **(A)** U937 and **(B)** HEL cells transduced with the control or PKCε overexpression constructs (Figure 4.3), following 48 hours of treatment as described in 2.8.8. The growth and viability were determined by flow cytometry using TOPRO-3 staining (2.8.2) and normalised to cells treated with the vehicle control (PBS; 2.8.8.1); n=2; data represents mean±1SD.

3.3.2 Determining whether PKCε-mediated DNR resistance is associated with increased efflux pump expression and activity

3.3.2.1 PKCε-mediated DNR resistance is associated with reduced drug accumulation

Having determined that resistance to ROS is not the mechanism of PKCε-mediated DNR resistance, alternative mechanisms were investigated. The anthracycline, DNR possesses fluorescent properties which can be detected by flow cytometry and used as an indicator of intracellular drug accumulation (2.8.8.2). To determine whether altered drug accumulation is the mechanism of PKCε-mediated DNR resistance, the fluorescence of cells treated with DNR was assessed following 2 hours of treatment; a timepoint where the intracellular concentration of DNR has been shown to reach equilibrium (Den Boer, *et al.*, 1999). In addition, DNR accumulation was assessed after 2 days of treatment, to reflect the drug sensitivity assays previously conducted (4.3.2.2).

Following 2 hours of DNR treatment, the change in fluorescence in relation to cells treated with the vehicle control, was 1.8-fold lower in the DNR resistant PKCε overexpression cell lines, compared to the control cell lines (U937 and HEL; Figure 5.5). The same trend was observed at the 2-day timepoint, although, in this case significance was not achieved (Figure 5.5). Furthermore, compared to the control cell lines, no differences in the DNR fluorescence were observed in NOMO-1 or TF-1 cells overexpressing PKCε, following 2 hours or 2 days of DNR treatment (Figure 5.5). The lack of significance following 2-days of drug exposure for U937 and HEL cells is likely due to the complexities associated with longer-term drug exposure, such as the induction of cell death which is negated upon shorter lengths of exposure. As a result, the 2-hour time point was used for subsequent analysis. Overall, this pattern of altered DNR accumulation reflects the findings of the drug sensitivity assays (4.3.2.2), with the DNR resistant cell lines also exhibiting reduced DNR accumulation. Therefore, these data demonstrate that the mechanism of PKCε-mediated DNR resistance is related to aspects of cell biology which regulate drug accumulation.

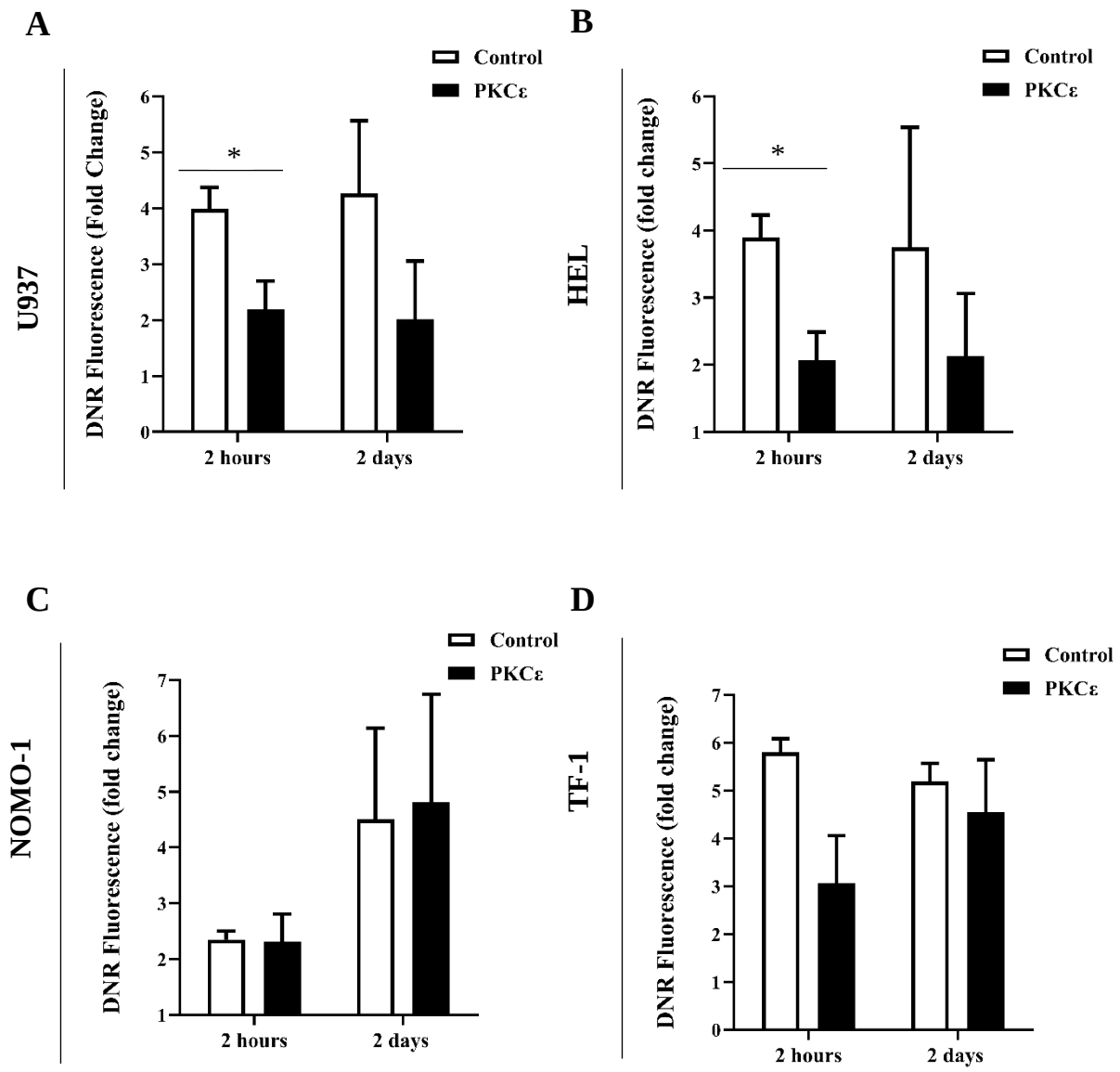

Figure 5.5: PKCε overexpression reduces DNR accumulation in U937 and HEL cells

Bar charts showing the DNR accumulation (fold change relative to cells treated with the vehicle control, (PBS)) of **(A)** U937, **(B)** HEL, **(C)** NOMO-1 and **(D)** TF-1 cells transduced with the control and PKCε overexpression constructs (Figure 4.3), following 2 hours or 2 days of treatment with 100nM DNR: 2 hours (n=3); 2 days; U937 and HEL (n=4) and NOMO-1 and TF-1 (n=3). Data represents mean+1SD. The statistical significance between the DNR accumulation in the control and PKCε overexpression cell lines at each time point was determined using Mann-Whitney tests; * $p<0.05$.

3.3.2.2 PKCε-mediated DNR resistance is associated with P-GP upregulation

As described above, PKCε-mediated chemoresistance in AML cell lines was associated with reduced DNR accumulation (3.3.2.1). This can arise through a range of processes including decreased drug uptake or increased expulsion via efflux pumps or SLC proteins (1.4.3). As DNR enters the cell by passive diffusion, uptake is unlikely to be affected by factors such as reduced cell growth. Therefore, it was deemed unlikely that the reduction in DNR accumulation was due to decreased drug uptake. Instead, it was hypothesised that the reduction in DNR accumulation in the DNR resistant lines (U937 and HEL) was due to increased drug efflux. P-GP is the best characterised efflux pump and in AML high P-GP function is associated with poor risk cytogenetics and reduced OS (Wuchter, *et al.*, 2000). P-GP has several substrates including vincristine and DNR and is known to reduce DNR accumulation *in vitro* (Nooter, *et al.*, 1990). Importantly, Ara-C is not a substrate for P-GP (Norgaard, *et al.*, 1998) and therefore upregulation and/or activation of P-GP would explain the differential phenotypes observed with respect to Ara-C and DNR in these lines. Although not fully established mechanistically, a link between PKC signalling and P-GP has long been recognised (1.6.5.3). Furthermore, PKCε has been implicated in the induction of P-GP expression, in a prostate cancer cell line, in response to aspirin (Flescher and Rotem, 2002b).

To determine whether PKCε-mediated DNR resistance is a result of P-GP drug efflux, the expression of this efflux pump was evaluated by flow cytometry and western blot analysis. Endogenous P-GP protein expression was first evaluated by western blot in AML cell lines. As a glycosylated protein, P-GP was not detected as a discrete band but instead as a smear with a molecular weight of 140kDa-170kDa. Of the cell lines investigated, KG-1 cells showed the highest degree of P-GP expression and was used as a positive control in subsequent analyses (Figure 5.6). Having identified a positive control, the ability to determine P-GP expression by flow cytometry was assessed. KG-1 cells stained with the P-GP antibody showed modest but uniform positive staining for P-GP (Figure 5.7). Thus, demonstrating the ability of this methodology to determine P-GP protein expression.

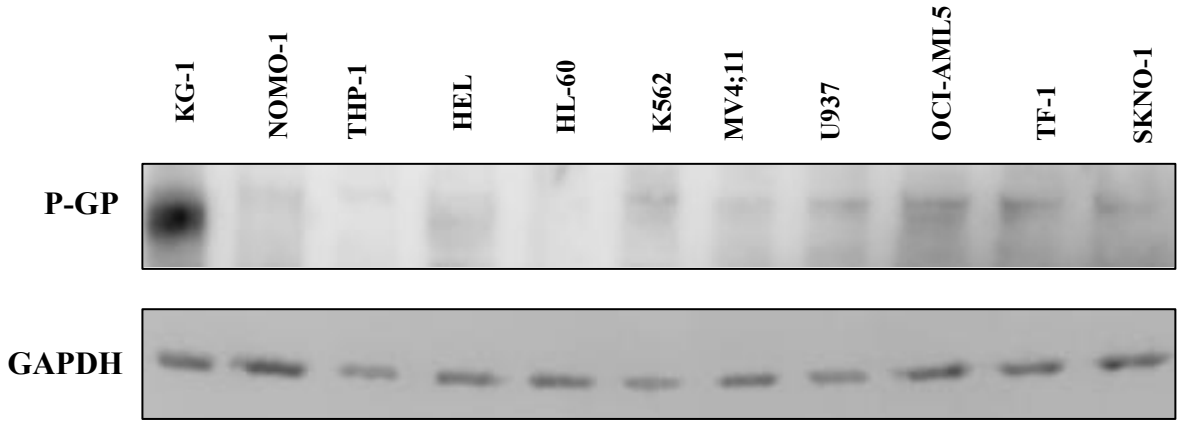

Figure 5.6: P-GP protein expression in AML cell lines

(A) Western blot showing P-GP (MW140-170kDa) expression in AML cell lines where P-GP was detected using the Insight C219 antibody (Table 2.10) and is shown alongside GAPDH (MW-36kDa) expression, which was used as a loading control and detected using the ThermoFisher Scientific GAPDH antibody (Table 2.10); n=1.

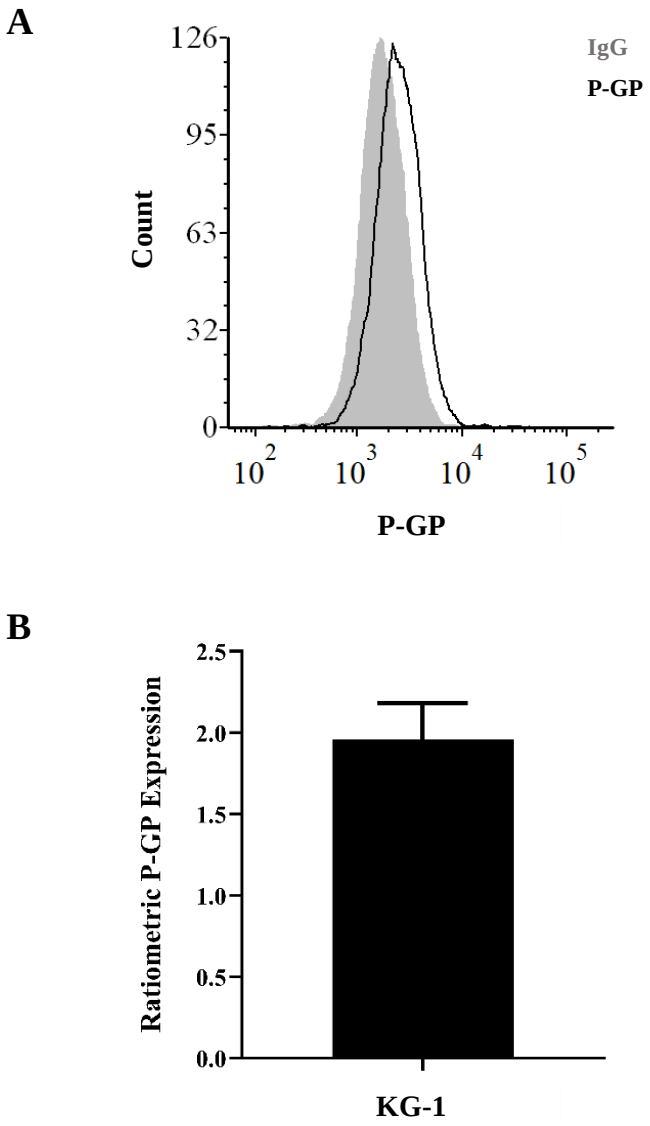

Figure 5.7: Validating the UIC2 P-GP flow cytometry antibody in KG-1 cells

(A) Representative histogram showing P-GP expression (clone UIC2; Table 2.12) of KG-1 cells compared to the staining of a matched isotype control (IgG2a,κ; Table 2.12). **(B)** Bar chart showing ratiometric P-GP expression in KG-1 cells. This was calculated by dividing the arithmetic mean of cells stained with the P-GP UIC2 antibody by the arithmetic mean of cells stained with the isotype control. Data represents mean+1SD; n=3.

Having validated the flow cytometric methodology in KG-1 cells, P-GP expression was determined in the PKCε overexpression cell lines. This analysis showed that U937 and HEL cells overexpressing PKCε, had a respective 3.0-fold and 3.5-fold increase in P-GP expression compared to the control cell lines (Figure 5.8 and Figure 5.9). Furthermore, no significant differences in P-GP expression were observed in NOMO-1 and TF-1 cells which did not exhibit DNR resistance upon PKCε overexpression (Figure 5.8 and Figure 5.9). P-GP expression in U937 and HEL overexpressing PKCε was validated by western blot analysis. Although the glycosylated nature of P-GP made quantification and clear demonstration of altered P-GP expression difficult, P-GP expression in the U937 and HEL cells overexpressing PKCε was c1.2-fold higher than the control lines (Figure 5.10). This supports the flow cytometry data and together implicate P-GP upregulation in PKCε-mediated DNR resistance.

3.3.2.3 P-GP inhibition reverses PKCε-mediated DNR resistance

To determine whether there is a causal association between P-GP and PKCε-mediated DNR resistance (3.3.2.2), P-GP inhibition assays were conducted using the selective P-GP inhibitor, Zosuquidar hydrochloride (ZSQ; Dantzig, *et al.*, 1999) and DNR uptake and cytotoxicity was assessed in the DNR resistant cell lines (U937 and HEL), as previously described (3.3.2.1). In the control and PKCε overexpression cell lines investigated, ZSQ treatment alone did not significantly impact the fluorescence of the cells, compared to cells treated with the vehicle control (Figure 5.11). Furthermore, DNR accumulation in the control U937 and HEL cell lines was not significantly different upon co-treatment with DNR and ZSQ, than when treated with DNR alone (Figure 5.11). This suggests that in these control lines P-GP is not intrinsically activated in response to DNR in these lines. In contrast, in the PKCε overexpression cell lines where DNR accumulation was reduced with DNR treatment alone (3.3.2.1), the addition of ZSQ increased DNR accumulation to levels equivalent with the control cell lines (Figure 5.11).

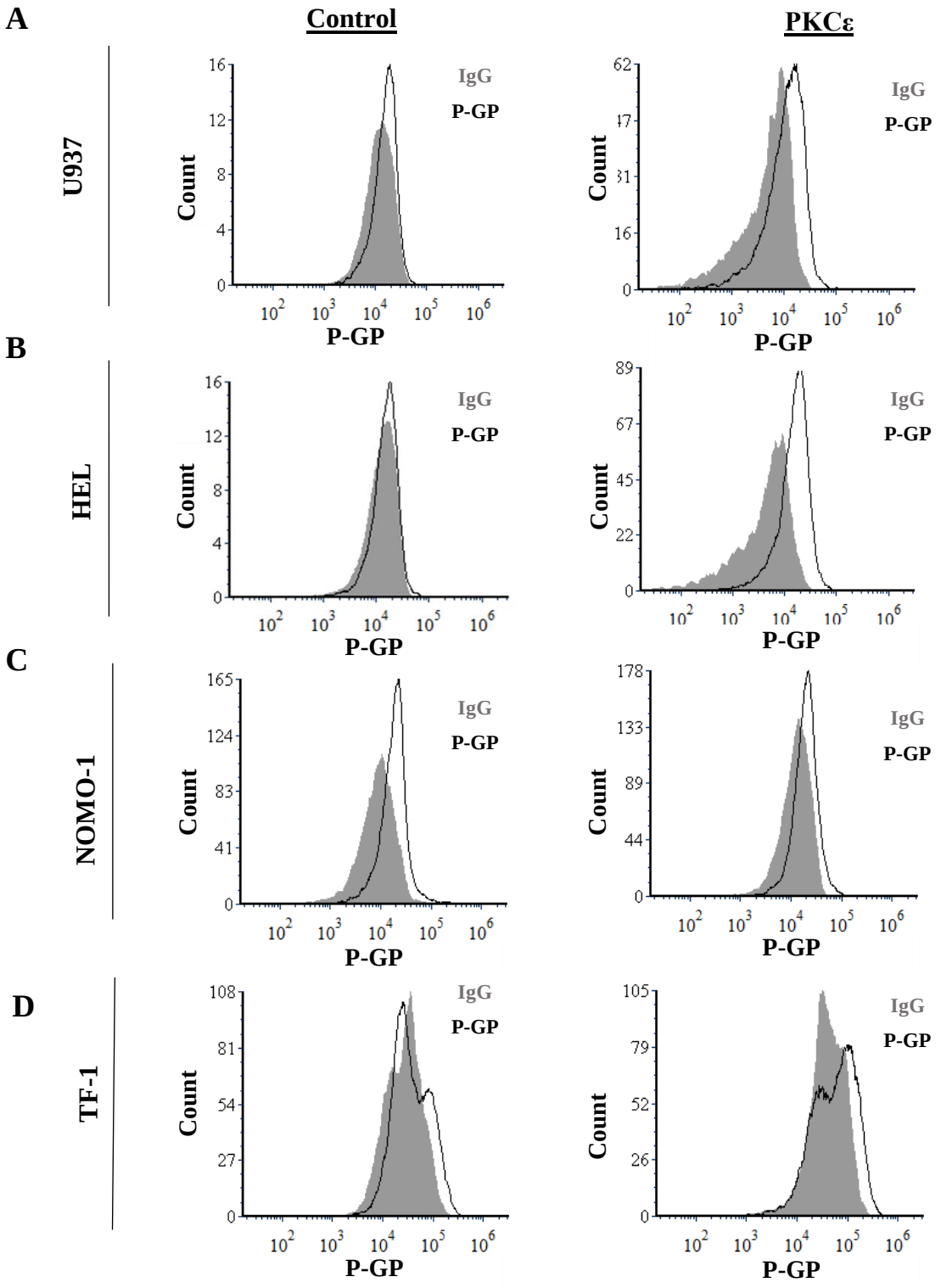

Figure 5.8: P-GP expression in PKCε overexpression AML cell lines

Representative histograms showing P-GP expression (MFI) in **(A)** U937, **(B)** HEL, **(C)** NOMO-1 and **(D)** TF-1 cells transduced with the control (left) or PKCε overexpression (right) constructs (Figure 4.3). P-GP expression was detected by flow cytometry using the CD243-APC (UIC2) antibody and was compared to an isotype control (IgG2k-APC; grey; Table 2.12).

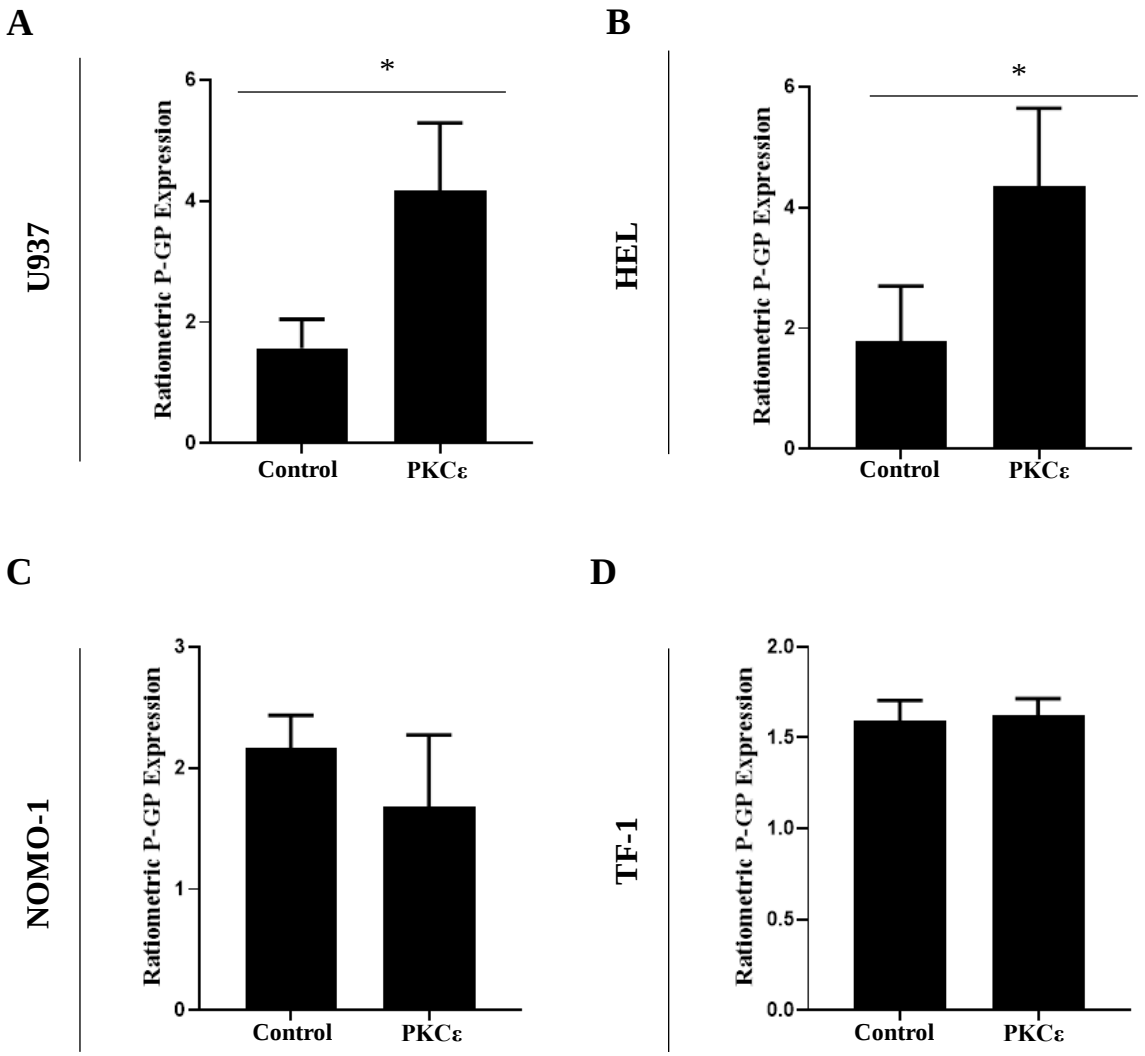

Figure 5.9: PKCε overexpression promotes P-GP upregulation in U937 and HEL cells

Bar charts representing P-GP expression (**A)** U937, **(B)** HEL, **(C)** NOMO-1 and **(D)** TF-1 cells transduced with the control or PKCε overexpression constructs (Figure 4.3). P-GP expression was determined by flow cytometry (2.8.4); U937 and HEL (n=4), NOMO-1 and TF-1 (n=3), data represents mean+1SD. The statistical significance between P-GP expression on the control and PKCε overexpression cell lines was determined by using Mann-Whitney tests; *$p<0.05$.

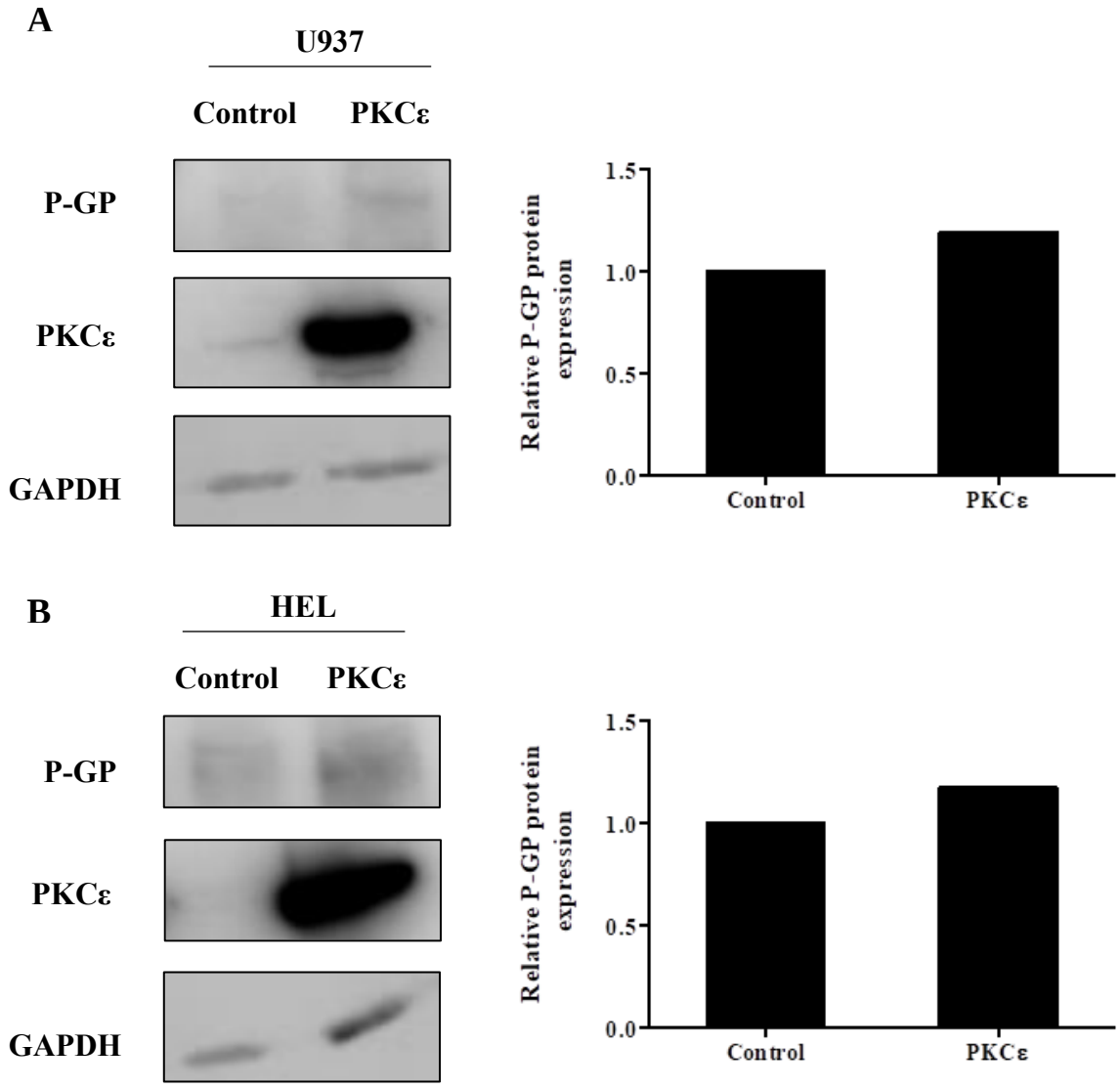

Figure 5.10: PKCε overexpression promotes P-GP upregulation in U937 and HEL cells

Western blot showing P-GP (MW140-170kDa) expression in **(A)** U937 and **(B)** HEL cells transduced with the control and PKCε overexpression constructs (Figure 4.3). P-GP was detected using the Insight C219 antibody (Table 2.10) and is shown alongside PKCε (Mw-84kDa) expression which was detected the Cell Signalling Technologies antibody #2683 (clone 22B10) and GAPDH (MW-36kDa) expression which was used as a loading control and detected using the ThermoFisher Scientific GAPDH antibody (Table 2.10). P-GP protein expression was quantified by densitometry using AIDA (2.7.5) and is shown relaive to loading; n=1.

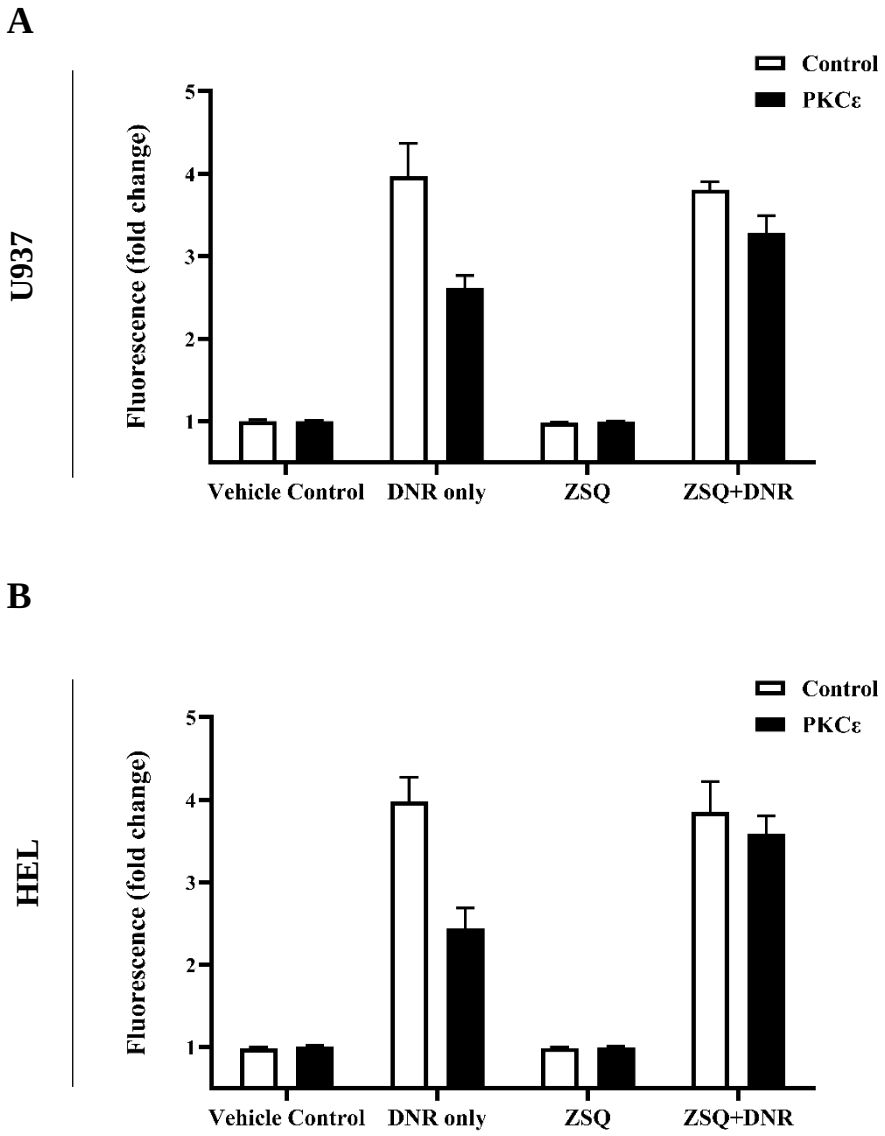

Figure 5.11: P-GP inhibition promotes DNR accumulation in U937 and HEL cells overexpressing PKCε

Bar charts showing the DNR fluorescence (fold change) of **(A)** U937 and **(B)** HEL cells transduced with the control and PKCε overexpression constructs (Figure 4.3), following 2 hours of treatment with 100nM DNR and 100nM ZSQ. DNR and ZSQ co-treatment is shown alongside the fluorescence of cells treated with the vehicle control (PBS+0.025% (*v/v*) DMSO) or 100nM ZSQ alone. The fold change in DNR fluorescence is relative to the fluorescence of cells treated with the vehicle control; n=3 data represents mean +1SD. The statistical significance of DNR accumulation in the control and PKCε overexpression cell lines treated with ZSQ was determined using Mann-Whitney tests and was deemed non-significant.

To ensure that the effects of P-GP inhibition using ZSQ were not due to off-target effects, titration assays were conducted. In KG-1 cells, which were used as a positive control for P-GP expression, a dose-dependent increase in DNR accumulation with increasing ZSQ concentration was observed (Figure 5.12). Furthermore, DNR accumulation plateaued at 30nM-100nM, suggesting that maximal P-GP inhibition had been achieved (Figure 5.12). When applied to the U937 and HEL cell lines, a concordant dose-dependent increase in DNR accumulation was observed in the PKCε overexpression cells upon ZSQ treatment (Figure 5.13). In both these cell lines, DNR accumulation also plateaued at 30nM-100nM, suggesting that in these three cell lines the same molecule is being inhibited. This also indicates that the increase in DNR fluorescence seen when using 100nM ZSQ (Figure 5.11) is not due to off target effects. Furthermore, ZSQ did not affect DNR accumulation in the control U937 and HEL cell lines (Figure 5.13), or the NOMO-1 and TF-1 PKCε overexpression cells (Figure 5.14), which did not present with altered DNR accumulation or DNR resistance. Overall, these data show that P-GP inhibition can fully restore DNR accumulation in the resistant PKCε overexpression cell lines, thus implicating P-GP in PKCε-mediated DNR resistance.

Having determined that P-GP inhibition restores drug accumulation in the DNR resistant cell lines (U937 and HEL; Figure 5.11), the effect of ZSQ treatment on the cytotoxicity of DNR following 2 days of treatment was evaluated. Compared to the vehicle control, ZSQ treatment alone did not affect the growth or viability of any of the cell lines investigated (Figure 5.15). As anticipated from the DNR accumulation assays, co-treatment with DNR and ZSQ did not significantly impact the $EC50^{G}$ (Figure 5.16) or $EC50^{V}$ (Figure 5.17) of DNR in the control U937 and HEL cell lines. However, in the lines overexpressing PKCε, P-GP inhibition by ZSQ enhanced the cytotoxicity of DNR, as demonstrated by the restoration of the $EC50^{G}$ (Figure 5.16) and $EC50^{V}$ (Figure 5.17) to equivalent levels of the control cell lines. Therefore, along with the drug accumulation analysis, these data demonstrate that drug efflux via P-GP fully accounts for the chemoresistant phenotype in these PKCε overexpression cell lines.

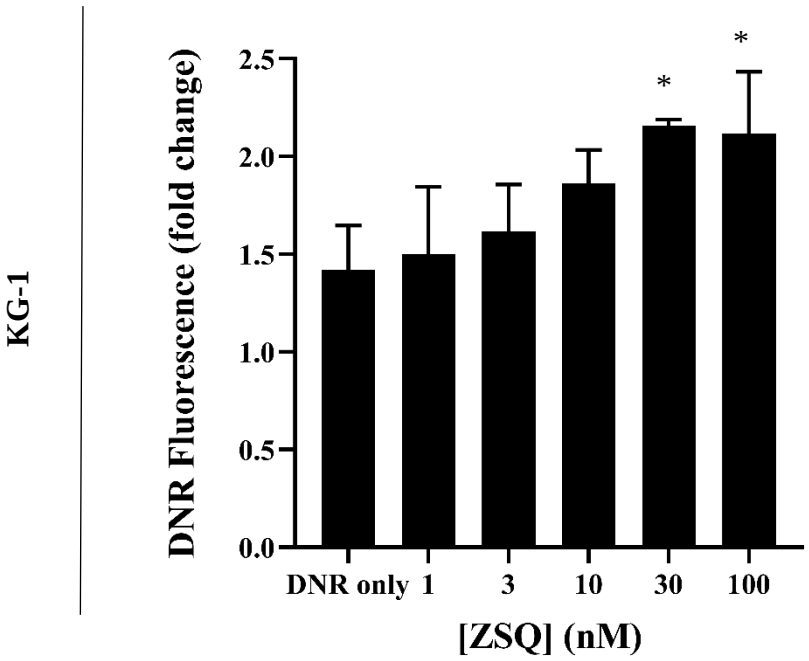

Figure 5.12: DNR accumulation in KG-1 cells increases in a dose-dependent manner in response to ZSQ

Bar chart showing the effect of ZSQ treatment (0-100nM) on DNR accumulation following 2 hours of treatment with 100nM DNR, following 2 hours of treatment with 100nM DNR. DNR fluorescence was normalised to the autofluorescence of cells treated with the vehicle control (PBS+0.025% (*v/v*) DMSO; 2.8.8); n=3; data represents mean+1SD. The statistical significance of DNR accumulation in KG-1 cells was determined using a one-way ANOVA with Bonferroni post-test comparison where comparisons were made to DNR treatment alone; *$p<0.05$.

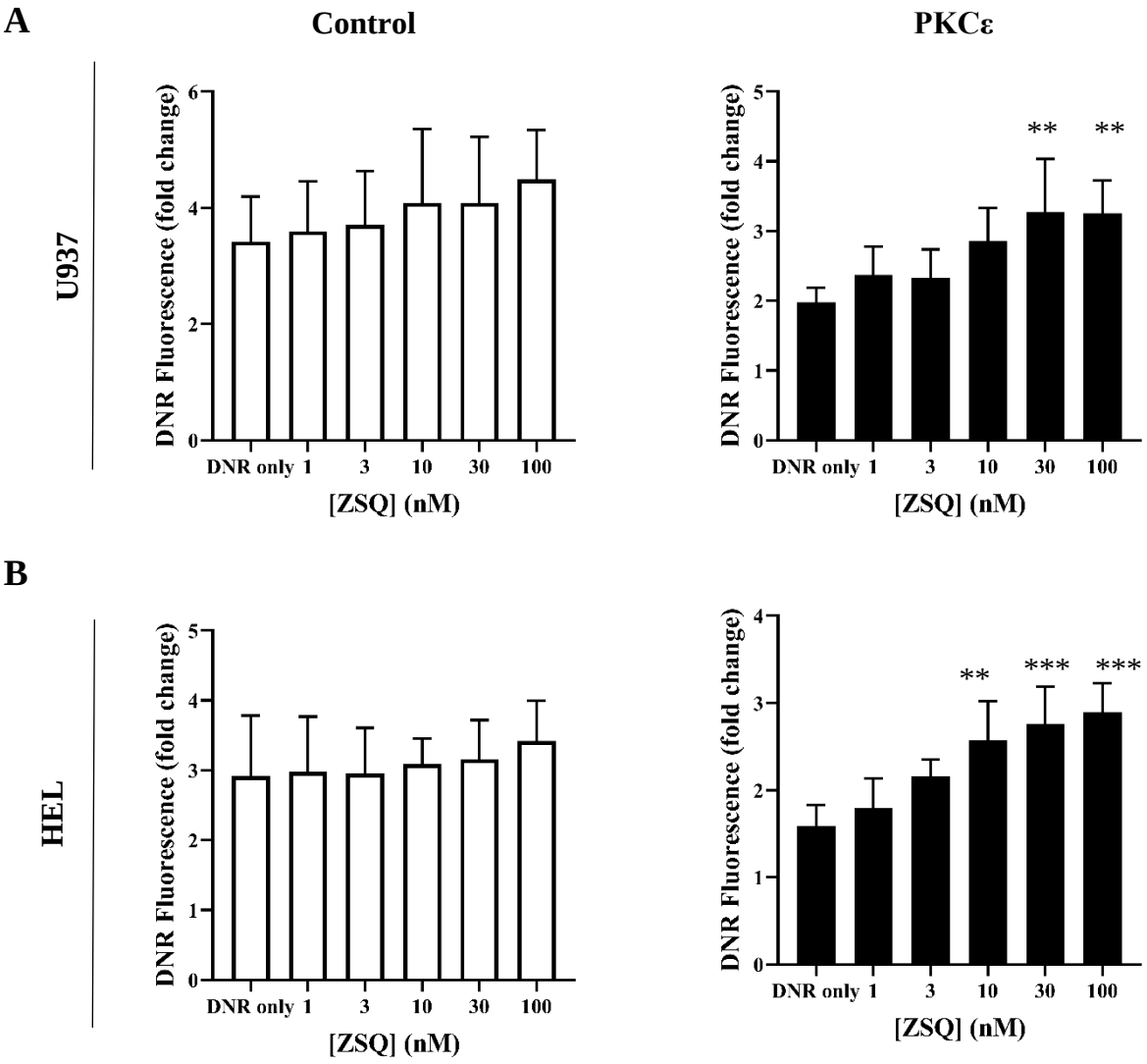

Figure 5.13: P-GP inhibition increases DNR accumulation in U937 and HEL cells overexpressing PKCε

Bar chart showing the effect of ZSQ treatment (0-100nM) on DNR accumulation following 2 hours of treatment with 100nM DNR in **(A)** U937 and **(B)** HEL cells transduced with the control (left; Figure 4.3) or PKCε overexpression constructs (Figure 4.3). DNR accumulation was determined by measuring DNR fluorescence (2.8.8.2) and is normalised to the fluorescence of treated with the vehicle control (PBS+0.025% (*v/v*) DMSO; 2.8.8); n=3; data represents mean+1SD. The statistical significance of DNR accumulation in the cell lines was determined using a one-way ANOVA with Bonferroni post-test comparison where comparisons were made to DNR treatment alone; *p<0.05, **p<0.01,***p<0.001.

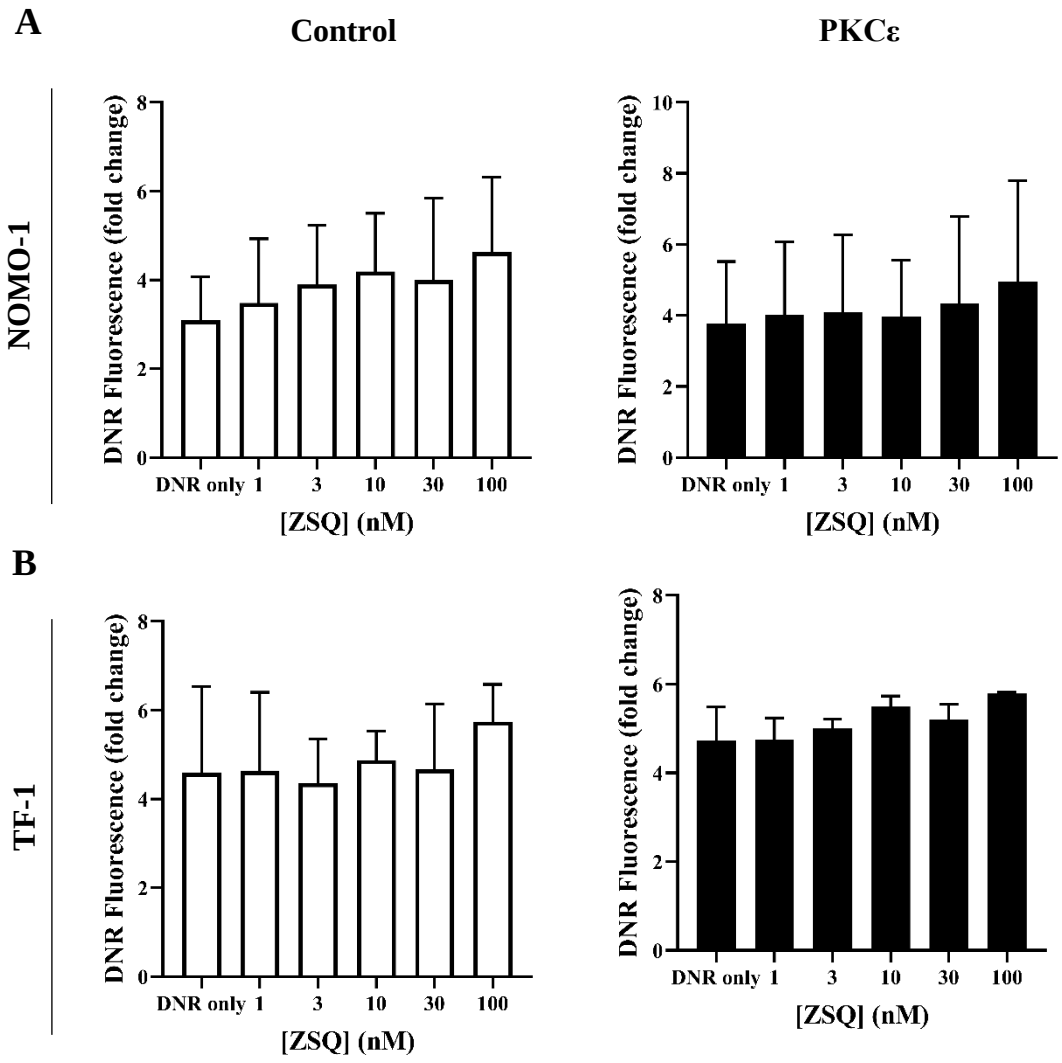

Figure 5.14: DNR accumulation does not increase with ZSQ concentration in NOMO-1 and TF-1 cells

Bar charts showing the effect of ZSQ treatment (0-100nM) on DNR accumulation following 2 hours of treatment with 100nM DNR in **(A)** NOMO-1 and **(B)** TF-1 cells transduced with the control or PKCε overexpression constructs (Figure 4.3). DNR accumulation was determined by measuring DNR fluorescence (PBS+0.025% (*v/v*) DMSO; 2.8.8.2) and is normalised to the fluorescence of cells treated with the vehicle control (2.8.8); NOMO-1; n=4 and TF-1; n=2; data represents mean+1SD. The statistical significance of DNR accumulation in the NOMO-1 cell lines was determined using a one-way ANOVA with Bonferroni post-test comparison where comparisons were made to DNR treatment alone and was deemed non-significant.

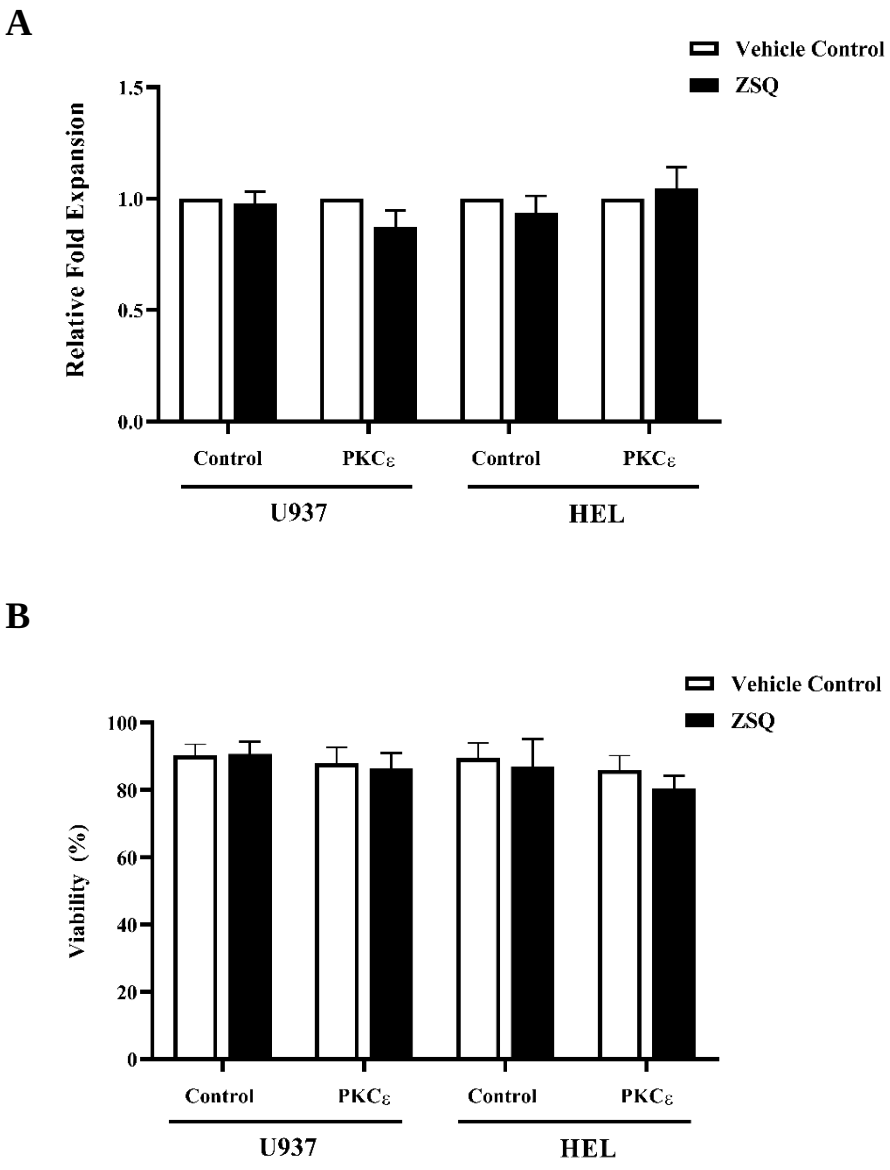

Figure 5.15: ZSQ treatment alone has no impact on the growth or viability of AML cells

Bar charts showing the effect of ZSQ treatment (100nM) on the **(A)** growth and **(B)** viability of U937 and HEL cells transduced with the control or PKCε overexpression (red) constructs (Figure 4.3), following 48 hours of treatment (2.8.8). The growth and viability were determined by flow cytometry using TOPRO-3 staining (2.8.2) and the fold expansion data is normalised to cells treated with the vehicle control (PBS+0.025% (*v/v*) DMSO; 2.8.8); n=4; data represents mean +1SD. The statistical significance of the differences in the fold expansion and viability of the control and PKCε overexpression cell lines was determined using Mann-Whitney tests and was deemed non-significant.

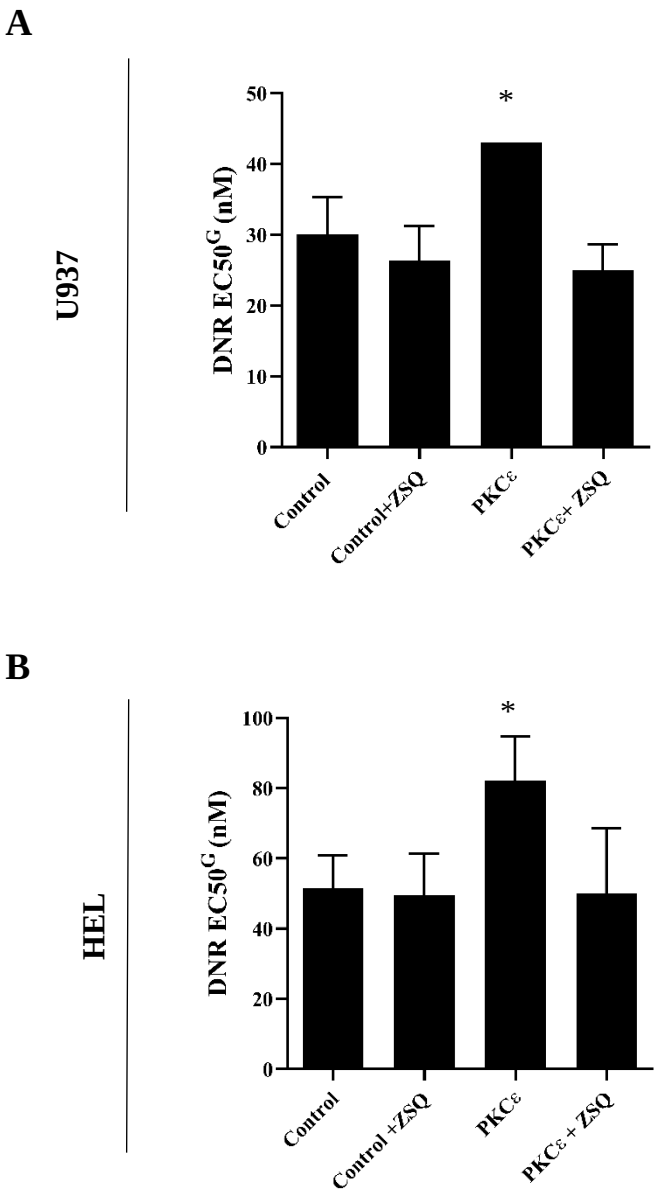

Figure 5.16: P-GP inhibition overcomes the impact of PKCε overexpression on the growth in U937 and HEL cells in response to DNR

Bar charts showing the effect of ZSQ treatment (100nM) on the $EC50^G$ (nM) of DNR in **(A)** U937 and **(B)** HEL cells transduced with the control or PKCε overexpression constructs (Figure 4.3), following 48 hours of treatment (2.8.8). The growth and viability were determined by flow cytometry using TOPRO-3 staining (2.8.2) and normalised to cells treated with the vehicle control (PBS+0.025% (*v/v*) DMSO; 2.8.8); n=3; data represents mean+1SD. The statistical significance in the $EC50^G$ was determined using one-way ANOVA with Bonferroni post-test comparison, where comparisons were made to the control lines treated with DNR alone and was deemed significant; *$p<0.05$.

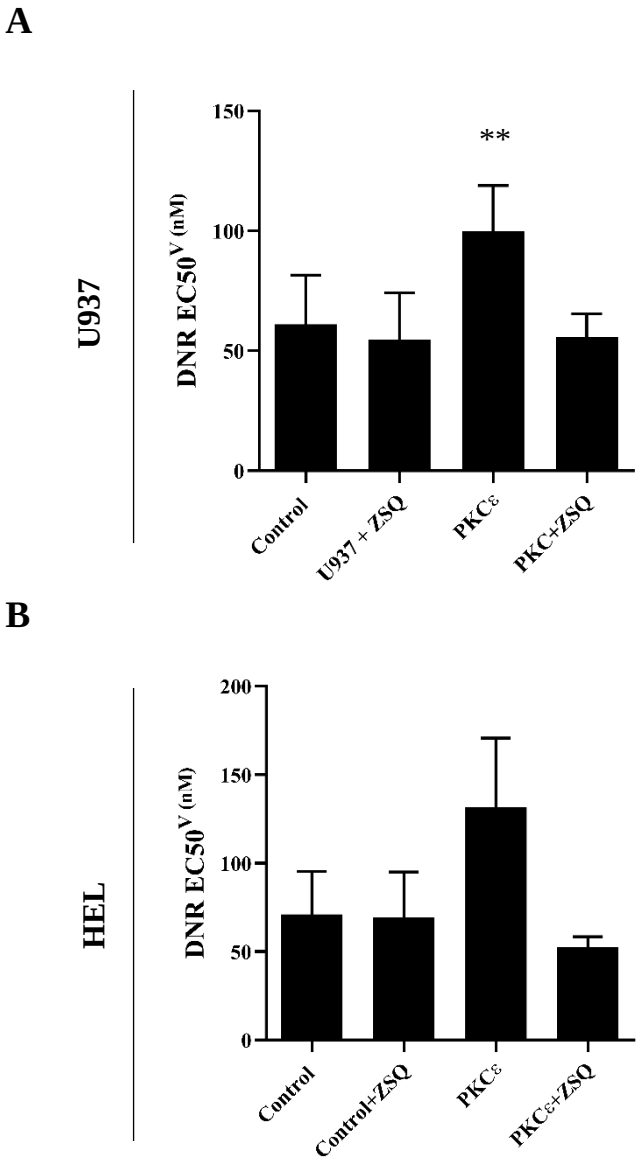

Figure 5.17: P-GP inhibition overcomes the impact of PKCε overexpression on the viability of U937 and HEL cells in response to DNR

Bar charts showing the effect of ZSQ treatment (100nM) on the $EC50^G$ (nM) of DNR in **(A)** U937 and **(B)** HEL cells transduced with the control or PKCε overexpression constructs (Figure 4.3), following 48 hours of treatment (2.8.8). The growth and viability were determined by flow cytometry using TOPRO-3 staining (2.8.2) and normalised to cells treated with the vehicle control (PBS+0.025% (*v/v*) DMSO; 2.8.8); n=3; data represents mean+1SD. The statistical significance in the $EC50^V$ was determined using one-way ANOVA with Bonferroni post-test comparison, where comparisons were made to the control lines treated with DNR alone and was deemed significant; **p<0.01.

Throughout the overexpression assays, the U937 and HEL cell lines showed concordant phenotypes, which were not observed in the NOMO-1 or TF-1 lines, despite showing similar degrees of PKCε overexpression (Figure 4.3). Both NOMO-1 and TF-1 cells showed endogenous P-GP expression (3.3.2.2) however there was no evidence of P-GP activity in the control or PKCε overexpression lines (Figure 5.13 and Figure 5.14). Thus, the levels of intrinsic P-GP expression and activity do not explain the lack of PKCε-mediated DNR resistance in these lines. It was also proposed that reducing PKCε expression may only sensitise cells to DNR in lines where P-GP is intrinsically active in response to DNR. In the PKCε knockdown and knockout lines (U937, Mv4;11, and OCIAML5; 4.3.3.1 and 4.3.3.2), P-GP protein was detected by western blot, with the caveat that this does not represent cell surface expression. However, there was no evidence of intrinsic activity in response to DNR (Figure 5.13 and Figure 5.18). Therefore, reducing PKCε expression in these lines may not have effected DNR sensitivity as P-GP is not intrinsically active.

3.3.2.4 PKCε does not promote drug efflux through increasing P-GP activity

Having established the involvement of P-GP in PKCε-mediated DNR resistance (3.3.2.3), experiments were conducted to investigate how PKCε promotes P-GP drug efflux. As previously described, western blot and flow cytometric analysis indicated the contribution of P-GP upregulation to this phenotype (3.3.2.2). However, the activity of this efflux pump is also central to its function. P-GP contains several PKC consensus phosphorylation sites (1.6.5.3) and despite conflicting evidence, phosphorylation of P-GP by PKC isoforms has been associated with P-GP activation and drug efflux (Chambers, *et al.*, 1994). To determine whether PKCε overexpression might confer DNR resistance through promoting P-GP activity, the impact of PKC agonists and inhibitors on DNR accumulation was assessed.

PMA is a potent activator of cPKC and nPKC isoforms, including PKCε, and acts through mimicking the effects of DAG (Jain and Trivedi, 2014). The ability of PMA to activate these PKC isoforms was assessed by measuring NOX2-derived superoxide using a Diogenes™ assay, as NOX2-derived ROS production is dependent on cPKC and nPKC activity (Rastogi, *et al.*, 2017). This analysis was conducted in NOMO-1 cells which produce extracellular superoxide. NOMO-1 cells treated with PMA showed a 4.45±2.45-fold increase in the rate of superoxide photon production, compared to cells treated with the vehicle control (Figure 5.19), suggesting that PMA treatment can promote PKC activity. Therefore, the impact of PMA treatment on DNR uptake, which was used as an indicator of P-GP activity, was assessed.

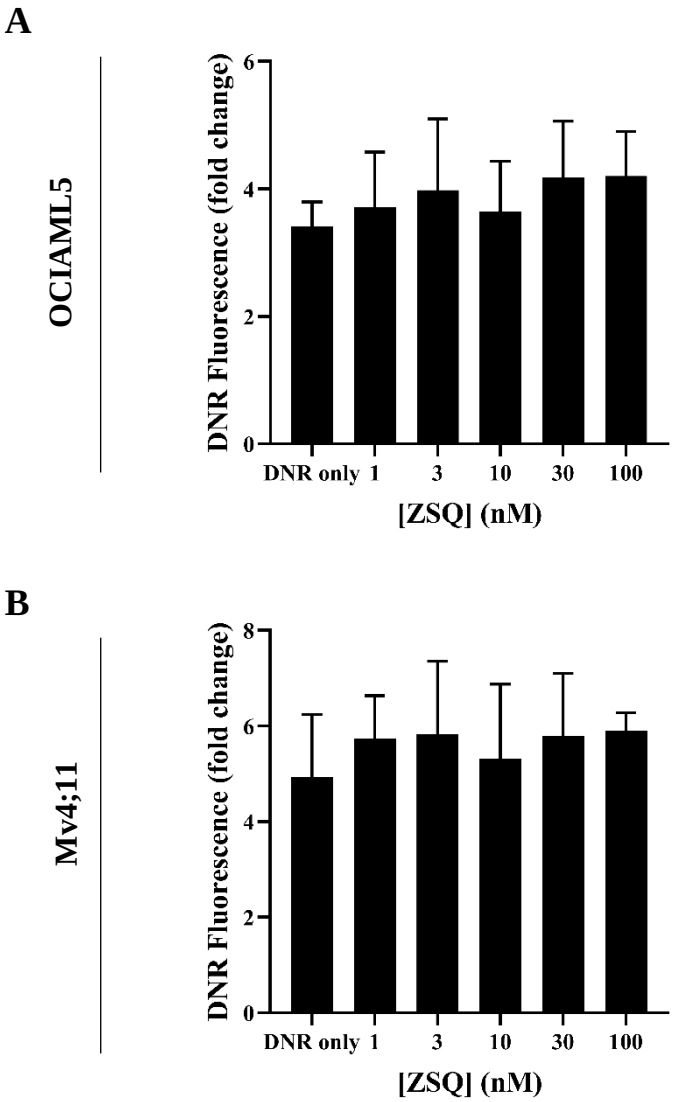

Figure 5.18: ZSQ treatment does not promote DNR accumulation in OCIAML5 or Mv4;11 cells

Bar charts showing the effect of ZSQ treatment (0-100nM) on DNR accumulation following 2 hours of treatment with 100nM DNR in **(A)** OCIAML5 and **(B)** Mv4;11 cells. DNR accumulation was determined by measuring DNR fluorescence (2.8.8.2) and is normalised to the fluorescence of cells treated with the vehicle control (PBS+0.025% (*v/v*) DMSO; 2.8.8); OCIAML5(n=3), Mv4;11 (n=2); data represents mean+1SD. The statistical significance of DNR accumulation in OCIAML5 cells was determined using a one-way ANOVA with Bonferroni post-test comparison where comparisons were made to DNR treatment alone and was deemed non-significant.

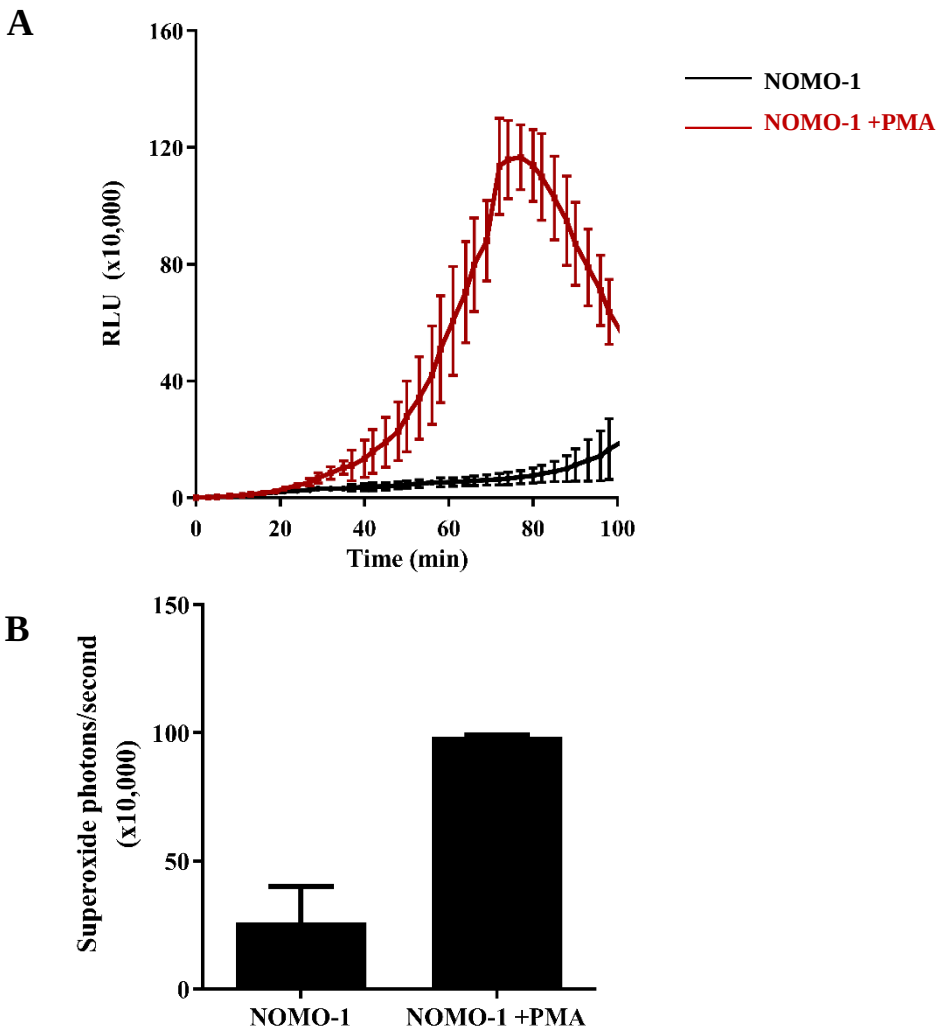

Figure 5.19: PMA treatment stimulates NOX2 superoxide production in NOMO-1 cells

(A) Chemiluminescent traces (relative light units (RLU) x10,000) and **(B)** rate of superoxide production (x10,000) of NOMO-1 cells in the presence and absence of PMA (100nM) which was measured, over 100 min, using the Diogenes™ superoxide probe (2.8.6); n=3.

In KG-1 cells, which previously demonstrated intrinsic P-GP activity in response to DNR (Figure 5.12), co-treatment with DNR and PMA reduced DNR accumulation by c20% compared to DNR treatment alone; an effect which was reversed by ZSQ treatment (Figure 5.20). These data demonstrate the capacity for PMA treatment to promote P-GP mediated DNR efflux in KG-1 cells. However, PMA treatment did not have a significant impact on the DNR accumulation of either the control or PKCε overexpression U937 or HEL cell lines (Figure 5.21). This suggests PKCε-mediated DNR resistance is not a consequence of increased in P-GP activity. Similarly, in the NOMO-1 and TF-1 (control and PKCε overexpression) lines, PMA treatment did not reduce DNR accumulation compared to DNR treatment alone (Figure 5.22), indicating that the reason that these lines do not exhibit the same phenotypes as the U937 and HEL overexpression lines, is not due to a lack of PKCε activation in these cells.

The PKC activation data (above) were supported by the reciprocal experiments where cPKC and nPKC isoforms were inhibited by Calphostin C (CC), a competitive inhibitor of the DAG binding site (Bruns, *et al.*, 1991). As with PMA, the ability of CC to inhibit PKC activity was assessed indirectly through the Diogenes ™ assay. NOMO-1 cells treated with CC showed a reduced rate of superoxide production, compared to NOMO-1 cells treated with the vehicle control (Figure 5.23). However, when applied to the drug uptake assay, CC treatment did not increase DNR accumulation, compared to DNR treatment alone (Figure 5.24). Therefore, these data further support the hypothesis that PKCε does not promote P-GP drug efflux through directly increasing P-GP activation.

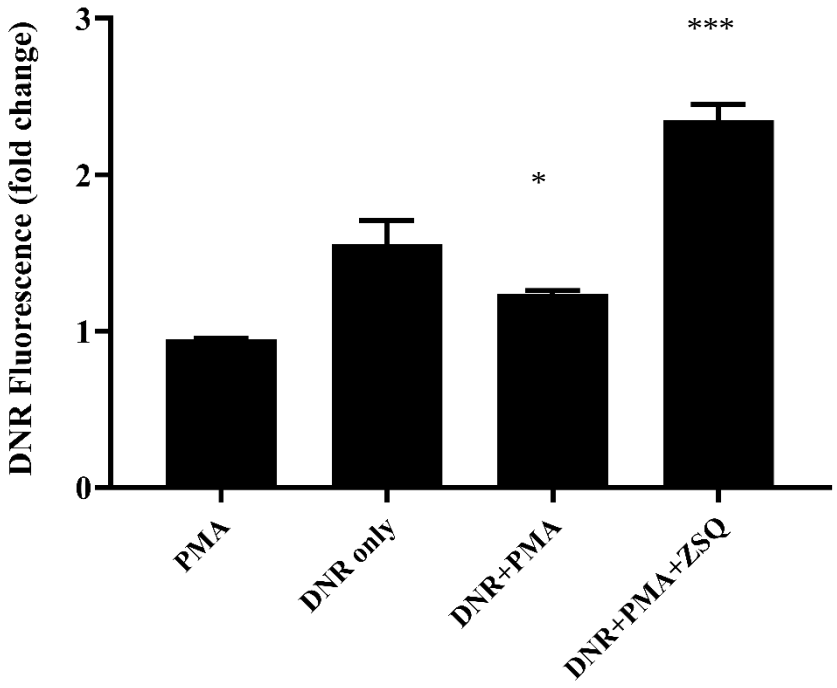

Figure 5.20: PMA treatment reduced DNR accumulation in KG-1 cells

Bar chart showing the effect of PMA treatment (100nM) on DNR fluorescence following 2 hours of treatment with 100nM DNR in KG-1 cells. DNR accumulation was determined by measuring DNR fluorescence (2.8.8.2) and is normalised to the fluorescence of cells treated with the vehicle control (PBS; 2.8.8); n=3; data represents mean+1SD. The statistical significance was determined using one-way ANOVA with Bonferroni post-test comparison where comparisons were made to DNR treatment alone, and were deemed significant; *$p<0.05$, *** $p<0.001$.

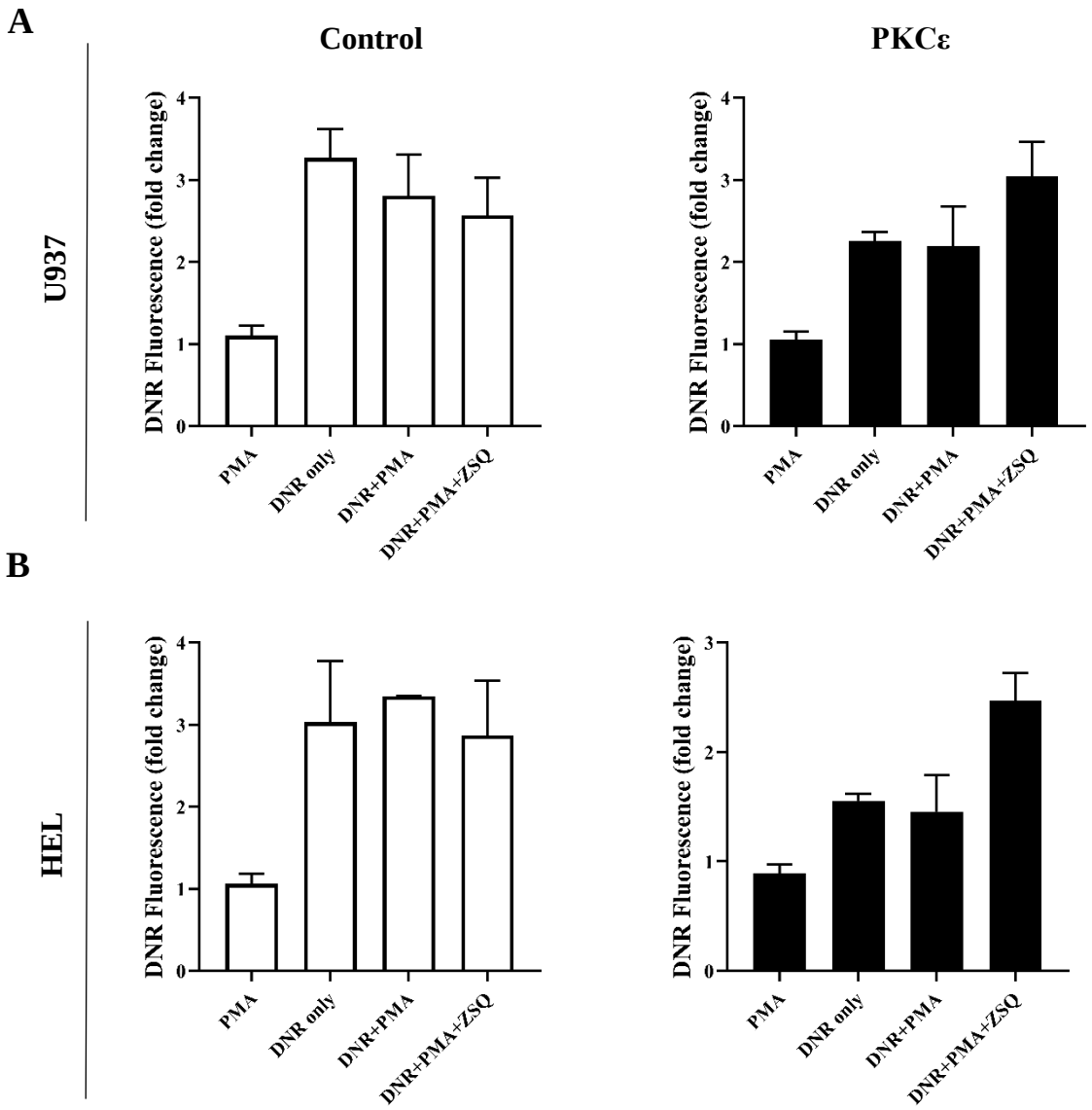

Figure 5.21: PMA treatment does not reduce DNR accumulation in U937 or HEL cells

Bar chart showing the effect of PMA treatment (100nM) on DNR fluorescence following 2 hours of treatment with 100nM DNR in **(A)** U937 and **(B)** HEL cells transduced with the control (left) or PKCε overexpression (right) constructs (Figure 4.3). DNR accumulation was determined by measuring DNR fluorescence (2.8.8.2) and is normalised to the fluorescence of cells treated with the vehicle control (PBS; 2.8.8); U937 n=3 except DNR+PMA+ZSQ treatment where n=2; HEL n=2; data represents mean+1SD. The statistical significance of DNR accumulation in the U937 cell lines was determined using one-way ANOVA with Bonferroni post-test comparison, where comparisons were made to DNR treatment alone, and were deemed non-significant.

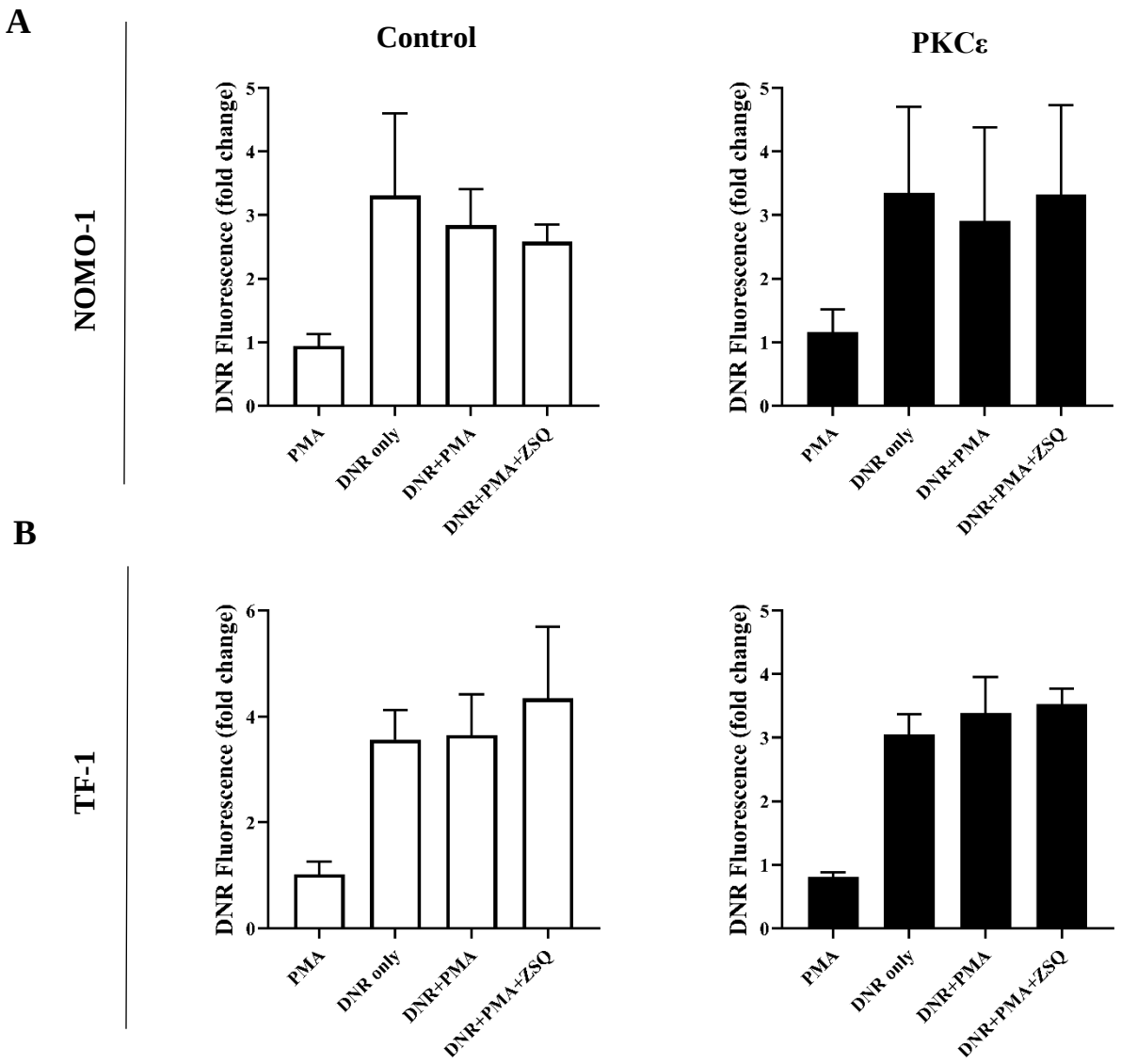

Figure 5.22: PMA does not affect DNR accumulation in NOMO-1 or TF-1 cells

Bar chart showing the effect of PMA treatment (100nM) on DNR fluorescence following 2 hours of treatment with 100nM DNR in **(A)** NOMO-1 and **(B)** TF-1 cells transduced with the control (left) or PKCε overexpression (right) constructs (Figure 4.3). DNR accumulation was determined by measuring DNR fluorescence (2.8.8.2) and is normalised to the fluorescence of cells treated with the vehicle control (PBS; 2.8.8); NOMO-1 n=4 except DNR+PMA+ZSQ treatment where n=3; TF-1 n=3 except DNR+PMA+ZSQ where n=2; data represents mean+1SD. The statistical significance of DNR accumulation was determined using one-way ANOVA with Bonferroni post-test comparison, where comparisons were made to DNR treatment alone, and were deemed non-significant.

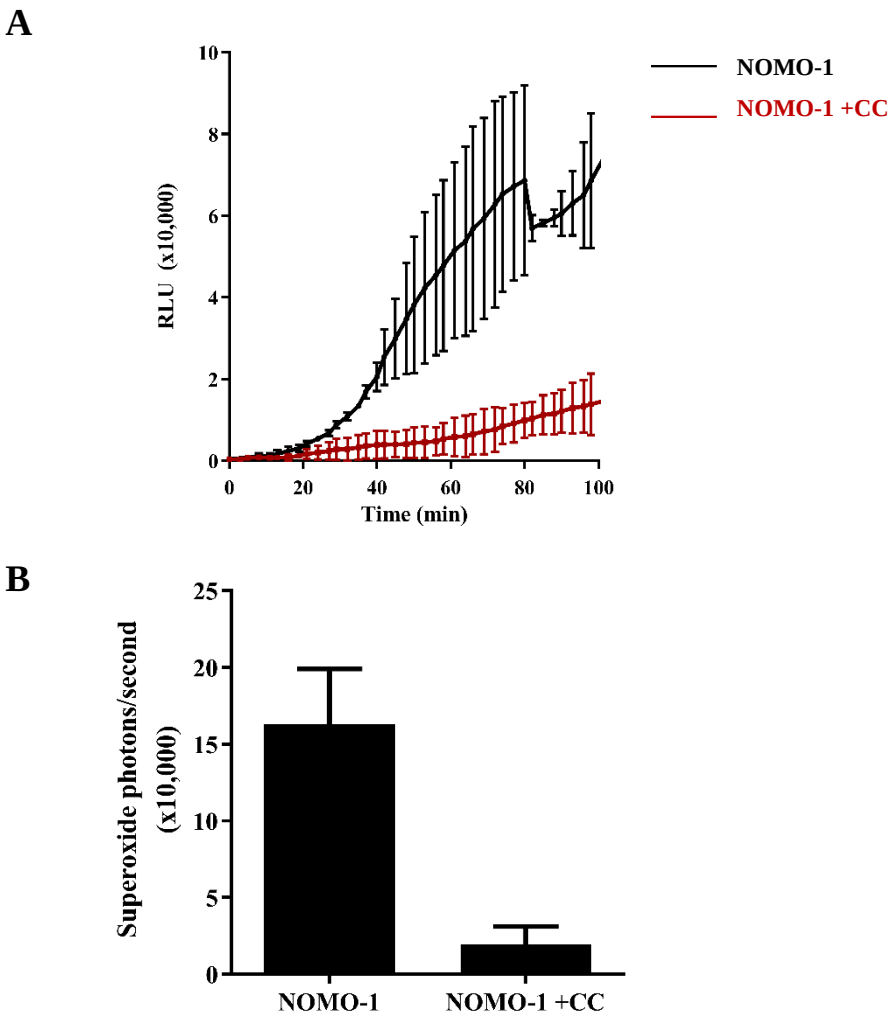

Figure 5.23: CC treatment reduces NOX2 superoxide production in NOMO-1 cells

(A) Chemiluminescent traces (RLU x10,000) and **(B)** rate of superoxide production (x10,000) of NOMO-1 cells in the presence and absence of PMA (100nM) which was measured, over 100 min, using the Diogenes™ assay (2.8.6); n=2.

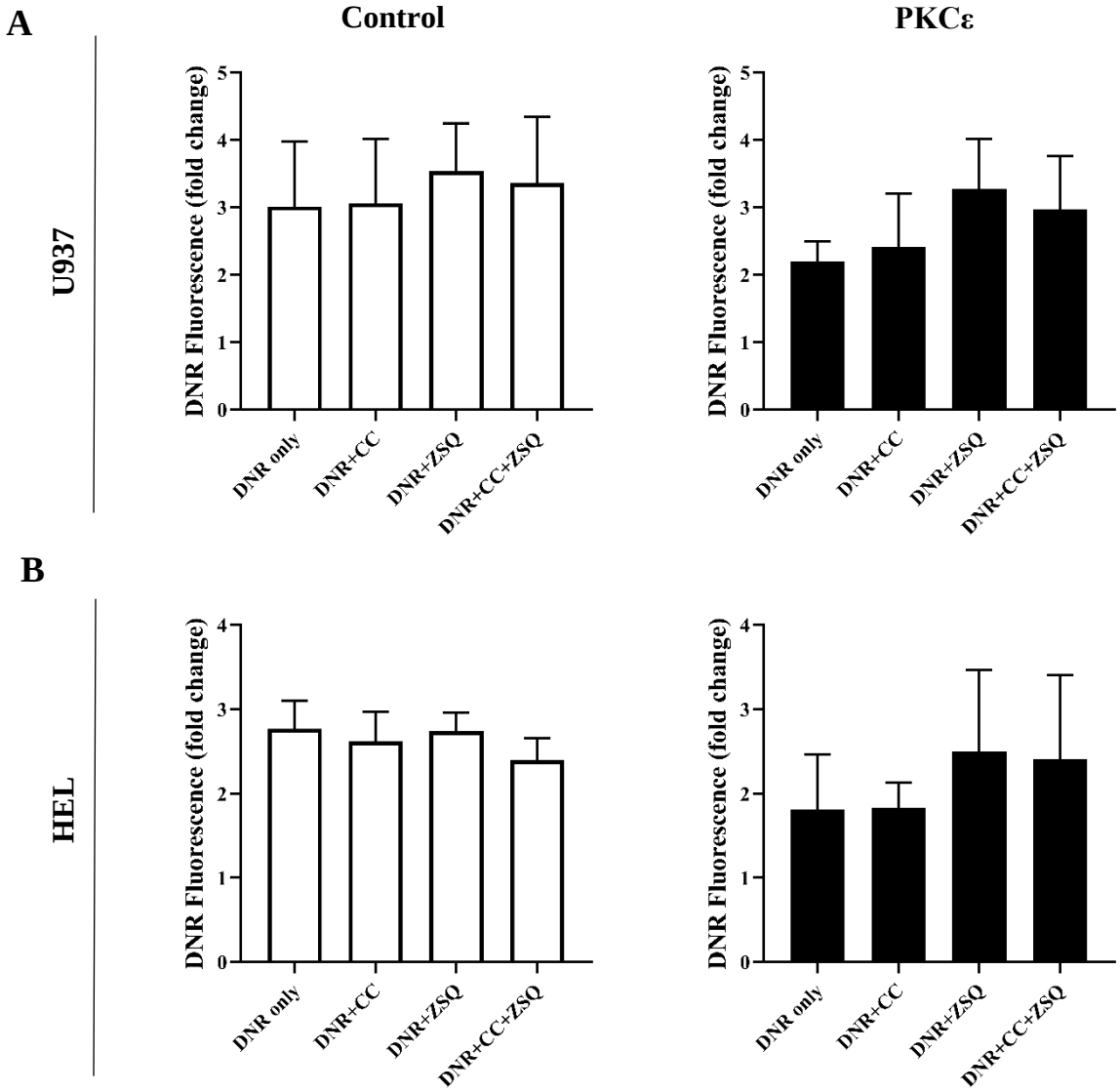

Figure 5.24: Calphostin C does not affect DNR accumulation in U937 and HEL cells

Bar chart showing the effect of Calphostin C (CC) treatment (100nM) on DNR fluorescence following 2 hours of treatment with 100nM DNR in **(A)** NOMO-1 and **(B)** TF-1 cells transduced with the control (left) or PKCε overexpression (right) constructs (Figure 4.3). DNR accumulation was determined by measuring DNR fluorescence (2.8.8.2). As the fluorescence of CC is detected in the same channel as DNR, the fluorescence of cells treated with CC alone was subtracted from any sample treated with CC, before the MFI was normalised to the vehicle control (PBS; 2.8.8); U937 (n=4), HEL (n=3). The statistical significance of DNR accumulation was determined using one-way ANOVA with Bonferroni post-test comparison, where comparisons were made to DNR treatment alone, and were deemed non-significant.

3.3.3 Determining the relationship between PKCε and P-GP in AML cell lines and patient samples

Having determined that P-GP drug efflux underpins the chemoresistant phenotype observed in the PKCε overexpression cell lines, the relationship between PKCε and P-GP was investigated further. Specifically, the endogenous expression of these two factors in AML cell lines and patient samples was assessed at an mRNA and protein level. mRNA expression in AML cell lines was assessed using data obtained from DepMap (2.11.3) and did not show a positive correlation between *P-GP* (*ABCB1*) and *PKCε* (*PRKCE*) across the AML cell lines investigated (Figure 5.25). Studies have shown that P-GP protein expression does not necessarily correlate with mRNA expression (Yague, *et al.*, 2003). Therefore, the relationship between P-GP and PKCε protein expression in AML cell lines was also examined. Western blot analysis showed that P-GP protein was heterogeneously expressed across the AML cell lines investigated. The highest level of P-GP expression was observed in KG-1 cells, but endogenous protein expression was also observed in HEL, NOMO-1, Mv4;11, U937, OCIAML5, and SKNO-1 cells (Figure 5.6); with the caveat that this does not represent surface P-GP expression. Correlation analysis between PKCε and P-GP protein expression could not be conducted as only 3 of the lines investigated had detectable levels of PKCε protein by western blot analysis (Figure 4.1).

Given the limitations of the AML cell line analysis, the relationship between P-GP and PKCε mRNA and protein expression was examined in patient samples. Using the TCGA 2013 dataset (Ley, *et al.*, 2013), *P-GP* mRNA expression was not significantly upregulated in the high *PKCε* cohort (Figure 5.25). This finding is concordant with the cell line analysis, in not supporting a relationship between *P-GP* and *PKCε* at an mRNA level. For the reasons described above, the relationship between PKCε and P-GP was also investigated at a protein level. P-GP expression and functionality data in samples from the AML14 and AML15 clinical trials, which was determined by flow cytometry, was kindly provided by Claire Seedhouse from Nottingham University. From this cohort of patients for which complete or partial P-GP expression and function data were available, PKCε expression had been determined by our group in 38 samples (2.12.3).

Patient samples were stratified into 2 groups based on their PKCε expression; those with undetectable PKCε expression by western blot (low PKCε), and samples which overexpressed PKCε compared to normal $CD34^+$ blasts (high PKCε; Figure 3.1). This analysis

showed that the proportion of patients with above median P-GP expression was 2.8-fold higher in the high PKCε cohort (23%) than in samples with low PKCε expression (8%; Figure 5.26A). This supports the PKCε overexpression cell lines in indicating an association between PKCε and P-GP protein expression. P-GP function had been assessed using a functional assay where rhodamine-123 efflux was modulated using the selective P-GP inhibitor PSC-833 (Seedhouse, *et al.*, 2007). The impact of PSC-833 on rhodamine-123 accumulation was evaluated by calculating a Psc ratio, as described in Pallis and Das-Gupta, 2005 where the fluorescence of cells treated with rhodamine-123 and PSC-833 was divided by the fluorescence of the cells treated with rhodamine-123 and the vehicle control. Samples which had a Psc ratio <1.7 were considered negative for P-GP function, while samples with a Psc$\geq$1.7 and Psc>3.4 were classified as having low and high P-GP function, respectively. Unlike the expression analysis, in patients with high and low PKCε expression no significant difference in P-GP function was observed (Figure 5.26B). This is likely due to the number of samples with functional P-GP, given that c70% of samples in each cohort were negative (Psc<1.7) for P-GP function. Combined with the small sample size this meant that only between 3-5 samples in each cohort had functional P-GP (Figure 5.26B). Despite this, overall, these data are not inconsistent with the PKCε overexpression analysis in indicating a positive relationship between PKCε and P-GP protein expression in AML cells.

To support this, PKCε and P-GP protein expression were determined in 8 AML patient-derived samples (Table 2.3) from the AML15 NCRI UK clinical trial using western blot analysis. PKCε was detected in 5 of the 8 samples, while P-GP was heterogeneously expressed (Figure 5.27). Across the samples, P-GP expression appeared to be greatest in the samples with the highest endogenous PKCε expression (AML165 and AML172) with the caveat that western blot analysis does not indicate the level of surface expression of P-GP (Figure 5.27). To investigate whether this relationship was causal, shRNA-mediated PKCε knockdown studies were conducted. In the AML165 and AML172 samples, PKCε knockdown did not affect DNR accumulation (Figure 5.28), although only a single shRNA construct (486) was investigated and because of the very small amount of material available, the degree of PKCε knockdown could not be validated. In addition, DNR accumulation was not impacted by ZSQ treatment (Figure 5.28), suggesting that these cells do not have intrinsically active P-GP in response to DNR (which would be required for PKCε knockdown to alter DNR sensitivity).

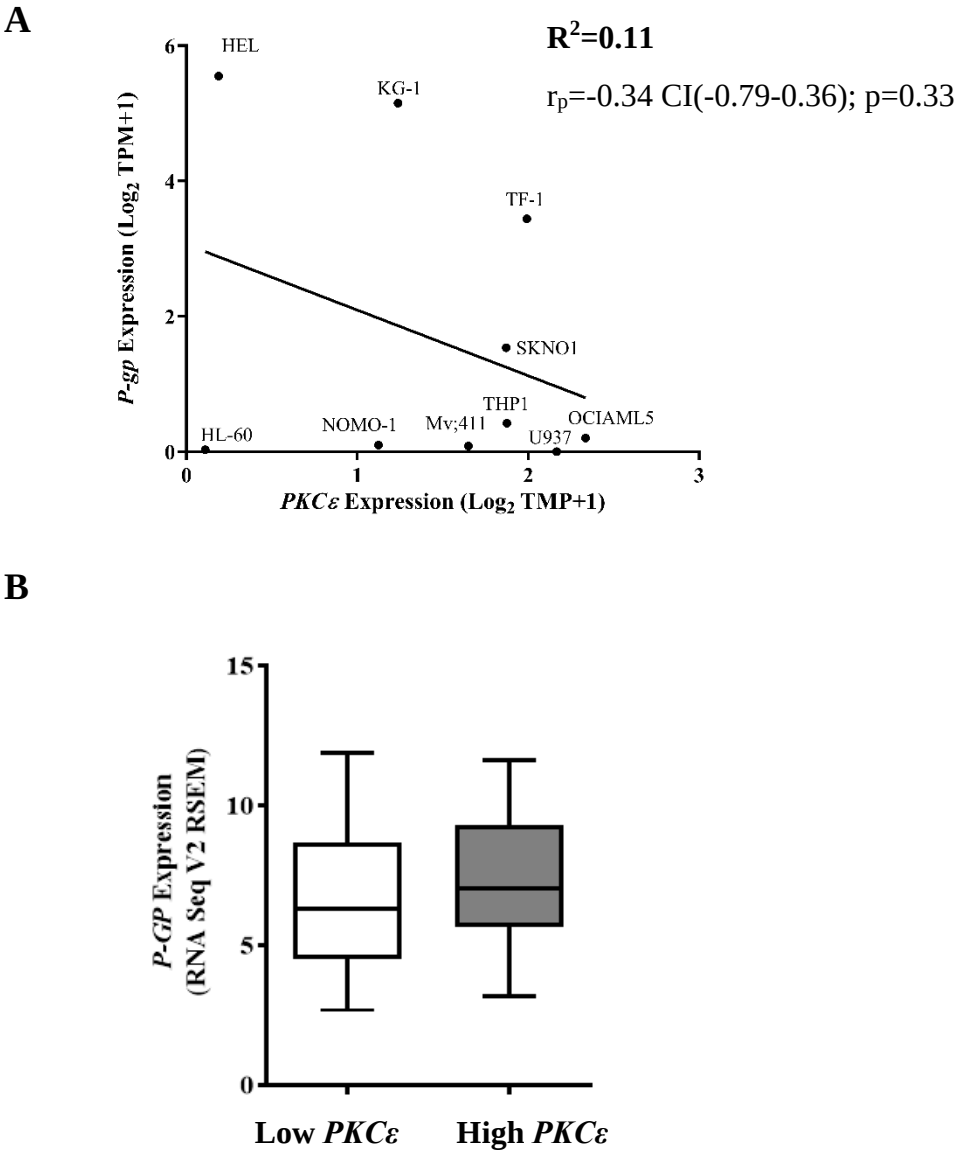

Figure 5.25: *P-GP* mRNA expression is not associated with *PKCε expression* in AML cell lines and patient samples

(A) Dot plot showing the correlation between *PKCε* (*PRKCE*) and *P-GP* (*ABCB1*) mRNA expression in AML cell lines. Gene expression data was obtained from DEPMAP using the Public 20Q1 dataset (Broad, 2020, Ghandi, *et al.*, 2019). The black line represents the linear regression line (R^2=0.11), while and the degree of correlation assessed using Pearson's correlation analysis (r_p=-0.34 CI(-0.79-0.36); p=0.33) which was deemed non-significant. (**B**) Box and whisker plot showing *P-GP* (*ABCB1*) mRNA expression (RNASeq V2 RSEM on a linear scale) in AML patients with low (lower quartile, n=35) and high (upper quartile, n=36) *PKCε* (*PRKCE*) expression. Patient data was obtained from the TCGA 2013 dataset Ley, *et al.*, 2013; 2.11.2). The median is represented with the black line, the box represents the interquartile range, and the whiskers represent the minimum and maximum values. Statistical significance was determined using Mann-Whitney test; and was deemed non-significant. A*bbreviations; TPM; transcripts per million*.

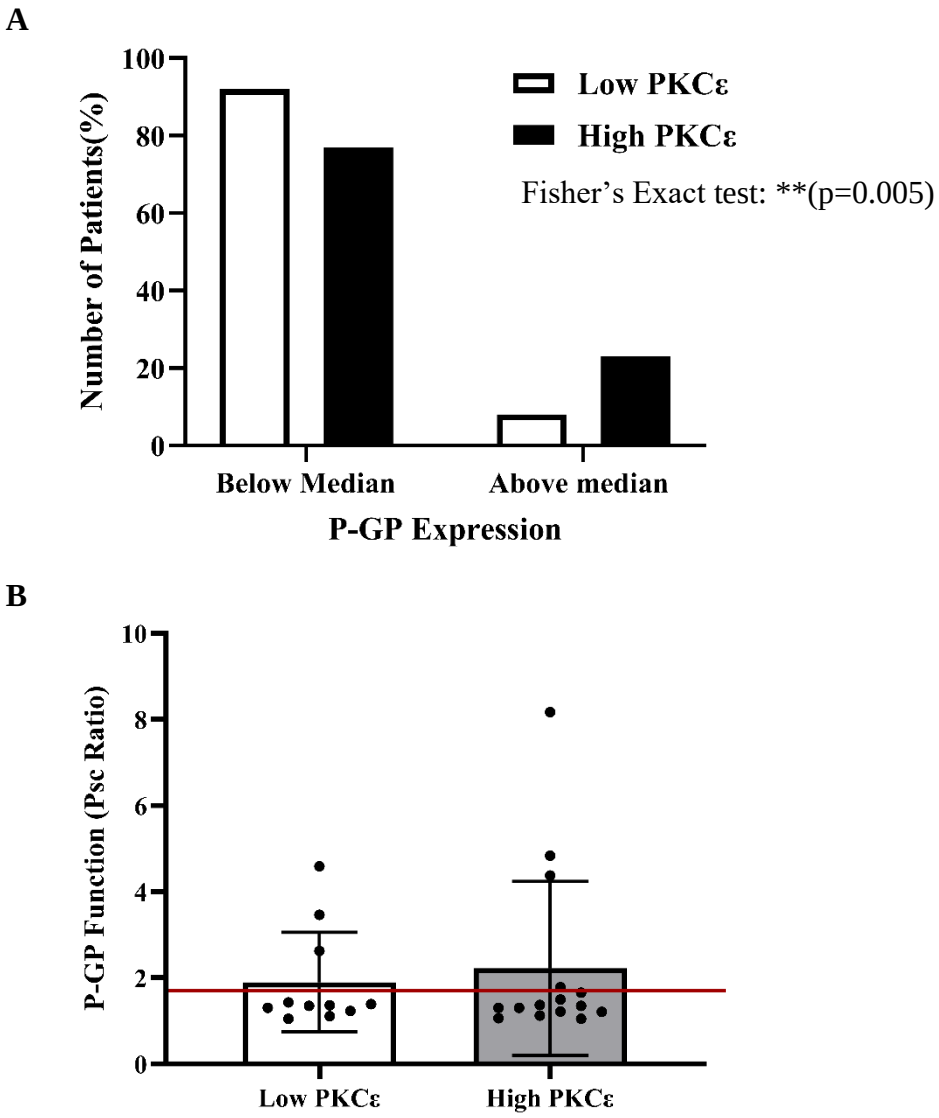

Figure 5.26: High PKCε protein expression is associated with high P-GP expression in AML patient samples

(A) Bar chart showing the number of patients (%) with above or below median P-GP expression, determined by MRK16 staining, in AML14 and AML15 samples with low (undetectable PKCε expression n=12), and high PKCε (overexpression compared to normal $CD34^+$ blasts; >108fg/1000 cells; n=14). Statistical significance was determined using a Fisher's Exact test and was deemed significant; **p<0.01. (**B**) Bar chart showing the P-GP function (Psc ratio) in AML14 and AML15 samples with low (undetectable PKCε expression n=11), and high PKCε (overexpression compared to normal $CD34^+$ blasts (>108fg/1000 cells; n=15) expression. The red line represents a Psc Ratio of 1.7. Samples with a Psc ratio $\geq$1.7 were deemed to have low P-GP function while those with a Psc >3.4 had high P-GP function (2.12.3). Statistical significance was determined using a Mann-Whitney test and was deemed non-significant.

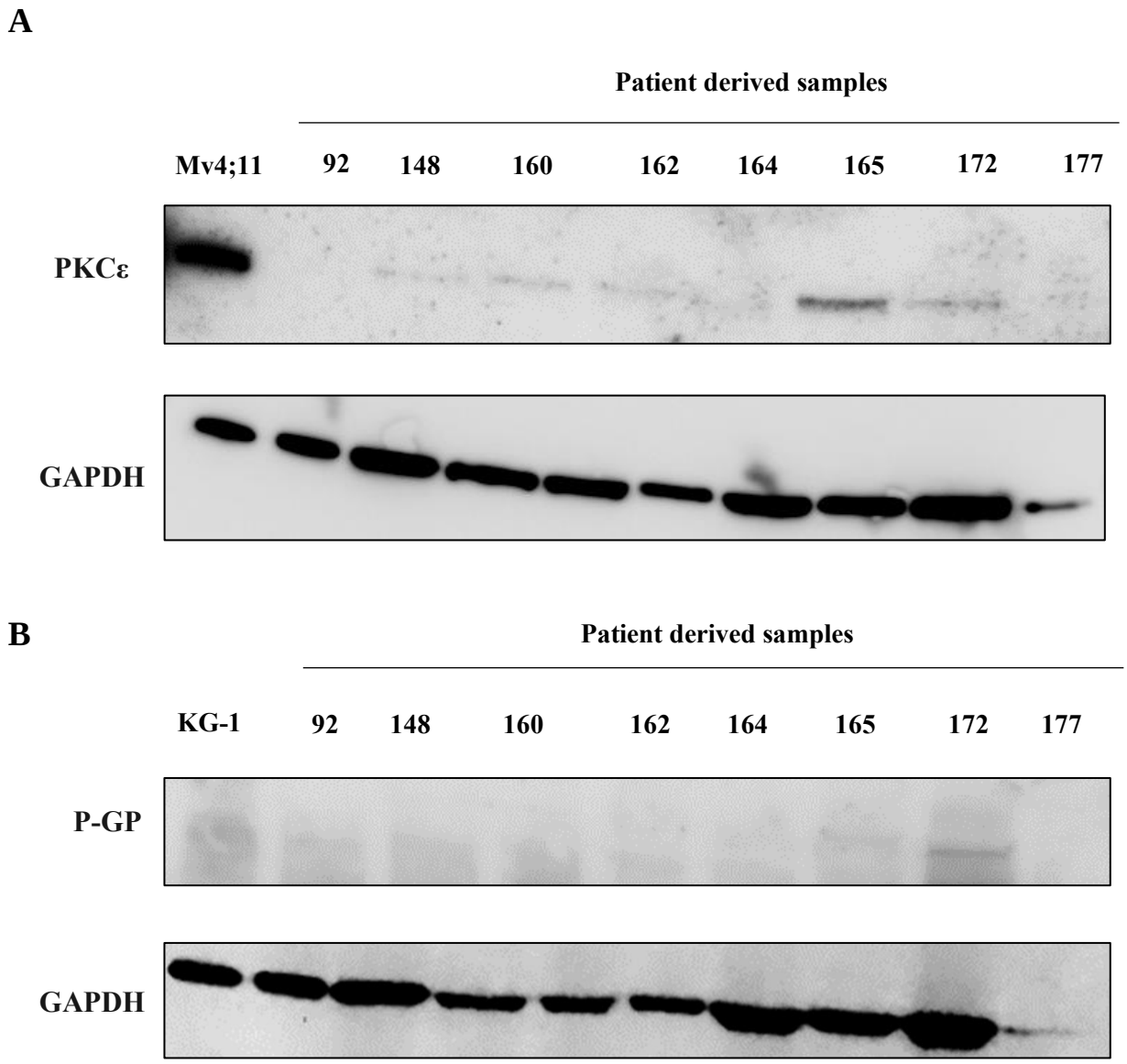

Figure 5.27: PKCε protein expression in AML patient-derived samples

Western blot showing the expression of **(A)** PKCε (MW-84kDa) and **(B)** P-GP (MW140-170kDa) expression in AML patient derived cells (2.3). PKCε expression was detected using the Cell Signalling Technologies antibody #2683 (clone 22B10) while P-GP was detected using the Insight C219 antibody (Table 2.10) and is shown alongside GAPDH (MW-36kDa) expression, which was used as a loading control and detected using the ThermoFisher Scientific GAPDH antibdy (Table 2.10).

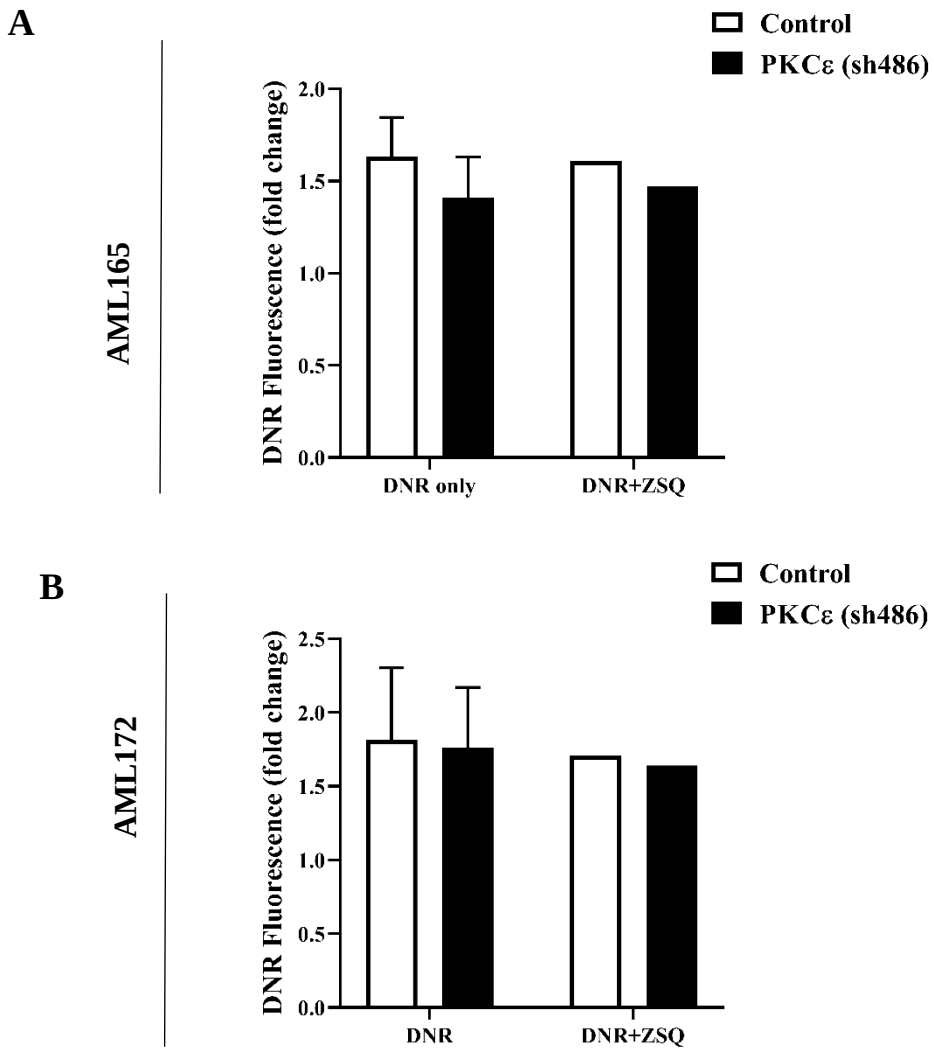

Figure 5.28: PKCε knockdown has no impact on DNR accumulation in AML patient samples

Bar chart showing the DNR fluorescence in the presence and absence of the P-GP inhibitor ZSQ (100nM), following 2 hours of treatment with 100nM DNR in AML patient samples; **(A)** AML165 and **(B)** AML172 transduced with the control or PKCε knockdown (486) constructs (Table 2.4). DNR fluorescence was normalised to the fluorescence of untreated treated with the vehicle controls (PBS or PBS+0.025% (*v/v*) DMSO; 2.8.8); DNR n=3. DNR+ZSQ n=1; data represents mean+1SD. Statistical significance was determined using a Mann-Whitney test and was deemed non-significant.

3.4 Discussion

The aim of this chapter was to establish the mechanisms through which PKCε confers DNR resistance in AML cells, as demonstrated in Chapter 4. As PKCε overexpression did not confer resistance to Ara-C, initial studies focused on mechanisms of chemoresistance which relate to the mode of action of DNR. The cytotoxicity of DNR is thought to be primarily mediated through DNA intercalation and interactions with topoisomerase II. However, ROS generation accounts at least in part, for the mode of action of anthracyclines (Jung and Reszka, 2001, Mansat-de Mas, *et al.*, 1999). Reduction of DNR by NADPH results in the production of the semiquinone radical daunorubicin aglycone. This subsequently reacts with oxygen to generate superoxide radicals and H_2O_2 and promotes cell death through JNK/stress-activated protein kinase (SAPK) apoptotic signalling (Pelicano, *et al.*, 2004). The cytoprotective capacity of PKCε has been demonstrated in cardiac cells. Treatment of cardiac cells with ATM promotes PKCε activation (Barnett, *et al.*, 2007), which subsequently contributes to cardio-protection through interacting with several proposed mitochondrial substrates including, mitochondrial K_{ATP} channels and cytochrome c oxidase subunit IV (Kabir, *et al.*, 2006, Kornfeld, *et al.*, 2015). Altered redox homeostasis and resistance to oxidative stress therefore represents a potential mechanism of PKCε-mediated DNR resistance.

Mitochondrial ROS are intrinsic products of oxidative metabolism and are generated when electrons, flowing down the ETC, prematurely react with oxygen to form superoxide radicals (Murphy, 2009). In the context of AML, modulating PKCε expression has been shown to disrupt mitochondrial ROS homeostasis and protect against oxidative stress (Di Marcantonio, *et al.*, 2018). Specifically, in response to the mitochondrial ROS-generating agents, thenoyltrifluoroacetone (TTFA) and ATM, PKCε overexpression conferred a survival advantage in OCIAML3 and THP-1 cells and promoted colony formation in MLLAF9 mouse leukaemic cells. Furthermore, PKCε knockdown in these cell lines resulted in significant increases in CellROX™ and MitoSOX™ fluorescence, suggesting increased levels of cytosolic ROS and mitochondrial superoxide, respectively. The role of PKCε in regulating mitochondrial ROS homeostasis was further supported in the Di Marcantonio *et al.* study through proteomic analysis. Nanoscale liquid chromatography coupled to tandem mass spectrometry, showed that 15% of the differentially expressed genes identified in the PKCε knockdown OCIAML3 cell line were related to mitochondrial biology (Di Marcantonio, *et al.*, 2018). These include proteins which are involved in regulating outer mitochondrial membrane

potential (e.g.UQCR10) and mitochondrial membrane transport (e.g.SLC25A1; Di Marcantonio, *et al.*, 2018).

To address whether altered redox homeostasis contributes to PKCε-mediated DNR resistance, this study investigated the propensity of PKCε to modulate mitochondrial ROS homeostasis. The reduced levels of detectable superoxide in U937 and HEL cells overexpressing PKCε (3.3) is supportive of a role in REDOX homeostasis. However, the homeostatic regulation of mitochondrial superoxide levels is ultimately underpinned by a balance between the rate of superoxide production and antioxidant capacity, hence, this data could be explained by a decrease in superoxide production as well as an increase in antioxidant capacity. The reduced rate of proliferation exhibited by the DNR resistant cell lines (U937 and HEL) is therefore a confounding factor as this, in itself, is likely to influence superoxide production. These data cannot therefore be attributed to increased antioxidant capacity arising from PKCε overexpression. To address this point specifically, the impact of PKCε overexpression on the sensitivity of these cell lines to ROS-generating agents was investigated.

In response to GOx, an oxi-reductase which generates H_2O_2, PKCε overexpression resulted in an increased sensitivity in both U937 and HEL cells, rather than promoting resistance. This result contradicts the findings of Di Marcantonio *et al.*, although these authors used agents which selectively provoke an increase in mitochondrial ROS. Thus, the impact of PKCε overexpression on the sensitivity of these cell lines to the mitochondrial ROS-generating agents, ATM and ATO was assessed. ATM causes the accumulation of ROS within the intermediate space of the mitochondrial membranes by inhibiting complex III of the ETC (Kabir, *et al.*, 2006). In this study, the growth inhibitory effects of ATM were diminished by PKCε overexpression in U937 and HEL cells compared to the control cell lines. However, no significant impact on cell viability was observed. This contrasts with the findings of Di Marcantonio *et al.* where PKCε overexpression conferred a significant survival advantage in OCIAML3 overexpressing PKCε, in response to 100μM ATM. The use of such high concentrations of ATM is however questionable given that the maximum impact of ATM on superoxide production is achieved at sub-micromolar levels (Votyakova and Reynolds, 2001) which is consistent with our own data. This suggests that the effect on survival of the high concentrations of ATM used by Di Marcantonio *et al.* could be due to off-target mechanisms.

Given the discrepancies between the present study and the Di Marcantonio *et al.* study, the impact of PKCε overexpression on the sensitivity of U937 and HEL cells to ATO was assessed. Unlike ATM, ATO generates ROS through the inhibition of complex I and complex III (Pourahmad, *et al.*, 2016). However, PKCε overexpression did not confer resistance to ATO. This supported the ATM analysis and are therefore is also at variance to the Di Marcantonio *et al.* study. Together, the data presented in this chapter show that PKCε overexpression does not confer resistance to ROS generating agents and that perturbed ROS homeostasis is unlikely to contribute to PKCε-mediated DNR resistance. Hence, alternative mechanisms of PKCε-mediated DNR resistance were investigated.

Using the fluorescent properties of DNR as an indicator of drug accumulation, the DNR resistant PKCε overexpression cell lines (U937and HEL) had reduced DNR accumulation compared to the control lines. Furthermore, this was not observed in NOMO-1 and TF-1 lines which did not exhibit DNR resistance upon PKCε overexpression. Intercalation of anthracyclines with DNA can cause endogenous quenching of its fluorescence, however, at low doses (<5μg/mL) DNR fluorescence and DNR intercalation has a linear relationship (Smeets, *et al.*, 1999). Therefore, the contribution of DNR intercalation with DNA is unlikely to contribute to discrepancies in DNR accumulation in these cell lines. However, DNR is a substrate for several efflux pumps, such as P-GP and MRP1 (de Jonge-Peeters, *et al.*, 2007). P-GP is one of the best characterised efflux pumps for which anthracyclines are a substrate and has been shown to reduce DNR accumulation *in vitro* (Nooter, *et al.*, 1990). Clinically, the upregulation of efflux pumps such as P-GP is a central mediator of multidrug resistance and is associated with poor CR induction in this malignancy (van der Kolk, *et al.*, 2000). Furthermore, this mechanism would explain why PKCε overexpression did not promote resistance to Ara-C, as this nucleoside analogue is not transported by P-GP (Norgaard, *et al.*, 1998).

Associations between PKC and P-GP expression and function have largely been studied using PKC agonists and inhibitors (Mayati, *et al.*, 2017). However, some PKC inhibitors, including Chelerythrine and Enzastaurin are thought to supress P-GP-mediated drug resistance by directly binding P-GP and inhibiting its function (Chambers, *et al.*, 1992, Michaelis, *et al.*, 2015). This has made determining a causal relationship between PKC activity and P-GP mediated drug efflux difficult. However, PKCε has been associated with the induction of P-GP expression in LNCaP cells; an androgen-sensitive human prostate adenocarcinoma cell line. Treatment of these cells with the PKCε-specific translocation

inhibitor, εV1–2, significantly supressed the fraction of cells which expressed P-GP in response to aspirin (Flescher and Rotem, 2002a).

Western blot and flow cytometric analysis showed P-GP upregulation in the U937 and HEL cell lines overexpressing PKCε, compared to the control lines. To determine whether a causal relationship existed between DNR resistance exhibited by these cells and P-GP drug efflux, P-GP inhibition assays were conducted using ZSQ, a third-generation inhibitor which binds allosterically to P-GP (Starling, *et al.*, 1997). In the DNR resistant PKCε overexpression cell lines, ZSQ treatment restored DNR accumulation and cytotoxicity to levels comparable with the control lines. These findings are in-line with the existing literature regarding ZSQ treatment in AML blasts (Tang, *et al.*, 2008). Furthermore, these data demonstrate that drug efflux via P-GP fully accounts for PKCε-mediated DNR resistance in this context. ZSQ has previously been shown to have a high specificity to P-GP with an EC50 of 59nM and limited effects on other multidrug transporters such as MRP1 (Starling, *et al.*, 1997). This was supported by the dose-dependent increase of DNR accumulation in response to ZSQ, in the U937 and HEL PKCε overexpression cells, indicating that the effects of ZSQ (100nM) were not due to off-target effects. Having determined that PKCε promotes DNR resistance via P-GP drug efflux in AML cell lines, the relationship between PKCε and P-GP was investigated in AML patient samples from the AML14 and AML15 clinical trials. A significant association between PKCε and P-GP expression was observed, supporting a relationship between these two factors. Although P-GP expression was not associated with increased P-GP function, around 70% of samples within each cohort were negative for functional P-GP, and as a result, the number of samples with active P-GP were too small to draw meaningful conclusions. However, these data are not inconsistent with an association between PKCε and P-GP expression in AML cells.

Regulation of P-GP expression can occur through transcriptional and post-translational mechanisms. PKC isoforms have been implicated in this process as PKCα and PKCθ can bind to the *MDR1* promoter directly (Gill, *et al.*, 2001), while PKCε can modulate the activity of transcription factors implicated in the transcriptional regulation of P-GP such as AP-1 and NF-κB (Garg, *et al.*, 2012, Katayama, *et al.*, 2014, Li, *et al.*, 2000). Despite this, the data presented in this chapter suggest that a transcriptional mechanism of P-GP induction by PKCε is unlikely. However, an association between PKCε and P-GP was indicated at a protein level in both AML cell lines and patient samples, suggesting a post-translational mechanism of P-GP regulation by PKCε.

A central post-translational modification involved in the regulation of P-GP is phosphorylation. Several PKC consensus phosphorylation sites have been identified in the linker region of P-GP Chambers, *et al.*, 1992. Treatment of a multidrug resistance human carcinoma cell line (KB-V1), with TPA induced P-GP phosphorylation and reduced vinblastine accumulation; a finding that was not observed in the vinblastine sensitive cell line (KB-3; Chambers, *et al.*, 1992). In addition, inhibition of PKC using the inhibitors, CC and ET-18-OCH_3, which do not bind directly to P-GP, resulted in reduced basal levels of P-GP phosphorylation (Chambers, *et al.*, 1992). Together, these data suggest that P-GP is a physiological substrate of PKC isoforms, and that in drug resistant cells PKC-mediated phosphorylation can promote P-GP activity. However, there is some conflicting evidence to this, as site-directed mutagenesis of the major PKC phosphorylation sites of P-GP (Ser661, Ser667 and Ser671) to alanine residues, preventing phosphorylation, did not affect vinblastine accumulation or doxorubicin drug efflux compared with lung fibroblasts expressing wild type P-GP (Goodfellow, *et al.*, 1996).

To investigate whether PKCε overexpression conferred DNR resistance by promoting P-GP activity, PMA was used to promote PKC (cPKC and nPKC) activity. The resulting impact on DNR uptake was used to infer the effect on P-GP activity. In KG-1 cells, which have intrinsic P-GP expression and activity, PMA treatment significantly reduced DNR accumulation, compared to DNR treatment alone. Furthermore, this effect was reversed by P-GP inhibition using ZSQ. The reduction in DNR accumulation of c20% in the PMA treated KG-1 cells was modest compared to the effect sizes described in the literature. For example, in a breast cancer cell line (KB-V1) TPA treatment promoted a 75% reduction in verapamil-induced vinblastine accumulation (Chambers, *et al.*, 1992). However, these data support the ability of PKC activation to promote P-GP activation and drug efflux in AML cells. When applied to the PKCε overexpression cell lines, PMA did not significantly reduce DNR accumulation. This finding was supported by PKC inhibition assays, where CC, treatment did not significantly affect DNR accumulation. Although the level of PKCε inhibition was not specifically determined, the ability of CC to inhibit PKC activity had been validated through the Diogenes™ assay. Together, these data suggest that PKCε-mediated DNR resistance is not a result of increased P-GP activity. Therefore, other post-translational mechanisms of regulation including increased stability or altered subcellular localisation of P-GP may contribute to PKCε-mediated DNR resistance.

The U937 and HEL PKCε overexpression cell lines, showed increased P-GP protein expression, compared to the controls, by flow cytometry and western blot analysis. The level of P-GP protein detected through western blot analysis represents P-GP expression within the cells as a whole, while flow cytometric analysis indicates expression at the cell surface. While the western blot analysis was difficult to quantitate, there was some indication that P-GP expression was upregulated in both analyses, and therefore it is more likely that PKCε is promoting P-GP stability opposed to altering the subcellular localisation of this efflux pump. The half-life of P-GP protein is in the order of hours to days (Muller, *et al.*, 1995, Pétriz, *et al.*, 2004, Xie, *et al.*, 2010). An inducible *EGFP-MDR1* vector in a drug resistant breast cancer cell line showed that P-GP had a half-life of 2.2 days, and that stability increased to 3.7 days for P-GP protein expressed at the cell surface (Pétriz, *et al.*, 2004), while in vincristine resistant HL-60 cells (HL-60/VCR) a half-life of 9 hours was observed (Xie, *et al.*, 2010). P-GP stability has in part been linked to glycosylation, as inhibiting glycosylation reduces membrane associated protein (Kramer, *et al.*, 1995), and increases P-GP degradation (Zhang, *et al.*, 2004).

Changes in P-GP stability and glycosylation is unlikely to be a direct consequence of PKCε overexpression as a previous study has shown that activation of PKC by TPA or mutagenesis of P-GP phosphorylation sites (including the PKC residues) did not affect P-GP ubiquitination (Zhang, *et al.*, 2004). However, the impact of serine/threonine kinases on P-GP stability appears to be context dependent. For example, Pro-viral integration site for Moloney murine leukaemia virus 1 (PIM-1) is a serine/threonine kinase which can phosphorylate P-GP at the Ser683 residue (Xie, *et al.*, 2010). In the above study, mutating the phosphorylation sites in P-GP, including Ser683, did not affect P-GP expression and degradation (Zhang, *et al.*, 2004), however, in HL-60/VCR cells which overexpress P-GP compared to vincristine sensitive HL-60 cells, PIM-1 knockdown reduced the half-life of P-GP from 9 hours to 5 hours, and caused an increased level of P-GP ubiquitination (Xie, *et al.*, 2010).

A study in Mv4;11 cells has shown that phosphorylation of the PIM-1L isoform by PKCα promotes PIM-1 stability and activity (Takami, *et al.*, 2018). Thus PKC-PIM1 interactions could represent an indirect mechanism for PKCε to promote P-GP stability. The possibility that PKCε overexpression is increasing P-GP stability would also explain why no differences in DNR accumulation were observed in the PKC inhibition and activation studies. These assays were conducted at a short (2 hour) time-point and therefore would not allow effects of altered P-GP stability to be observed and these assays could not be extended to a

longer time point as prolonged exposure to PMA treatment results in PKC downregulation and the induction of apoptosis (Henrich and Simpson, 1988).

One issue that this study raises is while the U937 and HEL cell lines showed concordant phenotypes, no phenotype was observed in the NOMO-1 or TF-1 lines, despite showing similar degrees of PKCε overexpression. The analysis conducted in this chapter suggests that differences in P-GP expression and activity between these lines is unlikely to contribute to this discrepancy. Furthermore, there is some data to suggest that different levels of PKC activity do not contribute to this, as PMA treatment did not reduce DNR accumulation in the NOMO-1 or TF-1 PKCε overexpression lines. However, given the limitations of these assays, described above, this hypothesis cannot be ruled out completely. Alternatively, different levels of intrinsic P-GP stability or rates of protein turnover could contribute to the discrepancies between the PKCε overexpression cell lines. This premise is potentially supported by the flow cytometric analysis conducted in this study. Although all four cell lines showed endogenous P-GP expression by western blot analysis, the flow cytometry data showed that U937 and HEL cells endogenously have little to no surface expression, whereas P-GP surface staining was observed in NOMO-1 and TF-1 cells. As P-GP expressed at the cell surface is thought to have a longer half-life, the intrinsic stability of P-GP in NOMO-1 and TF-1 cells may explain the different phenotypic consequences of PKCε overexpression.

Identifying a functional association between PKCε and P-GP-mediated chemoresistance, in a context other than the PKCε overexpression cell lines, was limited by the number of lines which endogenously expressed PKCε and P-GP. In the cell lines with endogenous PKCε expression that were used in the knockdown and knockout studies (U937, Mv4;11 and OCI1ML5), *P-GP* mRNA expression was low (Figure 5.25), however, P-GP protein expression was detected to some extent by western blot analysis. Reducing PKCε expression using genetic shRNA and CRISPR/Cas9 systems did not affect the DNR sensitivity of the cell lines (U937, Mv4;11 and OCIAML5) and patient samples (AML165 and AML172) investigated. Compared to the pharmacological inhibition studies, these genetic systems better reflect the longer-term consequences of reduced PKCε expression. However, there was no evidence of intrinsic P-GP activity in any of these lines which would be required for PKCε knockdown to alter DNR sensitivity. Therefore, modulating PKCε expression in AML cells with intrinsic P-GP activity would be required to substantiate the findings of the overexpression analysis, and to determine the therapeutic potential of this relationship.

In conclusion, the data presented in this chapter demonstrate that PKCε-mediated DNR resistance in AML cell lines can be fully explained by P-GP mediated drug efflux. Together, the evidence suggests that PKCε induces P-GP upregulation through post-translational mechanisms, as opposed to promoting P-GP activity, and suggest that the poor outcomes of patients with high expression of this kinase could, in part, be caused by the propensity of PKCε to promote P-GP mediated chemoresistance.

Chapter 6: Conclusions and Future Directions

6.1 Background

AML is a heterogeneous group of haematological malignancies that are characterised by the infiltration of the BM, PB, and organs, by clonal, abnormally differentiated myeloid cells (Döhner, *et al.*, 2015). Conventionally, AML is treated with intensive chemotherapy regimens, comprising of Ara-C and DNR infusions, and achieves CR in c70% of younger patients (<60 years; Ferrara and Schiffer, 2013). Despite this, such intensive treatment strategies are often poorly tolerated by older individuals who represent the majority of AML patients. As a result, prognosis remains poor. Outcomes can be improved through the application of targeted therapies. For example, ATRA and ATO have improved CR rates and long-term survival to >90% for patients with APL (Sanz, *et al.*, 2019), while the targeted BCL-2 inhibitor Venetoclax has shown promising improvements in patient outcome across AML subtypes (DiNardo, *et al.*, 2019). As a result, continued research into the molecular pathogenesis of AML with a view of identifying novel therapeutic targets is an important area of AML research.

PKCε is a member of the PKC family of serine/threonine kinases that is expressed in most mammalian tissues and is a central regulator of cell signalling. This signalling protein has been implicated in mediating cell survival, proliferation, differentiation adhesion and migration, while aberrant PKCε expression has been described in several pathologies, including cancer (1.6). Uniquely, PKCε is the only isoform within its family to have demonstrated transforming oncogenic properties Cacace, *et al.*, 1996, Mischak, *et al.*, 1993. In solid cancers, PKCε is frequently upregulated and is associated with aggressive disease phenotypes (Table 1.5). In terms of how PKCε may contribute to these findings, *in vitro* and *in vivo* models have implicated PKCε in modulating survival signalling which can lead to chemoresistance (Ding, *et al.*, 2002, McJilton, *et al.*, 2003, and promoting metastasis and invasion Caino, *et al.*, 2012, Gutierrez-Uzquiza, *et al.*, 2015, Hafeez, *et al.*, 2011, Jain and Basu, 2014b). Thus, highlighting PKCε as a potentially attractive therapeutic target in these contexts. However, compared to solid cancers, the role of PKCε in haematological malignancies including AML is poorly understood.

6.2 Conclusions

6.2.1 PKCε is frequently overexpressed in AML and is associated with poor patient outcomes

The initial aim of this study was to determine the frequency of PKCε overexpression in AML and characterise the pathophysiological attributes associated with PKCε upregulation in this malignancy. This was achieved through analysis of existing protein and mRNA datasets from AML patient samples, as outlined in Chapter 3. This highlighted, for the first time, that PKCε is frequently upregulated in AML patient samples and that high PKCε expression is associated with poor clinical outcomes in this malignancy (3.3.1.1). At a mRNA level, high *PKCε* expression in AML blasts was associated with poor OS and DFS. However, a trend of co-occurrence with poor prognostic cytogenetic and molecular abnormalities was observed (Figure 3.9). Therefore, it cannot be ruled out that the poor outcome of these patients is, in part, driven by the presence of known adverse risk aberrations. At a protein level, no difference in OS between patients with high and low PKCε protein expression was observed, although, it is important to note that the association with poor risk abnormalities was not observed in this dataset. Here, risk-adjusted analysis suggested that PKCε overexpression was an independent indicator of reduced CR induction (3.3.1.1).

The discrepancies between the mRNA and protein analysis could in part, be due to the strength of correlation between these factors, which can be variable. Although a significant correlation between PKCε mRNA and protein expression in AML patient samples was observed (r_p=0.6), means that c40% of protein expression cannot be accounted for from the level of mRNA. This suggests that protein levels are mostly regulated at a post-transcriptional level. Ultimately, a larger cohort of patients would be required to determine the statistical significance of the association between PKCε and adverse risk aberrations and whether PKCε is an independent predictor of poor patient outcomes in AML. However, across the mRNA and protein datasets analysed there is some consistent evidence that high PKCε expression in AML cells is associated with poor outcome, specifically in terms of treatment response. This is not only in-line with solid cancer studies (Pan, *et al.*, 2005) but also a study which used a risk prediction model with multiple AML molecular datasets (RNAseq, methylation, GEP and SNP) which highlighted PKCε as a potential poor risk marker in this malignancy (Hieke, *et al.*, 2016).

6.2.2 PKCε does not contribute to the pathogenesis of AML by disrupting myeloid cell development

Having characterised the expression of PKCε in AML patient samples, the mechanisms through which PKCε could contribute to the pathogenesis of this malignancy were investigated. Given the known roles of other PKC isoforms in haematopoiesis (1.6.6) and PKCε in solid cancers (1.6.5), experiments were conducted to determine whether PKCε acts as an oncogene in haematopoietic cells by disrupting myeloid growth and development.

Analysis of PKCε mRNA and protein in haematopoietic progenitor cells showed endogenous expression in normal haematopoietic cells and highlighted an expression profile which is indicative of a role in myeloid cell differentiation (3.3.2). Functional analysis in human HSPC showed that PKCε overexpression promotes monocyte differentiation, as demonstrated by the increased expression of the differentiation markers CD11b and CD14 on monocyte progenitors (Figure 3.23). This differentiation phenotype is concordant with the literature regarding PKC activity and other PKC isoforms in myeloid cell differentiation (Hass, *et al.*, 1997, Lin, *et al.*, 2007, Rossi, *et al.*, 1996, Whetton, *et al.*, 1994). This phenotype is, however, inconsistent with a role for PKCε in leukaemogenesis as arrested myeloid development is a defining characteristic of AML.

To determine the requirement of PKCε in monocyte differentiation, knockdown studies were conducted. Although a trend towards reduced expression CD11b and CD14 was observed, significance was not achieved. This suggests that although PKCε promotes monocyte differentiation, this isoform does not play an essential role in this process. The small effect size observed following PKCε knockdown in HSPC could be a result of redundancy in terms of other PKC isoforms. Of particular interest are the other nPKC isoforms (PKCδ, PKCθ and PKCη). From these, PKCη is the most closely related PKC isoform to PKCε (Littler, *et al.*, 2006), although there are differences in the lipid binding capacity of these two nPKC isoforms (Kazanietz, *et al.*, 1993). *PKCη* is highly expressed in immature human and murine haematopoietic progenitors (HSC, MPP, GMP) at an mRNA level; a finding which has also been validated in murine cells at a protein level (Porter and Magee, 2017). A competitive transplantation assay in irradiated mice showed that deletion of *PKCη* impaired HSC function (Porter and Magee, 2017), implicating a role for PKCη in regulating HSC biology. Although this paper did not address the impact of modulating PKCη expression on haematopoietic cell

differentiation, analysis of microarray datasets highlighted a pattern of expression which is not inconsistent with a role for *PKCη* in myeloid cell differentiation. Furthermore, this pattern of expression was similar to that of *PKCε* (Figure 3.13), suggesting that these isoforms may be co-ordinately expressed in haematopoietic cells and raises the possibility of redundancy in function between these two nPKC isoforms.

6.2.3 PKCε overexpression confers selective DNR resistance in AML through P-GP-mediated drug efflux

As the HSPC analysis indicated that PKCε is unlikely to contribute to the pathogenesis of AML through disrupting myeloid differentiation, alternative mechanisms of contribution were assessed. The propensity of PKCε to confer chemoresistance has been described in models of solid cancers (1.6.5). The clinical data from the AML patient samples was indicative of a chemoresistant phenotype as elevated PKCε expression was associated with reduced responses to first-line therapy and reduced DFS, an indicator of increased risk of relapse. Therefore, Chapter 4 aimed to address whether PKCε overexpression could confer chemoresistance. By assessing the chemosensitivity of AML cell lines to Ara-C and DNR, PKCε was found to confer selective DNR resistance (4.3.2.2). As Ara-C sensitivities were unaffected, it was initially proposed that the mechanism of PKCε-mediated chemoresistance was related to the mode of action of DNR.

DNR primarily acts through the inhibition of topoisomerase II; however, this anthracycline can also promote oxidative stress through the generation of H_2O_2 and superoxide radicals (Doroshow, 2019, Pommier, *et al.*, 2010). PKC isoforms may be able to promote DNR resistance through direct interactions with topoisomerase II which was identified as a downstream target of the aPKC isoform PKCζ in U937 cells (Plo, *et al.*, 2002). Furthermore, in lysates of *Drosophila melanogaster* Kc tissue cells, PKC-mediated phosphorylation promoted ATP hydrolysis and catalytic activity of topoisomerase II (Corbett, *et al.*, 1993). Such modifications can reduce the ability of topoisomerase inhibitors to stabilise topoisomerase-DNA complexes and induce apoptosis (DeVore, *et al.*, 1992). However, topoisomerase II hypo-phosphorylation has also been attributed to chemoresistant phenotypes (Ganapathi, *et al.*, 1996). Therefore, this mechanism of resistance was not investigated in this study. Instead, the ability of PKCε overexpression to confer resistance to oxidative stress was assessed. The cytoprotective capacity of PKCε has been described in cardiac cells Kabir, *et*

al., 2006, while a relatively recent study implicated a role for PKCε in maintaining mitochondrial ROS homeostasis in AML cells, and suggested that PKCε overexpression can confer a survival advantage in response to mitochondrial ROS-generating agents (Di Marcantonio, *et al.*, 2018). However, in the cell lines used in the present study no conclusive evidence was found to support this premise (3.3.1).

Further work showed that chemoresistance in the PKCε overexpression cell lines was accompanied by a reduction in DNR accumulation (3.3.2.1). As DNR enters the cell by passive diffusion, uptake is unlikely to be affected by factors such as reduced cell growth (which was observed in both DNR resistant cell lines). Furthermore, as the quenching of fluorescence upon DNA intercalation at low doses (<5μg/mL) has shown a linear relationship (Smeets, *et al.*, 1999), this was unlikely to contribute to the discrepancies in DNR accumulation observed. However, DNR is a substrate for several efflux pumps, such as P-GP and MRP1 (de Jonge-Peeters, *et al.*, 2007). P-GP is one of the best characterised efflux pumps for which anthracyclines are a substrate and has been shown to reduce DNR accumulation *in vitro* (Nooter, *et al.*, 1990). Clinically, the upregulation of efflux pumps, such as P-GP, is a central mediator of multidrug resistance and is associated with poor CR induction in AML (van der Kolk, *et al.*, 2000). Furthermore, this mechanism would explain why PKCε overexpression did not promote resistance to Ara-C, as this nucleoside analogue is not transported by P-GP (Norgaard, *et al.*, 1998). Functional inhibition of P-GP with the specific inhibitor ZSQ, restored DNR accumulation and ablated DNR resistance in the PKCε overexpression cell lines (U937 and HEL; 3.3.2.3). Together, these data demonstrated that drug efflux by P-GP fully accounts for PKCε-mediated DNR resistance in this context.

Considering the chemoresistant phenotype observed in the PKCε overexpression cell lines, the effect of high *PKCε* expression on patient outcome (OS and DFS) was re-analysed using the TCGA 2013 dataset, excluding patients who received induction therapy that did not contain DNR. Removing these non 7+3 induction regimes modestly solidified the significance of the reduced OS and DFS in the high *PKCε* expression cohort (Figure 6.1A). Given the small size of these cohorts even before the exclusion of additional samples, this analysis was extended by classifying high and low *PKCε* expression as above and below the median, respectively. Despite the smaller separation between the cohorts in terms of *PKCε* expression using this stratification system, excluding non 7+3 induction regimes resulted in significantly worse DFS for patients with high PKCε expression; a finding which was not achieved using the original analysis that included all treated, non-APL patients (Figure 6.1B).

A

	OS					DFS			
PKCε Expression	Cases	Deceased	Median OS (months)	p-value		Cases	Recurred/ Progressed	Median DFS (months)	p-value
LQ	37	22	30.6	**0.0271**		37	16	20.8	**0.0299**
UQ	38	29	11.2			38	21	11.6	
LQ (LDAC+Dec excluded)	30	15	32.3	**0.0229**		30	14	20.8	**0.0225**
UQ (LDAC+Dec excluded)	31	23	17.40			31	21	11.6	

B

	OS					DFS			
PKCε Expression	Cases	Deceased	Median OS (months)	p-value		Cases	Recurred/ Progressed	Median DFS (months)	p-value
Below median	75	45	30.6	**		75	38	16.6	NS
Above median	76	58	11.5	**0.003**		75	41	13.4	0.070
Below median (LDAC+Dec excluded)	61	33	52.7	*		61	32	18.2	*
Above median (LDAC+Dec excluded)	62	44	17.1	**0.0174**		61	38	11.6	**0.0455**

Figure 6.1: Exclusion of non-DNR induction therapies consolidates the poor outcomes associated with high *PKCε* expression

Tables comparing the OS and DFS of patients within the TCGA 2013 dataset (Ley, *et al.*, 2013) with high and low *PKCε* mRNA expression which were defined as **(A)** upper quartile (UQ) and lower quartile (LQ) or **(B)** above and below median. Tables show the outcome of patients using the analysis strategy described in 2.11.2 where untreated and APL treated patients were excluded (top two rows of each table) and the re-analysis of this dataset where patients who did not receive DNR containing induction therapies such as LDAC or decitabine were excluded. Statistical significance was determined using Log Rank tests; NS-not significant, *p<0.05, **p<0.01.

The mechanism of PKCε-mediated chemoresistance may also explain some of the findings from the original AML14 and AML15 analysis. As described previously, fewer patients with high PKCε protein expression achieved CR following first-line therapy, but no differences in OS were observed. The different observations in terms of OS and treatment response could be because CR refers to the response to induction chemotherapy whereas OS will depend on the response to subsequent rounds of chemotherapy, including salvage therapy which incorporate agents that the patient was not exposed to during induction therapy. The most common salvage therapy is FLAG-Ida (Fludarabine+Ara-C+G-CSF+Idarubicin). As this does not utilise DNR, the capacity of PKCε to confer DNR resistance would not affect a patient's response to this strategy. Although idarubicin is an anthracycline like DNR, there is evidence in AML cell lines and patient samples that idarubicin is at least in part resistant to P-GP efflux. In an accumulation assay using vincristine resistant HL-60 cells, 36% of the DNR concentration remained compared with 51% of Idarubicin (Berman and McBride, 1992). Furthermore, in patients from the AML15 clinical trial CR in patients with P-GP$^+$ blasts treated with FLAG-Ida was 86% compared to 78% for P-GP$^+$ AML treated with DNR containing induction regimes (Pallis, *et al.*, 2011). The different responses of P-GP$^+$ AML blasts to FLAG-Ida and DNR regimens in this trial could be pertinent to the original PKCε protein analysis, as most of the samples were from patients enrolled in the AML15 clinical trial (60/70; 86%). In this trial, patients were randomly divided into two induction therapy arms: DNR+Ara-C or FLAG-Ida (Burnett, *et al.*, 2013). Therefore, in a similar manner to the TCGA dataset, it would be interesting to see if the impact of PKCε overexpression on CR is greatest within patients that received DNR at induction. However, the induction treatment data was unavailable at the time of writing.

In terms of the mechanism through which PKCε promotes P-GP-mediated chemoresistance, no correlation between *PKCε* and *P-GP* mRNA expression was observed in AML cell lines or patient samples. This suggests that PKCε is not promoting P-GP expression through transcriptional mechanisms of regulation in this context. However, post-translational mechanisms of regulation were supported by the cell line and patient analysis. Through modulating PKC activity using the cPKC and nPKC agonist, PMA, and inhibitor, CC, there was no evidence to suggest that PKCε overexpression contributes to DNR resistance through promoting P-GP activity, with the caveat that these assays could only be conducted with short end points due to the toxicity of these agents. PKCε may instead be affecting the stability of

P-GP, which could not be assessed within the time frame of these assays, however, approaches which could be employed to establish this are outlined below.

Clinically, the efficacy of P-GP inhibitors has been limited (Baer, *et al.*, 2002, Cripe, *et al.*, 2010, Kolitz, *et al.*, 2010). It has been proposed that this could be due to the contribution of efflux-independent mechanisms of resistance and the activation of multiple efflux pumps. Although in the cell line models used in this study, P-GP efflux fully accounted for PKCε-mediated DNR resistance, PKC isoforms may also promote the expression or activity of other efflux pumps. From the TCGA dataset analysis *PKCε, PKCθ* and *PKCη* significantly correlated with *BRP1*, while *PKCθ* and *PKCη* also showed significant correlations with *MRP1* (Table 4.1); an efflux pump which has been associated with DNR resistance in AML cells (Legrand, *et al.*, 1999a, Legrand, *et al.*, 1999b). These findings are supported by similar observations in breast and ovarian cancer (Beck, *et al.*, 1998, Beck, *et al.*, 1996). Interestingly, treatment strategies for AML now incorporate the potent PKC inhibitor, Midostaurin. This inhibitor is only approved for the treatment of FLT3 mutated disease; however, it has a higher potency of inhibition to PKC (Levis, 2017) so the efficacy of Midostaurin may be down to its multi-targeted nature. In support of this, Midostaurin also shows efficacy against nonmutant *FLT3* AML (Fischer, *et al.*, 2010) and more specific FLT-3 inhibitors such as Sorafenib have not improved clinical efficacy (Majothi, *et al.*, 2020). Thus, if functional associations between PKC isoforms and other efflux pumps can be established, then PKC inhibition using Midostaurin or more specific PKC inhibitors (1.7) could potentially be effective in improving drug responsiveness in AML patients more broadly.

In contrast to the overexpression analysis, reducing PKCε expression using knockdown or knockout systems did not affect the intrinsic survival of AML cell lines or their sensitivities to chemotherapeutic agents. A major limitation of this study was the lack of cell lines which endogenously expressed PKCε. Particularly pertinent to these studies is the fact that none of the cell lines with endogenous PKC expression displayed functional (inhibitable) P-GP activity, which would be required to establish a functional link between these factors in a context other than the PKCε overexpression cell lines.

Studies have shown that pan PKC inhibitors can induce apoptosis in AML cells (Ruvolo, *et al.*, 2011, Zabkiewicz, *et al.*, 2014), supporting potential redundancy in function between PKC isoforms in AML cells and suggests that targeting multiple PKC isoforms or reducing overall PKC activity could have therapeutic potential in this malignancy. To try and

address the issue of redundancy, PKCθ knockdown studies were conducted as co-expression of PKCε and PKCθ was observed in the cell line models (Figure 4.26). However, reducing PKCθ in concert with reduced PKCε expression did not affect cell survival or chemosensitivity (4.3.4.1). Although this was not supportive of redundancy between these two isoforms, this does not rule out redundancy in function with respect to other PKC isoforms.

As described above, PKCη is the most closely related PKC isoform to PKCε and shows a similar expression profile in haematopoietic progenitor cells. In AML, a study which analysed the TCGA 2013 dataset showed that high *PKCη* expression (above median) was associated with significantly worse OS than patients with below-median expression(Porter and Magee, 2017). While there was co-occurrence with high-risk molecular aberrations, when survival analysis was restricted to patients with intermediate-risk cytogenetics, above median *PKCη* expression was still associated with poor outcomes (Porter and Magee, 2017). This profile of expression in AML patient samples is analogous to the observations made with high *PKCε* expression (upper quartile) in this study using the same dataset (3.3.1.3). My analysis of the TCGA data set using cBioPortal showed that out of the PKC isoforms *PKCε* expression correlated most strongly with *PKCη* expression in AML patient samples (Spearman's Correlation Coefficient: 0.2; p=0.012; Pearson's Correlation Coefficient; 0.15; p=0.05), suggesting that these two isoforms are co-expressed in AML blasts. Furthermore, a significant correlation between *P-GP* and *PKCη* was observed (Table 4.1) suggesting a potential association between *PKCη* and chemoresistant phenotypes in AML. Although functional substantiation is required, these findings are indicative of potential redundancy between these nPKC isoforms. Alternatively, given the correlated expression of these isoforms in haematopoietic and AML cells, it could be that the phenotypes associated with PKCε overexpression are a result of increased PKCη expression or activity. This was not investigated in the present study because, at least at an mRNA level, *PKCη* expression in AML cell lines was low (Figure 4.25). Nevertheless, determining whether modulating PKCε affects PKCη expression and whether overexpression of PKCη confers homologous phenotypes to PKCε would be of interest.

In conclusion, this study has shown that PKCε upregulation occurs frequently in AML and is a poor prognostic indicator in this malignancy. While functional studies did not support an oncogenic role for PKCε in normal haematopoietic cells or AML cell lines, my data suggests that PKCε could causally contribute to poor outcomes in this malignancy by decreasing the chemosensitivity of AML cells through promoting P-GP expression and drug efflux.

6.3 Future Directions

This thesis has provided a potential mechanism through which PKCε upregulation could contribute to poor outcomes in AML. Due to the limitations outlined previously, functional studies characterising the relationship between PKCε and P-GP drug efflux was restricted. Therefore, assessing the impact of modulating PKCε expression in AML patient samples with intrinsically active P-GP is required to consolidate the relationship between these two factors in a more clinically relevant model, and determine the therapeutic potential of this mechanism of chemoresistance. Furthermore, additional studies are needed to establish the mechanism through which PKCε promotes P-GP upregulation.

The data presented in this thesis suggest that PKCε overexpression promotes P-GP upregulation through post-translational mechanisms, without directly promoting P-GP activity. To further elucidate the mechanism of regulation, the impact of PKCε overexpression on P-GP stability and degradation could be assessed through pulse-chase assays (Simon and Kornitzer, 2014), while P-GP localisation could be determined by immunocytochemistry or confocal analysis. There is also the potential that PKCε could be acting through indirect mechanisms, therefore, evaluating the effect of PKCε overexpression on other kinases could be of interest. Conducting a PKCε interactome analysis could be used to direct this. Alternatively, given the evidence outlined in 6.2, redundancy between PKCε and PKCη could be evaluated through the application of PKCη-targeted shRNA constructs in primary AML cells. Lastly, it would be interesting to assess the effect of PKCε overexpression on idarubicin accumulation to see whether the chemosensitivity to this drug is also impaired by PKCε, and more broadly whether PKC isoforms can modulate the expression and activity of other efflux pumps, contributing to poor-treatment responses.

The data presented in this thesis suggest that PKCε overexpression promotes P-GP upregulation through post-translational mechanisms, without directly promoting P-GP activity. To further elucidate the mechanism of regulation, the impact of PKCε overexpression on P-GP

stability and degradation could be assessed through pulse-chase assays Simon and Kornitzer, 2014, while P-GP localisation could be determined by immunocytochemistry or confocal analysis. There is also the potential that PKCε could be acting through indirect mechanisms, therefore, evaluating the effect of PKCε overexpression on other kinases could be of interest. Conducting PKCε interactome analysis could be used to direct this. Alternatively, given the evidence outlined in **6.2** redundancy between PKCε and PKCη could be evaluated through the application of PKCη-targeted inhibitors or shRNA constructs in AML cells. Lastly, it would be interesting to assess the effect of PKCε overexpression on idarubicin accumulation and chemosensitivity, given the higher efficacy of idarubicin in P-GP expressing cells, as well as whether PKC isoforms are able to modulate the expression and activity of other efflux pumps, contributing to poor-treatment responses more broadly.

References

Abelson, S., Collord, G., Ng, S. W. K., Weissbrod, O., Mendelson Cohen, N., Niemeyer, E., *et al.* (2018) Prediction of acute myeloid leukaemia risk in healthy individuals. *Nature* **559** (7714) p.400-404. 10.1038/s41586-018-0317-6.

Aftab, D. T., Yang, J. M. and Hait, W. N. (1994) Functional role of phosphorylation of the multidrug transporter (P-glycoprotein) by protein kinase C in multidrug-resistant MCF-7 cells. *Oncol Res* **6** (2) p.59-70.

Aihara, H., Asaoka, Y., Yoshida, K. and Nishizuka, Y. (1991) Sustained activation of protein kinase C is essential to HL-60 cell differentiation to macrophage. *Proceedings of the National Academy of Sciences* **88** (24) p.11062-11066. 10.1073/pnas.88.24.11062.

Akashi, K., Traver, D., Miyamoto, T. and Weissman, I. L. (2000) A clonogenic common myeloid progenitor that gives rise to all myeloid lineages. *Nature* **404** (6774) p.193-7. 10.1038/35004599.

Akita, Y. (2002) Protein kinase C-epsilon (PKC-epsilon): its unique structure and function. *J Biochem* **132** (6) p.847-52.

Alessi, D. R., James, S. R., Downes, C. P., Holmes, A. B., Gaffney, P. R., Reese, C. B., *et al.* (1997) Characterization of a 3-phosphoinositide-dependent protein kinase which phosphorylates and activates protein kinase Balpha. *Curr Biol* **7** (4) p.261-9. 10.1016/s0960-9822(06)00122-9.

Alexandrov, L. B., Nik-Zainal, S., Wedge, D. C., Aparicio, S. A. J. R., Behjati, S., Biankin, A. V., *et al.* (2013) Signatures of mutational processes in human cancer. *Nature* **500** (7463) p.415-421. 10.1038/nature12477.

Antman, K. S., Griffin, J. D., Elias, A., Socinski, M. A., Ryan, L., Cannistra, S. A., *et al.* (1988) Effect of Recombinant Human Granulocyte-Macrophage Colony-Stimulating Factor on Chemotherapy-Induced Myelosuppression. *New England Journal of Medicine* **319** (10) p.593-598. 10.1056/NEJM198809083191001.

Arai, F., Hirao, A., Ohmura, M., Sato, H., Matsuoka, S., Takubo, K., *et al.* (2004) Tie2/angiopoietin-1 signaling regulates hematopoietic stem cell quiescence in the bone marrow niche. *Cell* **118** (2) p.149-61. 10.1016/j.cell.2004.07.004.

Arber, D. A., Orazi, A., Hasserjian, R., Thiele, J., Borowitz, M. J., Le Beau, M. M., *et al.* (2016) The 2016 revision to the World Health Organization classification of myeloid neoplasms and acute leukemia. *Blood* **127** (20) p.2391-405. 10.1182/blood-2016-03-643544.

Aslam, N. and Alvi, F. (2019) A systems biology-based molecular model of the protein kinase C life cycle. *bioRxiv* p.652628. 10.1101/652628.

Aziz, M. H., Manoharan, H. T., Church, D. R., Dreckschmidt, N. E., Zhong, W., Oberley, T. D., *et al.* (2007) Protein kinase Cepsilon interacts with signal transducers and activators of transcription 3 (Stat3), phosphorylates Stat3Ser727, and regulates its constitutive activation in prostate cancer. *Cancer Res* **67** (18) p.8828-38. 10.1158/0008-5472.Can-07-1604.

Bae, K. M., Wang, H., Jiang, G., Chen, M. G., Lu, L. and Xiao, L. (2007) Protein kinase C epsilon is overexpressed in primary human non-small cell lung cancers and functionally required for proliferation of non-small cell lung cancer cells in a p21/Cip1-dependent manner. *Cancer Res* **67** (13) p.6053-63. 10.1158/0008-5472.Can-06-4037.

Baer, M. R., George, S. L., Dodge, R. K., O'Loughlin, K. L., Minderman, H., Caligiuri, M. A., *et al.* (2002) Phase 3 study of the multidrug resistance modulator PSC-833 in previously untreated patients 60 years of age and older with acute myeloid leukemia: Cancer and Leukemia Group B Study 9720. *Blood* **100** (4) p.1224-32.

Bagger, F. O., Sasivarevic, D., Sohi, S. H., Laursen, L. G., Pundhir, S., Sonderby, C. K., *et al.* (2016) BloodSpot: a database of gene expression profiles and transcriptional programs for healthy and malignant haematopoiesis. *Nucleic Acids Res* **44** (D1) p.D917-24. 10.1093/nar/gkv1101.

Bain, B. J. and Béné, M. C. (2019) Morphological and Immunophenotypic Clues to the WHO Categories of Acute Myeloid Leukaemia. *Acta Haematol* **141** (4) p.232-244. 10.1159/000496097.

Baines Christopher, P., Zhang, J., Wang, G.-W., Zheng, Y.-T., Xiu Joanne, X., Cardwell Ernest, M., *et al.* (2002) Mitochondrial PKCε and MAPK Form Signaling Modules in the Murine Heart. *Circulation Research* **90** (4) p.390-397. 10.1161/01.RES.0000012702.90501.8D.

Barboule, N., Lafon, C., Chadebech, P., Vidal, S. and Valette, A. (1999) Involvement of p21 in the PKC-induced regulation of the G2/M cell cycle transition. *FEBS Letters* **444** (1) p.32-37. 10.1016/s0014-5793(99)00022-8.

Bark, H. and Choi, C.-H. (2010) PSC833, cyclosporine analogue, downregulates MDR1 expression by activating JNK/c-Jun/AP-1 and suppressing NF-κB. *Cancer Chemotherapy and Pharmacology* **65** (6) p.1131-1136. 10.1007/s00280-009-1121-7.

Barnett, M. E., Madgwick, D. K. and Takemoto, D. J. (2007) Protein kinase C as a stress sensor. *Cellular signalling* **19** (9) p.1820-1829. 10.1016/j.cellsig.2007.05.014.

Barretina, J., Caponigro, G., Stransky, N., Venkatesan, K., Margolin, A. A., Kim, S., *et al.* (2012) The Cancer Cell Line Encyclopedia enables predictive modelling of anticancer drug sensitivity. *Nature* **483** (7391) p.603-7. 10.1038/nature11003.

Basharat, M., Khan, S. A., Din, N. U. and Ahmed, D. (2019) Immunophenotypic characterisation of morphologically diagnosed cases of Acute Myeloid

Leukaemia (AML). *Pak J Med Sci* **35** (2) p.470-476. 10.12669/pjms.35.2.614.

Bassini, A., Zauli, G., Migliaccio, G., Migliaccio, A. R., Pascuccio, M., Pierpaoli, S., *et al.* (1999) Lineage-restricted expression of protein kinase C isoforms in hematopoiesis. *Blood* **93** (4) p.1178-1188.

Basu, A. and Weixel, K. M. (1995) Comparison of protein kinase C activity and isoform expression in cisplatin-sensitive and -resistant ovarian carcinoma cells. *International Journal of Cancer* **62** (4) p.457-460. 10.1002/ijc.2910620416.

Baum, C. M., Weissman, I. L., Tsukamoto, A. S., Buckle, A. M. and Peault, B. (1992) Isolation of a candidate human hematopoietic stem-cell population. *Proceedings of the National Academy of Sciences of the United States of America* **89** (7) p.2804-2808. 10.1073/pnas.89.7.2804.

Beck, J., Bohnet, B., Brügger, D., Bader, P., Dietl, J., Scheper, R. J., *et al.* (1998) Multiple gene expression analysis reveals distinct differences between G2 and G3 stage breast cancers, and correlations of PKC eta with MDR1, MRP and LRP gene expression. *Br J Cancer* **77** (1) p.87-91. 10.1038/bjc.1998.13.

Beck, J., Handgretinger, R., Klingebiel, T., Dopfer, R., Schaich, M., Ehninger, G., *et al.* (1996) Expression of PKC isozyme and MDR-associated genes in primary and relapsed state AML. *Leukemia* **10** (3) p.426-33.

Beckmann, R., Lindschau, C., Haller, H., Hucho, F. and Buchner, K. (1994) Differential nuclear localization of protein kinase C isoforms in neuroblastoma x glioma hybrid cells. *Eur J Biochem* **222** (2) p.335-43. 10.1111/j.1432-1033.1994.tb18872.x.

Ben-David, U., Siranosian, B., Ha, G., Tang, H., Oren, Y., Hinohara, K., *et al.* (2018) Genetic and transcriptional evolution alters cancer cell line drug response. *Nature* **560** (7718) p.325-330. 10.1038/s41586-018-0409-3.

Benavides, F., Blando, J., Perez, C. J., Garg, R., Conti, C. J., DiGiovanni, J., *et al.* (2011) Transgenic overexpression of PKCε in the mouse prostate induces preneoplastic lesions. *Cell Cycle* **10** (2) p.268-77. 10.4161/cc.10.2.14469.

Bennett, J. M., Catovsky, D., Daniel, M. T., Flandrin, G., Galton, D. A., Gralnick, H. R., *et al.* (1976) Proposals for the classification of the acute leukaemias. French-American-British (FAB) co-operative group. *Br J Haematol* **33** (4) p.451-8. 10.1111/j.1365-2141.1976.tb03563.x.

Benveniste, P., Frelin, C., Janmohamed, S., Barbara, M., Herrington, R., Hyam, D., *et al.* (2010) Intermediate-term hematopoietic stem cells with extended but time-limited reconstitution potential. *Cell Stem Cell* **6** (1) p.48-58. 10.1016/j.stem.2009.11.014.

Berman, E. and McBride, M. (1992) Comparative cellular pharmacology of daunorubicin and idarubicin in human multidrug-resistant leukemia cells. *Blood* **79** (12) p.3267-73.

Bertolotto, C., Maulon, L., Filippa, N., Baier, G. and Auberger, P. (2000) Protein kinase C theta and epsilon promote T-cell survival by a rsk-dependent phosphorylation and inactivation of BAD. *J Biol Chem* **275** (47) p.37246-50. 10.1074/jbc.M007732200.

Besson, A., Davy, A., Robbins, S. M. and Yong, V. W. (2001) Differential activation of ERKs to focal adhesions by PKC epsilon is required for PMA-induced adhesion and migration of human glioma cells. *Oncogene* **20** (50) p.7398-407. 10.1038/sj.onc.1204899.

Bhatia, M., Wang, J. C. Y., Kapp, U., Bonnet, D. and Dick, J. E. (1997) Purification of primitive human hematopoietic cells capable of repopulating immune-deficient mice. *Proceedings of the National Academy of Sciences* **94** (10) p.5320-5325. 10.1073/pnas.94.10.5320.

Bhayat, F., Das-Gupta, E., Smith, C., McKeever, T. and Hubbard, R. (2009) The incidence of and mortality from leukaemias in the UK: a general population-based study. *BMC Cancer* **9** p.252. 10.1186/1471-2407-9-252.

Black, J. D. (2000) Protein kinase C-mediated regulation of the cell cycle. *Front Biosci* **5** p.D406-23. 10.2741/black.

Blay, P., Astudillo, A., Buesa, J. M., Campo, E., Abad, M., García-García, J., *et al.* (2004) Protein kinase C theta is highly expressed in gastrointestinal stromal tumors but not in other mesenchymal neoplasias. *Clin Cancer Res* **10** (12 Pt 1) p.4089-95. 10.1158/1078-0432.Ccr-04-0630.

Boddu, P., Kantarjian, H. M., Garcia-Manero, G., Ravandi, F., Verstovsek, S., Jabbour, E., *et al.* (2017) Treated secondary acute myeloid leukemia: a distinct high-risk subset of AML with adverse prognosis. *Blood advances* **1** (17) p.1312-1323. 10.1182/bloodadvances.2017008227.

Bonnet, D. and Dick, J. E. (1997) Human acute myeloid leukemia is organized as a hierarchy that originates from a primitive hematopoietic cell. *Nat Med* **3** (7) p.730-7. 10.1038/nm0797-730.

Bose, P., Vachhani, P. and Cortes, J. E. (2017) Treatment of Relapsed/Refractory Acute Myeloid Leukemia. *Curr Treat Options Oncol* **18** (3) p.17. 10.1007/s11864-017-0456-2.

Bourguignon, L. Y., Peyrollier, K., Xia, W. and Gilad, E. (2008) Hyaluronan-CD44 interaction activates stem cell marker Nanog, Stat-3-mediated MDR1 gene expression, and ankyrin-regulated multidrug efflux in breast and ovarian tumor cells. *J Biol Chem* **283** (25) p.17635-51. 10.1074/jbc.M800109200.

Bourguignon, L. Y. W., Spevak, C. C., Wong, G., Xia, W. and Gilad, E. (2009) Hyaluronan-CD44 interaction with protein kinase C(epsilon) promotes oncogenic signaling by the stem cell marker Nanog and the Production of microRNA-21, leading to down-regulation of the tumor suppressor protein PDCD4, anti-apoptosis, and chemotherapy resistance in breast tumor cells. *The Journal of biological chemistry* **284** (39) p.26533-26546. 10.1074/jbc.M109.027466.

Broad, D. (2020) DepMap 20Q1 Public. 10.6084/m9.figshare.11791698.v2

Brognard, J. and Newton, A. C. (2008) PHLiPPing the switch on Akt and protein kinase C signaling. *Trends Endocrinol Metab* **19** (6) p.223-30. 10.1016/j.tem.2008.04.001.

Bromberg, O., Frisch, B. J., Weber, J. M., Porter, R. L., Civitelli, R. and Calvi, L. M. (2012) Osteoblastic N-cadherin is not required for microenvironmental support and regulation of hematopoietic stem and progenitor cells. *Blood* **120** (2) p.303-13. 10.1182/blood-2011-09-377853.

Brownlow, N., Pike, T., Zicha, D., Collinson, L. and Parker, P. J. (2014) Mitotic catenation is monitored and resolved by a PKCε-regulated pathway. *Nature Communications* **5** (1) p.5685. 10.1038/ncomms6685.

Bruns, R. F., Miller, F. D., Merriman, R. L., Howbert, J. J., Heath, W. F., Kobayashi, E., *et al.* (1991) Inhibition of protein kinase C by calphostin C is light-dependent. *Biochem Biophys Res Commun* **176** (1) p.288-93. 10.1016/0006-291x(91)90922-t.

Burnett, A. K., Milligan, D., Goldstone, A., Prentice, A., McMullin, M.-F., Dennis, M., *et al.* (2009) The impact of dose escalation and resistance modulation in older patients with acute myeloid leukaemia and high risk myelodysplastic syndrome: the results of the LRF AML14 trial. *British Journal of Haematology* **145** (3) p.318-332. https://doi.org/10.1111/j.1365-2141.2009.07604.x.

Burnett, A. K., Russell, N. H., Hills, R. K., Hunter, A. E., Kjeldsen, L., Yin, J., *et al.* (2013) Optimization of chemotherapy for younger patients with acute myeloid leukemia: results of the medical research council AML15 trial. *J Clin Oncol* **31** (27) p.3360-8. 10.1200/jco.2012.47.4874.

Buscarlet, M., Provost, S., Zada, Y. F., Barhdadi, A., Bourgoin, V., Lépine, G., *et al.* (2017) DNMT3A and TET2 dominate clonal hematopoiesis and demonstrate benign phenotypes and different genetic predispositions. *Blood* **130** (6) p.753-762. 10.1182/blood-2017-04-777029.

Cabezas-Wallscheid, N., Klimmeck, D., Hansson, J., Lipka, Daniel B., Reyes, A., Wang, Q., *et al.* (2014) Identification of Regulatory Networks in HSCs and Their Immediate Progeny via Integrated Proteome, Transcriptome, and DNA Methylome Analysis. *Cell Stem Cell* **15** (4) p.507-522. https://doi.org/10.1016/j.stem.2014.07.005.

Cacace, A. M., Guadagno, S. N., Krauss, R. S., Fabbro, D. and Weinstein, I. B. (1993) The epsilon isoform of protein kinase C is an oncogene when overexpressed in rat fibroblasts. *Oncogene* **8** (8) p.2095-2104.

Cacace, A. M., Ueffing, M., Han, E. K., Marmè, D. and Weinstein, I. B. (1998) Overexpression of PKCepsilon in R6 fibroblasts causes increased production of active TGFbeta. *J Cell Physiol* **175** (3) p.314-22. 10.1002/(sici)1097-4652(199806)175:3<314::Aid-jcp9>3.0.Co;2-r.

Cacace, A. M., Ueffing, M., Philipp, A., Han, E. K., Kolch, W. and Weinstein, I. B. (1996) PKC epsilon functions as an oncogene by enhancing activation of the Raf kinase. *Oncogene* **13** (12) p.2517-26.

Caino, M. C., Lopez-Haber, C., Kissil, J. L. and Kazanietz, M. G. (2012) Non-small cell lung carcinoma cell motility, rac activation and metastatic dissemination are mediated by protein kinase C epsilon. *PLoS One* **7** (2) p.e31714. 10.1371/journal.pone.0031714.

Calvi, L. M., Adams, G. B., Weibrecht, K. W., Weber, J. M., Olson, D. P., Knight, M. C., *et al.* (2003) Osteoblastic cells regulate the haematopoietic stem cell niche. *Nature* **425** (6960) p.841-6. 10.1038/nature02040.

Campos, L., Rouault, J. P., Sabido, O., Oriol, P., Roubi, N., Vasselon, C., *et al.* (1993) High expression of bcl-2 protein in acute myeloid leukemia cells is associated with poor response to chemotherapy. *Blood* **81** (11) p.3091-6.

Casey, E. M., Harb, W., Bradford, D., Bufill, J., Nattam, S., Patel, J., *et al.* (2010) Randomized, Double-Blinded, Multicenter, Phase II Study of Pemetrexed, Carboplatin, and Bevacizumab with Enzastaurin or Placebo in Chemonaïve Patients with Stage IIIB/IV Non-small Cell Lung Cancer: Hoosier Oncology Group LUN06-116. *Journal of Thoracic Oncology* **5** (11) p.1815-1820. https://doi.org/10.1097/JTO.0b013e3181ee820c.

Castrillo, A., Pennington, D. J., Otto, F., Parker, P. J., Owen, M. J. and Bosca, L. (2001) Protein kinase Cepsilon is required for macrophage activation and defense against bacterial infection. *J Exp Med* **194** (9) p.1231-42.

Castro, A. F., Horton, J. K., Vanoye, C. G. and Altenberg, G. A. (1999) Mechanism of inhibition of P-glycoprotein-mediated drug transport by protein kinase C blockers. *Biochem Pharmacol* **58** (11) p.1723-33. 10.1016/s0006-2952(99)00288-9.

Cenni, V., Döppler, H., Sonnenburg, E. D., Maraldi, N., Newton, A. C. and Toker, A. (2002) Regulation of novel protein kinase C epsilon by phosphorylation. *The Biochemical journal* **363** (Pt 3) p.537-545. 10.1042/0264-6021:3630537.

Cerami, E., Gao, J., Dogrusoz, U., Gross, B. E., Sumer, S. O., Aksoy, B. A., *et al.* (2012) The cBio cancer genomics portal: an open platform for exploring multidimensional cancer genomics data. *Cancer Discov* **2** (5) p.401-4. 10.1158/2159-8290.CD-12-0095.

Certo, M., Del Gaizo Moore, V., Nishino, M., Wei, G., Korsmeyer, S., Armstrong, S. A., *et al.* (2006) Mitochondria primed by death signals determine cellular addiction to antiapoptotic BCL-2 family members. *Cancer Cell* **9** (5) p.351-65. 10.1016/j.ccr.2006.03.027.

Challen, G. A., Sun, D., Jeong, M., Luo, M., Jelinek, J., Berg, J. S., *et al.* (2012) Dnmt3a is essential for hematopoietic stem cell differentiation. *Nature Genetics* **44** (1) p.23-31. 10.1038/ng.1009.

Chambers, T. C., Pohl, J., Glass, D. B. and Kuo, J. F. (1994) Phosphorylation by protein kinase C and cyclic AMP-dependent protein kinase of synthetic

peptides derived from the linker region of human P-glycoprotein. *Biochemical Journal* **299** (1) p.309-315. 10.1042/bj2990309.

Chambers, T. C., Zheng, B. and Kuo, J. F. (1992) Regulation by phorbol ester and protein kinase C inhibitors, and by a protein phosphatase inhibitor (okadaic acid), of P-glycoprotein phosphorylation and relationship to drug accumulation in multidrug-resistant human KB cells. *Mol Pharmacol* **41** (6) p.1008-15.

Chang, Z. L. and Beezhold, D. H. (1993) Protein kinase C activation in human monocytes: regulation of PKC isoforms. *Immunology* **80** (3) p.360-366.

Chattopadhyay, R., Dyukova, E., Singh, N. K., Ohba, M., Mobley, J. A. and Rao, G. N. (2014) Vascular endothelial tight junctions and barrier function are disrupted by 15(S)-hydroxyeicosatetraenoic acid partly via protein kinase C ε-mediated zona occludens-1 phosphorylation at threonine 770/772. *J Biol Chem* **289** (6) p.3148-63. 10.1074/jbc.M113.528190.

Chaudhary, P. M. and Roninson, I. B. (1992) Activation of MDR1 (P-glycoprotein) gene expression in human cells by protein kinase C agonists. *Oncol Res* **4** (7) p.281-90.

Chen, Q., Bian, Y. and Zeng, S. (2014) Involvement of AP-1 and NF-κB in the up-regulation of P-gp in vinblastine resistant Caco-2 cells. *Drug Metab Pharmacokinet* **29** (2) p.223-6. 10.2133/dmpk.dmpk-13-sh-068.

Cheng, H., Zheng, Z. and Cheng, T. (2020) New paradigms on hematopoietic stem cell differentiation. *Protein & Cell* **11** (1) p.34-44. 10.1007/s13238-019-0633-0.

Conway O'Brien, E., Prideaux, S. and Chevassut, T. (2014) The epigenetic landscape of acute myeloid leukemia. *Adv Hematol* **2014** p.103175. 10.1155/2014/103175.

Corbett, A. H., Fernald, A. W. and Osheroff, N. (1993) Protein kinase C modulates the catalytic activity of topoisomerase II by enhancing the rate of ATP hydrolysis: evidence for a common mechanism of regulation by phosphorylation. *Biochemistry* **32** (8) p.2090-7. 10.1021/bi00059a029.

Corcoran, A. and Cotter, T. G. (2013) Redox regulation of protein kinases. *Febs j* **280** (9) p.1944-65. 10.1111/febs.12224.

Cornford, P., Evans, J., Dodson, A., Parsons, K., Woolfenden, A., Neoptolemos, J., *et al.* (1999) Protein kinase C isoenzyme patterns characteristically modulated in early prostate cancer. *The American journal of pathology* **154** (1) p.137-144. 10.1016/S0002-9440(10)65260-1.

Costa, A. D., Jakob, R., Costa, C. L., Andrukhiv, K., West, I. C. and Garlid, K. D. (2006) The mechanism by which the mitochondrial ATP-sensitive K+ channel opening and H2O2 inhibit the mitochondrial permeability transition. *J Biol Chem* **281** (30) p.20801-8. 10.1074/jbc.M600959200.

Cousins, M. J., Pickthorn, K., Huang, S., Critchley, L. and Bell, G. (2013) The Safety and Efficacy of KAI-1678— An Inhibitor of Epsilon Protein Kinase C (εPKC)—Versus Lidocaine and Placebo for the Treatment of

Postherpetic Neuralgia: A Crossover Study Design. *Pain Medicine* **14** (4) p.533-540. 10.1111/pme.12058.

Cripe, L. D., Uno, H., Paietta, E. M., Litzow, M. R., Ketterling, R. P., Bennett, J. M., *et al.* (2010) Zosuquidar, a novel modulator of P-glycoprotein, does not improve the outcome of older patients with newly diagnosed acute myeloid leukemia: a randomized, placebo-controlled trial of the Eastern Cooperative Oncology Group 3999. *Blood* **116** (20) p.4077-4085. 10.1182/blood-2010-04-277269.

Csukai, M., Chen, C. H., De Matteis, M. A. and Mochly-Rosen, D. (1997) The coatomer protein beta'-COP, a selective binding protein (RACK) for protein kinase Cepsilon. *J Biol Chem* **272** (46) p.29200-6. 10.1074/jbc.272.46.29200.

Dantzig, A. H., Shepard, R. L., Law, K. L., Tabas, L., Pratt, S., Gillespie, J. S., *et al.* (1999) Selectivity of the multidrug resistance modulator, LY335979, for P-glycoprotein and effect on cytochrome P-450 activities. *J Pharmacol Exp Ther* **290** (2) p.854-62.

Daver, N., Schlenk, R. F., Russell, N. H. and Levis, M. J. (2019) Targeting FLT3 mutations in AML: review of current knowledge and evidence. *Leukemia* **33** (2) p.299-312. 10.1038/s41375-018-0357-9.

Davis, A., Gao, R. and Navin, N. (2017) Tumor evolution: Linear, branching, neutral or punctuated? *Biochimica et Biophysica Acta (BBA) - Reviews on Cancer* **1867** (2) p.151-161. https://doi.org/10.1016/j.bbcan.2017.01.003.

de Jonge-Peeters, S. D., Kuipers, F., de Vries, E. G. and Vellenga, E. (2007) ABC transporter expression in hematopoietic stem cells and the role in AML drug resistance. *Crit Rev Oncol Hematol* **62** (3) p.214-26. 10.1016/j.critrevonc.2007.02.003.

Den Boer, M. L., Pieters, R., Kazemier, K. M., Janka-Schaub, G. E., Henze, G. and Veerman, A. J. (1999) Relationship between the intracellular daunorubicin concentration, expression of major vault protein/lung resistance protein and resistance to anthracyclines in childhood acute lymphoblastic leukemia. *Leukemia* **13** (12) p.2023-30. 10.1038/sj.leu.2401576.

Deschler, B. and Lubbert, M. (2006) Acute myeloid leukemia: epidemiology and etiology. *Cancer* **107** (9) p.2099-107. 10.1002/cncr.22233.

DeVore, R. F., Corbett, A. H. and Osheroff, N. (1992) Phosphorylation of topoisomerase II by casein kinase II and protein kinase C: effects on enzyme-mediated DNA cleavage/religation and sensitivity to the antineoplastic drugs etoposide and 4'-(9-acridinylamino)methane-sulfon-m-anisidide. *Cancer Res* **52** (8) p.2156-61.

Di Marcantonio, D., Martinez, E., Sidoli, S., Vadaketh, J., Nieborowska-Skorska, M., Gupta, A., *et al.* (2018) Protein Kinase C Epsilon Is a Key Regulator of Mitochondrial Redox Homeostasis in Acute Myeloid Leukemia. *Clin Cancer Res* **24** (3) p.608-618. 10.1158/1078-0432.CCR-17-2684.

DiNardo, C. D., Pratz, K., Pullarkat, V., Jonas, B. A., Arellano, M., Becker, P. S., *et al.* (2019) Venetoclax combined with decitabine or azacitidine in treatment-naive, elderly patients with acute myeloid leukemia. *Blood* **133** (1) p.7-17. 10.1182/blood-2018-08-868752.

Ding, L., Ley, T. J., Larson, D. E., Miller, C. A., Koboldt, D. C., Welch, J. S., *et al.* (2012) Clonal evolution in relapsed acute myeloid leukaemia revealed by whole-genome sequencing. *Nature* **481** (7382) p.506-510. 10.1038/nature10738.

Ding, L., Wang, H., Lang, W. and Xiao, L. (2002) Protein kinase C-epsilon promotes survival of lung cancer cells by suppressing apoptosis through dysregulation of the mitochondrial caspase pathway. *J Biol Chem* **277** (38) p.35305-13. 10.1074/jbc.M201460200.

Disatnik, M. H., Buraggi, G. and Mochly-Rosen, D. (1994) Localization of protein kinase C isozymes in cardiac myocytes. *Exp Cell Res* **210** (2) p.287-97. 10.1006/excr.1994.1041.

Doench, J. G., Fusi, N., Sullender, M., Hegde, M., Vaimberg, E. W., Donovan, K. F., *et al.* (2016) Optimized sgRNA design to maximize activity and minimize off-target effects of CRISPR-Cas9. *Nature Biotechnology* **34** (2) p.184-191. 10.1038/nbt.3437.

Döhner, H., Estey, E., Grimwade, D., Amadori, S., Appelbaum, F. R., Büchner, T., *et al.* (2017) Diagnosis and management of AML in adults: 2017 ELN recommendations from an international expert panel. *Blood* **129** (4) p.424-447. 10.1182/blood-2016-08-733196.

Döhner, H., Weisdorf, D. J. and Bloomfield, C. D. (2015) Acute myeloid leukemia. *New England Journal of Medicine* **373** (12) p.1136-1152.

Dombret, H., Seymour, J. F., Butrym, A., Wierzbowska, A., Selleslag, D., Jang, J. H., *et al.* (2015) International phase 3 study of azacitidine vs conventional care regimens in older patients with newly diagnosed AML with >30% blasts. *Blood* **126** (3) p.291-9. 10.1182/blood-2015-01-621664.

Doroshow, J. H. (2019) Mechanisms of Anthracycline-Enhanced Reactive Oxygen Metabolism in Tumor Cells. *Oxidative Medicine and Cellular Longevity* **2019** p.9474823. 10.1155/2019/9474823.

Du, W., Lu, C., Zhu, X., Hu, D., Chen, X., Li, J., *et al.* (2019) Prognostic significance of CXCR4 expression in acute myeloid leukemia. *Cancer medicine* **8** (15) p.6595-6603. 10.1002/cam4.2535.

Dumontet, C., Fabianowska-Majewska, K., Mantincic, D., Callet Bauchu, E., Tigaud, I., Gandhi, V., *et al.* (1999) Common resistance mechanisms to deoxynucleoside analogues in variants of the human erythroleukaemic line K562. *Br J Haematol* **106** (1) p.78-85. 10.1046/j.1365-2141.1999.01509.x.

Eckford, P. D. W. and Sharom, F. J. (2009) ABC Efflux Pump-Based Resistance to Chemotherapy Drugs. *Chemical Reviews* **109** (7) p.2989-3011. 10.1021/cr9000226.

Elmore, S. (2007) Apoptosis: a review of programmed cell death. *Toxicologic pathology* **35** (4) p.495-516. 10.1080/01926230701320337.

Estey, E. and Döhner, H. (2006) Acute myeloid leukaemia. *Lancet* **368** (9550) p.1894-1907. https://doi.org/10.1016/S0140-6736(06)69780-8.

Estey, E. H. (2018) Acute myeloid leukemia: 2019 update on risk-stratification and management. *American Journal of Hematology* **93** (10) p.1267-1291. 10.1002/ajh.25214.

Evans, C. A., Lord, J. M., Owen-Lynch, P. J., Johnson, G., Dive, C. and Whetton, A. D. (1995) Suppression of apoptosis by v-ABL protein tyrosine kinase is associated with nuclear translocation and activation of protein kinase C in an interleukin-3-dependent haemopoietic cell line. *Journal of Cell Science* **108** (7) p.2591-2598.

Fabbro, D., Buchdunger, E., Wood, J., Mestan, J., Hofmann, F., Ferrari, S., *et al.* (1999) Inhibitors of protein kinases: CGP 41251, a protein kinase inhibitor with potential as an anticancer agent. *Pharmacol Ther* **82** (2-3) p.293-301. 10.1016/s0163-7258(99)00005-4.

Facchinetti, V., Ouyang, W., Wei, H., Soto, N., Lazorchak, A., Gould, C., *et al.* (2008) The mammalian target of rapamycin complex 2 controls folding and stability of Akt and protein kinase C. *Embo j* **27** (14) p.1932-43. 10.1038/emboj.2008.120.

Ferrara, F. and Schiffer, C. A. (2013) Acute myeloid leukaemia in adults. *Lancet* **381** (9865) p.484-495.

Ferri, S., Kojima, K. and Sode, K. (2011) Review of glucose oxidases and glucose dehydrogenases: a bird's eye view of glucose sensing enzymes. *Journal of diabetes science and technology* **5** (5) p.1068-1076. 10.1177/193229681100500507.

Fischer, T., Stone, R. M., Deangelo, D. J., Galinsky, I., Estey, E., Lanza, C., *et al.* (2010) Phase IIB trial of oral Midostaurin (PKC412), the FMS-like tyrosine kinase 3 receptor (FLT3) and multi-targeted kinase inhibitor, in patients with acute myeloid leukemia and high-risk myelodysplastic syndrome with either wild-type or mutated FLT3. *J Clin Oncol* **28** (28) p.4339-45. 10.1200/jco.2010.28.9678.

Fleming, R. A., Capizzi, R. L., Rosner, G. L., Oliver, L. K., Smith, S. J., Schiffer, C. A., *et al.* (1995) Clinical pharmacology of cytarabine in patients with acute myeloid leukemia: a cancer and leukemia group B study. *Cancer Chemother Pharmacol* **36** (5) p.425-30. 10.1007/bf00686192.

Flescher, E. and Rotem, R. (2002a) Protein kinase C epsilon mediates the induction of P-glycoprotein in LNCaP prostate carcinoma cells. *Cell Signal* **14** (1) p.37-43. 10.1016/s0898-6568(01)00215-7.

Flescher, E. and Rotem, R. (2002b) Protein kinase C ε mediates the induction of P-glycoprotein in LNCaP prostate carcinoma cells. *Cellular Signalling* **14** (1) p.37-43. https://doi.org/10.1016/S0898-6568(01)00215-7.

Forsström, B., Axnäs, B. B., Rockberg, J., Danielsson, H., Bohlin, A. and Uhlen, M. (2015) Dissecting antibodies with regards to linear and conformational epitopes. *PloS one* **10** (3) p.e0121673-e0121673. 10.1371/journal.pone.0121673.

Fridovich, I. (1995) Superoxide radical and superoxide dismutases. *Annu Rev Biochem* **64** p.97-112. 10.1146/annurev.bi.64.070195.000525.

Fukunaga, R., Ishizaka-Ikeda, E. and Nagata, S. (1993) Growth and differentiation signals mediated by different regions in the cytoplasmic domain of granulocyte colony-stimulating factor receptor. *Cell* **74** (6) p.1079-87. 10.1016/0092-8674(93)90729-a.

Gabrilove, J. L., Jakubowski, A., Fain, K., Grous, J., Scher, H., Sternberg, C., *et al.* (1988) Phase I study of granulocyte colony-stimulating factor in patients with transitional cell carcinoma of the urothelium. *J Clin Invest* **82** (4) p.1454-61. 10.1172/jci113751.

Gaidzik, V. I., Bullinger, L., Schlenk, R. F., Zimmermann, A. S., Röck, J., Paschka, P., *et al.* (2011) RUNX1 mutations in acute myeloid leukemia: results from a comprehensive genetic and clinical analysis from the AML study group. *J Clin Oncol* **29** (10) p.1364-72. 10.1200/jco.2010.30.7926.

Gallay, N., Dos Santos, C., Cuzin, L., Bousquet, M., Simmonet Gouy, V., Chaussade, C., *et al.* (2009) The level of AKT phosphorylation on threonine 308 but not on serine 473 is associated with high-risk cytogenetics and predicts poor overall survival in acute myeloid leukaemia. *Leukemia* **23** (6) p.1029-38. 10.1038/leu.2008.395.

Galmarini, C. M., Thomas, X., Calvo, F., Rousselot, P., Jafaari, A. E., Cros, E., *et al.* (2002) Potential mechanisms of resistance to cytarabine in AML patients. *Leukemia Research* **26** (7) p.621-629. https://doi.org/10.1016/S0145-2126(01)00184-9.

Galmarini, C. M., Thomas, X., Graham, K., El Jafaari, A., Cros, E., Jordheim, L., *et al.* (2003) Deoxycytidine kinase and cN-II nucleotidase expression in blast cells predict survival in acute myeloid leukaemia patients treated with cytarabine. *British Journal of Haematology* **122** (1) p.53-60. 10.1046/j.1365-2141.2003.04386.x.

Ganapathi, R., Constantinou, A., Kamath, N., Dubyak, G., Grabowski, D. and Krivacic, K. (1996) Resistance to etoposide in human leukemia HL-60 cells: reduction in drug-induced DNA cleavage associated with hypophosphorylation of topoisomerase II phosphopeptides. *Molecular Pharmacology* **50** (2) p.243-248.

Gao, J., Aksoy, B. A., Dogrusoz, U., Dresdner, G., Gross, B., Sumer, S. O., *et al.* (2013) Integrative analysis of complex cancer genomics and clinical profiles using the cBioPortal. *Sci Signal* **6** (269) p.pl1. 10.1126/scisignal.2004088.

Gao, T., Brognard, J. and Newton, A. C. (2008) The phosphatase PHLPP controls the cellular levels of protein kinase C. *J Biol Chem* **283** (10) p.6300-11. 10.1074/jbc.M707319200.

Garg, R., Benedetti, L. G., Abera, M. B., Wang, H., Abba, M. and Kazanietz, M. G. (2014) Protein kinase C and cancer: what we know and what we do not. *Oncogene* **33** (45) p.5225-5237. 10.1038/onc.2013.524.

Garg, R., Blando, J., Perez, C. J., Wang, H., Benavides, F. J. and Kazanietz, M. G. (2012) Activation of nuclear factor kappaB (NF-kappaB) in prostate cancer is mediated by protein kinase C epsilon (PKCepsilon). *J Biol Chem* **287** (44) p.37570-82. 10.1074/jbc.M112.398925.

Garg, R., Cooke, M., Benavides, F., Abba, M. C., Cicchini, M., Feldser, D. M., *et al.* (2020) Requirement for PKC Epsilon in Kras-Driven Lung Tumorigenesis. *Cancer Research* **80** (23) p.5166-5173. 10.1158/0008-5472.Can-20-1300.

Geiger, T. R. and Peeper, D. S. (2009) Metastasis mechanisms. *Biochim Biophys Acta* **1796** (2) p.293-308. 10.1016/j.bbcan.2009.07.006.

Genovese, G., Kähler, A. K., Handsaker, R. E., Lindberg, J., Rose, S. A., Bakhoum, S. F., *et al.* (2014) Clonal hematopoiesis and blood-cancer risk inferred from blood DNA sequence. *The New England journal of medicine* **371** (26) p.2477-87.

George, P. (1947) Reaction Between Catalase and Hydrogen Peroxide. *Nature* **160** (4054) p.41-43. 10.1038/160041a0.

Gerrard, G., Payne, E., Baker, R. J., Jones, D. T., Potter, M., Prentice, H. G., *et al.* (2004) Clinical effects and P-glycoprotein inhibition in patients with acute myeloid leukemia treated with zosuquidar trihydrochloride, daunorubicin and cytarabine. *Haematologica* **89** (7) p.782-90.

Ghandi, M., Huang, F. W., Jané-Valbuena, J., Kryukov, G. V., Lo, C. C., McDonald, E. R., *et al.* (2019) Next-generation characterization of the Cancer Cell Line Encyclopedia. *Nature* **569** (7757) p.503-508. 10.1038/s41586-019-1186-3.

Gill, P. K., Gescher, A. and Gant, T. W. (2001) Regulation of MDR1 promoter activity in human breast carcinoma cells by protein kinase C isozymes alpha and theta. *Eur J Biochem* **268** (15) p.4151-7. 10.1046/j.1432-1327.2001.02326.x.

Gilliland, D. G. and Griffin, J. D. (2002) The roles of FLT3 in hematopoiesis and leukemia. *Blood* **100** (5) p.1532-42. 10.1182/blood-2002-02-0492.

Giorgi, C., Agnoletto, C., Baldini, C., Bononi, A., Bonora, M., Marchi, S., *et al.* (2010) Redox control of protein kinase C: cell- and disease-specific aspects. *Antioxid Redox Signal* **13** (7) p.1051-85. 10.1089/ars.2009.2825.

Giorgione, J. R., Lin, J.-H., McCammon, J. A. and Newton, A. C. (2006) Increased Membrane Affinity of the C1 Domain of Protein Kinase Cδ Compensates for the Lack of Involvement of Its C2 Domain in

Membrane Recruitment *. *Journal of Biological Chemistry* **281** (3) p.1660-1669. 10.1074/jbc.M510251200.

Gobbi, G., Mirandola, P., Carubbi, C., Micheloni, C., Malinverno, C., Lunghi, P., *et al.* (2009) Phorbol ester-induced PKCepsilon down-modulation sensitizes AML cells to TRAIL-induced apoptosis and cell differentiation. *Blood* **113** (13) p.3080-7. 10.1182/blood-2008-03-143784.

Gobbi, G., Mirandola, P., Sponzilli, I., Micheloni, C., Malinverno, C., Cocco, L., *et al.* (2007) Timing and expression level of protein kinase C epsilon regulate the megakaryocytic differentiation of human CD34 cells. *Stem Cells* **25** (9) p.2322-9. 10.1634/stemcells.2006-0839.

Goodfellow, H. R., Sardini, A., Ruetz, S., Callaghan, R., Gros, P., McNaughton, P. A., *et al.* (1996) Protein kinase C-mediated phosphorylation does not regulate drug transport by the human multidrug resistance P-glycoprotein. *J Biol Chem* **271** (23) p.13668-74. 10.1074/jbc.271.23.13668.

Gorin, M. A. and Pan, Q. (2009) Protein kinase Cε: an oncogene and emerging tumor biomarker. *Molecular cancer* **8** (1) p.9.

Goulard, M., Dosquet, C. and Bonnet, D. (2018) Role of the microenvironment in myeloid malignancies. *Cell Mol Life Sci* **75** (8) p.1377-1391. 10.1007/s00018-017-2725-4.

Gould, C. M., Kannan, N., Taylor, S. S. and Newton, A. C. (2009) The Chaperones Hsp90 and Cdc37 Mediate the Maturation and Stabilization of Protein Kinase C through a Conserved PXXP Motif in the C-terminal Tail *[♦]. *Journal of Biological Chemistry* **284** (8) p.4921-4935. 10.1074/jbc.M808436200.

Grandage, V. L., Gale, R. E., Linch, D. C. and Khwaja, A. (2005) PI3-kinase/Akt is constitutively active in primary acute myeloid leukaemia cells and regulates survival and chemoresistance via NF-kB, MAPkinase and p53 pathways. *Leukemia* **19** (4) p.586-594. 10.1038/sj.leu.2403653.

Grassinger, J., Haylock, D. N., Storan, M. J., Haines, G. O., Williams, B., Whitty, G. A., *et al.* (2009) Thrombin-cleaved osteopontin regulates hemopoietic stem and progenitor cell functions through interactions with alpha9beta1 and alpha4beta1 integrins. *Blood* **114** (1) p.49-59. 10.1182/blood-2009-01-197988.

Gray, M. O., Karliner, J. S. and Mochly-Rosen, D. (1997) A Selective ε-Protein Kinase C Antagonist Inhibits Protection of Cardiac Myocytes from Hypoxia-induced Cell Death*. *Journal of Biological Chemistry* **272** (49) p.30945-30951. https://doi.org/10.1074/jbc.272.49.30945.

Greaves, M. and Maley, C. C. (2012) Clonal evolution in cancer. *Nature* **481** (7381) p.306-313. 10.1038/nature10762.

Gribar, J. J., Ramachandra, M., Hrycyna, C. A., Dey, S. and Ambudkar, S. V. (2000) Functional characterization of glycosylation-deficient human P-glycoprotein using a vaccinia virus expression system. *J Membr Biol* **173** (3) p.203-14. 10.1007/s002320001020.

Grimwade, D., Walker, H., Harrison, G., Oliver, F., Chatters, S., Harrison, C. J., *et al.* (2001) The predictive value of hierarchical cytogenetic classification in older adults with acute myeloid leukemia (AML): analysis of 1065 patients entered into the United Kingdom Medical Research Council AML11 trial. *Blood* **98** (5) p.1312-20. 10.1182/blood.v98.5.1312.

Griner, E. M. and Kazanietz, M. G. (2007) Protein kinase C and other diacylglycerol effectors in cancer. *Nature Reviews Cancer* **7** (4) p.281-294.

Grove, C. S. and Vassiliou, G. S. (2014) Acute myeloid leukaemia: a paradigm for the clonal evolution of cancer? *Disease Models & Mechanisms* **7** (8) p.941-951. 10.1242/dmm.015974.

Gupta, K. P., Ward, N. E., Gravitt, K. R., Bergman, P. J. and O'Brian, C. A. (1996) Partial reversal of multidrug resistance in human breast cancer cells by an N-myristoylated protein kinase C-alpha pseudosubstrate peptide. *J Biol Chem* **271** (4) p.2102-11. 10.1074/jbc.271.4.2102.

Gustafson, M. P., Lin, Y., Maas, M. L., Van Keulen, V. P., Johnston, P. B., Peikert, T., *et al.* (2015) A method for identification and analysis of non-overlapping myeloid immunophenotypes in humans. *PloS one* **10** (3) p.e0121546-e0121546. 10.1371/journal.pone.0121546.

Gutierrez-Uzquiza, A., Lopez-Haber, C., Jernigan, D. L., Fatatis, A. and Kazanietz, M. G. (2015) PKCepsilon Is an Essential Mediator of Prostate Cancer Bone Metastasis. *Mol Cancer Res* **13** (9) p.1336-46. 10.1158/1541-7786.MCR-15-0111.

Hafeez, B. B., Zhong, W., Weichert, J., Dreckschmidt, N. E., Jamal, M. S. and Verma, A. K. (2011) Genetic ablation of PKC epsilon inhibits prostate cancer development and metastasis in transgenic mouse model of prostate adenocarcinoma. *Cancer research* **71** (6) p.2318-2327. 10.1158/0008-5472.CAN-10-4170.

Hamdorf, M., Berger, A., Schule, S., Reinhardt, J. and Flory, E. (2011) PKCdelta-induced PU.1 phosphorylation promotes hematopoietic stem cell differentiation to dendritic cells. *Stem Cells* **29** (2) p.297-306. 10.1002/stem.564.

Hanahan, D. and Weinberg, Robert A. (2011) Hallmarks of Cancer: The Next Generation. *Cell* **144** (5) p.646-674. 10.1016/j.cell.2011.02.013.

Hansra, G., Garcia-Paramio, P., Prevostel, C., Whelan, R. D., Bornancin, F. and Parker, P. J. (1999) Multisite dephosphorylation and desensitization of conventional protein kinase C isotypes. *The Biochemical journal* **342 (Pt 2)** (Pt 2) p.337-344.

Hart, S. M., Ganeshaguru, K., Scheper, R. J., Prentice, H. G., Hoffbrand, A. V. and Mehta, A. B. (1997) Expression of the human major vault protein LRP in acute myeloid leukemia. *Experimental hematology* **25** (12) p.1227-1232.

Hasle, H., Clemmensen, I. H. and Mikkelsen, M. (2000) Risks of leukaemia and solid tumours in individuals with Down's syndrome. *Lancet* **355** (9199) p.165-9. 10.1016/s0140-6736(99)05264-2.

Hass, R., Pfannkuche, H. J., Kharbanda, S., Gunji, H., Meyer, G., Hartmann, A., *et al.* (1991) Protein kinase C activation and protooncogene expression in differentiation/retrodifferentiation of human U-937 leukemia cells. *Cell Growth Differ* **2** (11) p.541-8.

Hass, R., Prudovsky, I. and Kruhøffer, M. (1997) Differential effects of phorbol ester on signaling and gene expression in human leukemia cells. *Leuk Res* **21** (7) p.589-94. 10.1016/s0145-2126(97)00010-6.

Haug, J. S., He, X. C., Grindley, J. C., Wunderlich, J. P., Gaudenz, K., Ross, J. T., *et al.* (2008) N-cadherin expression level distinguishes reserved versus primed states of hematopoietic stem cells. *Cell Stem Cell* **2** (4) p.367-79. 10.1016/j.stem.2008.01.017.

Hazen, A. L., Diks, S. H., Wahle, J. A., Fuhler, G. M., Peppelenbosch, M. P. and Kerr, W. G. (2011) Major remodelling of the murine stem cell kinome following differentiation in the hematopoietic compartment. *J Proteome Res* **10** (8) p.3542-50. 10.1021/pr2001594.

Hazlehurst, L. A., Argilagos, R. F. and Dalton, W. S. (2007) β1 integrin mediated adhesion increases Bim protein degradation and contributes to drug resistance in leukaemia cells. *British Journal of Haematology* **136** (2) p.269-275. https://doi.org/10.1111/j.1365-2141.2006.06435.x.

Henrich, C. J. and Simpson, P. C. (1988) Differential acute and chronic response of protein kinase C in cultured neonatal rat heart myocytes to alpha 1-adrenergic and phorbol ester stimulation. *J Mol Cell Cardiol* **20** (12) p.1081-5. 10.1016/0022-2828(88)90588-3.

Herrmann, J., Lerman, L. O. and Lerman, A. (2007) Ubiquitin and Ubiquitin-Like Proteins in Protein Regulation. *Circulation Research* **100** (9) p.1276-1291. doi:10.1161/01.RES.0000264500.11888.f0.

Hieke, S., Benner, A., Schlenl, R. F., Schumacher, M., Bullinger, L. and Binder, H. (2016) Integrating multiple molecular sources into a clinical risk prediction signature by extracting complementary information. *BMC Bioinformatics* **17** (1) p.327. 10.1186/s12859-016-1183-6.

Hodge, C. W., Mehmert, K. K., Kelley, S. P., McMahon, T., Haywood, A., Olive, M. F., *et al.* (1999) Supersensitivity to allosteric GABA(A) receptor modulators and alcohol in mice lacking PKCepsilon. *Nat Neurosci* **2** (11) p.997-1002. 10.1038/14795.

Hogan, C. J., Shpall, E. J. and Keller, G. (2002) Differential long-term and multilineage engraftment potential from subfractions of human CD34+ cord blood cells transplanted into NOD/SCID mice. *Proc Natl Acad Sci U S A* **99** (1) p.413-8. 10.1073/pnas.012336799.

Hole, P. S., Zabkiewicz, J., Munje, C., Newton, Z., Pearn, L., White, P., *et al.* (2013) Overproduction of NOX-derived ROS in AML promotes proliferation and is associated with defective oxidative stress signaling. *Blood* **122** (19) p.3322-30. 10.1182/blood-2013-04-491944.

Hongpaisan, J., Xu, C., Sen, A., Nelson, T. J. and Alkon, D. L. (2013) PKC activation during training restores mushroom spine synapses and memory in the aged rat. *Neurobiology of Disease* **55** p.44-62. https://doi.org/10.1016/j.nbd.2013.03.012.

Hosokawa, K., Arai, F., Yoshihara, H., Iwasaki, H., Hembree, M., Yin, T., *et al.* (2010) Cadherin-based adhesion is a potential target for niche manipulation to protect hematopoietic stem cells in adult bone marrow. *Cell Stem Cell* **6** (3) p.194-8. 10.1016/j.stem.2009.04.013.

Hu, Z. B., Ma, W., Uphoff, C. C., Lanotte, M. and Drexler, H. G. (1993) Modulation of gene expression in the acute promyelocytic leukemia cell line NB4. *Leukemia* **7** (11) p.1817-23.

Ihle, J. N. (1992) Interleukin-3 and hematopoiesis. *Chem Immunol* **51** p.65-106. 10.1159/000420755.

Iliodromitis, E. K., Lazou, A. and Kremastinos, D. T. (2007) Ischemic preconditioning: protection against myocardial necrosis and apoptosis. *Vascular health and risk management* **3** (5) p.629-637.

Isakov, N., Galron, D., Mustelin, T., Pettit, G. R. and Altman, A. (1993) Inhibition of phorbol ester-induced T cell proliferation by bryostatin is associated with rapid degradation of protein kinase C. *J Immunol* **150** (4) p.1195-204.

Ito, T., Deng, X., Carr, B. and May, W. S. (1997) Bcl-2 Phosphorylation Required for Anti-apoptosis Function*. *Journal of Biological Chemistry* **272** (18) p.11671-11673. https://doi.org/10.1074/jbc.272.18.11671.

Ivanova, N. B., Dimos, J. T., Schaniel, C., Hackney, J. A., Moore, K. A. and Lemischka, I. R. (2002) A stem cell molecular signature. *Science* **298** (5593) p.601-4. 10.1126/science.1073823.

Ivanovs, A., Rybtsov, S., Ng, E. S., Stanley, E. G., Elefanty, A. G. and Medvinsky, A. (2017) Human haematopoietic stem cell development: from the embryo to the dish. *Development* **144** (13) p.2323-2337.

Ivaska, J., Bosca, L. and Parker, P. J. (2003) PKCepsilon is a permissive link in integrin-dependent IFN-gamma signalling that facilitates JAK phosphorylation of STAT1. *Nat Cell Biol* **5** (4) p.363-9. 10.1038/ncb957.

Ivaska, J., Whelan, R. D., Watson, R. and Parker, P. J. (2002) PKC epsilon controls the traffic of beta1 integrins in motile cells. *Embo j* **21** (14) p.3608-19. 10.1093/emboj/cdf371.

Ivey, A., Hills, R. K., Simpson, M. A., Jovanovic, J. V., Gilkes, A., Grech, A., *et al.* (2016) Assessment of Minimal Residual Disease in Standard-Risk AML. *New England Journal of Medicine* **374** (5) p.422-433. 10.1056/NEJMoa1507471.

Iwasaki, H. and Akashi, K. (2007) Hematopoietic developmental pathways: on cellular basis. *Oncogene* **26** (47) p.6687-6696. 10.1038/sj.onc.1210754.

Jabůrek, M., Costa, A. D., Burton, J. R., Costa, C. L. and Garlid, K. D. (2006) Mitochondrial PKC epsilon and mitochondrial ATP-sensitive K+ channel

copurify and coreconstitute to form a functioning signaling module in proteoliposomes. *Circ Res* **99** (8) p.878-83. 10.1161/01.RES.0000245106.80628.d3.

Jain, A. and Trivedi, V. (2014) Docking and virtual screening to identify PKC agonists: potentials in anticancer therapeutics. *Curr Comput Aided Drug Des* **10** (1) p.50-8. 10.2174/15734099113096660035.

Jain, K. and Basu, A. (2014a) The Multifunctional Protein Kinase C-epsilon in Cancer Development and Progression. *Cancers (Basel)* **6** (2) p.860-78. 10.3390/cancers6020860.

Jain, K. and Basu, A. (2014b) Protein Kinase C-epsilon Promotes EMT in Breast Cancer. *Breast Cancer (Auckl)* **8** p.61-7. 10.4137/BCBCR.S13640.

Jaiswal, S., Jamieson, C. H., Pang, W. W., Park, C. Y., Chao, M. P., Majeti, R., *et al.* (2009) CD47 is upregulated on circulating hematopoietic stem cells and leukemia cells to avoid phagocytosis. *Cell* **138** (2) p.271-85. 10.1016/j.cell.2009.05.046.

Jasinski, P., Terai, K., Zwolak, P. and Dudek, A. Z. (2008) Enzastaurin renders MCF-7 breast cancer cells sensitive to radiation through reversal of radiation-induced activation of protein kinase C. *European Journal of Cancer* **44** (9) p.1315-1322. https://doi.org/10.1016/j.ejca.2008.03.024.

Jiffar, T., Kurinna, S., Suck, G., Carlson-Bremer, D., Ricciardi, M. R., Konopleva, M., *et al.* (2004) PKC alpha mediates chemoresistance in acute lymphoblastic leukemia through effects on Bcl2 phosphorylation. *Leukemia* **18** (3) p.505-12. 10.1038/sj.leu.2403275.

Jin, L., Hope, K. J., Zhai, Q., Smadja-Joffe, F. and Dick, J. E. (2006) Targeting of CD44 eradicates human acute myeloid leukemic stem cells. *Nat Med* **12** (10) p.1167-74. 10.1038/nm1483.

Jin, L., Lee, E. M., Ramshaw, H. S., Busfield, S. J., Peoppl, A. G., Wilkinson, L., *et al.* (2009) Monoclonal antibody-mediated targeting of CD123, IL-3 receptor alpha chain, eliminates human acute myeloid leukemic stem cells. *Cell Stem Cell* **5** (1) p.31-42. 10.1016/j.stem.2009.04.018.

Johnson, J. A., Gray, M. O., Chen, C. H. and Mochly-Rosen, D. (1996) A protein kinase C translocation inhibitor as an isozyme-selective antagonist of cardiac function. *J Biol Chem* **271** (40) p.24962-6. 10.1074/jbc.271.40.24962.

Johnstone, R. W., Ruefli, A. A., Tainton, K. M. and Smyth, M. J. (2000) A role for P-glycoprotein in regulating cell death. *Leuk Lymphoma* **38** (1-2) p.1-11. 10.3109/10428190009060314.

Juliusson, G., Antunovic, P., Derolf, Å., Lehmann, S., Möllgård, L., Stockelberg, D., *et al.* (2009) Age and acute myeloid leukemia: real world data on decision to treat and outcomes from the Swedish Acute Leukemia Registry. *Blood* **113** (18) p.4179-4187. 10.1182/blood-2008-07-172007.

Juliusson, G., Jädersten, M., Deneberg, S., Lehmann, S., Möllgård, L., Wennström, L., *et al.* (2020) The prognostic impact of FLT3-ITD and

NPM1 mutation in adult AML is age-dependent in the population-based setting. *Blood advances* **4** (6) p.1094-1101. 10.1182/bloodadvances.2019001335.

Jung, K. and Reszka, R. (2001) Mitochondria as subcellular targets for clinically useful anthracyclines. *Adv Drug Deliv Rev* **49** (1-2) p.87-105. 10.1016/s0169-409x(01)00128-4.

Kabir, A. M. N., Clark, J. E., Tanno, M., Cao, X., Hothersall, J. S., Dashnyam, S., *et al.* (2006) Cardioprotection initiated by reactive oxygen species is dependent on activation of PKCε. *American Journal of Physiology-Heart and Circulatory Physiology* **291** (4) p.H1893-H1899. 10.1152/ajpheart.00798.2005.

Kadia, T. M., Jain, P., Ravandi, F., Garcia-Manero, G., Andreef, M., Takahashi, K., *et al.* (2016) TP53 mutations in newly diagnosed acute myeloid leukemia: Clinicomolecular characteristics, response to therapy, and outcomes. *Cancer* **122** (22) p.3484-3491. 10.1002/cncr.30203.

Kantarjian, H. M., Thomas, X. G., Dmoszynska, A., Wierzbowska, A., Mazur, G., Mayer, J., *et al.* (2012) Multicenter, randomized, open-label, phase III trial of decitabine versus patient choice, with physician advice, of either supportive care or low-dose cytarabine for the treatment of older patients with newly diagnosed acute myeloid leukemia. *J Clin Oncol* **30** (21) p.2670-7. 10.1200/jco.2011.38.9429.

Katayama, K., Noguchi, K. and Sugimoto, Y. (2014) Regulations of P-Glycoprotein/ABCB1/MDR1 in Human Cancer Cells. *New Journal of Science* **2014** p.476974. 10.1155/2014/476974.

Kaufmann, S. H., Karp, J. E., Svingen, P. A., Krajewski, S., Burke, P. J., Gore, S. D., *et al.* (1998) Elevated expression of the apoptotic regulator Mcl-1 at the time of leukemic relapse. *Blood* **91** (3) p.991-1000.

Kazanietz, M. G., Areces, L. B., Bahador, A., Mischak, H., Goodnight, J., Mushinski, J. F., *et al.* (1993) Characterization of ligand and substrate specificity for the calcium-dependent and calcium-independent protein kinase C isozymes. *Mol Pharmacol* **44** (2) p.298-307.

Khwaja, A., Bjorkholm, M., Gale, R. E., Levine, R. L., Jordan, C. T., Ehninger, G., *et al.* (2016) Acute myeloid leukaemia. *Nature Reviews Disease Primers* **2** (1) p.16010. 10.1038/nrdp.2016.10.

Kiel, M. J., Acar, M., Radice, G. L. and Morrison, S. J. (2009) Hematopoietic stem cells do not depend on N-cadherin to regulate their maintenance. *Cell Stem Cell* **4** (2) p.170-9. 10.1016/j.stem.2008.10.005.

Kikkawa, U., Takai, Y., Tanaka, Y., Miyake, R. and Nishizuka, Y. (1983) Protein kinase C as a possible receptor protein of tumor-promoting phorbol esters. *J Biol Chem* **258** (19) p.11442-5.

Kim, A. D., Stachura, D. L. and Traver, D. (2014) Cell signaling pathways involved in hematopoietic stem cell specification. *Experimental cell research* **329** (2) p.227-233. 10.1016/j.yexcr.2014.10.011.

Kim, C. H. (2010) Homeostatic and pathogenic extramedullary hematopoiesis. *Journal of blood medicine* **1** p.13-19. 10.2147/JBM.S7224.

Knapp, D., Hammond, C. A., Hui, T., van Loenhout, M. T. J., Wang, F., Aghaeepour, N., *et al.* (2018) Single-cell analysis identifies a CD33(+) subset of human cord blood cells with high regenerative potential. *Nat Cell Biol* **20** (6) p.710-720. 10.1038/s41556-018-0104-5.

Knauf, J. A., Elisei, R., Mochly-Rosen, D., Liron, T., Chen, X. N., Gonsky, R., *et al.* (1999) Involvement of protein kinase Cepsilon (PKCepsilon) in thyroid cell death. A truncated chimeric PKCepsilon cloned from a thyroid cancer cell line protects thyroid cells from apoptosis. *J Biol Chem* **274** (33) p.23414-25. 10.1074/jbc.274.33.23414.

Knauf, J. A., Ward, L. S., Nikiforov, Y. E., Nikiforova, M., Puxeddu, E., Medvedovic, M., *et al.* (2002) Isozyme-Specific Abnormalities of PKC in Thyroid Cancer: Evidence for Post-Transcriptional Changes in PKC Epsilon. *The Journal of Clinical Endocrinology & Metabolism* **87** (5) p.2150-2159. 10.1210/jcem.87.5.8441.

Knock, G. A. and Ward, J. P. (2011) Redox regulation of protein kinases as a modulator of vascular function. *Antioxid Redox Signal* **15** (6) p.1531-47. 10.1089/ars.2010.3614.

Kolitz, J. E., George, S. L., Marcucci, G., Vij, R., Powell, B. L., Allen, S. L., *et al.* (2010) P-glycoprotein inhibition using valspodar (PSC-833) does not improve outcomes for patients younger than age 60 years with newly diagnosed acute myeloid leukemia: Cancer and Leukemia Group B study 19808. *Blood* **116** (9) p.1413-21. 10.1182/blood-2009-07-229492.

Kondo, M., Weissman, I. L. and Akashi, K. (1997) Identification of clonogenic common lymphoid progenitors in mouse bone marrow. *Cell* **91** (5) p.661-72. 10.1016/s0092-8674(00)80453-5.

Konieczny, J. and Arranz, L. (2018) Updates on Old and Weary Haematopoiesis. *Int J Mol Sci* **19** (9) 10.3390/ijms19092567.

Kornfeld, O. S., Hwang, S., Disatnik, M.-H., Chen, C.-H., Qvit, N. and Mochly-Rosen, D. (2015) Mitochondrial Reactive Oxygen Species at the Heart of the Matter. *Circulation Research* **116** (11) p.1783-1799. doi:10.1161/CIRCRESAHA.116.305432.

Kortmansky, J. and Schwartz, G. K. (2003) Bryostatin-1: A Novel PKC Inhibitor in Clinical Development. *Cancer Investigation* **21** (6) p.924-936. 10.1081/CNV-120025095.

Kosaka, C., Sasaguri, T., Ishida, A. and Ogata, J. (1996) Cell cycle arrest in the G2 phase induced by phorbol ester and diacylglycerol in vascular endothelial cells. *Am J Physiol* **270** (1 Pt 1) p.C170-8. 10.1152/ajpcell.1996.270.1.C170.

Kottaridis, P. D., Gale, R. E., Frew, M. E., Harrison, G., Langabeer, S. E., Belton, A. A., *et al.* (2001) The presence of a FLT3 internal tandem duplication in patients with acute myeloid leukemia (AML) adds important prognostic

information to cytogenetic risk group and response to the first cycle of chemotherapy: analysis of 854 patients from the United Kingdom Medical Research Council AML 10 and 12 trials. *Blood* **98** (6) p.1752-9. 10.1182/blood.v98.6.1752.

Kraft, A. S., Smith, J. B. and Berkow, R. L. (1986) Bryostatin, an activator of the calcium phospholipid-dependent protein kinase, blocks phorbol ester-induced differentiation of human promyelocytic leukemia cells HL-60. *Proc Natl Acad Sci U S A* **83** (5) p.1334-8. 10.1073/pnas.83.5.1334.

Kramer, R., Weber, T. K., Arceci, R., Ramchurren, N., Kastrinakis, W. V., Steele, G., *et al.* (1995) Inhibition of N-linked glycosylation of P-glycoprotein by tunicamycin results in a reduced multidrug resistance phenotype. *British Journal of Cancer* **71** (4) p.670-675. 10.1038/bjc.1995.133.

Kurinna, S., Konopleva, M., Palla, S. L., Chen, W., Kornblau, S., Contractor, R., *et al.* (2006) Bcl2 phosphorylation and active PKC α are associated with poor survival in AML. *Leukemia* **20** (7) p.1316-1319. 10.1038/sj.leu.2404248.

Lai, B., Lai, Y., Zhang, Y., Zhou, M., Sheng, L. and OuYang, G. (2020) The Solute Carrier Family 2 Genes Are Potential Prognostic Biomarkers in Acute Myeloid Leukemia. *Technology in cancer research & treatment* **19** p.1533033819894308-1533033819894308. 10.1177/1533033819894308.

Lancet, J. E., Uy, G. L., Cortes, J. E., Newell, L. F., Lin, T. L., Ritchie, E. K., *et al.* (2018) CPX-351 (cytarabine and daunorubicin) Liposome for Injection Versus Conventional Cytarabine Plus Daunorubicin in Older Patients With Newly Diagnosed Secondary Acute Myeloid Leukemia. *J Clin Oncol* **36** (26) p.2684-2692. 10.1200/jco.2017.77.6112.

Lansdorp, P. M., Sutherland, H. J. and Eaves, C. J. (1990) Selective expression of CD45 isoforms on functional subpopulations of CD34+ hemopoietic cells from human bone marrow. *Journal of Experimental Medicine* **172** (1) p.363-366. 10.1084/jem.172.1.363.

Le Good, J. A., Ziegler, W. H., Parekh, D. B., Alessi, D. R., Cohen, P. and Parker, P. J. (1998) Protein kinase C isotypes controlled by phosphoinositide 3-kinase through the protein kinase PDK1. *Science* **281** (5385) p.2042-5. 10.1126/science.281.5385.2042.

Ledford, J. G., Kovarova, M. and Koller, B. H. (2007) Impaired Host Defense in Mice Lacking ONZIN. *The Journal of Immunology* **178** (8) p.5132-5143. 10.4049/jimmunol.178.8.5132.

Lee, H. W., Smith, L., Pettit, G. R. and Bingham Smith, J. (1996) Dephosphorylation of activated protein kinase C contributes to downregulation by bryostatin. *Am J Physiol* **271** (1 Pt 1) p.C304-11. 10.1152/ajpcell.1996.271.1.C304.

Lee, S.-K., Shehzad, A., Jung, J.-C., Sonn, J.-K., Lee, J.-T., Park, J.-W., *et al.* (2012) Protein kinase Cα protects against multidrug resistance in human

colon cancer cells. *Molecules and Cells* **34** (1) p.61-69. 10.1007/s10059-012-0087-1.

Lee, W., Hyun Boo, J., Whan Jung, M., Dai Park, S., Ho Kim, Y., Kim, S. U., *et al.* (2004) Amyloid beta peptide directly inhibits PKC activation. *Molecular and Cellular Neuroscience* **26** (2) p.222-231. https://doi.org/10.1016/j.mcn.2003.10.020.

Legrand, O., Simonin, G., Beauchamp-Nicoud, A., Zittoun, R. and Marie, J. P. (1999a) Simultaneous activity of MRP1 and Pgp is correlated with in vitro resistance to daunorubicin and with in vivo resistance in adult acute myeloid leukemia. *Blood* **94** (3) p.1046-56.

Legrand, O., Zittoun, R. and Marie, J. P. (1999b) Role of MRP1 in multidrug resistance in acute myeloid leukemia. *Leukemia* **13** (4) p.578-84. 10.1038/sj.leu.2401361.

Lehel, C., Olah, Z., Jakab, G. and Anderson, W. B. (1995) Protein kinase C epsilon is localized to the Golgi via its zinc-finger domain and modulates Golgi function. *Proceedings of the National Academy of Sciences* **92** (5) p.1406-1410. 10.1073/pnas.92.5.1406.

Levis, M. (2017) Midostaurin approved for FLT3-mutated AML. *Blood* **129** (26) p.3403-3406. https://doi.org/10.1182/blood-2017-05-782292.

Ley, T. J., Miller, C., Ding, L., Raphael, B. J., Mungall, A. J., Robertson, A., *et al.* (2013) Genomic and epigenomic landscapes of adult de novo acute myeloid leukemia. *N Engl J Med* **368** (22) p.2059-74. 10.1056/NEJMoa1301689.

Li, B. and Dewey, C. N. (2011) RSEM: accurate transcript quantification from RNA-Seq data with or without a reference genome. *BMC Bioinformatics* **12** (1) p.323. 10.1186/1471-2105-12-323.

Li, R. C., Ping, P., Zhang, J., Wead, W. B., Cao, X., Gao, J., *et al.* (2000) PKCepsilon modulates NF-kappaB and AP-1 via mitogen-activated protein kinases in adult rabbit cardiomyocytes. *Am J Physiol Heart Circ Physiol* **279** (4) p.H1679-89. 10.1152/ajpheart.2000.279.4.H1679.

Li, S., Phong, M., Lahn, M., Brail, L., Sutton, S., Lin, B. K., *et al.* (2007) Retrospective analysis of protein kinase C-beta (PKC-beta) expression in lymphoid malignancies and its association with survival in diffuse large B-cell lymphomas. *Biol Direct* **2** p.8. 10.1186/1745-6150-2-8.

Li, Y., Davis, K. L. and Sytkowski, A. J. (1996) Protein kinase C-epsilon is necessary for erythropoietin's up-regulation of c-myc and for factor-dependent DNA synthesis. Evidence for discrete signals for growth and differentiation. *J Biol Chem* **271** (43) p.27025-30.

Li, Y., Huang, T.-T., Carlson, E. J., Melov, S., Ursell, P. C., Olson, J. L., *et al.* (1995) Dilated cardiomyopathy and neonatal lethality in mutant mice lacking manganese superoxide dismutase. *Nature Genetics* **11** (4) p.376-381. 10.1038/ng1295-376.

Li, Z., Guo, J.-R., Chen, Q.-Q., Wang, C.-Y., Zhang, W.-J., Yao, M.-C., *et al.* (2017) Exploring the Antitumor Mechanism of High-Dose Cytarabine through the Metabolic Perturbations of Ribonucleotide and Deoxyribonucleotide in Human Promyelocytic Leukemia HL-60 Cells. *Molecules (Basel, Switzerland)* **22** (3) p.499. 10.3390/molecules22030499.

Lieschke, G. J., Grail, D., Hodgson, G., Metcalf, D., Stanley, E., Cheers, C., *et al.* (1994) Mice lacking granulocyte colony-stimulating factor have chronic neutropenia, granulocyte and macrophage progenitor cell deficiency, and impaired neutrophil mobilization. *Blood* **84** (6) p.1737-46.

Lima, C. D. and Mondragón, A. (1994) Mechanism of type II DNA topoisomerases: a tale of two gates. *Structure* **2** (6) p.559-560. 10.1016/S0969-2126(00)00055-1.

Lin, C. S., Lim, S. K., D'Agati, V. and Costantini, F. (1996) Differential effects of an erythropoietin receptor gene disruption on primitive and definitive erythropoiesis. *Genes Dev* **10** (2) p.154-64. 10.1101/gad.10.2.154.

Lin, Y. F., Lee, H. M., Leu, S. J. and Tsai, Y. H. (2007) The essentiality of PKCalpha and PKCbetaI translocation for CD14+monocyte differentiation towards macrophages and dendritic cells, respectively. *J Cell Biochem* **102** (2) p.429-41. 10.1002/jcb.21305.

Lin, Y. F., Leu, S. J., Huang, H. M. and Tsai, Y. H. (2011) Selective activation of specific PKC isoforms dictating the fate of CD14(+) monocytes towards differentiation or apoptosis. *J Cell Physiol* **226** (1) p.122-31. 10.1002/jcp.22312.

Littler, D. R., Walker, J. R., She, Y. M., Finerty, P. J., Jr., Newman, E. M. and Dhe-Paganon, S. (2006) Structure of human protein kinase C eta (PKCeta) C2 domain and identification of phosphorylation sites. *Biochem Biophys Res Commun* **349** (4) p.1182-9. 10.1016/j.bbrc.2006.08.160.

Liu, B., Li, L.-J., Gong, X., Zhang, W., Zhang, H. and Zhao, L. (2018) Co-expression of ATP binding cassette transporters is associated with poor prognosis in acute myeloid leukemia. *Oncology letters* **15** (5) p.6671-6677. 10.3892/ol.2018.8095.

Liu, J., Wang, L., Zhao, F., Tseng, S., Narayanan, C., Shura, L., *et al.* (2015) Pre-Clinical Development of a Humanized Anti-CD47 Antibody with Anti-Cancer Therapeutic Potential. *PLOS ONE* **10** (9) p.e0137345. 10.1371/journal.pone.0137345.

Loi, T. H., Dai, P., Carlin, S., Melo, J. V. and Ma, D. D. F. (2016) Pro-survival role of protein kinase C epsilon in Philadelphia chromosome positive acute leukemia. *Leukemia & Lymphoma* **57** (2) p.411-418. 10.3109/10428194.2015.1043545.

Lu, D., Huang, J. and Basu, A. (2006) Protein kinase Cepsilon activates protein kinase B/Akt via DNA-PK to protect against tumor necrosis factor-alpha-induced cell death. *J Biol Chem* **281** (32) p.22799-807. 10.1074/jbc.M603390200.

Macanas-Pirard, P., Broekhuizen, R., González, A., Oyanadel, C., Ernst, D., García, P., *et al.* (2017) Resistance of leukemia cells to cytarabine chemotherapy is mediated by bone marrow stroma, involves cell-surface equilibrative nucleoside transporter-1 removal and correlates with patient outcome. *Oncotarget* **8** (14)

Madeira, F., Park, Y. M., Lee, J., Buso, N., Gur, T., Madhusoodanan, N., *et al.* (2019) The EMBL-EBI search and sequence analysis tools APIs in 2019. *Nucleic acids research* **47** (W1) p.W636-W641. 10.1093/nar/gkz268.

Maier, T., Güell, M. and Serrano, L. (2009) Correlation of mRNA and protein in complex biological samples. *FEBS Letters* **583** (24) p.3966-3973. https://doi.org/10.1016/j.febslet.2009.10.036.

Maissel, A., Marom, M., Shtutman, M., Shahaf, G. and Livneh, E. (2006) PKCeta is localized in the Golgi, ER and nuclear envelope and translocates to the nuclear envelope upon PMA activation and serum-starvation: C1b domain and the pseudosubstrate containing fragment target PKCeta to the Golgi and the nuclear envelope. *Cell Signal* **18** (8) p.1127-39. 10.1016/j.cellsig.2005.09.003.

Majeti, R., Chao, M. P., Alizadeh, A. A., Pang, W. W., Jaiswal, S., Gibbs, K. D., Jr., *et al.* (2009) CD47 is an adverse prognostic factor and therapeutic antibody target on human acute myeloid leukemia stem cells. *Cell* **138** (2) p.286-99. 10.1016/j.cell.2009.05.045.

Majeti, R., Park, C. Y. and Weissman, I. L. (2007) Identification of a hierarchy of multipotent hematopoietic progenitors in human cord blood. *Cell Stem Cell* **1** (6) p.635-45. 10.1016/j.stem.2007.10.001.

Majothi, S., Adams, D., Loke, J., Stevens, S. P., Wheatley, K. and Wilson, J. S. (2020) FLT3 inhibitors in acute myeloid leukaemia: assessment of clinical effectiveness, adverse events and future research—a systematic review and meta-analysis. *Systematic Reviews* **9** (1) p.285. 10.1186/s13643-020-01540-1.

Majumder, P. K., Mishra, N. C., Sun, X., Bharti, A., Kharbanda, S., Saxena, S., *et al.* (2001) Targeting of protein kinase C delta to mitochondria in the oxidative stress response. *Cell Growth Differ* **12** (9) p.465-70.

Maksimovic, N., Zaric, M., Gazibara, T., Trajkovic, G., Maric, G., Miljus, D., *et al.* (2018) Incidence and Mortality Patterns of Acute Myeloid Leukemia in Belgrade, Serbia (1999–2013). *Medicina (Kaunas)* **54** (1) 10.3390/medicina54010005.

Mancini, E., Sanjuan-Pla, A., Luciani, L., Moore, S., Grover, A., Zay, A., *et al.* (2012) FOG-1 and GATA-1 act sequentially to specify definitive megakaryocytic and erythroid progenitors. *The EMBO journal* **31** (2) p.351-365. 10.1038/emboj.2011.390.

Mansat-de Mas, V., Bezombes, C., Quillet-Mary, A., Bettaieb, A., D'Orgeix A, D., Laurent, G., *et al.* (1999) Implication of radical oxygen species in

ceramide generation, c-Jun N-terminal kinase activation and apoptosis induced by daunorubicin. *Mol Pharmacol* **56** (5) p.867-74.

Marbeuf-Gueye, C., Ettori, D., Priebe, W., Kozlowski, H. and Garnier-Suillerot, A. (1999) Correlation between the kinetics of anthracycline uptake and the resistance factor in cancer cells expressing the multidrug resistance protein or the P-glycoprotein. *Biochimica et Biophysica Acta (BBA) - Molecular Cell Research* **1450** (3) p.374-384. https://doi.org/10.1016/S0167-4889(99)00060-9.

Martínez-Gimeno, C., Díaz-Meco, M. T., Domínguez, I. and Moscat, J. (1995) Alterations in levels of different protein kinase C isotypes and their influence on behavior of squamous cell carcinoma of the oral cavity: epsilon PKC, a novel prognostic factor for relapse and survival. *Head Neck* **17** (6) p.516-25. 10.1002/hed.2880170609.

Martini, S., Soliman, T., Gobbi, G., Mirandola, P., Carubbi, C., Masselli, E., *et al.* (2018) PKCepsilon Controls Mitotic Progression by Regulating Centrosome Migration and Mitotic Spindle Assembly. *Mol Cancer Res* **16** (1) p.3-15. 10.1158/1541-7786.MCR-17-0244.

Masso-Welch, P. A., Winston, J. S., Edge, S., Darcy, K. M., Asch, H., Vaughan, M. M., *et al.* (2001) Altered expression and localization of PKC eta in human breast tumors. *Breast Cancer Res Treat* **68** (3) p.211-23. 10.1023/a:1012265703669.

Matsunaga, T., Takemoto, N., Sato, T., Takimoto, R., Tanaka, I., Fujimi, A., *et al.* (2003) Interaction between leukemic-cell VLA-4 and stromal fibronectin is a decisive factor for minimal residual disease of acute myelogenous leukemia. *Nat Med* **9** (9) p.1158-65. 10.1038/nm909.

May, W. S., Tyler, P. G., Ito, T., Armstrong, D. K., Qatsha, K. A. and Davidson, N. E. (1994) Interleukin-3 and bryostatin-1 mediate hyperphosphorylation of BCL2 alpha in association with suppression of apoptosis. *Journal of Biological Chemistry* **269** (43) p.26865-26870. https://doi.org/10.1016/S0021-9258(18)47099-8.

Mayati, A., Moreau, A., Le Vee, M., Stieger, B., Denizot, C., Parmentier, Y., *et al.* (2017) Protein Kinases C-Mediated Regulations of Drug Transporter Activity, Localization and Expression. *Int J Mol Sci* **18** (4) 10.3390/ijms18040764.

McJilton, M. A., Van Sikes, C., Wescott, G. G., Wu, D., Foreman, T. L., Gregory, C. W., *et al.* (2003) Protein kinase Cepsilon interacts with Bax and promotes survival of human prostate cancer cells. *Oncogene* **22** (39) p.7958-68. 10.1038/sj.onc.1206795.

McKenzie, J. L., Gan, O. I., Doedens, M., Wang, J. C. and Dick, J. E. (2006) Individual stem cells with highly variable proliferation and self-renewal properties comprise the human hematopoietic stem cell compartment. *Nat Immunol* **7** (11) p.1225-33. 10.1038/ni1393.

Medeiros, B. C., Tanaka, T. N., Balaian, L., Bashey, A., Guzdar, A., Li, H., *et al.* (2018) A Phase I/II Trial of the Combination of Azacitidine and Gemtuzumab Ozogamicin for Treatment of Relapsed Acute Myeloid Leukemia. *Clin Lymphoma Myeloma Leuk* **18** (5) p.346-352.e5. 10.1016/j.clml.2018.02.017.

Medinger, M. and Passweg, J. R. (2017) Acute myeloid leukaemia genomics. *Br J Haematol* **179** (4) p.530-542. 10.1111/bjh.14823.

Michaelis, M., Rothweiler, F., Loschmann, N., Sharifi, M., Ghafourian, T. and Cinatl, J., Jr. (2015) Enzastaurin inhibits ABCB1-mediated drug efflux independently of effects on protein kinase C signalling and the cellular p53 status. *Oncotarget* **6** (19) p.17605-20. 10.18632/oncotarget.2889.

Midic, D., Rinke, J., Perner, F., Müller, V., Hinze, A., Pester, F., *et al.* (2020) Prevalence and dynamics of clonal hematopoiesis caused by leukemia-associated mutations in elderly individuals without hematologic disorders. *Leukemia* **34** (8) p.2198-2205. 10.1038/s41375-020-0869-y.

Mirandola, P., Gobbi, G., Ponti, C., Sponzilli, I., Cocco, L. and Vitale, M. (2006) PKCepsilon controls protection against TRAIL in erythroid progenitors. *Blood* **107** (2) p.508-13. 10.1182/blood-2005-07-2676.

Mischak, H., Goodnight, J. A., Kolch, W., Martiny-Baron, G., Schaechtle, C., Kazanietz, M. G., *et al.* (1993) Overexpression of protein kinase C-delta and -epsilon in NIH 3T3 cells induces opposite effects on growth, morphology, anchorage dependence, and tumorigenicity. *J Biol Chem* **268** (9) p.6090-6.

Mochly-Rosen, D., Das, K. and Grimes, K. V. (2012) Protein kinase C, an elusive therapeutic target? *Nat Rev Drug Discov* **11** (12) p.937-57. 10.1038/nrd3871.

Mochly-Rosen, D., Khaner, H. and Lopez, J. (1991) Identification of intracellular receptor proteins for activated protein kinase C. *Proc Natl Acad Sci U S A* **88** (9) p.3997-4000. 10.1073/pnas.88.9.3997.

Morita, K., Wang, F., Jahn, K., Hu, T., Tanaka, T., Sasaki, Y., *et al.* (2020) Clonal evolution of acute myeloid leukemia revealed by high-throughput single-cell genomics. *Nature Communications* **11** (1) p.5327. 10.1038/s41467-020-19119-8.

Morrison, S. J. and Weissman, I. L. (1994) The long-term repopulating subset of hematopoietic stem cells is deterministic and isolatable by phenotype. *Immunity* **1** (8) p.661-673. https://doi.org/10.1016/1074-7613(94)90037-X.

Morschhauser, F., Seymour, J. F., Kluin-Nelemans, H. C., Grigg, A., Wolf, M., Pfreundschuh, M., *et al.* (2008) A phase II study of enzastaurin, a protein kinase C beta inhibitor, in patients with relapsed or refractory mantle cell lymphoma. *Annals of Oncology* **19** (2) p.247-253. https://doi.org/10.1093/annonc/mdm463.

Mrózek, K., Marcucci, G., Nicolet, D., Maharry, K. S., Becker, H., Whitman, S. P., *et al.* (2012) Prognostic significance of the European LeukemiaNet standardized system for reporting cytogenetic and molecular alterations in adults with acute myeloid leukemia. *Journal of clinical oncology : official journal of the American Society of Clinical Oncology* **30** (36) p.4515-4523. 10.1200/JCO.2012.43.4738.

Muller, C., Laurent, G. and Ling, V. (1995) P-glycoprotein stability is affected by serum deprivation and high cell density in multidrug-resistant cells. *J Cell Physiol* **163** (3) p.538-44. 10.1002/jcp.1041630314.

Murphy, M. P. (2009) How mitochondria produce reactive oxygen species. *The Biochemical journal* **417** (1) p.1-13. 10.1042/BJ20081386.

Naci, D., Berrazouane, S., Barabé, F. and Aoudjit, F. (2019) Cell adhesion to collagen promotes leukemia resistance to doxorubicin by reducing DNA damage through the inhibition of Rac1 activation. *Scientific reports* **9** (1) p.19455-19455. 10.1038/s41598-019-55934-w.

Nerlov, C. and Graf, T. (1998) PU.1 induces myeloid lineage commitment in multipotent hematopoietic progenitors. *Genes & development* **12** (15) p.2403-2412. 10.1101/gad.12.15.2403.

Nerlov, C., McNagny, K. M., Döderlein, G., Kowenz-Leutz, E. and Graf, T. (1998) Distinct C/EBP functions are required for eosinophil lineage commitment and maturation. *Genes Dev* **12** (15) p.2413-23. 10.1101/gad.12.15.2413.

Newton, A. C. (2003) Regulation of the ABC kinases by phosphorylation: protein kinase C as a paradigm. *Biochemical Journal* **370** (Pt 2) p.361.

Newton, A. C. (2010) Protein kinase C: poised to signal. *American Journal of Physiology-Endocrinology and Metabolism* **298** (3) p.E395-E402. 10.1152/ajpendo.00477.2009.

Nilsson, S. K., Johnston, H. M. and Coverdale, J. A. (2001) Spatial localization of transplanted hemopoietic stem cells: inferences for the localization of stem cell niches. *Blood* **97** (8) p.2293-9. 10.1182/blood.v97.8.2293.

Nishizuka, Y. (1984) The role of protein kinase C in cell surface signal transduction and tumour promotion. *Nature* **308** (5961) p.693-698. 10.1038/308693a0.

Nooter, K., Sonneveld, P., Oostrum, R., Herweijer, H., Hagenbeek, T. and Valerio, D. (1990) Overexpression of the MDRL gene in blast cells from patients with acute myelocytic leukemia is associated with decreased anthracycline accumulation that can be restored by cyclosporin-A. *International Journal of Cancer* **45** (2) p.263-268. 10.1002/ijc.2910450210.

Norgaard, J. M., Bukh, A., Langkjer, S. T., Clausen, N., Palshof, T. and Hokland, P. (1998) MDR1 gene expression and drug resistance of AML cells. *Br J Haematol* **100** (3) p.534-40. 10.1046/j.1365-2141.1998.00593.x.

Notta, F., Doulatov, S., Laurenti, E., Poeppl, A., Jurisica, I. and Dick, J. E. (2011) Isolation of Single Human Hematopoietic Stem Cells Capable of Long-Term Multilineage Engraftment. *Science* **333** (6039) p.218-221. 10.1126/science.1201219.

Notta, F., Zandi, S., Takayama, N., Dobson, S., Gan, O. I., Wilson, G., *et al.* (2016) Distinct routes of lineage development reshape the human blood hierarchy across ontogeny. *Science* **351** (6269) p.aab2116. 10.1126/science.aab2116.

Ohmori, Y., Tanabe, J., Terashima, M., Shoji, W., Takada, S. and Obinata, M. (1992) Role of c-Myc on erythroid differentiation. *Tohoku J Exp Med* **168** (2) p.203-10. 10.1620/tjem.168.203.

Ohno, S., Konno, Y., Akita, Y., Yano, A. and Suzuki, K. (1990) A point mutation at the putative ATP-binding site of protein kinase C alpha abolishes the kinase activity and renders it down-regulation-insensitive. A molecular link between autophosphorylation and down-regulation. *J Biol Chem* **265** (11) p.6296-300.

Okada, S., Nakauchi, H., Nagayoshi, K., Nishikawa, S., Miura, Y. and Suda, T. (1992) In vivo and in vitro stem cell function of c-kit- and Sca-1-positive murine hematopoietic cells. *Blood* **80** (12) p.3044-50.

Okhrimenko, H., Lu, W., Xiang, C., Hamburger, N., Kazimirsky, G. and Brodie, C. (2005) Protein kinase C-epsilon regulates the apoptosis and survival of glioma cells. *Cancer Res* **65** (16) p.7301-9. 10.1158/0008-5472.Can-05-1064.

Osawa, M., Hanada, K., Hamada, H. and Nakauchi, H. (1996) Long-term lymphohematopoietic reconstitution by a single CD34-low/negative hematopoietic stem cell. *Science* **273** (5272) p.242-5. 10.1126/science.273.5272.242.

Ottone, T., Ammatuna, E., Lavorgna, S., Noguera, N. I., Buccisano, F., Venditti, A., *et al.* (2008) An allele-specific rt-PCR assay to detect type A mutation of the nucleophosmin-1 gene in acute myeloid leukemia. *J Mol Diagn* **10** (3) p.212-6. 10.2353/jmoldx.2008.070166.

Pallis, M. and Das-Gupta, E. (2005) Flow cytometric measurement of functional and phenotypic P-glycoprotein. *Methods Mol Med* **111** p.167-81. 10.1385/1-59259-889-7:167.

Pallis, M., Hills, R., White, P., Grundy, M., Russell, N., Burnett, A., *et al.* (2011) Analysis of the interaction of induction regimens with p-glycoprotein expression in patients with acute myeloid leukaemia: results from the MRC AML15 trial. *Blood Cancer Journal* **1** (6) p.e23-e23. 10.1038/bcj.2011.23.

Pallis, M. and Russell, N. (2000) P-glycoprotein plays a drug-efflux-independent role in augmenting cell survival in acute myeloblastic leukemia and is associated with modulation of a sphingomyelin-ceramide apoptotic pathway. *Blood* **95** (9) p.2897-904.

Pallis, M., Zhu, Y. M. and Russell, N. H. (1997) Bcl-x(L) is heterogenously expressed by acute myeloblastic leukaemia cells and is associated with autonomous growth in vitro and with P-glycoprotein expression. *Leukemia* **11** (7) p.945-9. 10.1038/sj.leu.2400705.

Pan, G., O'Rourke, K., Chinnaiyan, A. M., Gentz, R., Ebner, R., Ni, J., *et al.* (1997) The receptor for the cytotoxic ligand TRAIL. *Science* **276** (5309) p.111-3. 10.1126/science.276.5309.111.

Pan, Q., Bao, L. W., Kleer, C. G., Sabel, M. S., Griffith, K. A., Teknos, T. N., *et al.* (2005) Protein kinase C epsilon is a predictive biomarker of aggressive breast cancer and a validated target for RNA interference anticancer therapy. *Cancer Res* **65** (18) p.8366-71. 10.1158/0008-5472.Can-05-0553.

Pan, Q., Bao, L. W., Teknos, T. N. and Merajver, S. D. (2006) Targeted disruption of protein kinase C epsilon reduces cell invasion and motility through inactivation of RhoA and RhoC GTPases in head and neck squamous cell carcinoma. *Cancer Res* **66** (19) p.9379-84. 10.1158/0008-5472.Can-06-2646.

Pan, R., Hogdal, L. J., Benito, J. M., Bucci, D., Han, L., Borthakur, G., *et al.* (2014) Selective BCL-2 inhibition by ABT-199 causes on-target cell death in acute myeloid leukemia. *Cancer Discov* **4** (3) p.362-75. 10.1158/2159-8290.Cd-13-0609.

Papaemmanuil, E., Gerstung, M., Bullinger, L., Gaidzik, V. I., Paschka, P., Roberts, N. D., *et al.* (2016) Genomic Classification and Prognosis in Acute Myeloid Leukemia. *N Engl J Med* **374** (23) p.2209-2221. 10.1056/NEJMoa1516192.

Pardee, T. S., Zuber, J. and Lowe, S. W. (2011) Flt3-ITD alters chemotherapy response in vitro and in vivo in a p53-dependent manner. *Exp Hematol* **39** (4) p.473-485.e4. 10.1016/j.exphem.2011.01.009.

Pardo, O. E., Wellbrock, C., Khanzada, U. K., Aubert, M., Arozarena, I., Davidson, S., *et al.* (2006) FGF-2 protects small cell lung cancer cells from apoptosis through a complex involving PKCepsilon, B-Raf and S6K2. *Embo j* **25** (13) p.3078-88. 10.1038/sj.emboj.7601198.

Pass, J. M., Gao, J., Jones, W. K., Wead, W. B., Wu, X., Zhang, J., *et al.* (2001) Enhanced PKC beta II translocation and PKC beta II-RACK1 interactions in PKC epsilon-induced heart failure: a role for RACK1. *Am J Physiol Heart Circ Physiol* **281** (6) p.H2500-10. 10.1152/ajpheart.2001.281.6.H2500.

Passegué, E. and Wagers, A. J. (2006) Regulating Quiescence: New Insights into Hematopoietic Stem Cell Biology. *Developmental Cell* **10** (4) p.415-417. https://doi.org/10.1016/j.devcel.2006.03.002.

Patel, J. P., Gönen, M., Figueroa, M. E., Fernandez, H., Sun, Z., Racevskis, J., *et al.* (2012) Prognostic Relevance of Integrated Genetic Profiling in Acute Myeloid Leukemia. *New England Journal of Medicine* **366** (12) p.1079-1089. 10.1056/NEJMoa1112304.

Paul, F., Arkin, Y., Giladi, A., Jaitin, D. A., Kenigsberg, E., Keren-Shaul, H., *et al.* (2015) Transcriptional Heterogeneity and Lineage Commitment in Myeloid Progenitors. *Cell* **163** (7) p.1663-77. 10.1016/j.cell.2015.11.013.

Pearn, L., Fisher, J., Burnett, A. K. and Darley, R. L. (2007) The role of PKC and PDK1 in monocyte lineage specification by Ras. *Blood* **109** (10) p.4461-4469.

Peled, A., Kollet, O., Ponomaryov, T., Petit, I., Franitza, S., Grabovsky, V., *et al.* (2000) The chemokine SDF-1 activates the integrins LFA-1, VLA-4, and VLA-5 on immature human CD34(+) cells: role in transendothelial/stromal migration and engraftment of NOD/SCID mice. *Blood* **95** (11) p.3289-96.

Pelicano, H., Carney, D. and Huang, P. (2004) ROS stress in cancer cells and therapeutic implications. *Drug Resist Updat* **7** (2) p.97-110. 10.1016/j.drup.2004.01.004.

Perander, M., Bjorkoy, G. and Johansen, T. (2001) Nuclear import and export signals enable rapid nucleocytoplasmic shuttling of the atypical protein kinase C lambda. *J Biol Chem* **276** (16) p.13015-24. 10.1074/jbc.M010356200.

Perletti, G. P., Concari, P., Brusaferri, S., Marras, E., Piccinini, F. and Tashjian, A. H., Jr. (1998) Protein kinase Cepsilon is oncogenic in colon epithelial cells by interaction with the ras signal transduction pathway. *Oncogene* **16** (25) p.3345-8. 10.1038/sj.onc.1201871.

Perveen, K., Quach, A., McPhee, A., Prescott, S. L., Barry, S. C., Hii, C. S., *et al.* (2019) Validation of monoclonal anti-PKC isozyme antibodies for flow cytometry analyses in human T cell subsets and expression in cord blood T cells. *Scientific Reports* **9** (1) p.9263. 10.1038/s41598-019-45507-2.

Pétriz, J., Gottesman, M. M. and Aran, J. M. (2004) An MDR-EGFP gene fusion allows for direct cellular localization, function and stability assessment of P-glycoprotein. *Curr Drug Deliv* **1** (1) p.43-56. 10.2174/1567201043480072.

Piekny, A., Werner, M. and Glotzer, M. (2005) Cytokinesis: welcome to the Rho zone. *Trends Cell Biol* **15** (12) p.651-8. 10.1016/j.tcb.2005.10.006.

Pierce, A., Heyworth, C. M., Nicholls, S. E., Spooncer, E., Dexter, T. M., Lord, J. M., *et al.* (1998) An Activated Protein Kinase C α Gives a Differentiation Signal for Hematopoietic Progenitor Cells and Mimicks Macrophage Colony-stimulating Factor–stimulated Signaling Events. *The Journal of Cell Biology* **140** (6) p.1511-1518.

Pinho, S. and Frenette, P. S. (2019) Haematopoietic stem cell activity and interactions with the niche. *Nature Reviews Molecular Cell Biology* **20** (5) p.303-320. 10.1038/s41580-019-0103-9.

Piskernik, C., Haindl, S., Behling, T., Gerald, Z., Kehrer, I., Redl, H., *et al.* (2008) Antimycin A and lipopolysaccharide cause the leakage of superoxide

radicals from rat liver mitochondria. *Biochim Biophys Acta* **1782** (4) p.280-5. 10.1016/j.bbadis.2008.01.007.

Plo, I., Hernandez, H., Kohlhagen, G., Lautier, D., Pommier, Y. and Laurent, G. (2002) Overexpression of the atypical protein kinase C zeta reduces topoisomerase II catalytic activity, cleavable complexes formation, and drug-induced cytotoxicity in monocytic U937 leukemia cells. *J Biol Chem* **277** (35) p.31407-15. 10.1074/jbc.M204654200.

Pogoda, J. M., Preston-Martin, S., Nichols, P. W. and Ross, R. K. (2002) Smoking and risk of acute myeloid leukemia: results from a Los Angeles County case-control study. *Am J Epidemiol* **155** (6) p.546-53. 10.1093/aje/155.6.546.

Pommier, Y., Leo, E., Zhang, H. and Marchand, C. (2010) DNA Topoisomerases and Their Poisoning by Anticancer and Antibacterial Drugs. *Chemistry & Biology* **17** (5) p.421-433. https://doi.org/10.1016/j.chembiol.2010.04.012.

Pongracz, J., Clark, P., Neoptolemos, J. P. and Lord, J. M. (1995) Expression of protein kinase C isoenzymes in colorectal cancer tissue and their differential activation by different bile acids. *International Journal of Cancer* **61** (1) p.35-39. https://doi.org/10.1002/ijc.2910610107.

Porter, S. N. and Magee, J. A. (2017) PRKCH regulates hematopoietic stem cell function and predicts poor prognosis in acute myeloid leukemia. *Exp Hematol* **53** p.43-47. 10.1016/j.exphem.2017.05.006.

Potocnik, A. J., Brakebusch, C. and Fässler, R. (2000) Fetal and adult hematopoietic stem cells require beta1 integrin function for colonizing fetal liver, spleen, and bone marrow. *Immunity* **12** (6) p.653-63. 10.1016/s1074-7613(00)80216-2.

Pourahmad, J., Salimi, A. and Seydi, E. (2016) Role of Oxygen Free Radicals in Cancer Development and Treatment. 10.5772/64787

Prekeris, R., Mayhew, M. W., Cooper, J. B. and Terrian, D. M. (1996) Identification and localization of an actin-binding motif that is unique to the epsilon isoform of protein kinase C and participates in the regulation of synaptic function. *J Cell Biol* **132** (1-2) p.77-90. 10.1083/jcb.132.1.77.

Racke, F. K., Wang, D., Zaidi, Z., Kelley, J., Visvader, J., Soh, J. W., *et al.* (2001) A potential role for protein kinase C-epsilon in regulating megakaryocytic lineage commitment. *J Biol Chem* **276** (1) p.522-8. 10.1074/jbc.M005236200.

Ramos, N. R., Mo, C. C., Karp, J. E. and Hourigan, C. S. (2015) Current Approaches in the Treatment of Relapsed and Refractory Acute Myeloid Leukemia. *J Clin Med* **4** (4) p.665-95. 10.3390/jcm4040665.

Rapin, N., Bagger, F. O., Jendholm, J., Mora-Jensen, H., Krogh, A., Kohlmann, A., *et al.* (2014) Comparing cancer vs normal gene expression profiles identifies new disease entities and common transcriptional programs in AML patients. *Blood* **123** (6) p.894-904. 10.1182/blood-2013-02-485771.

Rastogi, R., Geng, X., Li, F. and Ding, Y. (2017) NOX Activation by Subunit Interaction and Underlying Mechanisms in Disease. *Frontiers in cellular neuroscience* **10** p.301-301. 10.3389/fncel.2016.00301.

Ray, P. D., Huang, B.-W. and Tsuji, Y. (2012) Reactive oxygen species (ROS) homeostasis and redox regulation in cellular signaling. *Cellular signalling* **24** (5) p.981-990. 10.1016/j.cellsig.2012.01.008.

Redig, A. J. and Platanias, L. C. (2008) Protein kinase C signalling in leukemia. *Leukemia & Lymphoma* **49** (7) p.1255-1262. 10.1080/10428190802007726.

Regala, R. P., Weems, C., Jamieson, L., Khoor, A., Edell, E. S., Lohse, C. M., *et al.* (2005) Atypical Protein Kinase Cι Is an Oncogene in Human Non–Small Cell Lung Cancer. *Cancer Research* **65** (19) p.8905-8911. 10.1158/0008-5472.Can-05-2372.

Rein, L. A. M. and Rizzieri, D. A. (2014) Clinical potential of elacytarabine in patients with acute myeloid leukemia. *Therapeutic advances in hematology* **5** (6) p.211-220. 10.1177/2040620714552615.

Rieger, M. A. and Schroeder, T. (2012) Hematopoiesis. *Cold Spring Harbor perspectives in biology* **4** (12) p.a008250. 10.1101/cshperspect.a008250.

Rizvi, M. A., Ghias, K., Davies, K. M., Ma, C., Weinberg, F., Munshi, H. G., *et al.* (2006) Enzastaurin (LY317615), a protein kinase Cbeta inhibitor, inhibits the AKT pathway and induces apoptosis in multiple myeloma cell lines. *Mol Cancer Ther* **5** (7) p.1783-9. 10.1158/1535-7163.Mct-05-0465.

Robb, L. (2007) Cytokine receptors and hematopoietic differentiation. *Oncogene* **26** (47) p.6715-23. 10.1038/sj.onc.1210756.

Robert-Moreno, A., Guiu, J., Ruiz-Herguido, C., López, M. E., Inglés-Esteve, J., Riera, L., *et al.* (2008) Impaired embryonic haematopoiesis yet normal arterial development in the absence of the Notch ligand Jagged1. *Embo j* **27** (13) p.1886-95. 10.1038/emboj.2008.113.

Roboz, G. J., Ritchie, E. K., Dault, Y., Lam, L., Marshall, D. C., Cruz, N. M., *et al.* (2018) Phase I trial of plerixafor combined with decitabine in newly diagnosed older patients with acute myeloid leukemia. *Haematologica* **103** (8) p.1308-1316. 10.3324/haematol.2017.183418.

Ron, D., Chen, C. H., Caldwell, J., Jamieson, L., Orr, E. and Mochly-Rosen, D. (1994) Cloning of an intracellular receptor for protein kinase C: a homolog of the beta subunit of G proteins. *Proc Natl Acad Sci U S A* **91** (3) p.839-43. 10.1073/pnas.91.3.839.

Ross, D. D. (2000) Novel mechanisms of drug resistance in leukemia. *Leukemia* **14** (3) p.467-73.

Rossi, F., McNagny, M., Smith, G., Frampton, J. and Graf, T. (1996) Lineage commitment of transformed haematopoietic progenitors is determined by the level of PKC activity. *Embo j* **15** (8) p.1894-901.

Ruijtenberg, S. and van den Heuvel, S. (2016) Coordinating cell proliferation and differentiation: Antagonism between cell cycle regulators and cell type-

specific gene expression. *Cell cycle (Georgetown, Tex.)* **15** (2) p.196-212. 10.1080/15384101.2015.1120925.

Russell, B., Curtis, M. W., Koshman, Y. E. and Samarel, A. M. (2010) Mechanical stress-induced sarcomere assembly for cardiac muscle growth in length and width. *J Mol Cell Cardiol* **48** (5) p.817-23. 10.1016/j.yjmcc.2010.02.016.

Ruvolo, P. P., Deng, X., Carr, B. K. and May, W. S. (1998) A functional role for mitochondrial protein kinase Calpha in Bcl2 phosphorylation and suppression of apoptosis. *J Biol Chem* **273** (39) p.25436-42. 10.1074/jbc.273.39.25436.

Ruvolo, P. P., Deng, X. and May, W. S. (2001) Phosphorylation of Bcl2 and regulation of apoptosis. *Leukemia* **15** (4) p.515-522. 10.1038/sj.leu.2402090.

Ruvolo, P. P., Zhou, L., Watt, J. C., Ruvolo, V. R., Burks, J. K., Jiffar, T., *et al.* (2011) Targeting PKC-mediated signal transduction pathways using enzastaurin to promote apoptosis in acute myeloid leukemia-derived cell lines and blast cells. *Journal of cellular biochemistry* **112** (6) p.1696-1707. 10.1002/jcb.23090.

Sallman, D. A., Al Malki, M., Asch, A. S., Lee, D. J., Kambhampati, S., Donnellan, W. B., *et al.* (2020) Tolerability and efficacy of the first-in-class anti-CD47 antibody magrolimab combined with azacitidine in MDS and AML patients: Phase Ib results. *Journal of Clinical Oncology* **38** (15_suppl) p.7507-7507. 10.1200/JCO.2020.38.15_suppl.7507.

Sallmyr, A., Fan, J., Datta, K., Kim, K.-T., Grosu, D., Shapiro, P., *et al.* (2008) Internal tandem duplication of FLT3 (FLT3/ITD) induces increased ROS production, DNA damage, and misrepair: implications for poor prognosis in AML. *Blood* **111** (6) p.3173-3182. 10.1182/blood-2007-05-092510.

Samuel, V. T., Liu, Z.-X., Qu, X., Elder, B. D., Bilz, S., Befroy, D., *et al.* (2004) Mechanism of Hepatic Insulin Resistance in Non-alcoholic Fatty Liver Disease*. *Journal of Biological Chemistry* **279** (31) p.32345-32353. https://doi.org/10.1074/jbc.M313478200.

Samuel, V. T., Liu, Z.-X., Wang, A., Beddow, S. A., Geisler, J. G., Kahn, M., *et al.* (2007) Inhibition of protein kinase Cε prevents hepatic insulin resistance in nonalcoholic fatty liver disease. *The Journal of Clinical Investigation* **117** (3) p.739-745. 10.1172/JCI30400.

Sanz, M. A., Fenaux, P., Tallman, M. S., Estey, E. H., Löwenberg, B., Naoe, T., *et al.* (2019) Management of acute promyelocytic leukemia: updated recommendations from an expert panel of the European LeukemiaNet. *Blood* **133** (15) p.1630-1643. 10.1182/blood-2019-01-894980.

Sardina, J. L., López-Ruano, G., Sánchez-Abarca, L. I., Pérez-Simón, J. A., Gaztelumendi, A., Trigueros, C., *et al.* (2010) p22phox-dependent NADPH oxidase activity is required for megakaryocytic differentiation. *Cell Death Differ* **17** (12) p.1842-54. 10.1038/cdd.2010.67.

Sardina, J. L., López-Ruano, G., Sánchez-Sánchez, B., Llanillo, M. and Hernández-Hernández, A. (2012) Reactive oxygen species: Are they important for haematopoiesis? *Critical Reviews in Oncology/Hematology* **81** (3) p.257-274. 10.1016/j.critrevonc.2011.03.005.

Sattler, M., Winkler, T., Verma, S., Byrne, C. H., Shrikhande, G., Salgia, R., *et al.* (1999) Hematopoietic growth factors signal through the formation of reactive oxygen species. *Blood* **93** (9) p.2928-35.

Saurin, A. T., Brownlow, N. and Parker, P. J. (2009) Protein kinase C epsilon in cell division: control of abscission. *Cell Cycle* **8** (4) p.549-55. 10.4161/cc.8.4.7653.

Saurin, A. T., Durgan, J., Cameron, A. J., Faisal, A., Marber, M. S. and Parker, P. J. (2008) The regulated assembly of a PKCepsilon complex controls the completion of cytokinesis. *Nat Cell Biol* **10** (8) p.891-901. 10.1038/ncb1749.

Schneider, E., Cowan, K. H., Bader, H., Toomey, S., Schwartz, G. N., Karp, J. E., *et al.* (1995) Increased expression of the multidrug resistance-associated protein gene in relapsed acute leukemia. *Blood* **85** (1) p.186-93.

Schofield, R. (1978) The relationship between the spleen colony-forming cell and the haemopoietic stem cell. *Blood Cells* **4** (1-2) p.7-25.

Schwende, H., Fitzke, E., Ambs, P. and Dieter, P. (1996) Differences in the state of differentiation of THP-1 cells induced by phorbol ester and 1,25-dihydroxyvitamin D3. *J Leukoc Biol* **59** (4) p.555-61.

Schwendt, M. and Olive, M. F. (2017) Protein kinase Cε activity regulates mGluR5 surface expression in the rat nucleus accumbens. *J Neurosci Res* **95** (4) p.1079-1090. 10.1002/jnr.23868.

Seedhouse, C. H., Grundy, M., White, P., Li, Y., Fisher, J., Yakunina, D., *et al.* (2007) Sequential influences of leukemia-specific and genetic factors on p-glycoprotein expression in blasts from 817 patients entered into the National Cancer Research Network acute myeloid leukemia 14 and 15 trials. *Clin Cancer Res* **13** (23) p.7059-66. 10.1158/1078-0432.Ccr-07-1484.

Seymour, J. F., Döhner, H., Butrym, A., Wierzbowska, A., Selleslag, D., Jang, J. H., *et al.* (2017) Azacitidine improves clinical outcomes in older patients with acute myeloid leukaemia with myelodysplasia-related changes compared with conventional care regimens. *BMC Cancer* **17** (1) p.852. 10.1186/s12885-017-3803-6.

Shirai, Y., Kashiwagi, K., Yagi, K., Sakai, N. and Saito, N. (1998) Distinct effects of fatty acids on translocation of gamma- and epsilon-subspecies of protein kinase C. *J Cell Biol* **143** (2) p.511-21. 10.1083/jcb.143.2.511.

Shivdasani, R. A., Fujiwara, Y., McDevitt, M. A. and Orkin, S. H. (1997) A lineage-selective knockout establishes the critical role of transcription factor GATA-1 in megakaryocyte growth and platelet development. *Embo j* **16** (13) p.3965-73. 10.1093/emboj/16.13.3965.

Shysh, A. C., Nguyen, L. T., Guo, M., Vaska, M., Naugler, C. and Rashid-Kolvear, F. (2017) The incidence of acute myeloid leukemia in Calgary, Alberta, Canada: a retrospective cohort study. *BMC Public Health* **18** (1) p.94. 10.1186/s12889-017-4644-6.

Simon, E. and Kornitzer, D. (2014) Pulse-chase analysis to measure protein degradation. *Methods Enzymol* **536** p.65-75. 10.1016/b978-0-12-420070-8.00006-4.

Sivaprasad, U., Shankar, E. and Basu, A. (2007) Downregulation of Bid is associated with PKCε-mediated TRAIL resistance. *Cell Death & Differentiation* **14** (4) p.851-860. 10.1038/sj.cdd.4402077.

Slupsky, J. R., Kamiguti, A. S., Harris, R. J., Cawley, J. C. and Zuzel, M. (2007) Central role of protein kinase Cepsilon in constitutive activation of ERK1/2 and Rac1 in the malignant cells of hairy cell leukemia. *Am J Pathol* **170** (2) p.745-54. 10.2353/ajpath.2007.060557.

Smeets, M. E. P., Raymakers, R. A. P., Vierwinden, G., Pennings, A. H. M., Boezeman, J., Minderman, H., *et al.* (1999) Idarubicin DNA intercalation is reduced by MRP1 and not Pgp. *Leukemia* **13** (9) p.1390-1398. 10.1038/sj.leu.2401496.

Socinski, M. A., Raju, R. N., Stinchcombe, T., Kocs, D. M., Couch, L. S., Barrera, D., *et al.* (2010) Randomized, Phase II Trial of Pemetrexed and Carboplatin with or without Enzastaurin versus Docetaxel and Carboplatin as First-Line Treatment of Patients with Stage IIIB/IV Non-small Cell Lung Cancer. *Journal of Thoracic Oncology* **5** (12) p.1963-1969. https://doi.org/10.1097/JTO.0b013e3181fd42eb.

Soh, J. W. and Weinstein, I. B. (2003) Roles of specific isoforms of protein kinase C in the transcriptional control of cyclin D1 and related genes. *J Biol Chem* **278** (36) p.34709-16. 10.1074/jbc.M302016200.

Spangler, J. B., Moraga, I., Mendoza, J. L. and Garcia, K. C. (2015) Insights into cytokine-receptor interactions from cytokine engineering. *Annu Rev Immunol* **33** p.139-67. 10.1146/annurev-immunol-032713-120211.

Speidel, D., Wellbrock, J. and Abas, M. (2017) RUNX1 Upregulation by Cytotoxic Drugs Promotes Apoptosis. *Cancer Res* **77** (24) p.6818-6824. 10.1158/0008-5472.Can-17-0319.

Sprick, M. R., Weigand, M. A., Rieser, E., Rauch, C. T., Juo, P., Blenis, J., *et al.* (2000) FADD/MORT1 and caspase-8 are recruited to TRAIL receptors 1 and 2 and are essential for apoptosis mediated by TRAIL receptor 2. *Immunity* **12** (6) p.599-609. 10.1016/s1074-7613(00)80211-3.

Srivastava, J., Procyk, K. J., Iturrioz, X. and Parker, P. J. (2002) Phosphorylation is required for PMA- and cell-cycle-induced degradation of protein kinase Cdelta. *Biochem J* **368** (Pt 1) p.349-55. 10.1042/bj20020737.

Stanley, E. R. (2009) Lineage commitment: cytokines instruct, at last! *Cell Stem Cell* **5** (3) p.234-6. 10.1016/j.stem.2009.08.015.

Starling, J. J., Shepard, R. L., Cao, J., Law, K. L., Norman, B. H., Kroin, J. S., *et al.* (1997) Pharmacological characterization of LY335979: A potent cyclopropyldibenzosuberane modulator of P-glycoprotein. *Advances in Enzyme Regulation* **37** p.335-347. https://doi.org/10.1016/S0065-2571(96)00021-0.

Staudinger, J., Zhou, J., Burgess, R., Elledge, S. J. and Olson, E. N. (1995) PICK1: a perinuclear binding protein and substrate for protein kinase C isolated by the yeast two-hybrid system. *J Cell Biol* **128** (3) p.263-71. 10.1083/jcb.128.3.263.

Steensma, D. P., Bejar, R., Jaiswal, S., Lindsley, R. C., Sekeres, M. A., Hasserjian, R. P., *et al.* (2015) Clonal hematopoiesis of indeterminate potential and its distinction from myelodysplastic syndromes. *Blood* **126** (1) p.9-16. 10.1182/blood-2015-03-631747.

Steinberg, S. F. (2008) Structural Basis of Protein Kinase C Isoform Function. *Physiological Reviews* **88** (4) p.1341-1378. 10.1152/physrev.00034.2007.

Steinberg, S. F. (2015) Mechanisms for redox-regulation of protein kinase C. *Frontiers in Pharmacology* **6** (128) 10.3389/fphar.2015.00128.

Stone, R. M., Mandrekar, S. J., Sanford, B. L., Laumann, K., Geyer, S., Bloomfield, C. D., *et al.* (2017) Midostaurin plus Chemotherapy for Acute Myeloid Leukemia with a FLT3 Mutation. *The New England journal of medicine* **377** (5) p.454-464. 10.1056/NEJMoa1614359.

Stone, R. M., Manley, P. W., Larson, R. A. and Capdeville, R. (2018) Midostaurin: its odyssey from discovery to approval for treating acute myeloid leukemia and advanced systemic mastocytosis. *Blood advances* **2** (4) p.444-453. 10.1182/bloodadvances.2017011080.

Sugiyama, T., Kohara, H., Noda, M. and Nagasawa, T. (2006) Maintenance of the hematopoietic stem cell pool by CXCL12-CXCR4 chemokine signaling in bone marrow stromal cell niches. *Immunity* **25** (6) p.977-88. 10.1016/j.immuni.2006.10.016.

Sun, M. K. and Alkon, D. L. (2012) Activation of protein kinase C isozymes for the treatment of dementias. *Adv Pharmacol* **64** p.273-302. 10.1016/b978-0-12-394816-8.00008-8.

Sun, Y., Chen, B.-R. and Deshpande, A. (2018) Epigenetic Regulators in the Development, Maintenance, and Therapeutic Targeting of Acute Myeloid Leukemia. *Frontiers in oncology* **8** p.41-41. 10.3389/fonc.2018.00041.

Swaminathan, M., Bannon, S. A., Routbort, M., Naqvi, K., Kadia, T. M., Takahashi, K., *et al.* (2019) Hematologic malignancies and Li-Fraumeni syndrome. *Cold Spring Harb Mol Case Stud* **5** (1) 10.1101/mcs.a003210.

Tabe, Y. and Konopleva, M. (2015) Role of Microenvironment in Resistance to Therapy in AML. *Curr Hematol Malig Rep* **10** (2) p.96-103. 10.1007/s11899-015-0253-6.

Takami, M., Katayama, K., Noguchi, K. and Sugimoto, Y. (2018) Protein kinase C alpha-mediated phosphorylation of PIM-1L promotes the survival and

proliferation of acute myeloid leukemia cells. *Biochem Biophys Res Commun* **503** (3) p.1364-1371. 10.1016/j.bbrc.2018.07.049.

Takubo, K., Nagamatsu, G., Kobayashi, C. I., Nakamura-Ishizu, A., Kobayashi, H., Ikeda, E., *et al.* (2013) Regulation of glycolysis by Pdk functions as a metabolic checkpoint for cell cycle quiescence in hematopoietic stem cells. *Cell Stem Cell* **12** (1) p.49-61. 10.1016/j.stem.2012.10.011.

Tang, R., Faussat, A.-M., Perrot, J.-Y., Marjanovic, Z., Cohen, S., Storme, T., *et al.* (2008) Zosuquidar restores drug sensitivity in P-glycoprotein expressing acute myeloid leukemia (AML). *BMC cancer* **8** p.51-51. 10.1186/1471-2407-8-51.

Taussig, D. C., Miraki-Moud, F., Anjos-Afonso, F., Pearce, D. J., Allen, K., Ridler, C., *et al.* (2008) Anti-CD38 antibody-mediated clearance of human repopulating cells masks the heterogeneity of leukemia-initiating cells. *Blood* **112** (3) p.568-75. 10.1182/blood-2007-10-118331.

Tavor, S., Petit, I., Porozov, S., Avigdor, A., Dar, A., Leider-Trejo, L., *et al.* (2004) CXCR4 regulates migration and development of human acute myelogenous leukemia stem cells in transplanted NOD/SCID mice. *Cancer Res* **64** (8) p.2817-24. 10.1158/0008-5472.can-03-3693.

Teicher, B. A. and Fricker, S. P. (2010) CXCL12 (SDF-1)/CXCR4 Pathway in Cancer. *Clinical Cancer Research* **16** (11) p.2927-2931. 10.1158/1078-0432.Ccr-09-2329.

Thomas, H. and Coley, H. M. (2003) Overcoming multidrug resistance in cancer: an update on the clinical strategy of inhibiting p-glycoprotein. *Cancer Control* **10** (2) p.159-65. 10.1177/107327480301000207.

Till, J. E., McCulloch, E. A. and Siminovitch, L. (1964) A STOCHASTIC MODEL OF STEM CELL PROLIFERATION, BASED ON THE GROWTH OF SPLEEN COLONY-FORMING CELLS. *Proc Natl Acad Sci U S A* **51** (1) p.29-36. 10.1073/pnas.51.1.29.

Tong, H., Chen, W., Steenbergen, C. and Murphy, E. (2000) Ischemic Preconditioning Activates Phosphatidylinositol-3-Kinase Upstream of Protein Kinase C. *Circulation Research* **87** (4) p.309-315. doi:10.1161/01.RES.87.4.309.

Tonks, A., Pearn, L., Musson, M., Gilkes, A., Mills, K. I., Burnett, A. K., *et al.* (2007) Transcriptional dysregulation mediated by RUNX1-RUNX1T1 in normal human progenitor cells and in acute myeloid leukaemia. *Leukemia* **21** (12) p.2495-2505. 10.1038/sj.leu.2404961.

Tonks, A., Tonks, A. J., Pearn, L., Mohamad, Z., Burnett, A. K. and Darley, R. L. (2005) Optimized retroviral transduction protocol which preserves the primitive subpopulation of human hematopoietic cells. *Biotechnol Prog* **21** (3) p.953-8. 10.1021/bp0500314.

Tóthová, E., Fricova, M., Stecová, N., Kafková, A. and Elbertová, A. (2002) High expression of Bcl-2 protein in acute myeloid leukemia cells is associated with poor response to chemotherapy. *Neoplasma* **49** (3) p.141-4.

Totoń, E., Ignatowicz, E., Skrzeczkowska, K. and Rybczyńska, M. (2011) Protein kinase Cε as a cancer marker and target for anticancer therapy. *Pharmacol Rep* **63** (1) p.19-29. 10.1016/s1734-1140(11)70395-4.

Tuomi, S., Mai, A., Nevo, J., Laine, J. O., Vilkki, V., Ohman, T. J., *et al.* (2009) PKCepsilon regulation of an alpha5 integrin-ZO-1 complex controls lamellae formation in migrating cancer cells. *Sci Signal* **2** (77) p.ra32. 10.1126/scisignal.2000135.

Uy, G. L., Rettig, M. P., Motabi, I. H., McFarland, K., Trinkaus, K. M., Hladnik, L. M., *et al.* (2012) A phase 1/2 study of chemosensitization with the CXCR4 antagonist plerixafor in relapsed or refractory acute myeloid leukemia. *Blood* **119** (17) p.3917-24. 10.1182/blood-2011-10-383406.

Valeriote, F. and van Putten, L. (1975) Proliferation-dependent cytotoxicity of anticancer agents: a review. *Cancer Res* **35** (10) p.2619-30.

Valko, M., Leibfritz, D., Moncol, J., Cronin, M. T., Mazur, M. and Telser, J. (2007) Free radicals and antioxidants in normal physiological functions and human disease. *Int J Biochem Cell Biol* **39** (1) p.44-84. 10.1016/j.biocel.2006.07.001.

van der Kolk, D. M., de Vries, E. G. E., Müller, M. and Vellenga, E. (2002) The Role of Drug Efflux Pumps in Acute Myeloid Leukemia. *Leukemia & Lymphoma* **43** (4) p.685-701. 10.1080/10428190290016773.

van der Kolk, D. M., de Vries, E. G. E., van Putten, W. L. J., Verdonck, L. F., Ossenkoppele, G. J., Verhoef, G. E. G., *et al.* (2000) P-glycoprotein and Multidrug Resistance Protein Activities in Relation to Treatment Outcome in Acute Myeloid Leukemia. *Clinical Cancer Research* **6** (8) p.3205-3214.

Vannini, N., Girotra, M., Naveiras, O., Nikitin, G., Campos, V., Giger, S., *et al.* (2016) Specification of haematopoietic stem cell fate via modulation of mitochondrial activity. *Nat Commun* **7** p.13125. 10.1038/ncomms13125.

Varga, A., Czifra, G., Tállai, B., Németh, T., Kovács, I., Kovács, L., *et al.* (2004) Tumor grade-dependent alterations in the protein kinase C isoform pattern in urinary bladder carcinomas. *European urology* **46** (4) p.462-465. 10.1016/j.eururo.2004.04.014.

Verma, A. K., Wheeler, D. L., Aziz, M. H. and Manoharan, H. (2006) Protein kinase Cepsilon and development of squamous cell carcinoma, the nonmelanoma human skin cancer. *Mol Carcinog* **45** (6) p.381-8. 10.1002/mc.20230.

Vermeulen, K., Van Bockstaele, D. R. and Berneman, Z. N. (2003) The cell cycle: a review of regulation, deregulation and therapeutic targets in cancer. *Cell proliferation* **36** (3) p.131-149. 10.1046/j.1365-2184.2003.00266.x.

Visnjic, D., Kalajzic, Z., Rowe, D. W., Katavic, V., Lorenzo, J. and Aguila, H. L. (2004) Hematopoiesis is severely altered in mice with an induced osteoblast deficiency. *Blood* **103** (9) p.3258-64. 10.1182/blood-2003-11-4011.

Vosberg, S. and Greif, P. A. (2019) Clonal evolution of acute myeloid leukemia from diagnosis to relapse. *Genes, chromosomes & cancer* **58** (12) p.839-849. 10.1002/gcc.22806.

Votyakova, T. V. and Reynolds, I. J. (2001) ΔΨm-Dependent and -independent production of reactive oxygen species by rat brain mitochondria. *Journal of Neurochemistry* **79** (2) p.266-277. https://doi.org/10.1046/j.1471-4159.2001.00548.x.

Wall, N. R., Mohammad, R. M., Reddy, K. B. and Al-Katib, A. M. (2000) Bryostatin 1 induces ubiquitination and proteasome degradation of Bcl-2 in the human acute lymphoblastic leukemia cell line, Reh. *Int J Mol Med* **5** (2) p.165-71. 10.3892/ijmm.5.2.165.

Wang, E. S., Aplenc, R., Chirnomas, D., Dugan, M., Fazal, S., Iyer, S., *et al.* (2020) Safety of gemtuzumab ozogamicin as monotherapy or combination therapy in an expanded-access protocol for patients with relapsed or refractory acute myeloid leukemia. *Leukemia & Lymphoma* **61** (8) p.1965-1973. 10.1080/10428194.2020.1742897.

Wang, H., Gutierrez-Uzquiza, A., Garg, R., Barrio-Real, L., Abera, M. B., Lopez-Haber, C., *et al.* (2014) Transcriptional regulation of oncogenic protein kinase Cϵ (PKCϵ) by STAT1 and Sp1 proteins. *The Journal of biological chemistry* **289** (28) p.19823-19838. 10.1074/jbc.M114.548446.

Wang, Q.-s., Wang, Y., Lv, H.-y., Han, Q.-w., Fan, H., Guo, B., *et al.* (2015) Treatment of CD33-directed chimeric antigen receptor-modified T cells in one patient with relapsed and refractory acute myeloid leukemia. *Molecular therapy : the journal of the American Society of Gene Therapy* **23** (1) p.184-191. 10.1038/mt.2014.164.

Warren, M., Luthra, R., Yin, C. C., Ravandi, F., Cortes, J. E., Kantarjian, H. M., *et al.* (2012) Clinical impact of change of FLT3 mutation status in acute myeloid leukemia patients. *Modern Pathology* **25** (10) p.1405-1412. 10.1038/modpathol.2012.88.

Wattad, M., Weber, D., Döhner, K., Krauter, J., Gaidzik, V. I., Paschka, P., *et al.* (2017) Impact of salvage regimens on response and overall survival in acute myeloid leukemia with induction failure. *Leukemia* **31** (6) p.1306-1313. 10.1038/leu.2017.23.

Weichert, W., Gekeler, V., Denkert, C., Dietel, M. and Hauptmann, S. (2003) Protein kinase C isoform expression in ovarian carcinoma correlates with indicators of poor prognosis. *Int J Oncol* **23** (3) p.633-639. 10.3892/ijo.23.3.633.

Welch, J. S., Ley, T. J., Link, D. C., Miller, C. A., Larson, D. E., Koboldt, D. C., *et al.* (2012) The origin and evolution of mutations in acute myeloid leukemia. *Cell* **150** (2) p.264-78. 10.1016/j.cell.2012.06.023.

Whetton, A. D., Heyworth, C. M., Nicholls, S. E., Evans, C. A., Lord, J. M., Dexter, T. M., *et al.* (1994) Cytokine-mediated protein kinase C activation

is a signal for lineage determination in bipotential granulocyte macrophage colony-forming cells. *J Cell Biol* **125** (3) p.651-9. 10.1083/jcb.125.3.651.

Wilson, A., Laurenti, E., Oser, G., van der Wath, R. C., Blanco-Bose, W., Jaworski, M., *et al.* (2008) Hematopoietic stem cells reversibly switch from dormancy to self-renewal during homeostasis and repair. *Cell* **135** (6) p.1118-29. 10.1016/j.cell.2008.10.048.

Wilson, A. and Trumpp, A. (2006) Bone-marrow haematopoietic-stem-cell niches. *Nature Reviews Immunology* **6** (2) p.93-106. 10.1038/nri1779.

Wu, D., Foreman, T. L., Gregory, C. W., McJilton, M. A., Wescott, G. G., Ford, O. H., *et al.* (2002) Protein kinase cepsilon has the potential to advance the recurrence of human prostate cancer. *Cancer Res* **62** (8) p.2423-9.

Wu, M., Li, C. and Zhu, X. (2018) FLT3 inhibitors in acute myeloid leukemia. *Journal of Hematology & Oncology* **11** (1) p.133. 10.1186/s13045-018-0675-4.

Wu, S. F., Huang, Y., Hou, J. K., Yuan, T. T., Zhou, C. X., Zhang, J., *et al.* (2010) The downregulation of onzin expression by PKCepsilon-ERK2 signaling and its potential role in AML cell differentiation. *Leukemia* **24** (3) p.544-51. 10.1038/leu.2009.280.

Wuchter, C., Leonid, K., Ruppert, V., Schrappe, M., Buchner, T., Schoch, C., *et al.* (2000) Clinical significance of P-glycoprotein expression and function for response to induction chemotherapy, relapse rate and overall survival in acute leukemia. *Haematologica* **85** (7) p.711-721. 10.3324/%x.

Xie, Y., Burcu, M., Linn, D. E., Qiu, Y. and Baer, M. R. (2010) Pim-1 Kinase Protects P-Glycoprotein from Degradation and Enables Its Glycosylation and Cell Surface Expression. *Molecular Pharmacology* **78** (2) p.310-318. 10.1124/mol.109.061713.

Xu, T.-R., He, G., Dobson, K., England, K. and Rumsby, M. (2007) Phosphorylation at Ser729 specifies a Golgi localisation for protein kinase C epsilon (PKCε) in 3T3 fibroblasts. *Cellular Signalling* **19** (9) p.1986-1995. https://doi.org/10.1016/j.cellsig.2007.05.009.

Xu, T. R. and Rumsby, M. G. (2004) Phorbol ester-induced translocation of PKC epsilon to the nucleus in fibroblasts: identification of nuclear PKC epsilon-associating proteins. *FEBS Lett* **570** (1-3) p.20-4. 10.1016/j.febslet.2004.05.080.

Yague, E., Armesilla, A. L., Harrison, G., Elliott, J., Sardini, A., Higgins, C. F., *et al.* (2003) P-glycoprotein (MDR1) expression in leukemic cells is regulated at two distinct steps, mRNA stabilization and translational initiation. *J Biol Chem* **278** (12) p.10344-52. 10.1074/jbc.M211093200.

Yamamoto, R., Morita, Y., Ooehara, J., Hamanaka, S., Onodera, M., Rudolph, Karl L., *et al.* (2013) Clonal Analysis Unveils Self-Renewing Lineage-Restricted Progenitors Generated Directly from Hematopoietic Stem Cells. *Cell* **154** (5) p.1112-1126. https://doi.org/10.1016/j.cell.2013.08.007.

Yanada, M., Matsuo, K., Suzuki, T., Kiyoi, H. and Naoe, T. (2005) Prognostic significance of FLT3 internal tandem duplication and tyrosine kinase domain mutations for acute myeloid leukemia: a meta-analysis. *Leukemia* **19** (8) p.1345-1349. 10.1038/sj.leu.2403838.

Yang, X., Boehm, J. S., Yang, X., Salehi-Ashtiani, K., Hao, T., Shen, Y., *et al.* (2011) A public genome-scale lentiviral expression library of human ORFs. *Nat Methods* **8** (8) p.659-61. 10.1038/nmeth.1638.

Yen, H.-C., Oberley, T. D., Gairola, C. G., Szweda, L. I. and St. Clair, D. K. (1999) Manganese Superoxide Dismutase Protects Mitochondrial Complex I against Adriamycin-Induced Cardiomyopathy in Transgenic Mice. *Archives of Biochemistry and Biophysics* **362** (1) p.59-66. https://doi.org/10.1006/abbi.1998.1011.

Yoshihara, H., Arai, F., Hosokawa, K., Hagiwara, T., Takubo, K., Nakamura, Y., *et al.* (2007) Thrombopoietin/MPL signaling regulates hematopoietic stem cell quiescence and interaction with the osteoblastic niche. *Cell Stem Cell* **1** (6) p.685-97. 10.1016/j.stem.2007.10.020.

Zabkiewicz, J., Pearn, L., Hills, R. K., Morgan, R. G., Tonks, A., Burnett, A. K., *et al.* (2014) The PDK1 master kinase is over-expressed in acute myeloid leukemia and promotes PKC-mediated survival of leukemic blasts. *Haematologica* **99** (5) p.858-64. 10.3324/haematol.2013.096487.

Zeidman, R., Trollér, U., Raghunath, A., Påhlman, S. and Larsson, C. (2002) Protein kinase Cepsilon actin-binding site is important for neurite outgrowth during neuronal differentiation. *Mol Biol Cell* **13** (1) p.12-24. 10.1091/mbc.01-04-0210.

Zeng, Z., Samudio, I. J., Munsell, M., An, J., Huang, Z., Estey, E., *et al.* (2006) Inhibition of CXCR4 with the novel RCP168 peptide overcomes stroma-mediated chemoresistance in chronic and acute leukemias. *Molecular Cancer Therapeutics* **5** (12) p.3113-3121. 10.1158/1535-7163.Mct-06-0228.

Zha, J., Harada, H., Osipov, K., Jockel, J., Waksman, G. and Korsmeyer, S. J. (1997) BH3 domain of BAD is required for heterodimerization with BCL-XL and pro-apoptotic activity. *J Biol Chem* **272** (39) p.24101-4. 10.1074/jbc.272.39.24101.

Zhang, J., Niu, C., Ye, L., Huang, H., He, X., Tong, W. G., *et al.* (2003) Identification of the haematopoietic stem cell niche and control of the niche size. *Nature* **425** (6960) p.836-41. 10.1038/nature02041.

Zhang, Z., Wu, J. Y., Hait, W. N. and Yang, J. M. (2004) Regulation of the stability of P-glycoprotein by ubiquitination. *Mol Pharmacol* **66** (3) p.395-403. 10.1124/mol.104.001966.

Zhu, J. and Emerson, S. G. (2002) Hematopoietic cytokines, transcription factors and lineage commitment. *Oncogene* **21** (21) p.3295-3313. 10.1038/sj.onc.1205318.

Zisopoulou, S., Asimaki, O., Leondaritis, G., Vasilaki, A., Sakellaridis, N., Pitsikas, N., *et al.* (2013) PKC-epsilon activation is required for recognition memory in the rat. *Behav Brain Res* **253** p.280-9. 10.1016/j.bbr.2013.07.036.